In theory, theory and practice are the same.
In practice, they are not.

A. Einstein

Members of the Examination Committee:

Prof. dr. P. Van Oostveldt (Chairman)

Prof. dr. ir. N. De Kimpe

Prof. dr. J. Marchand-Brynaert

Prof. dr. F. De Proft

Prof. dr. J. Van der Eycken

Prof. dr. ir. B. De Meulenaer

Prof. dr. M. Waroquier

Dr. S. Catak

Prof. dr. ir. C. Stevens (Promoter)

Prof. dr. ir. V. Van Speybroeck (Promoter)

Promoters: Prof. dr. ir. C. Stevens
Research Group SynBioC, Department of Organic Chemistry,
Faculty of BioScience Engineering, Ghent University
Prof. dr. ir. V. Van Speybroeck, Centre for Molecular Modeling, Ghent University

Dean: Prof. dr. ir. G. Van Huylenbroeck

Rector: Prof. dr. P. Van Cauwenberghe

ir. Diederica D. Claeys

COMBINATION OF EXPERIMENTAL AND COMPUTATIONAL CHEMISTRY IN THE SYNTHESIS OF NEW AZAHETEROCYCLES

Thesis submitted in fulfillment of the requirements
For the degree of Doctor (PhD) in Applied Biological Sciences:
Chemistry

Dutch translation of the title:

Combinatie van experimentele en computationele chemie in de synthese van nieuwe azaheterocyclische verbindingen

ISBN-number: 978-90-5989-332-0

Ghent, September 2009

The author:

ir. Diederica Claeys

The promoters:

Prof. dr. ir. V. Van Speybroeck

Prof. dr. ir. C. Stevens

Woord Vooraf

Vanaf mijn prille jeugd is keuzes maken altijd al een moeilijk te overwinnen berg geweest. Het brede gamma van wetenschappen bij de bio-ingenieurs sprak me aan, aangezien het nog vele wegen openliet. Na het verzamelen van deze ruime bagage, koos ik voor het pad van de scheikunde. Deze richting begon met uren labowerk en experimenteren, maar lag me niet helemaal. Tijdens mijn doctoraat kwam het spoor naar de computationele chemie er bij om zo het energetische landschap op een andere manier te kunnen bekijken.
Het was een hele uitdaging om vertrouwd te geraken met deze twee werelden, maar dit alles smaakt nog naar meer.

Het afleggen van een doctoraat is meer dan onderzoek alleen. Op twee labo's werken is een hele klus, maar bezorgt je ook dubbel zoveel collega's en sterke persoonlijkheden die de goede sfeer garanderen tijdens binnen- en buitenactiviteiten, zoals de ekidens, etentjes, trouwfeesten ...
Onderzoek gaat met ups en downs en net dan is overleg of een babbel met collega's zo verrijkend, daarom zou ik een aantal mensen extra in de verf willen zetten. Dank je: Nicolai, voor de begeleiding tijdens mijn thesis en aan het begin van mijn doctoraat; Bart, Kristof en Pieter, voor de samenwerking rond de Diels-Alder reacties; Kurt en Bart, voor de orde en de chaos aan de labotafel en trekkast; Ann, voor het Ninofs tussendoortje; Toon en Ewald voor het brainstormen, de tips en het programmeerwerk; An, als bureaugenote en assertief klankbord; Karen en Bart, voor de geduldige uitleg en de peptalk; Eva en Ruben voor de discussies op dezelfde golflengte over zoveel meer dan chemie alleen.

Tijdens de vier jaar van mijn doctoraat kon ik steeds rekenen op de steun van mijn promotor, professor Chris Stevens. Proffen hebben het druk, altijd, maar toch kon ik steeds binnenwaaien met een vraag of een tekst die nog net voor de deadline binnen moest.
Verder wil ik zeker ook mijn co-promotor, professor Veronique Van Speybroeck bedanken om me vanaf mijn derde jaar van het doctoraat de mogelijkheid te geven om me te verdiepen in de computationele chemie.

Tevens wil ik de leden van de examencommissie bedanken voor hun tijd die ze staken in het lezen en kritisch evalueren van mijn werk. I would also like to thank professor J. Marchand-Brynaert, professor F. De Proft and dr. S. Catak for their critical reading of this

thesis. Verder wens ik ook professor Bracke en dr. Vanhoecke te bedanken voor de biotesting, die een meerwaarde gaf aan dit onderzoek. Ook een dankjewel aan professor Bultinck en dr. Debie om me de eerste stappen in de kwantumchemie te helpen zetten.

And last, but not least, mijn vrienden en familie. De wandelgenoten, atletiekliefhebbers en Rode Kruisfanaten, om me met mijn neus van tussen de boeken of van achter het scherm te halen en samen fantastische adrenaline en endorfine producerende momenten te beleven. Mijn zus Dakerlia, (schoon)broer Karel, Hanne, Wout en Lotte; jullie tonen me de echte waarden van het leven en laten me mee genieten en veel relativeren. En ten slotte mijn trouwste supporters: mama en papa, voor wie Gent en Ninove slechts een telefoontje van elkaar verwijderd zijn.

Diederica Claeys

Gent, Oktober 2009

Table of Contents

List of Abbreviations

Ac	Acetyl
ADF	Amsterdam Density Functional package
Ar	Aryl
B3LYP	Becke, three-parameter, Lee-Yang-Parr functional
BB1K	Becke88-Becke95 one-parameter model for kinetics functional
BLYP	Becke Lee-Yang-Parr functional
Bn	Benzyl
Boc	*t*-Butoxycarbonyl
BS	Basis set
CCSD	Coupled-cluster with single and double excitations
CCSD(T)	Coupled-cluster with single and double and perturbutive triple excitations
COD	Cycloocta-1,5-diene
COSY	Correlated spectroscopy
Cy	Cyclohexyl
DABCO	1,4-Diazabicyclo[2.2.2]octane
DBU	1,8-Diazabicyclo[5.4.0]undec-7-ene
DEPT	Distortionless enhancement by polarization transfer
DFT	Density functional theory
DIFNOE	Difference nuclear Overhauser effect
DMAP	4-(Dimethylamino)pyridine
DMF	Dimethyl formamide
DMP	Dimethyl phosphite
DMSO	Dimethyl sulfoxide
DMTSF	Dimethyl(methylthio)sulfonium tetrafluorborate
DPPF	1,1'-Bis(diphenylphosphino)ferrocene
EGA	Electrogenerated acids
FMO	Frontier molecular orbital
GGA	Generalized gradient approximation
HF	Hartree-Fock
HMBA	Hexamethylenebis(acetamide)

HMBC	Heteronuclear multiple bond correlation
HOMO	Highest occupied molecular orbital
HPLC	High performance liquid chromatography
HSAB	Hard-soft, acid-base
HSQC	Heteronuclear single quantum correlation
IMDA	Intramolecular Diels-Alder reaction
IMDAF	Intramolecular Diels-Alder reaction of furan
IR	Infra red
IRC	Intrinsic reaction coordinate
KHMDS	Potassium 1,1,1,3,3,3-hexamethyldisilazane
KT	Kamertemperatuur
LDA	Lithium diisopropylamide
LiHMDS	Lithium 1,1,1,3,3,3-hexamethyldisilazane
LOT	Level of theory
LUMO	Lowest unoccupied molecular orbital
MD	Molecular dynamics
Mes	Mesityl, 2,4,6-Trimethylphenyl
MM	Molecular mechanics
Mp.	Melting Point
MP2	Møller–Plesset perturbation theory to second order
MP3	Møller–Plesset perturbation theory to third order
MS	Mass Spectrometry
NICS	Nucleus-independent chemical shift
NOE	Nuclear Overhauser effect
NMR	Nuclear magnetic resonance
NVE	Number of particles, volume, total energy
NVT	Number of particles, volume, temperature
On	overnight
PCA	Principal component analysis
PE	Petroleum ether
PES	Potential energy surface
Ph	Phenyl
PHF	Precultured heart fragment

PM3	Parametric Method 3
Py	Pyridine
QCISD	Quadratic configuration interaction with single and double excitation
RCM	Ring-closing metathesis
RMSD	Root-mean-square deviation
RT	Room temperature
SCF	Self-consistent field
SDD	Stuttgart-Dresden effective core potential
THF	Tetrahydrofuran
TLC	Thin layer chromatography
TOT	Tetrahedral octahedral tetrahedral
TPSS(h)	Tao, Perdew, Staroverov and Scuseria (hybrid) functional
Tr	Trityl, Triphenylmethane
TS	Transition state

Chapter 1 – Introduction and Goal

1 Computational Chemistry

The science of chemistry has been an experimental subject for a long time, strongly distinct from mathematical considerations. In 1830 August Comte wrote that "Every attempt to employ mathematical methods in the study of chemical questions must be considered profoundly irrational and contrary to the spirit of chemistry".[1] With the dawn of quantum theory, however, the potential of quantum mechanics as a predictive theory in chemistry was recognized; but the remaining problem is that the applications of these physical laws lead to equations that are too complicated to be soluble, as Paul Dirac said in 1929. Since then approximate methods have been developed and implemented in software packages. Experimental chemists can use these packages, but should get knowledge of the different methods and their ways of applications in this very young and fast developing science. Moreover, the reliability of the results of different methods and approximations should be validated.

In this way computational chemistry can bring insight into the mechanisms of chemical reactions, or, after validation, the same method can be used in a predictive way for similar reactions.

2 Goal of the Current Research

This PhD was planned as a combination of experimental and computational chemistry. The goal was to synthesize new azaheterocyclic compounds with an interesting potential for biological activity starting from pyroglutamates and α-aminophosphonates, as the *SynBioC* research group has a lot of experience with these compounds, and to investigate different ways of conformational restriction via cyclization. The use of the computational methods to explain observed isomer ratios, stereoselectivities and reactivities, is supposed to bring insights that improve the chemical intuition. Meanwhile the applicability of the methods is evaluated and its use in a predictive way for similar reactions, can lead to the final goal of computational chemistry, i.e. to have predictive power.

2.1 Pyrroglutamate-Hydantoin Rearrangement

The PhD-project started with the functionalisation[2,3,4] and functional group migration[5] of pyroglutamates as a tool for the synthesis of constrained azaheterocyclic compounds. In an introductory study it was assumed that after carbamoylation of pyroglutamates, the pyrrolidinone ring underwent ring expansion to 1,3-diazepine-2,4-diones.[6] Full spectroscopic and X-ray studies revealed, however, that the products were functionalised imidazolidine-2,4-diones or hydantoins (**2**).[7]

Also the ring expansion of pyrrolidinone (**3**) derivatives was tested along with some closely related derivatives.

Hydantoins possess a wide range of biological activities, with applications in the agrochemical sector and in human medicine. Phenytoin (**4**), for example, was introduced as a pharmaceutical in the 1950s and is still the drug of choice for the treatment of certain types of epileptic seizures.[8]

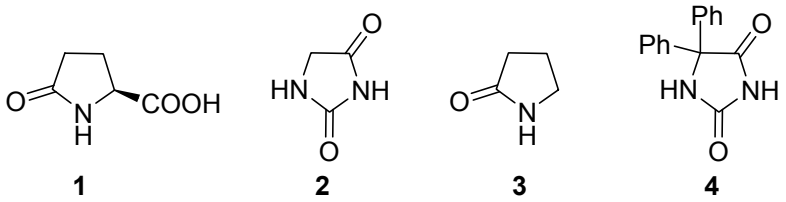

Figure 1. (2*S*)-Pyroglutamic acid (1), the hydantoin nucleus (2), pyrrolidin-2-one (3) and phenytoin (4)

Because of its biological importance, constrained bicyclic hydantoin derivatives were decided to be synthesized using biselectrophiles, which could form an alternative for the use of ring-closing metathesis (RCM).[9]

In cooperation with dr. ir. Dieltiens the idea was set to apply the pyroglutamate-hydantoin rearrangement in the synthesis of bis-hydantoins **5** which are hexamethylenebis(acetamide) (HMBA, **6**) analogues. HMBA has potential anti-cancer activity by inducing tumor cells to differentiate to non-malignant phenotypes.[10]

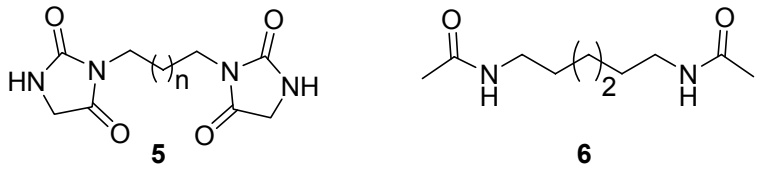

Figure 2. Bis-hydantoins (5) and hexamethylenebis(acetamide) (HMBA, 6)

These bishydantoins are very flexible molecules. To restrict the rotational freedom, the hydantoins would be incorporated in larger ring structures using RCM, as this has shown to be a valuable method for the synthesis of macrocycles. At the same time the limits of the applicability of RCM and the Grubbs' catalyst would be explored.

The thermodynamic stability of the double bond isomers of these macrocyclic alkenes will be investigated *in silico*. This is an apparently evident, but computational challenging task given the still remaining, large number of degrees of freedom. A suitable methodology to easily generate molecular conformations that span the potential energy surface will be looked for. This will be done in cooperation with dr. ir. Verstraelen using MD-Tracks.[11]

2.2 α-Amino Phosphonates

In order to prepare medium-sized amino phosphonates using isocyanates and RCM, a route towards diazepinediones was outlined, starting from β,γ-unsaturated α-aminophosphonates (Scheme 1). Azaheterocyclic phosphonates are a class of compounds with a high biological potential. Moreover, the experience in the *SynBioC* group on the synthesis of α-aminophosphonates[12,13] could be used and the ring closure methodology could be modelled.

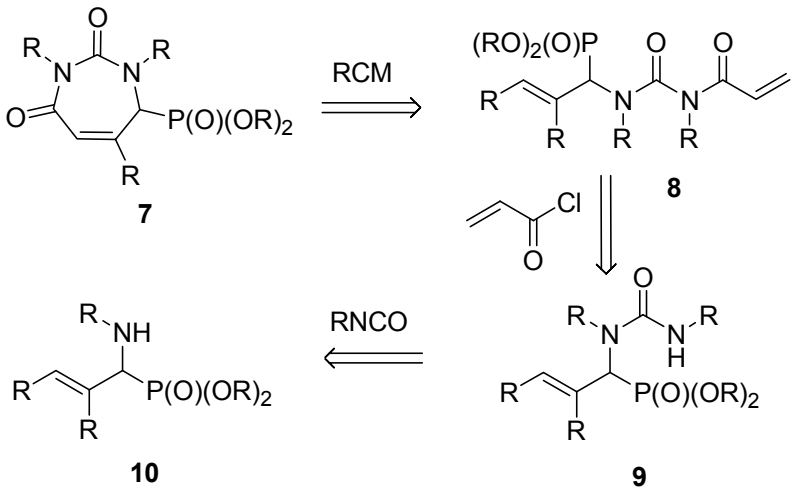

Scheme 1

During the PhD, my attention was more and more attracted to computational chemistry. The developed intramolecular Diels-Alder reaction with furanyl amino phosphonates that resulted in a mixture of *C*(2)-epimers **12** (Scheme 2), seemed an ideal steppingstone to the *in silico* chemistry, as the Diels-Alder reaction has been the subject of a lot of theoretical studies.

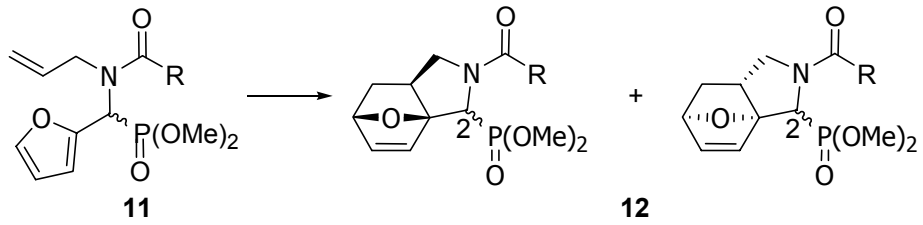

Scheme 2

The aim of the study was to use the transition state theory to predict the observed diastereomeric ratio and to explain the origin of the observed stereoselectivity. Once the appropriate level of theory has been evaluated, the influence of the position of the carbonyl group on the tether will be investigated, as this appeared to have an influence on the observed selectivity.

Experimentally, new derivatives will be synthesized using different dienophiles and other heterocyclic dienes. Ring opening of IMDAF (Intramolecular Diels-Alder reaction of furan) adducts will be tried. The cleavage of the oxygen bridge is a crucial synthetic transformation to produce functionalized cyclohexene derivatives that can be used in natural product synthesis. Hereby, focus will be on the Lewis acid catalyzed reactions which could yield ketones, alcohols or undergo further aromatization (Scheme 3).

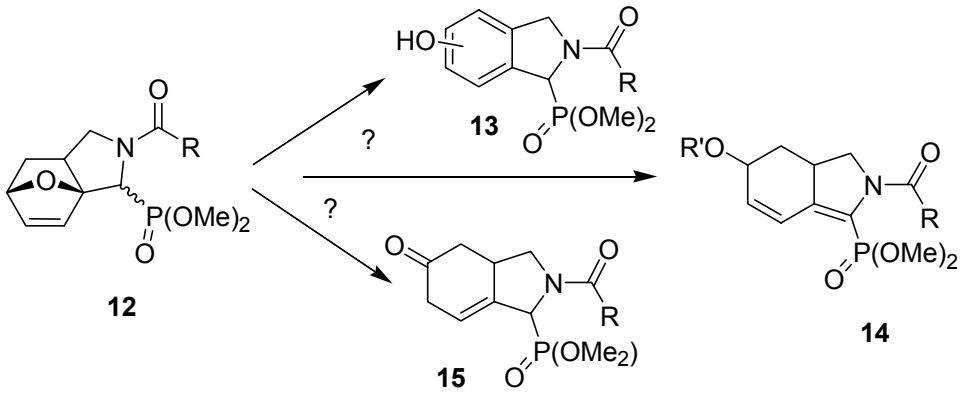

Scheme 3

These reactions will be modelled, trying to give a qualitative view of the relative rate of the reactions and possible product formation. The combination of transition metals together with main-group elements make this a computationally difficult task.

Using the modelling methods, it was tried to get information on quite difficult cyclization strategies of hydantoins and α-amino phosphonates, two classes of compounds that form an important subject of research in the department.

Chapter 2 – Literature Overview

In this chapter a short introduction is given on the two classes of the azaheteroclyclic compounds that occupy an important place in this thesis. The next paragraph gives a profound study of the experimental and theoretical intramolecular Diels-Alder or IMDA reaction, with a focus on furan as diene. In a final part, the literature on the opening of the oxygen bridge in IMDAF adducts is discussed.

1 Hydantoins

A general introduction on hydantoins and their synthesis is given to illustrate the importance of this class of compounds and to place the newly developed straightforward route into the right perspective.

Hydantoins, first detected as products of undesired side-reactions in peptide chemistry, have attracted much interest in drug discovery because of their wide range of therapeutic properties: antiarrhythmic,[14] anticonvulsant,[15] antitumor,[16] antidiabetic,[17] antimuscarinic[18]… activities. Several clinically important pharmaceuticals are based upon this heterocyclic scaffold, such as phenytoin **4** (Figure 3) which is used to treat certain types of epileptic seizures[8] and nilutamide **16**, an antiandrogen medication used in the treatment of prostate cancer. Hydantoins are useful not only for human medicine, but also for agriculture. Hydantocidin **17** is a naturally occurring spirohydantoin with herbicidal activities,[19] iprodion **18** is a commercially used fungicide.

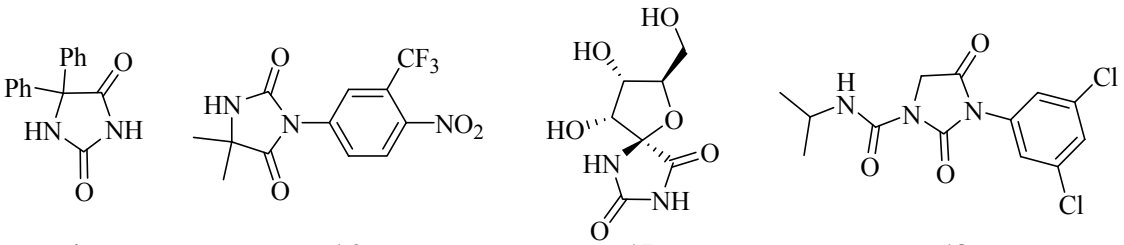

4 **16** **17** **18**

Figure 3. Phenytoin (4), nilutamide (16), hydantocidin (17) and iprodion (18)

Hydantoins may be regarded as cyclic ureides of α-amino acids and these two types of compounds are readily interconvertible. A number of methods exists to synthesize hydantoins.[20,21] Reactions of α-amino acids, nitriles or amides with alkali cyanates (Scheme 4) are used mainly for the preparation of hydantoins with substituents at the *C*(5)-position or also for *N*(1)-substituted hydantoins.

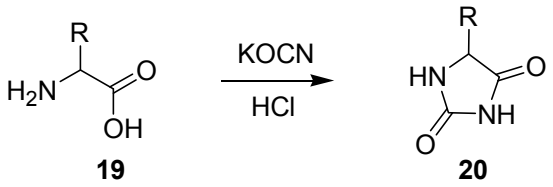

19 **20**

Scheme 4. Urech reaction[22]

Reaction of free α-amino acids, esters or nitriles with isocyanates is valuable when hydantoins with a substituent at the *N*(3)-position are desired. Urea can be reacted with α-amino acids, α-hydroxy acids, α-hydroxy nitriles, α-dicarbonyl compounds or unsaturated acids. Further a range of other methods was described starting from amino acids or derivatives with carbonic acid derivatives like phosgene, alkyl chloroformates, 1,1'-carbonyldiimidazole. Another general method is the Bucherer-Bergs synthesis (Scheme 5) of *C*(5)-substituted hydantoins from aldehydes and ketones through the action of potassium cyanide and ammonium carbonate.[23]

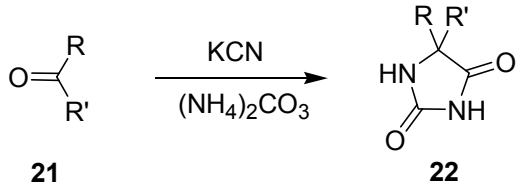

21 **22**

Scheme 5. Bucherer-Bergs reaction

New synthetic methods are still being developed or older ones further investigated; like a palladium catalyzed reaction,[24] a rearrangement reaction of 2,3-epoxydiaryl ketones,[25] or a modified Bucherer-Bergs reaction with nitriles and organometallic reagents.[26] In solid-phase synthesis the hydantoins are mostly synthesized using natural and unnatural acyclic α-amino acids or dipeptides as starting materials.[27]

Several *N*(3),*N'*(3)-polymethylene-bis-hydantoins have been evaluated as hexamethylenebis(acetamide) (HMBA) analogues.[28] HMBA is a compound that induces cancer cells to differentiate to a less malignant phenotype.[10] This provides an attractive area for the development of new anticancer drugs, these differentiation agents are expected to exhibit reduced toxicity relative to conventional chemotherapeutic agents.

The bis-hydantoins were synthesized via an *N*(3)-selective alkylation of the hydantoin with a 1,6-dihalohexane. The problem of this selectivity and the low yields can be circumvented using the protocol described in this thesis.

2 α-Amino Phosphonates[29]

α-Amino phosphonic acids hardly need an introduction, as these are structural analogues of α-amino acids, obtained by substitution of the planar carboxylic acid by a tetrahedral and more bulky phosphonic acid functionality. Many natural and synthetic aminophosphonic acids, phosphonate esters and peptide derivatives exhibit a broad spectrum of biological properties, including enzyme inhibition, antibody generation, antibiotic, antibacterial, antiviral, antifungal, antitumor and herbicide activities. A lot of synthetic effort is spent on the synthesis of cyclic amino acids and amino acid derivatives. They can be used for the synthesis of conformationally constrained peptidomimetics, which form a major tool in modern drug discovery.[30]

They also have applications in hydrometallurgy, due to their metal complexing properties, and in diagnostic medicine as screening agents.[30]

A more thorough introduction on aminophosphonates can be found in reference 29 in the PhD theses of Vanderhoydonck[31] and Moonen[12] and in reviews by Redmore[32] and by Moonen.[33]

3 The Intramolecular Diels-Alder Reaction: Theory and Experiment

3.1 Intro

The Diels-Alder reaction[34] is a Nobel Prize winning reaction that efficiently synthesizes complex ring structures via a pericyclic [4+2]-addition of a conjugated diene and a dienophile (Scheme 6).

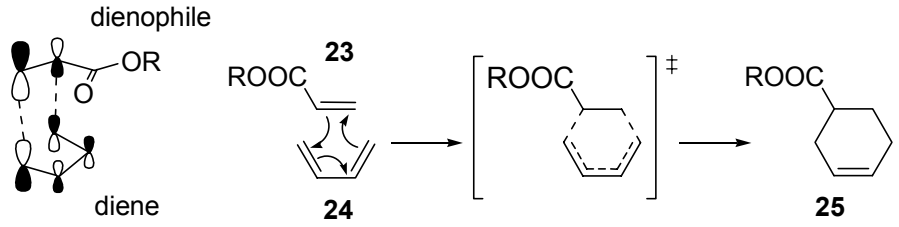

Scheme 6. The pericyclic Diels-Alder reaction

Furans can be used as the 4π diene components despite their aromaticity and hence expected decrease in reactivity.[35] The intramolecular Diels-Alder reaction of furan (the IMDAF reaction) is particularly attractive as two or more rings can be constructed in a

single step. The concerted character of the reaction, the mild conditions and the constraints, imposed by the connecting chain, result in high regio- and stereocontrol.

This part on the intramolecular Diels-Alder (IMDA) reaction starts describing the search for the mechanism of the Diels-Alder reaction and formulation of its general rules, as it shows the nice interplay between experimental and computational chemistry. Then the IMDAF reaction is discussed with a focus on the type I[i] reaction with a short, 3-atom tether, which is used for the synthesis of the heterocyclic amino phosphonates in this thesis. The history of the reaction shows the effect of the tether and its substituents on the reaction rate and selectivity. This is combined with and followed by computational studies of the furan Diels-Alder reaction. Next, different dienophyles encountered in literature are given. The last paragraph illustrates possibles ways to achieve asymmetric synthesis.

3.2 General Rules of Diels-Alder Reactions

After the discovery of the Diels-Alder reaction, the search for its mechanism and the nature of the transition state started. In an animated article Houk et al. gave an overview of the debate on the concerted versus stepwise mechanism of the Diels-Alder reaction.[36] In a concerted reaction, the two new bonds are partially formed in a single transition state. If both bonds are formed to the same extent, it is a synchronous reaction, otherwise, it is asynchronous. The stepwise process can either be diradical or zwitterionic. Experimental evidence was mainly based on the determination of reaction rates and stereoselectivity. Small Arrhenius A factors and stereospecifity point into the direction of a concerted mechanism.

The Diels-Alder reaction implies a stereospecific *syn* addition, so the stereochemistry of the diene and dienophile is retained. Generally *trans* dienophiles react faster than *cis* dienophiles. Another stereochemical aspect is given in the *endo* rule. In most intermolecular reactions, the activating group of the dienophile prefers being oriented towards the diene, due to a favourable interaction between the conjugating group and the diene, allowing secondary orbital interactions, and resulting in the so-called *endo* product. The more familiar terms *endo* and *exo* refer to the orientation of the activating group of the dienophile relative to the diene. For IMDA reactions this nomenclature can get confusing and the terms *syn* en a*nti* are used as well to name the orientation of the tether connection to

[i] In type I IMDA reactions, the tether is attached at the 4-position of the diene; in type II at the 3-position.

the dienophile in the transition state. They result in *endo* and *exo* fused products, with *cis* and *trans* fused rings.

From 1965 to 1969, Woodward and Hoffmann developed the concept of pericyclic reactions. They defined pericyclic reactions as "reactions in which all first-order changes in bonding relationships take place in concert on a closed curve";[37] all bonds are made or broken around a circle.

According to these rules, the Diels-Alder reaction is a concerted $[_{\pi}4_s + _{\pi}2_s]$ process. In a thermal pericyclic reaction, like the Diels-Alder reaction, the total number of $(4q+2)_s$ and $(4r)_a$ components must be odd. A component is a bond or orbital taking part in the pericyclic reaction as a single unit. The prefix π gives the type of electrons, the number refers to the number of electrons in the component. The suffix s stands for suprafacial. In a suprafacial component, new bonds are formed at the same face at both ends; this in contrast with an antarafacial component. For the Diels-Alder there is one $(4q+2)_s$ component, and the reaction is symmetry allowed.

The allowed reactions can maintain bonding all along the concerted pathway, while forbidden reactions necessarily pass through a nonbonding electronic structure along the reaction path and a stepwise mechanism is involved. Allowed reactions are not required to be concerted, but the concerted pathway that maintains bonding is expected to be favoured.[36]

The Woodward-Hoffmann theory had a large influence on the development of the frontier molecular orbital (FMO) theory by Fukui. Fukui assumed that "a majority of chemical reactions should take place at the position and in the direction of maximum overlapping of the HOMO or highest occupied molecular orbital and the LUMO or lowest unoccupied molecular orbital of the reacting species". He realised that for pericyclic reactions, not only the density distribution, but also the nodal property of the particular orbitals has significance.[38] The symmetry is correct for bond formation between the diene HOMO and dienophile LUMO, but also between the diene LUMO and dienophile HOMO, as shown in Figure 4.

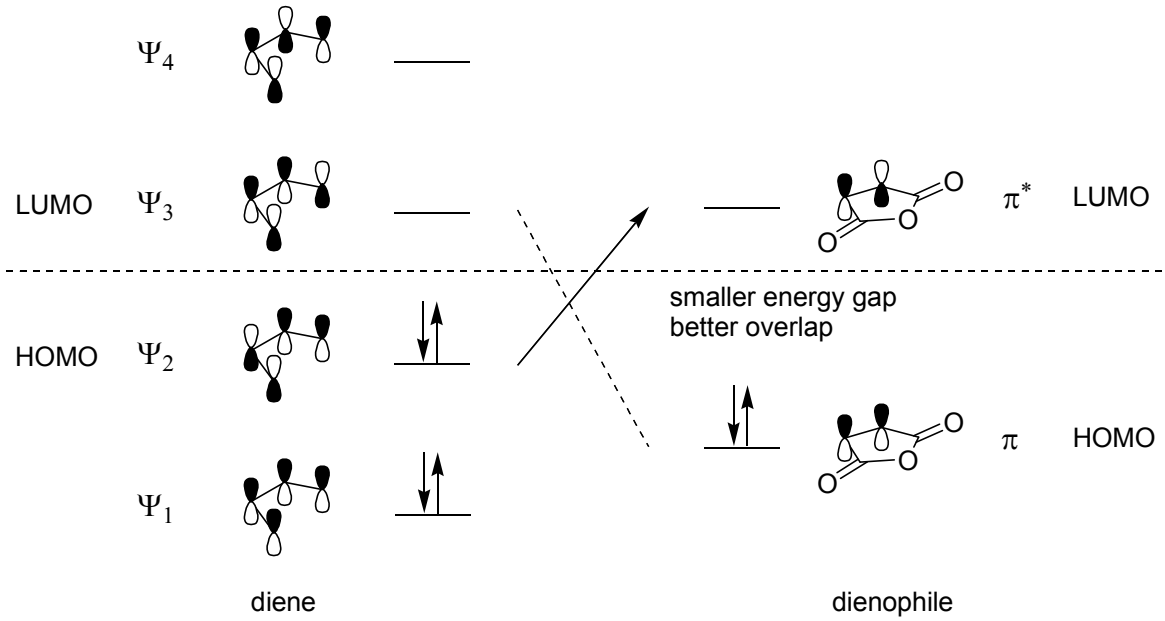

Figure 4. Orbital description of the cycloaddition between butadiene and maleic anhydride

Klopman[39] and Salem[40] derived a mathematical expression for the energy gain, when the orbitals of both reactants interact, by using the perturbation theory. The energy gain is inversely correlated with the energy difference between the HOMO and LUMO orbitals. A large energy gain implies a strong stabilization of the transition state, which promotes its formation and accelerates the reaction. In Figure 4, the electron-deficient dienophile has a low-energy LUMO and the electron-rich diene has a high-energy HOMO, so that this combination is preferred over the combination of the dienophile HOMO and the diene LUMO, which also has the right symmetry.

These theoretical studies provided backing to the concerted mechanism of pericyclic reactions. Early computational studies using semi-empirical methods predicted, however, the two-step mechanism, but this was due to parameterization deficiencies and approximations. Ab-initio methods predict a synchronous, concerted mechanism, with a transition state with aromatic character, to be the most stable.[41] The studies of kinetic isotope effects allow comparing theoretical and experimental results and are in very good agreement with the concerted mechanism.[36]

The FMO theory can be used to explain the *endo* rule, as the symmetry of the orbitals is correct for a bonding interaction[42] at the back of the diene, as shown for the cyclopentadiene dimerisation in Figure 5.

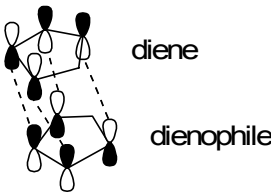

Figure 5

Regioselectivity and rate acceleration by substitution can also be explained using frontier orbitals. The energy difference between the frontier orbitals can be lowered by substitution. Conjugating groups compress FMO separation, electron-donating groups raise FMO energies, while electron-withdrawing groups lower FMO energies. Most electron-withdrawing substituents are conjugating groups as well, so that the overall lowering of the HOMO is much less than that of the LUMO. The change in energy falls in the order of ethylene, 1-substituted diene, 2-substituted diene.[43] This makes electron-withdrawing groups on the dienophile more effective.

Peeters et al. did a more detailed computational investigation of the transition state (TS) stabilization by substitution of the diene and found a correlation with steric, mesomeric, inductive and polarizability properties of the substituents.[44] Steric factors play a major role for 1-dienes, inductive groups have similar influences at 1- and 2-postitions, mesomeric effects appear to dominate in 1-dienes. Elements of the third and fourth periods in the substituents seem to favour TS-stabilization.

Olefin activation causes some asymmetry in the frontier orbitals, which is expressed in the magnitude of the orbital coefficients, obtained from ab-initio calculations. Conjugating substituents increase the coefficient of the unsubstituted terminus of ethylene at the expense of the coefficient of the other terminus in both FMOs. Electron-donating groups increase the remote coefficient of the HOMO and the nearby one in the LUMO, but for alkyl groups, the LUMO coefficients are nearly identical. If electron-withdrawing groups interact only inductively, their effect is the opposite of the donor groups. Conjugation of electron-withdrawing groups, further increases the remote LUMO coefficient, but diminishes or reverses the difference in HOMO coefficients (Figure 6).[43]

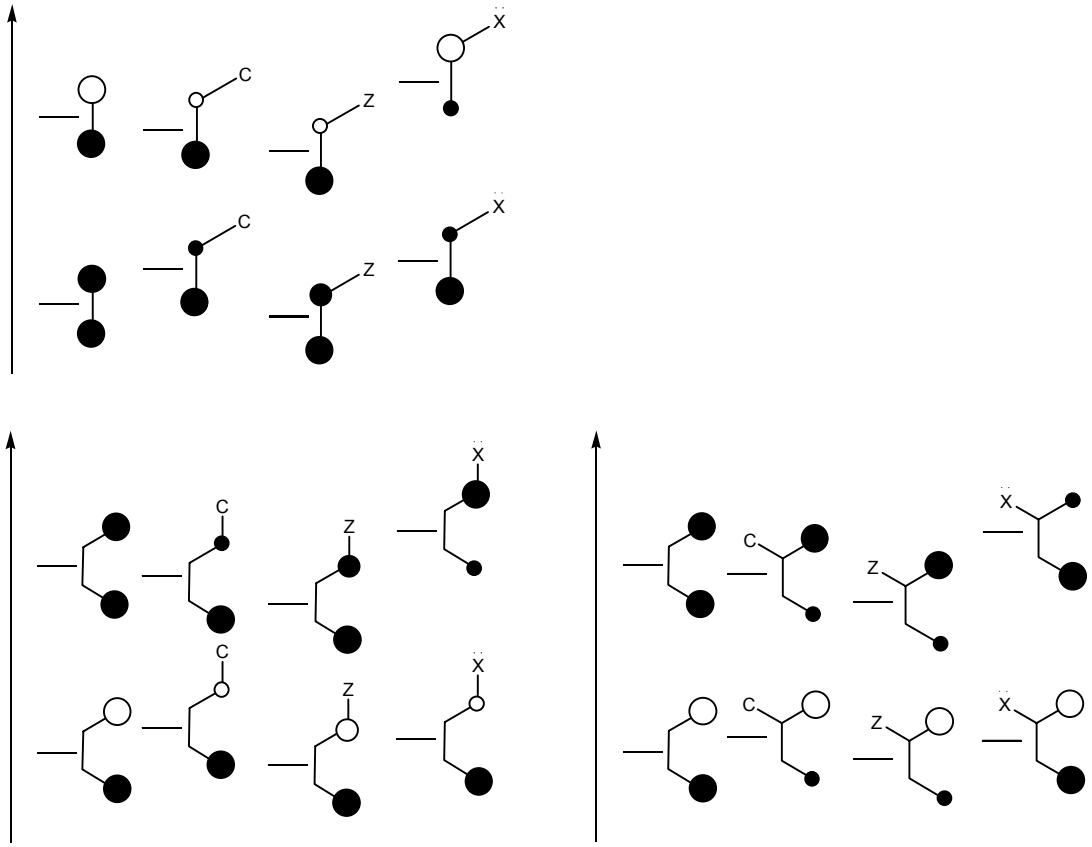

Figure 6. Frontier orbitals for dienophiles, 1-dienes and 2-dienes; C = conjugating group; Z = electron-withdrawing group; X = electron-donating group (after ref. 43)

Bond formation between the largest coefficients in the HOMO and the LUMO will be more advanced and determine the regioselectivity. For 1-substituted dienes, the 'ortho' regioisomer is favoured, for 2-substituted dienes, the 'para' regioisomer is.

However, not all Diels-Alder reactions follow the FMO rules of regiochemistry or reactivity, in which only the dominant FMO interaction is taken into account. Spino and Dory[45] reconstructed the butadiene-ethylene reaction pathway by means of the intrinsic reaction coordinate (IRC) approach. From this energy and orbital mixing profile (Figure 7), they conclude that in many cases there is no ground in taking only the dominant interaction into account. If the transition state has a well-developed *C*(2)-*C*(3) π-bond, which is an indication for a late transition state, conjugating substituents at *C*(2) or *C*(3) or aromatic systems like *o*-quinodimethanes will decrease the TS energy. Moreover, the $HOMO_{dienophile}$-$LUMO_{diene}$ interaction in the reagents differs a lot from that in the transition state, which makes it less reliable. Their new perception of the orbital interaction in the Diels-Alder mechanism is given in Scheme 7.

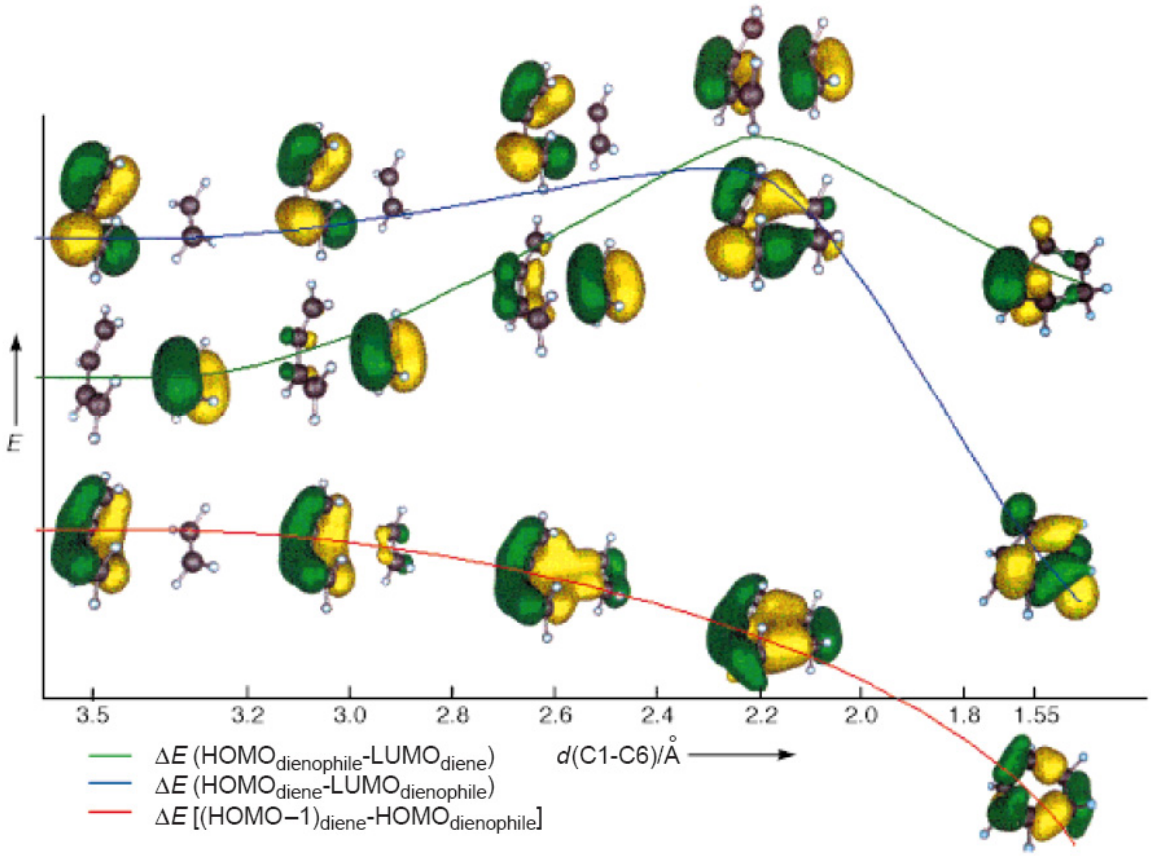

Figure 7. Energy profiles and chronology of orbital mixing for the three occupied π-orbitals during the Diels-Alder reaction of butadiene and ethylene. (Taken from ref. 45)

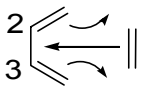

Scheme 7

3.3 IMDA(F) Reaction

In the next part, the focus is on type I[ii] intramolecular Diels-Alder reactions (with furans) or IMDA(F) reactions with a 3-membered connecting chain, also called a 3-atom tether. Mainly for the computational part, the methodology used for larger tethers is discussed as well.

3.3.1 Mechanism

Asynchronous Bond Formation

As predicted by the FMO theory, the bond formation between the diene and dienophile will be more advanced where the HOMO and LUMO have the largest coefficients. This leads to

[ii] In type I IMDA reactions, the tether is attached at the 4-position of the diene; in type II at the 3-position.

not symmetrically synchronous reactions. Constraints imposed by the tether reinforce this asynchronity; for 3-atom chains synchronous bond formation is unlikely.[46] Despite the asymmetry, it is generally accepted to remain a concerted reaction.

Thermodynamic parameters

As the Diels-Alder reaction proceeds through a highly ordered transition state, it has large negative activation entropies, typically in the range of -35 to -45 cal/mol/K.[46] In the intramolecular version some degree of ordering is already present, resulting in less negative activation entropies of -13 to -27 cal/mol/K, increase of reaction rates and milder reaction conditions. Dienes with an inherent s-*cis* configuration, like furan, even enhance this effect. Entropically seen, 3-atom tethers should cyclize faster than 4- and 5-membered chains. However, the substrates with a 4-membered chain have a cyclohexane-like transition state that suffers fewer nonbonded interactions.

3.3.2 Selectivity

Regioselectivity

The regioselectivity depends on the length of the connecting tether. Type I IMDA reactions with short 3-atom tethers (Figure 8), result in fused ring products. Bridged products are rarely observed and require a tether of at least five atoms.[46] This is in contrast with the intermolecular reactions, in which the substitution of the alkenes has a major influence on the regioselectivity.

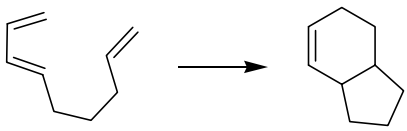

26 **27**

Figure 8. Formation of fused rings

Stereoselectivity : *Syn*/*Anti* Selectivity

In contrast with the intermolecular Diels-Alder reaction, the IMDA reaction has a higher tendency for *exo* or *anti* addition, so the *endo* rule is not valid. It is again the length of the connecting chain that has a major influence on the ring fusion of the adduct. When the 3-atom tether has a *cis* connection to the diene, the dienophile is forced into an *anti* transition state, resulting in *cis*-annelated adducts (Figure 9, left). The *syn* transition state is highly

strained. So, if *cis*-fused products are desired, one would employ *cis* dienes, however, these are prone to undergo 1,5-hydrogen shifts at elevated temperatures.

If the tether is *trans* connected to the diene, as with the furan as diene, both *anti* and *syn* transition states can occur, and steric effects cause the *anti* addition being preferred (Figure 9, right). Brown and Houk described a twist asynchronity model, after a computational study.[47] Any substitution in a (3*E*)-1,3,8-nonatriene-type system which leads to shorter developing internal *C*(4)-*C*(8) bonds in IMDA transition states favours *trans*-fused products over *cis*-fused ones. This preference arises from conformational requirements about the developing internal bond which results in a twist of the dienophile about this axis. This twist-asynchronity is more readily accommodated in *exo* than in *endo* transition states.[48] With furan as diene, only formation of *trans*-fused products has been reported,[46] which is based on steric strain factors. This is not valid for 4-atom tethers with furan as diene, in which both *cis*- and *trans*-fused rings can be formed depending on the tether.[49,50]

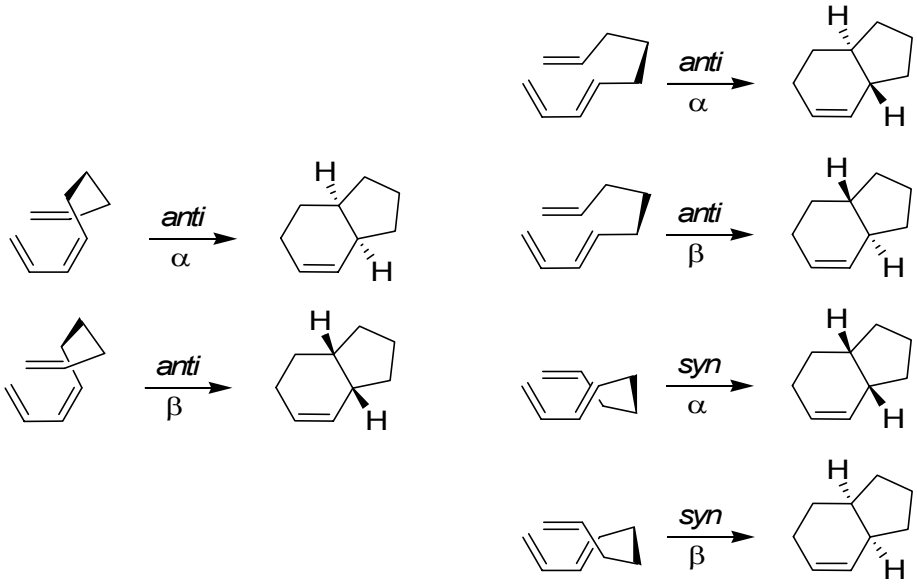

Figure 9. *Anti* & *syn* addition of the dienophile and π-diastereofacial approach in the IMDA reaction

Stereoselectivity: π-diastereofacial selectivity

The π-diastereofacial selectivity is related to the efficiency to direct the cyclization to one enantioface of the diene, indicated with α and β in Figure 9, and will have an influence on the position of the tether substituents, regularly giving isomeric mixtures.[51,52] This is mainly governed by the reaction temperature, chain length, steric interactions, e.g. related with the bulkiness and the location of the tether substituents, and ring strain in the transition states.[46] The reaction temperature is important as the furan adducts have the propensity to undergo

retro Diels-Alder reaction. So, the products can be the result of thermodynamic control and may not be the major isomer formed in the initial mixture. Examples are given in the next paragraph.

3.3.3 Kinetic and Thermodynamic Effects of the Tether and its Substituents

The first report of an IMDAF reaction with a 3-atom amide tether was the addition of maleic anhydride to secondary furfurylamines, by Bilovic in 1966 (Scheme 8).[53]

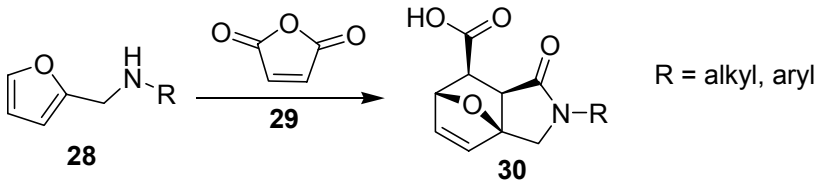

Scheme 8

Gschwend reported one of the first IMDAF reactions on tertiary *N*-furfurylacrylamides (Scheme 9).[54] The presence of the methyl substituent is a prerequisite for ring closure. Secondary amides without substituents on the tether do not cyclize, just like the esters. Moreover, the presence of the amide function, with its conformational implications is more important than its position in the tether.[55] Ring closure of the corresponding amine of **31** failed, because of fast retro Diels-Alder reaction and energetic preference of the starting material. This was shown by reduction of adduct **32** with $LiAlH_4$, which resulted in the ring-open furfurylamine.[54] However, the ring closure of a tertiary pentadienylallylamine, reported a few years earlier, was successful, yielding a ratio of 16/84 of the *trans*- and *cis*-fused adducts.[56]

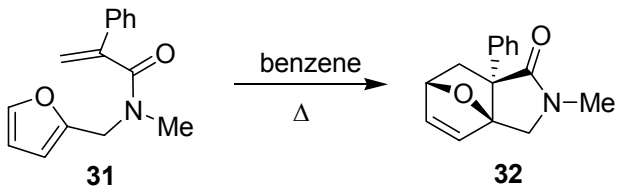

Scheme 9

The IMDAF reaction of the less sterically hindered allylamine analogues **33b,c,d** was published by Bilovic et al., but they ring opened too upon distillation (Scheme 10).[57]

Later, Choony et al.[58] reinvestigated the IMDA reaction of furfurylamines using even more steric buttresses (Scheme 10). The secondary amine **33a** did not ring close at all. As just mentioned methyl, methoxy and phenyl substituted reactants (**33b,c,d**) form unstable cycloadducts. Only very bulky buttresses like the trityl group (**33e**) can shift the equilibrium to the IMDAF adduct. Moreover, the protecting trityl group can be easily removed. The benzhydryl derivative **33f** is already too small, leaving a larger conformational space. Amide-type protecting groups (**33i,j**) enhance the adduct formation.

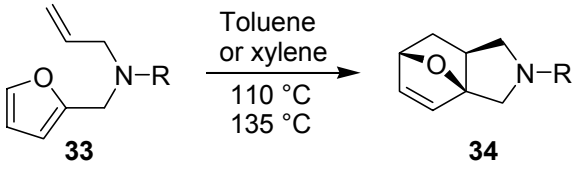

		% conversion
nr a	R = H	0
nr b,c,d	R = Me, OMe, Ph	unstable
nr e	R = Ph_3C	97.5
nr f	R = Ph_2CH	50
nr g	R = $PhCH_2$	2
nr h	R = 2,4,6-$Me_3C_6H_2$	10
nr i,j	R = tosyl, benzoyl	80

Scheme 10

Sternbach et al. studied the rate acceleration of an IMDA reaction due to geminal dialkyl substitution of the *C*(2) atom of a 3-atom tether (Scheme 11).[59] The geminal dialkoxy substitution has a larger influence than the geminal dialkyl substitution and acyclic geminal substitution is somewhat faster than cyclic geminal substitution. In this study, the increase in rates parallels the increase in equilibrium constants.

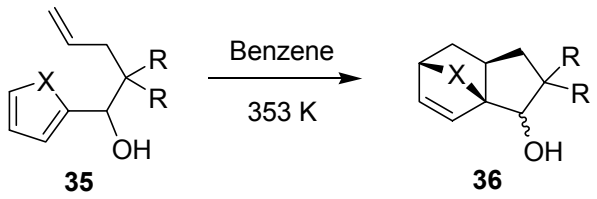

	relative *k*
R, R' = Cyclopentyl	1
R = R' = Bu	1.8
R, R' = -SCH_2CH_2S-	4.1
R = R' = -SEt	4.8
R = R' = -OEt	9.8

Scheme 11

A similar acceleration was reported for the IMDAF reactions of *N*-furfuryl-β-chloroacrylamides **37** (Scheme 12).[60] The methyl substituent R^3 on the connecting tether reduced the reaction time from 8 hours to 1 hour, and at the same time the reaction was directed to one diastereomer, with the methyl in *endo* position. This rate increase did not eliminate the need for a tertiary amide or an imide for the IMDAF to complete.

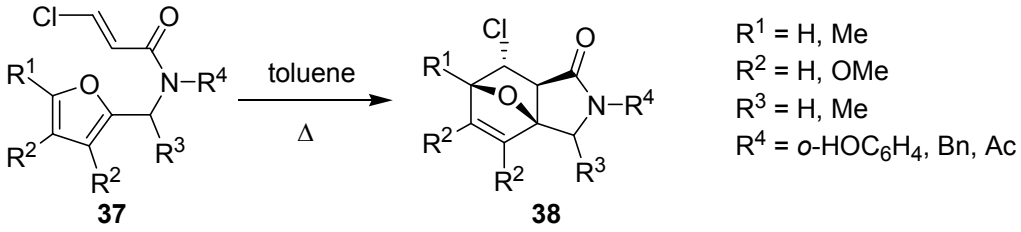

37 **38**

Scheme 12

Jung investigated a similar effect for the cycloaddition of the fumarates in Scheme 13 experimentally.[61] The large rate enhancement was linked with the presence of an oxygen atom adjacent to the substituted carbon atom. The forward rate constants for the fumarates are larger than for the corresponding keto esters and the rate increase in the keto ester series from mono- to dimethyl substitution is 7, while for the esters it is 310.[62,63]

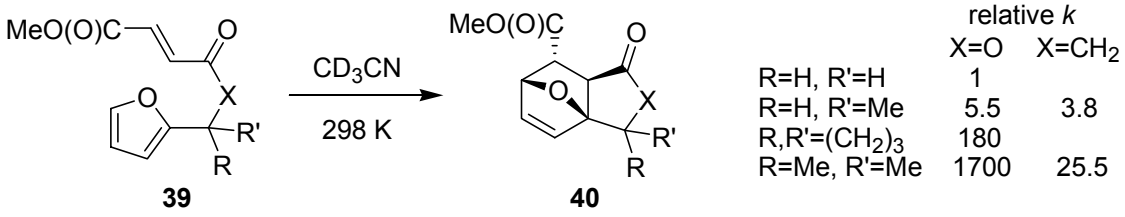

	relative *k*	
	X=O	X=CH_2
R=H, R'=H	1	
R=H, R'=Me	5.5	3.8
R,R'=$(CH_2)_3$	180	
R=Me, R'=Me	1700	25.5

39 **40**

Scheme 13

Tether substitutions

These examples show that substitution on the tether has a large effect on the reaction rate. The origin of this effect is the subject of much debate. The rate enhancement was found to be proportional to the steric bulk. The rate acceleration caused by one bulky substituent is generally called the *t*-butyl effect; if it is caused by geminal disubstitution on the tether it is called the *gem*-dialkyleffect.

The classic rationale for the *gem*-dialkyleffect is based on angle compression, known as the Thorpe-Ingold effect. Jung concludes from his experiments with spiro substrates (Scheme 13) that the rate acceleration has a strong enthalpic basis and is due primarily to the reactive rotamer effect,[64] which refers to an increased population of reactive *syn* rotamers that have a gauche conformation in the tether (Figure 10).

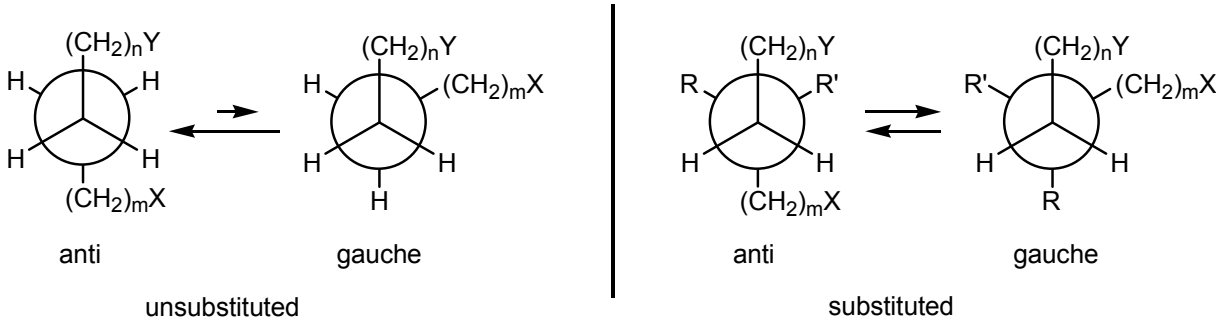

Figure 10. Illustration of the reactive rotamer effect by the Newman projection

A third and most recent hypothesis behind the *gem*-dialkyleffect is the facilitated transition theory, based on computational experiments for systems in which five-membered rings are formed: the IMDA reactions in Scheme 11 and Scheme 13 and a lactonisation reaction.[65] A conformational search of the starting material was done, but no relationship was found between the rate increase and a change in the concentration of the reactive rotamers. As the conversions between the conformations is not rate limiting, this result should be expected, based on the Curtin-Hammet principle (given in Appendix 1). Increasing the steric complexity around sp^3-sp^3 or sp^3-sp^2 bonds does not only change the relative energies of the staggered reactants A and B, but it can lower the rotational barrier of the reactant and facilitate rotation from a staggered resting state to an eclipsed transition state. This can be explained by a larger destabilization of the anti and gauche, staggered conformations than the eclipsed conformations. This leads to an overall lowering of the $\Delta H_T^{\ddagger}$ which results in an overall decrease of $\Delta G_T^{\ddagger}$, and thus in an increase of the reaction rate (Figure 11). This is valid if five-membered rings are formed, as the transition state is more eclipsed than the ground state conformations, but can not be extrapolated as such to six-membered rings with a chairlike transition state. The importance of conventional steric effects as the largest factor in rate acceleration caused by geminal tether substitution was shown earlier by Loudon and Wilcox.[66]

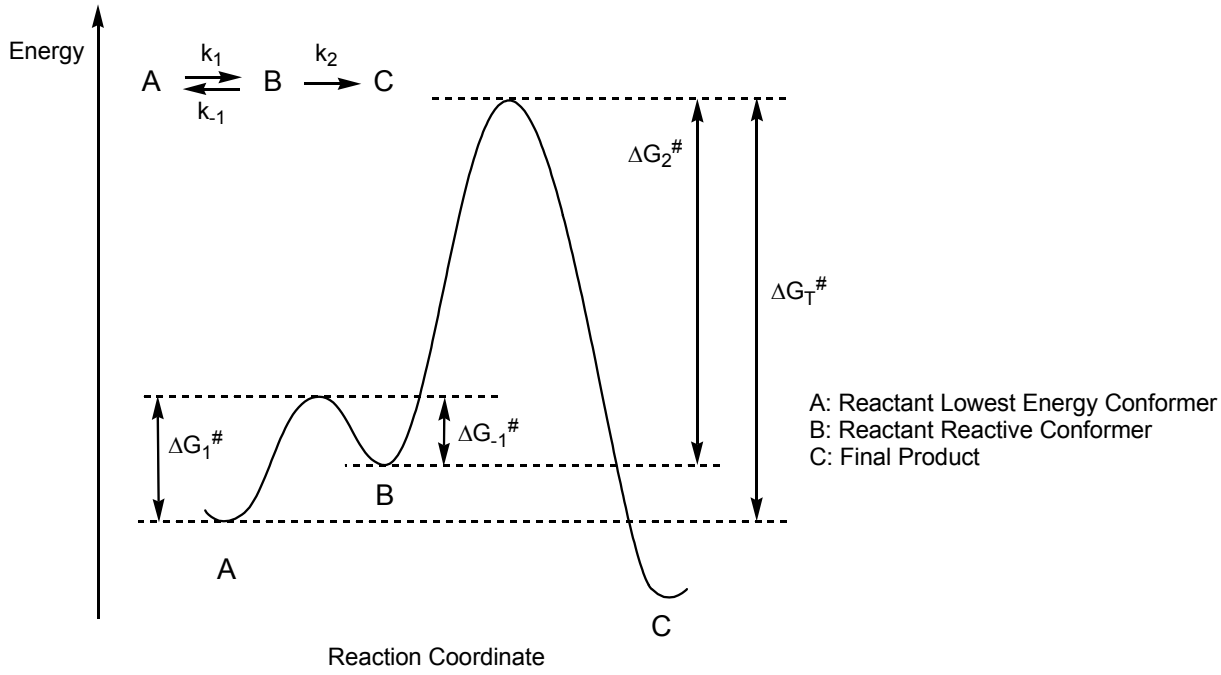

Figure 11. Reaction Energy Diagram

Very large groups are able to constrict the conformational space available to the dienophile. An analogue effect is the *t*-butyl-effect, which involves the substitution of the tether by a bulky group. The IMDA reaction of pentadienylacrylamides succeeded at lower temperatures by substitution of the *N*-atom with more sterically hindered groups. For the *t*-butyl derivatives NMR studies proved that exclusively the amide rotamer with the diene and dienophile having a *cis* orientation was present.[56]

In their kinetic study of amine buttressing by a trityl group (Scheme 10), Choony et al. confirmed that both an enthalpic and an entropic effect are operating: the ground state energy of the tritylated amine is raised by steric interference and, entropically, there are fewer degrees of freedom.

Planar Functional Groups

Previous examples show that amide tethers, whether the carbonyl is part of the tether or a substituent on the tether, enhance the adduct formation. The change from sp^3 to sp^2 hybridization has an influence on the extent of orbital overlap of diene and dienophile and introduction of one or two sp^2-centres reduces the nonbonded interactions.

A B3LYP model of the ground- and transition states of the additions in Scheme 14 shows that the incorporation of the amide carbonyl in the tether system places the dienophile in closer proximity to the furan ring, thereby reducing the activation energy.[67]

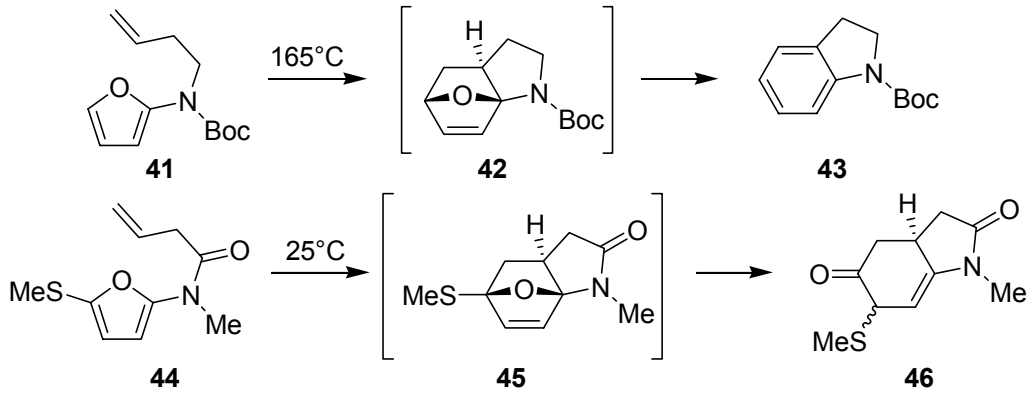

Scheme 14

This effect is counterbalanced if the carbonyl group cannot become coplanar with the dienophile in the transition state. This was suggested by Gschwend to explain the modest increase in reactivity on going from the allylpentadienylamine to the acryloyl derivative.[56] The subtle influence of the hybridization state of the tether centres is illustrated in Scheme 15. Ketofuran **47** did not react until the carbonyl group was protected.[68] In this case a change from sp^2 to sp^3 hybridization is beneficial as it is combined with the *gem*-dialkoxy effect.

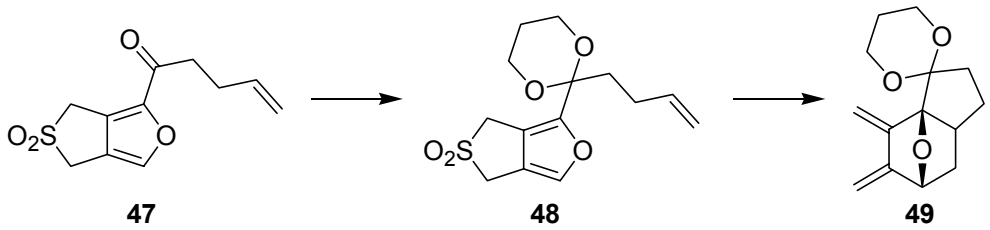

Scheme 15

Ghelfi investigated the steric and electronic effects of the R substituents of *N*-allyl-*N*-furfurylamides **50** on the IMDAF reaction rate. As shown before, the presence of an acyl substituent is a prerequisite for ring closure, as it is a steric buttress and influences the hybridization of *N*. The change of one or more chlorine atoms to methyl groups (going from **50a** to **50b**, **50c** to **50d**, **50a** to **50e**) slows down the reaction (Scheme 16).[69] Because the Van der Waals radius of Cl (1.75 Å) is 13 % smaller than that of CH_3 (2.0 Å), this cannot be attributed to steric factors.

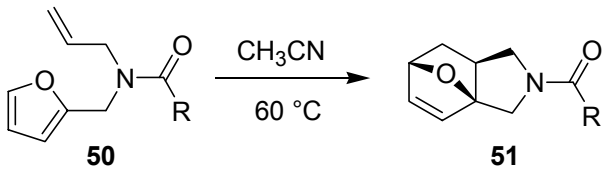

R	Conversion (%)
a CCl_3	80
b $C(CH_3)_3$	47
c $CHCl_2$	41
d $CH(CH_3)_2$	9
e $C(CH_3)Cl_2$	52

Scheme 16

The subtle effect was ascribed to the electronegativity of the R substituent. An increase in the electron-withdrawing strength of R, shortens the C=O bond, and thus lengthens the *N*-*C* bond, giving the *N*-atom a larger sp^3-hybridized character.[69]

Ring Constraints

The s-*cis* conformation of the tether bonds can also be established by internal coordination with metal salts, which exert a weak Lewis activity at the same time, as e.g. shown for the amide in Figure 12.[70,71]

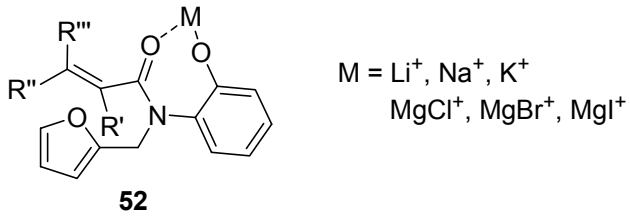

Figure 12. Internal coordination of metal salts, used to accelerate the IMDAF reaction

Adding a cyclic constraint to the furanyl system has an influence on the reaction rates of the addition of the furanylamides in Scheme 17. A DFT study of the reactants and transition states reveals that the six-membered ring in **53** adopts a half-chair conformation, imposing a *C*(3)-*C*(2)-*N*-*C*(4') dihedral angle of 156°. The seven-membered ring system has two low-energy conformations with a dihedral angle of 120° and 133°, which is closer to the transition state conformation. This study indicates there is a correlation of the reactivity with the rotation about the *C*(2)-*N* bond.[67]

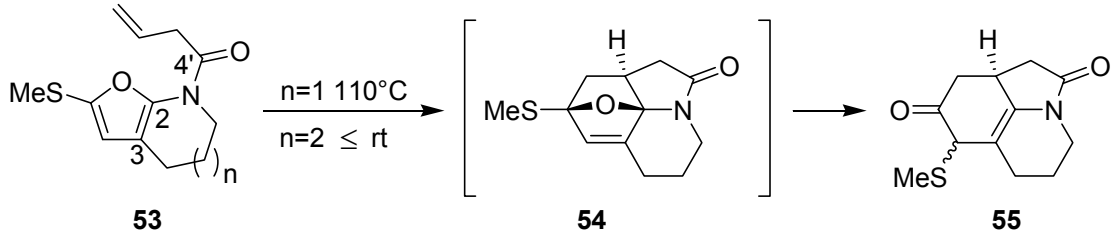

Scheme 17

π-Diastereofacial Selectivity

For the IMDAF reaction of *N*-furfuryl-β-chloroacrylamides (Scheme 12) force field calculations using a modified MM2 program indicate that the *endo* methyl isomer (**38**, R^3 = Me) is about 1.2 kcal/mol more stable than the *exo* isomer. Heating a 1:1 mixture of both isomers caused a very slow epimerisation of the *exo* to the *endo* isomer. So, apart from a kinetic preference, there is a thermodynamic preference as well.[60]

In a computational investigation of pentadienylacrylates **56**, the *C*(5)-methyl substituent favoured formation of *trans*-fused rings (**57** and **58**). Moreover, the methyl group preferred an *exo* position (**57**) in the *trans*-fused rings due to a reduced ^{1,3}A-strain between the methyl group and *H*(3) of the diene in its transition state (Scheme 18).[48]

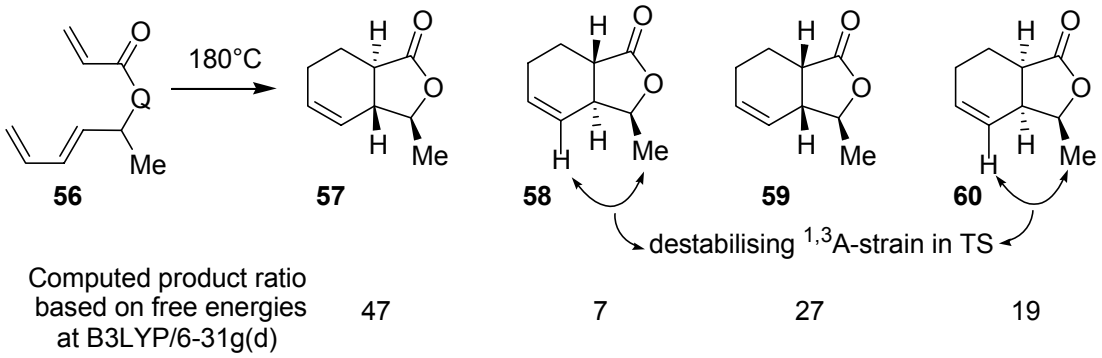

Scheme 18

Several other computational studies have shown that steric interactions, electrostatic effects and ring strain in the transition states are the source of stereoselectivity in intramolecular Diels-Alder reactions.[72]

The substituents on the tether and the nature of the connecting chain are of major importance in the IMDA(F) reaction. Tether substitutions, ring constraints and (planar) functional groups are known to alter the conformational distribution, to restrict the rotations of the reactants and change the energy barrier $\Delta H_T^{\ddagger}$ of the reaction. Steric and strain factors have an influence on the stability and orbital overlap in the transition state, electronic effects are less important.

3.3.4 Furan as Diene: Computational Studies

The general concepts of diene and dienophile substitution have been explained in § 3.2 of the Literature Overview. It has an effect on both, the regioselectivity of the intermolecular reaction and the rate of the Diels-Alder reaction. In this paragraph, computational studies on furan Diels-Alder reactions are given.

Furan is less aromatic than thiophene and pyrrole as e.g. expressed in the nucleus-independent chemical shifts (NICS) by Schleyer.[73] It has a higher electron density in the π-system than butadiene, reflected in a HOMO energy that is 0.09 eV higher than that of butadiene at the HF/6-31g* level, the LUMO is 1.26 eV higher in energy. Following the FMO theory, the energy gap for the normal Diels-Alder reaction between etheen and furan is smaller than that for the inverse electron demand Diels-Alder reaction and is in accord with the quantum of charge transfer at the transition state.[74] Reaction enthalpies for furan are significantly smaller for furan Diels-Alder reactions than for reactions involving unsubstituted hydrocarbon dienes ($\Delta\Delta H$ = 14-28 kcal/mol).[75] This explains the tendency for the products to undergo retro-cycloadditions.

A computational benchmark study on the Diels-Alder reactivity of butadiene with cyclic five-membered dienes revealed that CCSD(T)/6-31g* gives quantitative results for activation barriers and reaction energies; B3LYP and MP3 showed very good agreement. According to these authors changes as a function of basis set in energetics are rather small at B3LYP level of theory.[74]

Incorporation of a halogen at the 5-position of furan accelerates the IMDAF reaction 80 times.[76] The rate acceleration and higher yield by incorporating a halogen at the 3- or 5-position appear to be general. High-accuracy CBS-QB3 computations of the intermolecular reaction and isodesmic equations were used to investigate this effect. There is an increase of the exothermicity of the reaction by 4-9 kcal/mol, accompanied by a smaller decrease of the activation barriers of 2-3 kcal/mol. The stabilizing effect increases during bond formation and creates larger barriers to retro-cycloadditions. The effect of halogenation on the exothermicity is greater at the 2-position than at the 3-position. The origin of the effect is the energetic preference for the electronegative halogens to be attached to a more alkylated carbon framework. Electropositive groups stabilize carbon centres carrying electronegative substituents via hyperconjugation and σ-inductive effects. The trifluormethylgroup, with comparable electronegativity to chlorine and bromine, has a similar effect.[75] B3LYP/6-31g(d) has been used to investigate the same effect for

intramolecular cylcoadditions. B3LYP correctly predicts the changes in activation enthalpies upon halogenation, but has problems predicting the relative stabilities of reactants and products.[77]

3.3.5 Nature of the Dienophile

All the previous examples use alkenes as dienophiles, flanked by different electron-withdrawing functionalities. Terminal phenylsulfonyl groups have been used as acitivating groups,[78] and vinylsulfonic acids **61**, with the activating group incorporated in the tether, undergo smooth cycloaddition as well towards the *exo* adduct (Scheme 19).[79]

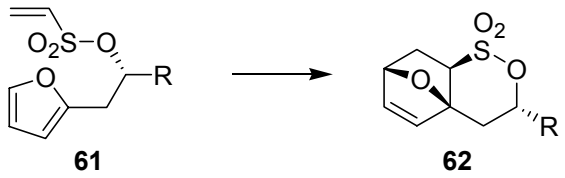

61 **62**

Scheme 19

Alkynes can react as the triple bond species, or as the isomeric allenes. If the alkynyl is (di)activated a 7-oxabicyclo[2.2.1]hepta-2,5-diene is typically obtained as e.g. in the synthesis of functionalized gibbanes (Scheme 20).[80]

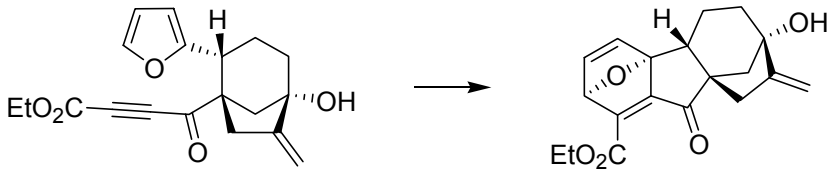

63 **64**

Scheme 20

The carbomethoxy allene **65** undergoes cycloaddition to **66**, although FMO theory predicts a higher reactivity for the double bond in α-position of the carboxylate.[81] This approach was used in the synthesis of gibberellins (+)-GA_1 and (+)-GA_3.[82]

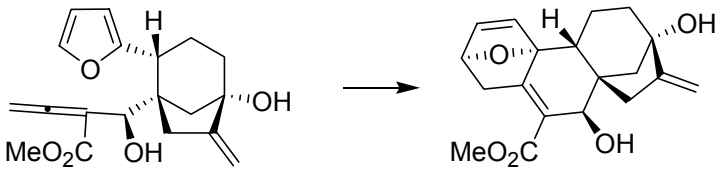

65 **66**

Scheme 21

Benzyne is less frequently used as dienophile, but it has been applied in natural product synthesis of biflorin and mansonone E, I and F.[83]

3.3.6 Asymmetric Synthesis

In IMDAF reactions with a 3-atom tether the regioselectivity is fixed and only *trans*-fused rings can be formed. The π-diastereofacial selectivity remains to be controlled. Several ways exist to impose a π-stereofacial selective addition.

The synthesis of optically pure products can be achieved by the insertion of chiral diene or dienophile substituents, as in the menthyl ester **67**.[84] In an analogue reaction, (-)-phenylmenthol, was used for IMDA reactions of deca-2,7,9,-trienoate esters and the final diastereomeric ratio was influenced by the use of different achiral catalysts.[85] The best diastereomeric excess of 72% was obtained with $TiCl_4$, but the yield dropped to 8%.

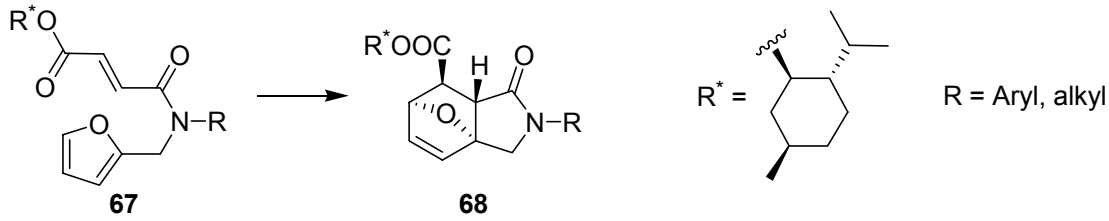

67 **68**

Scheme 22

A computational investigation of the effect of a chiral inductor on the diene was done for the ester **69** in Scheme 23 using DFT (B3LYP/6-31g(d)). Different rotamers of the transition states were modelled and their Boltzmann distribution at 110 °C was calculated. The most stable conformation is drawn in Scheme 23. Only *trans*-fused rings were formed. A better selectivity can be obtained by increasing the size of the alkyl group and by increasing the electron density at the oxygen atom of the X group, as there is an attractive electrostatic interaction between the oxygen and the hydrogen at the diene. Thus, metal alkoxides are predicted to enhance selectivity.[72a]

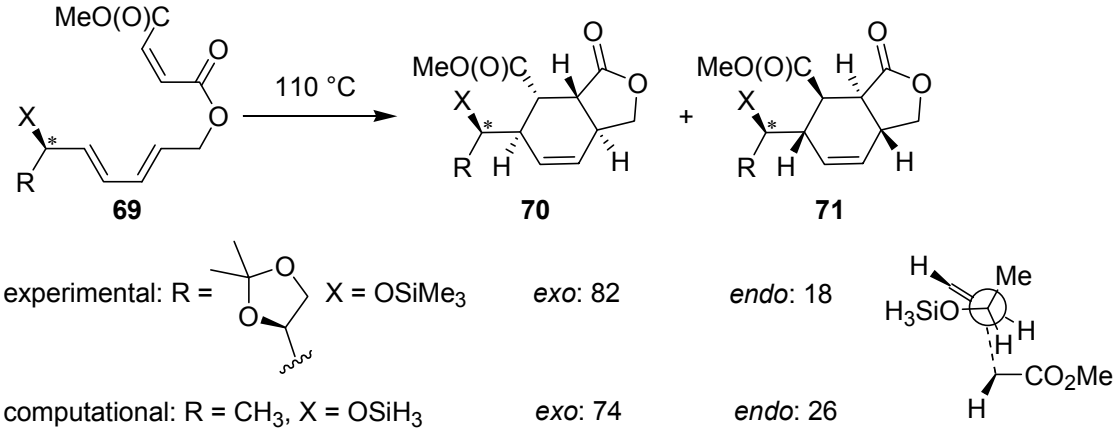

Scheme 23

The chiral auxiliary can be attached to the tether, but as the distance with the reactive centres increases, the selectivity decreases. The chiral α-methylbenzyl group attached to *N* in an amide tether, for instance, has a limited influence on the π-stereofacial selective addition.[86] Mukaiyama used (*R*)-phenylglycinol as a chiral inductor in the synthesis of natural (+)-farnesiferol C[71] and this approach was applied in the synthesis of solanoeclepin A derivatives.[87] In this case, only upon forming an internal chelate by using the Mg salt of **72**, the chirality was transferred and the diastereomeric ratio shifted from 50/50 to 88/12 (Scheme 24).

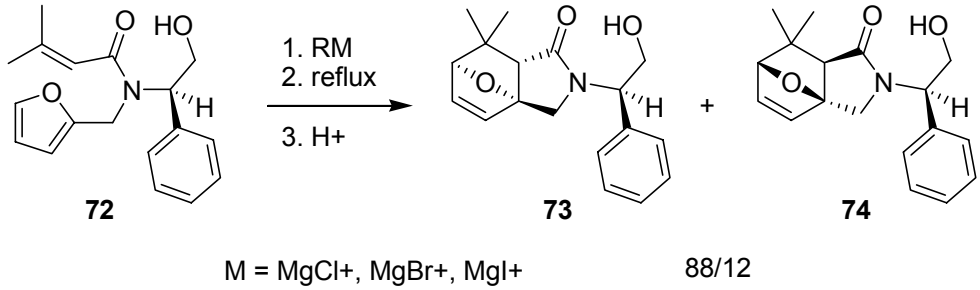

Scheme 24

Placing the chiral centre in the tether works as well. As mentioned before, generally a kinetic mixture of diastereomers is obtained, that can be converted to one product under thermodynamic conditions. The furyl enone **75** yielded oxanorbornene **76** as the sole product, in which the methyl group has an equatorial position (Scheme 25).[88]

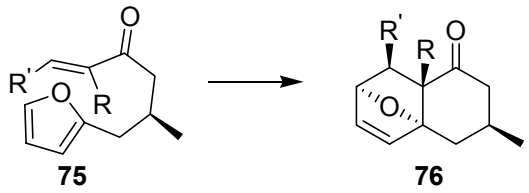

75 **76**

Scheme 25

4 Cleavage of the Oxanorbornene Oxygen Bridge

The IMDAF reaction provides a convenient entry into polycyclic targets including natural products[89] like prostaglandins and terpenoids. The formed 7-oxabicyclo[2.2.1]heptane skeleton is present in biologically active natural products, but, moreover, the 7-oxanorbornanes and their unsaturated derivatives can undergo a variety of reactions making them quite useful synthetic intermediates in the synthesis of natural products and analogues.[90]

An important synthetic transformation involves ethereal bridge cleavage. Many groups have developed different approaches, including treatment with acids or bases, nucleophilic additions and reductive processes. In the next paragraph focus is on IMDAF reactions with a 3-atom tether. At the same time some applications in the synthesis of natural and medicinal products are given.

4.1 Brønsted Acids

Protonation of the oxabridge and heating leads to ring opening, mostly followed by aromatization, a nucleophilic addition or (pinacolic) rearrangement in the absence of a nucleophile. The furfurylamines in Scheme 26 require treatment with HCl and aromatization to drive the reaction to completion.[91]

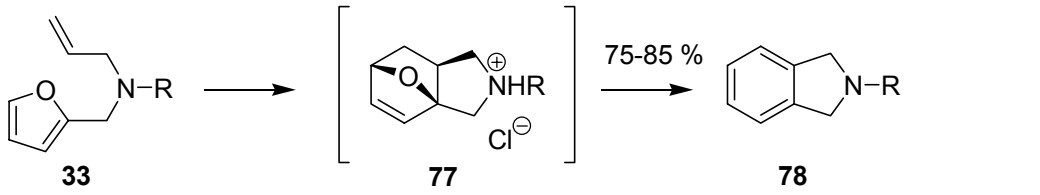

33 **77** **78**

R = Ph, *t*-Bu, *i*-Pr, *n*-Bu, Et, Me, H

Scheme 26

Also in adducts **79** that are very reluctant to ring opening, the oxabridge was cleaved applying harsh conditions using phosphoric acid, resulting in dihydroisoindolone **80** after aromatization (Scheme 27).[52]

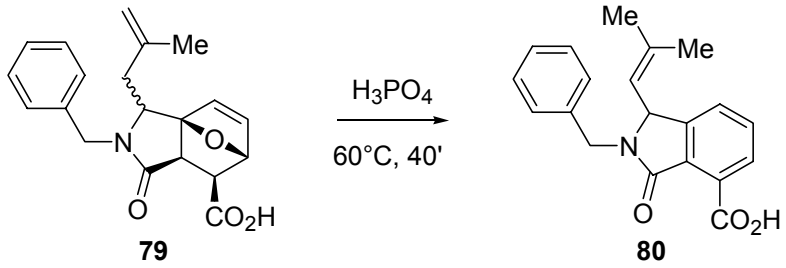

79 **80**

Scheme 27

The electrogenerated acids (EGA) can be considered as mild acids, as the area round the anode becomes acidic, while overall neutral conditions are maintained. This electrochemical ring opening of a 7-oxanorbornene with formation of a carbenium ion has been applied as the first step in a modified Ritter reaction (Scheme 28).[92]

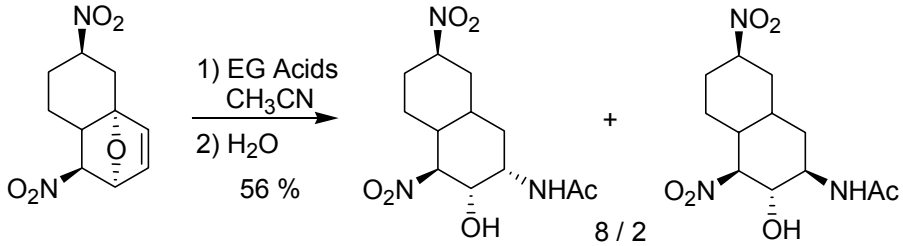

81 **82** **83**

Scheme 28

4.2 Lewis Acids

Different Lewis acids have been used to ring open IMDAF adducts, like $TiCl_4$, Me_2AlCl,[77] $SnCl_2$.[93] Treatment of **84** with $BF_3.OEt_2$ afforded β,γ-enone **85** (Scheme 29).[51]

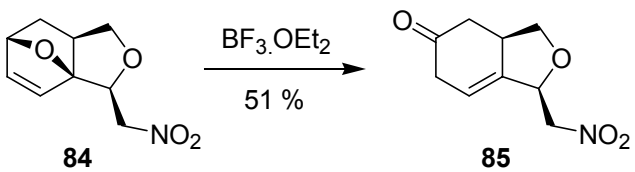

84 **85**

Scheme 29

After catalytic hydrogenation, the oxabridge of **86** was cleaved using BF_3/Ac_2O. Under these conditions the alkoxide was quenched via acetylation; neutralization of the carbeniumion yielded a mixture of two double bond isomers **87** and **88** (Scheme 30).[54]

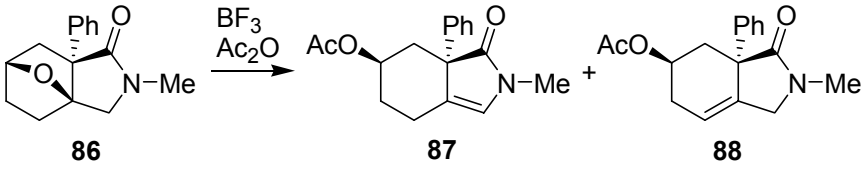

86 **87** **88**

Scheme 30

4.3 Base-induced Ring Opening

Mild basic conditions, e.g. Et_3N, LDA, KHMDS, can induce ring opening if an acidic proton is present in β-position of the oxygen atom of the oxanorbornane.[94,95]

The Diels-Alder reaction is often involved in the construction of the BC ring system of steroids in a D → BCD → ABCD route. De Clercq et al. applied this method in the synthesis of adrenosterone derivative **91** (Scheme 31).[96]

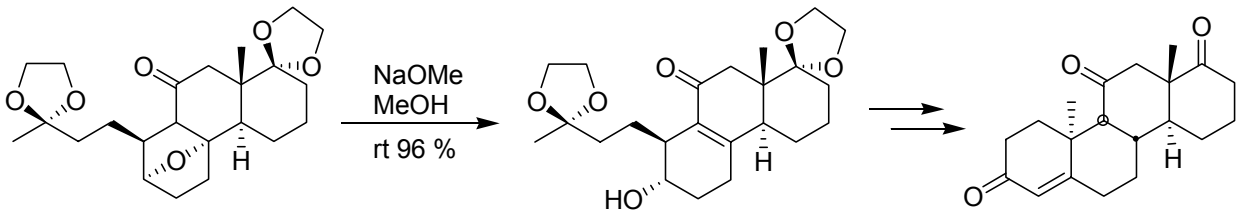

89 **90** **91**

Scheme 31

4.4 Internal Electron Donor and Geminal Leaving Group

The IMDAF adducts of *N*-homoallyl-2-aminofurans are hard to isolate, as they ring open easily by assistance of the mesomeric *N*-atom, certainly when the addition occurs above room temperature. Padwa et al. used these compounds in the synthesis of octahydroindole-based alkaloids.[97,98] Cyclization of **92** to the oxabicycle **94** was limited to systems containing an angular substituent, if R^2 = H, aromatic products were isolated (Scheme 32).

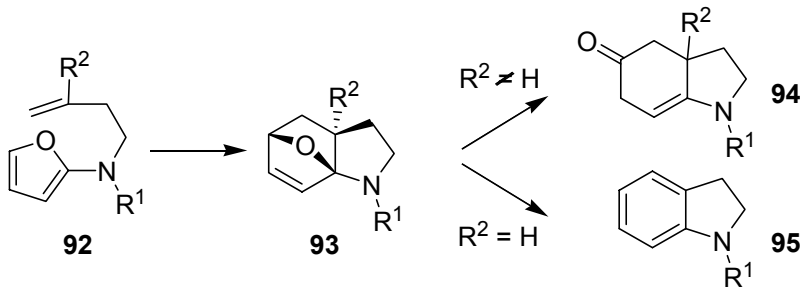

Scheme 32

A geminal leaving group can be used to prevent aromatization.[67b] An example is the synthesis of the *Stemona* alkaloid (±)-stenine, in which the cycloadduct undergoes a nitrogen-assisted ring opening to generate the zwitterionic intermediate **99**. A subsequent 1,2-thiomethyl shift provides tricyclic lactam **100** (Scheme 33).[99] The high stereoselectivity suggests a concerted 1,2-shift of the thiomethyl group.

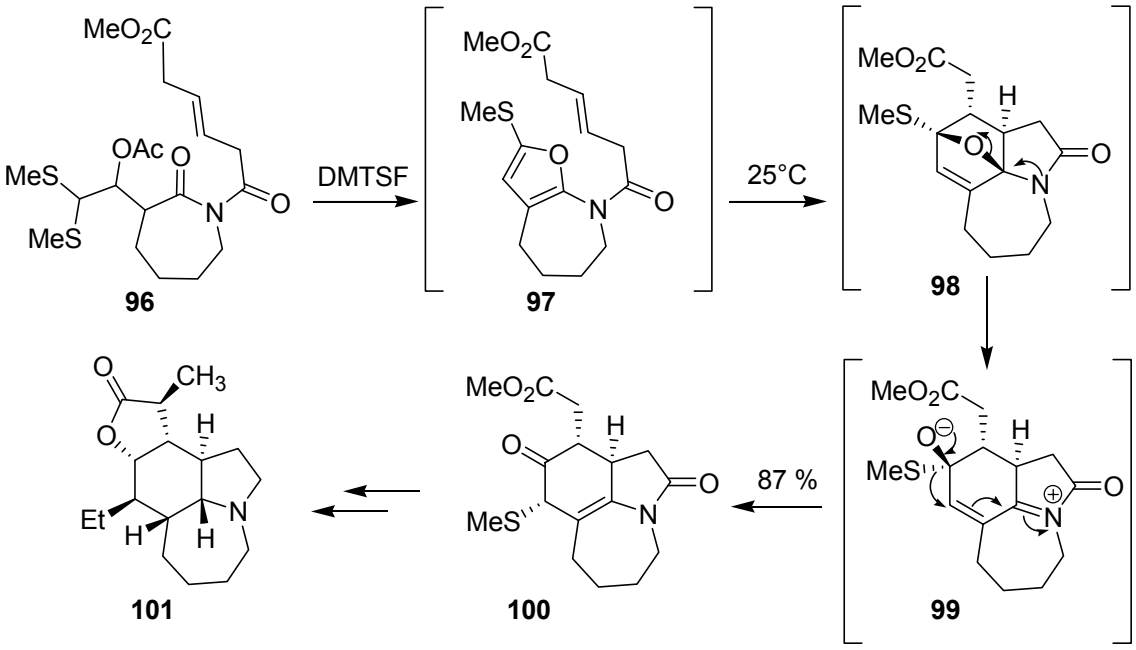

Scheme 33

Earlier a 1,4-thiomethyl shift had been described by Wu et al.[100]

4.5 Nucleophilic Additions

To allow the construction of carbon-carbon bonds throughout the bridge cleavage, the oxabridge can be opened via an S_N2' mechanism with organometallic reagents. In this way, a range of cyclohexenes **104** could be obtained with 68 to 85 % yield (Scheme 34).[101] The

complete stereoselectivity of this *exo* conjugate addition was explained by chelation of the organometal with the oxygen bridge. Regioselectivity can be introduced by placing electron withdrawing substituents on the double bond.[102]

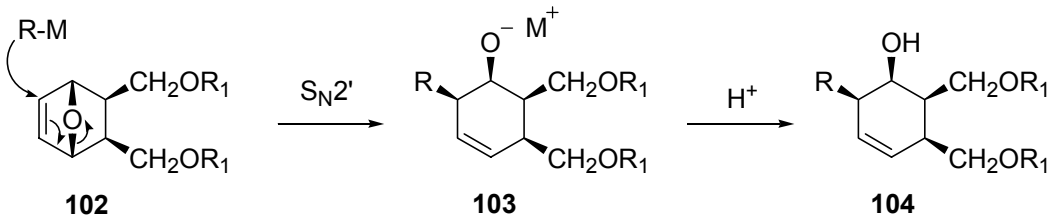

102 **103** **104**

Scheme 34

A review on S_N2' and S_N2'-like openings of oxa-n-cyclo systems was written by Woo and Keay.[103] The ring opening can be Lewis-acid catalyzed.[104] Lautens and coworkers investigated the enantioselective ring opening of oxabicycloheptenes by Pd(0)[105] and Rh(I)-catalysts.[106] A broad range of nucleophiles can be used, including alcohols, fenols, amines, anilines, carboxylates, arylboronic acids and were successfully applied to the IMDAF adducts **105** by Padwa et al. (Scheme 35).[93] The same methodology was used to construct the A and B ring of erythrina alkaloids.[107]

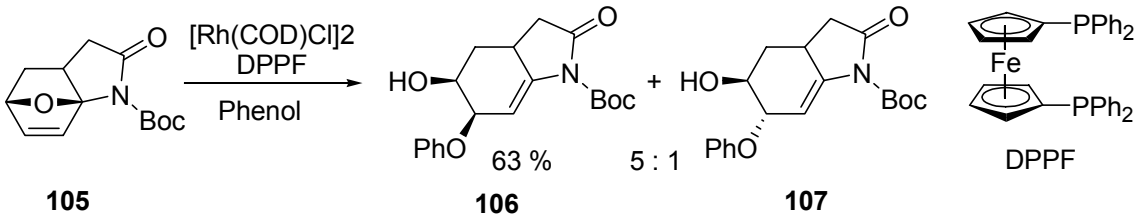

105 **106** **107**

Scheme 35

4.6 Metal Reduction of Halides

Halides and sulfones β to the 7-oxa bridge are reduced with metals and lead to ethereal bond cleavage. In their study of the synthesis of avermectin, Jung et al. ring opened norbornane **109** by reductive elimination using Na in THF after double bond oxidation with OsO_4 (Scheme 36).[60]

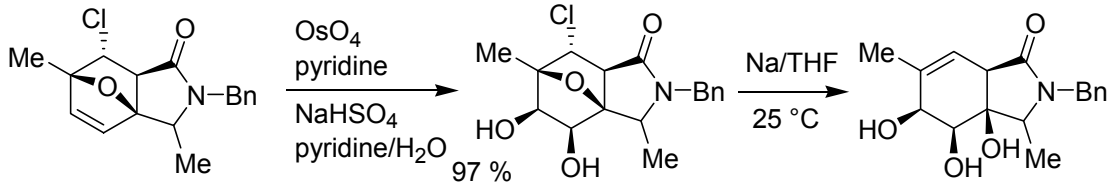

Scheme 36

4.7 Hydrogenolysis

The usual methods to cleave the oxygen bridge do not work for the adducts of furan with maleic anhydride or acetylene carboxylates. Using Lewis acids, the starting material is recovered. Me_3SiI in acetonitrile causes partial ring opening after 70 hours of reflux in acetonitrile. Only acidic conditions, like concentrated H_2SO_4 at 0°C, result in ring opening followed by aromatization.[108] A better solution is hydrogenolysis with Raney Nickel with retention of stereochemistry (Scheme 37), as applied in the synthesis of *Podophyllum* lignans.[109] Palladium / charcoal has been used as well.[110]

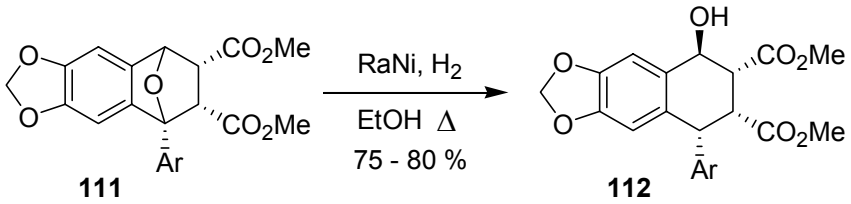

Scheme 37

Chapter 3 – Results and Discussion

1 Synthesis of Hydantoin Derivatives

1.1 The Pyroglutamate-Hydantoin Rearrangement

Small heterocyclic cores with skeletal and stereochemical diversity are important in drug discovery. In this framework, the use of pyroglutamate as a synthetic building block was investigated.

When a mixture of the pyroglutamate **113** and an isocyanate is treated with NaH in diethyl ether, a precipitate is formed almost immediately. Work-up after 30 minutes, confirms this is the sodium salt of the carbamoyl-2-pyrrolidinone **114** that is obtained in high purity (Scheme 38). Stirring the reaction overnight in ether yielded the same product **114**.

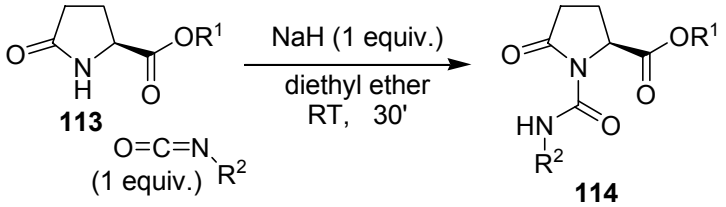

Scheme 38

If the same reaction is repeated in THF and stirred overnight, a different product is formed that has very similar 1D NMR spectra. This product was firstly misidentified as the perhydro-1,3-diazepine-2,4-dione **119**.[6,111] This was supposed to be formed via an intramolecular nucleophilic attack of the carbamoyl anion on the lactam ring, with formation of the strained bicyclic intermediate **116** that decomposes to the seven-membered ring anions **117** and **118**. A D_2O-quenching experiment proved both anions are in equilibrium with each other and cause the racemisation observed in the final product **119** (Scheme 39).

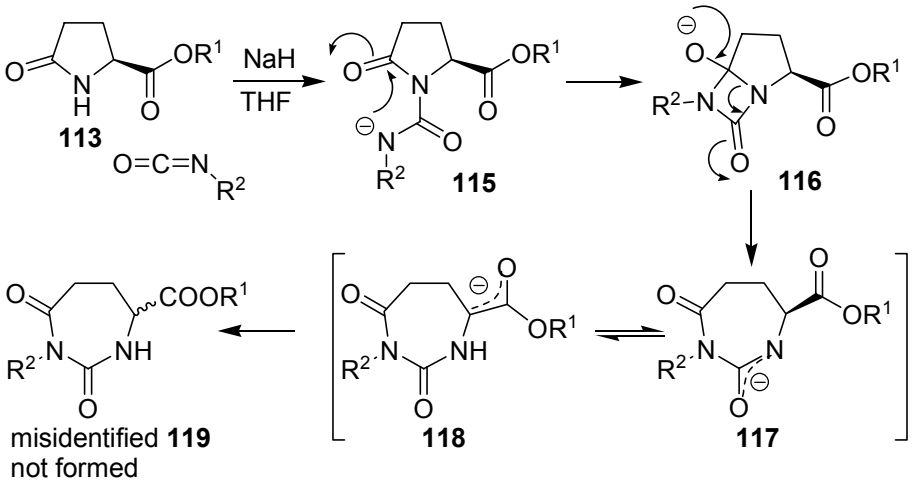

Scheme 39

In the past, 1-carbamoyl-2-pyrrolidinones of type **120** were incorrectly identified as perhydro-1,3-diazepine-2,4-diones of type **121** (Figure 13). For example the natural product squamolone was originally identified as a seven-membered ring (of type **121** but later turned out to be a five-membered ring (of type **120)**.[112] Also a claim of the preparation of these seven-membered rings by cyclisation of 4-ureidobutyric acids with thionyl chloride[113] was later on corrected by another research group.[114]

Since we had both the carbamoyllactam **120** and what we believed to be **121** in hands, their spectral data could be compared. Although both ^{1}H NMR and ^{13}C spectra clearly showed they were two different compounds, no conclusions could be made judging these spectra alone. The decisive proof was given by comparing both COSY and HMBC coupled spectra (Figure 13).

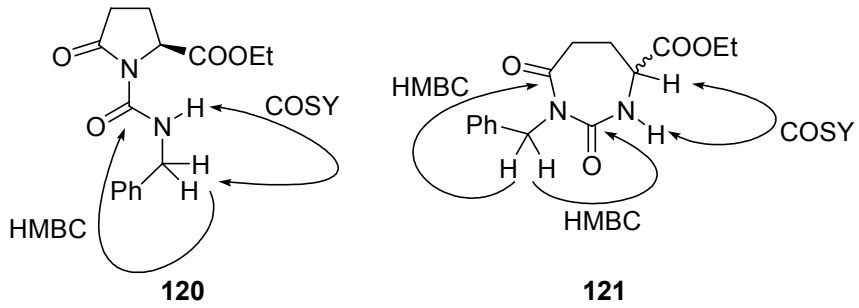

Figure 13. The COSY and HMBC couplings of 120 and 121 used for their structure determination

In the case of **120**, there is a coupling in the COSY spectrum between the proton on the *N*-atom and the two protons of the benzyl group, so the proton on nitrogen appears as an incompletely resolved triplet. In the case of **121** however, the proton on the *N*-atom couples

with the proton next to the ester function and not with the protons of the benzyl group. This proves that the benzyl group is attached to a tertiary nitrogen. Furthermore in the HMBC spectrum, the protons of the benzyl group of **120** only couple to the urea carbonyl, which is easily distinguishable from both other carbonyl groups, whereas in the case of **121** they couple to both the urea and the lactam carbonyl.

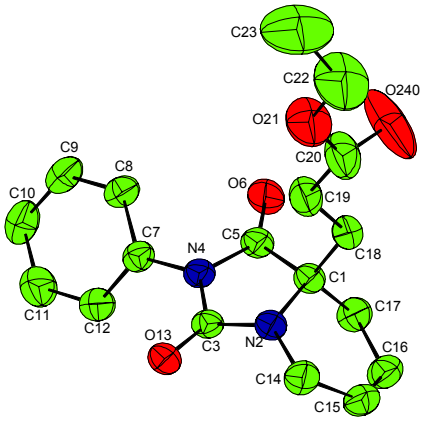

Figure 14

However, another rearranged product can be formed by reacting pyroglutamates with isocyanates. X-ray analysis of a bicyclic compound that was synthesized later (Figure 14) proved that no perhydrodiazepines were formed, but hydantoins were (Scheme 40). Several derivatives were synthesized (Table 1).

Table 1. Synthesis of hydantoins 122

N°	R^1	R^2	Yield
a	Bn	Ph	56
b	Bn	CH_2CH_2Cl	50
c	Et	Ph	89
d	Et	Bn	87
e	Et	CH_2CH_2Cl	81
f	Et	Allyl	48
g	Me	Ph	81

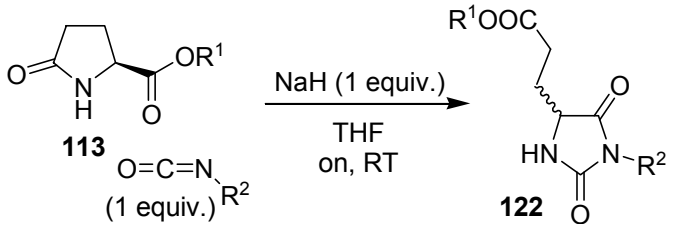

Scheme 40

The HMBC and COSY couplings for both rearranged products are analogue, which explains the misinterpretation of the spectral data (Figure 15). An article by Senior et al explains the spectral analysis of the possible products of the reaction of pyroglutamates with isocyanates in detail.[115]

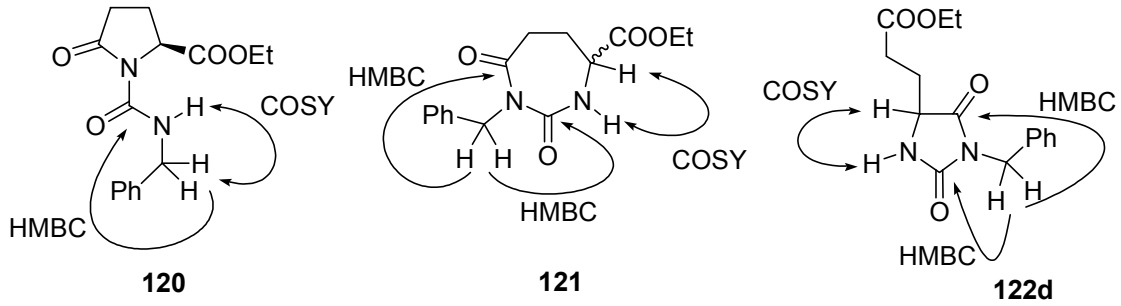

Figure 15. Structure determinating 2D spectral data of the three possible products of the reaction of pyroglutamates with isocyanates

Once both the carbamoyllactam **120** and the hydantoin **122d** have been fully determined, they can be quickly identified using the ^{1}H NMR spectra. The N*H* of the hydantoins **122** appears mostly between 6 and 7.25 ppm, while for the carbamoylpyrrolidinones it is much more downfield between 8 and 11 ppm. In the pyrrolidinone ring, all methylene protons are AB-systems, while for the hydantoin, the methylene protons next to the ester appear as a triplet due to the possibility of free rotation.

1.2 Reaction Pathway: One- and Two-Step Procedure

Two possible reaction pathways are given in Scheme 41 and Scheme 42. In the first one (Scheme 41), the carbamoyl anion reacts intramolecularly by a nucleophilic attack on the carbonyl of the ester function followed by expulsion of an alkoxide anion resulting in the formation of the bicyclic intermediate **123**. The alkoxide anion in turn can open this

bicyclic intermediate with formation of anions **124** and **125** that are in equilibrium and cause racemization of the chiral centre.

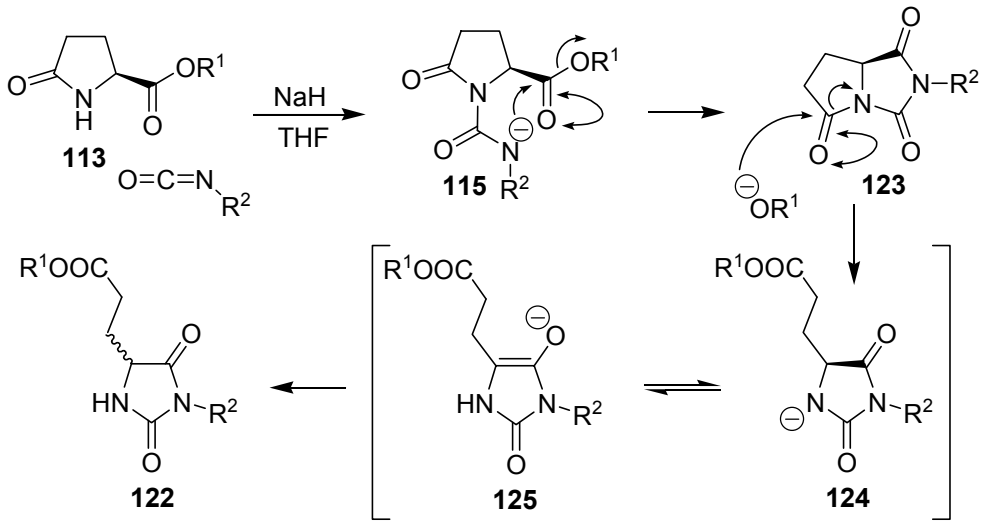

Scheme 41

Another reaction pathway, depicted in Scheme 42, can be proposed. The overnight reaction in THF can be initiated by slow decomposition of the ester in **113**. The alkoxide anion opens the lactam ring in the next step. The lactam carbonyl is activated by the electron-withdrawing properties of the carbamoyl group. Ring opening of pyroglutamates is usually performed by the treatment of *N*-acyl or *N*-alkoxycarbonyl pyroglutamates with $LiOH_{(aq)}$ in THF.[116,117] The ring opening of the lactam is followed by an intramolecular formation of a 5-membered ring and generation of a new alkoxide anion.

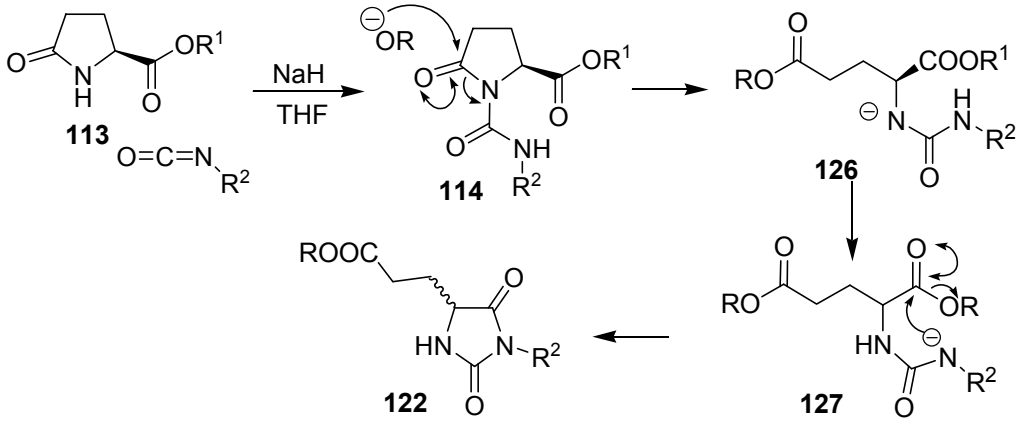

Scheme 42

Ester decomposition of the pyroglutamate has been observed during evaluation of the alkyation of the *N*-unprotected benzyl pyroglutamate **128** at *C*(2) (Scheme 43).[118]

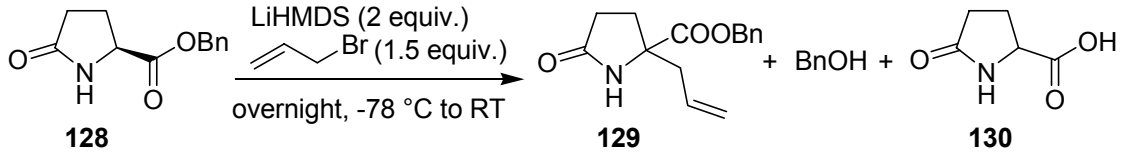

Scheme 43

Also during the evaluation of the Boc-migration of *N*-Boc-protected pyroglutamates **131** ester decomposition occurred for some of the derivatives. Compounds that are acylated at *C*(4) undergo Boc-migration, but without a *C*(4)-acyl group, ring opening towards the acyclic glutamate is observed (Scheme 44). Apparently, in the latter case, the dianions are unstable and the esters fragment with formation of the alkoxide anions.[5] Presumably, the *C*(4)-acyl group in **132** stabilizes the anion at *C*(4) as its 6-membered Li-salt complex and the anion at *C*(2) is stabilized by the Boc-group. In absence of the *C*(4)-acyl group, the Boc-group stabilizes the anion at *C*(4), via a 6-membered Li-complex and the anion at *C*(2) is not stabilized, which causes fragmentation. Analoguous stabilized counter-ion complexes have already been proposed to explain the regioselectivity of different alkylation procedures of the pyroglutamate.[3]

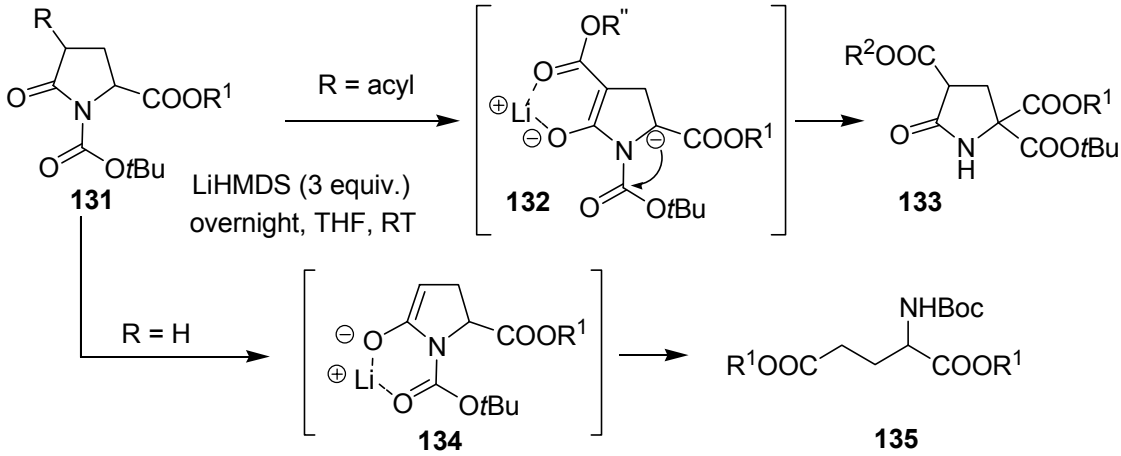

Scheme 44

To investigate the mechanism, the reaction towards **122c** in dry THF was sampled after 1h40'. This showed that 80 % of the product was the carbamoyllactam **114** and 20 % had further rearranged towards the hydantoin **122c**, but neither the bicyclic intermediate **123** nor

the ring open product **126** was observed. This only confirms that a fast carbamoylation occurs, followed by a slow rearrangement reaction.

Towards a two-step procedure

Normally the reaction of pyroglutamates **113** with isocyanates in diethyl ether yields the carbamoylated pyroglutamates, even after stirring overnight. If ethyl pyroglutamate and benzylisocyanate were stirred overnight in dry ether with NaH and the reaction was quenched with water instead of saturated $NH_4Cl_{(aq)}$, 69 % of carbamoylpyrrolidinon **120** was formed and no rearranged products were observed in the organic layer. Because of the low yield, the aqueous layer was analysed and found to contain the rearranged product **137**, which was identified by its ^{1}H NMR (Scheme 45).

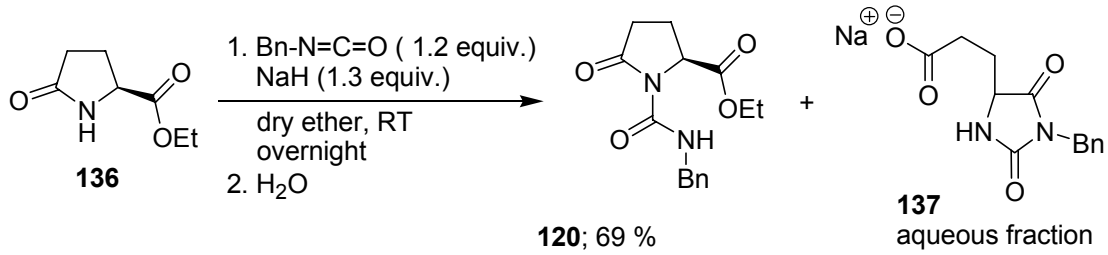

Scheme 45

The same reaction in THF that was not freshly distilled, furnished the rearranged product in 87 % yield after only 30 minutes (Scheme 46).

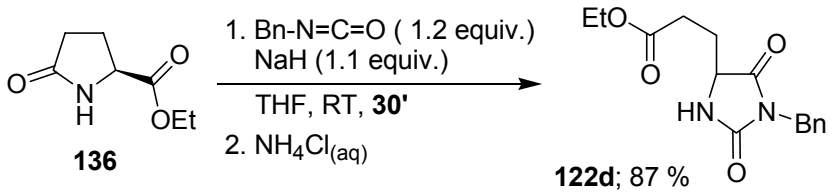

Scheme 46

These experiments suggest that the presence of traces of hydroxyl ions leads to a fast ring opening of the lactam, followed by ring closure towards the hydantoin and generation of a new alkoxide ion, analogous to the second reaction pathway depicted in Scheme 42.

Given these results, a 2-step procedure was developed in which the carbamoylation of the pyrrolidinone was performed in dry ether and after isolation of the carbamoyllactam, the

rearrangement reaction was performed in the presence of the desired alkoxide anions (Scheme 47). In this second step a transesterification can be done. This was exemplified in the synthesis of macrocyclic bishydantoins, given in § 1.3.3 of the Results and Discussion, in which one can start from the ethyl pyroglutamate and form the allylester of the hydantoin.

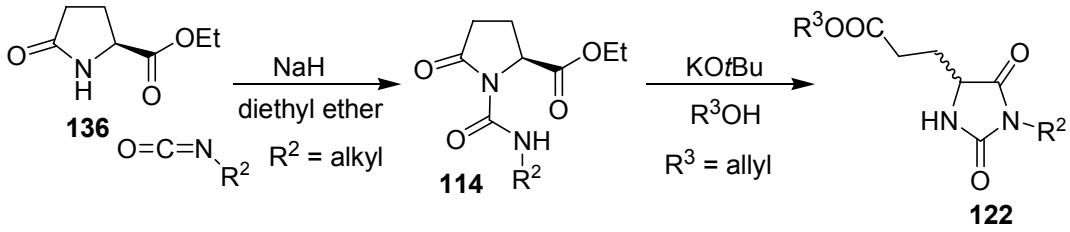

Scheme 47

Application of the 2-step procedure

To test the possibility to form crown-like structures, transesterification with ethylene glycol was evaluated using the carbamoylated ethyl pyroglutamate **138** (Scheme 48). However, it is hard to remove this high boiling solvent: extraction with benzene, in wich the excess of ethylene glycol is only slightly soluble, barely returned any product; via distillation, ethylene glycol was only partially removed. The residue, after distillation, was further purified by column chromatography, resulting in low yields. The selective *N*(3)-alkylation of the hydantoin was first evaluated using pyridine, but only starting material was recovered. The reaction with KO*t*Bu was successful, but again, the yield dropped by purification. Because of the low yields, the ethylene glycol derivatives were not further investigated.

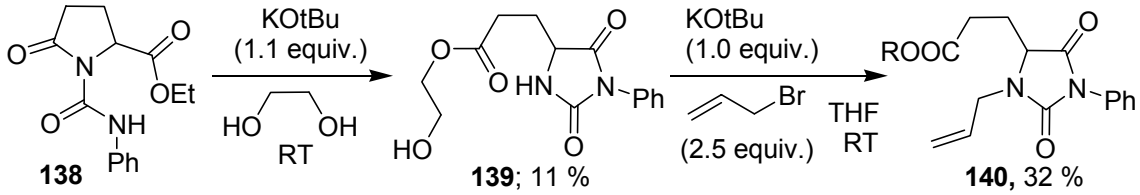

Scheme 48

In the framework of the synthesis of constrained bicyclic hydantoins (§ 1.3.1 of the Results and Discussion) the 2-step pyroglutamate-hydantoin rearrangement was evaluated for a

C(2)-alkylated pyroglutamate. The methyl pyroglutamate was allylated with allylbromide using 2 equivalents of LiHMDS (Scheme 49). Pyroglutamates are versatile building blocks, as the site of alkylation can be directed by changing the protecting group on nitrogen.[116,119] Without a protecting group on nitrogen, alkylation with 2 equivalents of base occurs at the 2-position, and no alkylation on nitrogen is observed.[120]

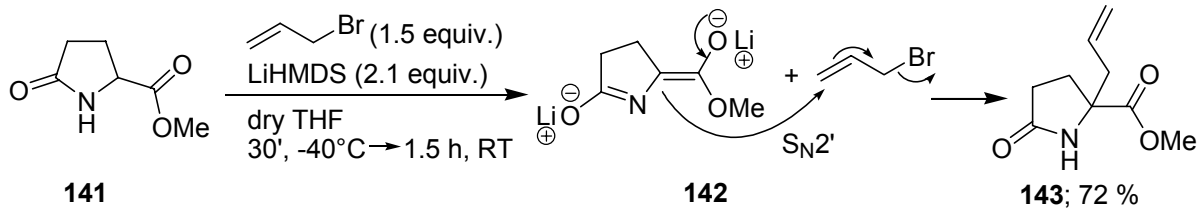

Scheme 49

This 2-alkylpyroglutamate ester **143** was reacted with propylisocyanate in dry ether with addition of NaH. After 25 minutes, work-up delivered the hydantoin **144**, the carbamoylated hydantoin **145** and a tiny amount of what is most probably the carbamoyllactam **146** (Scheme 50). A completely selective carbamoylation without further rearrangement failed for the *C*(2)-substituted pyroglutamate. This can be caused by a higher solubility of the sodium salt of the carbamoylated lactam **146** or by the *C*(2) substituent that changes the orientation of the ester group if the pathway in Scheme 41 is followed. Another explanation would be the hygroscopicity of the 2-alkylpyroglutamates, as traces of water initiate the rearrangement reaction given in the pathway in Scheme 42.

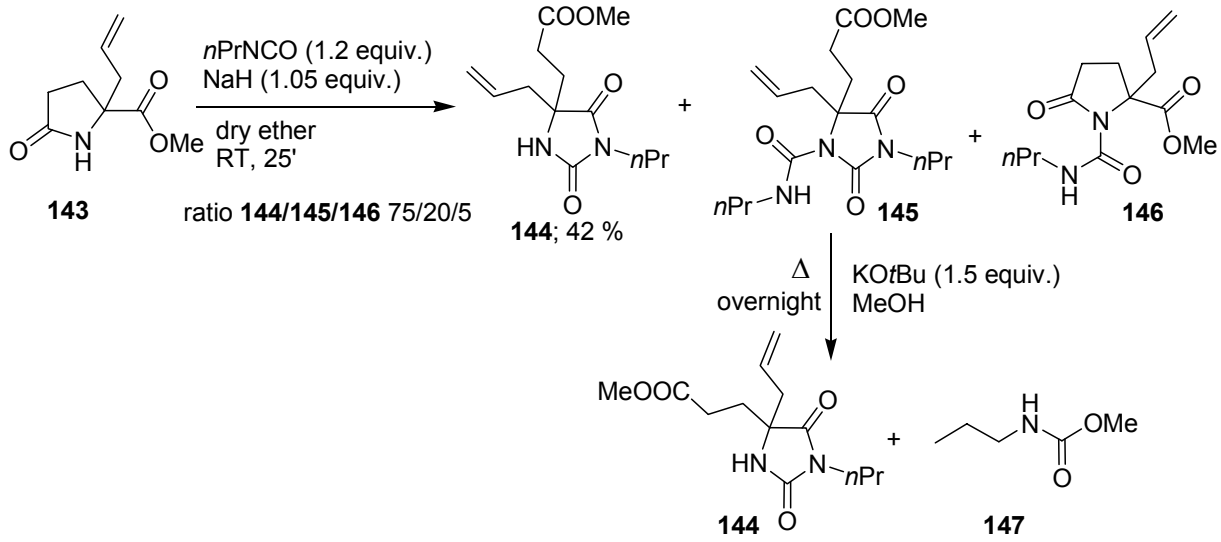

Scheme 50

The carbamoyl group of the carbamoylated hydantoin **145** can be easily removed by overnight reflux with potassium methoxide. If the same reaction was performed at room temperature, no decarbamoylation was observed. The side-product, urethane **147** can be removed by heating the residue under reduced pressure and was identified by its ^{1}H NMR spectrum.

Reaction of the methyl 2-allylpyroglutamate **143** with 2 equivalents of isocyanate results in a complete conversion to the carbamoylated hydantoin **145 (**Scheme 51**)**. After extraction 79 % of the crude product was isolated, probably a part of the product dissolved in the aqueous layer after ester hydrolysis. Removal of the minor impurities by column chromatography caused a drop in yield to 52 %. The addition of a second equivalent of isocyanate to the carbamoyl group of **146**, was never observed. The insertion of a single isocyanate molecule, was also reported for the carbamoylation of 2-pyrrolidone.[121]

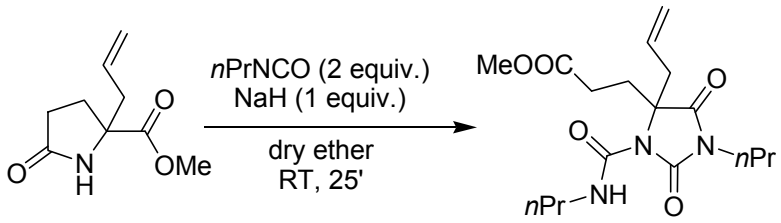

143 **145**; 52 %

Scheme 51

Looking back at the transamidation reaction performed in THF, the effect of the use of a slight excess of isocyanate was analysed again. Indeed the carbamoylated hydantoin derivative could be observed. This product was isolated for the reaction of ethyl pyroglutamate **136** with allylisocyanate (Scheme 52).

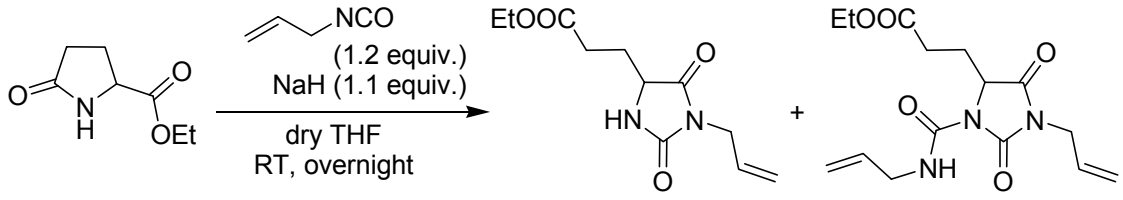

136 **122f**; 48 % **148**; 5 %

Scheme 52

Again 2D spectra were needed for the full identification of the carbamoylated hydantoins and to assure that no second carbamoylation of the pyroglutamate had occurred. Both NCH_2 hydrogen atoms couple to 1 urea carbonyl only and not to the same carbonyl atom, which means they are not part of the same urea (Figure 16).

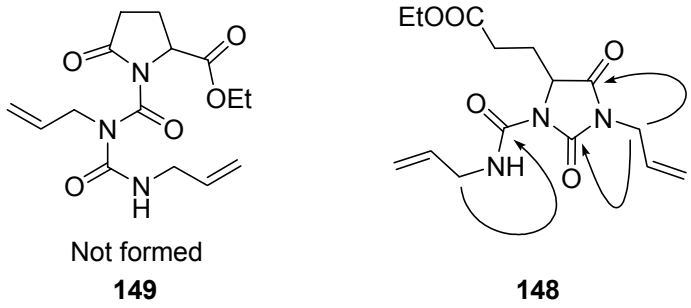

Figure 16. HMBC couplings used for identification of 148

Hydantoins were synthesized in medium to high yields via a rearrangement reaction of carbamoylated pyroglutamates. Two pathways for the one-pot carbamoylation and rearrangement reaction were proposed: one via the bicyclic imidazolidine intermediate **123** and another that starts via ester decomposition. The first one is more probable for the one-step reaction. The latter mechanism led to a faster two-step procedure that starts with the ring opening of the lactam ring, following the pathway in Scheme 42. It is important that the carbamoylation is done in completely dry circumstances; otherwise a rearrangement reaction occurs, initiated by hydroxyl ions.

1.3 Conformational restriction

1.3.1 Using Biselectrophiles

The pyroglutamate hydantoin rearrangement can be used as the key step in the synthesis of more complex hydantoins. The goal was the synthesis of more constrained bicyclic derivatives. Compounds like **153** have attracted the attention of a number of research groups due to their potential biological application and as a template in organic synthesis.[122,123]

For this purpose, the pyroglutamate **113** was alkylated at *C*(2) with 3-chloro-2-chloromethyl-1-propene, following the procedure in reference 118. Pyrrolizidinone **151** was formed as a side-product. This side reaction could be reduced by shortening the reaction time at room temperature from 2 to 1.5 hours and by avoiding heating during evaporation

of the solvent under reduced pressure. The alkylated pyroglutamate was obtained by recrystallization in petroleum ether.

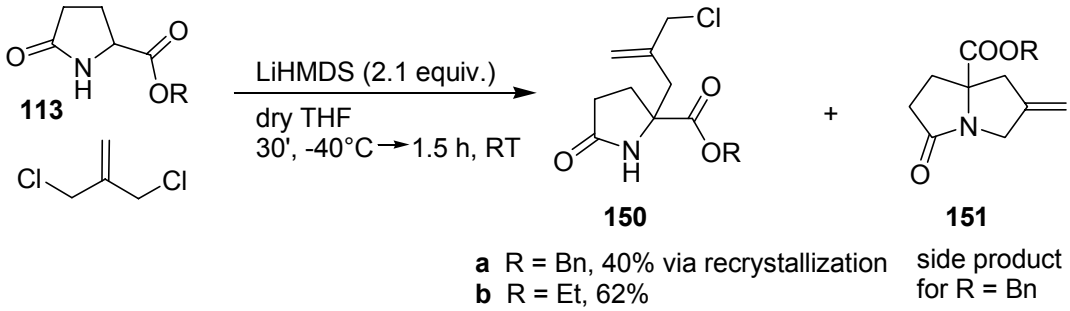

Scheme 53

Reaction of **150a** with propylisocyanate leads to a mixture of compounds from which the desired bicyclic imidazolidine **153** could be isolated. Another fraction was the carbamoylated hydantoin **154**. Apparently, the carbamoylation of the formed hydantoin is so fast that it can compete with the intramolecular alkylation reaction (Scheme 54).

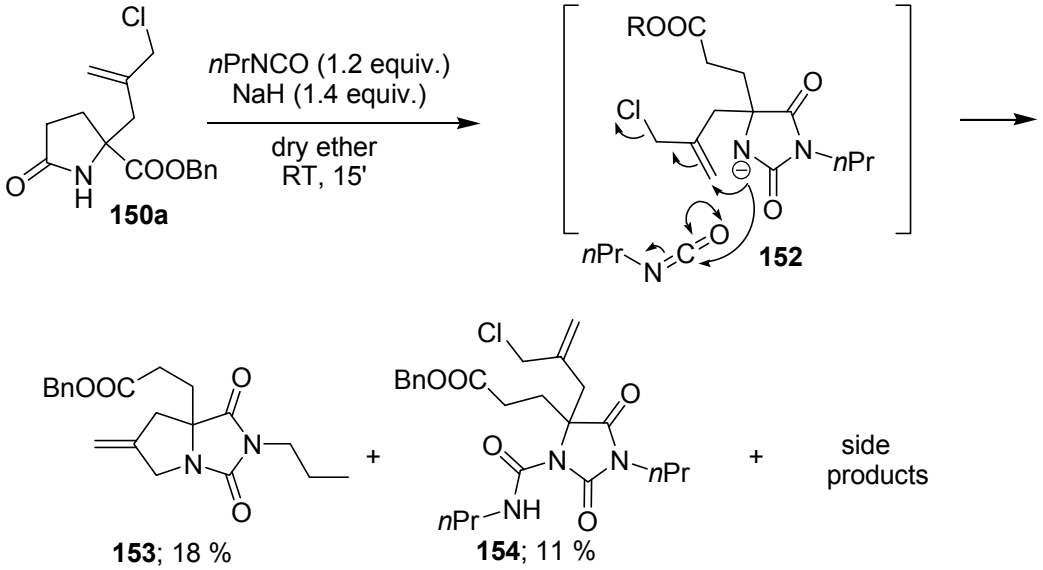

Scheme 54

To avoid the formation of a mixture of compounds, a two-step approach was taken for the ethyl derivative **150b**, in which the carbamoylpyroglutamate would be isolated again. As the reaction of the methyl 2-allylpyroglutamate **143** had shown, the use of ether as a solvent could not completely inhibit the rearrangement reaction of the *C*(2)-substituted pyroglutamate.

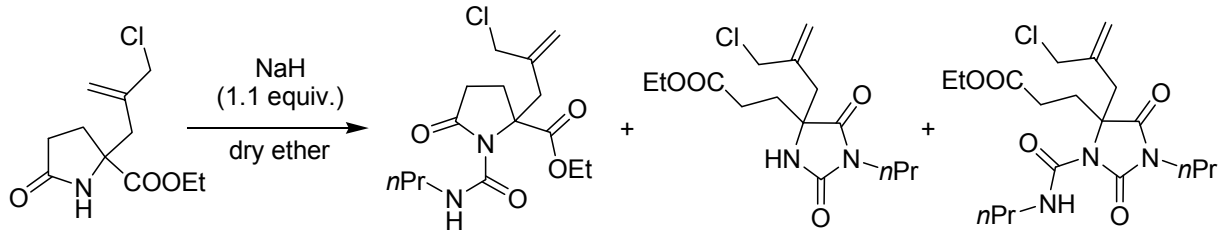

150b **155** **156** **157**

Ratio / Yield			
RT, 30', *n*PrNCO (1 equiv.)	52 / 13 %	38 / 10 %	10 / 8 %
0° C, 15', *n*PrNCO (1 equiv.)	80 / 35 %	0	20 / 6 %
RT, 30', *n*PrNCO (2 equiv.)	20 / 6%	0	80 / 31%

Scheme 55

Several reaction conditions were evaluated, and the highest conversion to the carbamoylpyroglutamate **155** was obtained using 1 equivalent of isocyanate in diethylether, reducing the reaction time to 15 minutes and lowering the temperature to 0°C. In less polar solvents like toluene or petroleum ether, the carbamoylation did not complete. Moreover, the pyroglutamate was badly soluble in the latter solvent. Unfortunately, less than 50 % of product was obtained after purification via column chromatography.

Similar to the reaction of the methyl 2-allylpyroglutamate **143** with two equivalents of isocyanate (Scheme 51), pyroglutamate **150b** yielded mainly the carbamoylated hydantoin **157**. In this case, also the carbamoyl lactam **155** was isolated. Probably the rearrangement reaction was slowed down because of the sterical hindrance, caused by the substituent on the glutamate. The hydantoin **156** with an unsubstituted *N*(1) position was not observed, again indicating that the second carbamoylation is fast, once the rearrangement towards the hydantoin has occurred.

Once the carbamoylpyroglutamate **155** had been isolated, a clean conversion to the pure bicyclic imidazolidinedione **158** was observed by stirring it with 1.2 equivalents of KO*t*Bu in ethanol. No side-products were formed during this one-pot sequence of the pyroglutamate-hydantoin rearrangement and an intramolecular substitution of the allylic chloride (Scheme 56).

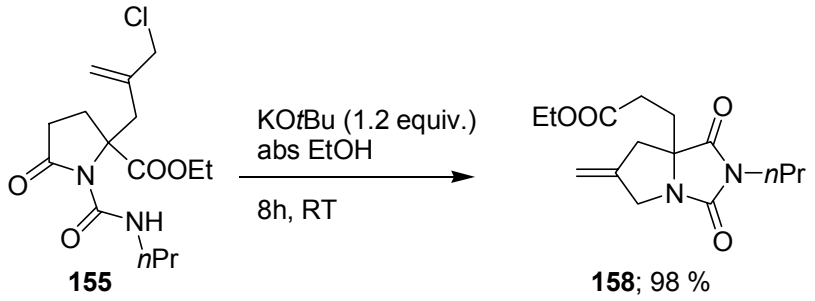

155 **158**; 98 %

Scheme 56

The same reaction sequence was then followed for the synthesis of bicycle **163**. After alkylation of the pyroglutamate with *cis*-1,4-dichloro-2-butene, the carbamoylation led to a mixture of the desired carbamoylpyroglutamate **161** and the usual hydantoin derivatives. Also ring closure towards the tetrahydro-1*H*-indolizine derivative **160** was unavoidable. After different purification steps, the yield dropped to 13 %. After isolation of the carbamoyl pyroglutamate, treatment with 1.3 equivalents of potassium ethoxide yielded the pure bicycle **163** (Scheme 57). Compound **163** can also be obtained via a ring-closing metathesis procedure, which avoids formation of the indolizidine derivative **160**. This method is shortly reviewed in the next paragraph and is given in paper IV in appendix 2.

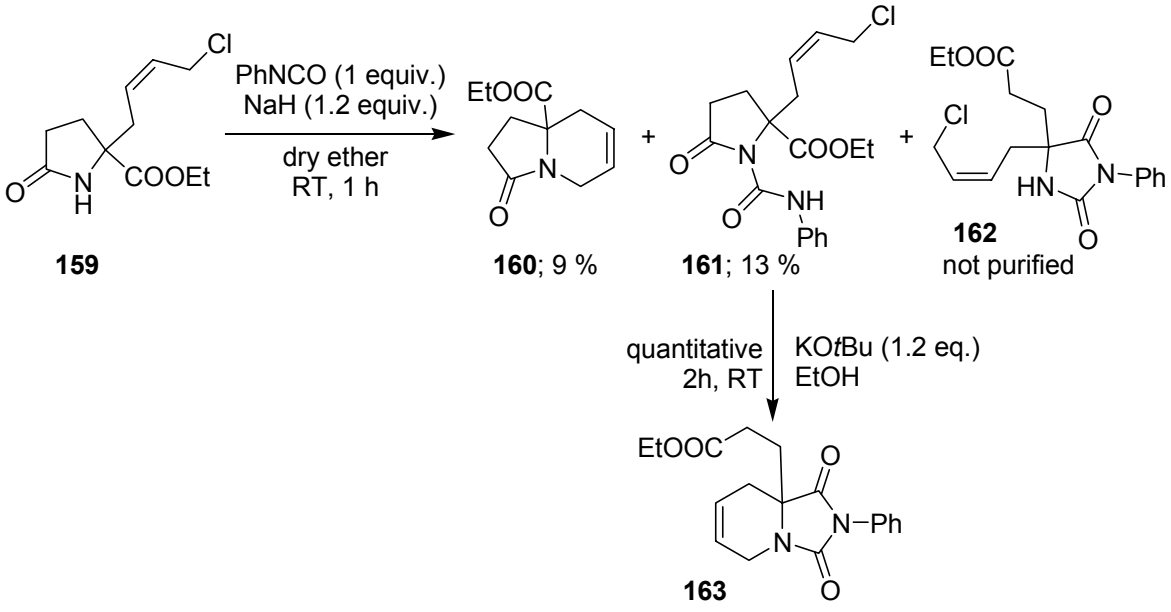

159 **160**; 9 % **161**; 13 % **162** not purified

163

Scheme 57

Bicyclic hydantoin derivatives can be formed via alkylation of the pyroglutamate ester at the *C*(2)-position with biselectrophiles before the rearrangement reaction. However, two undesired side reactions occur: internal ring closure of the alkylated pyroglutamate, before the isocyanate addition, and a fast carbamoylation of the hydantoin. Once the 2-alkyl-1-

carbamoylpyroglutamate esters were isolated, quantitative rearrangement and cycloaddition occurred to furnish the pure bicyclic imidazolidinediones.

1.3.2 Using RCM: Synthesis of Small Rings

As mentioned before, constrained bicyclic hydantoins can also be obtained via ring-closing metathesis of double-allylated hydantoins **166**. The first allyl group was introduced at *C*(2) of the pyroglutamate ester. Next, carbamoylation and double ring-transformation delivered the hydantoin. After alkylation of the hydantoin at *N*(1) with 2 equivalents of electrophile and K_2CO_3, RCM furnished bicyclic compound **167** (Scheme 58). The details of this transformation are described in Paper IV in appendix 2. The work was done in collaboration with dr. ir. Dieltiens, who was studying different metathesis applications for the construction of new azaheterocycles.

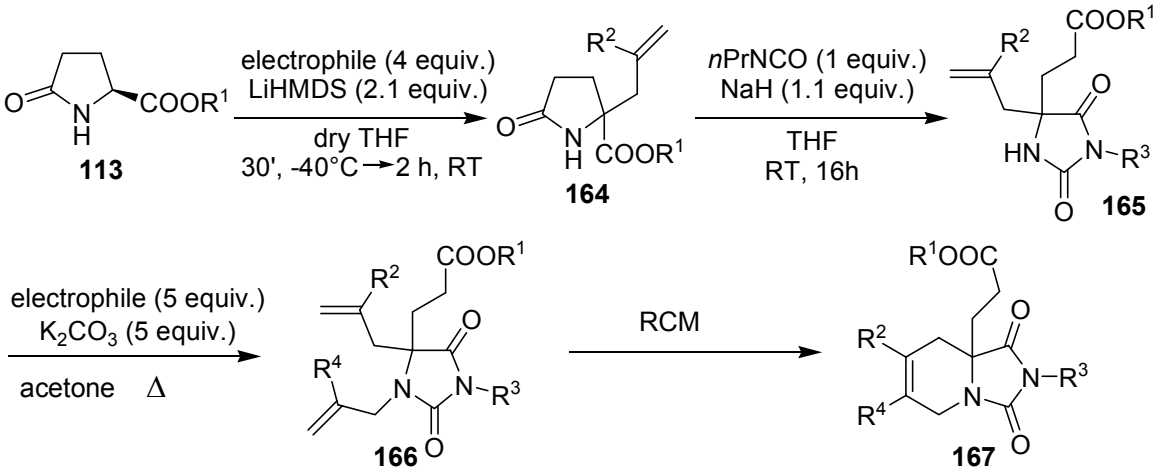

Scheme 58

1.3.3 Using RCM: Synthesis of Large Rings

The idea was set to apply the pyroglutamate-hydantoin rearrangement in the synthesis of bis-hydantoins **5** which are hexamethylenebis(acetamide) (HMBA, **6**) analogues. HMBA has potential anti-cancer activity by inducing tumor cells to differentiate to non-malignant phenotypes.[10] This implies that it works not by killing the cancer cells but by inducing them to differentiate and to express characteristics of the normal non-transformed counterpart. This is a promising approach to cancer therapy, potentially without many of the disadvantages of cytotoxic agents. HMBA has even had some modest success in clinical trials.[124] The doses required to achieve sufficient blood levels in human patients, however,

led to some undesirable side effects.[125] It was found that compounds **5a** and **5d** were 10 times more potent than HMBA itself, but the activity of **5b** however was low, probably due to its insolubility.[10,28,126]

Compound **5c** was found to show anti-epileptic activity in the maximal electroshock seizure test.[127]

The synthesis of these compounds usually involves the reaction of a hydantoin with a ω-dihaloalkane under basic conditions. The problems with this reaction are the need for *N*(3)-selective alkylation and the yield which is usually quite low. Starting from pyroglutamates would avoid the problem of *N*(3)-selectivity and would allow the synthesis of highly functionalized derivatives since pyroglutamates can easily be derivatized.[116,119]

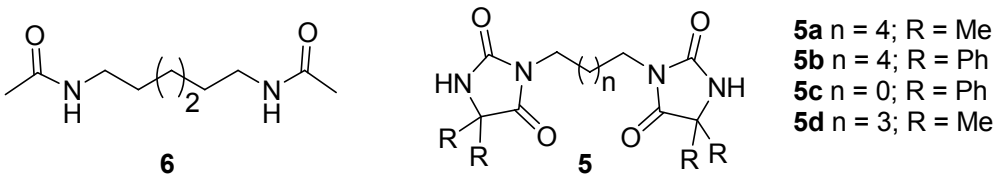

Figure 17. HMBA (6) and bis-hydantoins (5)

The hydantoins **169** were synthesized using the previously described two-step protocol, since the more straightforward one-step ring closing ring opening did not complete in THF and some side reactions occurred. So, NaH was added to a mixture of the pyroglutamate and the diisocyanate in dry ether (Scheme 59). Almost immediately after the addition of the base, a white precipitate was formed. The reaction was quenched with a saturated $NH_4Cl_{(aq)}$ solution after two hours and furnished **168** in good yields.

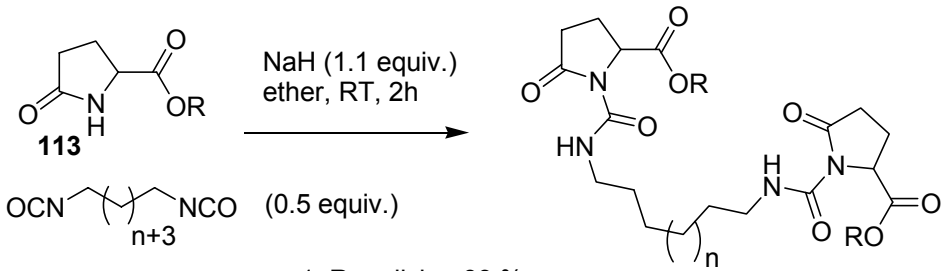

a *n* = 1; R = allyl; 83 %
b *n* = 1; R = ethyl; 93 %
c *n* = 3; R = allyl; not isolated
d *n* = 3; R = ethyl; 99 %
e *n* = 7; R = allyl; 91 %
f *n* = 7; R = ethyl; 99 %

Scheme 59

Stirring of the bis(carbamoyllactam) **168a** in allylalcohol with 2.1 equivalents KO*t*Bu, afforded the bis(hydantoin) **169a** (Scheme 60).

It was investigated whether one could start from ethyl pyroglutamate and perform a transesterification simultaneously with the pyroglutamate-hydantoin rearrangement. For this purpose the ethyl pyroglutamate was carbamoylated in ether with 1,6-diisocyanatohexane and then rearranged in allyl alcohol by treatment with KO*t*Bu. This sequence resulted in pure bis(hydantoins) **169b** and **d**. However, partial rearrangement of the carbamoylated product occurred in the first step and therefore the procedure starting from the allyl pyroglutamate is preferred.

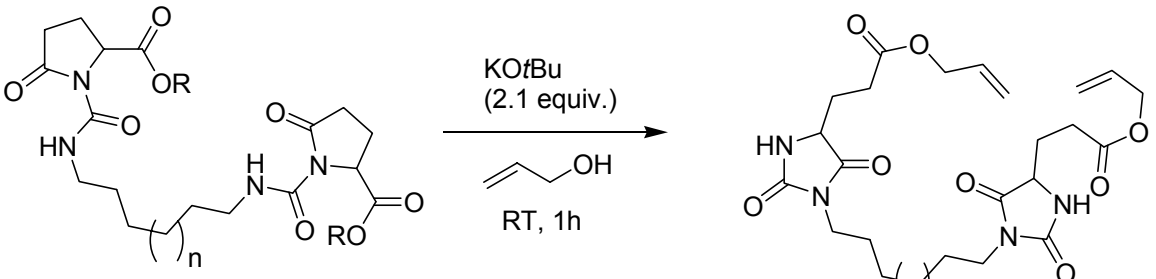

168

168a *n* = 1; R = allyl; **169a** 86 %
168b *n* = 1; R = ethyl; **169a** 91 %
168c *n* = 3; R = allyl; **169b** 86 %
168d *n* = 3; R = ethyl; **169b** 96 %
168e *n* = 7; R = allyl; **169c** 49 %

169

Scheme 60

The obtained hydantoins can be further derivatised by alkylation at nitrogen (Scheme 61). To introduce *N*-benzyl groups, the imidazolidinediones **169** were heated at reflux overnight in acetone with an excess of electrophile (mostly the corresponding bromide) and ground K_2CO_3. The alkylation had a 100% conversion, but the chromatographic removal of the excess of electrophile caused the yield to drop. For the methylation, iodomethane and NaH in DMF were used. The yields presented in Scheme 61 are those after purification of **170**.

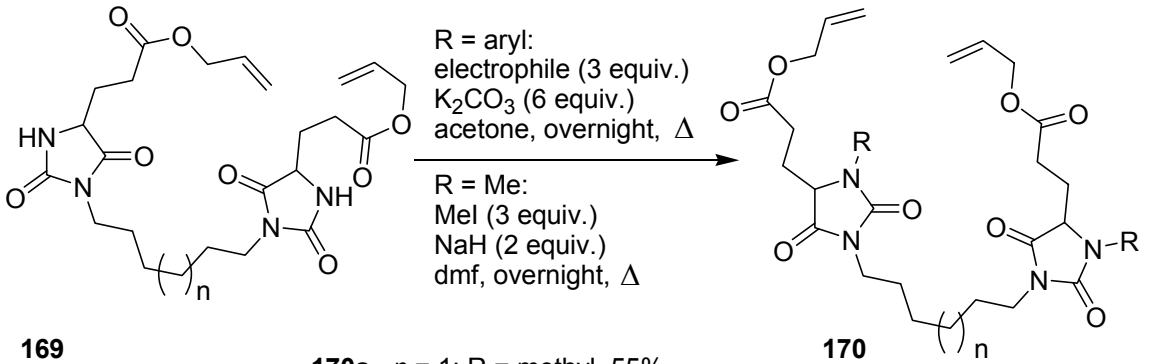

169 **170**

170a *n* = 1; R = methyl, 55%
170b *n* = 1; R = benzyl, 73%
170c *n* = 1; R = *p*-bromobenzyl, 78%
170d *n* = 3; R = *p*-chlorobenzyl, 68%
170e *n* = 3; R = *p*-bromobenzyl, 54%
170f *n* = 7; R = benzyl, 55%

Scheme 61

These bishydantoins are very flexible molecules. To restrict the rotational freedom, they were incorporated in large ring structures using RCM. The *N*-alkylation then also serves as protection methodology for the *N*-lactam to prevent deactivation of the catalyst used for the cyclisation. RCM is a powerful method to synthesise macrocyclic products; substrates devoid of any conformational constraints can be cyclized by it. Neither the conformational predisposition of the substrates nor the ring size play a decisive role, but the presence of polar relay substituents, their distance from the alkene groups and low steric hindrance close to the double bond are important.[128]

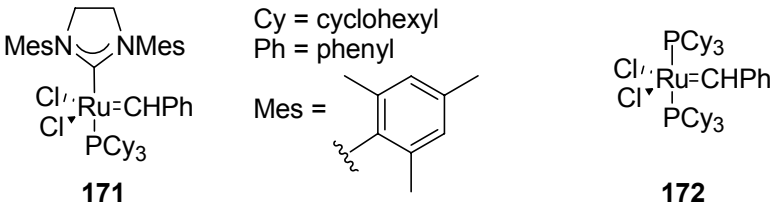

171 **172**

Figure 18. Second (171) and first (172) generation Grubbs' catalyst

The ring closure of **170a-f** was carried out using 5 mol-% of second generation Grubbs' catalyst **171** (Figure 18).[129] Simply heating the compounds at reflux overnight together with the ruthenium catalyst resulted in a quantitative conversion to the macrocycles (Scheme 62).

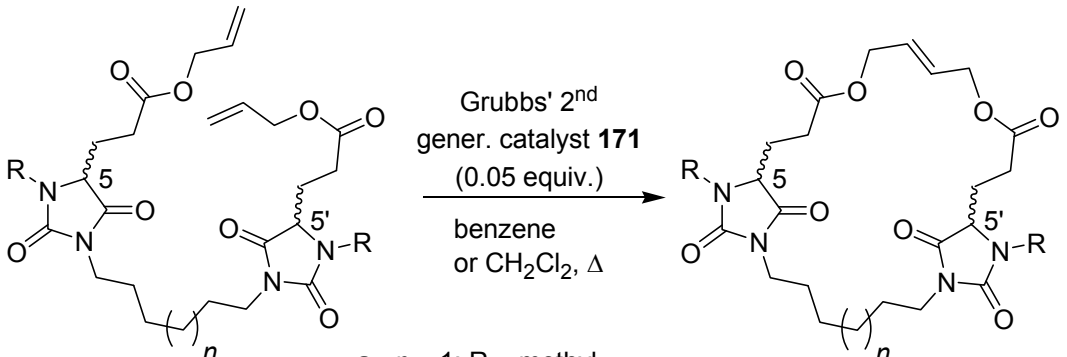

170 **173**

a *n* = 1; R = methyl
b *n* = 1; R = benzyl
c *n* = 1; R = *p*-bromobenzyl
d *n* = 3; R = *p*-chlorobenzyl
e *n* = 3; R = *p*-bromobenzyl
f *n* = 7; R = benzyl

Scheme 62

Usually RCM results in a mixture of *E* and *Z* isomers, but in some cases only *E* isomers have been formed.[130] The use of the second generation Grubbs' catalyst **171** affords a much higher *E*/*Z* ratio than the use of the standard Grubbs' carbene **172**.[131] This is caused by the ability of **171** to isomerize the initial product under the reaction conditions, thereby progressively enriching the mixture in the thermodynamically favoured *E* isomer.[132]

Also in this case, two separate signals were observed for the alkene protons of derivatives **173**. Since these macrocycles **173** have two chiral centers, these can be diastereomers as well. Usually the *E* and *Z* isomers are distinguished using $^{3}J_{HH}$ NMR coupling constants, but these are absent as the macrocycles are symmetrical. These $^{3}J_{HH}$ coupling constants, however, can be recovered when an *H*,*C*-inverse-detection spectrum is acquired without carbon-decoupling during acquisition. In the inverse-detected *H*,*C*-correlation spectra, the major component due to signals coming from H bonded to ^{12}C, which represents 99 % of the total number of *C* atoms in normal ^{1}H NMR spectra, is suppressed. By doing this, the $^{3}J_{HH}$ coupling constants between equivalent protons can be observed.[133]

The diastereomers of **173a** and **173c** were separated via preparative thin layer chromatography (TLC), though chromatography again caused a large drop in yield. For **173c,** coupling constants of 17.4 and 18.1 Hz were observed, pointing to a *trans* geometry for both isomers.

Further evidence that a mixture of diastereomers rather than *E* and *Z* isomers is formed, was provided by an experiment in which one of the diastereomers of **170e** could be isolated in pure form via column chromatography. This so-called 'diastereomer' is actually a mixture of two enantiomers, which cannot be distinguished in the NMR spectra. Heating of this

diastereomer at reflux with Grubbs' catalyst **171** gave one product in the ^{13}C NMR spectrum. So only the *E* or the *Z* isomer was formed, as otherwise two products should have been observed in the ^{13}C NMR spectrum. The coupling constant of **173e** was 17.7 Hz, again pointing to the formation of the *E* isomer.

The pyroglutamate-hydantoin rearrangement has been used to construct *N*(3),*N'*(3)-polymethylenebis(hydantoins), which are HMBA analogues. After *N*-alkylation or *N*-arylation, the bis(hydantoins) were ring closed to form 24- to 30-membered macrocycles, again indicating the power of ring-closing metathesis. The use of second generation Grubbs' catalyst **171** resulted in exclusive formation of the *trans* double bond isomers, as was confirmed by undecoupled HSQC.

1.4 Computational Investigation of Flexibility and Thermodynamic Stability of *Trans*-Fused Macrocyclic Alkenes[134]

The thermodynamic stability of the double bond isomers of the 24-membered cyclic alkene **173a**, containing two planar hydantoin rings, was investigated in silico. The macrocycle **173a** has two chiral centra and was obtained as a diastereomeric mixture. Therefore, both an S,S and an R,S isomer were modelled with an *E* or *Z* double bond, denoted respectively as *E*-(S,S), *Z*-(S,S), *E*-(R,S) and *Z*-(R,S) (Figure 19).

We can assume that a thermodynamic equilibrium was set. The second generation Grubbs' catalyst **171** (Figure 18)[129] that was used for the RCM reaction, is known to give higher *E*/*Z* ratios than the use of the standard Grubbs' carbene **172**,[131] as **171** is able to isomerize the initial product via backward and forward reactions, during the so called secondary metathesis process, thereby enriching the mixture in the thermodynamically favoured isomer.[132,135] As there are no substituents next to the double bond – dense substitution would cause kinetic control[136] – and the reaction was allowed to equilibrate, by stirring the reaction overnight under reflux, we can assume thermodynamic equilibrium and predict the ratio of the *E* and *Z* isomers based on their relative thermodynamic stability.

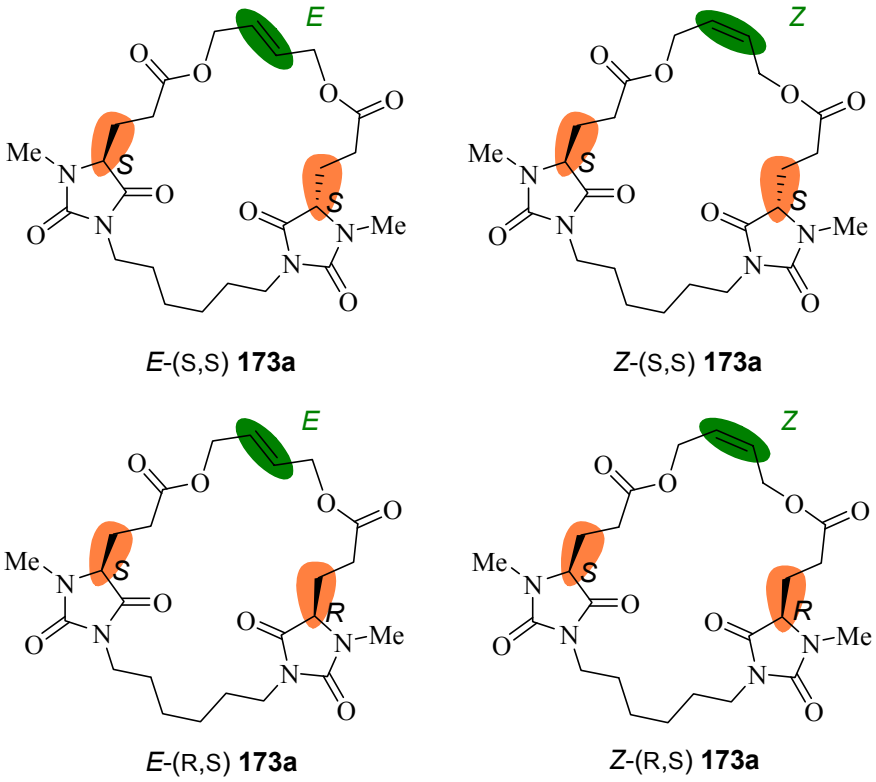

Figure 19. Different stereomers modelled by molecular dynamics

First the conformational sampling protocol is described. Given the computational demands of existing conformational sampling techniques, they are performed at relatively low levels of theory. We have chosen the very intuitive high temperature procedure to scan the potential energy surface at the low level of theory (LOT). More advanced methods should be used to scan the potential energy surface (PES) at the low LOT if the free energy is more sensitive to the temperature, like e.g. with proteins. Afterwards a higher LOT can be used on a selected training set. There are several possibilities to create the training set. The most simple procedure is to perform a random selection. However there is a risk that geometries of certain parts of the PES are not selected and that others are very similar. To make the step to a higher LOT and limit the computational cost, one should sample the obtained ensemble in a more uniform way. This will avoid calculation of similar structures at the computationally expensive level. Therefore, we have developed a new sampling procedure based on the Kennard-Stone algorithm.

The suitability of the methodology is then evaluated by predicting the thermodynamic stability of the double bond isomers of macrocycle **173a**. Finally, the effect of the double bond configuration on the conformation of the macrocycle is investigated by doing a conformational analysis.

1.4.1 Methods

Conformational sampling protocol

The conformational sampling protocol outlined below is applied to four isomers of the macrocycle: two *E* and two *Z* isomers. Within each type, two stereocentres can be equal (S,S) or different (R,S), as illustrated in Figure 19. The end result of the sampling procedure is a set of representative and diverse conformers for each of the four isomers. These sets can be used to characterize the effect of the double bond (*E* or *Z*) on the thermodynamic stability of the macrocycle.

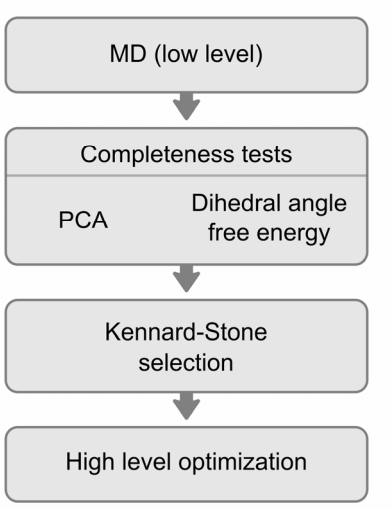

Figure 20. Flow chart of the conformational sampling protocol

The sampling procedure is applied to each stereomer and consists of four steps: (i) a quantum mechanical molecular dynamics simulation at a semi-empirical level, (ii) a first assessment of the completeness of the simulation based on the principal component analysis, (iii) a second assessment of the completeness of the simulation based on the sampling of dihedral angles, and (iv) the selection of configurations from the molecular dynamics trajectory with the Kennard-Stone algorithm.

The entire analysis and post-processing of the molecular dynamics simulation is implemented with the in-house developed trajectory analysis code, MD-Tracks.[11]

The molecular dynamics simulations are carried out with CP2K,[137] using the PM3 semi-empirical Hamiltonian[138] to compute the inter-atomic forces. The conformational space is explored with an NVT molecular dynamics run of 300 ps using an integration time step of 1 fs and the Nosé-Hoover thermostat[139,140] with a temperature of 1500 K and a time constant of 100 fs. The computational efficiency of the PM3 method and the high temperature make

the extensive sampling feasible. Prior to the production run, the system is initialized by means of an NVE simulation with a threshold in the instantaneous temperature, i.e. as soon as the temperature drops below 1400 K or rises above 1600 K, the velocities are scaled uniformly to obtain an instantaneous temperature of 1500 K. Although the initialization algorithm does not rigorously sample the NVT ensemble, it is an efficient tool to introduce the required amount of thermal energy before the actual production run.

The high temperature is not applicable in general, and one must carefully consider entropic side-effects. It is for example well-known that the preferred conformation of a protein is very sensitive to temperature, mainly because the entropic contribution to the free energy of the folded and the unfolded states is very dissimilar.[141,142] When this is the case, more advanced (and computationally expensive) sampling schemes[141,142,143 ,144] are required to perform the conformational search at the semi-empirical level.

It is essential to check the convergence of the molecular dynamics simulations. If the simulations were too short, the NVT ensemble of each conformer would not be sufficiently sampled and, by consequence, an ensemble average or a selection of conformers could never be representative. There is no golden standard to test convergence in general, but one can at least check that the ensemble averages of interest over the first and the second half of the simulation are equal within the statistical error margins. Another test is the absence of cosine content in a principal component analysis.[145,146] Both types of tests are discussed below. One must be aware that all these tests are necessary but not sufficient for the assessment of convergence. Strictly speaking, one can never avoid that a molecular dynamics simulation is trapped in a local free energy minimum with a mean residence time that is much longer than the actual simulation.

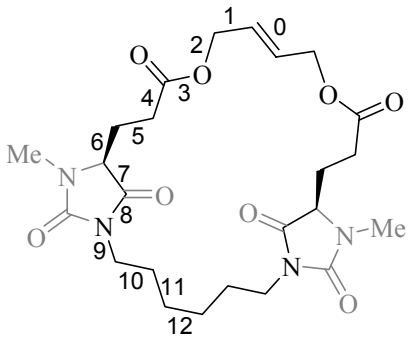

Figure 21. Indication of the backbone of macrocycle 173a in black and the dihedral angles of the *E*-(R,S) isomer.

The first convergence test is based on histograms of the dihedral angles of the macrocycle backbone, indicated in Figure 21. The backbone dihedral angles are labeled starting from the double bond. For each dihedral angle a histogram is constructed covering the whole range from -180° to 180° with bin widths of 20°. Also the error on the count of each bin is computed, taking into account the sampling inefficiency due to time correlations.[147] An example is given in Figure 22a. Based on the histogram, a free energy profile is derived using the following relation:

$$A_i = -k_B T \log(N_i) + C\,,$$

In which A_i is the free energy of the bin with index i, N_i is the corresponding count, k_B is the Boltzmann constant, T is the temperature and C is an arbitrary constant taken such that the lowest A_i becomes zero. First order estimates of the statistical errors on the free energy are estimated from the errors on the counts in the histogram. An example is given in Figure 22b. The red and the cyan curves give the histogram and free energy profiles for dihedral angle 2 positioned at one side of the double bond (closest to the R center) and the other side of the double bond (closest to the S center), respectively. If the molecular dynamics runs are complete, the two profiles should coincide as the dihedral angles are equivalent (Figure 21). The corresponding free energy profiles are indeed nearly identical (or reflected when chirality plays a role). This procedure was checked for each pair of equivalent dihedral angles in the four conformers.

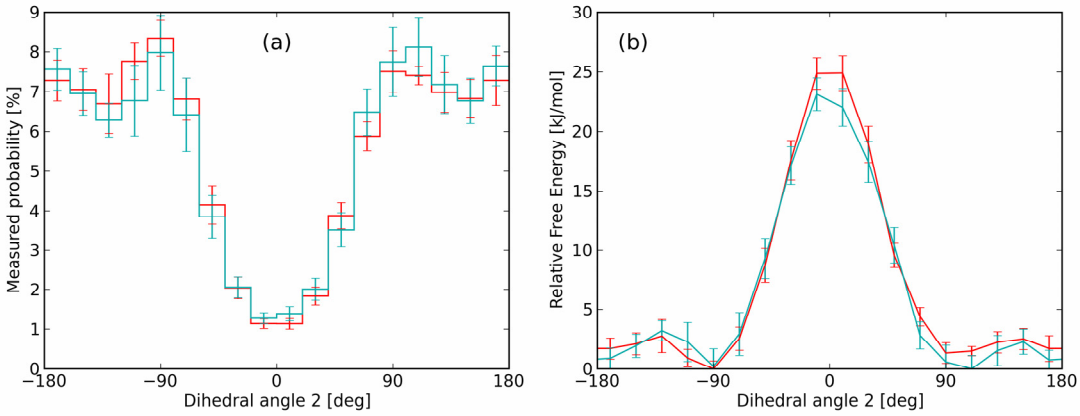

Figure 22. (a) A histogram with measured probabilities for dihedral angle 2 in conformer *E*-(R,S). The red and cyan curves correspond to the torsion along the R and S centres, respectively. (b) The corresponding free energy profiles.

The second convergence test is based on principal component analysis (PCA).[145,146] Each geometry from the trajectory is rotated and translated with the Kabsch algorithm[148] to have a minimal root-mean-square deviation (RMSD) in Cartesian coordinates from a reference structure. The fitting procedure avoids coupling of external and internal modes in the remainder of the analysis. The Cartesian coordinates of the transformed trajectory are used as input for a principal component analysis, i.e. the eigen value decomposition of covariance matrix of all the mass-weighted Cartesian coordinates is computed. One obtains the so-called principal components by transforming the Cartesian coordinates to the basis of eigenvectors. These principal components can be interpreted as time-dependent fluctuations along the eigen modes of the covariance matrix. Hess[145] showed that the principal components of an incomplete molecular dynamics simulation *can* have a significant overlap with a cosine function: $\cos(n\pi t / t_{total})$, for which n is the index of the eigen mode, t is the simulation time, and t_{total} is the length of the simulation. The cosine content of a PCA mode is defined as the square of the dot product of the normalized principal component with the normalized corresponding cosine function. This is a number between zero and one, and any significant deviation from zero for any of the principal components is an indicator for poor sampling. This is again only a necessary condition and one must be aware that false negatives are possible.

The last step in the protocol is the selection of distinct samples with the Kennard-Stone algorithm.[149] The goal of the Kennard-Stone algorithm is to select a maximally diverse subset from a large set of candidate samples. The algorithm assumes that one can define a "distance" between two samples, which is low when the two samples are similar and high otherwise. The samples are molecular geometries and the following distance measure between geometry μ and ν is defined:

$$D_{\mu\nu} = \sqrt{\sum_i \sum_{j>i} \left(\frac{r_{ij\nu} - r_{ij\mu}}{(r_{ij\nu} + r_{ij\mu})/2} \right)^2},$$

in which the double sum runs over all pairs of atoms, $r_{ij\nu}$ is the distance between atom i and atom j in sample ν and $r_{ij\mu}$ is the corresponding distance in sample μ. This distance measure expresses an RMSD between the distance matrices of the two geometries weighted

by the inverse of the average distance matrix. These weights are a mathematical expression of the intuitive notion that changes in short distances are more important.

Given a distance measure, the Kennard-Stone algorithm works as follows. One starts with a large set of candidate samples and an empty set of selected samples. The first two selected samples are the two candidates with the maximal pair distance. All subsequent samples are selected in an iterative way, until the number of selected samples reaches a desired value. In one iteration, the candidate with the largest minimum distance to all the previously selected samples is selected. In this case the set of candidates counts 30000 structures, sampled from the molecular dynamics trajectory with an interval of 10 fs. From this set 100 samples are selected with the Kennard-Stone algorithm.

The primary motivation for the Kennard-Stone algorithm is the selection of maximally diverse conformers. Duplicates or very similar structures are avoided in the computationally expensive post-processing steps. Although the molecular dynamics simulation samples the canonical ensemble, the structures selected by the Kennard-Stone algorithm are not distributed canonically. They are rather uniformly distributed over the accessible conformational space. This basic principle of the Kennard-Stone algorithm can best be compared with the behaviour pattern of asocial people entering the theatre one by one. They prefer to choose a seat as far as possible from each other. When a new person enters and finds a seat in a relatively vacant region, he will immediately occupy it. Hence all regions will be equally populated and the distribution of occupied seats becomes uniform over the entire room. This is independent of the original distribution of the seats. The uniformity of the selected samples is in our advantage since it will cancel out relative probabilities in the conformational space that are inherent to the semi-empirical method. When the samples are post-processed at a higher level of theory, the artefacts from the semi-empirical method on the selected geometries are reduced. The only remaining assumption is that both the semi-empirical level and the higher levels of theory used in the post-processing have a comparable accessible conformational space. This can be validated with an approximate correlation between PM3 energies with more accurate values. In some sense, this approach is comparable to importance sampling,[143] in which samples are generated with a computationally cheaper method and a correction is introduced afterwards to compensate for the differences between the cheaper and the more expensive method.

Thermodynamic analysis of the selected samples

Electronic structure optimizations were performed with GAUSSIAN 03[150] on all 400 selected conformations. For the optimizations a B3LYP[151,152] level of theory was used with a 6-31G(d)[153] basis set. For each of the four stereomeric configurations a frequency calculation was done for the 10 most stable conformations from each set of 100 samples. If necessary an additional optimization was performed using the 'Opt=tight' and 'Int=Ultrafine' options. In addition, for these 40 minimum energy conformations single point energies were calculated at an MP2/6-31G(d)[154] post Hartree Fock level as well. They should account for the dispersion interactions not present in the B3LYP functional. However for the MP2 free energy the entropic contribution is taken from the B3LYP frequency calculation.

Conformational analysis of the MD simulation

In addition to the conformational sampling protocol, one can also analyze the trajectory of the molecular dynamics simulation as such. The shape of the dihedral free energy profiles is compared among the different isomers and one can infer structural properties from these data. We also performed a similar molecular dynamics simulation on one half of the macrocycle, the chain molecule shown in Figure 23, to estimate the strain effects imposed by closing the macrocyle. Such strain effects should be absent in the open chain.

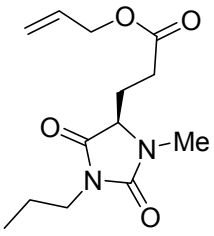

174

Figure 23. Half a macrocycle used to simulate the effect of the chiral centre on the dihedral angles close to the hydantoin ring

The relative orientation and position of the two hydantoins in the macrocycle is further examined with four specific internal coordinates. Based on the article of Cremer and Pople,[155] a time-dependent axes frame is attached to the five-membered ring in each hydantoin. The centres of the rings and the axes orthogonal to the ring planes are used as parameters to characterize the orientation and position of the hydantoins. The normal vector of a five-membered ring always points towards the CH_2 group connected to the stereocentre. The following coordinates were used: α, the angle between the two normal

vectors, d_{cc}, the distance between the two centres, and β_0 and β_1, the angles between each normal vector and the vector connecting the two centres.

1.4.2 Conformational Sampling and Analysis

Conformational sampling protocol

For each stereomer a molecular dynamics simulation has been carried out at the PM3 level. No significant drift in the conserved quantities is present. Multiple internal rotations are observed in all dihedral angles except for the double bond and the bonds in the five-membered rings. There were no transitions between R and S stereocentres.

All dihedral free energy profiles of the dihedral angles indicated in Figure 21 were plotted. A representative example (dihedral 5 of the *E*-(R,S) isomer) is given in Figure 24 resulting from simulations with varying length in time. As explained in Figure 22, the symmetrical equivalent angles on both side of the double bond are plotted. It is clear that for simulations shorter than 300 ps, statistical artefacts appear and the error bars on the free energies increase in size. The full simulation results in practically equal free energy profiles for symmetrically equivalent dihedral angles in all cases, confirming that a simulation time of 300 ps is sufficiently long for our sampling purposes. Note that due to differences in chirality of stereocentres in the (R,S) isomers, some free energy profiles are each other's mirror images. In these cases the reflected curves were also included to facilitate the comparison.

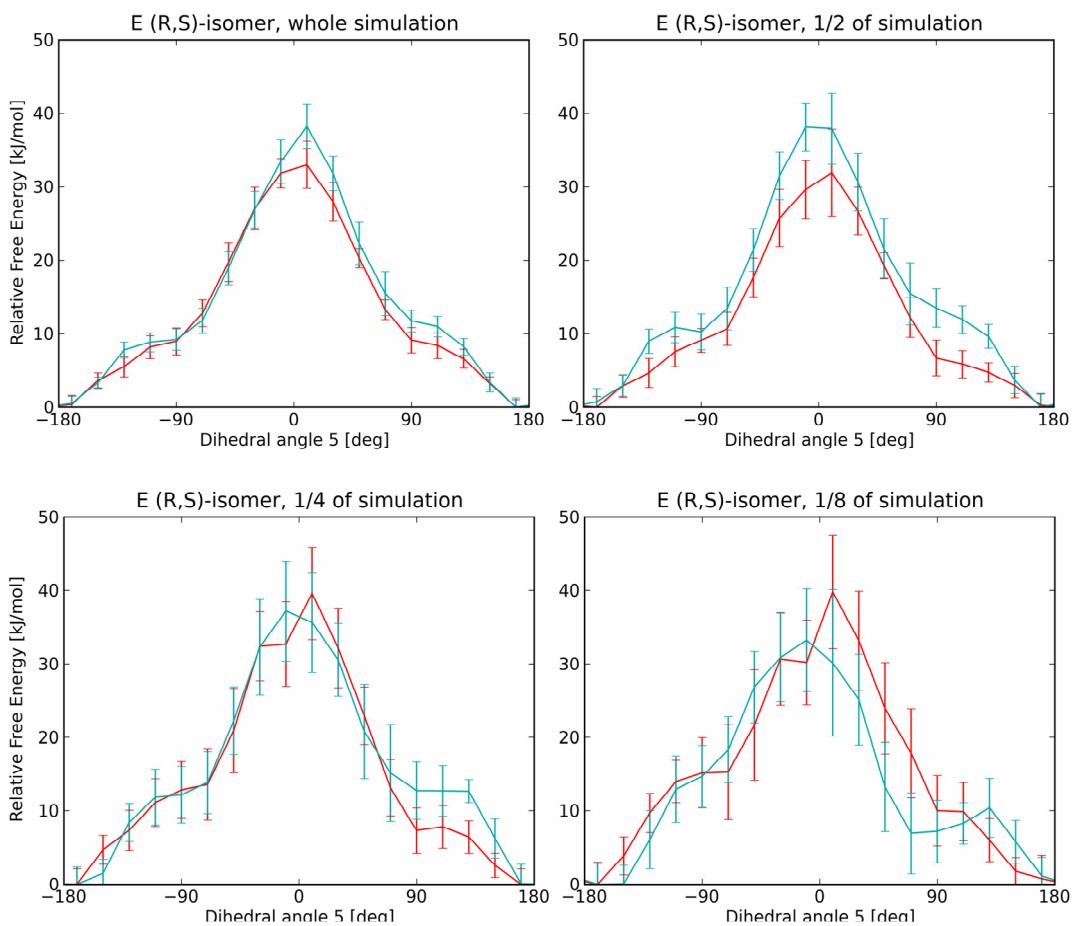

Figure 24. Free energy profiles for dihedral angle 5 of the *E*-(R,S) conformer, based on different fractions of the trajectory. (from left to right: 300 ps, 150 ps, 75 ps and 37.5 ps) The red and cyan curves correspond to the torsion along the R and S centres, respectively.

The most important results from the principal component analysis are summarized in Table 2. It is clear that all cosine content values are close to zero and there is no indication that the molecular dynamics simulations are too short.

Table 2. Cosine content (%) of the first five principal components from the 300 ps molecular dynamics simulation on each conformer.

Cosine content [%]	*E*-(S,S)	*E*-(R,S)	*Z*-(S,S)	*Z*-(R,S)
Mode 1	0.03	0.42	0.59	0.12
Mode 2	0.01	0.36	0.12	1.46
Mode 3	0.02	0.03	0.10	0.01
Mode 4	0.09	0.15	0.10	0.23
Mode 5	0.47	0.13	0.00	0.90

From each simulation 100 samples are selected following the Kennard-Stone procedure outlined above.

All 400 geometries selected with the Kennard-Stone algorithm are optimized at the B3LYP/6-31G(d) level of theory. Figure 25a and Figure 25b give an overview of the (optimized) potential energies for the (S,S) isomers and (R,S) isomers respectively. Before plotting, the energies are sorted and the lowest energy is taken as the reference value. The dashed lines are an estimate of the uncertainty on these curves. The error estimates are generated with a Monte Carlo procedure that is based on the approximation that the energies within each category are distributed uniformly over a range of 120 kJ/mol. Both in Figure 25a and Figure 25b, the *E* isomer has significantly more low-energy conformations than the *Z* isomer.

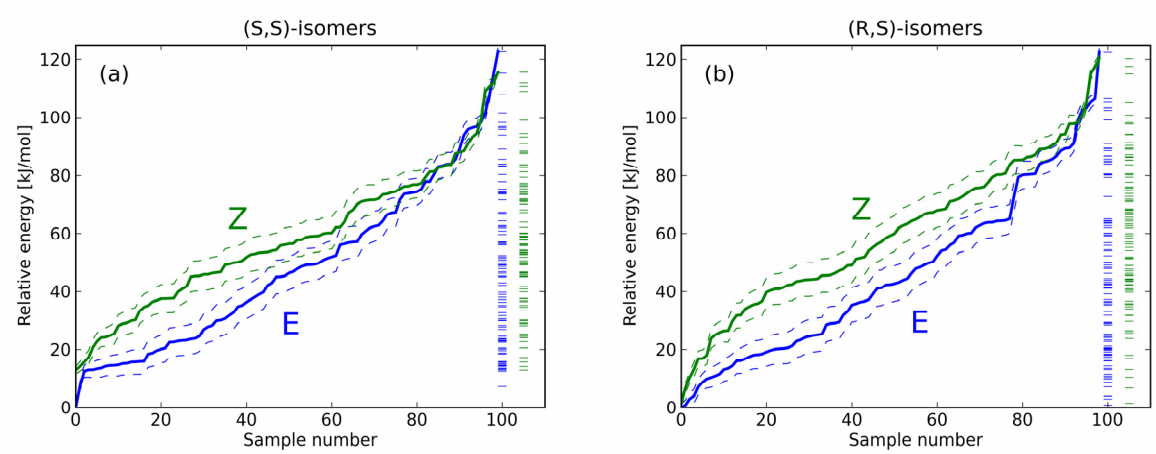

Figure 25. The solid line represents the sorted B3LYP/6-31G(d) energies for the four stereomers relative to the lowest energy conformation. The dashed lines are error estimates on the solid lines. In the right part of both plots, the potential energy of each sample is displayed for the *E* and *Z* conformations by a single dash.

To remove any ambiguity concerning LOT dependence of the obtained results, the free energies for the 10 most stable conformations of every stereomer are computed at the MP2/6-31G(d) level as discussed before and are plotted in Figure 26. The preference for the *E* isomers is even more pronounced at the MP2 level than at the B3LYP level. At MP2, there is a difference of 13 kJ/mol between the most stable *E* and *Z* isomer of the (S,S) stereomers. This is 10 kJ/mol for the (R,S) stereomers.

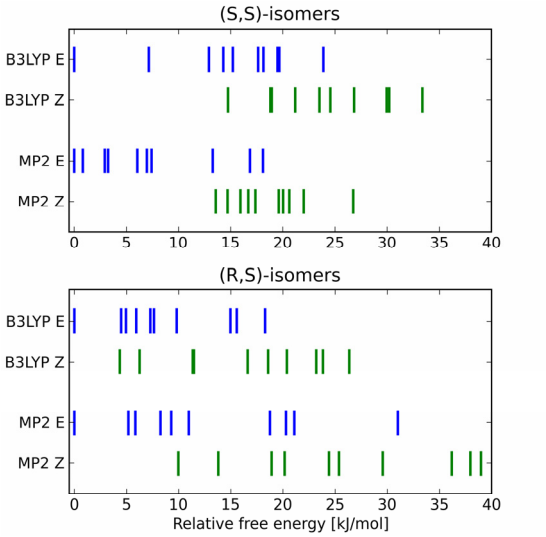

Figure 26. Comparison of B3LYP and MP2 free energies for the ten most stable samples of each conformer.

A Boltzmann distribution at 353.2 K is computed with these MP2 free energies for the (S,S) and the (R,S) isomers to make a coarse estimate of the relative prevalence of the *E* and the *Z* isomers in the experimental setup. The (R,S) and (S,S) stereomers are not compared to each other as these are interconvertible under basic conditions, as applied during the pyroglutamate-hydantoin ring transformation, but not during the RCM. The results are visualised in Figure 27 and show a clear preference for the *E* isomer, which is in accordance with the experimental results.

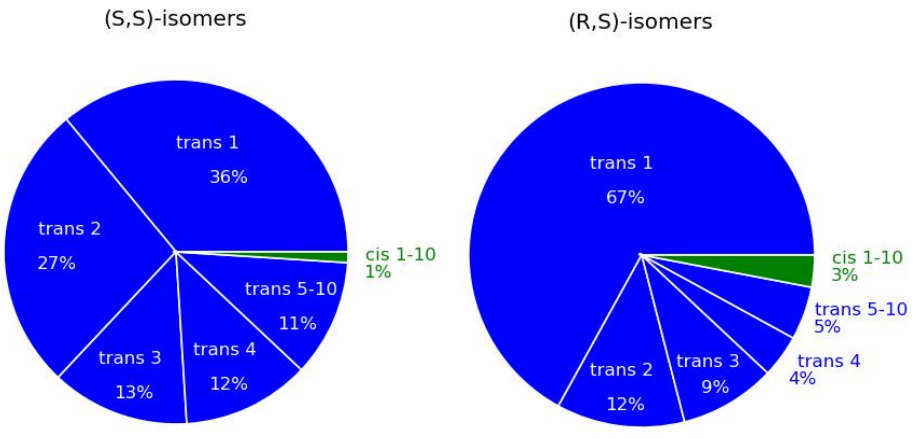

Figure 27. Boltzmann distribution of the MP2 free energies at 353.2 K of the 10 most stable conformations of both double bond isomers. *E*1 is the most stable *E* conformation among the samples, *E*2 the second most stable, and so on. The contributions of the *Z* conformations are small and combined into one segment.

Figure 28 clearly shows the correlation between the B3LYP and the PM3 energy based on the 400 optimized macrocycle geometries. It is therefore acceptable to analyze the molecular dynamics simulations used for the sampling procedure as such to gain more insights in the structural properties of the bishydantoins. In first instance we will analyze the free energy profiles of the backbone dihedral angles. In the remainder of the discussion the relative orientation and position of the hydantoin pair is examined.

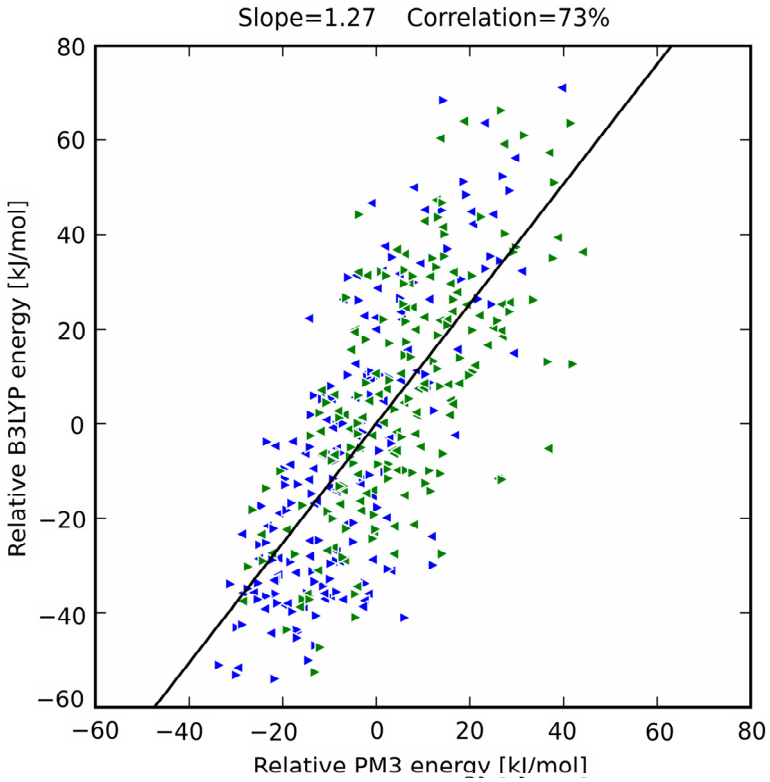

Figure 28. Correlation between PM3 and B3LYP energies. Blue and green triangles correspond to E and Z isomers respectively. Left and right triangles correspond to (S,S) and (R,S) isomers respectively. All energies are relative to the mean PM3 or B3LYP energy.

From the dihedral angle free energy profiles, flexible dihedral angles can be recognized by low free energy barriers, which correspond to a nearly uniform sampling of the dihedral angle.

The major difference between the *E* and *Z* isomers was found for dihedral angles 1 (next to the carbon-carbon double bond). For the *E* isomers, the energy barrier is lower than 10 kJ/mol. The higher barrier, about 20 kJ/mol, for the *Z* isomer is mainly caused by steric hindrance with moieties at opposite positions relative to the carbon-carbon double bond.

For the subsequent dihedral angles the differences between the double bond isomers become negligible.

A second type of differences can be observed between (R,S) and (S,S) isomers. Dihedral angle 6, 7 and 9 (Figure 29) have identical profiles in the (S,S) case, but in the (R,S) case the free energy profiles near the R stereocentre have an opposite dependence on the dihedral angle compared to the S centre. The origin of these differences is obviously related to the chirality of the hydantoin, but the mechanism for each case (6, 7 and 9) is slightly different. Case 7 is simply caused by the stiff valence interactions of the ring and of the bonds towards the stereocentre. In case of dihedral angle 6, the non-bonding interaction partners are chiral, which directly leads to an asymmetric dihedral angle profile. Dihedral angle 9 has no simple explanations based on local interactions. A molecular dynamics simulation on half a macrocycle (a single chain starting from the carbon-carbon double bond and ending at the opposite end of the cycle, see Figure 23), reveals no chirality at dihedral angle 9. Therefore the trends in this angle can only be explained by constraints due to the closed cycle or by hydantoin-hydantoin interactions.

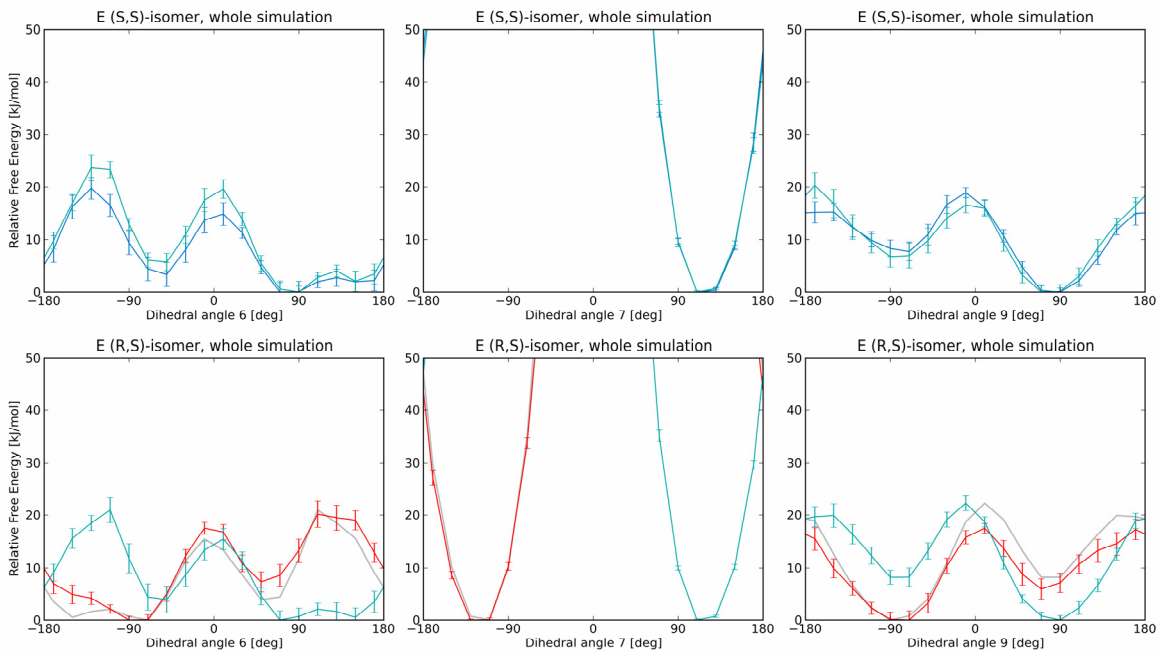

Figure 29. Free energy profiles of dihedral angles 6, 7 and 9 in conformers *E*-(S,S) and *E*-(R,S). The cyan or blue curves correspond to S stereocentres. The red curves correspond to R stereocentres. To facilitate the comparison with the red curve, the grey curve in the plots of the *E*-(R,S) isomer is the mirror image of the cyan curve.

Additional understanding of the macrocycle structure can be gained by analyzing the relative position and orientation of the two hydantoins. The average distance between the centres of the two five-membered rings is 7.82 ± 0.03 Å in the *E* case and 7.69 ± 0.03 Å in the *Z* case. Given the approximate radius of a hydantoin group, 2.5 Å, direct interactions between the hydantoin groups are unlikely to have a major effect on the structure. The time-average of the angle between the normal vectors attached to the five-membered rings ranges from 80° to 100° in the four cases. This average angle of approximately 90° corresponds to a negligible correlation of the two normal vectors. This is again an indication that the two hydantoins have no significant direct interactions.

During the whole simulation of the four isomers, the methyl substituents on the hydantoin rings point to the outer side of the macrocycle. The angle between the normal vector of a five-membered ring and the vector connecting the two ring centres is practically identical in all cases, on average 67.8° ± 0.7°. Note that the sense of the normal vector always points towards the CH_2 group connected to the stereocentre. Figure 30 gives a schematic representation of the average hydantoin orientation in both the (S,S) and (R,S) cases. It can be seen that the hydantoins are on average tilted with the CH_2 group on the stereocentres towards the double bond. This orientation imposes the least strain on the chain between the two hydantoins on the side of the carbon-carbon double bond. The alkyl chain that connects the two other ends of the hydantoins tries to relieve its own strain too. This is only possible when dihedral angle 9 synchronizes with the chirality of the stereocentres.

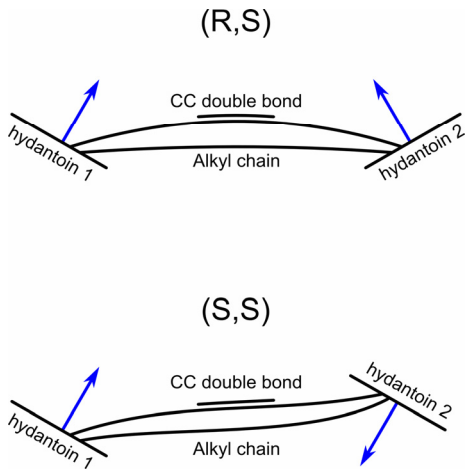

Figure 30. Schematic representation of the relative orientation of the hydantoin rings and the (S,S) and (R,S) case.

The experimentally observed thermodynamic stability of the double bond isomers of macrocycle **173a** was investigated computationally. Because of the large number of degrees of freedom of the macrocycle, a suitable methodology was outlined and implemented with MD-Tracks to easily generate molecular conformations that span the potential energy surface.

The method starts with a fast generation of molecular geometries covering the potential energy surface by a molecular dynamics simulation with a semi-empirical method at high temperature. Dihedral free energy distribution plots and principal component analysis are used to test the completeness of the molecular dynamics trajectory. Next a diverse set of molecules is selected by a Kennard-Stone algorithm with a distance measure based on the distance matrix. This selection of conformations is then optimized at a DFT or post-Hartree Fock level. By calculating probability distributions based on the post-Hartree Fock calculations that also cover long-range interactions, more insight was obtained in the number of conformers contributing to the experimentally observed findings. Indeed the *E* isomers are 10 kJ/mol more stable than the *Z* isomers and determine the overall distribution. This corresponds with the *E* isomer being the only experimentally observed double-bond stereoisomer.

Furthermore, the rotational free energy barriers were investigated for all dihedral angles. It was found that the bonds next to the double bond reflect the main difference between the double bond isomers and are probably the main cause of the energy difference between the *E* and *Z* isomers. The larger part of the ring backbone is rather flexible, except for the few bonds in the hydantoins, which is the reason for the large number of different conformations. Each stereocentre has three related dihedral angles that show asymmetric behaviour. Two can be explained with local interactions with the stereocentre, but the asymmetry of the third dihedral angle is only present when the macrocycle is closed. Further analysis shows this preference is caused by relieving strain in the chains that connect the two hydantoins.

1.5 Thiohydantoins

Thiohydantoins are the sulphur analogues of hydantoins in which one or both carbonyl groups are replaced by thiocarbonyl groups. The 2-thiohydantoins are best known, because of their broad range of applications as hypolipidemic, anticarcinogenic, antimutagenic, antithyroidal, antiviral, antimicrobial, anti-ulcer and anti-inflammatory agents, as well as

pesticides. They also have been used as reference standards for the development of C-terminal protein sequencing. Given this large field of applications, different methods have been developed to synthesize 2-thiohydantoins. The most commonly used methods involve the treatment of α-amino acids with acetic anhydride, followed by ammonium thiocyanate and the reaction beween α-amino acid derivatives and isothiocyanates.[156,157,158] Other possibilities are the reaction between thiourea and α-halo acids, α-amino acids[159] or benzil or the reaction of oxazolinone and thiocyanate, among others.

Despite sulphur and oxygen being members of the same group, they differ considerably as sulphur also possesses a d-orbital and the difference in electronegativity between sulphur and carbon is much smaller than between oxygen and carbon. Eventhough, analogous conditions were tested for the thiocarbamoylation as for the one-step carbamoylation and succeeding rearrangement of pyroglutamates. These experiments showed a difference according to the ester and the isothiocyanate used. The reactions resulted in mixtures of compounds: starting material, thiocarbamoylated product at nitrogen and at *C*(2), bis-thiocarbamoylated product and rearranged product (Scheme 63). From the reaction of benzyl pyroglutamate with phenylisothiocyanate, the thiohydantoin fraction could be isolated via crystallization in 42%. The reaction of ethyl pyroglutamate with phenylisothiocyanate furnished 31% of the *N*-thiocarbamoyl-pyroglutamate via recrystallization. This reaction was, later on, repeated by Stamford et al[115] using methylisothiocyanate and they isolated the thiohydantoins in 40 % yield. The biscarbamoylated pyroglutamate **177** was not fully identified, because of the presence of an aryl substituent which cannot be used to differentiate it from e.g. the carbamoylated thiohydantoin in the HMBC spectra. Its formation was assumed by comparison with literature data, in which formation of this biscarbamoylpyroglutamate was reported.[121]

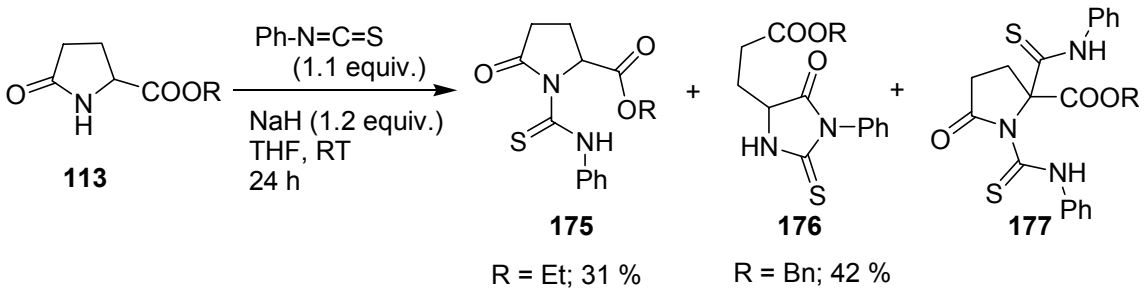

Scheme 63

To avoid the formation of side-products at the time the starting pyroglutamate is still being consumed, the two-step procedure was evaluated in which the thiocarbamoylpyroglutamate was isolated first. Reaction with NaH (Scheme 64) delivered the thiocarbamoylated pyroglutamate that could be isolated in pure form after recrystallization in acetone or column chromatography.

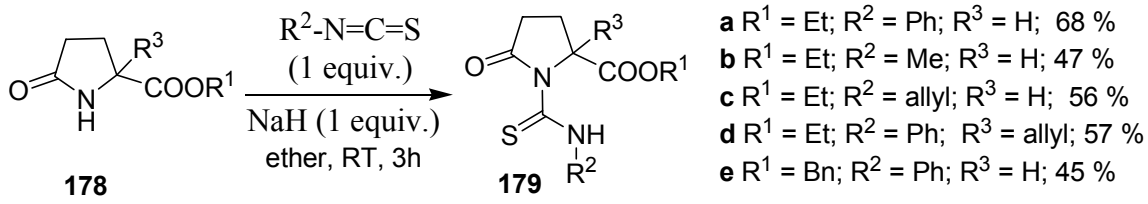

Scheme 64

The usual conditions for the rearrangement towards hydantoins with the potassium alkoxide furnished the thiohydantoin, but in a mixture with the thiourethane **181**, formed by removal of the thiocarbamoyl group, and other side-products. Product **182** was not fully determined, but with thioisocyanates, thiocarbamoylation at *C*(2) of the pyroglutamates has already been reported.[121] Other procedures for the formation of thiohydantoins were evaluated. Upon reflux in toluene with DBU a complex reaction mixture was formed. Microwave conditions – 150 to 300 Watt for 10 to 100 minutes - with K_2CO_3 in CH_2Cl_2 only lead to the recuperation of starting material.[157]

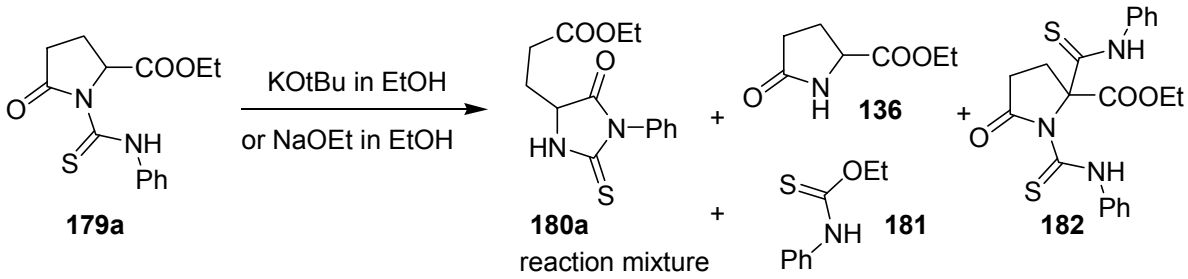

Scheme 65

Apparently, the thiocarbamoylation does not activate the lactam enough to cause stereoselective ring opening. So, literature procedures were screened. After acidic ester hydrolysis, the ring closure towards the hydantoin can be obtained by heating the isolated thiocarbamoylated derivatives to 200 °C.[156] As the thiohydantoins can be hydrolized under acidic conditions (20 % HCl, 150 °C), reaction with 2N HCl was first evaluated at room temperature, but only starting material was recovered. Reflux with 2N HCl for 24 hours

yielded the pure thiohydantoins **180** (Scheme 66). The starting product dissolved slowly upon hydrolysis.

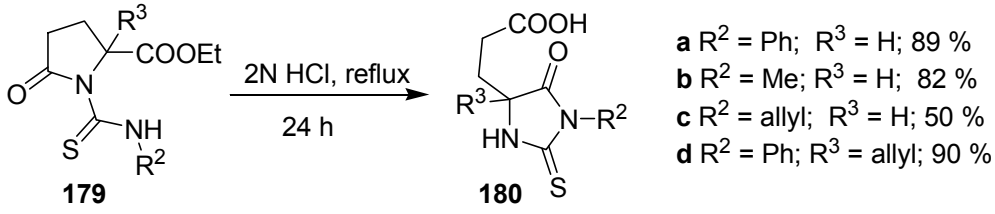

Scheme 66

Several derivatives were synthesized which shows that the same reaction conditions can be used with aryl- and alkylisothiocyanates and for pyroglutamates that are substituted at *C*(2). The bis-pyroglutamate **183** could not be rearranged, most probably due to solubility problems (Scheme 67).

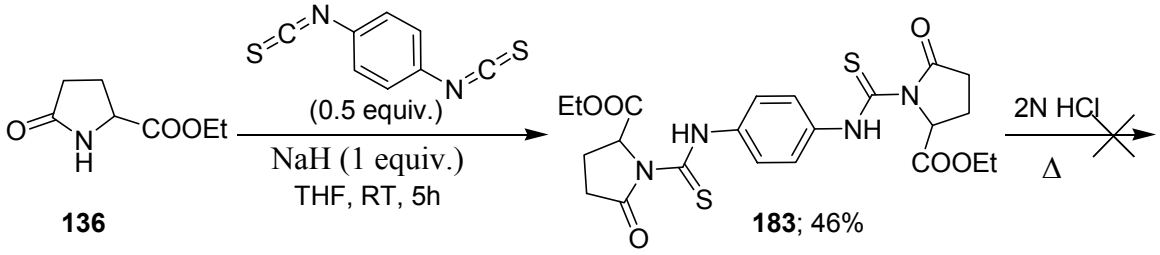

Scheme 67

The reaction conditions used to synthesize hydantoins from pyroglutamates and isocyanates yielded the thiohydantoins too, but in low yields, as side-products were formed.

The two-step procedure by treating a mixture of pyroglutamates and isothiocyanates with NaH, delivered the thiocarbamoylated lactams. The use of alkoxide ions for the subsequent rearrangement reaction gave no clean conversion. Therefore, classical acidic conditions were applied. Reflux with diluted $HCl_{(aq)}$ furnished, in most cases, the thiohydantoins.

1.6 Biotesting of Hydantoin Derivatives

Cancer is the result of genetic mutations that lead to alterations of certain cells. When a cancer develops, the cells start to divide in an uncontrolled way, penetrating and damaging the surrounding tissue.

As mentioned before, several *N*(3),*N'*(3)-polymethylene-bis-hydantoins have been evaluated as hexamethylenebis(acetamide) (HMBA) analogues. HMBA is a compound that induces cancer cells to differentiate to a less malignant phenotype.

There is interest from industry to test our bis(hydantoins) on a broad range of cancer cell lines and on the HIV-virus.

Another way to treat cancer is by limiting the invasion into healthy tissue surrounding the modified cells. Several hydantoin derivatives were screened for their anti-invasive activity in cooperation with the department of Gynaecological Oncology and the department of Experimental Cancerology at the Ghent University Hospital. The screening assay that was used, is based on the in vitro confrontation of invasive cancer cells with a fragment of normal tissue. Precultured heart fragments (PHFs) from chicken embryos are confronted with standard aggregates of invasive test cells like human MCF-7/6 mammary carcinoma cells. The aggregates get attached to the PHFs by overnight incubation. The cultures are treated with the compounds at concentrations ranging from 100 to 1 µm. After 8 days of incubation the cultures are analysed histologically. More details on the procedure can be found in references 160 and 161.

The observed invasion was scored from grade 0 to 4. In grade 0 only the PHF can be found and no confronting cells. In grade 1 the confronting cells are attached to the PHF and do not occupy the heart tissue. Grade 2 is given if the occupation of the PHF is limited to the outer fibroblast-like and myoblast cell layers. If the confronting cells have occupied the PHF, but left more than half of the original amount of heart tissue intact, it is grade 3; if it is less than half, it is grade 4.

The 15 compounds selected for the screening are given in Figure 31: *N*(3)-substituted (thio)hydantoins, *N*(1),*N*(3)-disubstituted hydantions, bis(hydantoins) and functionalized bis(hydantoins).

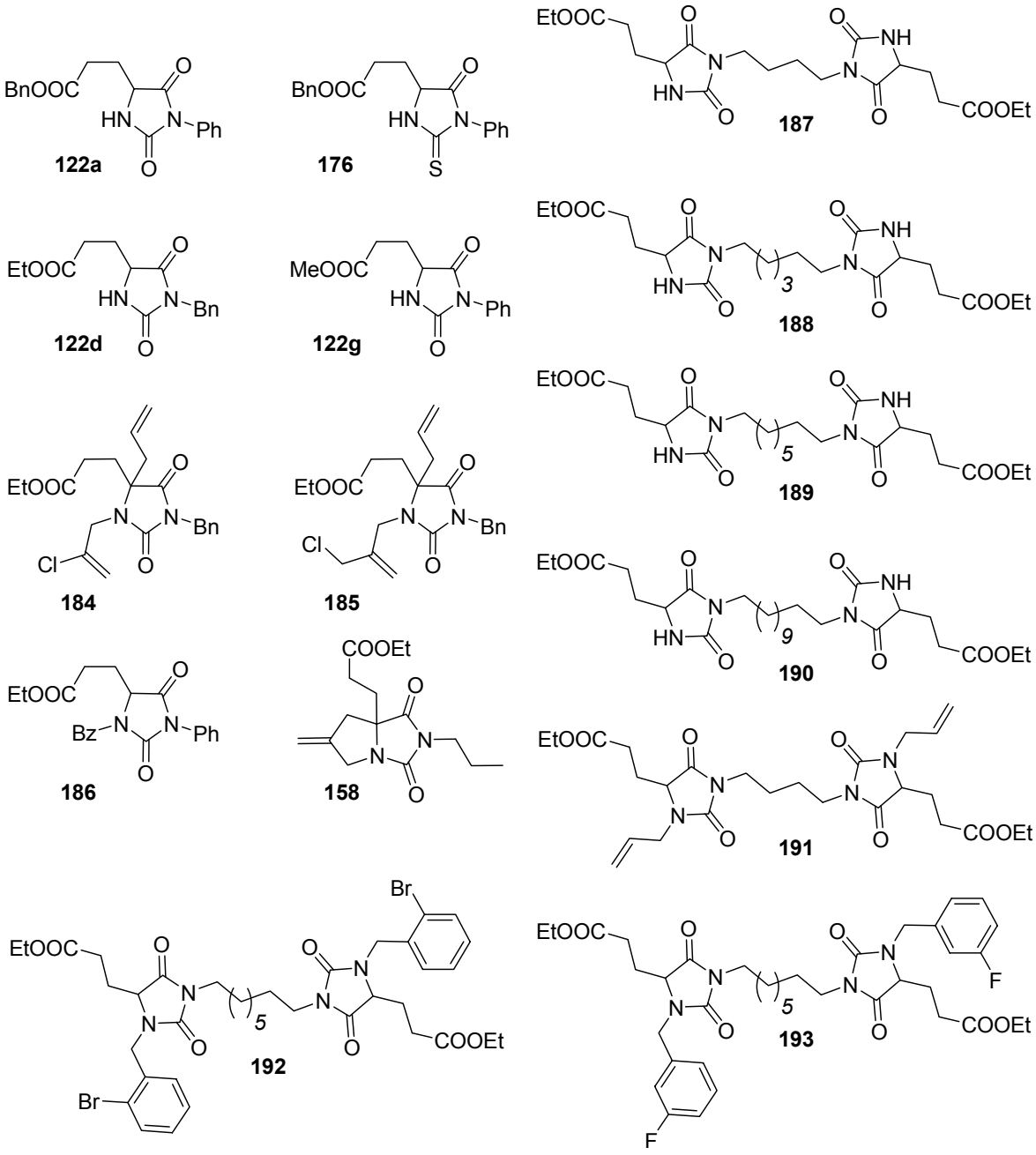

Figure 31

The first screening was done for 13 compounds at a concentration of 100 µm. This high concentration is well suited for selecting active compounds and detecting toxicity towards benign cells. The results in Table 3 show that a number of compounds completely block the invasion of the cancer cells into the heart tissue, whereas in the control experiments the heart fragments have grade 4. No obvious resemblance can be found between the active compounds.

Table 3. Anti-invasive activity of hydantoins from Figure 31 at 100, 10 and 1 µm

100 µm

Product	Invasion Grade	Remark
122a	4	
176	1	Toxic for PHF
122d	1	Toxic for PHF
122g	3	
184	1	
186	2	
187	4	
188	2	
189	1	
190	3	
191	3	
192	3	
193	1	
Control	4	
Control	4	

10 µm

Product	Invasion Grade Batch 1	Invasion Grade Batch 2
185	1	
158	2	
189	1	
190	1	0
193	1	2
186	1	
Control	2	2

1 µm

Product	Invasion Grade
189	3
190	2
193	3
Control	2

In a second screening at 10 µm the most active and untested compounds **185** and **158** were tested. In these tests the control experiments showed a decreased activity of the cancer cells. After a number of cell divisions mutations start to accumulate that alter the normal activity of the cancer cells. This made it hard to draw conclusions and to compare the results with the previous screening.

In the screening at 1 µm, the same decreased activity of the cancer cells was observed for the control experiment, but the strong invasion of grade 3 in the test experiments shows that the cancer cells are still reasonably active. However, the anti-invasive activity of the hydantoins is poor at this low concentration.

1.7 Evaluation of Ring Expansion Methods

To evaluate a possible ring expansion towards diazepines, 2-pyrrolidinone was carbamoylated with benzylisocyanate or propylisocyanate and left overnight at room temperature in DMF or CH_2Cl_2 or under reflux in THF, but mainly starting material was recovered.

In an attempt to activate the pyrrolidinone lactam for ring opening, a leaving group would be introduced at *C*(5). Via a literature procedure[162] succinimide was reduced to 5-ethoxypyrrolidin-2-one, but in very low yield. As only a small amount of pyrrolidinone **195** was obtained, the subsequent carbamoylation and rearrangement was attempted via the one-pot procedure in THF. Two equivalents of isocyanate were used to trap the possibly formed ethoxide ions. After stirring overnight only the carbamoylpyrrolidinone **198** was formed (Scheme 68) in a mixture with the 1,3-diphenylurea formed by the excess of isocyanate. A large part of the urea can be removed by filtration, as the urea crystallizes as tiny needles in acetone.

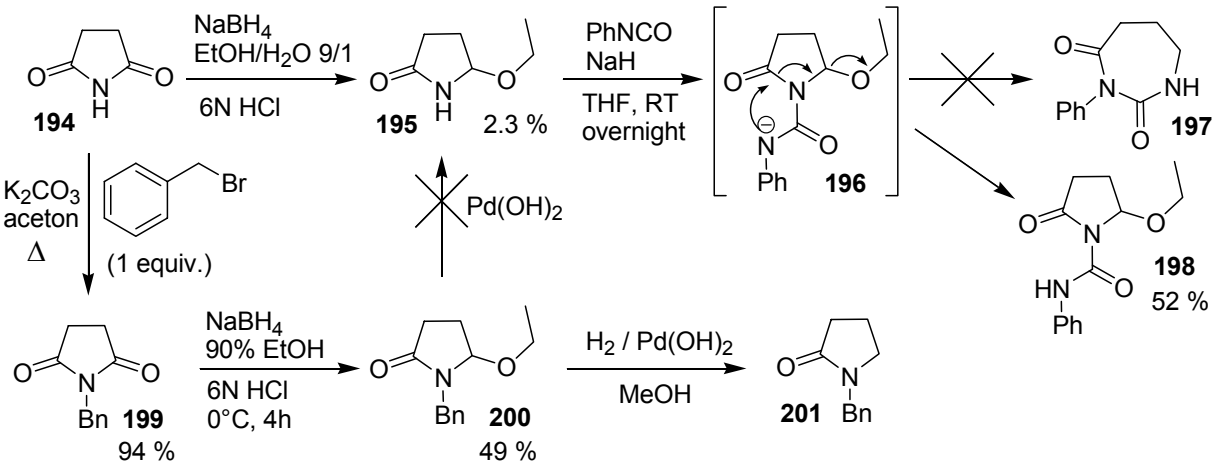

Scheme 68

To reduce the product loss upon reduction, the succinimide was benzylated first by reflux with benzylbromide and K_2CO_3 in acetone. Reduction at 0°C resulted in 1-benzyl-5-ethoxypyrrolidin-2-one **200** in 49 %, which was remarkably better than the reduction of the unprotected succinimide. However, hydrogenation of **200** over $Pd(OH)_2$ on charcoal, furnished pyrrolidinone **201**, from which the ethoxy group had been eliminated. It is known that good leaving groups like carbonitriles are easily eliminated, and apparently the same is valid for the ethoxide. Because of these low yields and the instability of the 5-ethoxy group

no further attempts were evaluated to synthesize the activated 1-carbamoyl-5-ethoxypyrrolidin-2-one.

2 α-Amino Phosphonates

2.1 Intro

In the *SynBioC* research group, a high-yielding procedure has been developed for the synthesis of α-alkylamino phosphonates[12] that will be used as the first step in the different pathways. In an attempt to synthesize diazepinones via RCM, the carbamoylation of these α-amino phosphonates is studied.

The IMDAF reaction of furfurylamine derivatives was investigated and has been reviewed in § 2.3.1. This reaction was further studied and includes the investigation of the stereoselectivity of the reaction in silico together with kinetic experiments and the synthesis of other derivatives. Finally, the ring opening reactions of the IMDAF adducts, as the next step towards biological active products, is explored both experimentally and computationally.

2.2 Carbamoylation Using Isocyanates

2.2.1 Evaluation of Diazepine Synthesis via RCM

As the synthesis of diazepines via ring expansion was not straightforward, another method using RCM would be evaluated. Its retro-synthesis is given in Scheme 69. It starts from α-alkylamino phosphonates **10** that are easily synthesized from α,β-unsaturated aldimines in high yields. This would be followed by reactions with isocyanates, then acylation or alkylation and RCM.

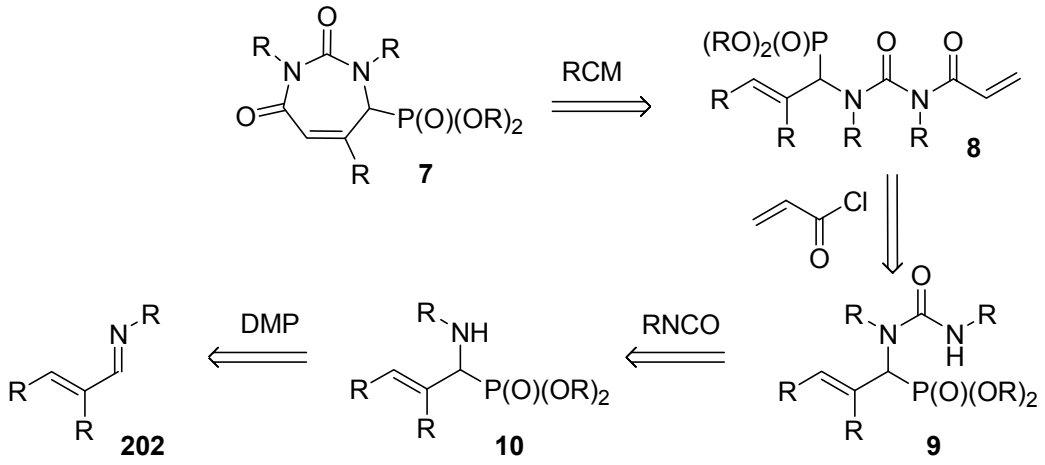

Scheme 69. Retrosynthetic route towards diazepines

The imination and subsequent Pudovik reaction with dimethyl phosphite in alcoholic solvent are given in Scheme 70. Methanol is used as the solvent for the phosphonylation, corresponding with dimethyl phosphite, since some transesterification occurs at higher temperatures. During the work-up via an acid base extraction, diethyl ether should be used as organic solvent during the acid extraction, as the HCl salts of the α-amino phosphonates containing two aromatic rings are very soluble in CH_2Cl_2.

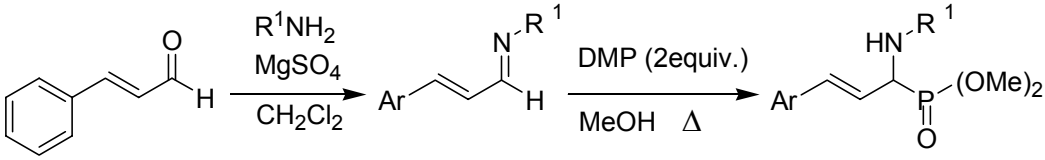

Scheme 70

These amines **205** are less nucleophilic due to the phosphonate group in α-position. Reaction of the amino phosphonates with phenyl isocyanate proceeded to completion when both compounds were stirred at RT in THF or chloroform. Only the *t*-butylamine is too sterically hindered to react.

In case of allyl or isopropyl isocyanate, only a part of the amine did react. It is well- known that aryl isocyanates are more reactive than their alkyl counterparts. For the reactions with alkyl isocyanates elevated temperatures or basic conditions are required. However, reflux conditions did not complete the reaction either (Table 4).

Several bases were tested (Table 4): strong bases like sodium hydride could not be used as they cause elimination of the phosphonate functionality with formation of the imine; other bases caused rearrangement of the double bond towards the more stable enamine under reflux conditions or even at room temperature after prolonged stirring.

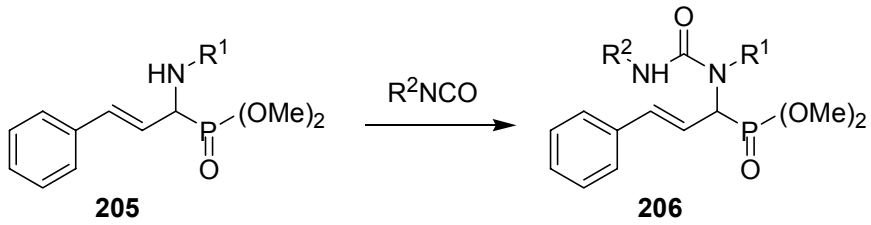

205 **206**

Scheme 71

Table 4. Different reaction conditions for the carbamoylation of amino phosphonate 205

	R^1	R^2	Conditions[A]	Remark / Yield[B]
A	Bn	Ph	RT, 5h, THF or $CHCl_3$	73 %
B	*n*-Pr	Ph	RT, on, THF or $CHCl_3$	72 %
C	*t*-Bu	Ph	Δ, on, THF	No reaction
	Bn	*n*-Pr	RT, 2d, THF	Equilibrium
	Bn	*n*-Pr	Δ, 5h, THF	Equilibrium
	Bn	*n*-Pr	Δ, 2.5h, toluene	Side reactions & decomposition
	Bn	*n*-Pr	Et_3N (1), Δ, 4h, THF	Side reaction & rearrangement
	Bn	*n*-Pr	Et_3N (1), RT, 2d, THF	Side reaction & rearrangement
	Bn	*n*-Pr	K_2CO_3 (3), Δ, 16h, acetone	Rearrangement
	Bn	*n*-Pr	Hünig's base (1), Δ, on, THF	Equilibrium
	Bn	Allyl	RT, on, THF	Equilibrium
D	Bn	*n*-Pr	Cu(I)Cl (0.1), PPh_3 (0.1), Δ, on, CH_2Cl_2	54 %
	Bn	*n*-Pr	Cu(I)Cl (0.1), Δ, on, CH_2Cl_2	66 %
E	Bn	Allyl	Cu(I)Cl (0.1), Δ, on, CH_2Cl_2	21 %
F	*n*-Pr	Allyl	Cu(I)Cl (0.1), Δ, on, CH_2Cl_2	73 %

[A] Equivalents are given in parentheses, on = overnight

[B] Purified by column chromatography

As the basic conditions cause too many side reactions, activation of the isocyanate was evaluated. Using 3 equivalents of isocyanate, 0.1 equivalent of copper(I)chloride and 0.1

equivalent of PPh_3 yielded the desired ureas after overnight reflux in dichloromethane. In the original reference, in which Cu(I)Cl activation of alkyl isocyanates was used for the formation of alkyl carbamates from primary, secondary and tertiary alcohols,[163] no PPh_3 was used. Also in our hands the amino phosphonates **205** did react without PPh_3. Addition of 1 equivalent of Cu(I)Cl shortened the reaction time. But still, an excess of isocyanate was required to force the reaction to completion. Unfortunately, this resulted in dimerisation of the isocyanate to the dialkylureas, which necessitated further purification. The yields of this procedure that gave quantitative carbamoylation of the amines with aliphatic isocyanates are shown at the end of Table 4. The low yields of the first three entries are due to the work-up procedure. Initially this was done by washing the reaction mixture repeatedly with brine or water to remove the copper catalyst. Direct purification by column chromatography, without previous washing, gave higher yields.

The next step was the acylation of these ureas **206** with an α,β-unsaturated acyl chloride or anhydride. For a first series of conditions, acryloyl chloride was used. When the acid chloride and the amino phosphonate were stirred in CH_2Cl_2 or THF for 5 hours to 1 day at different temperatures, no reaction was observed. Overnight reflux in toluene caused decomposition and double bond rearrangement towards the vinylic phosphonate.

As the carbamoylation, and subsequent acylation were investigated simultaneously, basic conditions, that are mostly used for the acylation of ureas, were evaluated here as well. Similar side reactions were observed. With butyllithium, a complex mixture was formed. Sodium hydride, applied under reflux conditions causes double bond isomerisation,[13] but at RT mainly starting material was recovered. Also reflux with K_2CO_3 caused clean double bond migration. With Et_3N, $(i\text{-Pr})_2EtN$, pyridine or DMAP no reaction occurred at RT. Heating or prolonged stirring caused rearrangement towards vinyl phosphonates. A modified Mitsunobu reaction, used for the alkylation of maleimides with alcohols[164] resulted in a complex reaction mixture, apparently due to incompatibility with the phosphonate group. Acylation of the ureido phosphonate **206b** with α –methylacryloyl anhydride in the presence of Et_3N and LiCl[165] failed as well and only starting product was recovered.

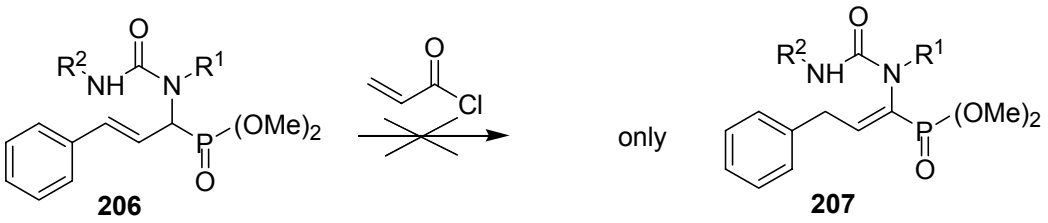

Scheme 72

Table 5. Different reaction conditions for the evaluation of the acylation of phosphorylated ureas 206

Entry	R^1	R^2	Conditions[A]	Remark
1	Bn	Ph	0 °C, RT, 5h, CH_2Cl_2	No reaction
2	Bn	Ph	0 °C, RT, 26h, THF	No reaction
3	*n*-Pr	Ph	Δ, on, THF	No reaction
4	*n*-Pr	Ph	Δ, on, toluene	Decomposition Rearrangement
5	Bn	Ph	BuLi (1), -78°C, 45min, THF	Side reactions Rearrangement
6	*n*-Pr	Ph	NaH (1.3), 0°C to RT, on, THF	No reaction
7	Bn	Ph	K_2CO_3 (3), Δ, 4.5h, acetone	Rearrangement
8	*n*-Pr	Ph	Et_3N (1.3), RT, on, THF or CH_2Cl_2	No reaction
9	*n*-Pr	Ph	Et_3N (3), RT, 16h, THF or dioxane	No reaction
10	*n*-Pr	Ph	Et_3N (1.2), on, Δ CH_2Cl_2 or molten DMSO	Starting product Rearrangement
11	*n*-Pr	Ph	Hünig's base (1), RT, 3d, THF	Starting product Rearrangement
12	Bn	Ph	Pyridine (solvent), RT, 3h	No reaction
13	Bn	Ph	Pyridine (solvent), Δ, 1.3h	Side reactions Rearrangement
14	*n*-Pr	Ph	DMAP (1.2), RT, 2d, THF or CH_3CN	Rearrangement
15	Bn	Ph	Mitsunobu[164]	Complex mixture
16	Bn	Ph	Acryloyl chloride (10), Δ, 27h, CH_3CN	Diazaphospholidinone
17	Bn	Ph	Acryloyl chloride (10), Δ, 7h, THF	Mainly starting product
18	Bn	*n*-Pr	Acryloyl chloride (10), Δ, 9h, CH_3CN	Diazaphospholidinone

[A] Equivalents are given in parentheses, on = overnight

The formation of the vinylphosphonate **207** can easily be followed by ^{31}P NMR as there is a shielding shift from 25 to 16 ppm. In the ^{1}H NMR spectrum the benzylic protons appear at

about 3.5 ppm and the CHP proton at 4.9 ppm disappears. The dimethyl 3-phenyl-1-(3-phenyl-1-propylureido)propenyl phosphonates from entry 14 in Table 5 have been fully characterized. From the $^3J_{CP}$ coupling of 13.9 Hz it can be concluded that the double bond has an *E* geometry. This was deducted by comparison with the coupling constants of acylamino phosphonate **208** (Figure 32).[13] The $^3J_{CP}$ values for dimethyl (*E*)-1-propenyl phosphonate **209** and di(*tert*-butyl) (*Z*)-1-propenyl phosphonate **210** also indicate that the heteronuclear coupling is about three times as large for the *E* isomer as for the *Z* isomer (Figure 32).[166]

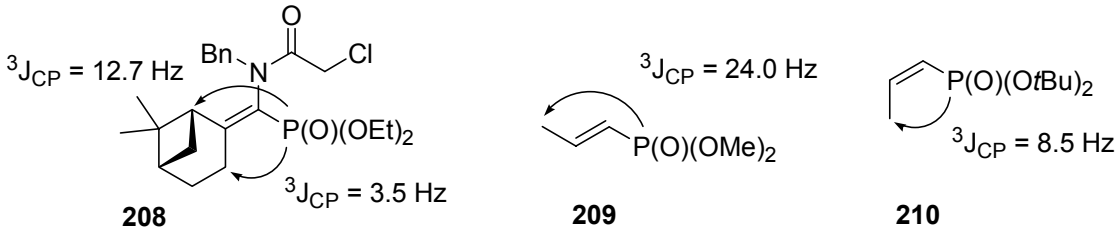

Figure 32

Finally a procedure was evaluated in which the phosphorylated ureas were refluxed with a large excess of the acid chloride.[167] In THF, mainly starting material was recovered. The same reaction in acetonitrile, that has a slightly higher boiling point and higher polarity, furnished the diazaphospholidinone **211a**. As the tetrahedral phosphorus atom in **211** is surrounded by four different substituents, these compounds include two chiral centres. Indeed a diastereomeric mixture was observed in ^{31}P NMR, the two peaks were at 28.1 and 29.3 ppm in a ratio of 1/0.8. The same reaction with **211b** was followed by ^{31}P NMR. Some side-products were formed during reflux, but they were removed by washing with saturated $NaHCO_3$ solution. In the ^{31}P NMR spectra two peaks remained at 24.0 and 25.6 ppm with a ratio of 0.6/1. This five-membered ring formation was observed with furfuryl ureido phosphonates too, as discussed in § 2.4.4 of the Results and Discussion.

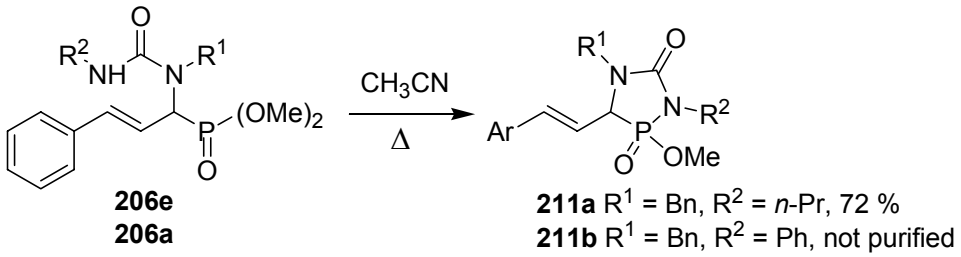

Scheme 73

Several methods exist for the synthesis of 1,4,2-diazaphospholidin-5-ones **211**. Mostly the *P-N* bond is formed first, followed by ring closure. The ring closure of α-ureido phosphonates has been reported. A first procedure involves reaction of diphenyl α-alkylamino phosphonates with alkyl isocyanates in the presence of DABCO. Under these rigid conditions immediate formation of the five-membered ring occurs.[168] Pudovik et al. used no base, but the cyclization was done with diphenyl α-alkylaminoalkyl phosphonates.[169] Immediate ring closure occurred with the easily leaving phenoxy groups. Our method allows isolation of the intermediate ureido phosphonates, no base is needed if the proper solvent, acetonitrile, is used and the resulting phospholidine is less acid sensitive.

The reaction products can be identified using IR spectroscopy: the α-ureido phosphonates show an absorbance peak at 1640 cm^{-1} for C=O and at 1530 for the NH deformation; the diazaphospholidinones have the carbonyl double bond stretching at 1700-1720 cm^{-1}. The carbonyl carbon signal in the ^{13}C NMR spectrum appears typically at about 155 ppm, which is the same as for the ring-open urea. For the ring-open ureido phosphonate, the coupling between the carbonyl carbon atom and phosphorous is very small or absent. In the diazaphospholidinone a $^{2}J_{PNC}$ coupling of 27.7 Hz (for compound **211a**) appears. The $^{1}J_{PC}$ constant shifts from 156.9 to 118.8 Hz for the major isomer of **211a** and to 121.2 Hz for the minor isomer, which is typical for the diazaphospholidinones.

This intramolecular substitution reaction indicates that the ureido phosphonate is probably too sterically hindered and activation of the ureas will lead to a faster intramolecular reaction. With this in mind, we did not further investigate the acylation of the ureido phosphonates. Moreover, after carbamoylation with allylisocyanate, RCM could be evaluated directly. With secondary amides some successful metathesis reactions have been reported.[170,171] Amines and pyridines are known to desactivate the Grubbs' catalyst. To circumvent this problem, free amines or pyridines can be protonated prior to addition.[170,171,172] The Grubbs' catalyst might be sequestered in the form of unproductive 5- or 6-membered chelate structures, as depicted in Figure 33. These complexes inhibit catalytic conversion, but can be avoided by coordination of the carbonyl with $Ti(O\textit{i}Pr)_4$.[173,174] This has been applied in the synthesis of tetrahydropyranyl-protected 1,3-diazepine-2,4-diones, in which the use of this binary catalyst system with first generation Grubbs' catalyst was required to perform the reaction.[165]

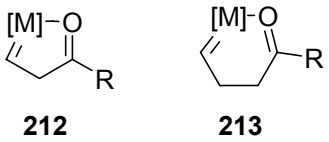

212 **213**

Figure 33

Using the 2nd generation Grubbs' catalyst under reflux conditions, catalytic amounts of Ti-catalyst were found to be sufficient.[173] Unfortunately, the application of this method to ureido phosphonate **206f** led to complex reaction mixtures and not to the desired diazepinone **214** (Scheme 74).

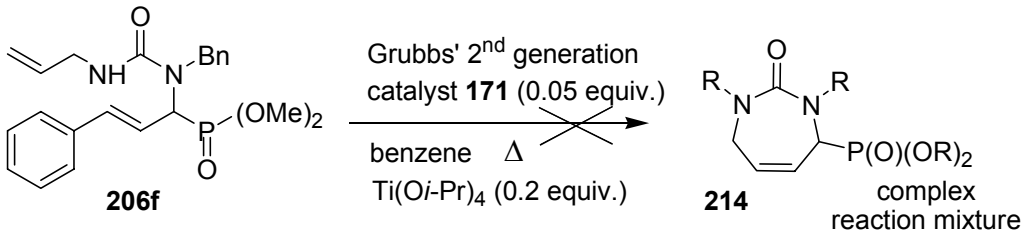

Scheme 74

Possible explanations for the failure of the RCM are the high planarity of the seven-membered ring with the conjugated carbamide. Analogue 1,3-diazepine-2,4-diones have been synthesized using RCM at room temperature. The higher temperature which was used, could cause further transformation to the pyrrolidinone, as has been described for the benzodiazepine analogues (Scheme 75).[175]

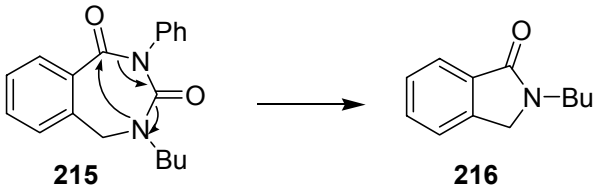

Scheme 75

The presence of a non-terminal alkene or a phosphonate substituent should not impose any problems to the RCM, as shown by the synthesis of phosphonopyrrolines and –pyrroles from α-allylamino β,γ-unsaturated alkyl phosphonates.[176] Styrene builds up and is dimerized to stilbene, which releases ethylene as well and drives the reaction.

As presented in Figure 33, Grubbs' catalyst can be sequestered in an unreactive complex. A short computational investigation was done towards the possible complexation of the catalyst by the ureido phosphonate.

Computational Details

Gas-phase density functional calculations were performed at the GGA level with Gaussian03.[150] Following Cavallo et al.,[177] the fast BP86 functional was used. For BP86 calculations, gradient corrections were taken from the work of Becke and Perdew.[178] The electronic configuration of the molecular systems was described by the split-valence basis set with polarization functions of Ahlirchs and co-worker (standard SVP basis set in gaussian03), for H, C, N, O, P and Cl.[179] For Ru the small-core, quasi-relativistic Stuttgart/Dresden effective core potential (standard SDD basis set in gaussian03) basis set was used, with an associated (8s7p6d)/[6s5p3d] valence basis set contracted according to a (311111/22111/411) scheme.[180] The ruthenium catalyst has a multiplicity of 1. Ruthenium can have an oxidation state zero, usually in metal-carbonyl complexes, or II, the most stable for ruthenium, both with paired electrons. Oxidation state III is not very common.[181]

For steric reasons, initiation of metathesis occurs on the terminal double bond. So, that ruthenium carbene complex was started with and different complexes with the ureido group were evaluated. All of them optimized towards the four-membered ring structure, with coordination of Ru towards the *N*-atom of the secondary amide, as presented in Figure 34.

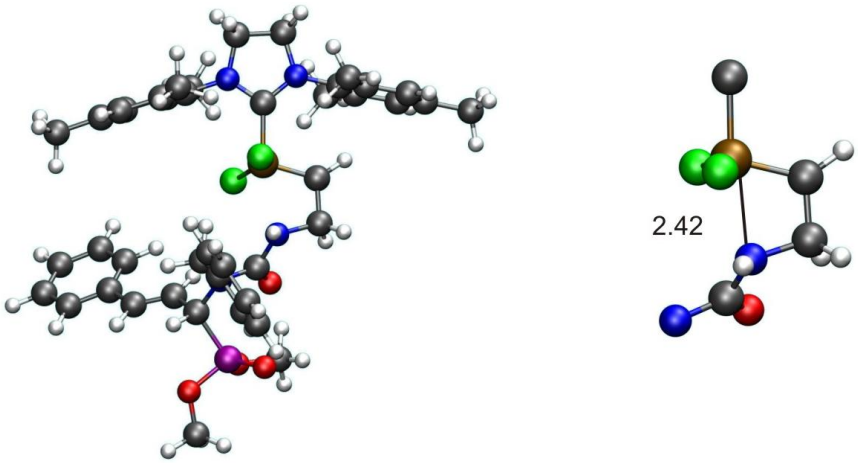

Figure 34. Optimized complex of amino phosphonate 206f with Grubbs' 2nd generation catalyst 171. The Ru-N distance is indicated in Å.

The Ru-N distance was 2.42 Å, which is large in comparison with Ru-N bonds in other complexes. The distance with the pyridine ligand, for instance, calculated at B3LYP, was 2.22 Å in the bottom bound complex **217** and 2.17 Å in the side bound complex **218**, shown in Figure 35.[182] This model also shows that there is no sterical interaction that would avoid carbene formation of the Grubbs' catalyst and the ureido phosphonate.

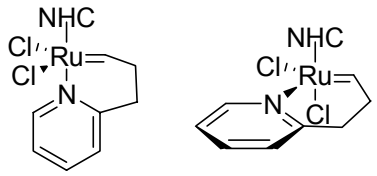

217 **218**

Figure 35

So, there will be a preferential coordination of the ruthenium carbene towards the proximate *N*-atom and not towards the carbonyl. This complexation is weaker than the one observed in other catalyst-deactivating complexes. Ti(O*i*Pr)$_4$-complexation is most effective to avoid coordination of the carbonyl and will probably have a smaller effect on the reduction of the basicity of the *N*-atom. This reaction should be evaluated again without Ti-catalyst at lower temperature.

The amino phosphonates **205** were successfully carbamoylated with both aryl and alkyl isocyanates using Cu(I)Cl as a catalyst. Acylation of the obtained ureido phosphonates **206** failed. 1,4,2-Diazaphospholidin-5-ones **211** were formed instead. Direct ring closure of the allyl derivative **206f** via metathesis was tried without success. A computational study of the obtained complex of **206f** and Grubbs' 2nd generation catalyst shows that the complexation is weaker than the one observed in known catalyst-deactivating complexes. Therefore, the latter reaction needs further investigation.

2.3 Furanyl Amino Phosphonates and the Diels-Alder Reaction

By replacing the cinnamyl group with a furfuryl group, ideal substrates for an intramolecular Diels-Alder reaction are obtained. In a first part the previous synthesis of these adducts is reviewed and the stereoselectivity and duality of the reaction is explained. Then a short evaluation of the solvent effect on the stereoselectivity is given. Next the Diels-Alder reaction is investigated computationally: the reaction energetics are studied and

linked with molecular properties. This is done for two substrates and allows the evaluation of the effect of the carbonyl substituent's position on the tether. In a fourth part the possibilities of this Diels-Alder reaction are explored experimentally by the use of other acylating reagents, activating the diene, using other dienes and expanding the tether.

2.3.1 Review of the Synthesis

The synthesis of tricyclic 2-phosphonopyrrolidines via an intramolecular Diels-Alder reaction of carefully designed furanyl-α-amino phosphonates (Paper VII in Appendix 2) is shortly reviewed here (Scheme 76).

The aminoalkyl phosphonates were synthesized via phosphonylation of the corresponding imines by refluxing with dimethyl phosphite in methanol. Subsequent acylations yielded the corresponding amides **11** in high purity.

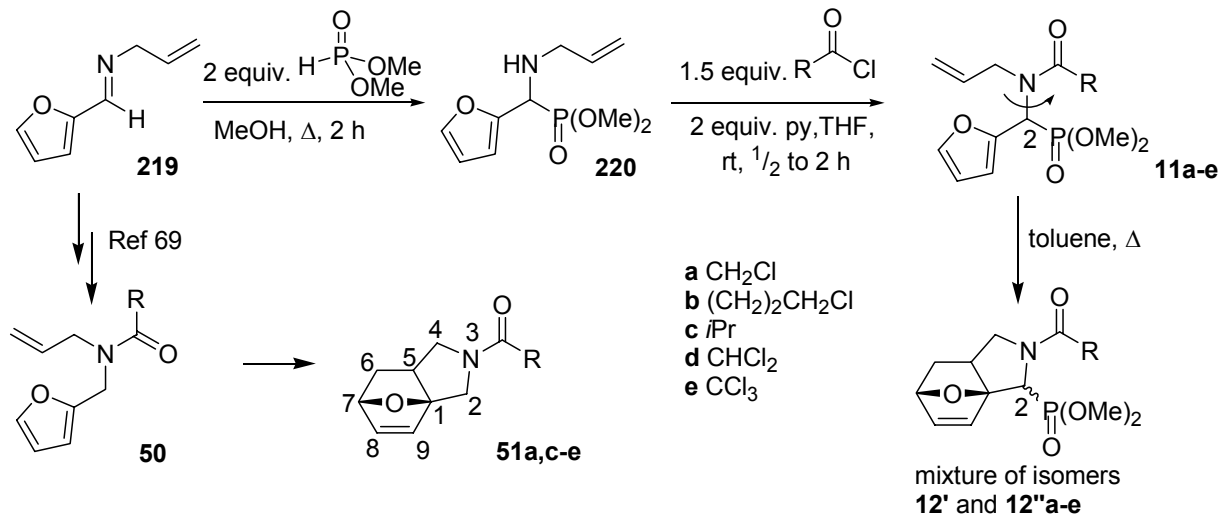

Scheme 76

As explained in the literature overview, the acyl group induces both a sterical and an electronical advantage to obtain a reactive substrate for the IMDAF reaction. When 1-(allylamino)-1-(furan-2-yl)methyl phosphonate **220** was refluxed overnight in toluene, only minimal amounts – 16 % – of Diels-Alder adducts could be detected by the typical peaks of C(6)H_aH_b at 1.4 and 1.7 ppm. Prolonged refluxing only resulted in a breakdown of the starting material. However, when the corresponding amides (**11a-e**) were refluxed in toluene, complete conversion to the ring-closed products was observed. The order of reactivity was in accordance with the results reported earlier for similar substrates **50** without the phosphonate group.[69] A remarkable influence of the phosphonate group could

be observed. While amides **51a** and **51c** could only be obtained in low yield[69] because of the poor conversion (Table 6), the corresponding phosphono amides **12** gave complete conversion. Experiments with toluene and acetonitrile showed that the first one was the solvent of choice in most cases: a faster formation of product and smaller amounts of side-products were observed, probably due to the higher boiling point of toluene.

Table 6. Acylation and IMDAF reaction of 1-(allylamino)-1-(furan-2-yl)methyl phosphonate 220

N°	R	Yield **11** (%)	Conversion/ Yield[A] **12** (%)	Isomer Ratio **12"/12'**	Time (h)	Temp (°C)	Conversion/ Yield[B] **50** to **51** (%)
a	CH_2Cl	99	100 / 75	27 / 73	20	110	43 / 40
b	$(CH_2)_2CH_2Cl$	88	100 / 47	20 / 80	4.5	110	-
c	*i*Pr	88	100 / 53	17 / 83	7	110	62 / 60
d	$CHCl_2$	96	100 / 94	35 / 65	3	110	100 / 97
e	CCl_3	99[C]	100 / 99	21 / 79	1[C]	82	100 / 99
b	$(CH_2)_2CH_2Cl$	88	100 / 47	20 / 80	4.5	110	-

[A] The reported yields are those of isolated products after column chromatography or crystallization.

[B] 30-40 h reflux in acetonitrile (results from Ref 69).

[C] The cycloadduct formed at room temperature, during acylation and subsequent work-up. The obtained mixture of **11e** and **12e** was further refluxed for 1 h to obtain complete conversion to **12e**.

In all cases, a mixture of isomers (**12'** and **12''**) was formed (Scheme 76). While absolute stereocontrol of substituents on the diene or dienophile is often observed, this is not the case for tether substituents, regularly giving mixtures of both isomers.[51,52] A detailed spectroscopic elucidation of the products and their stereochemistry was performed using NMR, including 2D and DIFNOE spectra, and X-ray analysis. Both isomers have an *exo*-fused skeleton, but the phosphonate substituent on the tether has an *exo* position in the major epimer and an *endo* position in the minor epimer of **12e** (Figure 36).

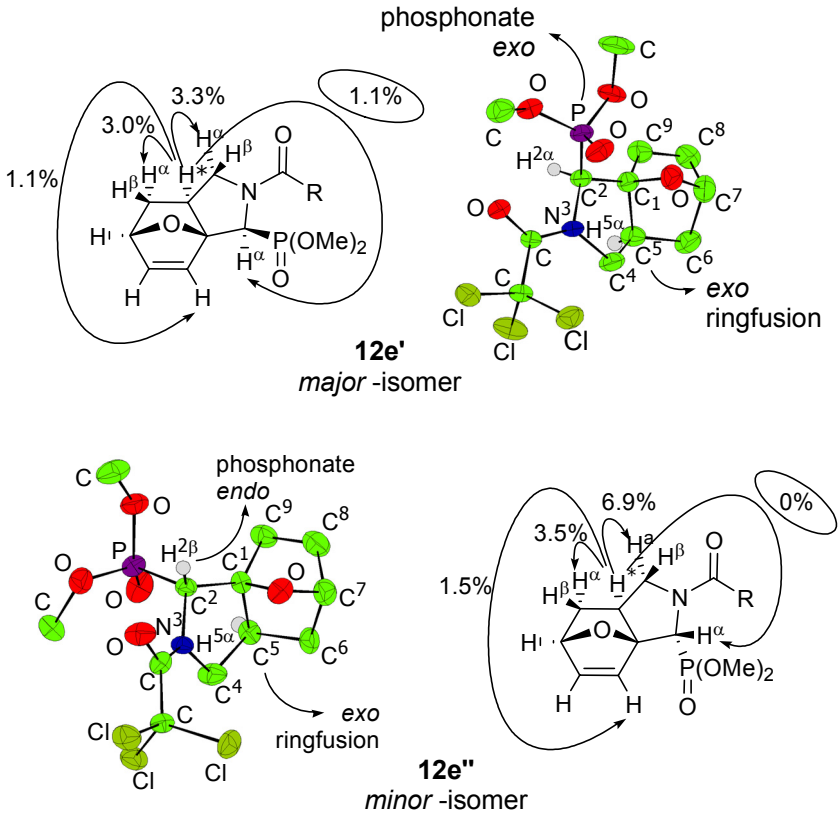

Figure 36. Stereochemical analysis of isomers 12e' and 12e''. The percentage of nuclear Overhauser effect with irradiation of C(5)*H* is indicated. The X-ray structures of both isomers are depicted as well.

Furthermore, the observed stereoisomer ratio may be the result of thermodynamic control and may not be the isomer ratio formed in the initial reaction mixture. Equilibration can occur under thermal conditions via a consecutive retro-Diels-Alder, Diels-Alder reaction. To investigate this kind of behaviour, pure samples of major **12e'** and minor **12e''** were heated in toluene (110°C). No change at all occurred to the minor isomer **12e''** over a 20 h period. The major isomer **12e'** on the other hand, was slowly converted to the minor isomer **12e''**. After 1 h at 110°C, only 2 % conversion was observed. This did not at all reflect the 21/79 ratio observed after 1 h at 110°C starting from the open precursor **11e**. When heating was continued for 20 h, 95 % conversion to **12e''** was observed. The slow conversion of the major isomer to the minor isomer suggests retrocycloaddition of the less stable cycloadduct. This is in agreement with the stereochemistry generally observed during IMDAF reactions: when a single bulky substituent is present in the tether, the most stable cycloadduct will be formed in such a way as to minimize nonbonded interactions.[51]

An additional experiment was performed using a substrate with the amide group included in the tether. In this case the dienophiles were inserted during acylation using acryloyl and cinnamoyl chloride. The corresponding pyrrolidinones **222** and **224** were obtained as single

isomers upon refluxing the amides **221** and **223** in toluene or THF (Scheme 77). However, the stereochemistry of the two stereocentres could not be determined via DIFNOE experiments. Refluxing of **222** in toluene during 60 h did not result in formation of the other epimer.

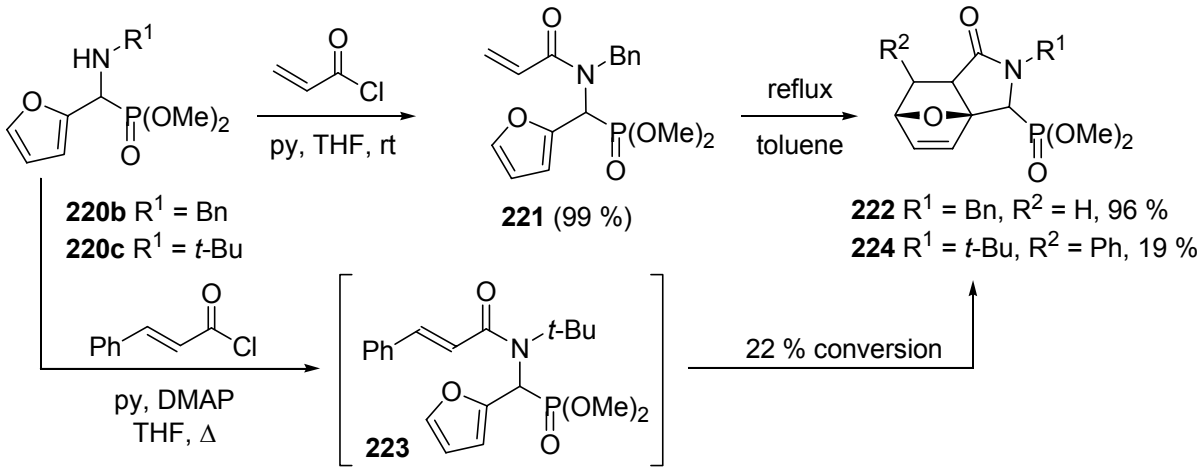

Scheme 77

As for the experimental part, it can be concluded that compounds **12** with the allyl group as dienophile, two isomers were formed, which are epimers at the *C*(2)-centre. The major isomer, with the phosphonate in *exo* position, is the thermodynamically less stable one. For the products **222** and **224** with the acyl group as dienophile, only one isomer was formed. This isomer could not be converted into the other *C*(2)-epimer by refluxing it in toluene.

2.3.2 Evaluation of Solvent Effect on the Stereoselectivity

Because computational experiments were aimed at reproducing the observed *endo*/*exo* product ratio of adducts **12e**, it was necessary to know if the solvent has a large effect on this ratio. At the same time, an idea was offered of the solvent effect on the reaction rate.

Therefore, the IMDAF reaction to pyrrolidine **12e** was repeated in methanol, acetonitrile and toluene at 65°C and stopped after 2h15'. In the respective solvents, the percentages of *endo* product, relative to the total amount of product, were 18, 23 and 33%. So, the solvent does not cause an inversion of stereoselectivity, only a small effect is observed: the *endo* ratio increases with a decrease of the solvent polarity.

These cycloadditions are relatively insensitive to changes in solvent polarity. The Diels-Alder reaction proceeds via a concerted, though slightly asymmetric formation of the two new σ-bonds. So, no large degree of charge separation is developed in the transition state.

Solvent effects on IMDA reactions are very often caused by a change in dipolarity of the substrate during the activation process, but, tertiary amides lack strong dipole effects. This in contrast to IMDAF reactions having an ester tether, where the IMDA reaction accelerates if more polar solvents are used due to a rotation of the ester from an s-*trans* conformation in the reactant to an s-*cis* conformation in the transition state and product.[61]

Given the limited influence of the solvent polarity on the stereoselectivity, only gas phase calculations, which represent an apolar medium, will be done.

2.3.3 Computational Investigation of Stereoselectivity

Computational Details

All ab initio calculations were carried out with the GAUSSIAN 03[150] software package. All geometries have been optimized at the B3LYP[151,152] level with the 6-31+G* basis set, and were followed by frequency calculations that confirmed the nature of the stationary points and were used in the thermochemical analysis. Diffuse functions were added as phosphorous is a third row element.[183] Previous studies have shown B3LYP is very accurate for many Diels-Alder reactions and performs well in reproducing the effects on activation energies,[74,77,67a,184] but shows systematic errors for hetero systems and incorrectly predicts the strain of the norbornene framework, leading to an underestimation of the reaction exothermicity.[185]

As a correct energy calculation of the TSs was relevant because of the small preference for one of the epimers, single-point energies were calculated with new generation functionals; i.e. the hybrid mPW1PW91[186] functional and the hybrid meta-GGA BB1K[187] functional as well as with post-HF MP2[154] and MP3[188] methods and these numbers were validated against CCSD.[189]

Theoretical Results and Discussion

As the tricyclic phosphono pyrrolidine **12e** was most easily formed, an X-ray was taken of both these isomers and to have a means for comparison, **12e** was used for the calculation as well. Also the acryloyl derivative **222** was used, because only one isomer was formed in excellent yield. The reactions considered and the numbering of atoms are presented in Scheme 78.

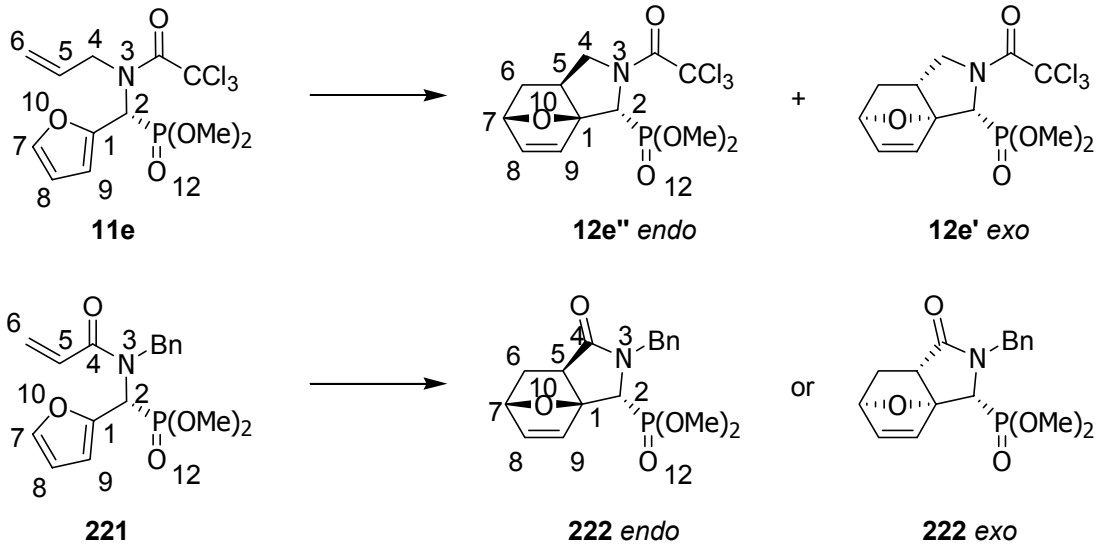

Scheme 78. Computationally studied Diels-Alder reactions

Till now the formation of one or two isomers was mentioned, but actually two or four different isomers are present (keeping in mind that the stereochemistry at positions 1, 5 and 7 are linked), since they appear as enantiomeric couples. The *R*-isomer was used for the calculations. For the product only the *exo*-oriented tether was modelled, which was based on the known stereochemical preference of the reaction. From now on, *exo* and *endo* always point at the orientation of the phosphonate group on the *C*(2)-position of the tether, respectively pointing towards the oxabridge or away from it.

i. Pyrrolidinone **222**

The energies and free energy differences with respect to the reactant of the *endo* and *exo* cycloadduct of **222**, their respective transition states and the reactant are given in Table 2. The product with the phosphonate in *endo* position is energetically more stable than the *exo* analogue due to reduced steric hindrance between the phosphonate group and the oxanorbornene and a higher distance between the electronegative oxygens of the phosphonate – in which the double bonded *O* is most electronegative – and the oxabridge of the oxanorbornene skeleton. These distances are given in Table 8.

Table 7. Relative[A] electronic (SCF without ZPE corrections) and free energies at 383.8 K (kJ/mol) for the stationary points of the IMDAF reaction of 221 to 222 with 6-31+g(d) basis

	B3LYP		BB1K		mPW1PW91	
	ΔE	ΔG	ΔE	ΔG	ΔE	ΔG
221	0.0	0.0	0.0	0.0	0.0	0.0
TS *endo*	111.3	118.5	98.0	105.3	89.1	96.4
TS *exo*	125.6	133.8	113.8	122.0	103.8	112.0
222 *endo*	-24.6	-6.1	-72.9	-54.4	-67.3	-48.8
222 *exo*	-8.9	11.6	-57.8	-37.2	-51.5	-31.0

[A] Relative to the energy of the reactant

Table 8. Geometric parameters for the stationary points of the IMDAF reaction of 221 to 222 of the B3LYP/6-31+g(d) optimized structures. Distances in Å, angles in degrees

	a_{O10P11}	a_{O10O12}	a_{O10Ocl}[A]	a_{HBnO12}[B]	a_{HarO12}[C]	$\varphi_{C1C2NC4}$	$\varphi_{C2NC4C5}$	$\varphi_{O10C1C2N}$
221	4.06	4.56	4.56	4.51	4.68	120.68	-168.43	-27.15
TS *endo*	4.08	5.22	4.30	2.46	3.37	-12.49	-12.99	-71.79
TS *exo*	3.21	4.61	2.93	2.37	2.51	18.04	6.05	70.33
222 *endo*	4.09	5.23	4.27	2.52	3.21	-10.81	-6.09	-84.27
222 *exo*	3.17	4.57	2.88	2.45	2.52	16.70	1.22	80.94

[A] O_{cl} is the oxygen of the methoxy groups closest to the oxabridge.

[B] HBn is the H-atom at the benzylic position closest to *O*(12).

[C] Har is the aromatic hydrogen atom closest to *O*(12).

Then, both pathways were explored to find an explanation for the formation of a single isomer of pyrrolidinone **222** (Table 7). This IMDAF reaction has a large energy barrier towards the transition state, which is in agreement with the high temperature required for the reaction. At 110 ˚C the precursor rotamers will be in equilibrium and the kinetic isomer ratio of the cycloadducts will depend only on the difference in the free energy of the transition state of both isomers (Curtin-Hammett principle[190]). The transition states are depicted in Figure 37 and relevant geometrical parameters for transition states and precursors are given in Table 8. The free energy of the transition state for the *exo* isomer is higher than for the *endo* isomer by 15 to 17 kJ/mol depending on the functional; causing the exclusive formation of the *endo* isomer.

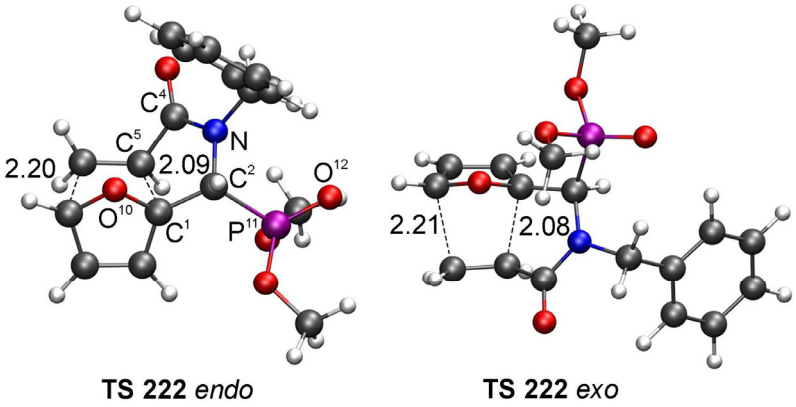

Figure 37. Structures of the transition states of the *endo* and *exo* isomer of 222 at B3LYP/6-31+g(d). Distances in Å

To trace the origin of this energetic difference the transition states and reactant conformations were screened. The major differences between the transition states of the different isomers are the dihedral angles $\varphi_{O10C1C2N}$ and $\varphi_{C1C2NC4}$. The first one corresponds to the rotation of the furan group and has an opposite value for both isomers. The latter is associated with the hindered *C*(2)-*N* rotation that was described previously.[191] This rotation has a barrier of about 70 kJ/mol at the HF/3-21+g* level and shows two minima at -45° and at 115° that have about the same energy. The *exo* transition state needs a larger distortion of the dihedral angle and this might be one of the origins for the higher energy of the transition state. This increase can be attributed to steric interactions, mainly of the benzyl and furan group with the phosphonate moiety as can be seen from the distances given in Table 8. The rotational potential in terms of the dihedral angle $\varphi_{C1C2NC4}$ was calculated at a B3LYP/6-31+g(d) LOT (Figure 38).

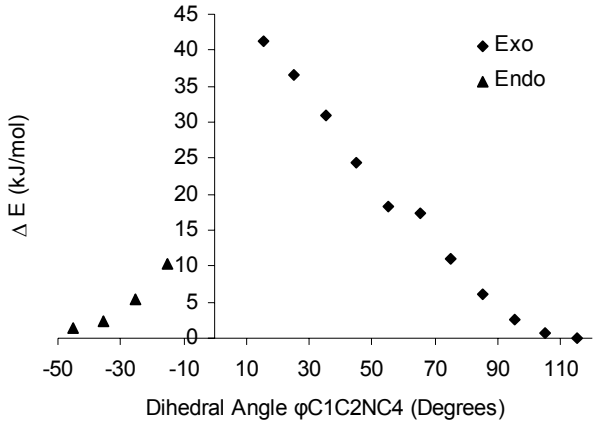

Figure 38. Rotational energy for the *endo* precursor – on the left – and the *exo* precursor – on the right – of 221 towards their respective transition states calculated at B3LYP/6-31+G*

For formation of pyrrolidinone **222** we find exclusive formation of the *endo* isomer in correspondence with the experimental results of full selectivity and this irrespective of the functional used.

i. Pyrrolidine **12e**

The energies and important geometrical parameters of the stationary points in the cycloaddition to the *exo* and *endo* isomer of **12e** are given in Table 9 and Table 10. Again B3LYP underestimates the free energy of the reaction, but the energy difference between both epimers is independent of the functional. The *endo* cycloadduct is energetically preferred in order to minimize the steric hindrance and electrostatic repulsion between the phosphonate group and the oxabridge of the oxanorbornene skeleton. These distances between the oxygen atoms are listed in Table 10. The energy difference between the *endo* and *exo* isomer of pyrrolidinone **222** is of the same order of magnitude as for the pyrrolidine **12e**. If the retro-Diels-Alder reaction is possible, this difference in stability between the two isomers can explain the conversion of the major isomer into the minor isomer under thermodynamic control.

Table 9. Relative[A] electronic (SCF without ZPE corrections) and free energies at 354.8 K (kJ/mol) for the stationary points of the IMDAF reaction of 11e to 12e with 6-31+g(d) basis

	B3LYP		BB1K		mPW1PW91		MP2		MP3		CCSD	
	ΔE	ΔG	ΔE	ΔG	ΔE	ΔG	ΔE	ΔG	ΔE	ΔG	ΔE	ΔG
11e	0.0	0.0	0.0	0.0	0.0	0.0						
TS *endo*	101.5	113.7	87.7	100.0	80.6	92.8	1.4	1.9	1.0	1.5	1.0	1.6
TS *exo*	101.9	113.6	85.4	97.2	78.7	90.4	0.0	0.0	0.0	0.0	0.0	0.0
12e'' *endo*	-26.0	-1.8	-76.2	-52.1	-67.7	-43.6						
12e' *exo*	-12.3	9.5	-63.8	-42.0	-54.6	-32.9						

[A] Relative to the energy of the reactant for DFT methods and to the TS *exo* for MPx and CCSD

Table 10. Geometric parameters for the stationary points of the IMDAF reaction of 11e to 12e of the B3LYP/6-31+g(d) optimized structures. Distances in Å, angles in degrees

	a_{O10P11}	a_{O10O12}	a_{O10Ocl}[A]	$\varphi_{C1C2NC4}$	$\varphi_{C2NC4C5}$	$\varphi_{O10C1C2N}$
11e	3.14	3.50	3.07	-43.52	80.24	85.95
TS *endo*	4.08	4.59	4.54	-32.26	8.59	-61.61
TS *exo*	3.06	3.42	2.96	-23.02	49.33	92.05
12e'' *endo*	4.09	4.57	4.58	-25.18	8.19	-75.71
12e' *exo*	3.02	3.37	2.90	-15.51	35.78	98.58

[A] O_{cl} is the oxygen of the methoxy groups closest to the oxabridge

Next, the experimentally observed isomer ratio during the synthesis of pyrrolidine **12e** was to be unravelled. To test whether the Curtin-Hammet conditions are fulfilled, the reaction was followed in methanol. Methanol was chosen because of its lower boiling point that does not allow the retro-Diels-Alder reaction to occur, as observed experimentally. Moreover, the ^{31}P NMR peaks of both isomers are better resolved. As the ratio of major and minor isomer remained constant throughout the course of the reaction, the Curtin-Hammet principle holds. So again the relative energies of the transition states were studied. The structures and parameters are given in Figure 39 and Table 9 and Table 10. The energetic difference of both transition states is very small and depends on the functional. Therefore, a higher level of theory was used to calculate these subtle differences. MP2[154] and MP3[188] calculations indeed predict a lower free energy of the *exo* transition state by 1.9 to 1.5 kJ/mol and these figures were validated using a CCSD[16] calculation. This confirms the formation of a mixture of the *endo* and *exo* cycloadduct.

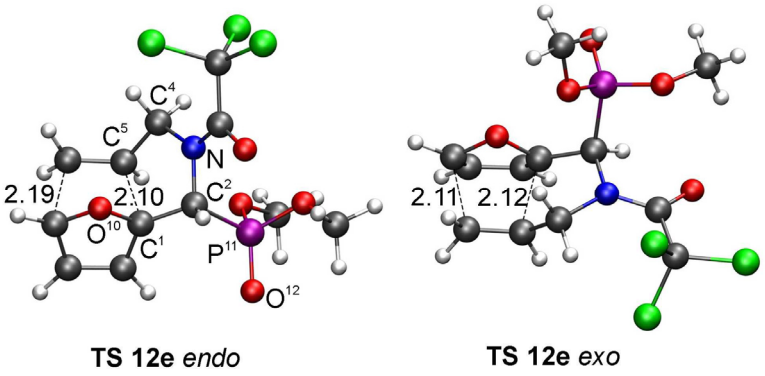

Figure 39. Structures of the transition states of the *endo* and *exo* isomer of 12e at B3LYP/6-31+g(d). Distances in Å.

The retro-Diels-Alder reaction of the *exo* isomer has an activation free energy that is, depending on the method, 33 to 42 kJ/mol more than the forward reaction and indicates that the slow thermodynamic conversion of the *exo* isomer to the *endo* epimer is possible.

The theoretical study for formation of pyrrolidine **12e** indeed shows that the *endo* cycloadduct is thermodynamically preferred and that there is a competition between the formation of both isomers. CCSD calculations confirm the experimentally observed preference for the epimer in which the phosphonate group is oriented towards the oxa-bridge.

Conclusions

The IMDAF reaction of 1-acyl-1-alkylamino(furan-2-yl)methyl phosphonates results in complex azaheterocyclic phosphonates in a small number of synthetic steps. These products might be used as novel conformationally-constrained amino acid analogues. The presence of a phosphonate substituent on the tether raises the conversion of the IMDAF reaction significantly. Furthermore a high degree of stereocontrol is observed during the cycloaddition reaction. Only the *exo*-fused products were obtained. For derivatives containing the carbonyl group in the tether two isomers were formed, originating from incomplete stereocontrol of the phosphite addition. If the allyl group serves as dienophile, four isomers are formed resulting from an incomplete kinetic control of the position of the phosphonate as tether substituent during the IMDAF reaction. However the most stable stereoisomers, having an *endo*-oriented phosphonate group, are formed under thermodynamic control.

This kinetic and thermodynamic control could be computationally reproduced. With the acyl group functioning as dienophile the isomers with the phosphonate group in *exo* position require a larger distortion from their minimum energy precursor than the *endo* isomers and are sterically more hindered, as can be seen in their respective transition states. For amino phosphonates **11** with the allyl group as dienophile the *endo* and *exo* position require about the same amide rotation and there is a subtle energy difference that requests a high level of theory calculation. From the calculations it is clear that B3LYP fails to estimate the reaction free energy of these strained cycloadducts.

2.4 Elaboration of the Synthesis

2.4.1 Acylation Using Maleic Acid Anhydride

Maleic anhydride is a very reactive acylating dienophile and the acylation and Diels-Alder reaction was evaluated with the α-aminofurfuryl phosphonates **224a** and **b** by simply refluxing both compounds in toluene or acetonitrile (Scheme 79). The isopropyl substituent causes more sterical hindrance, therefore a higher boiling solvent was used. The products were purified by recrystallization in acetone.

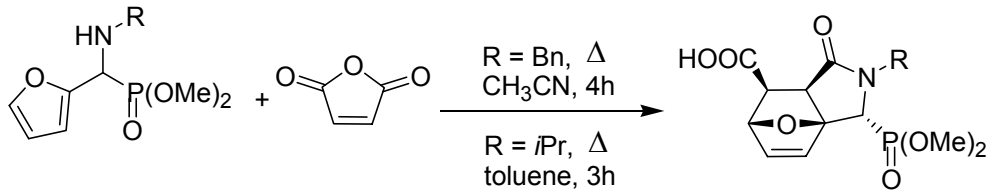

220b
220d

225a R = Bn, 67 %
225b R = *i*Pr, 63 %

Scheme 79

In theory an intermolecular Diels-Alder reaction can occur without previous acylation as well. This has been erroneously reported by Borisov et al.[192] Inspection of the IR-spectrum of the product of the isopropyl derivative shows two carbonyl peaks at 1693 and 1727 cm^{-1}, corresponding with an amide, which appears between 1690 and 1710 cm^{-1}, and an acid, at about 1730 cm^{-1}. Because of the larger ring strain, the anhydride carbonyl would appear round 1785 cm^{-1}.[89d]

The relative stereochemistry of the protons *H*(5) and *H*(6) is determined by the *cis* conformation of the maleic anhydride. Nevertheless, the acid at *C*(6) can easily epimerize.[193] The $J_{H(5),H(6)}$ coupling constant of 9.2 Hz indeed indicates that these *H*-atoms have an *s-cis* conformation; an *s-trans* conformation would have a coupling constant of about 3.5 Hz in agreement with the Karplus equation. The adducts are expected to be *exo*-ring-fused, which was confirmed by analysis of the coupling constants of the hydrogen atoms *H*(5), *H*(6) and *H*(7). If the proton *H*(6) has an *exo* orientation, $J_{H(6)exo\text{-}H(7)}$ is 4 to 5 Hz, otherwise $J_{H(6)endo\text{-}H(7)}$ is 0 Hz.[50] There was no coupling observed between *H*(6) and *H*(7), so *H*(6), and consequently *H*(5), has an *endo* position; which means the rings are *trans*-fused.

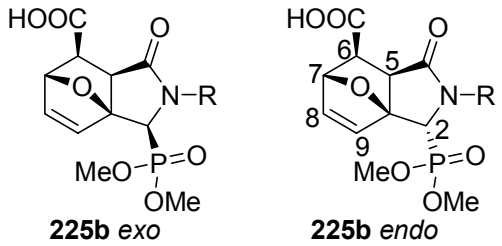

225b *exo* **225b** *endo*

Figure 40

Table 11. DIFNOE spectra show that the phosphonate is *endo*-oriented in the major adduct 225b

Saturated Proton	Observed Proton	NOE (%)
H(5)	*H*(6)	9.7
	H(2)	0
	H(9)	3.0
H(6)	*H*(5)	9.6
	H(2)	0.0
	H(7)	5.7
	H(8)	2.8

The conformation at *C*(2) was determined via NOE spectra, taken in $CDCl_3$ (Table 11). As there is no nuclear Overhauser effect between *H*(5) or *H*(6) and *H*(2), the major product has the phosphonate in *endo* position. Under reflux conditions, only the *endo* phosphonate was formed.

To determine whether the reaction is a tandem acylation/IMDAF reaction or the Diels-Alder reaction occurs before the acylation, the amino phosphonate and maleic anhydride were stirred at room temperature in toluene. Figure 41 shows the ^{1}H NMR spectrum after 4 days. All the starting product had disappeared and three new products were formed: the amide **226b** (45.6 %), the cycloadducts with an *endo* phosphonate (50.0 %) and with an *exo* phosphonate (4.4 %). The intermediate after acylation can be recognized by the vinylic protons at 6.5 and 6.8 ppm of the maleic acid, while the furanyl protons remain present as well. This confirmed the occurrence of the amide **226b** as intermediate (Scheme 80). Upon addition, the CHP proton shifts upfield and the $^2J_{HP}$ coupling gets smaller: from 22.2 Hz for the ring open amide to 9.4 Hz for the *exo* isomer and 6.1 for the *endo* isomer. The latter is a very small $^2J_{HP}$-value for α-amino phosphonates. Usually the *exo* isomer has a larger $^2J_{HP}$-coupling than the *endo* isomer.

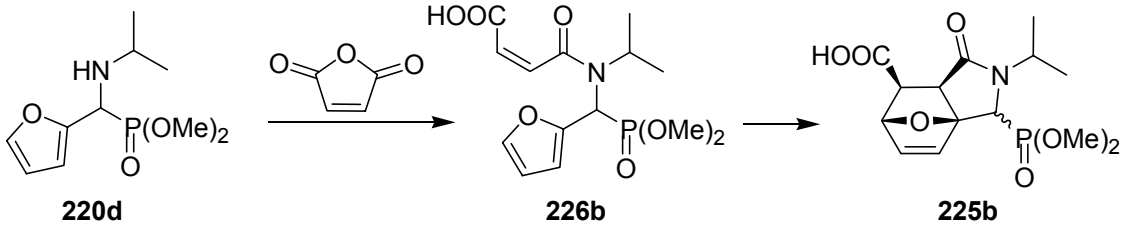

220d **226b** **225b**

Scheme 80

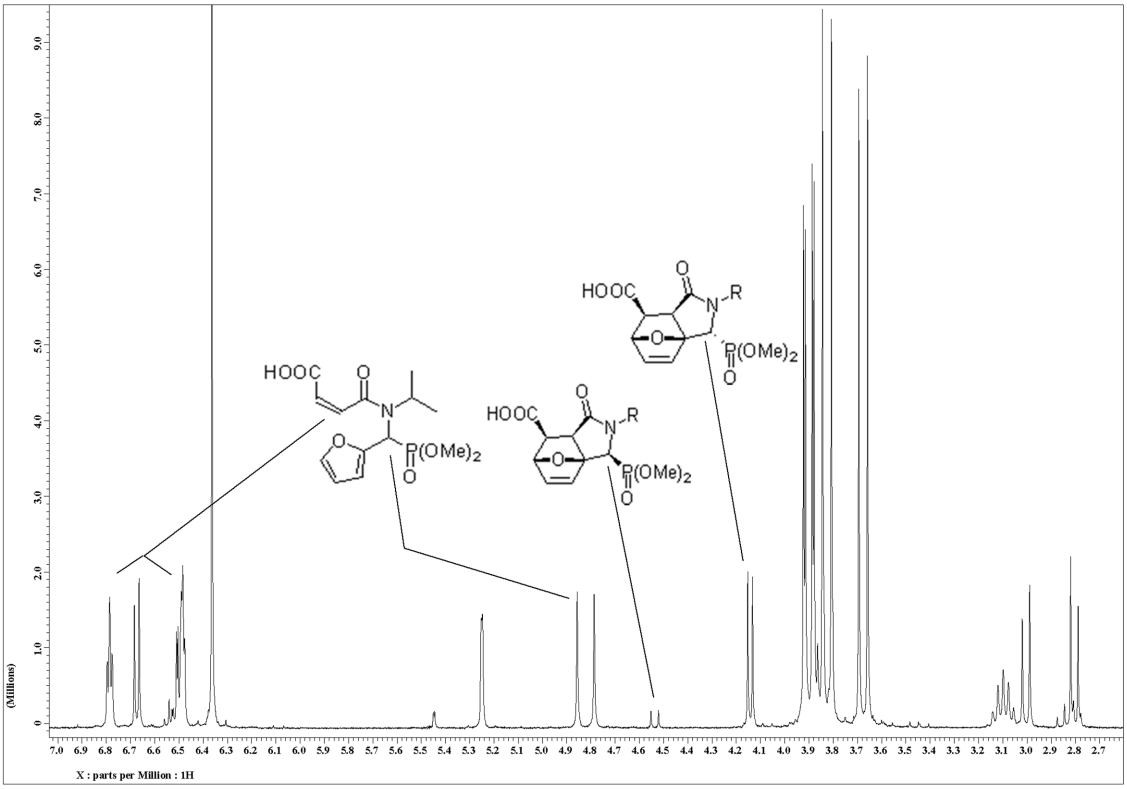

Figure 41. ^{1}H NMR during the addition of maleic anhydride and amino phosphonate 220d

The same year this research was done, an article was published that disclosed the same reaction, but it was performed at room temperature and required 3 days.[194] Very small amounts of product with the phosphonate in *exo* position (2-11 %) were observed. However, they did not use the more sterically demanding isopropyl substituent on nitrogen. After 4 days, the reaction didn't complete and heating was necessary. Reflux conditions assure that only the thermodynamically most stable *endo* phosphonate is obtained, but slow decomposition of the phosphonate occurs, as can be seen by the appearance of a dimethyl phosphite peak in the ^{31}P NMR spectra.

2.4.2 The Halo-Effect of 5-Bromofuranyl as Diene

Halogen substituents on the 3- and 5-position of the furanyl ring have been found to increase reaction rates and yields.[75,77] These halogen atoms can be used for C-C bond formation.[195] High accuracy CBS-QB3 computations on the intermolecular Diels-Alder reaction of furan and 2-bromofuran with ethylene have activation enthalpies of 20.5 and 18.4 kcal/mol respectively; the corresponding reaction enthalpies are -12.2 and -17.3

kcal/mol. So, there is an increase in exothermicity upon substitution and a smaller decrease in activation barriers. This was ascribed to the energetic preference for electronegative halogens to be attached to a more highly alkylated carbon framework and explains why the stabilizing effect of the halogens increases with bond formation between the diene and the dienophile. A similar study on the effect of 3- and 5-bromo substitution of the furan group on the rate of the IMDAF reaction at B3LYP level gave similar results. Moreover, the position of the halogen on the ring has minor consequences.

First the effect of bromine substitution at the 5-position of the furan on the π-diastereofacial selectivity of the IMDAF reaction of product **229** was tested. Therefore, the α-allylamino phosphonate **228a** was synthesized via the usual sequence of imination and Pudovik reaction. The next step is the acetylation. The ring closure, that had already started during the acylation, was completed by additional reflux for 1 hour in acetonitrile. Again a diastereomeric mixture was formed in a ratio of 65/35 *exo*/*endo*. There is no significant effect on the stereoselectivity of the addition. Apparently both the transition states to the *endo* and *exo* isomer are influenced to the same extent. The major *exo* isomer could be isolated via crystallization in acetone.

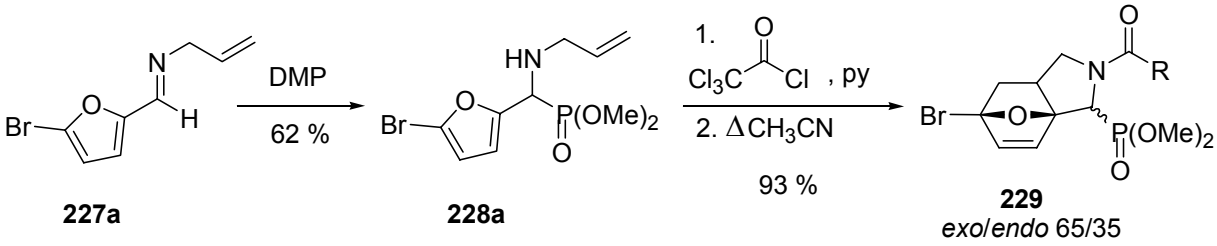

Scheme 81

In a second experiment, the rate enhancement of 5-bromosubstitution of furan was tested for the reaction with the acryloyl derivative. Both reactions were followed by ^{31}P NMR. The reaction time reduced from 70 to 40 minutes. Moreover, during the synthesis of the acylated product, a small amount of adduct was already formed. Again, only the *endo* isomer was formed.

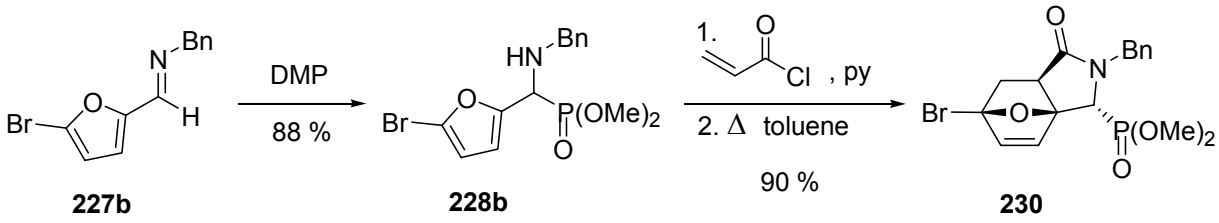

227b **228b** **230**

Scheme 82

2.4.3 Heterocycles Replacing Furan

In the continuation of the smooth intramolecular ring closing of aminophosphonates with a furanyl substituent, the same reaction was evaluated with an imidazole as diene. As for the furan derivatives the stereochemistry of these compounds should be favourable, but the Diels-Alder cycloaddition failed. There are two possible explanations: or the energy gap between the frontier orbitals is too big, or the retrocycloaddition is too fast.

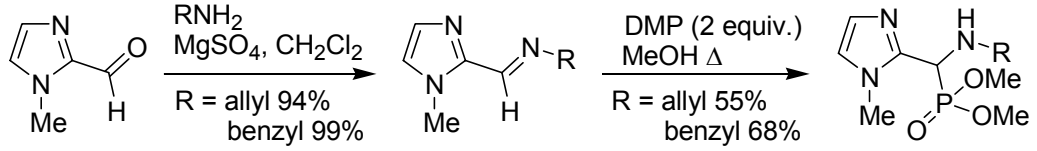

231 **232**

Scheme 83

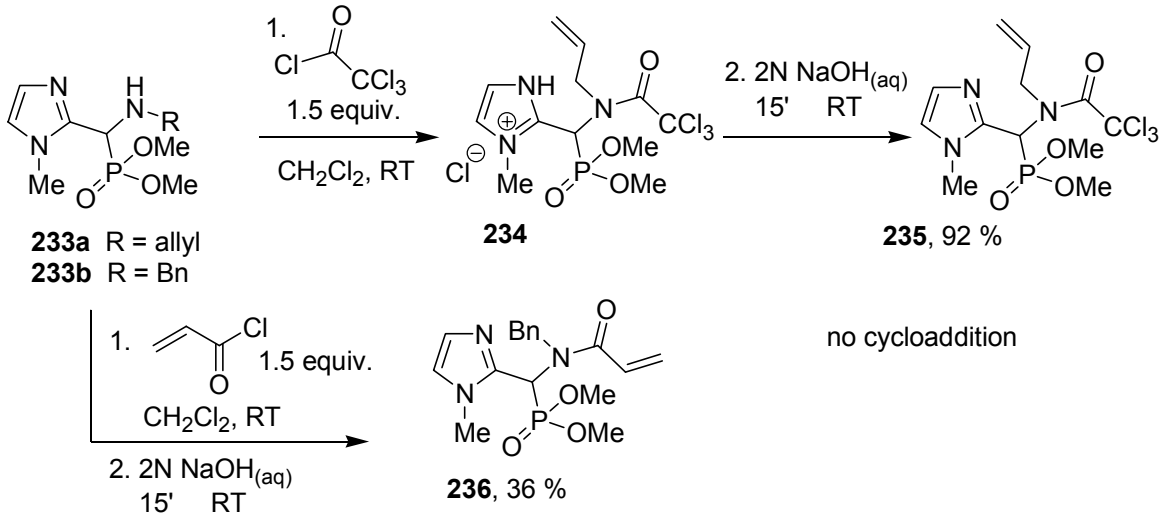

Scheme 84

The amino phosphonates were synthesized following the usual procedure (Scheme 83). If the acetylation of the allylamine was done with 2 equivalents of pyridine, it was impossible to isolate the imidazole derivative, so it remained in the aqueous layer after neutralization

of the reaction mixture with saturated $NaHCO_{3(aq)}$. Prolonged stirring with $NaOH_{(aq)}$ resulted in product breakdown.

The reaction was repeated without an additional base, as the imidazole itself was able to capture the HCl. Fast precipitation of the hydrochloric acid salt of the product was observed. After stirring for an additional 2.5 hours the very hygroscopic salt was filtered. To obtain the unprotected imidazole, the mixture was neutralised by adding 2 N $NaOH_{(aq)}$, stirring for 15' and extraction with CH_2Cl_2.

The intramolecular Diels-Alder reaction was then evaluated on both the hydrochloride salt and the deprotected form. The salt was refluxed in dichloroethane with Et_3N, no reaction was observed, only decomposition. The unprotected imidazole **235** was refluxed in toluene and CH_3CN only returning starting material. After stirring the unprotected product while microwave heating in toluene for 1h at 200°C only starting material was recovered; the decomposed material stuck to the vial. Also refluxing in toluene in a pressure vial at 200°C for 24h only gave decomposition and starting product.

After acylation of the benzyl derivative **232b** with acryloyl chloride, the Diels-Alder cycloaddition was evaluated by refluxing the amide **236** in toluene and with different Lewis acids: $BF_3(OEt)_2$, $LiClO_4$, $AlCl_3$. This only resulted in product breakdown; besides starting material, benzylacrylamide could be identified.

2.4.4 Evaluation of Diazepinedione Synthesis via IMDAF with a 5-Atom Tether

Usually IMDAF reactions are used to construct an oxanorbornene with a fused 5- or 6-membered ring. Sporadically a 7-membered ring is formed by the use of a 5-atom tether.[35a] Given the success of the previously described cycloaddition with the α-aminofurfuryl phosphonates, an analogous method was tested.

The *n*-propylimine was phosphonylated by refluxing the imine with dimethylphosphite for 4 hours. The usual acid base extraction furnished the expected amino phosphonate **220e** for 91 %, but 9 % of a minor side-product **237** was observed (Scheme 85). The ratio was measured by integration of the ^{31}P NMR. The carbamoylation with allyl isocyanate was performed on this mixture, as the urea would need chromatographic purification.

Heating in toluene under reflux, did not result in Diels-Alder cycloaddition, but again ring closure towards the diazaphospholidinones was observed. Both diastereomers were formed in equal amounts. To fully identify the products **239**, they were separated by preparative thin layer chromatography.

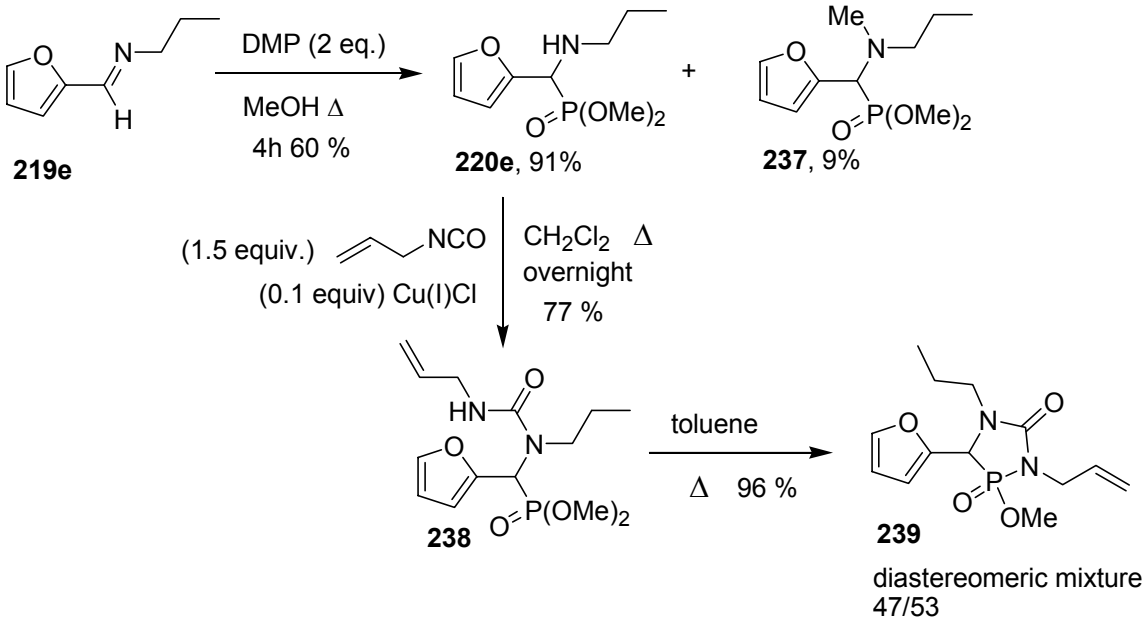

Scheme 85

Next a kinetic experiment was performed on product **240** to test which of the two cycloadditions would be preferred (Scheme 86). Reflux in toluene for 1 day delivered a mixture of 75 % of the *endo*-Diels-Alder adduct, 10 % of the *exo*-Diels-Alder adduct and 15% of the product with an allyl group. These data were deducted from the crude ^{1}H NMR spectrum. In the IR spectrum a carbonyl peak appeared at 1714 cm^{-1}, indicating a minor amount of the phosphorous containing heterocycle was formed. The major carbonyl peak was at 1643 cm^{-1} of the ring-open products. Heating at 100 °C in a pressure tube in acetonitrile for 2 days furnished 84 % of adduct **241** with the phosphonate in *endo* position and 16 % of *exo* **241**. In the IR spectrum no peak was observed between 1700 and 1720 cm^{-1}.

Thus there is a clear preference for the Diels-Alder addition if a 3-atom tether is used.

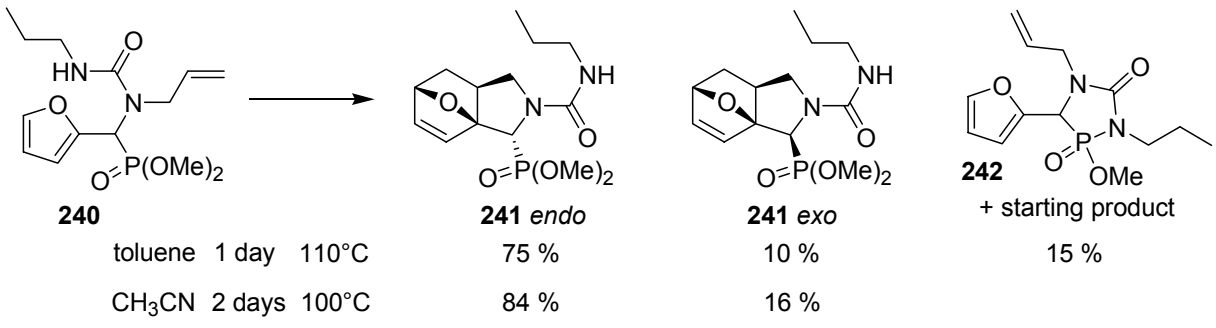

Scheme 86

2.5 Ring Opening of Oxanorbornenes

Because intramolecular cycloaddition reactions such as the IMDAF reaction can achieve high levels of both regio- and stereoselectivity, a synthetic approach based on that methodology allows for a concise construction of the perhydroisoindole skeleton. Therefore, it is necessary to ring open the oxygen bridge. Different methods to achieve this were described in paragraph 4 of the Literature Overview.

Using the synthesized amino phosphonates, Brønsted acids (such as p-toluene sulfonic acid, glacial acetic acid or HCl, which usually cause further aromatization) either lead to starting material or decomposition with formation of complex reaction mixtures. Bases like NaOMe and LDA, can deprotonate the α-position of the phosphonate. Formation of a vinylic phosphonate would open the oxygen bridge towards a cyclohexenol derivative, but again, no reaction occurred or the product decomposed. The ring opening with Lewis acids was more successful and is described in detail in the next part.

The complex formations with $TiCl_4$ and $FeCl_3$ were investigated computationally as different reaction products were formed. It is one of the first computational studies of the ring opening of IMDAF adducts. Few literature studies on the modelling of reactions of these transition metal catalysts with main group elements have been reported.[196,197,198,199]

2.5.1 Ring Opening with Lewis Acids

$BF_3.OEt_2$

The ring opening by activation with BF_3 was evaluated before in the *SynBioC* research group as one of the first successful methods, with a conversion of 40 %, however side-products were formed.[200] Optimization of these conditions, e.g. by raising the Lewis acid load to three equivalents as different oxygens can be complexed, resulted in a maximal conversion of 64 % and a negligible side-product formation (Scheme 87). Capturing the hydroxide anion of the product via acetylation with acetic anhydride, as described by Gschwend,[54] can bring a solution to drive the reaction to completion, but was not further investigated, as other Lewis acids gave better results.

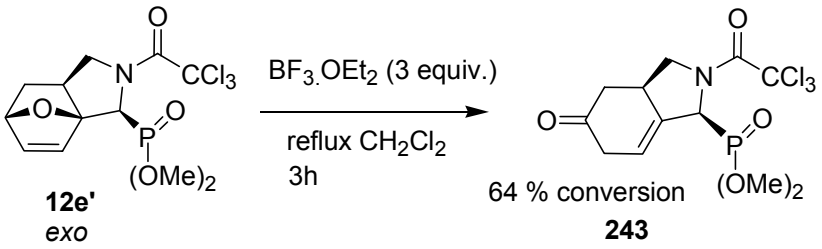

Scheme 87

At that moment the product was not purified, but full spectral analysis, done for the reaction with $FeCl_3$, led to the conclusion that product **243** had been formed. The CHP-proton is still present in the ^{1}H NMR, so no vinylic phosphonate is formed. Moreover, the ^{31}P-NMR shift of 22.6 ppm is too high to be a vinylic phosphonate, which usually appears round 16 ppm. The usually very sharp doublet of the CHP-proton is broadened, which is possibly caused by a very small, not resolved, allylic coupling. As only one olefinic hydrogen is present, this leads to the β,γ-unsaturated phosphonate as drawn in Scheme 87. A clearly unconjugated cyclic carbonyl appears at 207.5 ppm in the ^{13}C NMR and at 1718 cm^{-1} in the IR-spectrum.

$FeCl_3$

The ring opening with $FeCl_3$ gave a better conversion. However, the results can be slightly distorted as the reaction could not be followed directly by ^{31}P NMR. Fe^{3+} is paramagnetic and accelerates the longitudinal relaxation of all protons. Shorter relaxation times broaden the resonance lines and therefore $FeCl_3$ hinders the measurement of NMR spectra.[201] Therefore, the results are obtained after washing the reaction mixture several times with a saturated $NaHCO_{3(aq)}$ solution. It was assumed this did not change the ratio of the products, which involves the supposition that no phosphonic acids are formed and the side-products are mainly formed by further aromatization.

Different reaction conditions showed that catalytic amounts of Lewis acid are not sufficient. Higher reaction temperatures increase the side-product formation. The best conditions were one hour of reflux in dichloromethane with 1.5 equivalents of Lewis acid. Unfortunately, the work-up by washing the reaction mixture several times with $NaHCO_{3(aq)}$ or $CaCO_{3(aq)}$ caused large product losses, reducing the yield to 15 % only (Scheme 88).

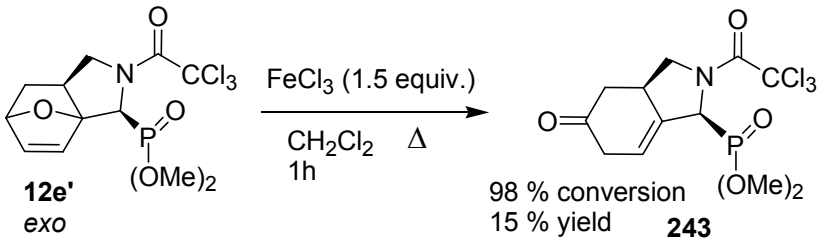

Scheme 88

If the reaction mixture was directly filtered over celite and washed twice with a saturated $NaHCO_{3(aq)}$ solution to remove the Fe-residue, two products were obtained in a ratio of 73/27 according to the integration of the ^{31}P NMR spectrum. After purification by column chromatography, they were identified as the benzopyrrolidine derivatives **244** and **245** (Scheme 89). Looking back at the spectra of the previous reactions with aqueous work-up, small amounts of phenol **245** were observed.

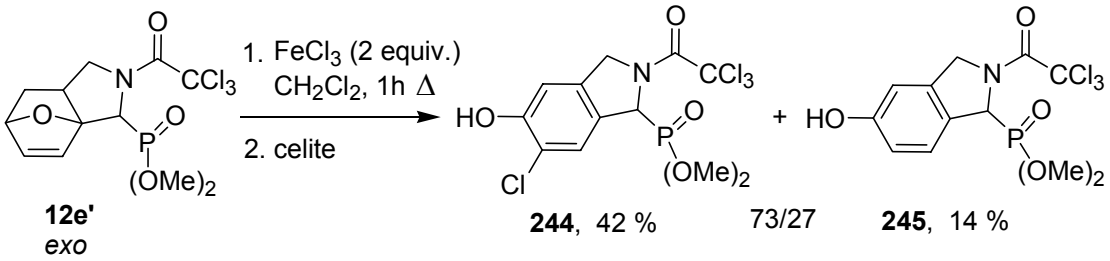

Scheme 89

The position of the chlorine and hydroxyl group on the aromatic ring of **244** can be easily deducted from the COSY spectrum. The aromatic hydrogen in ortho position of the hydroxyl group will have a larger shielding or upfield shift. The most upfield aromatic proton shows a small allylic coupling with the NCH_2 protons. The most downfield aromatic proton couples with the CHP proton, from which the position of the substituents can be determined. The same reasoning holds for phenol **245**, where the aromatic proton with the most upfield broad singlet couples with the NCH_2 proton.

Apparently the work-up procedure caused a very fast aromatization of the product after possible insertion of a chloride ion. Most probably, the allylic cation formed by ring opening of the oxygen bridge remained present until the work-up. By filtration over celite, the $FeCl_3$, of which 2 equivalents were used, bound to the silicate surface, releasing chloride ions that added to the cation **246** (Scheme 90).

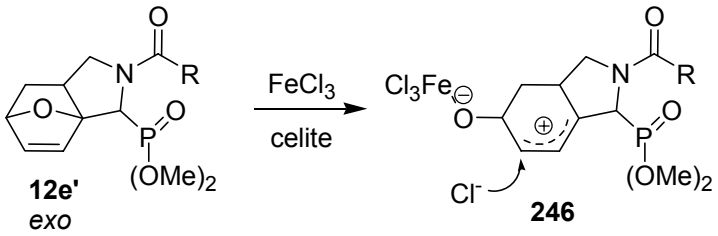

Scheme 90

A similar reaction was observed for a cholestane epoxide. Dry $FeCl_3$-SiO_2 reagent, formed by adsorption of $FeCl_3$ on a chromatographic silica gel, converted the epoxide **247** into a chlorohydrin **248** and a cholestan-6-one **249** (Scheme 91).[202]

The next step was a fast oxidation, in which the $FeCl_3/SiO_2$ reacts as an oxidant.[203]

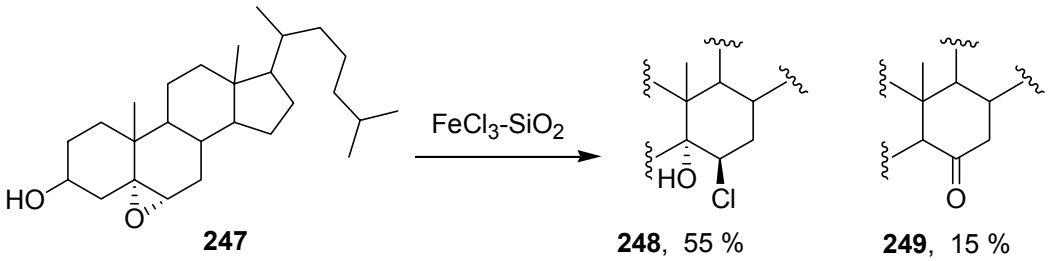

Scheme 91

Activated Montmorillonite

Because of the hygroscopicity of $FeCl_3$ and the tedious work-up required, with large product losses, an alternative procedure using a clay catalyst was evaluated. The Fe^{3+}-cation-exchanged montmorillonite has been used as an efficient heterogeneous catalyst for the alcoholysis of epoxides,[204] which made it worth to evaluate in the ring opening towards **243** in the absence of a nucleophile.

The catalytic use of Fe^{3+}-exchanged montmorillonite clay in organic synthesis is gaining importance and has many advantages over other catalysts, such as easy handling, non corrosiveness, low cost and recovery of the catalyst.[205] Montmorillonite is a smectite clay with an aluminosilicate structure: an internal layer of octahedral alumina groups is surrounded by two layers of tetrahedral silica groups in a TOT (tetrahedral octahedral tetrahedral) structure. In the montmorillonite clays, the TOT sheet retains a residual negative charge, caused by isomorphous substitution of e.g. Al(III) by Mg(II) or Fe(II) atoms. This charge is balanced by cations, like Na^+ or Ca^{2+} in the interlamellar layer, between the TOT layers, or at the broken edge sites. Montmorillonite K10 is acid-treated, which causes delamination of the structure and creates mesopores. This augments the

accessible catalytic surface, particularly at the sheet edges. A second way of activating the clay is cation exchange by metal cations such as Al^{3+} or Fe^{3+} in an aqueous medium.

This clay contains both brønsted acidic sites and Lewis acidic sites. Brønsted sites are mainly associated with the interlamellar region, and are only accessible in the presence of a clay-swelling solvent. Lewis sites are mainly present at the edges.[206] Heating to around 100 °C removes most of the interlamellar water until only one layer remains, increasing the Brønsted acidity. If the clay is heated to 200-300 °C, the interlayer structure collapses, resulting in a decrease of brønsted acidity and an increase in Lewis acidity. If Lewis acidity is concerned, which is achieved by using a non-swelling solvent and by clay activation at 250/280°C, Fe^{3+}-montmorillonite has been shown to be the most effective catalyst among metal-exchanged montmorillonites.[207,208] The higher activity of Fe^{3+}- than Al^{3+}-montmorillonite is surprising, given the reversal of reactivity in their homogeneous counterparts, and has been ascribed to the synergistic/antagonistic effect by its support.

The Fe^{3+}-montmorillonite K10 was prepared by the procedure reported by Laszlo,[209] and was activated overnight at 120 °C. This catalyst, K10-FeAA120, was evaluated for the ring opening of adduct **12e'**. The clay has an estimated amount of 0.075 mmol of exchanged Fe per 0.1 g of clay.[207] This value was used for the calculation of the added equivalents of catalyst.

The reaction was performed in CH_2Cl_2, in which the catalyst was suspended by stirring vigorously. At room temperature with 0.4 equivalents of catalyst after 1 day, only 8 % conversion to cyclohexenone **243** was obtained. The reaction under reflux with 0.4 equivalents of catalyst was followed by ^{31}P NMR. After 16 hours, all the starting material was consumed, yielding 80 % cyclohexenone **243** and 20 % side-products (Scheme 92). Reducing the catalyst load to 0.1 equivalents furnished 27 % ring opened cyclohexenone **243**, 14 % side-products and 59 % starting product after 2 days. Thus, reflux conditions are required and a catalyst load of 0.4 equivalents is necessary to reduce the reaction time and in this way, the side-product formation. Pure **243** could be obtained via column chromatography in 59 % yield.

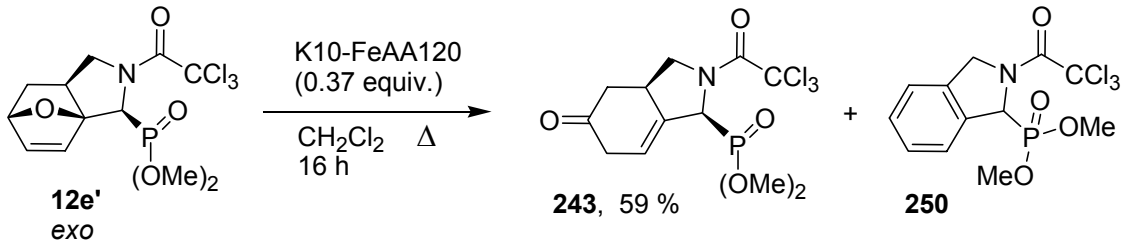

Scheme 92

The major side-product (14 %) was identified as the dihydroisoindole derivative **250**. Its formation can be explained by the oxidative activity of Fe(III) in the presence of the silicate. However, this time the aryl group has no substituents, in contrast with the reaction in Scheme 89.

Microwave conditions gave analogue ratios of the aromatic products and cyclohexenone derivative **243**, but the results on catalyst load and reaction time are hard to compare, because of suspension problems of the clay catalyst in the microwave reaction vessel.

The same reaction with the minor isomer **12e''** gave a conversion of 89 % to the *C*(2)-epimer of cyclohexenone **243**, 7 % of dihydroisoindole **250** was formed and 3 % of other side-products. The products were not isolated.

Ring opening of the IMDAF adduct **222** *endo* yielded two products in a ratio of 74/26. The major product was the cyclohexenone **251**, formed by the usual β-eliminative ring opening of the oxygen bridge; the minor product was the dihydroisoindolone **252** (Scheme 93).

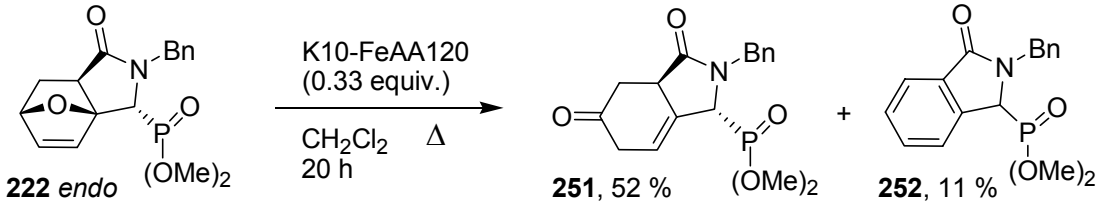

Scheme 93

Acids **225a** and **b** are reluctant to ring opening and after reflux with K10-FeAA120 in CH_2Cl_2 only starting material was recovered. After reflux in acetone or heating at 65°C in DMF with $NaHCO_3$, no reaction was observed (Scheme 94). Heating at higher temperatures most probably caused hydrolysis of the phosphonate, as all the product was extracted in the aqueous layer.

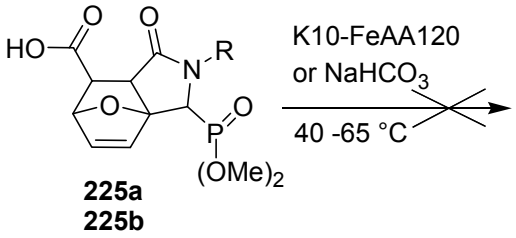

225a
225b

Scheme 94

Ferric chloride can also be adsorbed on montmorillonite K10, following a procedure by Pai et al.,[210] using an organic solvent. This procedure for the activation of the clay is much shorter. To leave mainly the Lewis acidity of the catalyst, it was activated at 280°C before use. This heating process liberates HCl, with some kind of bond formation of the catalyst on the clay, and removes physisorbed water from the catalyst surface.[211] Because of the release of minor amounts of $FeCl_3$, the interpretation and mainly integration of the NMR spectra is hindered by peak broadening and lack of a stable deuterium lock. The catalyst, referred to as K10-FeOO280, contains about 0.063 mmol of $FeCl_3$ per 250 mg.[212]

After 20h of reflux in CH_2Cl_2 with 0.2 equivalents of catalyst, all the starting material was consumed. Cyclohexenone **243** and dihydroisoindole **250** were formed as the only two products in a 85/15 ratio, according to the ^{31}P NMR values.

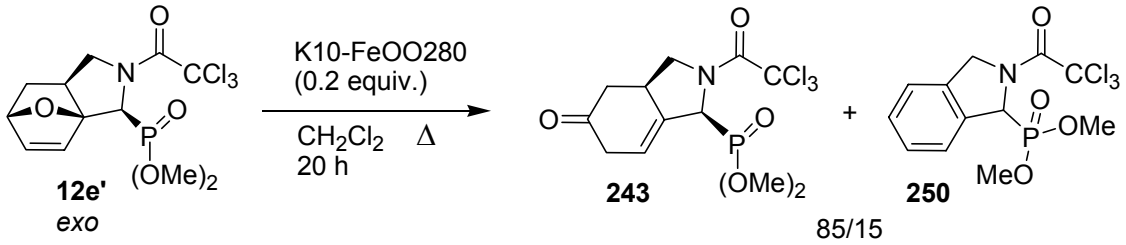

12e'
exo

243

250

85/15

Scheme 95

$TiCl_4$

The Lewis acid $TiCl_4$ promoted the ring opening, even at 0°C. After 2 hours, the reaction was quenched by pouring the reaction mixture in ice water. Extraction with EtOAc furnished three products: two epimers **254** and **255**, formed via β-eliminative bridge opening with addition of chloride, and the dihydroisoindole derivative **250** as a minor side-product (Scheme 96). Simple reflux of **254** and **255** in CH_2Cl_2 did not result in cis-trans-isomerisation or aromatization. The percentage of the aromatic compound **250**, was larger after chromatographic purification than before. This indicates that an acid catalyzed

aromatization of the cyclohexene derivative towards the dihydroisoindole occurs. Stirring **254** and **255** on silica did indeed convert these products slowly to the aromatic compound **250**, but other unidentified (aromatic) products were formed as well. Using $Ti(OEt)_4$ would create a less acidic environment, but no reaction occurred at 0°C, at room temperature or under reflux in CH_2Cl_2.

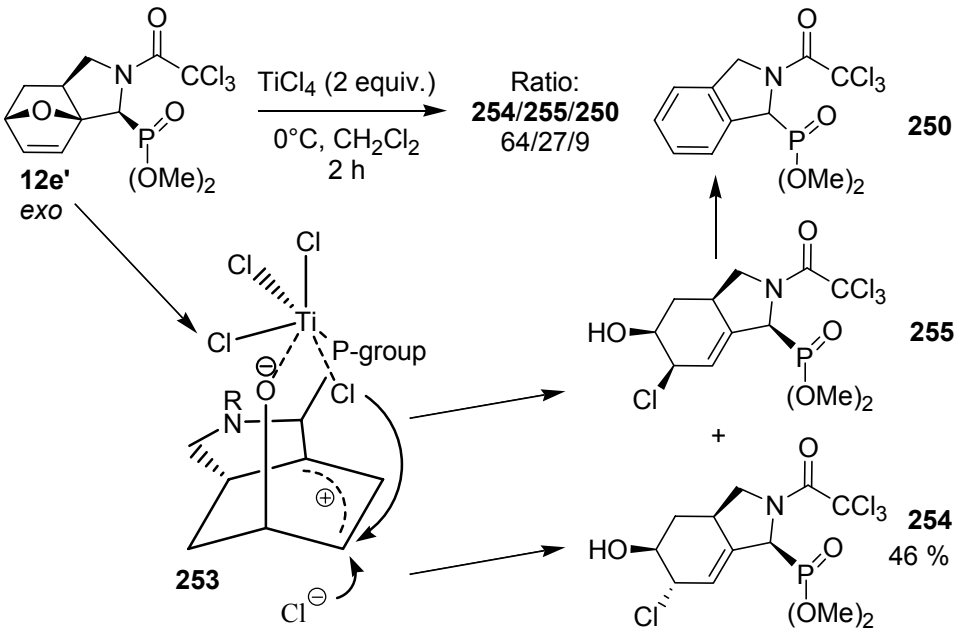

Scheme 96

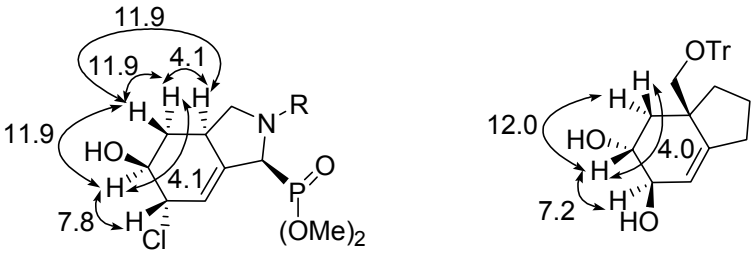

254, *trans*, major **256**

Figure 42. $^2J_{HH}$ coupling constants of the cyclohexene ring of the major isomer 254 and comparison with compound 256 from literature[213]

Given the complexation of the titanium catalyst with the oxygen bridge as depicted in Scheme 96, only the *cis* enantiomers **255** were expected, as they can be formed via an intramolecular reaction.[77] However, after chromatographical purification of the major compound and analysing the $^2J_{HH}$ coupling constants of the cyclohexene ring, the coupling of 7.8 Hz between the protons geminal to the hydroxyl and chloro substituent, indicates this

is the *trans* isomer. Comparison with literature data confirms this as shown in Figure 42, where a *trans* coupling of 7.2 Hz was observed.[213] The formation of the *trans* isomers requires the presence of free chloride ions. These can be formed via complexation of $TiCl_4$ with the amide or the phosphonate or by the presence of water. The use of a large excess of $TiCl_4$ catalyst slightly favoured the formation of the *trans* isomer: the *cis*/*trans* ratio was 23/70, leaving the possibility of chloride formation by functional group complexation. The crystalline adduct **12e'** showed a broad singlet at 1.56 ppm in the ^{1}H NMR that accounted for almost 0.5 equivalents of intercrystalline water. Attempts to remove it by drying with $MgSO_4$ or storing on P_2O_5 were not successful.

To evaluate the temperature effect on the product ratio, the reaction was stirred for 1 hour at -46°C. Formation of aromatics is most probably initiated by an elimination reaction and lowering the temperature would reduce the entropy contribution to the Gibbs free energy. Unfortunately, tiny peaks of the dihydroisoindole **250** appeared in the aromatic region at 7.35 and 7.55 ppm in the ^{1}H NMR, with still 35 % unreacted adduct **12e'** left. The ratio of the two epimers **254** and **255** was 72/28. Lowering the temperature slightly favours the intermolecular addition of the chloride ion. A decrease of the temperature, makes $-T\Delta S$ less positive, which makes the free energy of the addition reaction more negative. The intermolecular reaction has a larger, negative entropy and a lower reaction temperature will favour the intermolecular addition of the chloride ion.

The *endo* isomer **12e''**, was ring opened under the same reaction conditions. In this case no aromatic products were formed. Both products were purified by column chromatography. Again, the relative stereochemistry of the hydroxyl group and the chloro substituent was determined by the $^2J_{HH}$ coupling constants of their geminal protons and these are given in Hertz in Scheme 97. A coupling constant of 8 Hz points at an almost diaxial position of the hydrogen atoms, which is only possible for the *trans* isomer. Normally the diaxial coupling is between 10 and 13 Hz, but the two vicinal equatorial substituents reduce it. For the *cis* isomer a $^2J_{HH}$ coupling of 3.3 Hz is found, slightly larger than the usual 2 Hz. According to the ^{1}H NMR spectrum, about 15 % of intercrystalline water was present. This experiment suggests that a reduction of the water content of the reagent reduces the formation of the *trans* isomers and eliminates aromatization.

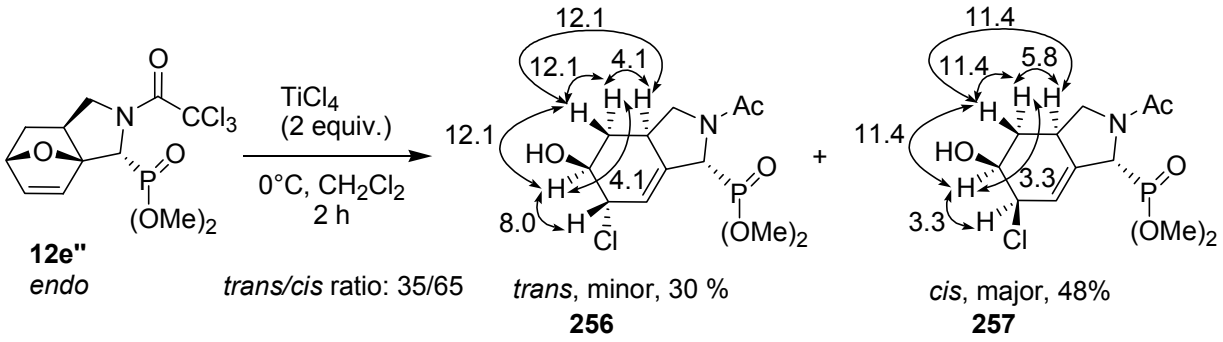

Scheme 97

Therefore, an attempt was made to perform the ring opening with $TiCl_4$ and to capture the free HCl with Et_3N. In literature, the compatibility of these reagents is described in the synthesis of titanium enolates from the corresponding carbonyl precursors with $TiCl_4$ and a tertiary amine base.[214] The addition of $TiCl_4$ precedes the addition of the base, leaving some time to allow complexation with the substrate before the base can bind irreversibly to the titanium catalyst. Titanium complexation was evaluated at -78°C for 10 minutes and was followed by addition of Et_3N. After leaving the reaction at 0°C for 2 hours, mainly starting material was recovered.

Preliminary experiments using $Yb(OTf)_3$ under the conditions of reference 215 only resulted in the isolation of starting material.

2.5.2 Computational Study of the Ring Opening

The reactions with Lewis acids $TiCl_4$ and $FeCl_3$ gave different, mainly non-aromatized reaction products. Different ways of complexation of the catalysts with oxanorbornene **12e'** were modelled to get an idea of the type of complex and its possible influence on the reaction. Then, the main pathways given in Scheme 96 and Scheme 88 were investigated computationally.

Computational details

All ab initio calculations were carried out with the GAUSSIAN 03 software package,[150] except for the calculation of the B3LYP-D[216] Van der Waals corrections that were calculated with ORCA 2.6.35.[217]

The geometries have been optimized at the B3LYP[151] level of theory (LOT) with a LanL2DZ[218] potential for the transition metals and a 6-31g(d)[153] basis set for the remaining atoms. This basis set is referred to as BS_1. As a check for the presence of spin contamination, the difference between the expectation value of the total spin $<S^2>$ was verified to differ from s(s+1) by less than 10%, where s equals 1/2 times the number of unpaired electrons. This was followed by frequency calculations that confirmed the nature of the stationary points and that were used in the thermochemical analysis.

Single point calculations were performed using a larger basis set: 6-311+g(3df)[219] for Ti or Fe and 6-311+g(d)[220] for the other atoms, which will be referred to as BS_2.

Different levels of theory (LOTs) have been used to model systems in which both main group elements and first row transition metals are present.[196] MP2[154] geometry optimizations have been done for small catalytic systems.[230] In this study they were used to model the catalyst dimers and catalyst solvent interactions, but they were too computationally demanding for the larger complexes. For these complexes, only single point energies were calculated at an MP2 LOT. The role of dispersion interactions was evaluated by calculating the B3LYP-D Van der Waals correction term.[216] This is an empirical $-C_6R^{-6}$ correction term that is added to the B3LYP functional to correct for the dispersion interactions. In more general terms this approach is defined as the DFT-D methodology and has been proven very successful in many different situations.

In literature, the performance of density functionals to study systems involving both first row transition metals and main group elements has been evaluated.[221,222,223,224] The TPSS[225] and TPSSh[226] functionals gave promising results.[222,224] The success of TPSSh was ascribed to the 10 % exact exchange by Jensen. In this thesis, this functional is mostly used with a 6-311+g[219] basis for the transition metals and a 6-31g(d)[153] basis for the other atoms, which is referred to as BS_3.

The bonding interactions of the catalyst monomers and the oxanorbornene **12e'** have been analyzed with the energy decomposition scheme of the program package ADF.[227] This was done on the B3LYP/BS_1 optimized structures. For the calculations in ADF, the non-hybrid BLYP functional was used with a DZP basis set for C, H and N, a TZ2P basis set for P, O and Cl, as these are the more crucial part of the ligands, and a TZ2P+ basis for the transition metals.

The bond dissociation energy (ΔE) between the Lewis acid and the oxanorbornene **12e'** is partitioned into several contributions to which a physical meaning can be given. First, ΔE is

separated into ΔE_{prep} and ΔE_{int}. ΔE_{prep} is the energy to promote the fragment from its equilibrium geometry to the geometry in the complex, and ΔE_{int} is the interaction energy between the fragments. This ΔE_{int} is further divided into three components: the electrostatic interaction energy, ΔE_{elstat}; the repulsive interaction ΔE_{Pauli} and the stabilizing orbital interaction term ΔE_{oi}.

$$\Delta E = \Delta E_{prep} + \Delta E_{int}$$

$$\text{with} \quad \Delta E_{int} = \Delta E_{elstat} + \Delta E_{Pauli} + \Delta E_{oi}$$

The fragments used for the bonding analysis, must be spin-restricted. As Fe(III) has five unpaired electrons, an unrestricted fragment was needed. Therefore, the same orbitals as in the restricted fragment were used, but the 5d-orbitals were occupied each by one electron. The unrestricted fragment that was built in this way, was used for the bonding analysis, although it is not self-consistent. Therefore, a correction term was added to the complexation energy. This was estimated as the opposite of the energy that was obtained by relaxing the unrestricted fragment to self-consistency.

Multiplicity of the catalysts

One of the difficulties in studying transition metal catalysts is the determination of their proper spin state. The periodic table is filled in the order [Ar] $4s^2$ $3d^{10}$, which is true for isolated metal atoms, but when a metal is surrounded with ligands, the d orbitals drop in energy and are filled first. Therefore, the electronic configuration of Fe(0), Fe with oxidation state zero, is [Ar] $4s^0$ $3d^8$; Fe(III) is [Ar] $4s^0$ $3d^5$ and Ti(IV) is [Ar] $4s^0$ $3d^0$. So, the tetrahedral $TiCl_4$ monomer has spin zero and thus multiplicity one.

The $FeCl_3$ catalyst has a high-spin ground state. It prefers a half-filled d shell and has multiplicity 6. This was reported in literature[228] and was verified by us at a HF/6-31g(d) level of theory. The bonds are formed using the Fe 4s and Cl 3p orbitals. The Fe 3d orbitals participate little in the bonding since they are much lower in energy than the Fe 4s and Cl 3p orbitals and much higher in energy than the Cl 3s orbital.[228] The dimer Fe_2Cl_6 has multiplicity 11, as we evaluated at HF/6-31g(d).

Benchmarking study

Before investigating the complexation between the oxanorbornene and the organometal catalysts, a LOT study was done. The performance of different levels of theory was evaluated for the geometry prediction of the seven-membered ring chelate structure of

diester **258** with $TiCl_4$ (Figure 43). X-ray data of this complex were published by Helmchen et al.[229]

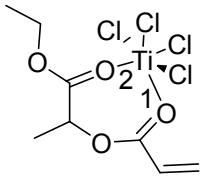

258

Figure 43. Complex between allyl lactate 258 and $TiCl_4$

Table 12. Experimental and computed distances (Å) for complex of 258 with $TiCl_4$ at different levels of theory. The bonds are indicated in Figure 43.

	TiO 1	TiO 2	average TiCl
Ref 229	2.109	2.136	2.26
B3LYP/BS_1	2.245	2.261	2.25
MP2/BS_1	2.247	2.250	2.23
TPSS/BS_3	2.206	2.237	2.27
TPSSh/BS_3	2.195	2.225	2.27
TPSSh/BS_2	2.196	2.234	2.26

The distances between Ti and its ligands were used as benchmark (Table 12). B3LYP and MP2 gave comparable distances, but overestimate the Ti-O bond lengths. The use of a larger basis set at MP2 (BS_2) only resulted in reduction of the bond length by 0.02 Å. So, the MP2 LOT will only be used for single point energy calculations on the B3LYP/BS_1 optimized geometries of the complexes.

The TPSS(h) functionals gave a little better results than B3LYP. The hybrid TPSSh is slightly preferred over its non-hybrid analogue and the smaller basis set BS_3 without extra polarization functions on the metals gave the same results as BS_2.

Keeping this in mind, the geometry optimizations were done at TPSSh/BS_3 and at B3LYP/BS_1.

No experimental data were found for a benchmarking study on the complexation energy. To evaluate long-range interactions, the dimerisation energy of the $TiCl_4$ catalyst computed at a CCSD(T)//MP2 level with an SBKP pseudopotential[230] was taken as a reference. These calculations are very sensitive towards the inclusion of dispersion interactions and B3LYP and TPSSh completely fail to reproduce these.

Table 13. Computed distances (Å) and dimerisation energy (kJ/mol) for the $TiCl_4$ dimer at different levels of theory.

	Ti-Cl	Ti- - Cl	Dimerisation Energy
Ref 229	2.17	4.51	-19.25
B3LYP/BS_1	2.16	6.05	-0.20
B3LYP/BS_3	2.19	6.05	-0.47
MP2/BS_1	2.16	2.53	-18.91
TPSSh/BS_3	2.18	5.30	-2.22

Dimerization and solvation

Next the dimerization and solvation energies were evaluated by optimization at a B3LYP and an MP2 LOT (Table 14). Within the dimer the geometry of the $TiCl_4$ moiety is hardly distorted from that of the monomer (Figure 44). The very low interactions of the dimer are apparent at the MP2 LOT (-19 kJ/mol, Table 14). The dimers are weakly bound Van der Waals complexes. Other computational studies confirm this low interaction energy.[230,231] $TiCl_4$ was shown to maintain its tetrahedral structure, even in bulk solvent.[231]

Solvation with one or two CH_2Cl_2 molecules did not cause any change in the conformation of the Lewis acid and positive solvation energies were obtained (Table 14). These low interactions are also reflected in the long distances between the molecules (Figure 44a and b).

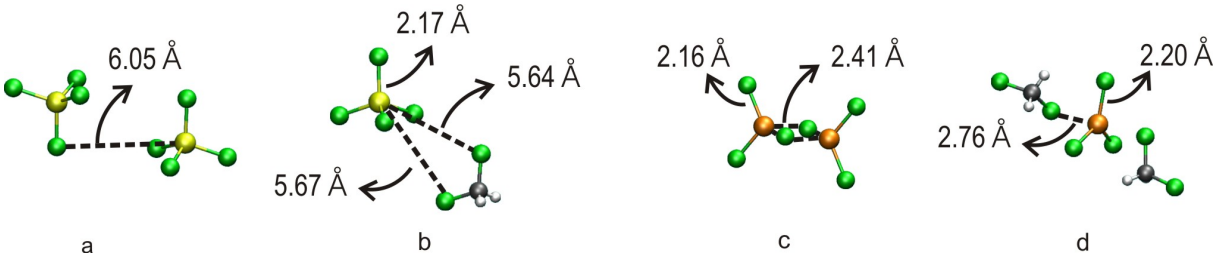

Figure 44. Dimer of the $TiCl_4$ (a) and $FeCl_3$ (c) catalyst and monosolvated $TiCl_4$ (b) and disolvated $FeCl_3$ (d) catalyst, with the respective bond lengths calculated at B3LYP/BS_1.

The $FeCl_3$ monomer is trigonal planar and is stabilized by solvent interactions (Figure 44d).[199] A second solvent molecule results in a further stabilization at MP2, but not at B3LYP (Table 14). According to an ab initio study at the HF LOT by Curtiss et al., the dimeric form of the catalyst has a tetrahedral geometry (Figure 44c). The two tetrahedra share a common edge, corresponding with a global D_{2h} symmetry.[232]

Table 14. Dimerisation and solvation energies with CH_2Cl_2 of the different catalysts in kJ/mol at the B3LYP/BS_1 and the MP2/BS_1 LOTs

	$TiCl_4$		$FeCl_3$	
Process	B3LYP	MP2	B3LYP	MP2
Dimerisation	-0.2	-19	-123	-171
Mono-solvation	19	8	-28	-40
Di-solvation	36	15	-27	-63

The catalyst dimer shows a strong interaction that is larger than the solvation energy. This explains the low solubility of the catalyst and is a possible explanation for the necessity of slightly higher reaction temperatures. The dimerisation and solvation energies change, however, a lot with the different LOTs. Mössbauer spectroscopy data show that $FeCl_3$ occurs as a monomer in very polar solvents with a high donicity like ethanol, but takes the dimeric or oligomeric form in solvents with a lower donicity.[233] Therefore, the reaction pathway with the $FeCl_3$ catalyst will be investigated with both the monomeric and the dimeric iron catalyst and solvent effects will be verified; whereas for the $TiCl_4$ catlyst, the latter will be less important.

Complex Formation

Next the complexation between oxanorbornene **12e'** and both Lewis acid monomers was evaluated at different positions at B3LYP/BS_1. Both catalysts prefer coordination towards the most electronegative P=O oxygen atom over coordination towards the amide by about 35 kJ/mol. A bidentate coordination (Figure 45) to the phosphonate and the oxygen bridge is slightly more stable (3 kJ/mol for $TiCl_4$ and 7 kJ/mol for $FeCl_3$).

The Ti catalyst takes an octahedron-like structure in the complex with the oxanorbornene **12e'**. This octahedral coordination of the $TiCl_4$ catalyst has been reported before (Figure 45a). An ab initio (HF and MP3) study on the complexation of $TiCl_4$ with formaldehyde showed that formation of a six-coordinate complex via coordination of two carbonyl compounds is energetically preferred over a 1:1 complex.[196] Experimental NMR spectroscopy[234] and X-ray absorption[235] studies confirm the formation of chelate intermediates with bidentate ligands (keto esters, alkoxy ketones or alkoxy aldehydes). Octahedral 1:1 complexes are formed, which is in accordance with our computational results.

The absolute complexation energies using the LANL2DZ pseudopotential were positive in case of the titanium catalyst (Table 15), while this is an exothermic reaction.[138] Therefore, the energies of the most stable, bidentate complexes were calculated without the use of an effective core potential (ECP) and at a larger basis set (BS_2). MP2 single point calculations give a complexation energy that is 46 kJ/mol lower in energy than the sum of the B3LYP dispersion correction and the B3LYP/BS_2 single point calculation. Optimization at TPSSh gives a complexation energy that is about the same as the one computed at B3LYP/BS_2// B3LYP/BS_1.

Table 15. Complexation energies of the $TiCl_4$, the monomeric and dimeric $FeCl_3$ catalysts (kJ/mol) with oxanorbornene 12e' calculated at different LOTs.

	$TiCl_4$-**12e'**	$FeCl_3$-**12e'**	Fe_2Cl_6-**12e'**
B3LYP/BS_1	9	-103	-76
B3LYP-D dispersion correction	-50	-37	-57
B3LYP/BS_2// B3LYP/BS_1	-53	-154	-114
MP2/6-311+g*// B3LYP/BS_1	-149	-239	-233
TPSSh/BS_3	-41	-120	-84

Iron(III) can coordinate three to eight ligands and often exhibits an octahedral coordination.[236] In this study, the Fe catalyst has a coordination number of 5 and has a trigonal bipyramidal structure. When an extra solvent molecule was added, it did not coordinate to the catalyst. Also in this case the MP2 single point calculation gives a larger complexation energy than the dispersion corrected B3LYP/BS_2 calculation.

For both catalysts the metal-Cl bond distances increase upon complexation. The average length of the Ti-Cl bond increases from 2.16 to 2.25 Å and the Fe-Cl distances increase from 2.16 to 2.23 Å for the B3LYP/BS_1 optimized complexes with the catalyst monomers. For these complexes, the distance between Ti and the oxygen bridge is 0.59 Å smaller than between Fe and the ethereal bridge. The complexation energies computed at B3LYP/BS_2 // B3LYP/BS_1 or TPSSh/BS_3 are also three times as large for the monomeric $FeCl_3$ catalyst than for $TiCl_4$ (Table 15). The complexation energy for the dimeric Fe_2Cl_6 catalyst was two times as large. Stabilization of the Fe catalyst by solvent interactions will further reduce the difference in complexation energy between the Ti and Fe catalyst.

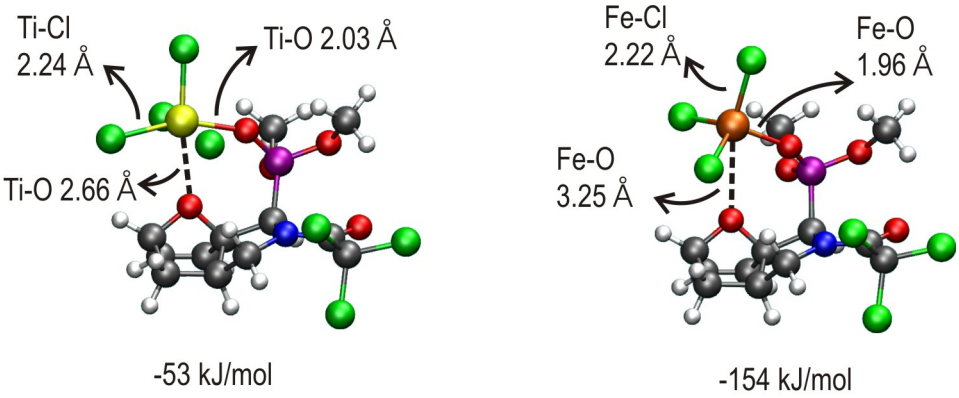

Figure 45. Most stable, bidentate complexes between oxanorbornene 12e' and the $TiCl_4$ (a) and $FeCl_3$ (b) catalyst. The bond lengths computed at B3LYP/BS_1 are given. The complexation energy (kJ/mol) was computed at B3LYP/BS_2 // B3LYP/BS_1.

To explain the difference in the complexation energy of the catalyst and the oxanorbornene **12e'**, the bonding interactions have been analyzed with the energy decomposition scheme implemented in ADF[227] (Table 16).

Table 16. Energy decomposition analysis of the Lewis acid monomers and oxanorbornene 12e' (kJ/mol)

		$TiCl_4$-**12e'**	$FeCl_3$-**12e'**
ΔE_{prep}	ΔE_{prep}(Catalyst)	108	29
	ΔE_{prep}(**12e'**)	25	16
	Total ΔE_{prep}	133	46
ΔE_{int}	ΔE_{elstat}	-353	-295
	ΔE_{Pauli}	439	339
	ΔE_{oi}	-232	-234
	Total ΔE_{int}	-146	-190
Correction			37
ΔE		**-12**	**-107**

This showed that the preparation energy for the Ti-catalyst is much larger than that for the Fe-catalyst. This is possibly caused by the repulsion between the larger number of ligands of the Ti-catalyst. The preparation energy was the main reason for the difference between the complexation energies.

Analysis of the interaction energy showed that there is a larger electrostatic interaction between $TiCl_4$ and the ligand **12e'** than between $FeCl_3$ and **12e'**. The Pauli repulsive

interactions between the fragments, which are caused by the fact that two electrons with the same spin cannot occupy the same space, were also much larger for the $TiCl_4$-complex than for the $FeCl_3$-complex. The orbital interaction terms were about the same.

The electrostatic term can be associated with the ionic bonding and the orbital interactions with the covalent contributions to the bonding.[237] The ratio of ΔE_{elstat} / ΔE_{oi} indicated that the complexation with $TiCl_4$ has a larger ionic character than the complexation with $FeCl_3$.

Ring Opening

Once the most stable complexes were identified different reaction pathways for both catalysts were evaluated.

For the $TiCl_4$ catalyzed reaction, three pathways were investigated. (1) The minor product is formed via a concerted C-O bond breaking and chloride transfer from the catalyst to the double bond as shown in Figure 46, pathway 1. An IRC calculation confirmed the concerted character of this transition state (TS **1**). (2) The energy barrier for the ring opening of the other side of the oxygen bridge was 21 kJ/mol higher than that of pathway 1 at the B3LYP/BS_1 LOT. (3) The major product can be formed via addition of free chloride anions to the $TiCl_4$ complex **253**, shown in pathway 2 in Figure 46. These chloride anions result either from a strong interaction between $TiCl_4$ and the phosphonate with elimination of chloride or from the reaction of intercrystalline water with the catalyst. After opening of the oxygen bridge, the product is formed after a fast oxidation of the catalyst with ice water.

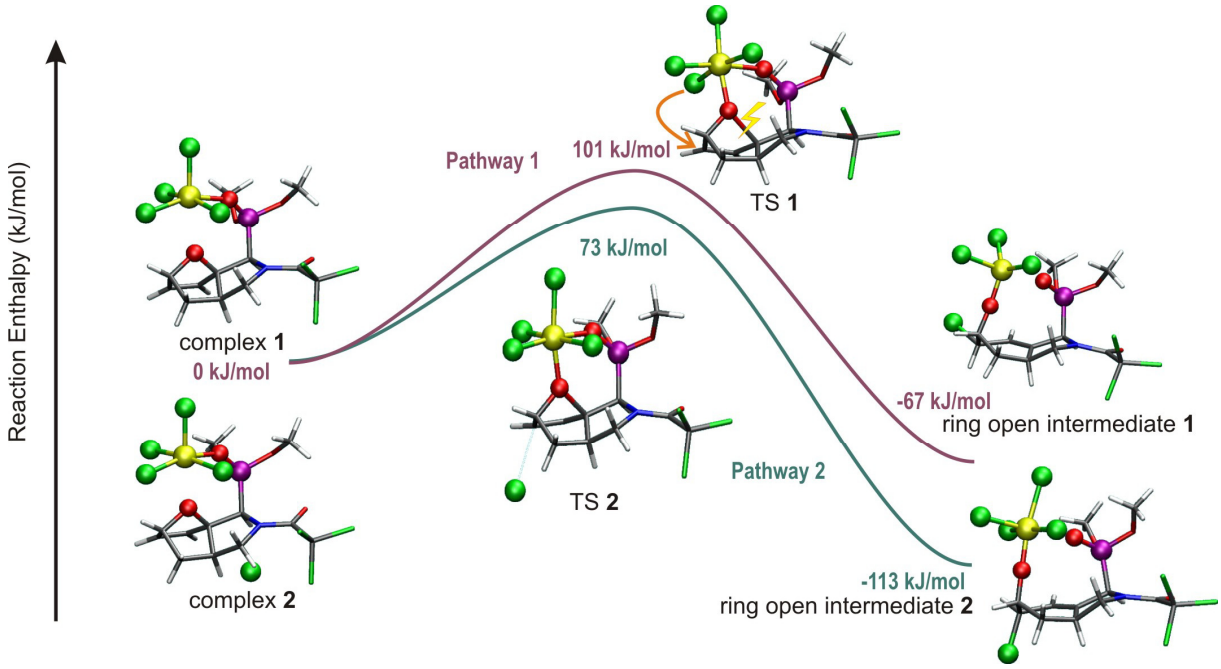

Figure 46. Reaction profile for the ring opening of oxanorbornene 12e' with $TiCl_4$. The reaction enthalpies (ΔH) (kJ/mol) at 273.15K were computed at the B3LYP/BS_1 LOT.

Table 17. The uncorrected electronic energies (ΔE) and reaction enthalpies (ΔH) (kJ/mol) at 273.15K for pathways 1 and 2 relative to the respective complexes 1 and 2 for the ring opening with $TiCl_4$

$TiCl_4$	Pathway 1				Pathway 2			
	TS		Product		TS		Product	
LOT	ΔE	ΔH	ΔE	ΔH	ΔE	ΔH	ΔE	ΔH
B3LYP/ BS_1	108	101	-68	-67	78	73	-116	-113
B3LYP-D dispersion correction	-8		2		5		6	
MP2/6-311+g* // B3LYP/ BS_1	122		-38		118		-84	
B3LYP/ BS_2 // B3LYP/ BS_1	98		-65		77		-109	
TPSSh/ BS_3	103	96	-38	-37	71	67	-99	-97

The energies of the ring opening at different LOTs are given in Table 17. The energy barrier for pathway **2**, which leads to the major product is clearly lower than that of pathway **1**. Although, both pathways start from a different complex and an external chloride anion is involved in pathway **2**, it will definitely compete with the formation of minor product **255**. Comparison of the reaction enthalpies gives a similar conclusion.

The electronic energy barriers computed at B3LYP and TPSSh are close to each other. The energies at MP2 are much higher. This is most probably due to the underestimation of the

oxanorbornene stability at B3LYP. Another explanation would be that MP2 is known to overestimate binding energies.

The ring opening of the oxygen bridge with ferric chloride was modelled using the catalyst dimer. When the oxygen bridge is broken, the bond between the alkoxide and iron tightens, and the distance between this iron atom and the phosphonate oxygen increases, but no chloride ion is eliminated from the Lewis acid. Instead, the carbocation is stabilized by formation of a 3-membered epoxide (Figure 47, pathway 3). This intermediate was also observed when the catalyst monomer was used in the model. The energy of the epoxide is about the same as the energy of the starting complex **3** when the catalyst dimer is modelled or almost 50 kJ/mol less stable if the monomeric catalyst is used. This difference is most probably due to the reduced stability of the dimeric complex **3**, in which the stabilization of the second $FeCl_3$ molecule via complexation is limited. Stabilization of the transition state by one or two solvent molecules was evaluated, but these did not stabilize the carbocation and could not avoid epoxide formation.

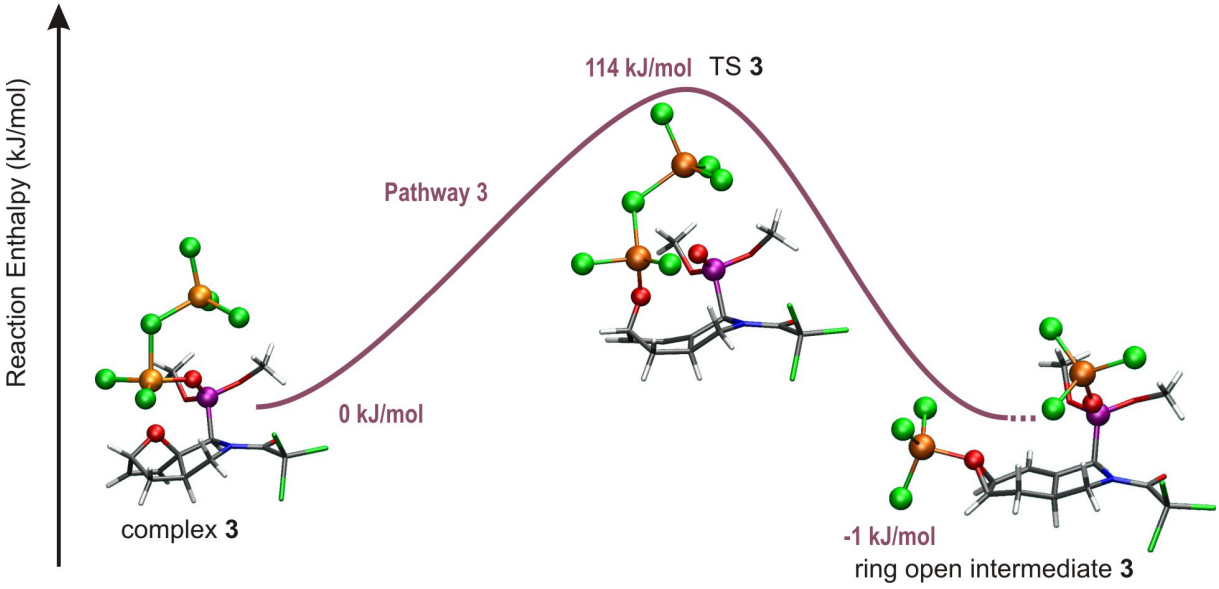

Figure 47. Reaction profile for the ring opening of oxanorbornene 12e' with $FeCl_3$. The reaction enthalpies (ΔH) (kJ/mol) at 313K were computed at the B3LYP/BS_1 LOT.

Table 18. The uncorrected electronic energies (ΔE) and reaction enthalpies (ΔH) (kJ/mol) at 313 K for pathway 3 relative to the respective complexes for the ring opening with the $FeCl_3$ monomer and dimer.

$FeCl_3$	Dimer				Monomer			
	TS		Product		TS		Product	
LOT	ΔE	ΔH	ΔE	ΔH	ΔE	ΔH	ΔE	ΔH
B3LYP/BS_1	122	114	-2	-1	135	127	51	51
B3LYP-D dispersion correction	0		20		-9		13	
B3LYP/ large // B3LYP/BS_1	118		-15		140		45	
MP2/6-311+g* // B3LYP/ BS_1	193		62		184		112	
TPSSh/BS_3	135	127	3	5	142	135	50	50

Possible further reaction paths involve a 1-step 1,2-hydride shift of the epoxide **259** or ring opening of the epoxide and a 1,2-hydride shift from *C*(7) to *C*(8) (first pathway in Scheme 98) or deprotonation of *C*(7) followed by keto-enol tautomerism (second pathway in Scheme 98). The latter pathway was proposed by Namboothiri et al.[51] Under the Lewis acidic conditions, however, it is less probable to happen.

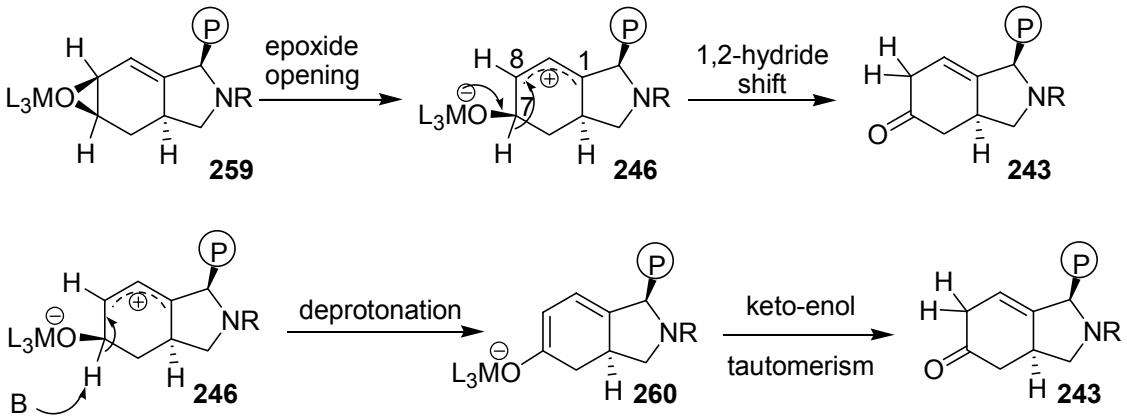

Scheme 98

The 1-step 1,2-hydride shift was evaluated, but a pseudo IRC analysis of the pathway at B3LYP/BS_1 predicted a large barrier of about 350 kJ/mol for this reaction.

The mechanism of a 2-step acid-induced rearrangement of epoxides to ketones has been proved experimentally and computationally.[238] Also for this Lewis acid catalyzed reaction, this is the preferred pathway. The reaction was modelled with the $FeCl_3$ monomer, as the second $FeCl_3$ molecule coordinates to the phosphonate group in ring-open intermediate **3** in

Figure 47 and will have a negligible influence on the further reaction pathway. The energy profile is drawn in Figure 48 and the corresponding energies are given in Table 19. The first step is the ring opening of the epoxide **259** (intermediate **4** in Figure 48) with formation of intermediate **5** in which the carbocation is stabilized by one of the chloride ligands of the Lewis acid. This step has an electronic energy barrier of 46 to 60 kJ/mol depending on the functional. So, whether the epoxide is formed as an intermediate or not, the pathway via a hydride shift remains possible.

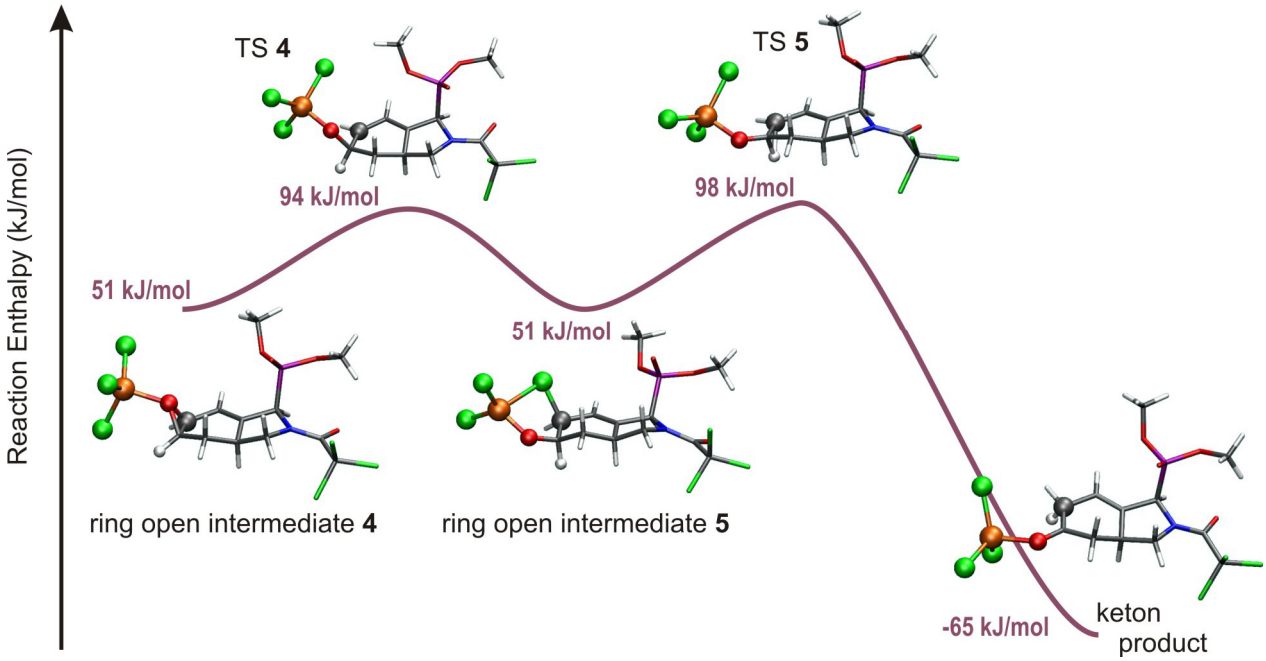

Figure 48. Reaction profile for the 2-step 1,2-hydride shift of epoxide 259 (ring-open intermediate 4) with the $FeCl_3$ monomer. The reaction enthalpies (ΔH) (kJ/mol) at 313K were computed at the B3LYP/BS_1 LOT.

Table 19. The uncorrected electronic energies (ΔE) and reaction enthalpies (ΔH) (kJ/mol) at 313 K relative to the $FeCl_3$-12e' oxanorbornene complex for the 2-step 1,2-hydride shift of epoxide 259 with the $FeCl_3$ monomer.

$FeCl_3$	Intermediate **5**				Product			
	TS **4**		Intermed **5**		TS **5**		Product	
LOT	ΔE	ΔH	ΔE	ΔH	ΔE	ΔH	ΔE	ΔH
B3LYP/BS_1	100	94	51	51	111	98	-64	-65
B3LYP-D dispersion correction	10		11		11		17	
B3LYP/ large // B3LYP/BS_1	94		50		101		-76	
TPSSh/BS_3	110	104	63	63	122	109	-48	-49

The next step is the 1,2-hydride shift with formation of the experimentally observed product, ketone **243** with an energy barrier of 51 to 59 kJ/mol. For the different functionals and basis sets, this barrier is much lower than the barrier for the ring opening of the oxanorbornene.

When the two catalysts are compared, one can see that the energy barrier for breaking the *C-O* bond with $FeCl_3$ is larger than with $TiCl_4$. This corresponds with the experimental observation that the titanium catalyzed reaction completes at 0°C and the reaction with the iron catalyst requires reflux conditions in CH_2Cl_2. The distances between *O*(10) and *C*(1) show that the iron catalyzed reaction has a later transition state, which is in accordance with the Hammond postulate.

Table 20. Bond distances (Å) calculated at B3LYP/BS_1 for the stationary points of the 3 pathways shown in Figure 46 and Figure 47. M is Ti or Fe; *O*(10) is the oxabridge and C(1)-O(10) the bond that is broken.

		M-O(10)	C(1)-O(10)	M-O(=P)
Complex 1	$TiCl_4$	2.66	1.45	2.03
Complex 2	$TiCl_4$ and Cl^-	2.38	1.48	1.97
Complex 3	$FeCl_3$ dimer	2.36	1.46	1.95
	$FeCl_3$ monomer	3.25	1.44	1.96
TS 1	$TiCl_4$	2.03	2.05	2.14
TS 2	$TiCl_4$ and Cl^-	2.01	1.84	2.09
TS 3	$FeCl_3$ dimer	1.86	2.71	2.67
	$FeCl_3$ monomer	1.92	2.38	2.81
Intermed 1	$TiCl_4$	1.75	2.95	2.19
Intermed 2	$TiCl_4$ and Cl^-	1.79	3.09	2.24
Intermed 3	$FeCl_3$ dimer	2.05	3.22	6.76
	$FeCl_3$ monomer	2.04	3.23	6.58

The main difference between the $TiCl_4$ and $FeCl_3$ as Lewis acids in the opening of the oxanorbornene oxygen bridge is their way of stabilizing the oxide anion. When the *C*(1)-*O*(10) bond is broken, the bond between the alkoxide anion and the transition metal tightens. In pathway 1 with $TiCl_4$, the alkoxide replaces a chloride that adds to the allyl cation in a concerted way. With $FeCl_3$, however, the carbocation is stabilized by the

alkoxide anion itself and no chloride transfer occurs; instead, the bond with the phosphonate is broken.

This can be linked with existing stability correlations for coordination compounds.[239] Following the classification of cationic species by Chatt, Ahrland and Davies, Ti is a 'class a' compound that forms more stable complexes with ligands in which the coordinating atom is a first-row element (N, O, F) than those of an analogous ligand in which the donor is a second-row element (P, S, Cl).[240] This was later extended to the HSAB (hard-soft acid-base) principle by Pearson.[241] Both Ti(IV) and Fe(III) lewis acids and the oxide and chloride ligands are hard atoms according to this chemical hardness classification. The features which bring out a 'class a' behaviour are small size and a high positive oxidation state or charge.[241] Thus, the oxide anion is a harder ligand than the chloride and Ti(IV) is expected to be harder than Fe(III). According to the ionic-covalent theory, 'class a' acids are assumed to bind bases with primarily ionic forces.[241] The bond analysis of the complexes has indeed shown that the Ti-complex has a larger ionic character. Thus, the relatively better stabilization of the oxide anion by the catalyst causes the different behaviour of the catalyst and in that way a different product formation.

Conclusion

Different reaction conditions were found for the ring opening of the oxanorbornene **12e'** and some analogues, as shown in Scheme 99. The use of $FeCl_3$ and $TiCl_4$ as Lewis acids resulted in the ring opening of the oxygen bridge without complete oxidation of the six-membered ring. Aromatization causes a loss of the stereocentres that were created by the stereoselectivity of the IMDAF reaction.

Coating of the Fe-catalyst on montmorillonite K10 eased the tedious work-up, but accelerated the aromatization.

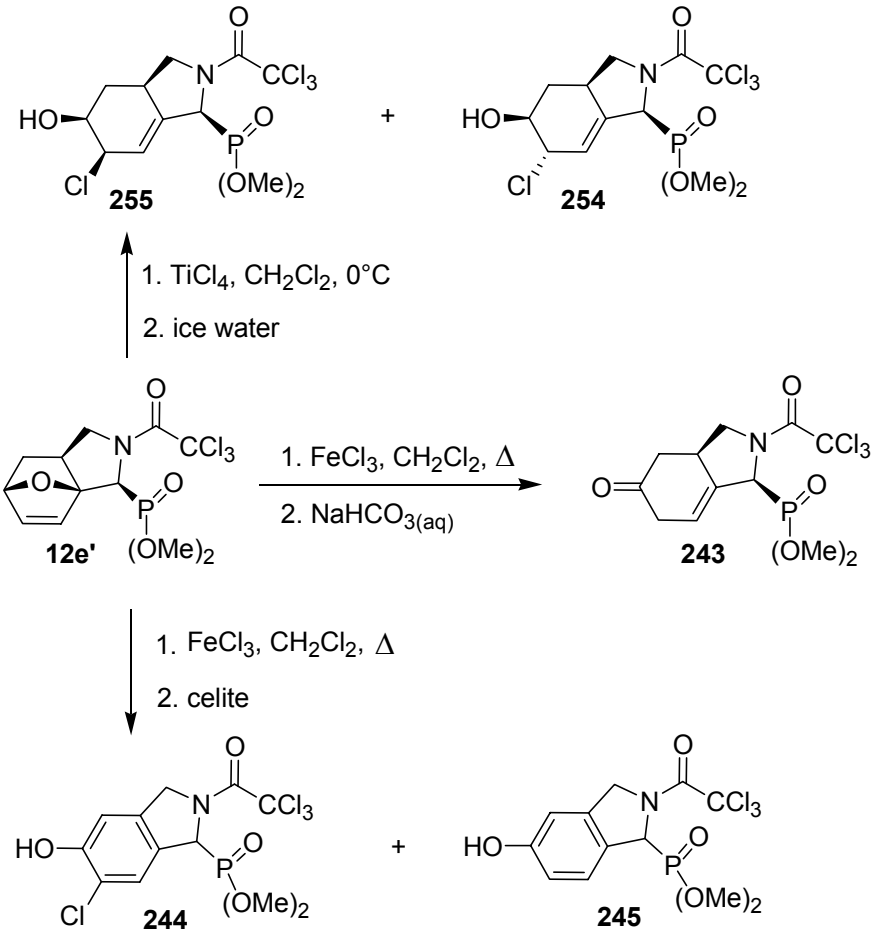

Scheme 99

The synthesized compounds contain the phosphonate analogue of a proline or glutamic acid skeleton. Proline determines the unique stereochemical structure of proteins and pyroglutamic acid is an important neurotransmitter. The bicyclic and ring-open structures can be useful in revealing the conformational requirements of biological receptors, e.g. L-glutamic-acid receptors, which play a role in neurodegenerate diseases like epilepsy, Huntington disease and Alzheimer.

The bonding of the transition metals with their ligands is a complex interplay between electrostatic interactions, donor-acceptor interactions between the ligand and the metal and formation of ligand group orbitals. Therefore, ab-initio calculations are ideal tools to study the result of these combined interactions. The different complexes between the oxanorbornenes and the transition metals were computationally investigated, as well as the pathways towards the different products. This ab-initio investigation revealed the mechanistic pathways and was able to reproduce the formation of the experimentally observed products.

The energy barrier was higher for the $FeCl_3$-catalyzed reaction than for the $TiCl_4$-catalyzed reaction. The different behaviour of both catalysts could be linked with their affinity to form complexes with oxide anions. Using $TiCl_4$, the alkoxide anion bound tightly to the metal and the bonding with one of the chloride ligands was weakened. This chloride anion was inserted in the heterocyclic ligand to neutralize the allylic carbocation. With $FeCl_3$ the oxide anion stabilized the allylic carbocation and the bond between the transition metal and the phosphonate was broken. This behaviour coincides with the stability correlation of complexes based on Pearson's HSAB principle. Ti(IV) is somewhat harder than Fe(III) and the bonding between Ti(IV) and its ligands has more ionic character.

Chapter 4 - Experimental Procedures

1 Instrumental Material

1.1 NMR Spectroscopy

^{1}H NMR spectra (300 MHz), ^{13}C NMR spectra (75 MHZ) and ^{31}P NMR spectra (121 MHz) were recorded with a Jeol Eclipse FT 300 NMR spectrometer. The compounds were diluted in deuterated solvents, with tetramethylsilane as internal standard. Peak assignments were accomplished by using COSY, DEPT, HSQC and HMBC spectra.

1.2 Infrared Spectrometry

Infrared spectra were measured with a Perkin-Elmer Spectrum One FT-IR spectrophotometer. For liquid samples, spectra were recorded by preparing a thin film of product between two sodium chloride plates. Solid compounds were mixed with potassium bromide and pressed at high pressure until a transparent disc was obtained. The recent infrared spectra were measured with a Perkin-Elmer Spectrum BX FT-IR System Spectrometer. Only selected absorbances (ν_{max}/cm^{-1}) were reported.

1.3 Mass Spectrometry

Low resolution mass spectra of pure compounds were recorded via direct injection on an Agilent 1100 Series LC/MSD type SL mass spectrometer with Electron Spray Ioniastion geometry (ESI 70 eV) and using a Mass Selective Detector (quadrupole). If crude reaction mixtures were analyzed, the mass spectrometer was preceded by an HPLC reversed phase column with a diode array UV/VIS detector.

1.4 Chromatographic Purification

Column chromatography was carried out using a glass column filled with silica gel (Acros, particle size 0.035-0.070 mm, pore diameter ca. 6 nm). Thin layer chromatography was performed on glass-backed silica plates (Merck Kieselgel 60 F_{254}, precoated 0.25 mm), which were developed using standard visualisation techniques or agents: UV fluorescence (254 nm and 366 nm), colouring with iodine vapours and permanganate solution.

1.5 Elemental Analysis

Elemental analyses were obtained by means of a Perkin Elmer 2400 Series II apparatus.

1.6 Melting Point

Melting points of crystalline products were measured with a Büchi B-540 apparatus.

1.7 Dry Solvents

Diethyl ether, tetrahydrofuran and toluene were distilled from sodium and sodium benzophenone ketyl. Dichloromethane was distilled over calcium hydride. Acetonitrile was distilled from calcium hydride and kept over molecular sieves.

1.8 Microwave Reactions

All microwave reactions were performed in the CEM Focused MicrowaveTM Synthesis System, Model Discover, with a selectable power output from 0-300 watts. The reactions were performed in 10 ml thick walled Pyrex reaction vessels closed with a Septa cap and equiped with a small stirring bar. The temperature control system uses a non-contact infrared sensor to measure temperature on the bottom of the vessel and is used in a feedback loop with the on-board computer to regulate the temperature from 25-250 °C by adjusting the power output (1 watt increments).

2 Synthesis of Hydantoin Derivatives

2.1 Alkylation of Pyroglutamates at *C*(2)

The alkyl pyroglutamate (14 mmol; 1 equiv.) and 1.5 equivalents of electrophile (21 mmol) were dissolved in 20 ml dry THF under an N_2-atmosphere. The mixtrure was cooled to -40°C in an acetone bath. LiHMDS (30 mmol; 2.1 equiv.; 1M solution in hexanes) was slowly added at this temperature. The mixture was stirred for an additional 1.5 hours at room temperature. The reaction was quenched by addition of saturated $NH_4Cl_{(aq)}$ until the pH was neutral. The mixture was extracted with EtOAc, and the organics were dried over $MgSO_4$ and filtered. The solvent and the excess of electrophile were removed under reduced pressure to deliver the pure product. In case that biselectrophiles were used, further purification by recrystallization or by column chromatography can be necessary.

The complete spectroscopic description of compounds **150a-b**, **151**, **159** and **160** were described in Paper II and Paper IV in Appendix 2.

2.2 One-pot Pyroglutamate-Hydantoin Rearrangement

The pyroglutamate ester (14.66 mmol) was dissolved in dry THF (70 mL) and 1 equivalent of the isocyanate was added with a syringe and stirred shortly. After addition of NaH (1.02 equivalents) the reaction mixture was stirred overnight at room temperature under a nitrogen atmosphere. The reaction was then quenched with saturated $NH_4Cl_{(aq)}$ solution until the pH was neutral or slightly acidic. The mixture was extracted 3 times with EtOAc, the organic layers were dried with $MgSO_4$ and filtered. It is important to work under completely dry circumstances. Use of excess of isocyanate caused partial carbamoylation of the formed hyantoin and those products need further purification via column chromatography.

For the more alkylated reagents or if traces of water are present, the one-pot reaction also starts in diethylether.

The complete spectroscopic description of compounds **122a-g** can be found in Paper IV in Appendix 2.

Methyl 3-(4-allyl-2,5-dioxo-1-propylimidazolidin-4-yl)propionate (144)

The synthesis of **144** was performed in ether.

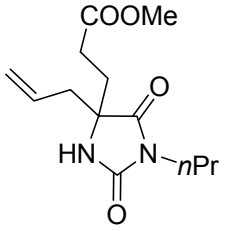

^{1}H NMR δ (300 MHz, $CDCl_3$, ppm): 0.92 (3H, t, J = 7.4 Hz, C<u>H</u>$_3$, propyl); 1.62 (2H, sextet, J = 7.4 Hz, C<u>H</u>$_2$CH$_3$); 2.03-2.22 (2H, m, CH$_2$C<u>H</u>$_2$C$_q$); 2.25-2.31 (2H, m, C(=O)C<u>H</u>$_2$); 2.39-2.54 (2H, m, CH$_2$, allyl); 3.44 (2H, t, J = 7.4 Hz, NC<u>H</u>$_2$); 3.67 (3H, s, OC<u>H</u>$_3$); 5.14-5.22 (2H, m, HC=C<u>H</u>$_2$); 5.59-5.74 (1H, m, <u>H</u>C=CH$_2$); 5.90 (1H, br s, N<u>H</u>). **^{13}C NMR δ (75 MHz, $CDCl_3$, ppm):** 11.28 (CH$_3$, propyl); 21.52 (<u>C</u>H$_2$CH$_3$); 28.51 (C(=O)<u>C</u>H$_2$); 31.05 (CH$_2$<u>C</u>H$_2$C$_q$); 40.38 (NCH$_2$); 41.55 (CH$_2$, allyl); 52.09 (OCH$_3$); 64.33 (C$_q$); 121.38 (HC=<u>C</u>H$_2$); 129.99 (H<u>C</u>=CH$_2$); 157.01 (C=O, urea); 173.27 (C=O); 175.24 (C=O). **IR ν (cm^{-1}):** 1712 (C=O); 1740 (C=O); 1775 (C=O); 3307 (NH). **MS m/z (%):** 269 (100, [M+H]$^+$). **Chromatography:** R_f = 0.31 (EtOAc/PE 1/1) **Yield:** 42 %. Yellow oil.

When 2 equivalents of isocyanate were used, the component **144** above was carbamoylated, under the same reaction conditions.

Methyl 3-(4-allyl-2,5-dioxo-1-propyl-3-propylcarbamoylimidazolidin-4-yl)propionate (145)

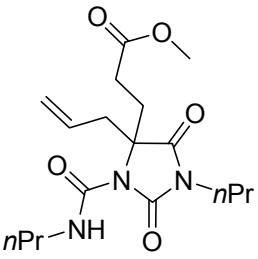

^{1}H NMR δ (300 MHz, $CDCl_3$, ppm): 0.93 (3H, t, J = 7.4 Hz, C$\underline{H}_3$, propyl); 0.96 (3H, t, J = 7.4 Hz, C$\underline{H}_3$, propyl); 1.53-1.69 (4H, m, 2 x C$\underline{H}_2$CH$_3$); 2.05-2.24 (2H, m, CH$_2$C$\underline{H}_2$C$_q$); 2.26-2.34 (1H, m, C(=O)C$\underline{H}_a$H$_b$); 2.57 (1H, dd, J = 7.2 Hz and J = 13.8 Hz, C$\underline{H}_a$H$_b$, allyl); 2.69-2.81 (1H, m, C(=O)CH$_a\underline{H}_b$); 3.17-3.29 (1H, m, CH$_a\underline{H}_b$, allyl); 3.19-3.36 (2H, m, NHC$\underline{H}_2$); 3.44 (2H, dt, J = 2.8 Hz and J = 7.3 Hz, NC$\underline{H}_2$); 3.64 (3H, s, OC$\underline{H}_3$); 5.08-5.18 (2H, m, HC=C$\underline{H}_2$); 5.41-5.55 (1H, m, $\underline{H}$C=CH$_2$); 8.08 (1H, t, J = 5.1 Hz, N$\underline{H}$). **^{13}C NMR δ (75 MHz, $CDCl_3$, ppm):** 11.28 (CH$_3$, propyl); 11.35 (CH$_3$, propyl); 21.25 (C$\underline{H}_2$CH$_3$); 22.88 (C$\underline{H}_2$CH$_3$); 28.93 (CH$_2$C$\underline{H}_2$); 30.18 (C$\underline{H}_2$CH$_2$); 39.39 (CH$_2$, allyl); 40.78 (NCH$_2$); 41.61 (NHCH$_2$); 51.87 (OCH$_3$); 69.25 (C$_q$); 121.31 (HC=C$\underline{H}_2$); 129.91 (H$\underline{C}$=CH$_2$); 151.10 (C=O, carbamoyl); 156.34 (C=O, urea, hydantoin); 172.22 (C=O); 173.44 (C=O). **IR ν (cm^{-1}):** 1696 (C=O); 1721 (C=O); 1776 (C=O); 3347 (NH). **MS m/z (%):** 354 (100, [M+H]$^+$). **Chromatography:** R_f = 0.47 (EtOAc/PE 1/3) **Yield:** 52 %. Yellow oil.

Ethyl 3-(1-allyl-3-allylcarbamoyl-2,5-dioxoimidazolidin-4-yl)-propionate (148)

This product was observed as a side-product of the carbamoylation reaction, because of the use of an excess of isocyanate.

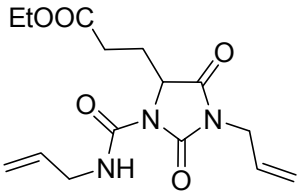

^{1}H NMR δ (300 MHz, $CDCl_3$, ppm): 1.24 (3H, t, J = 7.2 Hz, C$\underline{H}_3$); 2.30-2.50 (4H, m, C$\underline{H}_2$C$\underline{H}_2$); 3.94 (2H, m, NHC$\underline{H}_2$); 4.07-4.15 (2H, m, NC$\underline{H}_2$); 4.11 (2H, q, J = 7.2 Hz, OC$\underline{H}_2$); 4.64 (1H, dd, J = 2.1 Hz and J = 3.7 Hz, C$\underline{H}$); 5.17 (1H, qd, J = 1.4 Hz and J = 10.4 Hz, NHCH$_2$CH=C$\underline{H}_a$H$_b$); 5.23 (1H, qd, J = 1.4 Hz and J = 17.3 Hz, NHCH$_2$CH=CH$_a\underline{H}_b$); 5.27 (1H, d, J = 1.3 Hz, NCH$_2$CH=C$\underline{H}_a$H$_b$); 5.30 (1H, dd, J = 1.3 Hz and J = 16.5 Hz, NCH$_2$CH=CH$_a\underline{H}_b$); 5.82 (1H, dddd, J = 6.3 Hz, J = 6.3 Hz, J = 9.7 Hz and J = 16.5 Hz, NCH$_2$C$\underline{H}$=CH$_a$H$_b$); 5.88 (1H, dddd, J = 5.7 Hz, J = 5.7 Hz, J = 10.4 Hz and J = 17.3 Hz, NHCH$_2$C$\underline{H}$=CH$_a$H$_b$); 7.88 (1H, br t, J = 4.9 Hz, N$\underline{H}$). **^{13}C NMR δ (75 MHz, $CDCl_3$, ppm):** 14.15 (CH$_3$); 25.57 (C(=O)$\underline{C}$H$_2$); 28.82 ($\underline{C}$H$_2$CH); 41.19 (NHCH$_2$); 42.46 (NCH$_2$); 58.17 (CH); 60.75 (OCH$_2$); 116.51 (NHCH$_2$CH=$\underline{C}$H$_2$); 119.21 (NCH$_2$CH=$\underline{C}$H$_2$); 130.20 (NCH$_2\underline{C}$H=CH$_2$); 133.65 (NHCH$_2\underline{C}$H=CH$_2$); 150.71 (NHC=O,

urea); 155.35 (NC=O, urea); 170.60 (C=O, lactam); 172.01 (C=O, ester). **IR ν (cm^{-1}):** 1646 (C=C); 1701 (C=O); 1725 (C=O); 1781 (C=O); 3352 (br NH). **MS m/z (%):** 324.2 (100, $[M+H]^+$). **Chromatography:** R_f = 0.59 (EtOAc/PE 7/3) **Yield:** 5 %. Oil.

Benzyl 3-[4-(2-chloromethylallyl)-2,5-dioxo-1-propyl-3-propylcarbamoylimidazolidin-4-yl]propionate (154)

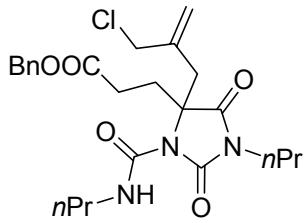

^{1}H NMR δ (300 MHz, $CDCl_3$, ppm): 0.90 (3H, t, J = 7.6 Hz, C<u>H</u>$_3$, propyl); 0.95 (3H, t, J = 7.4 Hz, C<u>H</u>$_3$, propyl); 1.48-1.66 (4H, m, 2 x C<u>H</u>$_2$CH$_3$); 2.04-2.36 (2H, m, CH$_2$C<u>H</u>$_2$); 2.31-2.39 (1H, m, C<u>H</u>$_a$H$_b$); 2.70 (1H, d, J = 14.0 Hz, C<u>H</u>$_a$H$_b$C=); 2.75-2.86 (1H, m, CH$_a$<u>H</u>$_b$); 3.12-3.36 (2H, m, NHC<u>H</u>$_2$); 3.36 (1H, d, J = 14.0 Hz, CH$_a$<u>H</u>$_b$C=); 3.33-3.52 (2H, m, NC<u>H</u>$_2$); 3.85 (2H, s, ClC<u>H</u>$_2$); 5.02 (1H, br s, C=C<u>H</u>$_a$H$_b$); 5.06 (2H, s, OC<u>H</u>$_2$); 5.30 (1H, br s, C=CH$_a$<u>H</u>$_b$); 7.28-7.39 (5H, m, C<u>H</u>$_{ar}$); 8.12 (1H, t, J = 5.5 Hz, N<u>H</u>). **^{13}C NMR δ (75 MHz, $CDCl_3$, ppm):** 11.29 (CH$_3$, propyl); 11.40 (CH$_3$, propyl); 21.22 (<u>C</u>H$_2$CH$_3$); 22.91 (<u>C</u>H$_2$CH$_3$); 28.99 (CH$_2$<u>C</u>H$_2$); 30.73 (<u>C</u>H$_2$CH$_2$); 38.09 (C$_q$<u>C</u>H$_2$C$_q$=); 40.88 (NCH$_2$); 41.72 (NCH$_2$); 47.80 (Cl<u>C</u>H$_2$); 66.81 (OCH$_2$); 69.13 (<u>C</u>$_q$CH$_2$); 120.46 (C=<u>C</u>H$_2$); 128.48 (3 x CH$_{ar}$); 128.67 (2 x CH$_{ar}$); 135.61 (C$_{q,ar}$); 138.93 (C$_q$=); 151.16 (C=O, carbamoyl); 156.23 (C=O, urea, hydantoin); 171.49 (C=O); 173.33 (C=O). **IR ν (cm^{-1}):** 1694 (C=O); 1721 (C=O); 1775 (C=O); 3346 (NH). **MS m/z (%):** 478/480 (100, $[M+H]^+$). **Chromatography:** R_f = 0.41 (EtOAc/PE 1/4) **Yield:** 11 %. Oil.

Ethyl 3-[4-(2-chloromethylallyl)-2,5-dioxo-1-propylimidazolidin-4-yl]propionate (156)

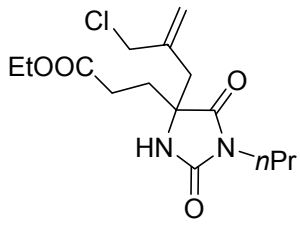

^{1}H NMR δ (300 MHz, $CDCl_3$, ppm): 0.90 (3H, t, J = 7.4 Hz, C<u>H</u>$_3$, propyl); 1.25 (3H, t, J = 7.2 Hz, C<u>H</u>$_3$, ethyl); 1.59 (2H, sextet, J = 7.4 Hz, C<u>H</u>$_2$CH$_3$, propyl); 2.07-2.31 (4H, m, C<u>H</u>$_2$CH$_2$C=O); 2.60 (1H, d, J = 13.8 Hz, C<u>H</u>$_a$H$_b$C=); 2.70 (1H, d, J = 13.8 Hz, CH$_a$<u>H</u>$_b$C=); 3.37-3.47 (2H, m, NC<u>H</u>$_2$); 4.00 (1H, d, J = 12.0 Hz, C<u>H</u>$_a$H$_b$Cl); 4.03 (1H, d, J = 12.0 Hz, CH$_a$<u>H</u>$_b$Cl); 4.13 (2H, q, J = 7.2 Hz, OC<u>H</u>$_2$); 5.11 (1H, s, C=C<u>H</u>$_a$H$_b$); 5.30 (1H, s, C=CH$_a$<u>H</u>$_b$); 6.93 (1H, br s, N<u>H</u>). **^{13}C NMR δ (75 MHz, $CDCl_3$, ppm):** 11.22 (CH$_3$, propyl); 14.13 (CH$_3$, ethyl); 21.43 (CH$_2$, propyl); 28.68 (CH$_2$<u>C</u>H$_2$); 32.04 (<u>C</u>H$_2$CH$_2$); 39.28 (<u>C</u>H$_2$C=); 40.35 (NCH$_2$); 48.78 (ClCH$_2$); 61.04 (OCH$_2$); 64.79 (HNC$_q$); 120.51 (C=<u>C</u>H$_2$); 138.81 (<u>C</u>=CH$_2$); 157.24 (C=O, urea); 172.69 (C=O); 175.26 (C=O). **Chromatography:** R_f = 0.14 (EtOAc/PE 1/4) **Yield:** 10 %.

Ethyl 3-[4-(2-chloromethylallyl)-2,5-dioxo-1-propyl-3-propylcarbamoylimidazolidin-4-yl]propionate (157)

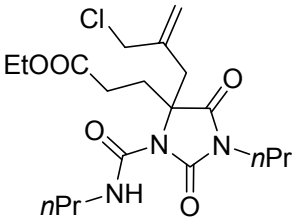

^{1}H NMR δ (300 MHz, $CDCl_3$, ppm): 0.92 (3H, t, J = 7.4 Hz, C<u>H</u>$_3$, propyl); 0.96 (3H, t, J = 7.4 Hz, C<u>H</u>$_3$, propyl); 1.24 (3H, t, J = 7.2 Hz, C<u>H</u>$_3$, ethyl); 1.50-1.71 (4H, m, 2 x C<u>H</u>$_2$CH$_3$, propyl); 2.02-2.29 (2H, m, CH$_2$C<u>H</u>$_2$); 2.25-2.37 (1H, m, C<u>H</u>$_a$H$_b$); 2.71 (1H, d, J = 14.0 Hz, C<u>H</u>$_a$H$_b$C=); 2.74-2.84 (1H, m, CH$_a$<u>H</u>$_b$); 3.16-3.40 (2H, m, NHC<u>H</u>$_2$); 3.36 (1H, d, J = 14.0 Hz, CH$_a$<u>H</u>$_b$C=); 3.35-3.55 (2H, m, NC<u>H</u>$_2$); 3.86 (2H, s, ClC<u>H</u>$_2$); 4.09 (2H, q, J = 7.2 Hz, OC<u>H</u>$_2$); 5.02 (1H, br s, C=C<u>H</u>$_a$H$_b$); 5.31 (1H, br s, C=CH$_a$<u>H</u>$_b$); 8.12 (1H, t, J = 5.5 Hz, N<u>H</u>). **^{13}C NMR δ (75 MHz, $CDCl_3$, ppm):** 11.29 (CH$_3$, propyl); 11.38 (CH$_3$, propyl); 14.18 (CH$_3$, ethyl); 21.22 (<u>C</u>H$_2$CH$_3$); 22.90 (<u>C</u>H$_2$CH$_3$); 29.03 (CH$_2$<u>C</u>H$_2$); 30.77 (<u>C</u>H$_2$CH$_2$); 38.07 (C$_q$<u>C</u>H$_2$C$_q$=); 40.88 (NCH$_2$); 41.72 (NHCH$_2$); 47.81 (ClCH$_2$); 60.90 (OCH$_2$); 69.16 (N<u>C</u>$_q$CH$_2$); 120.44 (C=<u>C</u>H$_2$); 138.93 (C$_q$=); 151.15 (C=O, carbamoyl); 156.25 (C=O, urea, hydantoin); 171.64 (C=O, ester); 173.38 (C=O, lactam). **IR ν (cm^{-1}):** 1694 (C=O); 1722 (C=O); 1776 (C=O); 3345 (NH). **MS m/z (%):** 416/418 (100, [M+H]$^+$). **Chromatography:** R_f = 0.40 (EtOAc/PE 1/4) **Yield:** 31 %. Oil.

If the reaction was quenched with water instead of saturated $NH_4Cl_{(aq)}$ the sodium salt of the hydantoin was formed in the aqueous layer.

Sodium 3-(1-benzyl-2,5-dioxoimidazolidin-4-yl)propionate (137)

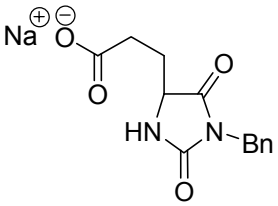

^{1}H NMR δ (300 MHz, D_2O, ppm): 1.59-1.74 (1H, m, C<u>H</u>$_a$H$_b$); 1.78-1.89 (1H, m, CH$_a$<u>H</u>$_b$); 2.02 (1H, t, J = 8.0 Hz, CH$_2$); 3.83 (2H, dd, J = 4.4 Hz en J = 8.5 Hz, C<u>H</u>); 4.12 (1H, d, J = 15.7 Hz, NC<u>H</u>$_a$H$_b$); 4.18 (1H, d, J = 15.7 Hz, NCH$_a$<u>H</u>$_b$); 7.12-7.26 (5H, m, CH$_{ar}$). **^{13}C NMR δ (75 MHz, D_2O, ppm):** 29.46 (CH$_2$); 34.26 (CH$_2$); 43.51 (NCH$_2$); 55.84 (CH); 127.01 (2 x CH$_{ar}$); 127.30 (CH$_{ar,para}$); 128.89 (2 x CH$_{ar}$); 139.76 (C$_{q,ar}$); 160.08 (C=O); 180.37 and 182.66 (C=O, carboxylate and lactam).

2.3 Two-Step Pyroglatamate-Hydantoin Rearrangement

2.3.1 Carbamoylation of Pyroglutamates at Nitrogen

The pyroglutamate ester (14.66 mmol) was dissolved in dry ether (70 mL) and 1 equivalent of the isocyanate was added with a syringe and stirred shortly. After addition of NaH (1.02 equivalents) the reaction mixture was stirred for 0.5 to 2 hours under a nitrogen atmosphere, while a white precipitate was formed. The reaction was then quenched with saturated $NH_4Cl_{(aq)}$ solution until the pH was neutral or slightly acidic. The mixture was extracted 3 times with EtOAc, the organic layers were dried with $MgSO_4$ and filtered. It is important to work under completely dry circumstances, possible traces of rearranged product can be present.

The complete spectroscopic description of compounds **114** can be found in reference 111.

For the *C*(2) alkylated derivatives, the reaction was stirred 15' at 0°C.

Ethyl 2-(2-chloromethylallyl)-5-oxo-1-propylcarbamoylpyrrolidine-2-carboxylate (155)

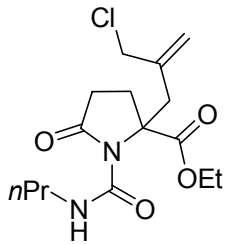

^{1}H NMR δ (300 MHz, $CDCl_3$, ppm): 0.93 (3H, t, J = 7.3 Hz, C$\underline{H}_3$, propyl); 1.27 (3H, t, J = 7.0 Hz, C$\underline{H}_3$, ethyl); 1.57 (2H, sextet, J = 7.3 Hz, C$\underline{H}_2$CH$_3$, propyl); 2.04-2.28 (2H, m, C$\underline{H}_2$CH$_2$); 2.52-2.72 (2H, m, CH$_2$C$\underline{H}_2$); 2.81 (1H, d, J = 14.9 Hz, C$\underline{H}_a$H$_b$C=); 3.16-3.34 (2H, m, NC$\underline{H}_2$); 3.45 (1H, d, J = 14.9 Hz, CH$_a$$\underline{H}_b$C=); 3.95-4.04 (2H, m, ClC$\underline{H}_2$); 4.17-4.29 (2H, m, OC$\underline{H}_2$); 5.08 (1H, s, C=C$\underline{H}_a$H$_b$); 5.40 (1H, s, C=CH$_a$$\underline{H}_b$); 8.45 (1H, br t, J = 6.1 Hz, N$\underline{H}$). **^{13}C NMR δ (75 MHz, $CDCl_3$, ppm):** 11.09 (CH$_3$, propyl); 13.84 (CH$_3$, ethyl); 22.65 (CH$_2$, propyl); 26.53 (CH$_2$$\underline{C}H_2$); 31.31 ($\underline{C}H_2CH_2$); 37.16 ($\underline{C}H_2$C=); 41.34 (NCH$_2$); 48.39 (ClCH$_2$); 61.68 (OCH$_2$); 67.86 (C$_q$); 120.60 (C=$\underline{C}H_2$); 140.35 ($\underline{C}$=CH$_2$); 152.05 (C=O, urea); 172.20 (C=O); 177.09 (C=O). **IR ν (cm^{-1}):** 1720 (C=O); 3312 (NH). **MS m/z (%):** 331/333 (100, [M+H + NH$_4$]$^{2+}$). **Chromatography:** R_f = 0.27 (EtOAc/PE 1/4) **Yield:** 35 %.

Ethyl 2-[(2*cis*)-4-chlorobut-2-enyl] -5-oxo-1-phenylcarbamoylpyrrolidine-2-carboxylate (161)

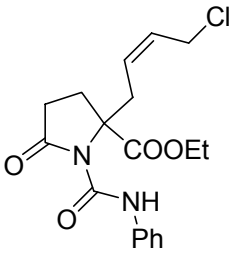

^{1}H NMR δ (300 MHz, $CDCl_3$, ppm): 1.27 (3H, t, J = 7.1 Hz, C$\underline{H}_3$); 2.01-2.27 (2H, m, C$\underline{H}_2$CH$_2$); 2.63-2.81 (2H, m, CH$_2$C$\underline{H}_2$); 2.90 (1H, ddd, J = 1.0 Hz, J = 8.2 Hz and J = 15.0 Hz, C$_q$C$\underline{H}_a$H$_b$CH=); 3.36 (1H, ddd, J = 1.2 Hz, J = 7.9 Hz and J = 15.0 Hz, C$_q$CH$_a\underline{H}_b$CH=); 4.04 (1H, dd, J = 7.2 Hz and J = 11.6 Hz, ClC$\underline{H}_a$H$_b$CH=); 4.17 (1H, dd, J = 8.7 Hz and J = 11.6 Hz, ClCH$_a\underline{H}_b$CH=); 4.20-4.33 (2H, m, OC$\underline{H}_2$); 5.52-5.63 (1H, m, C$\underline{H}$=CH); 5.81-5.92 (1H, m, CH=C$\underline{H}$); 7.10 (1H, br t, J = 7.4 Hz, C$\underline{H}_{ar}$); 7.27-7.34 (2H, m, C$\underline{H}_{ar}$); 7.46-7.54 (2H, m, C$\underline{H}_{ar}$); 10.56 (1H, br s, N$\underline{H}$). **^{13}C NMR δ (75 MHz, $CDCl_3$, ppm):** 14.18 (CH$_3$); 26.80 (C$\underline{H}_2$CH$_2$); 31.66 (CH$_2$C$\underline{H}_2$); 32.41 (C$\underline{H}_2$CH=); 39.00 (ClC$\underline{H}_2$CH=); 62.18 (OCH$_2$); 68.41 (C$_q$); 120.38 (2 x CH$_{ar}$); 124.44 (CH$_{ar}$); 127.10 (C$\underline{H}$=CH); 129.12 (2 x CH$_{ar}$); 130.63 (CH=C$\underline{H}$); 137.16 (C$_{q,ar}$); 149.58 (C=O, urea); 172.19 (C=O, ester); 177.64 (C=O, lactam). **IR ν (cm^{-1}):** 1723 (C=O); 3232 (NH). **MS m/z (%):** 365/367 (100, [M+H]$^+$). **Chromatography:** R_f = 0.25 (EtOAc/PE 3/7). **Yield:** 13 %.

2.3.2 Pyroglutamate-Hydantoin Rearrangement

The carbamoyl pyroglutamate (2.76 mmol) was dissolved in the alcohol (20 ml), corresponding with the desired alkoxide nucleophile, and 1.1 equivalents of KO*t*Bu were added. The mixture was stirred at room temperature for 1 hour, protected from moisture using a $CaCl_2$-tube. The reaction was quenched with a saturated $NH_4Cl_{(aq)}$ solution, extracted with EtOAc, dried over $MgSO_4$ and filtered. Removal of the solvent yielded the product. The products can be further purified by recrystallization from EtOAc or acetone or by column chromatography.

2-hydroxyethyl 3-(2,5-dioxo-1-phenylimidazolidin-4-yl)propionate (139)

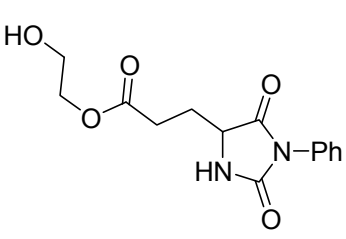

^{1}H NMR δ (300 MHz, $CDCl_3$, ppm): 1.25 (1H, s, O$\underline{H}$); 2.14-2.25 (1H, m, C$\underline{H}_a$H$_b$CH$_2$CO); 2.30-2.41 (1H, m, CH$_a\underline{H}_b$CH$_2$CO); 2.62 (2H, t, J = 7.0 Hz, C$\underline{H}_2$CO); 3.70 (2H, dd, J = 6.2 Hz en J = 5.1 Hz, HOC$\underline{H}_2$); 4.30 (1H, br t, J = 5.6 Hz, C$\underline{H}$); 4.38 (2H, dd, J = 6.2 Hz en J = 5.1 Hz, COOC$\underline{H}_2$); 6.05 (1H, s, N$\underline{H}$); 7.36-7.42 (3H, m, C$\underline{H}_{ar,\ meta\ en\ para}$); 7.45-7.51 (2H, m, C$\underline{H}_{ar,\ orhto}$). **^{13}C NMR δ (75 MHz, $CDCl_3$, ppm):** 27.00 (C$\underline{H}_2$CH); 29.66 (C$\underline{H}_2$CO); 41.61 (HOC$\underline{H}_2$); 56.27 (CH);

64.58 (COO<u>C</u>H_2); 126.23 (2 x $CH_{ar,ortho}$); 128.51 ($CH_{ar,para}$); 129.27 (2 x $CH_{ar,meta}$); 131.38 ($C_{ar,quat.}$); 156.10 (C=O, ureum); 172.34 (C=O, lactam); 172.48 (C=O, ester). **IR ν (cm^{-1}):** 1714 (C=O); 1741 (C=O); 1773 (C=O); 3248 (NH). **MS m/z (%):** 311 (100, $[M+H + NH_4]^{2+}$). **Mp.:** 118 °C. **Chromatography:** R_f = 0.19 (EtOAc/PE 1/1) **Yield:** 11 %. White crystals.

2.4 Alkylation of the Hydantoins at *N*(3)

The hydantoin (0.5 mmol) was dissolved in dry THF (15 ml) and 1.0 equivalent of KO*t*Bu and 2.5 equivalents of electrophile were added. The mixture was stirred at room temperature for 6.5 hours under an N_2-atmosphere. The reaction was quenched with a saturated $NH_4Cl_{(aq)}$ solution, extracted with EtOAc, dried over $MgSO_4$ and filtered. Removal of the solvent yielded the product. The product was purified by column chromatography.

2-Hydroxyethyl 3-(3-allyl-2,5-dioxo-1-phenylimidazolidin-4-yl)propionate (140)

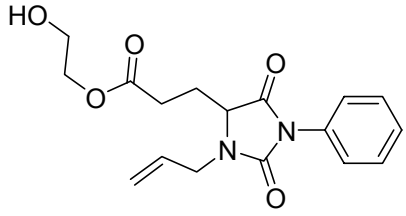

^{1}H NMR δ (300 MHz, $CDCl_3$, ppm): 1.25 (1H, s, O<u>H</u>); 2.14-2.26 (1H, m, C<u>H</u>$_a$H$_b$CH$_2$CO); 2.32-2.43 (1H, m, CH$_a$<u>H</u>$_b$CH$_2$CO); 2.53 (2H, t, J = 7.3 Hz, C<u>H</u>$_2$CO); 3.67 (2H, t, J = 5.6 Hz, HOC<u>H</u>$_2$); 3.71 (1H, ddt, J = 15.5 Hz, J = 7.7 Hz en J = 1.0 Hz, NC<u>H</u>$_a$H$_b$); 4.20 (1H, t, J = 5.5 Hz, C<u>H</u>); 4.34 (2H, t, J = 5.6 Hz, COOC<u>H</u>$_2$); 4.44 (1H, ddt, J = 15.5 Hz, J = 5.1 Hz en J = 1.4 Hz, NCH$_a$<u>H</u>$_b$); 5.32 (1H, br d, J = 9.5 Hz, =C<u>H</u>$_a$H$_b$); 5.33 (1H, br d, J = 17.6 Hz, =CH$_a$<u>H</u>$_b$); 5.77-5.90 (1H, m, =C<u>H</u>); 7.34-7.50 (5H, m, C<u>H</u>$_{ar}$). **^{13}C NMR δ (75 MHz, $CDCl_3$, ppm):** 23.88 (<u>C</u>H$_2$CH); 28.02 (<u>C</u>H$_2$CO); 41.45 (HO<u>C</u>H$_2$); 43.74 (N<u>C</u>H$_2$); 57.55 (<u>C</u>H); 64.38 (COO<u>C</u>H$_2$); 119.84 (=<u>C</u>H$_2$); 126.05 (2 x <u>C</u>H$_{ar,ortho}$); 128.27 (<u>C</u>H$_{ar,para}$); 129.08 (2 x <u>C</u>H$_{ar,meta}$); 131.46 (<u>C</u>$_{ar,quat.}$ or =<u>C</u>H); 131.52 (<u>C</u>$_{ar,quat.}$ or =<u>C</u>H); 155.13 (<u>C</u>=O, urea); 171.31 (<u>C</u>=O, lactam); 171.93 (<u>C</u>=O, ester). **IR ν (cm^{-1}):** 1645 (C=C); 1713 (C=O); 1735 (C=O); 1773 (C=O); 3471 (OH). **MS m/z (%):** 351 (100, $[M+H + NH_4]^{2+}$). **Chromatography:** R_f = 0.52 (EtOAc/PE 1/1) **Yield:** 32 %. Oil.

2.5 Synthesis of Imidazopyridine and Imidazopyrrolidine Derivatives using Biselectrophiles

The two-step procedure starts with the synthesis of the 2-alkyl-1-carbamoylpyroglutamate. However, partial rearrangement occurs, leading to hydantion side-products, as described in $ 2.1. After chromatographic purification, the carbamoylated lactam (0.5 mmol) was dissolved in 10 ml absolute ethanol and 1.2 equivalents KO*t*Bu was added. The mixture was stirred for 4 hours at room temperature under an N_2-atmosphere. The reaction was quenched with a saturated $NH_4Cl_{(aq)}$ solution, extracted with EtOAc, dried over $MgSO_4$ and filtered. Removal of the solvent yielded the pure product.

Benzyl 3-(6-methylene-1,3-dioxo-2-propyltetrahydropyrrolo[1,2-c]imidazol-7a-yl)propionate (153)

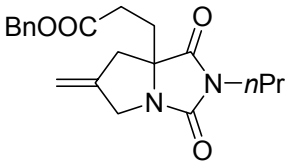

^{1}H NMR δ (300 MHz, $CDCl_3$, ppm): 0.88 (3H, t, J = 7.4 Hz, C<u>H</u>$_3$, propyl); 1.61 (2H, sextet, J = 7.4 Hz, C<u>H</u>$_2$CH$_3$); 2.04-2.36 (4H, m, CH$_2$C<u>H</u>$_2$); 2.49-2.60 (2H, m, C<u>H</u>$_2$C=); 3.40-3.47 (2H, m, NC<u>H</u>$_2$CH$_2$); 3.69 (1H, br d, J = 15.7 Hz, NC<u>H</u>$_a$H$_b$C=); 4.31 (1H, br d, J = 15.7 Hz, NCH$_a$<u>H</u>$_b$C=); 5.07 (1H, br s, C=C<u>H</u>$_a$H$_b$); 5.09 (2H, s, OCH$_2$); 5.13 (1H, pentuplet, J = 2.2 Hz, C=CH$_a$<u>H</u>$_b$); 7.29-7.40 (5H, m, C<u>H</u>$_{ar}$). **^{13}C NMR δ (75 MHz, $CDCl_3$, ppm):** 11.22 (CH$_3$, propyl); 21.38 (<u>C</u>H$_2$CH$_3$); 29.16 (CH$_2$<u>C</u>H$_2$); 29.37 (<u>C</u>H$_2$CH$_2$); 40.81 (C$_q$<u>C</u>H$_2$C$_q$=); 40.81 (N<u>C</u>H$_2$CH$_2$); 48.78 (N<u>C</u>H$_2$C$_q$=); 66.79 (OCH$_2$); 71.20 (C$_q$<u>C</u>H$_2$); 110.24 (C=<u>C</u>H$_2$); 128.43 (CH$_{ar}$); 128.51 (2 x CH$_{ar}$); 128.65 (2 x CH$_{ar}$); 135.70 (C$_{q,ar}$); 144.89 (C$_q$=); 159.84 (C=O, urea); 172.28 (C=O); 175.03 (C=O). **IR ν (cm^{-1}):** 1713 (C=O); 1774 (C=O). **MS m/z (%):** 357 (100, [M+H]$^+$). **Chromatography:** R_f = 0.28 (EtOAc/PE 1/4) **Yield:** 18 %. Oil.

Ethyl 3-(6-methylene-1,3-dioxo-2-propyltetrahydropyrrolo[1,2-c]imidazol-7a-yl)propionate (158)

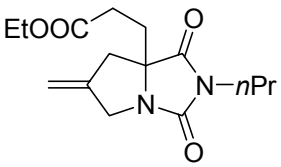

A complete spectroscopic description of this compound can be found in reference [242].

Ethyl 3-(1,3-dioxo-2-phenyl-2,3,5,8-tetrahydro-1H-imidazo[1,5-a]pyridin-8a-yl)-propionate (163)

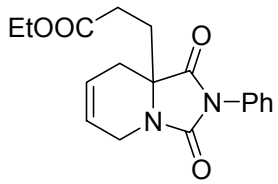

A complete spectroscopic description of this compound can be found in Paper IV of Appendix 2.

2.6 Synthesis of Macrocyclic Bis(hydantoins) using RCM

Typical procedures for the synthesis and complete spectroscopic description of compounds **168a-f**, **169a-c**, **170a-f** and **173a-f** can be found in Paper VI in Appendix 2.

2.7 Synthesis of Thiohydantoins

2.7.1 One-pot Procedure

The benzyl pyroglutamate (4.5 mmol) was dissolved in dry THF (10 mL) and 1 equivalent of phenylisothiocyanate (1 equivalent) was added with a syringe and stirred shortly. After addition of NaH (1.2 equivalents) the reaction mixture was stirred 1 day at room temperature under a nitrogen atmosphere. The reaction was then quenched with saturated $NH_4Cl_{(aq)}$ solution. The mixture was extracted 3 times with EtOAc, the organic layers were dried with $MgSO_4$ and filtered. Purification by recrystallization in ether furnished the 2-thiohydantoin.

Benzyl 3-(5-oxo-1-phenyl-2-thioxoimidazolidin-4-yl)propionate (176)

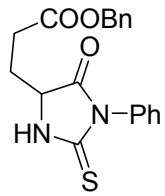

^{1}H NMR δ (300 MHz, $CDCl_3$, ppm): 2.13-2.26 (1H, m, C$\underline{H}_a$H$_b$CH); 2.33-2.44 (1H, m, CH$_a\underline{H}_b$CH); 2.63 (2H, t, J = 6.9 Hz, C$\underline{H}_2$C=O); 4.35 (1H, dd, J= 5.1 Hz and J= 6.5 Hz, C$\underline{H}$); 5.16 (2H, s, OC$\underline{H}_2$); 7.28-7.53 (10H, m, C$\underline{H}_{ar}$); 7.66 (1H, br s, N$\underline{H}$). **^{13}C NMR δ (75 MHz, $CDCl_3$, ppm):** 26.61 ($\underline{C}H_2$CH); 29.85 ($\underline{C}H_2$C=O); 59.00 (CH); 67.10 (OCH_2); 128.25 (2 x CH_{ar}); 128.50 (2 x CH_{ar}); 128.56 (CH_{ar}); 128.69 (2 x CH_{ar}); 129.18 (2 x CH_{ar}); 129.32 (CH_{ar}); 132.54 ($C_{q,ar}$); 135.29 ($C_{q,ar}$); 172.48 (C=O); 173.09 (C=O); 183.71 (C=S). **IR ν (cm^{-1}):** 1258 (C=S); 1697 (C=O); 1750 (C=O); 3234 (br NH). **MS m/z (%):** 353 (100, $[M-H]^+$). **Mp.:** 157 °C. **Yield:** 42 %. Crystals.

The bis(thiocarbamoylated) pyroglutamates were obtained as side products of this reaction.

Benzyl (5-oxo-1,2-bis(phenylthiocarbamoyl)pyrrolidine-2-carboxylate (177)

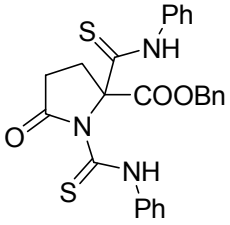

^{1}H NMR δ (300 MHz, $CDCl_3$, ppm): 2.48-2.78 (4H, m, C$\underline{H}_2C_q$ and C$\underline{H}_2$C=O); 5.14 (2H, s, OC$\underline{H}_2$); 7.27-7.54 (13H, m, C$\underline{H}_{ar}$); 7.73-7.78 (2H, m, C$\underline{H}_{ar}$); 8.31 (1H, br s, N$\underline{H}$); 10.42 (1H, br s, N$\underline{H}$). **^{13}C NMR δ (75 MHz, $CDCl_3$, ppm):** 28.94 (C$\underline{H}_2C_q$); 36.61 (C$\underline{H}_2$C=O); 67.34 (OCH_2); 72.24 (C_q); 123.02 (2 x CH_{ar}); 127.65 (CH_{ar}); 128.28 (2 x CH_{ar}); 128.67 (CH_{ar}); 128.72 (2 x CH_{ar}); 128.78 (2 x CH_{ar}); 129.25 (2 x CH_{ar}); 129.41 (2 x CH_{ar}); 129.89 (CH_{ar}); 131.93 ($C_{q,ar}$); 135.36 ($C_{q,ar}$); 137.65 ($C_{q,ar}$); 171.32 (C=O, ester); 173.58 (C=O, lactam); 181.52 (C=S, thiocarbamoyl), 190.77 (C=S, thioamide). **IR ν (cm^{-1}):** 1226 (C=S); 1504 (C_{arom}); 1706 (C=O); 1726 (C=O); 3257 (br NH). **MS m/z (%):** 490 (100, $[M+H]^+$). **Mp.:** 133-144 °C. **Yield:** 3 %. Crystals.

Ethyl (5-oxo-1,2-bis(phenylthiocarbamoyl)pyrrolidine-2-carboxylate (182)

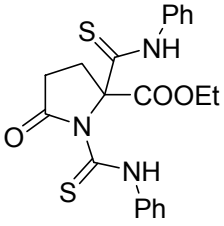

^{1}H NMR δ (300 MHz, $CDCl_3$, ppm): 1.27 (3H, t, J = 7.2 Hz, C$\underline{H}_3$); 2.43-2.71 (2H, m, C$\underline{H}_2C_q$); 2.49-2.77 (2H, m, C$\underline{H}_2$C=O); 4.17 (2H, q, J = 7.2 Hz, OC$\underline{H}_2$); 7.31 (1H, t, J = 7.4 Hz, C$\underline{H}_{ar}$); 7.32-7.38 (2H, m, C$\underline{H}_{ar}$); 7.39-7.47 (2H, m, C$\underline{H}_{ar}$); 7.48-7.57 (3H, m, C$\underline{H}_{ar}$); 7.76 (2H, d, J = 7.7 Hz, C$\underline{H}_{ar}$); 8.31 (1H, br s, N$\underline{H}$); 10.43 (1H, br s, N$\underline{H}$). **^{13}C NMR δ (75 MHz, $CDCl_3$, ppm):** 14.18 (CH_3); 28.84 (C$\underline{H}_2C_q$); 36.60 (C$\underline{H}_2$C=O); 61.36 (OCH_2); 72.19 (C_q); 122.92 (2 x CH_{ar}); 127.55 (CH_{ar}); 128.18 (2 x CH_{ar}); 129.14 (2 x CH_{ar}); 129.32 (2 x CH_{ar}); 129.79 (CH_{ar}); 131.87 ($C_{q,ar}$); 137.57 ($C_{q,ar}$); 171.35 (C=O, ester); 173.51 (C=O, lactam); 181.40 (C=S, thiocarbamoyl), 190.77 (C=S, thioamide). **IR ν (cm^{-1}):** 1233 (C=S); 1700 (C=O); 1732 (C=O); 3235 (br NH). **MS m/z (%):** 428 (100, $[M-H]^+$). **Mp.:** 130-140 °C. **Yield:** 38 % (from the 2-step procedure). Crystals.

2.7.2 Two-Step Procedure

Thiocarbamoylation of Pyroglutatmates

The pyroglutamate ester (5 mmol) was dissolved in dry ether (50 mL) and 1 equivalent of the isocyanate was added with a syringe and stirred shortly. After addition of NaH (1.02 equivalents) the reaction mixture was stirred for 3 hours under a nitrogen atmosphere. The reaction was then quenched with saturated $NH_4Cl_{(aq)}$ solution. The mixture was extracted 3 times with EtOAc, the organic layers were dried with $MgSO_4$ and filtered. The

thiocarbamoylpyroglutamate was obtained in pure form by recrystallization in acetone or ether or by column chromatography.

Ethyl 5-oxo-1-phenylthiocarbamoylpyrrolidine-2-carboxylate (179a)

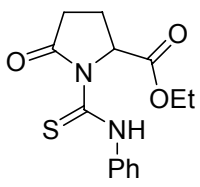

^{1}H NMR δ (300 MHz, $CDCl_3$, ppm): 1.31 (3H, t, J = 7.2 Hz, C$\underline{H}_3$); 2.11 (1H, dddd, J = 1.9 Hz, J = 2.3 Hz, J = 9.5 Hz and J = 13.4 Hz, C$\underline{H}_a$H$_b$CH); 2.38 (1H, dddd, J = 9.4 Hz, J = 9.5 Hz, J = 11.5 Hz and J = 13.4 Hz, CH$_a\underline{H}_b$CH); 2.73 (1H, ddd, J = 2.3 Hz, J = 9.4 Hz and J = 17.7 Hz, C$\underline{H}_a$H$_b$C=O); 2.96 (1H, ddd, J = 9.5 Hz, J = 11.5 Hz and J = 17.7 Hz, CH$_a\underline{H}_b$C=O); 4.19-4.36 (2H, m, OC$\underline{H}_2$); 5.42 (1H, dd, J = 1.9 Hz en J = 9.5 Hz, C$\underline{H}$); 7.25 (1H, br t, J = 7.4 Hz, C$\underline{H}_{ar}$); 7.36-7.41 (2H, m, C$\underline{H}_{ar}$); 7.60 (2H, d, J = 8.0 Hz, C$\underline{H}_{ar}$); 12.44 (1H, br s, N$\underline{H}$). **^{13}C NMR δ (75 MHz, $CDCl_3$, ppm):** 14.26 (CH_3); 21.20 ($\underline{C}H_2$CH); 33.22 ($\underline{C}H_2$C=O); 61.99 (OCH_2); 62.95 (CH); 124.72 (2 x CH_{ar}); 126.86 (CH_{ar}); 128.95 (2 x CH_{ar}); 138.03 ($C_{q,ar}$); 171.03 (C=O); 176.51 (C=O); 178.71 (C=S). **IR ν (cm^{-1}):** 1706 (C=O); 1732 (C=O); 3153 (br NH). **MS m/z (%):** 293 (100, $[M+H]^+$). **Mp.:** 145 °C. **Yield:** 68%. Crystals.

Ethyl 1-methylthiocarbamoyl-5-oxopyrrolidine-2-carboxylate (179b)

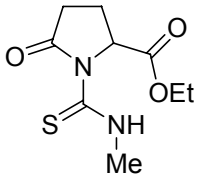

^{1}H NMR δ (300 MHz, $CDCl_3$, ppm): 1.31 (3H, t, J = 7.2 Hz, C$\underline{H}_3$); 2.05 (1H, dddd, J= 1.9 Hz, J = 2.2 Hz, J = 9.5 Hz and J = 13.4 Hz, C$\underline{H}_a$H$_b$CH); 2.35 (1H, dddd, J= 9.4 Hz, J = 9.6 Hz, J = 11.4 Hz and J = 13.4 Hz, CH$_a\underline{H}_b$CH); 2.65 (1H, ddd, J = 2.2 Hz, J = 9.4 Hz and J = 17.7 Hz, C$\underline{H}_a$H$_b$C=O); 2.87 (1H, ddd, J = 9.5 Hz, J = 11.4 Hz and J = 17.7 Hz, CH$_a\underline{H}_b$C=O); 3.16 (3H, d, J = 4.7 Hz, NC$\underline{H}_3$); 4.18-4.34 (2H, m, OC$\underline{H}_2$); 5.34 (1H, dd, J = 1.9 Hz en J = 9.6 Hz, C$\underline{H}$); 10.65 (1H, br s, N$\underline{H}$). **^{13}C NMR δ (75 MHz, $CDCl_3$, ppm):** 14.19 ($CH_2\underline{C}H_3$); 21.40 ($\underline{C}H_2$CH); 32.38 (N$\underline{C}H_3$); 32.90 ($\underline{C}H_2$C=O); 61.85 (OCH_2); 62.78 (CH); 171.24 (C=O); 176.29 (C=O); 180.92 (C=S). **IR ν (cm^{-1}):** 1705 (C=O); 1739 (C=O); 3232 (br NH). **MS m/z (%):** 231 (100, $[M+H]^+$). **Mp.:** 89-92 °C. **Chromatography:** R_f = 0.1 (EtOAc/PE 1/6). **Yield:** 47 %. Crystals.

Ethyl 1-allylthiocarbamoyl-5-oxopyrrolidine-2-carboxylate (179c)

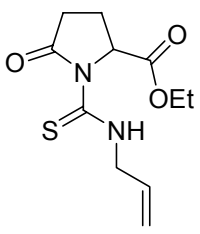

^{1}H NMR δ (300 MHz, $CDCl_3$, ppm): 1.30 (3H, t, J = 7.2 Hz, C$\underline{H}_3$); 1.99-2.10 (1H, m, C$\underline{H}_a$H$_b$CH); 2.28-2.45 (1H, m, CH$_a\underline{H}_b$CH); 2.66 (1H, ddd, J = 1.6 Hz, J = 9.2 Hz and J = 17.8 Hz, C$\underline{H}_a$H$_b$C=O); 2.86 (1H, ddd, J = 9.6

Hz, J = 10.9 Hz and J = 17.8 Hz, $CH_a\underline{H}_bC=O$); 4.16-4.32 (4H, m, $NC\underline{H}_2$ and $OC\underline{H}_2$); 5.06 (1H, br d, J = 10.5 Hz, $=C\underline{H}_aH_b$); 5.12 (1H, dd, J = 1.1 Hz and J = 17.3 Hz, $=CH_a\underline{H}_b$); 5.17 (1H, dd, J = 1.1 Hz and J = 9.6 Hz, $C\underline{H}$); 5.70-5.85 (1H, m, $=C\underline{H}$); 10.61 (1H, br s, $N\underline{H}$). **^{13}C NMR δ (75 MHz, $CDCl_3$, ppm):** 13.81 ($CH_2\underline{C}H_3$); 21.00 ($\underline{C}H_2CH$); 32.56 ($\underline{C}H_2C=O$); 47.49 ($N\underline{C}H_2$); 61.34 ($O\underline{C}H_2$); 62.44 ($\underline{C}H$); 116.92 ($=CH_2$); 131.77 (=CH); 170.72 (C=O); 175.99 (C=O); 179.69 (C=S). **IR ν (cm^{-1}):** 1714 (C=O); 1735 (C=O); 3202 (br NH). **MS m/z (%):** 257 (100, $[M+H]^+$). **Mp.:** 63-65 °C. **Chromatography:** R_f = 0.15 (EtOAc/PE 1/6). **Yield:** 56 %. Crystals.

Ethyl 2-allyl-5-oxo-1-phenylthiocarbamoylpyrrolidine-2-carboxylate (179d)

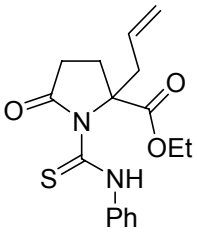

^{1}H NMR δ (300 MHz, $CDCl_3$, ppm): 1.29 (3H, t, J = 7.2 Hz, $C\underline{H}_3$); 2.10-2.28 (2H, m, $C\underline{H}_2C_q$); 2.66-2.88 (3H, m, $C\underline{H}_2C=O$ and $C\underline{H}_aH_bC_q$); 3.94 (1H, dd, J = 6.9 Hz and J = 14.6 Hz, $CH_a\underline{H}_bC_q$); 4.13-4.32 (2H, m, $OC\underline{H}_2$); 5.23 (1H, br d, J = 9.9 Hz $=C\underline{H}_aH_b$); 5.27 (1H, br d, J = 14.9 Hz $=CH_a\underline{H}_b$); 5.68-5.82 (1H, m, $=C\underline{H}$); 7.22-7.28 (1H, m, $C\underline{H}_{ar}$); 7.35-7.42 (2H, m, $C\underline{H}_{ar}$); 7.55 (2H, br d, J = 7.4 Hz, $C\underline{H}_{ar}$); 12.43 (1H, s, $N\underline{H}$). **^{13}C NMR δ (75 MHz, $CDCl_3$, ppm):** 14.12 (CH_3); 27.13 ($\underline{C}H_2C_q$); 31.81 ($\underline{C}H_2C=O$); 39.26 ($\underline{C}H_2C_q$); 61.94 (OCH_2); 71.43 (C_q); 120.95 ($=CH_2$); 125.02 (2 x CH_{ar}); 126.84 (CH_{ar}); 128.92 (2 x CH_{ar}); 131.57 (=CH); 138.02 ($C_{q,ar}$); 172.17 (C=O); 177.99 (C=O); 178.43 (C=S). **IR ν (cm^{-1}):** 1705 (C=O); 1737 (C=O); 3138 (br NH). **MS m/z (%):** 333 (100, $[M+H]^+$). **Chromatography:** R_f = 0.3 (EtOAc/PE 1/3). **Yield:** 57 %. Yellow oil.

Benzyl 5-oxo-1-phenylthiocarbamoylpyrrolidine-2-carboxylate (179e)

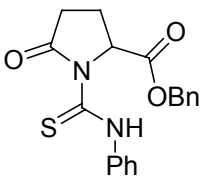

^{1}H NMR δ (300 MHz, $CDCl_3$, ppm): 1.94 (1H, dddd, J = 1.9 Hz, J = 2.2 Hz, J = 10.6 Hz and J = 13.9 Hz, $C\underline{H}_aH_bCH$); 2.14-2.19 (1H, m, $CH_a\underline{H}_bCH$); 2.59 (1H, ddd, J = 2.2 Hz, J = 9.4 Hz and J = 17.9 Hz, $C\underline{H}_aH_bC=O$); 2.81 (1H, ddd, J = 9.6 Hz, J = 10.6 Hz and J = 17.9 Hz, $CH_a\underline{H}_bC=O$); 5.14-4.23 (2H, m, $OC\underline{H}_2$); 5.40 (1H, dd, J = 1.9 Hz en J = 9.9 Hz, $C\underline{H}$); 7.17-7.37 (8H, m, $C\underline{H}_{ar}$); 7.56 (2H, br d, J = 7.7 Hz, $C\underline{H}_{ar}$); 12.43 (1H, br s, $N\underline{H}$). **^{13}C NMR δ (75 MHz, $CDCl_3$, ppm):** 20.67 ($\underline{C}H_2CH$); 32.82 ($\underline{C}H_2C=O$); 62.62 (CH); 67.22 (OCH_2); 124.37 (2 x CH_{ar}); 126.57 (CH_{ar}); 128.11 (2 x CH_{ar}); 128.31 (CH_{ar}); 128.46 (2 x CH_{ar}); 128.66 (2 x CH_{ar}); 135.10 ($C_{q,ar}$); 137.74 ($C_{q,ar}$); 170.66 (C=O); 176.27 (C=O); 178.30 (C=S). **IR ν (cm^{-1}):** 1706 (C=O); 1742 (C=O). **MS m/z (%):** 355 (100, $[M+H]^+$). **Mp.:** 81-83 °C. **Chromatography:** R_f = 0.25 (EtOAc/PE 3/10). **Yield:** 45%. Crystals.

1,4-Di-[(2-ethoxycarbonyl-5-oxopyrrolidine-1-carbothioyl)amino]benzene (183)

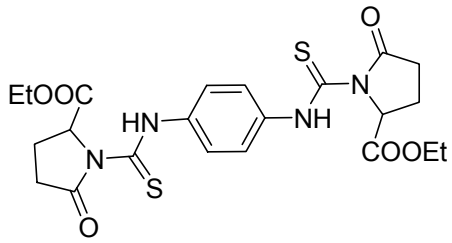

^{1}H NMR δ (300 MHz, $CDCl_3$, ppm): 1.31 (6H, t, J = 7.2 Hz, 2 x C$\underline{H}_3$); 2.09 (2H, tdd, J = 2.0 Hz, J = 9.5 Hz and J = 13.5 Hz, 2 x C$\underline{H}_a$H$_b$CH); 2.30-2.46 (2H, m, 2 x CH$_a\underline{H}_b$CH); 2.73 (2H, ddd, J = 2.0 Hz, J = 9.2 Hz and J = 17.8 Hz, 2 x C$\underline{H}_a$H$_b$C=O); 2.96 (2H, ddd, J = 9.5 Hz, J = 11.4 Hz and J = 17.8 Hz, 2 x CH$_a\underline{H}_b$C=O); 4.19-4.35 (4H, m, 2 x OC$\underline{H}_2$); 5.40 (2H, dd, J = 2.0 Hz en J = 9.8 Hz, 2 x C$\underline{H}$); 7.66 (4H, s, 4 x C$\underline{H}_{ar}$); 12.50 (2H, br s, 2 x N$\underline{H}$). **^{13}C NMR δ (75 MHz, $CDCl_3$, ppm):** 14.22 (2 x CH_3); 21.16 (2 x $\underline{C}H_2$CH); 33.16 (2 x $\underline{C}H_2$C=O); 61.95 (2 x OCH_2); 62.88 (2 x CH); 124.80 (4 x CH_{ar}); 136.11 (2 x $C_{q,ar}$); 170.94 (2 x C=O); 176.52 (2 x C=O); 178.40 (2 x C=S). **IR ν (cm^{-1}):** 1716 (C=O); 1751 (C=O); 3153 (NH). **MS m/z (%): 507** (100, $[M+H]^+$). **Mp.:** 191 °C. **Yield:** 46 %. Crystals.

Ringtransformation of thiocarbamoylpyroglutamates towards thiohydantoins

The thiocarbamoylpyroglutamate (0.5 mmol) was added to 15 ml of a 2N $HCl_{(aq)}$ solution and stirred under reflux for 1 day. During the reaction the product slowly dissolved. Then the solution was extracted three times with CH_2Cl_2. The organic layers were dried with $MgSO_4$, filtered and the solvent was removed under reduced pressure, yielding the product that can be recrystallized in acetone.

The derivatives **180a**[243], **180b**[244] and **180c**[245] were described in literature.

3-(4-Allyl-5-oxo-1-phenyl-2-thioxoimidazolidin-4-yl)propionic acid (180d)

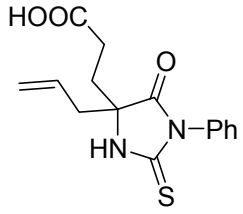

^{1}H NMR δ (300 MHz, $CDCl_3$, ppm): 2.09-2.26 (1H, m, C$\underline{H}_a$H$_b$C=O); 2.22-2.44 (1H, m, C$\underline{H}_a$H$_b$C$_q$); 2.43-2.65 (2H, m, CH$_a\underline{H}_b$C$_q$ and CH$_a\underline{H}_b$C=O); 4.53-2.70 (2H, m, C$\underline{H}_2$CH=); 5.23-5.33 (2H, m, =C$\underline{H}_2$); 5.71-5.87 (1H, m, =CH); 7.25-7.32 (2H, m, C$\underline{H}_{ar}$); 7.43-7.57 (3H, m, C$\underline{H}_{ar}$); 10.09 (1H, br s, N$\underline{H}$). **^{13}C NMR δ (75 MHz, $CDCl_3$, ppm):** 30.26 ($\underline{C}H_2C_q$); 32.58 ($\underline{C}H_2$C=O); 41.77 ($\underline{C}H_2$CH=); 68.84 (C_q); 122.28 (=$\underline{C}H_2$); 128.48 (2 x CH_{ar}); 129.13 (CH_{ar}); 129.41 (2 x CH_{ar}); 129.62 (=CH); 132.55 ($C_{q,ar}$); 174.98 (C=O); 178.92 (C=O); 184.10 (C=S). **IR ν (cm^{-1}):** 1712 (C=O); 1738 (C=O); 3189 (br NH). **MS m/z (%):** 305 (100, $[M+H]^+$). **Yield:** 90 %.

2.8 Carbamoylation of pyrrolidinone derivatives

The pyrrolidin-2-one (0.5 mmol) was dissolved in dry THF (10 mL) and 1 equivalent of the isocyanate was added with a syringe and stirred shortly. After addition of NaH (1.02 equivalents) the reaction mixture was stirred overnight under a nitrogen atmosphere. The reaction was then quenched with saturated $NH_4Cl_{(aq)}$ solution. The mixture was extracted 3 times with EtOAc, the organic layers were dried with $MgSO_4$ and filtered.

5-Ethoxy-1-phenylcarbamoylpyrrolidin-2-one (198)

This reaction was done with 2 equivalents of isocyanate, and minor amounts of diphenylurea are present in the sample. The compound was not completely pure, but identified by its 1D and 2D NMR spectra and its mass.

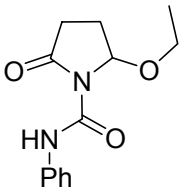

^{1}H NMR δ (300 MHz, $CDCl_3$, ppm): 1.21 (3H, t, J = 7.0 Hz, C$\underline{H}_3$); 2.03-2.24 (2H, m, C$\underline{H}_2$CH); 2.55 (1H, ddd, J = 1.5 Hz, J = 8.5 Hz and J = 17.8 Hz, C$\underline{H}_a$H$_b$C=O); 2.99 (1H, ddd, J = 8.8 Hz, J = 11.0 Hz and J = 17.8 Hz, CH$_a\underline{H}_b$C=O); 3.66-3.85 (2H, m, OC$\underline{H}_2$); 5.81 (1H, br d, J = 5.5 Hz, C$\underline{H}$); 7.11 (1H, br t, J = 7.4 Hz, C$\underline{H}_{ar}$); 7.29-7.36 (2H, m, C$\underline{H}_{ar}$); 7.50-7.55 (2H, m, C$\underline{H}_{ar}$); 10.48 (1H, br s, N$\underline{H}$). **^{13}C NMR δ (75 MHz, $CDCl_3$, ppm):** 15.49 (CH_3); 26.30 ($\underline{C}H_2$CH); 31.58 ($\underline{C}H_2$C=O); 65.43 (OCH_2); 87.32 (CH); 120.44 (2 x CH_{ar}); 124.40 (CH_{ar}); 129.13 (2 x CH_{ar}); 137.33 ($C_{q,ar}$); 150.14 (C=O, urea); 177.96 (C=O, lactam). **MS m/z (%):** 249 (100, $[M+H]^+$). **Chromatography:** R_f = 0.20 (EtOAc/PE 1/4) **Yield:** 52 %.

3 Synthesis of α-Amino Phosphonate Derivatives

3.1 Synthesis of Aldimines

2-Furfural (boiling point: 159 - 161 °C) was distilled under reduced pressure; 5-bromo-2-furfural is a crystalline product. The aldehyde was mixed with 1 equivalent of amine (1.1 equivalents were used for volatile amines) and 2 equivalents of $MgSO_4$ in dichloromethane. The mixture was then stirred at room temperature overnight and shielded from moisture using a $CaCl_2$-tube. The imines were obtained in high purity and yield after filtration of the solids and evaporation of the solvent under reduced pressure.

The imines **204a,c-d** and **219a-c** were described in reference 13 and their spectroscopic data matched those reported in the literature.

(2*E*)-*n*-Propyl-(3-phenylpropenylidene)amine (204b)

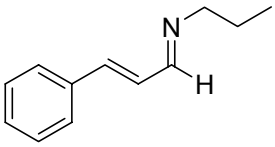

^{1}H NMR δ (300 MHz, $CDCl_3$, ppm): 0.94 (3H, t, J = 7.2 Hz, C$\underline{H}_3$); 1.70 (2H, sextet, J = 7.2 Hz, C$\underline{H}_2$); 3.48 (2H, dt, J = 1.2 Hz and J = 7.2 Hz, NC$\underline{H}_2$); 6.85-6.97 (2H, m, $\underline{H}$C=C$\underline{H}$); 7.27-7.39 (3H, m, C$\underline{H}_{arom}$); 7.45-7.49 (2H, m, C$\underline{H}_{arom}$); 8.00-8.04 (1H, m, N=C$\underline{H}$). **Yield:** 97 %. Yellow oil.

Isopropyl(furan-2-ylmethylidene)amine (219d)

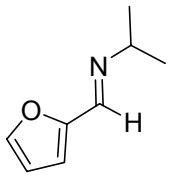

^{1}H NMR δ (300 MHz, $CDCl_3$, ppm): 1.27 (6H, d, J = 6.3 Hz, CH(C$\underline{H}_3$)$_2$); 3.49 (1H, septet, J = 6.3 Hz, C$\underline{H}$(CH$_3$)$_2$); 6.47 (1H, dd, J = 1.7 Hz and J = 3.4 Hz, $\underline{H}$C=CHO); 6.70 (1H, d, J = 3.4 Hz, =C$\underline{H}$); 7.50 (1H, d, J = 1.7 Hz, =C$\underline{H}$O); 8.11 (1H, s, N=C$\underline{H}$). **Yield:** 93 %. Yellow oil.

Allyl-(5-bromofuran-2-ylmethylidene)amine (227a)

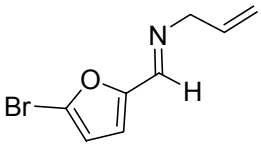

^{1}H NMR δ (300 MHz, $CDCl_3$, ppm): 4.22 (2H, dq, J = 6.1 Hz and J = 1.4 Hz, NC$\underline{H}_2$); 5.17 (1H, dq, J = 10.1 Hz and J = 1.4 Hz, =C$\underline{H}_A$H$_B$); 5.22 (1H, dq, J = 17.3 Hz and J = 1.7 Hz, =CH$_A$$\underline{H}_B$); 6.04 (1H, ddt, J = 17.3 Hz, J = 10.1 Hz and J = 6.1 Hz, CH$_2$C$\underline{H}$=); 6.42 (1H, d, J = 3.6 Hz, $\underline{H}$C=CBr); 6.73 (1H, d, J = 3.6 Hz, C$_q$=C$\underline{H}$); 8.00 (1H, t, J = 1.4 Hz, N=C$\underline{H}$). **Yield:** 96 %. Brown oil.

Benzyl-(5-bromofuran-2-ylmethylidene)amine (227b)

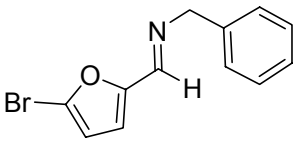

^{1}H NMR δ (300 MHz, $CDCl_3$, ppm): 4.78 (2H, br s, NC$\underline{H}_2$); 6.41 (1H, d, J = 3.4 Hz, $\underline{H}$C=CBr); 6.74 (1H, d, J = 3.4 Hz, C$_q$=C$\underline{H}$); 7.23-7.38 (5H, m, C$\underline{H}_{arom}$); 8.05 (1H, t, J = 1.4 Hz, N=C$\underline{H}$). **Yield:** 97 %. Brown oil.

Allyl-(1-methyl-1*H*-imidazol-2-ylmethylene)amine (233a)

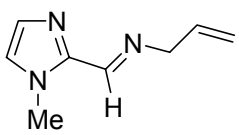

^{1}H NMR δ (300 MHz, $CDCl_3$, ppm): 4.01 (3H, s, C$\underline{H}_3$); 4.21-4.24 (2H, m, NC$\underline{H}_2$); 5.15 (1H, dq, J_{cis} = 10.3 Hz and J = 1.6 Hz, =C$\underline{H}_a$H$_b$); 5.22 (1H, dq, J_{trans} = 17.2 Hz and J = 1.6 Hz, =CH$_a$$\underline{H}_b$); 6.04 (1H, ddt, J_{trans} = 17.2 Hz and J_{cis} = 10.3 Hz en J_{vic} = 5.5 Hz, C$\underline{H}$=CH$_2$); 6.94 (1H, s, NC$\underline{H}$); 7.11 (1H, s, NC$\underline{H}$); 8.33 (1H, s, C$\underline{H}$=N). **Yield:** 94 %.

Benzyl-(1-methyl-1*H*-imidazol-2-ylmethylene)amine (233b)

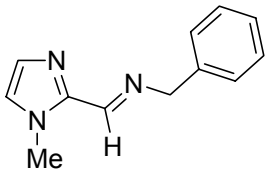

^{1}H NMR δ (300 MHz, $CDCl_3$, ppm): 4.02 (3H, s, C<u>H</u>$_3$); 4.80 (2H, s, C<u>H</u>$_2$); 6.94 (1H, s, NC<u>H</u>); 7.12 (1H, NC<u>H</u>); 7.27-7.36 (5H, m, C<u>H</u>$_{ar}$); 8.43 (1H, s, C<u>H</u>=N). **Yield:** 99 %.

3.2 Phosphonylation Using Diethyl Phosphite

To a solution of the aldimine (5 mmol) in methanol (10 ml), 2 equivalents of dimethyl phosphite were added and the mixture was refluxed for 2 to 3 hours, shielded from moisture using a $CaCl_2$-tube. After evaporation of the solvent, the residue was dissolved in 10 ml of diethyl ether and added to an equal amount of 1M $HCl_{(aq)}$ in a separatory funnel. After extraction, the organic layer was discarded. The water phase was washed twice with a small amount of diethyl ether, neutralized with 3M $NaOH_{(aq)}$ and extracted with dichloromethane. After drying with $MgSO_4$ and evaporation of the solvent under reduced pressure, the α-amino phosphonates are obtained in high purity.

The synthesis of amino phosphonates **205a,c-d** and **220a-c** was described in references 12 and 13 and their spectroscopic data matched those reported in the literature.

Dimethyl (2*E*)-3-phenyl-1-propylaminoprop-2-enyl phosphonate (205b)

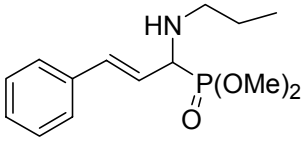

^{1}H NMR δ (300 MHz, $CDCl_3$, ppm): 0.91 (3H, t, J = 7.4 Hz, C<u>H</u>$_3$, propyl); 1.43-1.59 (2H, m, C<u>H</u>$_2$CH$_3$); 1.62 (1H, br s, N<u>H</u>); 2.44-2.57 (1H, m, NC<u>H</u>$_A$H$_B$); 2.62-2.75 (1H, m, NCH$_A$<u>H</u>$_B$); 3.70 (1H, ddd, J = 0.9 Hz, J = 8.5 Hz and J_{H-P} = 19.0 Hz, C<u>H</u>P); 3.80 (3H, d, J_{HP} = 10.5 Hz, C<u>H</u>$_3$O); 3.82 (3H, d, J_{HP} = 10.5 Hz, C<u>H</u>$_3$O); 6.13 (1H, ddd, J_{HP} = 5.8 Hz, J = 8.5 Hz and J_{trans} = 16.0 Hz, PhCH=C<u>H</u>); 6.64 (1H, dd, J = 4.7 Hz and J_{trans} = 16.0 Hz, PhC<u>H</u>=CH)); 7.22-7.36 (3H, m, C<u>H</u>$_{arom}$); 7.39-7.44 (2H, m, C<u>H</u>$_{arom}$). **^{13}C NMR δ (75 MHz, $CDCl_3$, ppm):** 11.75 (<u>C</u>H$_3$, propyl); 23.08 (CH$_3$<u>C</u>H$_2$); 50.07 (d, J_{CP} = 16.2 Hz, N<u>C</u>H$_2$); 53.49 (d, J_{CP} = 6.9 Hz, <u>C</u>H$_3$O); 53.71 (d, J_{CP} = 6.9 Hz, <u>C</u>H$_3$O,); 59.03 (d, J_{CP} = 155.8 Hz, <u>C</u>HP); 124.44 (d, J_{CP} = 6.9 Hz, PhCH=<u>C</u>H); 126.6 (2 x <u>C</u>H$_{arom}$); 127.99 (<u>C</u>H$_{arom}$); 128.67 (2 x <u>C</u>H$_{arom}$); 134.20 (d, J_{CP} = 13.9Hz, Ph<u>C</u>H=CH); 136.38 (<u>C</u>$_{q,arom}$). **^{31}P NMR δ (121 MHz, $CDCl_3$, ppm):** 26.72. **IR ν (cm^{-1}):** 1032 (P-O); 1057 (P-O); 1247 (P=O); 3307 (NH). **MS m/z (%):** 284 (100, $[M+H]^+$). **Yield:** 74 %. Brown liquid.

Dimethyl isopropylaminofuran-2-ylmethyl phosphonate (220d)

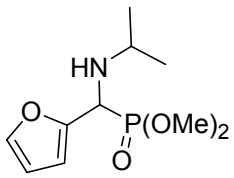

^{1}H NMR δ (300 MHz, $CDCl_3$, ppm): 1.02 (6H, t, J = 6.0 Hz, $CH(C\underline{H}_3)_2$); 2.74 (1H, septet, J = 6.0 Hz, $C\underline{H}(CH_3)_2$); 3.64 (3H, d, J_{HP} = 10.7 Hz, $OC\underline{H}_3$); 3.84 (3H, d, J_{HP} = 10.7 Hz, $OC\underline{H}_3$); 4.23 (1H, d, J_{HP} = 23.7 Hz, $C\underline{H}P$); 6.35-6.39 (2H, m, 2 x =$C\underline{H}$); 7.41-7.43 (1H, m, =$C\underline{H}O$). **^{13}C NMR δ (75 MHz, $CDCl_3$, ppm):** 21.42 (CH_3); 23.68 (CH_3); 46.36 (d, J_{CP} = 16.2 Hz, $\underline{C}H(CH_3)_2$), 51.70 (d, J_{CP} = 162.7 Hz, CHP); 53.39 (d, J_{CP} = 6.9 Hz, OCH_3); 54.10 (d, J_{CP} = 6.9 Hz, OCH_3), 108.85 (d, J_{CP} = 8.1 Hz, =$\underline{C}HC_qO$); 110.60 (d, J_{CP} = 2.3Hz, $\underline{C}H$=CHO); 142.52 (d, J_{CP} = 3.5 Hz, =CHO); 150.13 (d, J_{CP} = 2.3 Hz, =C_qO). **^{31}P NMR δ (121 MHz, $CDCl_3$, ppm):** 24.38. **IR ν (cm^{-1}):** 1038 (P-O); 1254 (P=O); 3294 (NH). **MS m/z (%):**248 (100, $[M+H]^+$). **Yield:** 87 %. Brown oil.

Dimethyl allylamino-(5-bromofuran-2-yl)methyl phosphonate (228a)

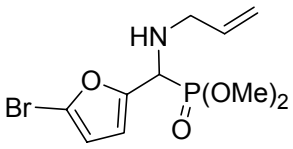

^{1}H NMR δ (300 MHz, $CDCl_3$, ppm): 2.10 (1H, br s, N$\underline{H}$); 3.11 (1H, dd, J = 13.9 Hz and J_{vic}= 6.8 Hz, $NC\underline{H}_AH_B$); 3.34 (1H, ddq, J = 13.9 Hz, J_{vic}= 5.4 Hz and J = 1.4 Hz, $NCH_A\underline{H}_B$); 3.72 (3H, d, J_{HP} = 10.7 Hz , $OC\underline{H}_3$); 3.84 (3H, d, J_{HP} = 10.7 Hz , $OC\underline{H}_3$); 4.15 (1H, d, J_{HP} = 22.3 Hz , $C\underline{H}P$); 5.14 (1H, dq, J = 10.2 Hz and J = 1.4 Hz, =$C\underline{H}_AH_B$); 5.17 (1H, dq, J = 17.1 Hz and J = 1.4 Hz, =$CH_A\underline{H}_B$); 5.81 (1H, dddd, J = 17.1 Hz, J = 10.2 Hz, J = 6.8 Hz and J = 5.4 Hz, $C\underline{H}$= CH_2); 6.31 (1H, d, J = 3.3 Hz, =$C\underline{H}$); 6.38 (1H, t, J = 3.3 Hz, =$C\underline{H}$). **^{13}C NMR δ (75 MHz, $CDCl_3$, ppm):** 50.16 (d, J_{CP} = 16.15 Hz, NCH_2); 52.91 (d, J_{CP} = 162.7 Hz, CHP) ; 53.63 (d, J_{CP} = 6.9 Hz, CH_3O); 54.06 (d, J_{CP} = 6.9 Hz, CH_3O); 112.13 (d, J_{CP} = 8.1 Hz, $\underline{C}H$=C_qO); 112.49 ($\underline{C}H$=C_qBr); 117.48 (=CH_2); 121.75 (d, J_{CP} = 3.5 Hz, C_qBrO); 135.44 ($CH_2\underline{C}H$=); 151.73 (C_qO). **^{31}P NMR δ (121 MHz, $CDCl_3$, ppm):** 23.32. **IR ν (cm^{-1}):** 1043 (P-O); 1251 (P=O); 3308 (NH). **MS m/z (%):**324/326 (100, $[M+H]^+$). **Yield:** 62 %. Brown oil.

Dimethyl benzylamino-(5-bromofuran-2-yl)methyl phosphonate (228b)

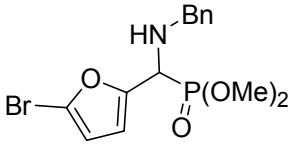

^{1}H NMR δ (300 MHz, $CDCl_3$, ppm): 2.12 (1H, br s, NH); 3.64 (1H, d, J = 13.3 Hz, $NC\underline{H}_AH_B$); 3.69 (3H, d, J_{HP} = 10.7 Hz , OCH_3); 3.82 (3H, d, J_{HP} = 10.7 Hz , OCH_3); 3.89 (1H, d, J = 13.3 Hz, $NCH_A\underline{H}_B$); 4.07 (1H, d, J_{HP} = 22.6 Hz , CHP); 6.32 (1H, d, J = 3.3 Hz, =CH); 6.37 (1H, t, J = 3.3 Hz, =CH); 7.23-7.35 (5H, m, CH_{arom}). **^{13}C NMR δ (75 MHz, $CDCl_3$, ppm):** 51.45 (d, J_{CP} = 16.2 Hz, CH_2); 52.88 (d, J_{CP} = 162.7 Hz, CHP); 53.62 (d, J_{CP} = 6.9 Hz, OCH_3); 54.15 (d, J_{CP} = 6.9 Hz, OCH_3); 112.27 (d, J_{CP} = 8.1 Hz, $\underline{C}H$=C_qO); 112.55 (d, J_{CP} = 2.3 Hz,

CH=C_qBrO); 121.83 (d, J_{CP} = 4.6 Hz, =C_qBr); 127.42 (CH_{arom}); 128.46 (2 x CH_{arom}); 128.55 (2 x CH_{arom}); 138.77 ($C_{q,arom}$); 151.76 (C_qO). **^{31}P NMR δ (121 MHz, $CDCl_3$, ppm):** 23.18. **IR ν (cm^{-1}):** 1035 (P-O); 1251 (P=O); 3320 (NH). **MS m/z (%):** 374/376 (100, $[M+H]^+$). **Yield:** 88 %. Yellow oil.

Dimethyl allylamino-(1-methyl-1*H*-imidazol-2-yl)methyl phosphonate (233a)

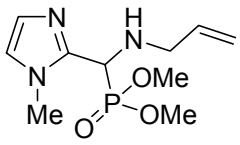

^{1}H NMR δ (300 MHz, $CDCl_3$, ppm): 2.37 (1H, br s, NH); 3.07 (1H, dd, J = 14.0 Hz and J = 7.0 Hz, NCH_aH_b); 3.34 (1H, dd, J = 14.0 Hz and J = 5.2 Hz, NCH_aH_b); 3.69 (3H, s, NCH_3); 3.75 (3H, d, J_{HP} = 10.7 Hz, OCH_3); 3.76 (3H, d, J_{HP} = 10.7 Hz, OCH_3); 4.25 (1H, d, J_{HP} = 22.0 Hz, CHP); 5.07-5.15 (2H, m, $=CH_2$); 5.75-5.89 (1H, m, $CH=CH_2$); 6.87 (1H, s, NCH); 7.03 (1H, s, NCH). **^{13}C NMR δ (75 MHz, $CDCl_3$, ppm):** 32.74 (NCH_3); 50.55 (d, J_{CP} = 16.2 Hz, CH_2N); 51.58 (d, J_{CP} = 162.7 Hz, CHP); 53.40 (d, J_{CP} = 6.9 Hz, OCH_3); 53.72 (d, J_{CP} = 6.9 Hz, OCH_3); 116.92 ($=CH_2$); 121.96 (NCH); 127.54 (NCH); 135.68 ($CH=CH_2$); 142.41 (N=C). **^{31}P NMR δ (121 MHz, $CDCl_3$, ppm):** 23.49. **IR ν (cm^{-1}):** 1032 (P-O); 1254 (P-O); 1250 (P=O); 3326 (NH). **MS m/z (%):** 260 (100, $[M+H]^+$). **Yield:** 55 %. Oil.

Dimethyl benzylamino-(1-methyl-1*H*-imidazol-2-yl)methyl phosphonate (233b)

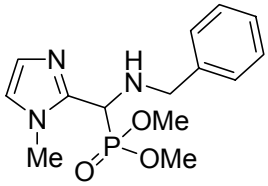

^{1}H NMR δ (300 MHz, $CDCl_3$, ppm): 3.50 (3H, s, NCH_3); 3.58 (1H, d, J = 13.1 Hz, NCH_aH_b); 3.68 (3H, d, J_{HP} = 10.5 Hz, OCH_3); 3.74 (3H, d, J_{HP} = 10.7 Hz, OCH_3); 3.89 (1H, d, J = 13.1 Hz, NCH_aH_b); 4.15 (1H, d, J_{HP} = 22.0 Hz, CHP); 6.85 (1H, s, NCH); 7.03 (1H, d, J = 1.1 Hz, NCH); 7.20-7.32 (5H, m, CH_{ar}). **^{13}C NMR δ (75 MHz, $CDCl_3$, ppm):** 32.84 (CH_3); 51.58 (d, J_{CP} = 161.5 Hz, CHP); 51.80 (d, J_{CP} = 16.2 Hz, CH_2N); 53.63 (d, J_{CP} = 6.9 Hz, OCH_3); 53.97 (d, J_{CP} = 6.9 Hz, OCH_3); 122.11 (NCH); 127.27 (CH_{arom}); 127.86 (NCH); 128.40 (4 x CH_{arom}); 138.66 (C_q, benzyl); 142.40 (N=C). **^{31}P NMR δ (121 MHz, $CDCl_3$, ppm):** 23.39. **IR ν (cm^{-1}):** 1031 (P-O); 1253 (P-O); 1250 (P=O); 3326 (NH). **MS m/z (%):** 310 (100, $[M+H]^+$). **Yield:** 68 %. Oil.

Dimethyl furan-2-yl(propylamino)methyl phosphonate (220e)

This product was obtained as a mixture with dimethyl furan-2-yl(methylpropylamino)methyl phosphonate (**237**) and was identified by its ^{1}H NMR spectrum

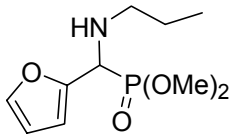

^{1}H NMR δ (300 MHz, $CDCl_3$, ppm): 0.88 (3H, t, J = 7.3 Hz, C<u>H</u>$_3$); 1.35-1.59 (2H, m, C<u>H</u>$_2$CH$_3$); 2.42-2.64 (2H, m, NC<u>H</u>$_2$); 3.66 (3H, d, J_{HP} = 10.5 Hz, OCH_3); 3.82 (3H, d, J_{HP} = 10.7 Hz, OCH_3); 4.13 (1H, d, J_{HP} = 22.0 Hz, CHP); 6.36-6.39 (2H, m, 2 x =CH); 7.42-7.44 (1H, m, CHO). **^{31}P NMR δ (121 MHz, $CDCl_3$, ppm):** 24.13. Oil.

Dimethyl furan-2-yl(methylpropylamino)methyl phosphonate (237)

This product was obtained in a mixture with dimethyl furan-2-yl(methylpropylamino)methyl phosphonate (**220e**) or 1,3-diallylurea and was identified by its ^{1}H NMR spectrum and its mass spectrum.

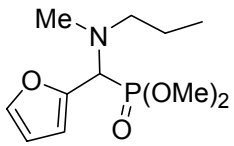

^{1}H NMR δ (300 MHz, $CDCl_3$, ppm): 0.91 (3H, t, J = 7.4 Hz, C<u>H</u>$_3$); 1.50 (2H, sextet, J = 7.4 Hz, C<u>H</u>$_2$CH$_3$); 2.29-2.38 (1H, m, NC<u>H</u>$_a$H$_b$); 2.34-2.38 (3H, m, NC<u>H</u>$_3$); 2.54-2.64 (1H, m, NCH$_a$<u>H</u>$_b$); 3.63 (3H, d, J_{HP} = 10.5 Hz, OCH_3); 3.88 (3H, d, J_{HP} = 10.5 Hz, OCH_3); 4.22 (1H, d, J_{HP} = 26.7 Hz, CHP); 6.37-6.39 (1H, m, =CH); 6.49-6.52 (1H, m, =CH); 7.43-7.45 (1H, m, CHO). **^{31}P NMR δ (121 MHz, $CDCl_3$, ppm):** 23.71. **MS m/z (%):** 262 (100, $[M+H]^+$). Oil.

3.3 Carbamoylation of 1-Aminoalkyl Phosphonates

The carbamoylation reaction with aryl isocyanates occurs without catalyst. The α-amino phosphonate (1 mmol) is dissolved in 20 ml of dry THF or $CHCl_3$ and stirred under a nitrogen atmosphere. One equivalent of the isocyanate is added using a syringe and the mixture is stirred for 5 hours at room temperature. The solvent is evaporated under reduced pressure. As a slight excess of isocyanate results in formation of the corresponding urea, the products are mostly purified using column chromatography.

For the reaction with alkyl isocyanates, 3 equivalents of the isocyanate are added with a syringe to a mixture of 1 mmol of the α-amino phosphonate and 0.1 equivalents of Cu(I)Cl in dry CH_2Cl_2. The reaction is kept under a nitrogen atmosphere during overnight reflux. Then, the mixture is concentrated under reduced pressure and chromatographed on a silica gel column to furnish the pure product.

Dimethyl (3*E*)-[1-(1-benzyl-3-phenylureido)-3-phenylprop-2-enyl] phosphonate (206a)

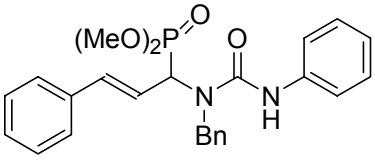

^{1}H NMR δ (300 MHz, $CDCl_3$, ppm): 3.80 (3H, d, J_{HP} = 10.5 Hz, C$\underline{H}_3$O); 3.82 (3H, d, J_{HP} = 10.7 Hz, C$\underline{H}_3$O); 4.61 (1H, d, J = 16.7 Hz, C$\underline{H}_A$H$_B$); 4.99 (1H, d, J = 16.7 Hz, CH$_A\underline{H}_B$); 5.25 (1H, dd, J = 7.8 Hz and J_{HP} = 22.6 Hz, C$\underline{H}$P); 6.34 (1H, td, J = 7.8 Hz and J_{trans} = 15.9 Hz, PhCH=C$\underline{H}$); 6.78 (1H, br d, J_{trans} = 15.9 Hz, PhC$\underline{H}$=CH)); 6.97-7.01 (1H, m, C$\underline{H}_{arom}$); 7.20-7.44 (14H, m, C$\underline{H}_{arom}$); 7.52 (1H, br s, N$\underline{H}$). **^{13}C NMR δ (75 MHz, $CDCl_3$, ppm):** 50.79 (N$\underline{C}$H$_2$); 53.72 (d, J_{CP} = 6.9 Hz, $\underline{C}$H$_3$O,); 53.89 (d, J_{CP} = 6.9 Hz, $\underline{C}$H$_3$O); 55.40 (d, J_{CP} = 156.9 Hz, $\underline{C}$HP); 119.77 (PhCH=$\underline{C}$H); 119.85 (2 x $\underline{C}H_{arom}$); 123.19 ($\underline{C}H_{arom}$); 126.84 (2 x $\underline{C}H_{arom}$); 127.68 (2 x $\underline{C}H_{arom}$); 128.12 ($\underline{C}H_{arom}$); 128.55 ($\underline{C}H_{arom}$); 128.73 (2 x $\underline{C}H_{arom}$); 128.90 (2 x $\underline{C}H_{arom}$); 129.15 (2 x $\underline{C}H_{arom}$); 135.93 ($\underline{C}_{q,arom}$); 137.05 (d, J_{CP} = 12.7 Hz, Ph$\underline{C}$H=CH); 137.28 ($\underline{C}_{q,arom}$); 139.09 ($\underline{C}_{q,arom}$); 155.59 (C=O). **^{31}P NMR δ (121 MHz, $CDCl_3$, ppm):** 25.51. **IR ν (cm^{-1}):** 1030 (P-O); 1051 (P-O); 1238 (P=O); 1662 (C=O, urea); 3318 (NH). **MS m/z (%):** 451 (100, $[M+H]^+$). **Mp.:** 102 °C. **Chromatography:** R_f = 0.25 (EtOAc/PE 50/50) **Yield:** 73 %. White solid.

Dimethyl (3*E*)-[3-phenyl-1-(3-phenyl-1-propyl-ureido)prop-2-enyl] phosphonate (206b)

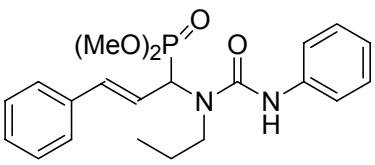

^{1}H NMR δ (300 MHz, $CDCl_3$, ppm): 0.96 (3H, t, J = 7.4 Hz, C$\underline{H}_3$, propyl); 1.63-1.83 (2H, m, C$\underline{H}_2$CH$_3$); 3.29-3.41 (1H, m, NC$\underline{H}_A$H$_B$); 3.49-3.61 (1H, m, NCH$_A\underline{H}_B$); 3.83 (3H, d, J_{HP} = 10.7 Hz, C$\underline{H}_3$O); 3.85 (3H, d, J_{HP} = 10.7 Hz, C$\underline{H}_3$O); 4.89 (1H, dd, J = 7.8 Hz and J_{HP} = 25.3 Hz, C$\underline{H}$P); 6.41 (1H, ddd, J = 7.8 Hz, J = 8.2 Hz and J_{trans} = 15.8 Hz, PhCH=C$\underline{H}$); 6.78 (1H, dd, J = 2.2 Hz and J_{trans} = 15.8 Hz, PhC$\underline{H}$=CH)); 7.02 (1H, t, J = 7.4 Hz, C$\underline{H}_{arom}$); 7.28-7.47 (9H, m, C$\underline{H}_{arom}$); 7.96 (1H, br s, N$\underline{H}$). **^{13}C NMR δ (75 MHz, $CDCl_3$, ppm):** 11.51 ($\underline{C}$H$_3$, propyl); 22.44 (CH$_3\underline{C}$H$_2$); 50.07 (N$\underline{C}$H$_2$); 53.83 (d, J_{CP} = 6.9 Hz, $\underline{C}$H$_3$O); 54.02 (d, J_{CP} = 8.1 Hz, $\underline{C}$H$_3$O); 56.78 (d, J_{CP} = 156.9 Hz, $\underline{C}$HP); 119.91 (2 x $\underline{C}H_{arom}$); 120.06 (PhCH=$\underline{C}$H); 123.01 ($\underline{C}H_{arom}$); 126.84 (2 x $\underline{C}H_{arom}$); 128.58 ($\underline{C}H_{arom}$); 128.81 (2 x $\underline{C}H_{arom}$); 128.90 (2 x $\underline{C}H_{arom}$); 135.91 ($\underline{C}_q$(Ph)); 136.20 (Ph$\underline{C}$H=CH, J_{CP} = 13.9 Hz); 139.42 ($\underline{C}_{q,arom}$); 155.19 (C=O). **^{31}P NMR δ (121 MHz, $CDCl_3$, ppm):** 25.59. **IR ν (cm^{-1}):** 1034 (P-O); 1053 (P-O); 1237 (P=O); 1655 (C=O, urea); 3327 (NH). **MS m/z (%):** 403 (100, $[M+H]^+$). **Mp.:** 107 °C. **Chromatography:** R_f = 0.37 (EtOAc/PE 25/10) **Yield:** 72 %. Slightly yellow powder.

Dimethyl (3*E*)-[1-(1-benzyl-3-propylureido)-3-phenylprop-2-enyl] phosphonate (206d)

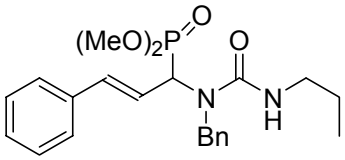

^{1}H NMR δ (300 MHz, $CDCl_3$, ppm): 0.71 (3H, t, J = 7.4 Hz, C$\underline{H}_3$, propyl); 1.29-1.41 (2H, m, C$\underline{H}_2$CH$_3$); 3.09-3.16 (2H, m, NC$\underline{H}_2$, propyl); 3.77 (3H, d, J_{HP} = 10.7 Hz, C$\underline{H}_3$O); 3.79 (3H, d, J_{HP} = 10.7 Hz, C$\underline{H}_3$O); 4.54 (1H, d, J = 17.2 Hz, NC$\underline{H}_A$H$_B$, benzyl); 4.86 (1H, d, J_{AB} = 17.2 Hz, NCH$_A\underline{H}_B$, benzyl); 4.86 (1H, br s, N$\underline{H}$); 5.52 (1H, dd, J = 8.4 Hz and J_{HP} = 22.8 Hz, C$\underline{H}$P); 6.28 (1H, ddd, J = 8.4 Hz, J = 9.1 Hz and J_{trans} = 15.8 Hz, PhCH=C$\underline{H}$); 6.74 (1H, dd, J = 2.9 Hz and J_{trans} = 15.8 Hz, PhC$\underline{H}$=CH)); 7.24-7.34 (10H, m, C$\underline{H}_{arom}$). **^{13}C NMR δ (75 MHz, $CDCl_3$, ppm):** 11.17 (C$\underline{H}_3$, propyl); 23.13 (CH$_3$C$\underline{H}_2$); 42.82 (NC$\underline{H}_2$, propyl); 49.55 (NC$\underline{H}_2$, benzyl); 53.29 (d, J_{CP} = 6.9 Hz, C$\underline{H}_3$O); 53.55 (d, J_{CP} = 6.9 Hz, C$\underline{H}_3$O); 54.49 (d, J_{CP} = 155.8 Hz, C$\underline{H}$P); 120.40 (PhCH=C$\underline{H}$); 126.69 (2 x C$\underline{H}_{arom}$); 126.90 (2 x C$\underline{H}_{arom}$); 127.64 (C$\underline{H}_{arom}$); 128.29 (C$\underline{H}_{arom}$); 128.63 (2 x C$\underline{H}_{arom}$); 128.89 (2 x C$\underline{H}_{arom}$); 136.09 (C$\underline{_{q,arom}}$); 136.36 (d, J_{CP} = 12.7 Hz, PhC$\underline{H}$=CH); 137.68 (C$\underline{_{q,arom}}$); 157.88 (d, J_{CP} = 2.3 Hz, C=O). **^{31}P NMR δ (121 MHz, $CDCl_3$, ppm):** 25.58. **IR ν (cm^{-1}):** 1032 (P-O); 1054 (P-O); 1247 (P=O); 1646 (C=O, urea); 3360 (NH). **MS m/z (%):** 417 (100, $[M+H]^+$). **Chromatography:** R_f = 0.1 (EtOAc/PE 3/1) **Yield:** 66 %. Yellow liquid.

Dimethyl (3*E*)-[1-(3-allyl-1-benzylureido)-3-phenylprop-2-enyl] phosphonate (206e)

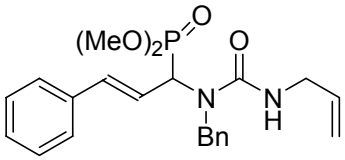

^{1}H NMR δ (300 MHz, $CDCl_3$, ppm): 3.76 (3H, d, J_{HP} = 10.7 Hz, C$\underline{H}_3$O); 3.76-3.83 (2H, m, NC$\underline{H}_2$, allyl); 3.78 (3H, d, J_{HP} = 10.7 Hz, C$\underline{H}_3$O); 4.58 (1H, d, J = 17.5 Hz, C$\underline{H}_A$H$_B$, benzyl); 4.89 (1H, d, J = 17.5 Hz, CH$_A\underline{H}_B$, benzyl); 4.92 (1H, dq, J_{trans} = 17.1 Hz and J = 1.7 Hz, =C$\underline{H}_A$H$_B$); 4.96 (1H, dq, J_{cis} = 10.5 Hz J and J = 1.5 Hz, =CH$_A\underline{H}_B$); 5.04 (1H, br s, N$\underline{H}$); 5.52 (1H, dd, J = 8.6 Hz and J_{HP} = 22.4 Hz, C$\underline{H}$P); 5.73 (1H, tdd, J = 5.2 Hz, J_{cis} = 10.5 Hz and J_{trans} = 17.1 Hz, CH$_2$=C$\underline{H}$); 6.28 (1H, td, J = 8.6 Hz and J_{trans} = 15.7 Hz, PhCH=C$\underline{H}$); 6.73 (1H, dd, J = 2.8 Hz and J_{trans} = 15.7 Hz, PhC$\underline{H}$=CH)); 7.16-7.43 (10H, m, C$\underline{H}_{arom}$). **^{13}C NMR δ (75 MHz, $CDCl_3$, ppm):** 43.30 (NC$\underline{H}_2$, allyl); 49.53 (NC$\underline{H}_2$, benzyl); 53.26 (d, J_{CP} = 6.9 Hz, C$\underline{H}_3$O); 53.58 (d, J_{CP} = 8.1 Hz, C$\underline{H}_3$O); 54.57 (d, J_{CP} = 156.9 Hz, C$\underline{H}$P); 115.05 (=C$\underline{H}_2$); 120.16 (PhCH=C$\underline{H}$); 126.66 (2 x C$\underline{H}_{arom}$); 126.82 (2 x C$\underline{H}_{arom}$); 127.64 (C$\underline{H}_{arom}$); 128.27 (C$\underline{H}_{arom}$); 128.57 (2 x C$\underline{H}_{arom}$); 128.88 (2 x C$\underline{H}_{arom}$); 134.99 (C$\underline{H}$=CH$_2$); 135.99 (C$\underline{_{q,arom}}$); 136.51 (d, J_{CP} = 13.8 Hz, PhC$\underline{H}$=CH); 137.38 (C$\underline{_{q,arom}}$); 157.64 (d, J_{CP} = 3.5 Hz, C=O). **^{31}P NMR δ (121 MHz, $CDCl_3$, ppm):** 25.46. **IR ν (cm^{-1}):**

1031 (P-O); 1052 (P-O); 1249 (P=O); 1653 (C=O, urea); 3347 (NH). **MS m/z (%):** 415 (100, $[M+H]^+$). **Chromatography:** R_f = 0.14 (EtOAc/PE 8/1) **Yield:** 21 %. Liquid.

Dimethyl (3*E*)-[1-(3-allyl-1-propylureido)-3-phenylprop-2-enyl] phosphonate (206f)

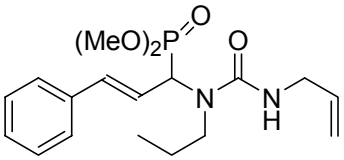

^{1}H NMR δ (300 MHz, $CDCl_3$, ppm): 0.91 (3H, t, J = 7.4 Hz, C$\underline{H}_3$, propyl); 1.52-1.81 (2H, m, C$\underline{H}_2$CH$_3$); 3.21-3.32 (1H, m, NC$\underline{H}_A$H$_B$, propyl); 3.38-3.49 (1H, m, NCH$_A\underline{H}_B$, propyl); 3.78 (3H, d, J_{HP} = 10.7 Hz, C$\underline{H}_3$O); 3.80 (3H, d, J_{HP} = 10.5 Hz, C$\underline{H}_3$O); 3.91 (2H, br t, J = 5.4 Hz, NC$\underline{H}_2$, allyl); 5.11 (1H, dq, J_{cis} = 10.2 Hz and J = 1.4 Hz, =C$\underline{H}_A$H$_B$); 5.20 (1H, dq, J_{trans} = 17.1 Hz and J = 1.6 Hz, =CH$_A\underline{H}_B$); 5.20-5.29 (2H, m, N$\underline{H}$ and C$\underline{H}$P); 5.90 (1H, tdd, J = 5.4 Hz, J_{cis} = 10.2 Hz and J_{trans} = 17.1 Hz, CH$_2$=C$\underline{H}$); 6.35 (1H, ddd, J = 8.0 Hz, J = 9.6 Hz and J_{trans} = 15.9 Hz, PhCH=C$\underline{H}$); 6.76 (1H, dd, J = 2.1 Hz and J_{trans} = 15.9 Hz, PhC$\underline{H}$=CH)); 7.24-7.42 (5H, m, C$\underline{H}_{arom}$). **^{13}C NMR δ (75 MHz, $CDCl_3$, ppm):** 11.51 (C$\underline{H}_3$, propyl); 22.64 (CH$_3\underline{C}$H$_2$); 43.61 (N$\underline{C}$H$_2$, allyl); 48.53 (N$\underline{C}$H$_2$, propyl), 53.52 (d, J_{CP} = 6.9 Hz, $\underline{C}$H$_3$O); 53.57 (d, J_{CP} = 6.9 Hz, $\underline{C}$H$_3$O); 55.11 (d, J_{CP} = 156.9 Hz, $\underline{C}$HP); 115.65 (=$\underline{C}$H$_2$); 120.52 (PhCH=$\underline{C}$H); 126.77 (2 x $\underline{C}$H$_{arom}$); 128.37 ($\underline{C}$H$_{arom}$); 128.73 (2 x $\underline{C}$H$_{arom}$); 135.51 ($\underline{C}$H=CH$_2$); 135.93 (d, J_{CP} = 13.8 Hz, Ph$\underline{C}$H=CH); 136.17 ($\underline{C}_{q,arom}$); 157.29 (d, J_{CP} = 3.5 Hz, C=O). **^{31}P NMR δ (121 MHz, $CDCl_3$, ppm):** 25.57. **IR ν (cm^{-1}):** 1034 (P-O); 1052 (P-O); 1248 (P=O); 1634 (C=O, urea); 3351 (NH). **MS m/z (%):** 367 (100, $[M+H]^+$). **Chromatography:** R_f = 0.16 (EtOAc/PE 8/1) **Yield:** 73 %. Crystals.

Dimethyl 3-phenyl-1-(3-phenyl-1-propylureido)propenyl phosphonate (207b)

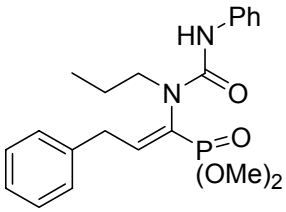

^{1}H NMR δ (300 MHz, $CDCl_3$, ppm): 0.95 (3H, t, J = 7.3 Hz, C$\underline{H}_3$, propyl); 1.59-1.81 (2H, m, C$\underline{H}_2$CH$_3$); 3.32-3.42 (1H, m, NC$\underline{H}_A$H$_B$); 3.59 (2H, dd, J = 3.2 Hz and J = 7.3 Hz, C$\underline{H}_2$); 3.67-3.80 (1H, m, NCH$_A\underline{H}_B$); 3.79 (3H, d, J_{HP} = 11.0 Hz, C$\underline{H}_3$O); 3.81 (3H, d, J_{HP} = 10.7 Hz, C$\underline{H}_3$O); 6.85 (1H, s, N$\underline{H}$); 6.97-7.07 (2H, m, =C$\underline{H}$ and C$\underline{H}_{arom}$); 7.12-7.16 (2H, m, C$\underline{H}_{arom}$); 7.21-7.33 (7H, m, C$\underline{H}_{arom}$). **^{13}C NMR δ (75 MHz, $CDCl_3$, ppm):** 11.54 (C$\underline{H}_3$, propyl); 21.92 (CH$_3\underline{C}$H$_2$); 34.58 (d, J_{CP} = 13.9 Hz, $\underline{C}$H$_2$); 50.10 (N$\underline{C}$H$_2$); 53.35 (d, J_{CP} = 5.8 Hz, $\underline{C}$H$_3$O); 53.42 (d, J_{CP} = 5.8 Hz, $\underline{C}$H$_3$O); 119.42 (2 x $\underline{C}$H$_{arom}$); 123.07 ($\underline{C}$H$_{arom}$); 127.09 ($\underline{C}$H$_{arom}$); 128.64 (2 x $\underline{C}$H$_{arom}$); 128.95 (2 x $\underline{C}$H$_{arom}$); 129.07 (2 x $\underline{C}$H$_{arom}$); 130.51 (d, J_{CP} = 216.9 Hz, $\underline{C}_q$P); 136.69 ($\underline{C}_{q,arom}$); 138.98 ($\underline{C}_{q,arom}$); 149.81 (d, J_{CP} = 28.8 Hz, =$\underline{C}$H); 153.94 (C=O). **^{31}P NMR δ (121 MHz, $CDCl_3$, ppm):**

15.84. **IR ν (cm^{-1}):** 1030 (P-O); 1052 (P-O); 1246 (P=O); 1672 (C=O, urea); 3316 (NH). **MS m/z (%):** 403 (100, $[M+H]^+$). **Chromatography:** R_f = 0.13 (EtOAc/PE 6/5) **Yield:** 37%.

Dimethyl (3-allyl-1-propylureido)furan-2-ylmethyl phosphonate (238)

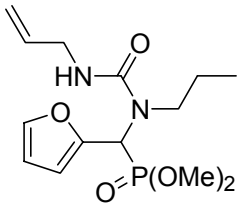

^{1}H NMR δ (300 MHz, $CDCl_3$, ppm): 0.85 (3H, t, J = 7.3 Hz, C$\underline{H}_3$, propyl); 0.94-1.14 (1H, m, C$\underline{H}_a$H$_b$CH$_3$); 1.56-1.73 (1H, m, CH$_a\underline{H}_b$CH$_3$); 3.30-3.40 (1H, m, NC$\underline{H}_a$H$_b$CH$_2$); 3.49-3.59 (1H, m, NCH$_a\underline{H}_b$CH$_2$); 3.81 (3H, d, J_{HP} = 10.7 Hz, OCH$_3$); 3.91 (3H, d, J_{HP} = 10.7 Hz, OCH$_3$); 3.97-4.04 (2H, m, NC$\underline{H}_2$, allyl); 5.12 (1H, dq, J_{cis} = 10.3 Hz and J = 1.6 Hz, =C$\underline{H}_A$H$_B$); 5.19 (1H, dq, J_{trans} = 17.3 Hz and J = 1.6 Hz, =CH$_A\underline{H}_B$); 5.27 (1H, t, J = 5.6 Hz, NH); 5.90 (1H, ddt, J_{cis} = 10.3 Hz, J_{trans} = 17.3 Hz and J = 5.2 Hz, CH$_2$=C$\underline{H}$); 6.20 (1H, d, J_{HP} = 23.7 Hz, CHP); 6.39-6.42 (1H, m, =CH); 6.68 (1H, br d, J = 3.3 Hz, =CH); 7.45-7.47 (1H, m, CHO). **^{13}C NMR δ (75 MHz, $CDCl_3$, ppm):** 11.09 (CH$_3$); 21.55 (CH$_2$); 43.42 (NCH$_2$, allyl); 46.68 (NCH$_2$, propyl); 48.24 (d, J_{CP} = 163.8 Hz, CHP); 53.37 (d, J_{CP} = 6.9 Hz, OCH$_3$); 53.46 (d, J_{CP} = 6.9 Hz, OCH$_3$), 110.67 (=$\underline{C}$H); 111.49 (d, J_{CP} = 3.5 Hz, =$\underline{C}$H); 115.21 (CH$_2$=); 135.51 (CH$_2$=$\underline{C}$H); 143.01 (=CHO); 147.36 (d, J_{CP} = 13.9 Hz, =C$_q$O); 156.99 (d, J_{CP} = 3.5 Hz, C=O). **^{31}P NMR δ (121 MHz, $CDCl_3$, ppm):** 22.61. **IR ν (cm^{-1}):** 1039 (P-O); 1249 (P=O); 1531 (NH); 1634 (C=O, urea); 3358 (NH). **MS m/z (%):** 331 (100, $[M+H]^+$). **Chromatography:** R_f = 0.1 (EtOAc/PE 8/2) **Yield:** 77 %. Oil.

Dimethyl (1-allyl-3-propylureido)furan-2-ylmethyl phosphonate (240)

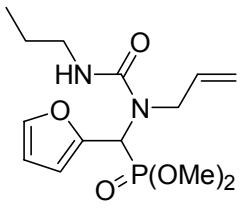

^{1}H NMR δ (300 MHz, $CDCl_3$, ppm): 0.89 (3H, t, J = 7.3 Hz, C$\underline{H}_3$, propyl); 1.49 (2H, sextet, J = 7.3 Hz, C$\underline{H}_2$CH$_3$); 3.20 (2H, dd, J = 6.6 Hz and J = 11.1 Hz, NC$\underline{H}_2$CH$_2$); 3.72 (3H, d, J_{HP} = 10.7 Hz, OCH$_3$); 3.82 (3H, d, J_{HP} = 10.7 Hz, OCH$_3$); 3.95 (1H, dd, J = 5.4 Hz and J = 17.6 Hz, NC$\underline{H}_a$H$_b$, allyl); 4.11 (1H, dd, J = 5.4 Hz and J = 17.6 Hz, NCH$_a\underline{H}_b$, allyl); 4.82 (1H, br s, NH); 5.08-5.16 (2H, m, =C$\underline{H}_2$); 5.60 (1H, ddt, J_{cis} = 10.3 Hz, J_{trans} = 17.2 Hz and J = 5.4 Hz, CH$_2$=C$\underline{H}$); 6.30 (1H, d, J_{HP} = 23.7 Hz, CHP); 6.33-6.36 (1H, m, =CH); 6.62 (1H, br d, J = 3.0 Hz, =CH); 7.40-7.43 (1H, m, CHO). **^{13}C NMR δ (75 MHz, $CDCl_3$, ppm):** 11.45 (CH$_3$); 23.28 (CH$_2$); 42.90 (NCH$_2$, allyl); 47.92 (NCH$_2$, propyl); 47.94 (d, J_{CP} = 163.8 Hz, CHP); 53.57 (d, J_{CP} = 6.9 Hz, 2 x OCH$_3$); 110.67 (=$\underline{C}$H); 111.52 (d, J_{CP} = 3.5 Hz, =$\underline{C}$H); 116.75 (CH$_2$=); 135.36 (CH$_2$=$\underline{C}$H); 143.18 (=CHO); 147.48 (d, J_{CP} = 13.9 Hz, =C$_q$O); 157.90 (d, J_{CP} = 3.5 Hz, C=O). **^{31}P NMR δ (121 MHz, $CDCl_3$,**

ppm): 22.59. **IR ν (cm^{-1}):** 1247 (P=O); 1547 (NH); 1643 (C=O, urea); 3380 (NH). **MS m/z (%):** 331 (100, $[M+H]^+$). **Mp.:** 71 °C. **Yield:** 65 %. Oil.

3.4 Synthesis of 1,4,2-Diazaphospholidin-5-ones

The α-ureido phosphonate (5 mmol) is dissolved in 5 ml of dry CH_3CN, freshly distilled from CaH_2, and heated under reflux for 9 hours, shielded from moisture with a $CaCl_2$-tube. The reaction mixture is concentrated under reduced pressure and purified using column chromatography.

4-Benzyl-2-methoxy-2-oxo-1-propyl-3-styryl-2λ^5-[1,4,2]-diazaphospholidin-5-one (211a)

This compound was obtained as a diastereomeric mixture (ratio: 45/55). Signals of the major and minor isomers are indicated as 'M' and 'm' whenever possible.

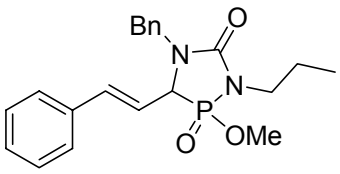

^{1}H NMR δ (300 MHz, $CDCl_3$, ppm): 0.97 (3H, t, J = 7.4 Hz, C$\underline{H}_3$, M); 0.98 (3H, t, J = 7.4 Hz, C$\underline{H}_3$, m); 1.65-1.81 (4H, m, C$\underline{H}_2$CH$_3$, M+m); 3.27-3.50 (4H, m, NC$\underline{H}_2$, M+m); 3.75 (3H, d, J_{HP} = 11.6 Hz, OCH_3, m); 3.78 (3H, d, J_{HP} = 11.3 Hz, OCH_3, M); 3.95 (1H, d, J = 15.0 Hz, NC$\underline{H}_a$H$_b$Ph, m); 3.95 (1H, dd, J = 9.3 Hz and J_{HP} = 17.8 Hz, CHP, m); 3.99 (1H, d, J = 14.7 Hz, NC$\underline{H}_a$H$_b$Ph, M); 4.15 (1H, dd, J = 9.5 Hz and J_{HP} = 16.8 Hz, CHP, M); 5.05 (1H, dd, J = 1.9 Hz and J = 14.7 Hz, NCH$_a\underline{H}_b$Ph, M); 5.18 (1H, dd, J = 2.2 Hz and J = 15.0 Hz, NC$\underline{H}_a$H$_b$Ph, m); 5.90 (1H, ddd, J = 5.4 Hz, J = 9.5 Hz and J_{trans} = 15.8 Hz, PhCH=C$\underline{H}$, M); 6.05 (1H, ddd, J = 6.0 Hz, J = 9.3 Hz and J_{trans} = 15.7 Hz, PhCH=C$\underline{H}$, m); 6.51 (1H, dd, J = 4.3 Hz and J_{trans} = 15.7 Hz, PhC$\underline{H}$=CH, m); 6.62 (1H, dd, J = 4.5 Hz and J_{trans} = 15.8 Hz, PhC$\underline{H}$=CH, M); 7.18-7.24 (4H, m, CH_{arom}, M+m); 7.27-7.41 (16H, m, CH_{arom}, M+m). **^{13}C NMR δ (75 MHz, $CDCl_3$, ppm):** 11.37 (CH_3, M+m); 22.94 ($\underline{C}H_2CH_3$, M); 23.05 ($\underline{C}H_2CH_3$, m); 42.35 (N$\underline{C}H_2$, M+m); 45.49 (d, J_{CP} = 10.4 Hz, N$\underline{C}H_2$Ph, m); 45.74 (d, J_{CP} = 11.5 Hz, N$\underline{C}H_2$Ph, M); 53.92 (d, J_{CP} = 6.9 Hz, CH_3O, m); 54.48 (d, J_{CP} = 121.2 Hz, CHP, m); 54.81 (d, J_{CP} = 6.9 Hz, CH_3O, M); 55.96 (d, J_{CP} = 118.8 Hz, CHP, M); 119.67 (d, J_{CP} = 6.9 Hz, PhCH=$\underline{C}$H, m); 199.90 (d, J_{CP} = 10.4 Hz, PhCH=$\underline{C}$H, M); 126.77 ($\underline{C}H_{arom}$, M+m); 127.04 ($\underline{C}H_{arom}$, M+m); 127.93 ($\underline{C}H_{arom}$, M+m); 127.97 ($\underline{C}H_{arom}$, M+m); 128.37 ($\underline{C}H_{arom}$, M+m); 128.64 ($\underline{C}H_{arom}$, M+m); 128.75 (2 x $\underline{C}H_{arom}$, M+m); 128.93 (2 x $\underline{C}H_{arom}$, M+m); 135.39 ($\underline{C}_{q,arom}$, M); 135.42 ($\underline{C}_{q,arom}$, m); 135.94 ($\underline{C}_{q,arom}$, M); 136.25 ($\underline{C}_{q,arom}$, m); 137.15 (d, J_{CP} = 12.7 Hz, Ph$\underline{C}$H=CH, m); 137.42 (d, J_{CP} = 11.5 Hz, Ph$\underline{C}$H=CH, M); 155.62 (d, J_{CP} = 27.7 Hz, C=O, m); 155.67 (d, J_{CP} = 27.7 Hz, C=O, M). **^{31}P NMR δ**

(121 MHz, $CDCl_3$, ppm): 28.05 (M) and 29.31 (m). **IR ν (cm^{-1}):** 1723 (C=O). **MS m/z (%):** 385 (100, $[M+H]^+$). **Chromatography:** R_f = 0.18 and 0.20 (EtOAc/PE 1/4) **Yield:** 72%.

1-Allyl-3-furan-2-yl-2-methoxy-2-oxo-4-propyl-2λ^5-[1,4,2]diazaphospholidin-5-one (239)

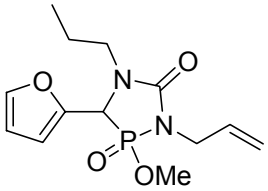

Diastereomer 1: **^{1}H NMR δ (300 MHz, $CDCl_3$, ppm):** 0.84 (3H, t, J = 7.4 Hz, C<u>H</u>$_3$, propyl); 1.34-1.53 (2H, m, C<u>H</u>$_2$CH$_3$); 2.80 (1H, ddd, J = 5.5 Hz, J = 8.5 Hz and J = 14.3 Hz, NC<u>H</u>$_a$H$_b$CH$_2$); 3.52 (3H, d, J_{HP} = 11.3 Hz, OCH$_3$); 3.56-3.68 (1H, m, NCH$_a$<u>H</u>$_b$CH$_2$); 4.01 (2H, br dd, J = 6.0 Hz and J = 10.2 Hz, NC<u>H</u>$_2$, allyl); 4.85 (1H, d, J_{HP} = 19.3 Hz, CHP); 5.21 (1H, dq, J_{cis} = 10.2 Hz and J = 1.4 Hz, =C<u>H</u>$_A$H$_B$); 5.32 (1H, dq, J_{trans} = 17.1 and Hz J = 1.4 Hz, =CH$_A$<u>H</u>$_B$); 5.92 (1H, ddt, J_{cis} = 10.2 Hz, J_{trans} = 17.1 Hz and J = 6.0 Hz, CH$_2$=C<u>H</u>); 6.43-6.45 (2H, m, =CH); 7.49-7.51 (1H, m, CHO). **^{13}C NMR δ (75 MHz, $CDCl_3$, ppm):** 11.12 (CH$_3$, propyl); 20.50 (<u>C</u>H$_2$CH$_3$); 42.79 (NCH$_2$); 44.30 (d, J = 9.2 Hz, NCH$_2$); 52.24 (d, J_{CP} = 117.7 Hz, CHP); 54.44 (d, J_{CP} = 6.9 Hz, OCH$_3$), 110.90 (d, J_{CP} = 6.9 Hz, =<u>C</u>H); 111.15 (d, J_{CP} = 3.5 Hz, =<u>C</u>H); 118.00 (CH$_2$=); 133.01 (CH$_2$=<u>C</u>H); 144.05 (=CHO); 144.77 (d, J_{CP} = 10.4 Hz, =C$_q$O); 155.39 (d, J_{CP} = 25.4 Hz, C=O). **^{31}P NMR δ (121 MHz, $CDCl_3$, ppm):** 24.63. **IR ν (cm^{-1}):** 1710 (C=O). **MS m/z (%):** 299 (100, $[M+H]^+$). **Chromatography:** R_f = 0.1 (EtOAc/PE 4/7) **Yield:** 21 %. Oil.

Diastereomer 2: ^{1}H NMR δ (300 MHz, $CDCl_3$, ppm): 0.86 (3H, t, J = 7.3 Hz, C<u>H</u>$_3$, propyl); 1.29-1.58 (2H, m, C<u>H</u>$_2$CH$_3$); 2.81 (1H, ddd, J = 5.3 Hz, J = 8.6 Hz and J = 14.0 Hz, NC<u>H</u>$_a$H$_b$CH$_2$); 3.60-3.70 (1H, m, NCH$_a$<u>H</u>$_b$CH$_2$); 3.84 (3H, d, J_{HP} = 11.8 Hz, OCH$_3$); 3.89-4.01 (1H, m, NC<u>H</u>$_a$H$_b$, allyl); 4.07-4.20 (1H, m, NCH$_a$<u>H</u>$_b$, allyl); 4.65 (1H, d, J_{HP} = 19.8 Hz, CHP); 5.22 (1H, dq, J_{cis} = 10.2 Hz and J = 1.4 Hz, =C<u>H</u>$_A$H$_B$); 5.34 (1H, dq, J_{trans} = 17.2 Hz and J = 1.4 Hz, =CH$_A$<u>H</u>$_B$); 5.86-5.99 (1H, m, CH$_2$=C<u>H</u>); 6.39-6.41 (1H, m, =CH); 6.43-6.46 (1H, m, =CH); 7.47-7.48 (1H, m, CHO). **^{31}P NMR δ (121 MHz, $CDCl_3$, ppm):** 26.38. **IR ν (cm^{-1}):** 1709 (C=O). **MS m/z (%):** 299 (100, $[M+H]^+$). **Chromatography:** R_f = 0.05 (EtOAc/PE 4/7) **Yield:** 15 %. Oil.

3.5 Acylation of 1-Aminoalkyl Phosphonates

To a solution of 5 mmol of the 1-aminoalkyl phosphonate and 10 mmol of pyridine in 10 ml dry THF, 1.5 equivalents of the acid chloride (7.5 mmol) was added dropwise, at room

temperature, under a nitrogen atmosphere. The reaction was stirred at room temperature for 0.5 to 3 hours, depending on the substrate and the acid chloride. Then, the reaction was quenched with 10 ml of a saturated $NaHCO_{3(aq)}$ solution and mixed with 10 ml of diethyl ether in a separatory funnel. The organic phase was collected and the remaining aqueous phase was washed twice with 5 ml of diethyl ether. The combined organic phases were mixed with 10 ml of a 1 M $HCl_{(aq)}$ solution. The organic phase was collected and the remaining aqueous phase was washed twice with 5 ml of diethyl ether. The combined organic phases were dried using $MgSO_4$, after filtration, the solvent was evaporated under reduced pressure. Only ^{31}P NMR data are given, as partial ring closure occurred during acylation.

The synthesis of **11a-e** and **221** and **223** was described in reference 13 and Paper VII in Appendix2.

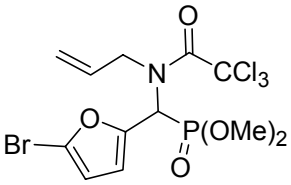

Dimethyl [allyl(trichloroacetyl)amino]-(5-bromofuran-2-yl)methyl phosphonate

^{31}P NMR δ (121 MHz, $CDCl_3$, ppm): 20.45. **Yield:** 96 %. Brown oil.

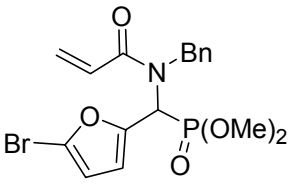

Dimethyl [benzyl(chloroacetyl)amino]furan-2-ylmethyl phosphonate

^{31}P NMR δ (121 MHz, $CDCl_3$, ppm): 20.75. **Yield:** 94 %. Brown oil.

To a solution of 8 mmol of the 1-aminoalkyl phosphonate in 15 ml dry CH_2Cl_2, 1.5 equivalents of the acid chloride (16 mmol) were added dropwise, at room temperature, under a nitrogen atmosphere. A precipitate was formed immediately. After stirring for 2.5 hours, 15 ml of 2N $NaOH_{(aq)}$ solution was added and stirred for an additional 15 minutes. After separation, the aqueous layer was extracted two times with CH_2Cl_2. After drying with $MgSO_4$, filtration and evaporation of the solvent under reduced pressure, the crude product was obtained, which was further purified using column chromatography.

Dimethyl [allyl-(2,2,2-trichloroacetyl)amino]-(1-methyl-1*H*-imidazol-2-yl)methyl phosphonate (235)

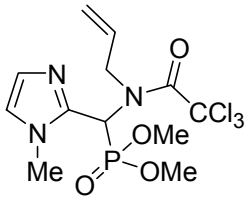

^{1}H NMR δ (300 MHz, $CDCl_3$, ppm): 3.55 (3H, s, C$\underline{H}_3$); 3.85 (3H, d, J_{HP} = 10.7 Hz, OC$\underline{H}_3$); 3.93 (3H, d, J_{HP} = 11.0 Hz, OC$\underline{H}_3$); 4.52 (1H, dd, J = 17.2 Hz and J = 8.0 Hz, NC$\underline{H}_a$H$_b$); 4.62 (1H, d, J_{trans} = 17.0 Hz, =C$\underline{H}_a$H$_b$); 4.72 (1H, d, J_{cis} = 10.2 Hz, =CH$_a\underline{H}_b$); 4.89 (1H, br d, J = 17.2 Hz, NCH$_a\underline{H}_b$); 5.12-5.28 (1H, m, C$\underline{H}$=CH$_2$); 6.35 (1H, d, J_{HP} = 22.8 Hz, C$\underline{H}$P); 6.86 (1H, s, NC$\underline{H}$); 7.01 (1H, d, J = 1.1 Hz, NC$\underline{H}$). **^{13}C NMR δ (75 MHz, $CDCl_3$, ppm):** 32.56 (C$\underline{H}_3$); 49.73 (d, J_{CP} = 165.0 Hz, C$\underline{H}$P); 50.07 (C$\underline{H}_2$N); 53.62 (d, J_{CP} = 6.9 Hz, OC$\underline{H}_3$); 54.45 (d, J_{CP} = 5.8 Hz, OC$\underline{H}_3$); 92.66 (C$\underline{C}$l$_3$); 116.86 (=C$\underline{H}_2$); 122.00 (NC$\underline{H}$); 128.40 (NC$\underline{H}$); 131.01 (C$\underline{H}$=CH$_2$); 138.97 (d, J_{CP} = 5.8 Hz, N=C$\underline{q}$); 161.04 (C=O). **^{31}P NMR δ (121 MHz, $CDCl_3$, ppm):** 20.95. **IR ν (cm^{-1}):** 1033 (P-O); 1249 (P=O); 1672 (C=O). **MS m/z (%):** 404/406/408/410 (100, $[M+H]^+$). **Yield:** 92 %. Oil.

Dimethyl (acryloylbenzylamino)-(1-methyl-1*H*-imidazol-2-yl)methyl phosphonate (236)

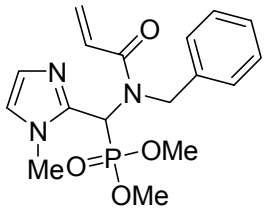

^{1}H NMR δ (300 MHz, $CDCl_3$, ppm): 3.53 (3H, s, C$\underline{H}_3$); 3.78 (3H, d, J_{HP} = 10.7 Hz, OC$\underline{H}_3$); 3.85 (3H, d, J_{HP} = 11.0 Hz, OC$\underline{H}_3$); 4.96 (1H, d, J = 17.8 Hz, NC$\underline{H}_a$H$_b$); 5.11 (1H, d, J = 17.8 Hz, NCH$_a\underline{H}_b$); 5.72 (1H, t, J = 6.1 Hz, C$\underline{H}$=CH$_2$); 6.50 (2H, d, J = 6.1 Hz, =C$\underline{H}_2$); 6.63 (1H, s, NC$\underline{H}$); 6.73 (1H, d, J_{HP} = 23.7 Hz, C$\underline{H}$P); 6.82 (2H, d, J = 6.9 Hz, 2 x C$\underline{H}_{ar}$); 6.89 (1H, NC$\underline{H}$); 7.08-7.17 (1H, m, C$\underline{H}_{ar}$); 7.12-7.20 (2H, m, C$\underline{H}_{ar}$). **^{13}C NMR δ (75 MHz, $CDCl_3$, ppm):** 33.05 (C$\underline{H}_3$); 45.46 (d, J_{CP} = 166.1 Hz, C$\underline{H}$P); 48.50 (C$\underline{H}_2$N); 53.68 (d, J_{CP} = 6.9 Hz, OC$\underline{H}_3$); 54.26 (d, J_{CP} = 6.9 Hz, OC$\underline{H}_3$); 121.83 (NC$\underline{H}$); 125.85 (2 x C$\underline{H}_{ar}$); 126.93 (C$\underline{H}_{ar}$); 127.24 (=C$\underline{H}_2$); 128.25 (2 x C$\underline{H}_{ar}$); 128.64 (NC$\underline{H}$); 130.32 (C$\underline{H}$=CH$_2$); 137.53 (C$\underline{q,ar}$); 139.91 (d, J_{CP} = 6.9 Hz, N=C$\underline{q}$); 166.88 (d, J_{CP} = 3.5 Hz, C=O). **^{31}P NMR δ (121 MHz, $CDCl_3$, ppm):** 22.03. **IR ν (cm^{-1}):** 1031 (P-O); 1055 (P-O); 1250 (P=O); 1651 (C=O). **MS m/z (%):** 264 (100, $[M+H]^+$). **Yield:** 36 %. Oil.

3.6 Intramolecular Diels-Alder with Furan (IMDAF)

A solution of the ring-open α-amino phosphonate was refluxed in CH_3CN (for **229**) or toluene (for **230**) until disappearance of the starting product was observed in the ^{31}P NMR

spectra: 1 hour for **229**, and 40 minutes for **230**. The solvent was removed under reduced pressure and after recrystallization in acetone the pure adducts ware obtained.

The synthesis of **12a-e** and **222** and **224** was described in reference 13 and Paper VII in Appendix2.

Dimethyl 7-bromo-3-(2,2,2-trichloroacetyl)-10-oxa-3-azatricyclo[5.2.1.0^{1,5}]dec-8-en-2-yl phosphonate (229)

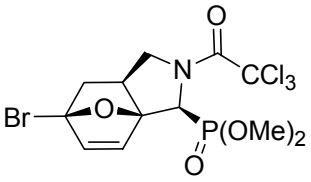

^{1}H NMR δ (300 MHz, $CDCl_3$, ppm): 2.05-2.18 (1H, m, $C\underline{H}_AH_B$); 2.09-2.12 (1H, m, $CH_A\underline{H}_B$); 2.20-2.30 (1H, m, CH); 3.52 (1H, t, J = 11.4 Hz, $NC\underline{H}_AH_B$); 3.82 (3H, d, J_{HP} = 11.0 Hz, OCH_3); 3.83 (3H, d, J_{HP} = 11.0 Hz, OCH_3); 4.78 (1H, dd, J = 11.4 Hz and J = 7.0 Hz, $NCH_A\underline{H}_B$); 5.06 (1H, d, J_{HP} = 14.9 Hz, CHP); 6.48 (1H, d, J = 5.8 Hz, =CH); 6.50 (1H, d, J = 5.8 Hz, =CH). **^{13}C NMR δ (75 MHz, $CDCl_3$, ppm):** 40.59 (CH_2); 48.17 (d, J_{CP} = 3.5 Hz, CH); 53.67 (d, J_{CP} = 5.8 Hz, OCH_3); 54.04 (d, J_{CP} = 5.8 Hz, OCH_3); 55.45 (NCH_2); 56.39 (d, J_{CP} = 161.5 Hz, CHP); 90.11 (CBrO); 92.84 (CCl_3); 93.30 (d, J_{CP} = 4.6 Hz, OC_q); 135.32 (=CH); 140.86 (=CH); 159.73 (C=O). **^{31}P NMR δ (121 MHz, $CDCl_3$, ppm):** 19.75. **IR ν (cm^{-1}):** 1025 (P-O); 1052 (P-O); 1255 (P=O); 1674 (C=O). **MS m/z (%):** 468/470/472/474/476 (100, $[M+H]^+$). **Mp.:** 182 °C. **Yield:** Major isomer 46 %. White crystals.

Dimethyl 3-benzyl-7-bromo-4-oxo-10-oxa-3-azatricyclo[5.2.1.0^{1,5}]dec-8-en-2-yl phosphonate (230)

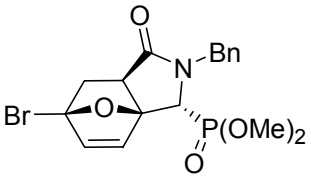

^{1}H NMR δ (300 MHz, $CDCl_3$, ppm): 2.27 (1H, dd, J = 12.0 Hz and J = 8.7 Hz, $C\underline{H}_AH_B$); 2.58 (1H, dd, J = 12.0 Hz and J = 3.5 Hz, $CH_A\underline{H}_B$); 2.84 (1H, dd, J = 8.7 Hz and J = 3.5 Hz, $C\underline{H}C_q$); 3.82 (3H, d, J_{HP} = 10.7 Hz, OCH_3); 3.83 (3H, d, J_{HP} = 10.7 Hz, OCH_3); 3.93 (1H, d, J_{HP} = 6.1 Hz, CHP); 4.25 (1H, d, J = 15.1 Hz, $NC\underline{H}_AH_B$); 5.31 (1H, J = 15.1 Hz, $NCH_A\underline{H}_B$); 6.43 (1H, d, J = 5.6 Hz, $=C\underline{H}C_qBrO$); 6.61 (1H, d, J = 5.6 Hz, $=C\underline{H}C_q$); 7.20-7.37 (5H, m, CH_{arom}). **^{13}C NMR δ (75 MHz, $CDCl_3$, ppm):** 39.97 (CH_2); 45.65 (NCH_2); 49.86 (CHC_q); 53.49 (d, J_{CP} = 6.9 Hz, OCH_3); 53.70 (d, J_{CP} = 8.1 Hz, OCH_3); 54.58 (d, J_{CP} = 161.5 Hz, CHP); 88.15 (C_qBrO); 88.98 (d, J_{CP} = 6.9 Hz, C_qO); 127.91 (CH_{arom}); 128.17 (2 x CH_{arom}); 128.90 (2 x CH_{arom}); 133.93 ($=\underline{C}HC_q$); 134.80 ($CH_{q,arom}$); 140.84 ($=\underline{C}HBrO$); 173.33 (C=O). **^{31}P NMR δ (121 MHz, $CDCl_3$, ppm):** 20.78.

IR ν (cm^{-1}): 1036 (P-O); 1239 (P=O); 1649 (C=O). **MS m/z (%):** 428/430 (100, $[M+H]^+$). **Yield:** 90 %.

3.7 Acylation with Maleic Anhydride and IMDAF

To a solution of 5 mmol of the alkylaminofuran-2-ylmethyl phosphonate in toluene (for **225b**) or CH_3CN (for **225a**) 1 equivalent of finely ground maleic andydride was added. The mixture was refluxed until maximal conversion to the Diels-Alder adduct was observed in the ^{31}P NMR spectra: 3 hours for **225b**, 4 hours for **225a**. The solvent was removed under reduced pressure and after recrystallization in acetone the pure adducts ware obtained.

3-Benzyl-2-(dimethoxyphosphoryl)-4-oxo-10-oxa-3-aza-tricyclo[5.2.1.0^{1,5}]dec-8-ene-6-carboxylic acid (225a)

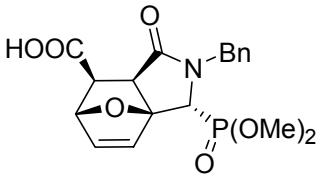

^{1}H NMR δ (300 MHz, $CDCl_3$, ppm): 2.81 (1H, d, J = 9.1 Hz, C<u>H</u>CO); 3.08 (1H, d, J = 9.1 Hz, C<u>H</u>CO); 3.83 (3H, d, J_{HP} = 10.7 Hz, OCH_3); 3.85 (3H, d, J_{HP} = 10.7 Hz, OCH_3); 3.97 (1H, d, J_{HP} = 5.5 Hz, CHP); 4.27 (1H, d, J = 15.1 Hz, NC<u>H</u>$_A$H$_B$); 5.18 (1H, d, J = 1.5 Hz, CHO); 4.27 (1H, d, J = 15.1 Hz, NCH$_A$<u>H</u>$_B$); 6.39 (1H, dd, J = 5.9 Hz, J = 1.5 Hz, =C<u>H</u>CHO); 6.65 (1H, d, J = 5.9 Hz, =CHC$_q$); 7.20-7.35 (5H, m, CH$_{arom}$). **^{13}C NMR δ (75 MHz, $CDCl_3$, ppm):** 45.75 (<u>C</u>HCO); 46.00 (NCH_2); 50.44 (<u>C</u>HCO); 53.59 (d, J_{CP} = 6.9 Hz, OCH_3); 53.91 (d, J_{CP} = 6.9 Hz, OCH_3); 54.59 (d, J_{CP} = 162.7 Hz, CHP); 81.28 (CHO); 89.34 (d, J_{CP} = 6.9 Hz, C_qO); 127.83 (CH_{arom}); 128.06 (2 x CH_{arom}); 128.89 (2 x CH_{arom}); 134.64 (=<u>C</u>HC$_q$); 134.78 ($C_{q,arom}$); 136.72 (=<u>C</u>HCHO); 172.50 (C=O); 173.90 (C=O). **^{31}P NMR δ (121 MHz, $CDCl_3$, ppm):** 21.15. **IR ν (cm^{-1}):** 1049 (P-O); 1261 (P=O); 1695 (C=O); 1721 (C=O). **MS m/z (%):** 394 (100, $[M+H]^+$). **Mp.:** 202 °C. **Yield:** 67 %. White crystals.

2-(Dimethoxyphosphoryl)-3-isopropyl-4-oxo-10-oxa-3-aza-tricyclo[5.2.1.0^{1,5}]dec-8-ene-6-carboxylic acid (225b)

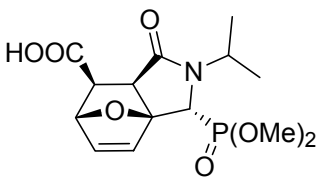

^{1}H NMR δ (300 MHz, $CDCl_3$, ppm): 1.33 (3H, d, J = 6.6 Hz, CHC<u>H</u>$_3$); 1.45 (3H, d, J = 6.9 Hz, CHC<u>H</u>$_3$); 2.79 (1H, d, J = 9.2 Hz, CHCO); 3.01 (1H, d, J = 9.2 Hz, CHCO); 3.79-3.93 (1H, m, C<u>H</u>$(CH_3)_2$); 3.90 (3H, d, J_{HP} = 6.1 Hz, CHP); 5.22 (1H, br s, CHO); 6.47 (1H, dd, J = 5.9 Hz and J = 1.5 Hz, =C<u>H</u>CHO); 6.68 (1H, d, J = 5.9 Hz, CHC$_q$).

^{13}C NMR δ (75 MHz, $CDCl_3$, ppm): 19.12 (2 x CH_3); 46.46 (CHCO); 49.59 ($CH(CH_3)_2$); 50.57 (CHCO); 53.54 (d, J_{CP} = 8.1 Hz, OCH_3); 54.03 (d, J_{CP} = 6.9 Hz, OCH_3); 57.19 (d, J_{CP} = 163.8 Hz, CHP); 81.35 (CHO); 89.99 (d, J_{CP} = 6.9 Hz, C_qO); 134.53 (=CHC_q); 136.71 (=CHCHO); 172.88 (C=O); 173.48 (C=O). **^{31}P NMR δ (121 MHz, $CDCl_3$, ppm):** 21.16. **IR ν (cm^{-1}):** 1033 (P-O); 1243 (P=O); 1693 (C=O); 1727 (C=O). **MS m/z (%):** 246 (100, $[M+H]^+$). **Mp.:** 194 °C. **Yield:** 63 %. White crystals.

3.8 Ring Opening of Oxanorbornenes

3.8.1 Ring opening with $FeCl_3$

To a solution of 0.5 mmol of the IMDAF adduct **12e'** in 10 ml dry CH_2Cl_2, 1.5 equivalents of $FeCl_3$ were added. Care should be taken as air contact of the catalyst causes its immediate hydrolysis. After reflux under an N_2-atmosphere for 1 hour, the reaction was quenched with 10 ml of a saturated $NaHCO_{3(aq)}$ solution and washed with saturated $NaHCO_{3(aq)}$ solution until the formation of yellowish $Fe(OH)_3$ complexes in the aqueous layer was no longer observed. This tedious work-up delivered 15 % of a 98 % pure cyclohexenone **243**.

Dimethyl (1*S*,3a*R*)- and (1*R*,3a*S*)-[5-oxo-2-(2,2,2-trichloroacetyl)-2,3,3a,4,5,7a-hexahydro-1H-isoindol-1-yl] phosphonate (243)

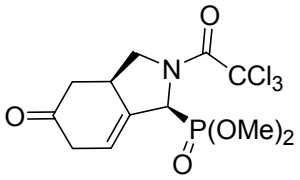

^{1}H NMR δ (300 MHz, $CDCl_3$, ppm): 2.29 (1H, dd, J = 15.1 Hz and J = 12.5 Hz, CH_AH_BCH); 2.73 (1H, dd, J = 15.1 Hz and J = 5.0 Hz, CH_AH_BCH); 2.86-2.99 (1H, m, CH_AH_BCH=); 3.03-3.16 (2H, m, CH_AH_BCH= and CH); 3.50 (1H, t, J = 11.2 Hz, NCH_AH_B); 3.79 (3H, d, J_{HP} = 10.7 Hz, OCH_3); 3.89 (3H, d, J_{HP} = 10.7 Hz, OCH_3); 4.75 (1H, dd, J = 11.2 Hz and J = 7.7 Hz, NCH_AH_B); 5.36 (1H, br d, J_{HP} = 13.8 Hz, CHP); 6.26 (1H, octuplet, J = 2.5 Hz, =CH). **^{13}C NMR δ (75 MHz, $CDCl_3$, ppm):** 39.13 (CH_2CH=); 39.68 (CH); 42.00 (CH_2CH); 53.68 (d, J_{CP} = 6.9 Hz, OCH_3); 53.94 (d, J_{CP} = 5.8 Hz, OCH_3); 54.81 (NCH_2); 57.28 (d, J_{CP} = 156.9 Hz, CHP); 92.67 (C_qCl_3); 119.15 (d, J_{CP} = 6.9 Hz, HC=C); 134.55 (d, J_{CP} = 4.6 Hz, C_q=CH); 159.01 (C=O, amide); 207.52 (C=O, keton). **^{31}P NMR δ (121 MHz, $CDCl_3$, ppm):** 22.60. **IR ν (cm^{-1}):** 1038 (P-O); 1254 (P=O); 1677 (C=O); 1718 (C=O). **MS m/z (%):** 390/392/394 (100, $[M+H]^+$). **Chromatography:** R_f = 0.21 (EtOAc). **Yield:** 15%.

3.8.2 Ring opening with $FeCl_3$ followed by filtration over celite

To a solution of 0.5 mmol of the IMDAF adduct **12e'** in 10 ml dry CH_2Cl_2, 2.0 equivalents of $FeCl_3$ were added. Care should be taken as air contact of the catalyst causes its immediate hydrolysis. After reflux under an N_2-atmosphere for 1 hour, the suspension was filtered directly over celite. The residue was washed with 10 ml CH_2Cl_2. The filtrate was washed 3 times with an equal amount of saturated $NaHCO_{3(aq)}$ solution. This yielded dihydroisondoles **244** and **245** in a ratio of 73/23. Purification by column chromatography furnished pure **244** and **245** in 42 and 14 % yield.

Dimethyl [6-chloro-5-hydroxy-2-(2,2,2-trichloroacetyl)-2,3-dihydro-1H-isoindol-1-yl]phosphonate (244)

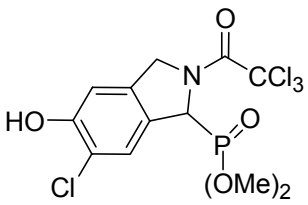

^{1}H NMR δ (300 MHz, $CDCl_3$, ppm): 3.72 (3H, d, J = 10.5 Hz, $OC\underline{H}_3$); 3.90 (3H, d, J = 11.0 Hz, $OC\underline{H}_3$); 5.00 (1H, dd, J = 14.6 Hz and J = 5.2 Hz, $C\underline{H}_aH_bN$); 5.35 (1H, dd, J = 14.6 Hz and J = 6.9 Hz, $CH_a\underline{H}_bN$); 5.78 (1H, d, J_{HP} = 8.8 Hz, $C\underline{H}P$); 6.71 (1H, s, $C\underline{H}_{ar}COH$); 7.43 (1H, d, J = 2.2 Hz, $C\underline{H}_{ar}CCl$). **^{13}C NMR δ (75 MHz, $CDCl_3$, ppm):** 53.86 (d, J_{CP} = 6.9 Hz, $O\underline{C}H_3$); 54.27 (d, J_{CP} = 6.9 Hz, $O\underline{C}H_3$); 54.82 ($\underline{C}H_2N$); 61.46 (d, J_{CP} = 156.9 Hz, $\underline{C}HP$); 92.64 (C_qCl_3); 110.29 ($\underline{C}H_{arom}C_{q,arom}OH$); 120.63 ($C_{q,arom}Cl$); 124.53 (d, J_{CP} = 5.8 Hz, $\underline{C}_{q,arom}CH_2$); 124.64 (d, J_{CP} = 3.5 Hz, $\underline{C}H_{arom}C_{q,arom}Cl$); 137.44 (d, J = 4.6 Hz, $\underline{C}_{q,arom}CHP$); 152.81 ($C_{q,arom}OH$); 159.61 (C=O). **^{31}P NMR δ (121 MHz, $CDCl_3$, ppm):** 21.78. **IR ν (cm^{-1}):** 1035 (P-O); 1687 (C=O); 3142 (OH). **MS m/z (%):** 422/424/426/428 (100, $[M+H]^+$). **Mp.:** 198 °C (carbonization). **Chromatography:** R_f = 0.27 (EtOAc/PE 12/5). **Yield:** 42 %. Colourless crystals.

Dimethyl [5-hydroxy-2-(2,2,2-trichloroacetyl)-2,3-dihydro-1H-isoindol-1-yl]-phosphonate (245)

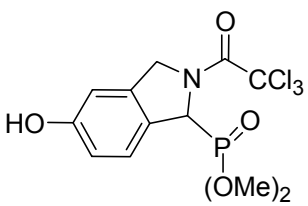

^{1}H NMR δ (300 MHz, $CDCl_3$, ppm): 3.72 (3H, d, J = 10.5 Hz, $OC\underline{H}_3$); 3.90 (3H, d, J = 11.0 Hz, $OC\underline{H}_3$); 5.02 (1H, dd, J = 14.3 Hz and J = 5.0 Hz, $C\underline{H}_aH_bN$); 5.35 (1H, dd, J = 14.3 Hz and J = 6.6 Hz, $CH_a\underline{H}_bN$); 5.80 (1H, d, J_{HP} = 7.7 Hz, $C\underline{H}P$); 6.55 (1H, s, $C_{q,ar}C\underline{H}_{ar}COH$); 6.63 (1H, d, J = 8.3 Hz, $CH_{ar}C\underline{H}_{ar}COH$); 7.21 (1H, dd, J = 8.3 Hz and J = 1.7 Hz, $C_{q,ar}C\underline{H}_{ar}CH_{ar}$). **^{13}C NMR δ (75 MHz, $CDCl_3$, ppm):** 53.69 (d, J_{CP} = 5.8 Hz, $O\underline{C}H_3$); 54.25 (d, J_{CP} = 6.9 Hz, $O\underline{C}H_3$); 55.12 ($\underline{C}H_2N$); 61.48 (d, J_{CP} = 158.1 Hz, $\underline{C}HP$); 92.68 ($\underline{C}_qCl_3$); 109.58 ($C_{q,ar}\underline{C}H_{ar}COH$); 115.84 ($CH_{ar}\underline{C}H_{ar}COH$); 122.40 (d, J_{CP} = 4.6 Hz,

$\underline{C}_{q,ar}CHP$); 124.54 ($C_{q,ar}\underline{C}H_{ar}CH_{ar}$); 138.61 (d, J_{CP} = 5.8 Hz, $\underline{C}_{q,ar}CH_2$); 157.84 ($C_{q,ar}OH$); 159.52 (C=O). **^{31}P NMR δ (121 MHz, $CDCl_3$, ppm):** 22.41. **IR ν (cm^{-1}):** 1032 (P-O); 1684 (C=O); 3205 (OH). **MS m/z (%): 388, 390, 392** (100, $[M+H]^+$). **Chromatography:** R_f = 0.15 (EtOAc/PE 12/5). **Yield:** 14 %. Yellow oil.

3.8.3 Ring opening using Fe^{3+}-montmorillonite

Preparation of the catalyst K10-FeAA120: Fe^{3+}-cation-exchanged clay

With deionised water, 125 ml of a 1M aqueous $FeCl_3$ solution was prepared. Then 10 g of montmorillonite K10 - purchased from the Fluka company – was added over a period of 10 minutes and the mixture was stirred for 18 hours. After centrifugation, the supernatant solution was decanted. The clay was washed with deionised water, centrifugated and decanted. This procedure was repeated until the filtrate was free from Cl^-ions, as indicated with a negative $AgNO_3$-test. Then the exchanged clay was dried overnight at 120 °C and ground in a mortar. Before every use the clay was placed in a drying oven at 120 °C for at least 7 hours.

Preparation of the catalyst K10-FeOO280

To immobilize the $FeCl_3$ on montmorillonite K10, 15 gram of ferric chloride was dissolved in 60 ml dry CH_3CN. Over a period of 10 minutes, 10 g of montmorillonite K10 was added and the mixture was stirred for 5 hours. The clay was filtered, washed with 10 ml of CH_3CN and 60 ml of benzene. Then the clay was dried overnight at 280 °C and ground in a mortar. It was stored at 100° C and before every use the clay was activated in a drying oven at 280 °C for at least 5 hours.

General Procedure for the Ring Opening with K10-FeAA120

To a solution of 0.5 mmol of the IMDAF adduct in dry dichloromethane, 0.25 g K10-FeAA120 was added. This mixture was stirred vigorously and refluxed for 16 to 20 hours depending on the substrate. After filtration of the clay catalyst, the solvent was evaporated under reduced pressure. Product **243** was purified via column chromatography in 59% yield, the aromatic side-product was fully identified in § 3.8.4. Cyclohexenone **251** and dihydroisoindole **252** were purified using preparative TLC.

Dimethyl (1*S*,3a*R*)- and (1*R*,3a*S*)-(2-benzyl-3,5-dioxo-2,3,3a,4,5,7a-hexahydro-1H-isoindol-1-yl) phosphonate (251)

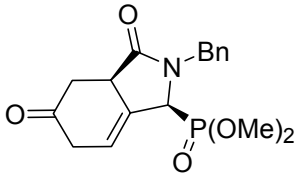

^{1}H NMR δ (300 MHz, $CDCl_3$, ppm): 2.33 (1H, dd, J = 15.4 Hz and J = 12.7 Hz, $C\underline{H}_AH_BCH$); 2.93-3.00 (2H, m, $C\underline{H}_2CH$=); 3.00 (1H, dd, J = 15.4 Hz and J = 5.8 Hz, $CH_A\underline{H}_BCH$); 3.51-3.63 (1H, m, CH); 3.80 (3H, d, J_{HP} = 10.7 Hz, OCH_3); 3.84 (3H, d, J_{HP} = 10.2 Hz, OCH_3); 4.18-4.22 (1H, m, CHP); 4.24 (1H, d, J = 14.9 Hz, $NC\underline{H}_AH_B$); 5.32 (1H, d, J = 14.9 Hz, $NCH_A\underline{H}_B$); 5.87-5.94 (1H, m, =CH); 7.22-7.39 (5H, m, CH_{arom}). **^{13}C NMR δ (75 MHz, $CDCl_3$, ppm):** 39.28 ($\underline{C}H_2CH$=); 39.46 ($\underline{C}H_2CH$); 40.93 ($CH_2\underline{C}H$); 45.28 (NCH_2); 53.38 (d, J_{CP} = 8.0 Hz, OMe); 54.26 (d, J_{CP} = 8.0 Hz, OMe); 56.60 (d, J_{CP} = 160.4 Hz, CHP); 121.77 (d, J_{CP} = 9.2 Hz, CH=); 128.11 (CH_{arom}); 128.43 (2 x CH_{arom}); 129.02 (2 x CH_{arom}); 130.41 (d, J_{CP} = 6.9 Hz, $\underline{C}_q$=); 135.38 ($\underline{C}_{q,arom}$); 173.29 (C=O, lactam); 206.62 (C=O, keton). **^{31}P NMR δ (121 MHz, $CDCl_3$, ppm):** 21.71. **IR ν (cm^{-1}):** 1033 (P-O); 1232 (P=O); 1686 (C=O); 1702 (C=O). **MS m/z (%):** 350 (100, $[M+H]^+$). **Chromatography:** R_f = 0.16 (EtOAc/PE 7/3). **Yield:** 52 %. Oil.

Dimethyl (2-Benzyl-3-oxo-2,3-dihydro-1H-isoindol-1-yl)phosphonate (252)

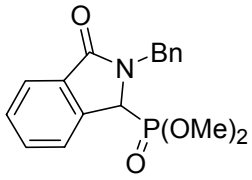

^{1}H NMR δ (300 MHz, $CDCl_3$, ppm): 3.56 (3H, d, J_{HP} = 10.7 Hz, OCH_3); 3.74 (3H, d, J_{HP} = 10.7 Hz, OCH_3); 4.55 (1H, d, J = 15.0 Hz, $NC\underline{H}_AH_B$); 4.69 (1H, d, J_{HP} = 13.2 Hz, CHP); 5.58 (1H, d, J = 15.0 Hz, $NCH_A\underline{H}_B$); 7.23-7.35 (5H, m, CH_{arom}); 7.51-7.61 (2H, m, CH_{arom}); 7.67-7.72 (1H, m, CH_{arom}); 7.91-7.96 (1H, m, CH_{arom}). **^{13}C NMR δ (75 MHz, $CDCl_3$, ppm):** 45.12 (NCH_2); 53.77 (d, J_{CP} = 6.9 Hz, 2 x OCH_3); 56.92 (d, J_{CP} = 155.8 Hz, CHP); 124.19 (CH_{arom}); 124.45 (d, J_{CP} = 2.3 Hz, CH_{arom}); 127.76 ($CH_{arom,benzyl}$); 128.39 (2 x $CH_{arom,benzyl}$); 128.79 (2 x $CH_{arom,benzyl}$); 129.03 (CH_{arom}); 131.84 (CH_{arom} and $C_{q,arom}$); 136.65 ($C_{q,arom,benzyl}$); 138.44 (d, J_{CP} = 5.8 Hz, $C_{q,arom}$); 168.83 (d, J_{CP} = 3.5 Hz, C=O). **^{31}P NMR δ (121 MHz, $CDCl_3$, ppm):** 21.05. **IR ν (cm^{-1}):** 1029 (P-O); 1257 (P=O); 1692 (C=O). **MS m/z (%):** (100, $[M+H]^+$). **Chromatography:** R_f = 0.29 (EtOAc/PE 7/3). **Yield:** 11 %. Oil.

3.8.4 Ring Opening with $TiCl_4$

A solution of 0.5 mmol of the IMDAF adduct in 20 ml of dry dichloromethane was cooled in an ice bath. With a syringe with a small amount of purified petroleum ether in it, 2

equivalents of $TiCl_4$ were added. (To purify the petroleum ether, it was washed with 18M H_2SO_4 in a separatory funnel, next the organic solvent was treated with K_2CO_3.) The reaction mixture was stirred for 2 hours at 0°C under an N_2-atmosphere, poured into 20 ml of ice water and extracted with EtOAc. The organic layer was dried over $MgSO_4$ and filtered. The solvent was removed under reduced pressure. The residue was subjected to column chromatography to yield the *cis* and *trans* cyclohexenones and the aromatized product in case IMDAF adduct **12e'** was used.

Dimethyl (1*S*,3a*R*,5*S*,6*S*)- and (1*R*,3a*S*,5*R*,6*R*)-[6-chloro-5-hydroxy-2-(2,2,2-trichloroacetyl)-2,3,3a,4,5,6-hexahydro-1H-isoindol-1-yl] phosphonate (254)

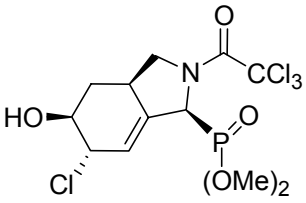

^{1}H NMR δ (300 MHz, $CDCl_3$, ppm): 1.57 (1H, q, J = 11.9 Hz, C$\underline{H}_a$H$_b$); 2.28 (1H, dt, J = 11.9 Hz and J = 4.1 Hz, CH$_a$$\underline{H}_b$); 2.58 (1H, br s, O$\underline{H}$); 2.80-2.97 (1H, m, C$\underline{H}$); 3.30 (1H, t, J = 11.1 Hz, C$\underline{H}_a$H$_b$N); 3.77 (3H, d, J = 11.0 Hz, OC$\underline{H}_3$); 3.87 (3H, d, J = 11.0 Hz, OC$\underline{H}_3$); 4.04 (1H, ddd, J = 11.9 Hz, J = 7.8 Hz and J = 4.1 Hz, C$\underline{H}$OH); 4.55-4.63 (1H, m, C$\underline{H}$Cl); 4.61 (1H, dd, J = 11.1 Hz and J = 7.7 Hz, CH$_a$$\underline{H}_b$N); 5.29 (1H, dq, J_{HP} = 14.6 Hz and J = 2.2 Hz, C$\underline{H}$P); 6.18-6.23 (1H, m, $\underline{H}$C=C). **^{13}C NMR δ (75 MHz, $CDCl_3$, ppm):** 33.57 ($\underline{C}H_2$); 40.97 (d, J_{CP} = 2.3 Hz, $\underline{C}$H); 53.85 (d, J_{CP} = 8.1 Hz, O$\underline{C}H_3$); 54.04 (d, J_{CP} = 5.8 Hz, O$\underline{C}H_3$); 54.40 ($\underline{C}H_2$N); 56.83 (d, J_{CP} = 158.1 Hz, $\underline{C}$HP); 63.95 (d, J_{CP} = 3.5 Hz, $\underline{C}$HCl); 74.00 ($\underline{C}$HOH); 92.70 (C_qCl_3); 122.38 (d, J_{CP} = 6.9 Hz, H$\underline{C}$=C); 137.79 (d, J_{CP} = 4.6 Hz, HC=$\underline{C}$); 159.24 (C=O). **^{31}P NMR δ (121 MHz, $CDCl_3$, ppm):** 22.14. **IR ν (cm^{-1}):** 1027 (P-O); 1677 (C=O); 3387 (OH). **MS m/z (%):** 426, 428, 430, 432 (100, $[M+H]^+$). **Chromatography:** R_f = 0.05 (EtOAc/PE 3/2). **Yield:** 46 %. Oil.

Dimethyl (1*S*,3a*R*,5*S*,6*R*)- and (1*R*,3a*S*,5*R*,6*S*)-[6-chloro-5-hydroxy-2-(2,2,2-trichloroacetyl)-2,3,3a,4,5,6-hexahydro-1H-isoindol-1-yl] phosphonate (255)

The spectrum was derived from the spectral data of the mixture of the cyclohexene derivatives.

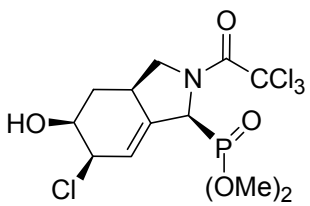

^{1}H NMR δ (300 MHz, $CDCl_3$, ppm): 1.65 (1H, q, J = 11.5 Hz, C$\underline{H}_a$H$_b$); 2.07 (1H, ddd, J = 11.5 Hz, J = 4.8 Hz and J = 3.4 Hz, CH$_a$$\underline{H}_b$); 2.72-2.97 (1H, m, C$\underline{H}$); 3.30 (1H, t, J = 11.6 Hz, C$\underline{H}_a$H$_b$N); 3.81 (3H, d, J = 11.0 Hz, OC$\underline{H}_3$); 3.86 (3H, d, J = 10.5 Hz, OC$\underline{H}_3$); 4.00-4.08 (1H, m, C$\underline{H}$OH); 4.55-4.65 (1H, m, CH$_a$$\underline{H}_b$N); 4.87 (1H, br s, C$\underline{H}$Cl); 5.27 (1H, d, J_{HP} = 14.3 Hz, C$\underline{H}$P); 6.44 (1H, br s, $\underline{H}$C=C). **^{13}C NMR δ (75 MHz, $CDCl_3$,**

ppm): 33.60 (<u>C</u>H_2); 42.33 (d, J_{CP} = 3.5 Hz, <u>C</u>H); 54.01 (d, J_{CP} = 5.8 Hz, O<u>C</u>H_3); 54.04 (<u>C</u>H_2N); 54.24 (d, J_{CP} = 6.9 Hz, O<u>C</u>H_3); 57.07 (d, J_{CP} = 156.9 Hz, <u>C</u>HP); 61.33 (<u>C</u>HCl); 68.30 (<u>C</u>HOH); 92.69 (C_qCl_3); 121.43 (d, J_{CP} = 5.8 Hz, H<u>C</u>=C); 137.48 (d, J_{CP} = 3.5 Hz, HC=<u>C</u>); 159.24 (C=O). **^{31}P NMR δ (121 MHz, $CDCl_3$, ppm):** 22.06. **MS m/z (%):** 426, 428, 430, 432 (100, $[M+H]^+$). **Chromatography:** R_f = 0.20 (EtOAc/PE 3/2). Oil.

Dimethyl [2-(2,2,2-trichloroacetyl)-2,3-dihydro-1H-isoindol-1-yl] phosphonate (250)

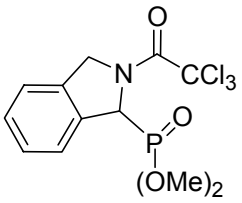

^{1}H NMR δ (300 MHz, $CDCl_3$, ppm): 3.55 (3H, d, J = 11.0 Hz, O<u>C</u>H_3); 3.86 (3H, d, J = 11.0 Hz, O<u>C</u>H_3); 5.09 (1H, dd, J = 14.3 Hz and J = 5.0 Hz, C<u>H</u>$_a$$H_b$N); 5.50 (1H, dd, J = 14.3 Hz and J = 6.6 Hz, CH_a<u>H</u>$_b$N); 5.88 (1H, d, J_{HP} = 9.4 Hz, C<u>H</u>P); 7.28-7.34 (1H, m, C<u>H</u>$_{ar}$); 7.35-7.39 (2H, m, C<u>H</u>$_{ar}$); 7.52-7.58 (1H, m, C<u>H</u>$_{ar}$). **^{13}C NMR δ (75 MHz, $CDCl_3$, ppm):** 53.65 (d, J_{CP} = 6.9 Hz, O<u>C</u>H_3); 53.86 (d, J_{CP} = 5.8 Hz, O<u>C</u>H_3); 54.97 (<u>C</u>H_2N); 62.03 (d, J_{CP} = 153.5 Hz, <u>C</u>HP); 92.77 (<u>C</u>$_q$$Cl_3$); 122.30 (d, J_{CP} = 2.3 Hz, <u>C</u>H$_{ar}$); 124.14 (d, J_{CP} = 3.5 Hz, <u>C</u>H$_{ar}$); 128.15 (d, J_{CP} = 2.3 Hz, <u>C</u>H$_{ar}$); 128.72 (d, J_{CP} = 3.5 Hz, <u>C</u>H$_{ar}$); 132.70 (d, J_{CP} = 4.6 Hz, <u>C</u>$_{q,ar}$); 137.16 (d, J_{CP} = 5.8 Hz, <u>C</u>$_{q,ar}$); 159.38 (<u>C</u>=O). **^{31}P NMR δ (121 MHz, $CDCl_3$, ppm):** 21.89. **IR ν (cm^{-1}):** 1029 (P-O); 1686 (C=O); 3471 (OH). **MS m/z (%):** 372, 374, 376 (100, $[M+H]^+$). **Chromatography:** R_f = 0.42 (EtOAc/PE 3/2). **Yield:** 11 %. Oil.

Dimethyl (1*R*,3a*R*,5*S*,6*R*)- and (1*S*,3a*S*,5*R*,6*S*)-[6-chloro-5-hydroxy-2-(2,2,2-trichloroacetyl)-2,3,3a,4,5,6-hexahydro-1H-isoindol-1-yl] phosphonate (257)

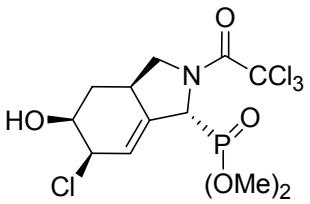

^{1}H NMR δ (300 MHz, $CDCl_3$, ppm): 1.62 (1H, q, J = 11.4 Hz, C<u>H</u>$_a$$H_b$); 2.11 (1H, ddd, J = 11.4 Hz, J = 5.8 Hz and J = 3.3 Hz, CH_a<u>H</u>$_b$); 2.33 (1H, d, J = 11.4 Hz, O<u>H</u>); 3.30-3.47 (1H, m, C<u>H</u>); 3.65 (1H, t, J = 9.6 Hz, C<u>H</u>$_a$$H_b$N); 3.78 (3H, d, J = 11.0 Hz, O<u>C</u>H_3); 3.82 (3H, d, J = 11.0 Hz, O<u>C</u>H_3); 4.06 (1H, tt, J = 11.4 Hz and J = 3.3 Hz, C<u>H</u>OH); 4.45 (1H, dt, J = 9.6 Hz and J = 1.8 Hz, CH_a<u>H</u>$_b$N); 4.80-4.87 (1H, m, C<u>H</u>Cl); 5.12 (1H, d, J_{HP} = 12.1 Hz,C<u>H</u>P); 6.03-6.10 (1H, m, <u>H</u>C=C). **^{13}C NMR δ (75 MHz, $CDCl_3$, ppm):** 30.14 (<u>C</u>H_2); 39.77 (<u>C</u>H); 53.77 (d, J_{CP} = 6.9 Hz, O<u>C</u>H_3); 53.87 (d, J_{CP} = 6.9 Hz, O<u>C</u>H_3); 54.57 (<u>C</u>H_2N); 60.64 (d, J_{CP} = 156.9 Hz, <u>C</u>HP); 60.73 (d, J_{CP} = 3.5 Hz, <u>C</u>HCl); 67.82 (<u>C</u>HOH); 92.74 (C_qCl_3); 122.37 (d, J_{CP} = 10.4 Hz, H<u>C</u>=C); 137.06 (d, J_{CP} = 6.9 Hz, HC=<u>C</u>); 159.43 (C=O). **^{31}P NMR δ (121 MHz, $CDCl_3$, ppm):** 21.02 **IR ν (cm^{-1}):** 1036 (P-O); 1675

(C=O); 3384 (OH). **MS m/z (%):** 426, 428, 430, 432 (100, $[M+H]^+$). **Mp.:** 150-152 °C. **Chromatography:** R_f = 0.05 (EtOAc/PE 2/1). **Yield:** 48 %. Colourless crystals.

Dimethyl (1*R*,3a*R*,5*S*,6*S*)- and (1*S*,3a*S*,5*R*,6*R*)-[6-chloro-5-hydroxy-2-(2,2,2-trichloroacetyl)-2,3,3a,4,5,6-hexahydro-1H-isoindol-1-yl] phosphonate (256)

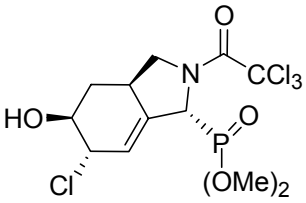

^{1}H NMR δ (300 MHz, $CDCl_3$, ppm): 1.52 (1H, q, J = 12.1 Hz, C$\underline{H}_a$H$_b$); 2.33 (1H, dt, J = 12.1 Hz en J = 4.1 Hz, CH$_a$$\underline{H}_b$); 3.08 (1H, br s, O$\underline{H}$); 3.39-3.56 (1H, m, C$\underline{H}$); 3.65 (1H, t, J = 9.8 Hz, C$\underline{H}_a$H$_b$N); 3.80 (3H, d, J = 11.0 Hz, OC$\underline{H}_3$); 3.83 (3H, d, J = 10.5 Hz, OC$\underline{H}_3$); 4.04 (1H, ddd, J = 12.1 Hz, J = 8.0 Hz and J = 4.1 Hz,C$\underline{H}$OH); 4.55-4.65 (1H, dd, J = 9.8 Hz and J = 1.7 Hz, CH$_a$$\underline{H}_b$N); 4.48-4.57 (1H, m, C$\underline{H}$Cl); 5.07 (1H, d, J_{HP} = 12.1 Hz, C$\underline{H}$P); 5.85 (1H, br s, $\underline{H}$C=C). **^{13}C NMR δ (75 MHz, $CDCl_3$, ppm):** 34.75 ($\underline{C}H_2$); 38.87 ($\underline{C}$H); 53.99 (d, J_{CP} = 6.9 Hz, O$\underline{C}H_3$); 54.26 (d, J_{CP} = 6.9 Hz, O$\underline{C}H_3$); 54.68 ($\underline{C}H_2$N); 60.93 (d, J_{CP} = 158.1 Hz, $\underline{C}$HP); 63.26 ($\underline{C}$HCl); 68.30 ($\underline{C}$HOH); 92.73 (C_qCl_3); 123.50 (d, J_{CP} = 10.4 Hz, H$\underline{C}$=C); 136.91 (d, J_{CP} = 6.9 Hz, HC=$\underline{C}$); 159.32 (C=O). **^{31}P NMR δ (121 MHz, $CDCl_3$, ppm):** 20.46 **IR ν (cm^{-1}):** 1047 (P-O); 1255 (P=O) ; 1649 (C=O); 3473 (OH). **MS m/z (%):** 426, 428, 430, 432 (100, $[M+H]^+$). **Mp.:** 149-151 °C. **Chromatography:** R_f = 0.12 (EtOAc/PE 2/1). **Yield:** 30 %. Colourless crystals.

Chapter 5 – Summary and Perspectives

All chemists use models. They can be plastic models or a set of pre-defined objects and rules to approximate real chemical entities and processes.
In a similar way, computational chemistry simulates chemical structures and reactions numerically, based on physical laws. Several methods have been developed and have been implemented in software packages and new methods are continuously generated.
These packages are available for experimental chemists who should get knowledge of the different methods and their applications and keep track of new developments in this young and fast developing science. Moreover, the reliability of the results should be evaluated for different fields of chemistry. After validation, the same method can be used in a predictive way for similar reactions. The simulations can bring insight into chemical reactions, confirm existing laws and indicative parameters or create new ones.

This thesis is a combination of both experimental and computational chemistry.
New azaheterocycles that are pyroglutamate and α-amino phosphonate derivatives were synthesized. Both classes have an interesting biological potential and form an important subject of investigation in the *SynBioC* research group. For both classes, different ways of conformational restriction via cyclization were evaluated.
Computational methods were applied to explain the observed isomer ratios, to evaluate and to predict stereoselectivities and to explain different reactivities. This was done at the *Center for Molecular Modeling*.

The first part started with the synthesis of hydantoins via a pyroglutamate-hydantoin rearrangement. Hydantoins possess a wide range of biological activities and have applications in both the agrochemical sector and human medicine.
When a mixture of a pyroglutamate **i** and an isocyanate is treated with NaH in diethyl ether, a precipitate is formed almost immediately. Work-up after 30 minutes, confirms this is the sodium salt of the carbamoyl-2-pyrrolidinone **(ii)** that has been obtained in high purity.

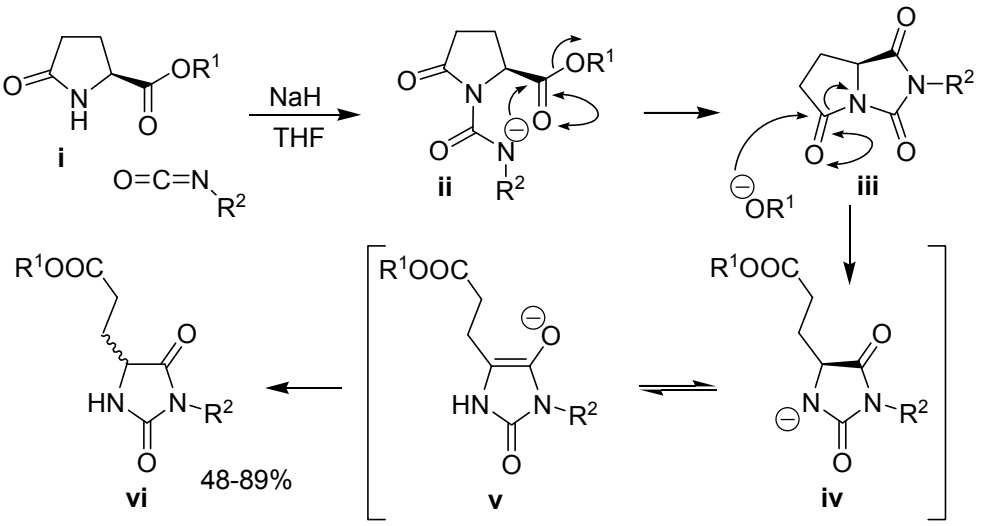

If the same reaction is repeated in THF and stirred overnight, a different class of products is formed that has very similar 1D NMR spectra. The products were misidentified at first as perhydro-1,3-diazepine-2,4-diones (e.g. **viii)**, but X-ray analysis and 2D NMR spectral data proved it to be hydantoin derivatives (e.g. **ix)**.

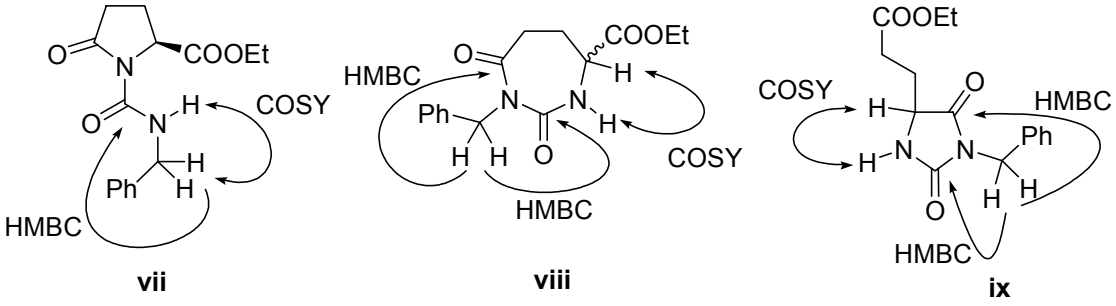

The hydantoins can be formed by an intramolecular nucleophilic attack of the carbamoyl anion **ii** on the carbonyl of the ester function followed by expulsion of an alkoxide anion, which results in the formation of the bicyclic intermediate **iii**. The alkoxide anion in turn can open this bicyclic intermediate with formation of anions **iv** and **v** that are in equilibrium and cause racemization of the chiral centre. Work-up results in hydantoin derivative **vi** as a 1:1 enantiomeric mixture.

When two equivalents of isocyanate are used, the resulting hydantoin is carbamoylated very fast. The addition of a second equivalent of isocyanate to the carbamoyl group of **ii**, was never observed.

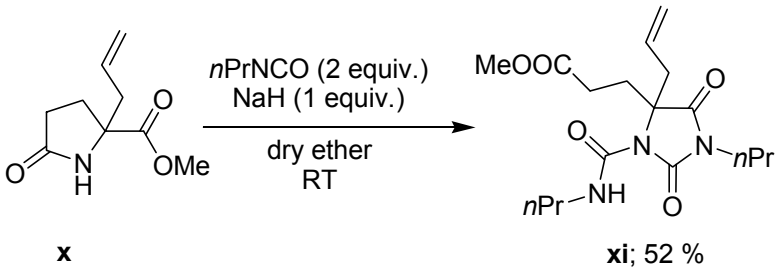

x **xi**; 52 %

If a two-step approach is taken, the carbamoyl pyroglutamate **xii** is isolated first and the ring-transformation is performed in the presence of the desired alkoxide anions. As a pool of alkoxide anions is present and the lactam carbonyl is activated by the electron-withdrawing properties of the carbamoyl group, another reaction pathway is proposed. The alkoxide anion opens the lactam ring. This is followed by an intramolecular formation of the five-membered hydantoin ring and a new alkoxide anion is generated. In the second step, a transesterification can be done. Unfortunately, partial rearrangement occurred during the first step when *C*(2)-alkylated pyroglutamates were used.

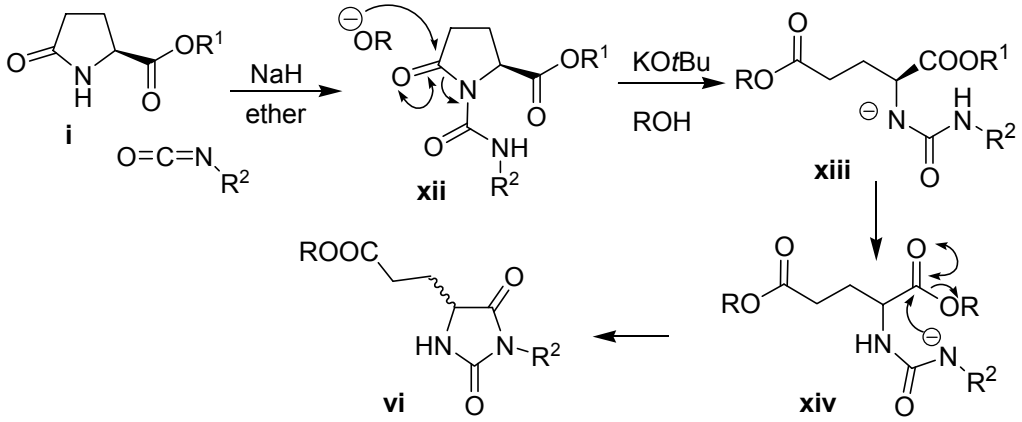

i **xii** **xiii** **vi** **xiv**

Pyroglutamate is a versatile building block, as the site of alkylation can be directed by changing the protecting group on nitrogen. So, the pyroglutamate-hydantoin rearrangement can be used as the key step in the synthesis of more complex hydantoins. Several hydantoins with an extra fused ring show interesting biological properties.

The rearrangement reaction was applied in the *SynBioC* research group for the synthesis of hydantoins that were annelated to a six-membered ring in a short 4-step approach, the six-membered rings were formed in the last step by ring-closing metathesis (RCM).

Small bicyclic hydantoin derivatives **xvi** can be formed via alkylation of the pyroglutamate ester at the *C*(2)-position with biselectrophiles before the rearrangement reaction. However, two undesired side reactions occur: internal ring closure of the alkylated pyroglutamate,

before the isocyanate addition, and a fast carbamoylation of the hydantoin at *N*(1). Once the 2-alkyl-1-carbamoylpyroglutamate esters **xv** were isolated, quantitative rearrangement and cycloaddition occurred to furnish the pure bicyclic imidazolidinediones.

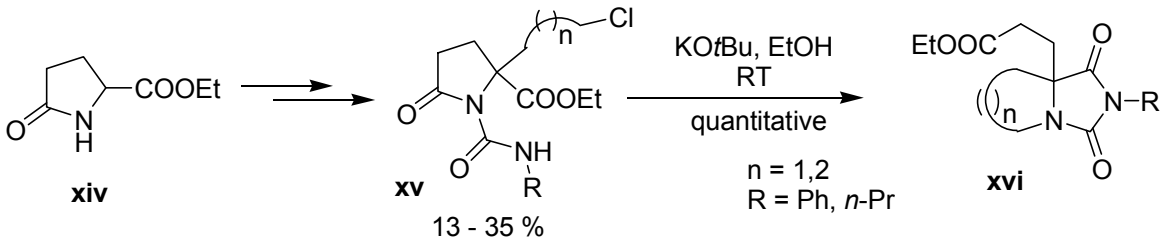

The ring-transformation was also used to construct *N*(3),*N'*(3)-polymethylene-bis(hydantoins) **xviii**, which are HMBA analogues and might prove effective in cancer treatment. The bis(hydantoins) were obtained by reaction of pyroglutamates with diisocyanates.

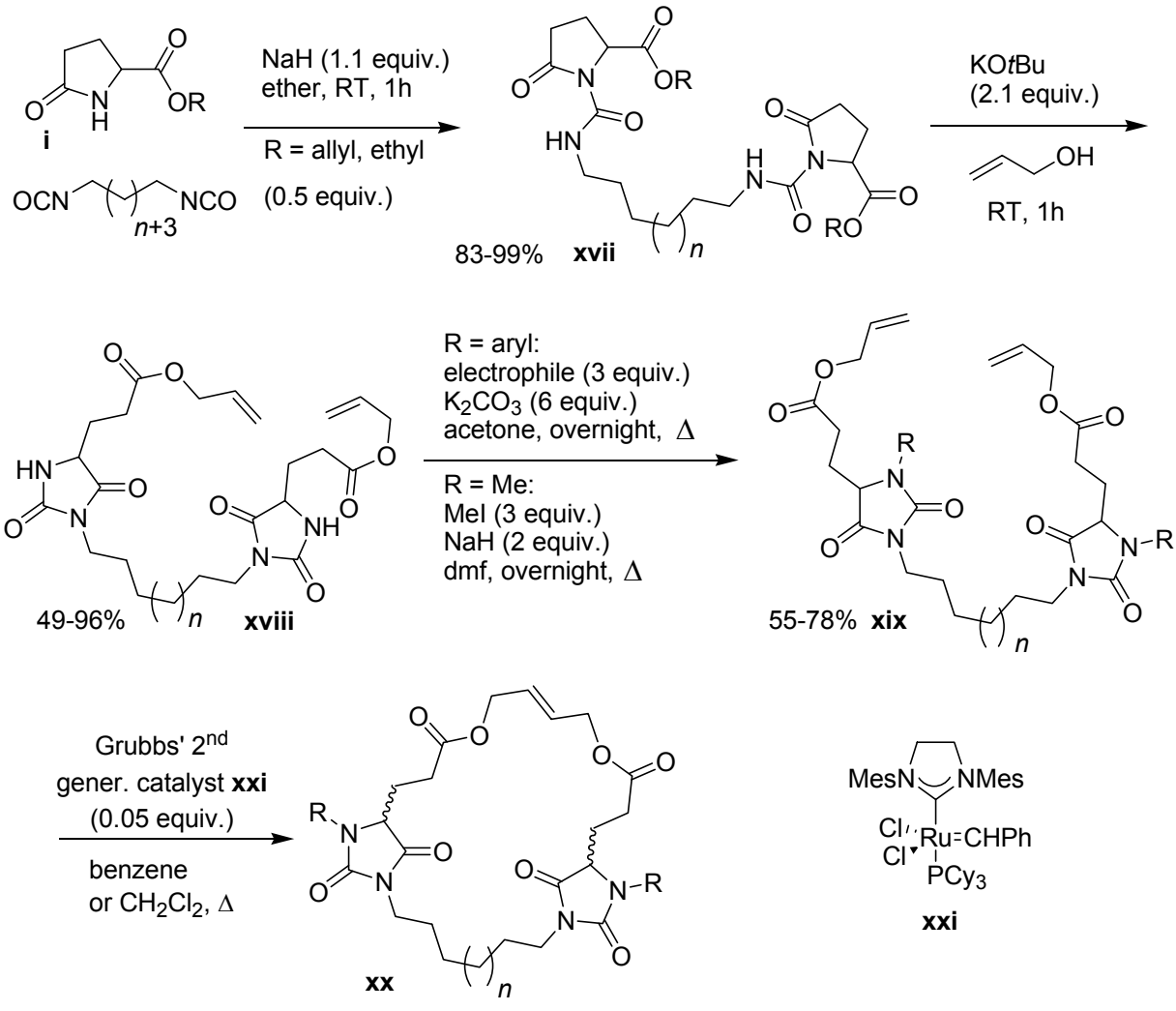

After *N*-alkylation or *N*-arylation of the bis(hydantoins) **xviii**, the allyl esters were ringclosed to form 24- to 30-membered macrocycles **xx** by RCM using the second generation Grubbs' catalyst **xxi**. RCM is a powerful method to synthesize macrocyclic products and most probably, the presence of polar relay substituents at a proper distance from the alkene groups contributed to the successful ring closure. Moreover, only the *trans* isomers were isolated. This can be explained by secondary metathesis reactions that isomerize the initial product to produce a thermodynamically controlled *E*/*Z* ratio.

This experimentally observed thermodynamic stability of the double bond isomers of these macrocycles was investigated computationally. Because of the large number of degrees of freedom of the macrocycle, a suitable methodology was outlined and implemented with MD-Tracks to easily generate molecular conformations that span the potential energy surface.

The method starts with a fast generation of molecular geometries covering the potential energy surface by a molecular dynamics simulation with a semi-empirical method at high temperature. Dihedral free energy distribution plots and principal component analysis are used to test the completeness of the molecular dynamics trajectory. Next a diverse set of molecules is selected by a Kennard-Stone algorithm with a distance measure based on the distance matrix. This selection of conformations is then optimized at a DFT or post-Hartree Fock level. By calculating probability distributions based on the post-Hartree Fock calculations that also cover long-range interactions, more insight was obtained in the number of conformers contributing to the experimentally observed findings. Indeed the *E* isomers are 10 kJ/mol more stable than the *Z* isomers and determine the overall distribution. This corresponds with the *E* isomer being the only experimentally observed double-bond stereoisomer.

Furthermore, the rotational free energy barriers were investigated for all dihedral angles. It was found that the bonds next to the double bond reflect the main difference between the double bond isomers and are probably the main cause of the energy difference between the *E* and *Z* isomers. The larger part of the ring backbone is rather flexible, except for the few bonds in the hydantoins, which is the reason for the large number of different conformations. Each stereocentre has three related dihedral angles that show asymmetric behaviour. Two can be explained with local interactions with the stereocentre, but the asymmetry of the third dihedral angle is only present when the macrocycle is closed.

Further analysis shows this preference is caused by relieving strain in the chains that connect the two hydantoins.

The hydantoin core has a high biological potential. A number of the synthesized (bis)hydantoins were screened for their anti-invasive activity on human breast cancer cell lines in cooperation with the department of Gynaecological Oncology and the department of Experimental Cancerology at the Ghent University Hospital. Some of these show good anti-invasive activity at a concentration of 100 and 10 μm in the embryonic chick heart assay.

As the synthesis of diazepines via ring expansion of pyrrolidin-2-one derivatives was not successful, another method was evaluated using RCM. It started from α-aminoalkyl phosphonates, a class with high biological potential. The α,β-unsaturated imines **xxii** were phosphonylated with complete 1,2 selectivity by treatment with dimethyl phosphite in refluxing methanol. The *N*-atom was carbamoylated with both aryl and alkyl isocyanates using Cu(I)Cl as a catalyst. Acylation of the obtained ureido phosphonates **xxiv** failed. Under basic conditions only double bond rearrangement towards the vinylic phosphonates was observed. The 1,4,2-diazaphospholidin-5-one **xxv** was formed under reflux in CH_3CN. Direct ring closure of the allyl derivative of **xxiv** via metathesis was evaluated without success. A computational study of the obtained complex of **xxiv** and Grubbs' 2nd generation catalyst shows that the complexation is weaker than the one observed in known catalyst-deactivating complexes. Therefore, the latter reaction needs further investigation.

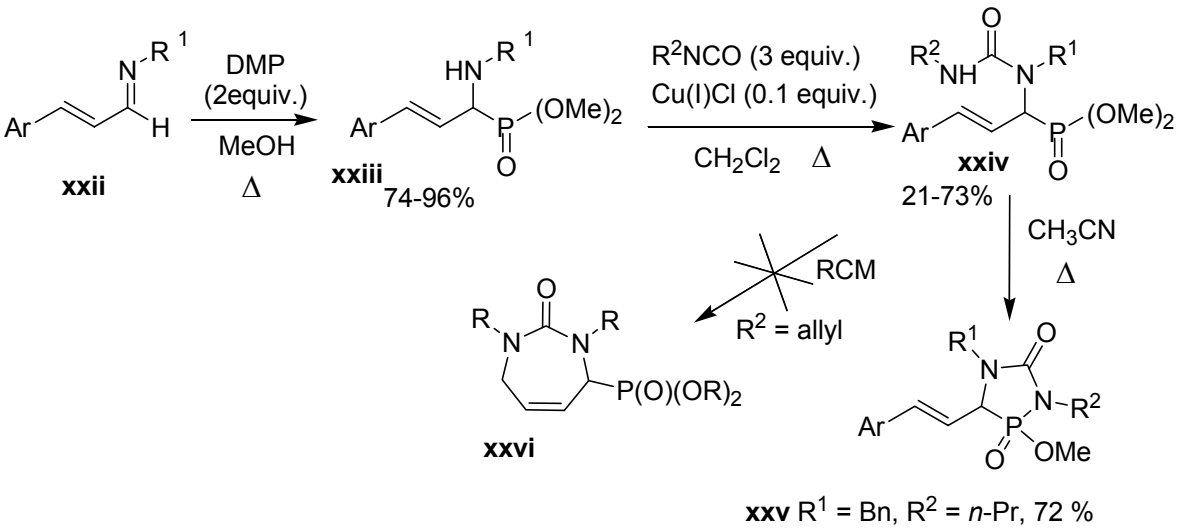

By replacing the cinnamyl group with a furfuryl group, ideal substrates for an IMDAF reaction (intramolecular Diels-Alder reaction with furans) were obtained. These products might be used as novel conformationally constrained amino acid analogues. The synthesis of these tricyclic phosphonates was developed within the *SynBioC* research group. A high degree of stereocontrol was observed during the cycloaddition. Only the *exo*-fused products were obtained. For derivatives of type **xxvii**, for which the allyl group serves as dienophile, a mixture of isomers was formed resulting from an incomplete kinetic control of the position of the phosphonate as tether substituent during the IMDAF reaction. The major isomer **xxix**, with the *C*(2)-phosphonate substituent in *exo* position, could be converted to the minor *endo* isomer **xxxi** under thermodynamic control via a retro-Diels-Alder reaction. For derivatives of type **xxxiii**, with an acyl group as dienophile, only one isomer **xxxiv** was observed.

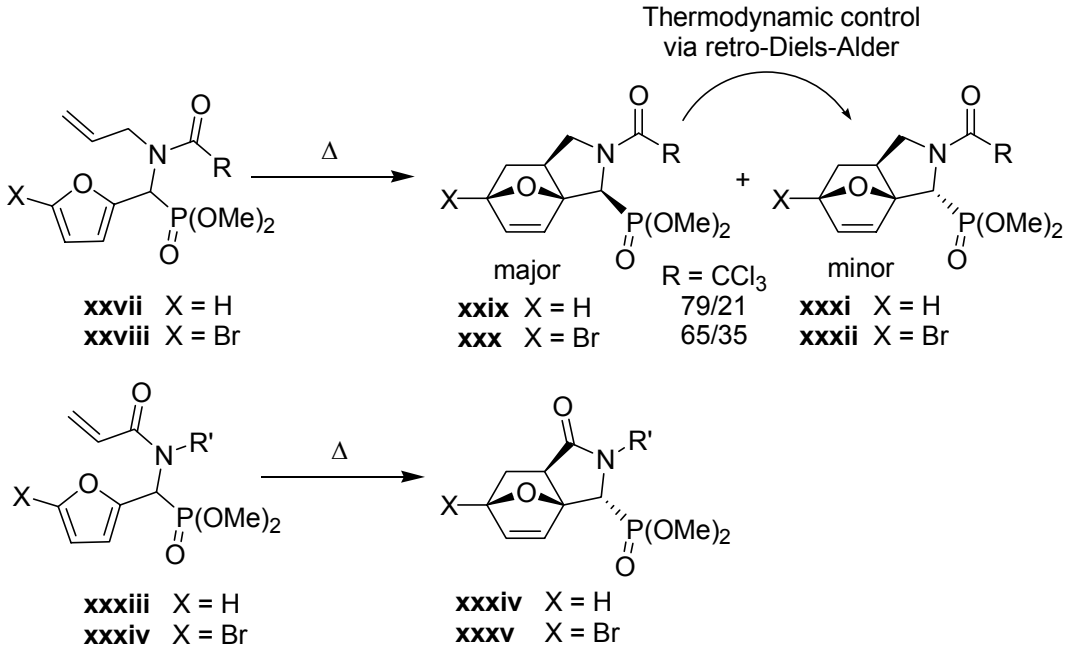

The kinetic and thermodynamic control could be reproduced computationally. With the acyl group functioning as dienophile the isomers with the phosphonate group in *exo* position require a larger distortion from their minimum energy precursor than the *endo* isomers and are sterically more hindered, as can be seen in their respective transition states. This causes exclusive formation of the *endo* isomer **xxxiv**. For amino phosphonates **xxvii** with the allyl group as dienophile the *endo* and *exo* position require about the same amide rotation and there is a subtle energy difference that requests a high level of theory calculation. From the calculations it is clear that B3LYP fails to estimate the reaction free energy of these strained cycloadducts.

This synthesis of azaheterocyclic phosphonates was further elaborated. Bromine substitution at the 5-position of the furan reduces the reaction time for ring closure of **xxxiv** with 40 %, but no significant effect on the π-diastereofacial selectivity of the IMDAF reaction with **xxviii** was observed.

The acylation of the amino phosphonates **xxxvi** with maleic anhydride and IMDAF reaction occur in one step. Using the IR and NMR spectra it was proved that the acylation occurred before ring closure. Also these adducts have *exo*-fused rings and the phosphonate substituent on the tether prefers an *endo* orientation.

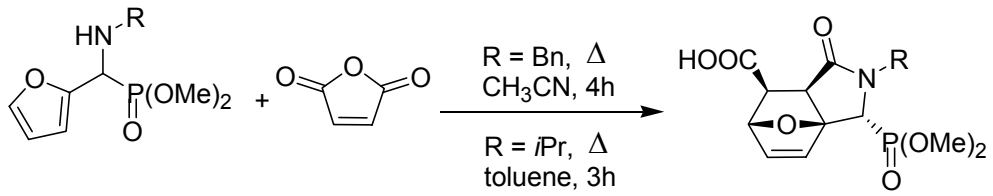

xxxvi

xxxvii R = Bn, 67 %
R = *i*Pr, 63 %

Because the IMDAF reaction can achieve high levels of both regio- and stereoselectivity, a synthetic approach based on that methodology allows for a concise construction of functionalized cyclohexene derivatives.

Different reaction conditions were found for the ring opening of the oxanorbornene **xxix** and some analogues. The use of $FeCl_3$ and $TiCl_4$ as Lewis acids resulted in the ring opening of the oxygen bridge without complete oxidation of the six-membered ring.

Coating of the Fe-catalyst on montmorillonite K10 eased the tedious work-up, but accelerated the aromatization, which caused a loss of the stereocentres that were created by the stereoselectivity of the IMDAF reaction.

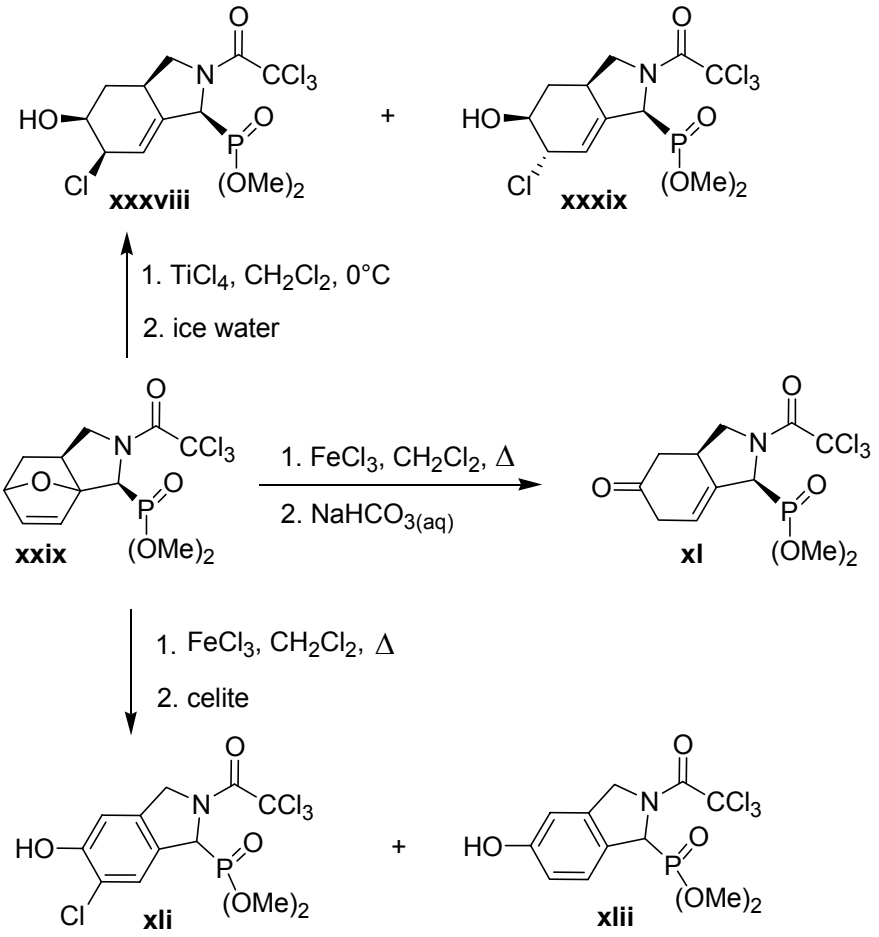

A computational study of the complexation and C-O bond breaking process showed that the energy barrier was higher for the $FeCl_3$-catalyzed reaction than for the $TiCl_4$-catalyzed reaction. The different behaviour of both catalysts could be linked with their affinity to form complexes with oxide anions. This behaviour coincides with the stability correlation of complexes based on Pearson's hard-soft acid-base principle. Using $TiCl_4$ a chloride anion was inserted to neutralize the allylic carbocation. With $FeCl_3$ the oxide anion stabilized the allylic carbocation and the reaction continues via a 2-step 1,2-hydride shift.

In this thesis, new azaheterocycles with biological potential were synthesized starting from pyroglutamates and α-amino phosphonates. For several synthetic routes computational studies were used to explain the stereoselectivities and evaluate different reaction pathways, for which traditional chemical models and the experimentally built chemical intuition fail. The same methodologies can be used in a more predictive way and can be extended with more advanced techniques.

In the intramolecular Diels-Alder reaction for example, the composition of the tether and its substituents all have different contributions to the (π-dia)stereoselectivity that counterbalance each other. The applied methodology could explain the observed product ratio and can be used in the future as a predictive tool; even for inverse electron demand Diels-Alder reactions for which the analysis of the transition state is even more important. The method can be extended by taking solvent effects into account.

The same holds for the reactions in which both transition metals and s- and p-block elements are involved, but further benchmarking of the methods is needed in this area.

Computational studies can contribute to the optimization of experimental conditions, but with the current techniques, chemical intuition is still needed to propose possible reaction pathways or to indicate important reaction coordinates. This synergy between experimental and computational chemistry makes future research fascinating, challenging, sometimes frustrating but very promising.

Chapter 6 – Samenvatting en Perspectieven

Elke scheikundige gebruikt modellen. Dit kunnen plastic modellen zijn of een geheel van structuren en voorstellingen met bijhorende mechanismen en principes om echte chemische entiteiten en processen te benaderen.
Op een gelijkaardige manier simuleert computationele chemie chemische structuren en reacties op numerieke wijze, vertrekkende van wetten uit de fysica. Verschillende methoden werden ontwikkeld en geïmplementeerd in softwarepakketten en er komen voortdurend nieuwe benaderingen bij.
Experimentele scheikundigen die deze pakketten willen gebruiken, moeten inzicht krijgen in deze verschillende methoden en hun mogelijke toepassingen en moeten op de hoogte blijven van nieuwe ontwikkelingen in deze jonge en snel evoluerende wetenschap. Daarbij komt dat de betrouwbaarheid van de methoden voor bepaalde chemische toepassingsdomeinen moet geëvalueerd worden. Na deze validatie kan dezelfde methode gebruikt worden om gelijkaardige reacties te voorspellen. Deze simulaties kunnen meer inzicht geven in chemische reacties, bestaande regels en wetten bevestigen en nieuwe parameters creëren.

Deze thesis is een combinatie van zowel experimentele als computationele chemie.
Nieuwe azaheterocyclische verbindingen werden gesynthetiseerd vertrekkende van pyroglutamaten en α-amino fosfonaten. Beide klassen van verbindingen hebben interessante biologische eigenschappen en vormen belangrijke onderzoeksonderwerpen binnen de *SynBioC* groep. Voor beide klassen werd gezocht naar verschillende ringsluitingsmethoden om de conformationele vrijheidsgraden van de molecules te beperken.
De computationele methoden werden gebruikt om de waargenomen verhoudingen van de isomeren te reproduceren, te voorspellen en te verklaren en om inzicht te krijgen in de verschillen in reactiviteit. Dit onderzoek werd uitgevoerd aan het *Centrum voor Moleculaire Modellering*.

In een eerste deel werden hydantoines gesynthetiseerd via een omleggingsreactie vertrekkende van pyroglutamaten. Hydantoines bezitten een waaier van biologische activiteiten met toepassingen zowel in de agrochemische sector als in de medische wereld.

Wanneer NaH toegevoegd wordt aan een mengsel van pyroglutamaat **i** en een isocyanaat in ether, wordt vrijwel onmiddellijk een neerslag gevormd. Opwerking na 30 minuten, leert dat dit het verwachte natriumzout is van het carbamoyl-2-pyrrolidinon (**ii)** dat zeer zuiver wordt verkregen.

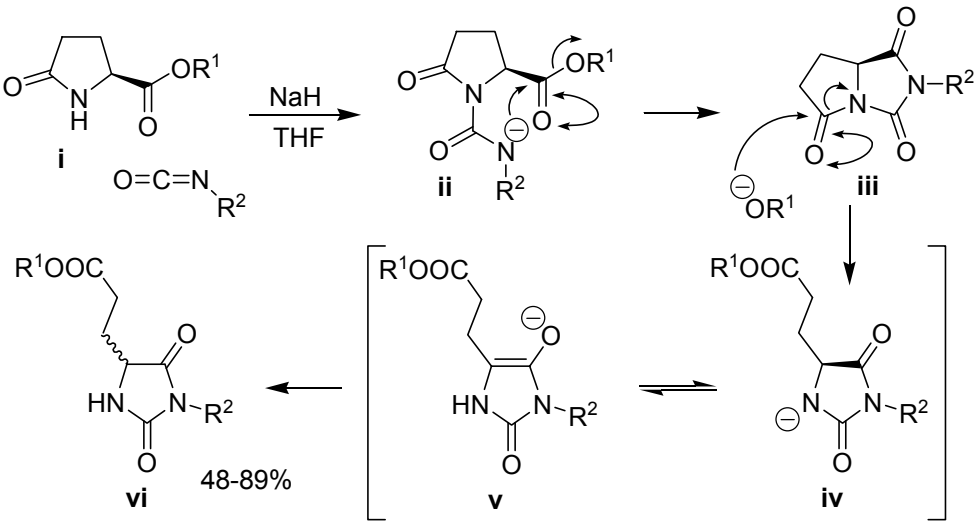

Als dezelfde reactie gedurende één nacht geroerd wordt in THF, wordt een andere klasse producten bekomen met een sterk gelijkend 1D NMR spectrum. Dit bleken geen perhydro-1,3-diazepine-2,4-dionen (e.g. **viii**) zoals oorspronkelijk werd aangenomen, maar hydantoines (e.g. **ix**) zoals met X-straalanalyse en 2D NMR spectra aangetoond werd.

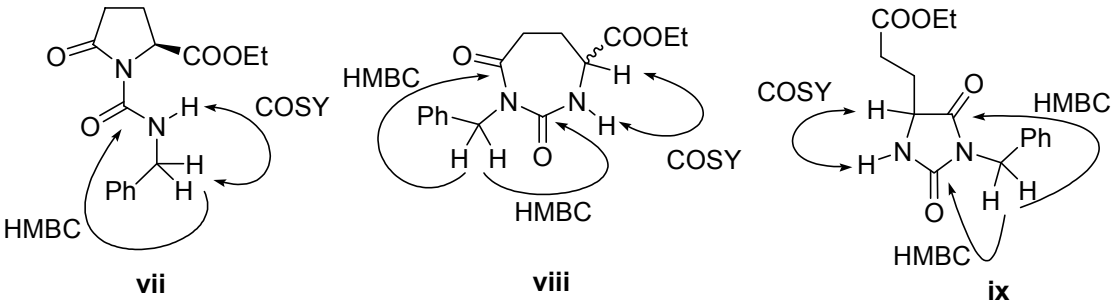

De hydantoines kunnen gevormd worden via een intramoleculaire nucleofiele aanval van het carbamoyl anion **ii** op de carbonylfunctie van het ester, gevolgd door uitstoot van het alkoxide anion met vorming van het bicyclisch intermediair **iii**. Het alkoxide anion kan op zijn beurt dit bicyclisch intermediair openen met vorming van anionen **iv** en **v**. Deze anionen zijn met elkaar in evenwicht. Door deze racemisatie van het chirale centrum worden de hydantoines **vi** verkregen als een 1:1 enantiomeer mengsel.

Als twee equivalenten isocyanaat gebruikt worden, wordt het gevormde hydantoine heel snel gecarbamoyleerd. De additie van een tweede equivalent isocyanaat aan de carbamoyl groep van **ii**, werd nooit waargenomen.

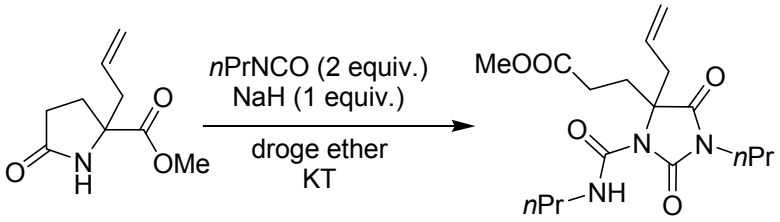

x **xi**; 52 %

Bij een tweestapsbenadering, wordt het gecarbamoyleerde pyroglutamaat **xii** eerst geïsoleerd en wordt de ringtransformatie uitgevoerd in aanwezigheid van de gewenste alkoxide anionen. Gezien een groot aantal alkoxide anionen aanwezig is en het lactam carbonyl geactiveerd wordt door de elektronenzuigende carbamoylgroep, werd een ander reactiemechanisme voorgesteld. Het alkoxide anion opent de lactam ring. Dit wordt gevolgd door een intramoleculaire additie aan het ester met vorming van het hydantoine en generatie van een nieuw alkoxide anion. Tijdens deze tweede stap kan een omestering gedaan worden. Jammer genoeg vond bij gebruik van *C*(2)-gealkyleerde pyroglutamaten al gedeeltelijke omlegging plaats tijdens de eerste stap.

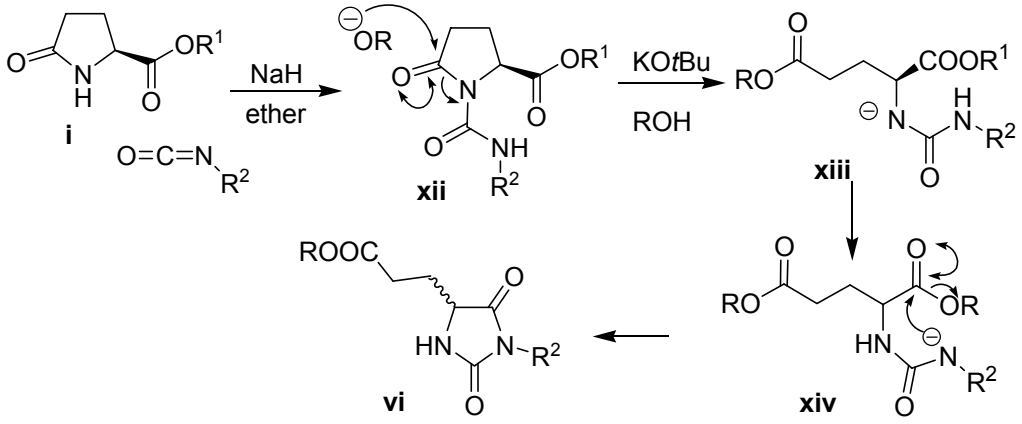

Pyroglutamaat is een veelzijdige bouwsteen aangezien de plaats van alkylering kan gestuurd worden door wijziging van de beschermende groep op het stikstofatoom. Op deze manier kan de pyroglutamaat-hydantoineomlegging gebruikt worden in de synthese van meer complexe hydantoines.

Dit werd toegepast binnen de *SynBioC* onderzoeksgroep in een korte vierstapssequentie voor de synthese van hydantoinederivaten die gefuseerd zijn met een zesring. De zesring werd gevormd in de laatste stap via RCM.

Kleine bicyclische hydantoinederivativen **xvi** kunnen gevormd worden na alkylering van het pyroglutamaat op de *C*(2)-positie met biselektrofielen voor de omlegging, hoewel twee nevenreacties plaatsvonden: interne ringsluiting van het gealkyleerde pyroglutamaat, voor additie van het isocyanaat, en een snelle carbamoylering van het hydantoine op *N*(1). Eens de 2-alkyl-1-carbamoylpyroglutamaten **xv** geïsoleerd waren, leidden omlegging en cycloadditie kwantitatief tot de zuivere bicyclische imidazolidinediones.

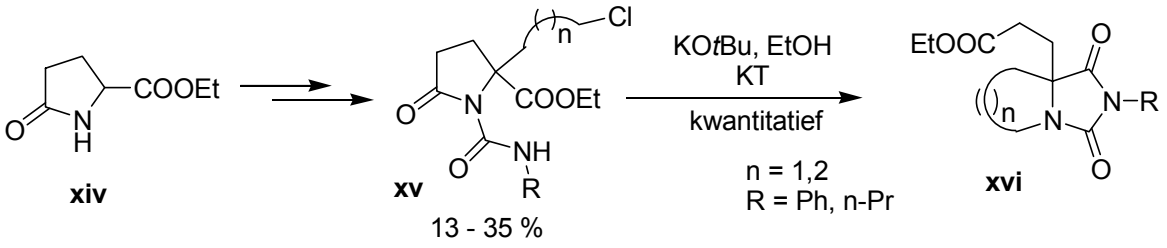

De ringtransformatie werd ook gebruikt in de synthese van *N*(3),*N'*(3)-polymethyleen-bis(hydantoines) **xviii**. Dit zijn HMBA analogen met mogelijk nut in de behandeling van kanker. De bis(hydantoines) werden verkregen via reactie van pyroglutamaten met diisocyanaten.

Na *N*-alkylering van de bis(hydantoines) **xviii**, werden de allylesters ringgesloten met vorming van 24- tot 30-ringen **xx** via RCM met de 2de generatie Grubbs' katalysator **xxi**. RCM is een krachtige methode om macrocyclische producten te synthetiseren en hoogst waarschijnlijk zorgt de aanwezigheid van polaire relaysubstituenten op de gepaste afstand van de dubbele binding voor het succes van de ringsluiting. Bovendien werden enkel de *trans* isomeren geïsoleerd. Dit kan verklaard worden doordat secundaire metathesereacties plaatsvinden, die het initiële product isomeriseren tot hun thermodynamisch gecontroleerde *E*/*Z* ratio.

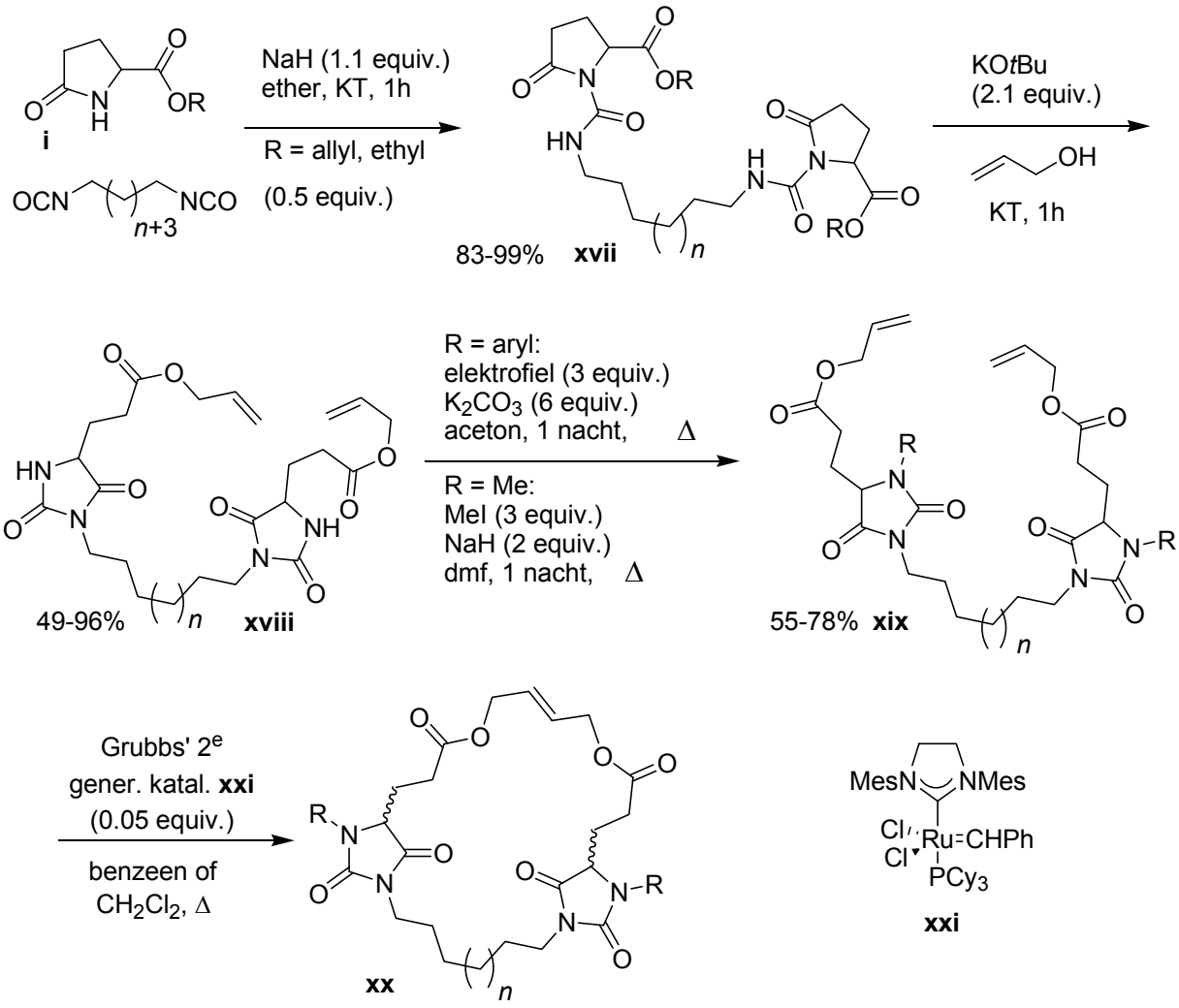

Deze experimenteel waargenomen thermodynamische stabiliteit van de isomeren van de dubbele binding werd computationeel onderzocht. Gezien het grote aantal vrijheidsgraden van de verbinding, werd een geschikte methodologie uitgewerkt om moleculaire conformaties te genereren die het volledige potentieelenergieoppervlak overspannen. De implementatie gebeurde met MD-Tracks, dat ontwikkeld werd binnen het CMM.

De methode begon met een snelle generatie van moleculaire geometrieën via een moleculairedynamicasimulatie met een semi-empirische methode op hoge temperatuur. De volledigheid van de simulatie werd getest door het plotten van de dihedrale vrije energieprofielen en met een principal component analyse. Daarna werd een diverse set van molecules geselecteerd met een nieuw ontwikkeld Kennard-Stone algoritme, waarbij de maat voor verscheidenheid tussen de molecules gebaseerd is op de afstandsmatrix. Deze selectie van conformaties werd dan geoptimaliseerd op DFT of post-Hartree Fock niveau. De *E* isomeren waren 10 kJ/mol stabieler dan de *Z* isomeren en vormden het overgrote aandeel in de distributie van de conformeren, wat overeenkomt met het experiment.

Een aantal van de gesynthetiseerde (bis)hydantoines werd getest op hun anti-invasieve activiteit tegen een humane borstkankercellijn in samenwerking met het departement Gynaecologische Oncologie en het departement Experimenteel Kankeronderzoek aan het Universitair Ziekenhuis in Gent. Sommige van deze verbindingen vertoonde goede anti-invasieve activiteit bij een concentratie van 100 en 10 µm in het *embryonic chick heart assay*.

Aangezien de synthese van diazepines via ringexpansie van pyrrolidin-2-on derivaten niet succesvol bleek, werd een andere methode geëvalueerd via RCM vertrekkende van α-aminoalkyl phosphonaten, een andere klasse verbindingen met groot biologisch potentieel.
De α,β-onverzadigde imines **xxii** werden gefosfonyleerd met volledige 1,2 selectiviteit door behandeling met dimethyl fosfiet in methanol. Het *N*-atoom werd gecarbamoyleerd met zowel aryl- als alkylisocyanaten met Cu(I)Cl als katalysator. Acylering van de verkregen ureido phosphonaten **xxiv** mislukte. Onder basische condities werd verplaatsing van de dubbele binding tot vinylische fosfonaten waargenomen. Het 1,4,2-diazaphospholidin-5-on **xxv** werd gevormd onder reflux in CH_3CN. Ringsluiting van het allylderivaat van **xxiv** via metathese leverde een complex reactiemengsel. Een computationele studie van het verkregen complex van **xxiv** met Grubbs' 2de generatie katalysator toonde dat de complexatie zwakker was dan deze in gekende katalysator-desactiverende complexen. Verder onderzoek van deze reactie is dus aangewezen.

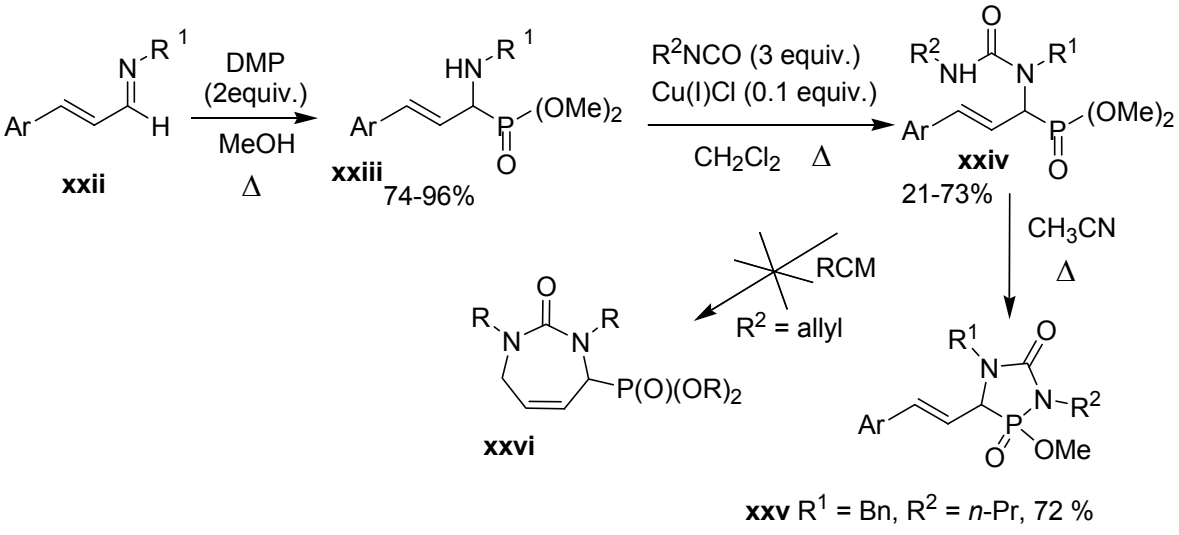

Furfurylamino fosfonaten zijn ideale substraten voor de IMDAF reactie (intramoleculaire Diels-Alder reactie met furan). De producten kunnen gebruikt worden als nieuwe conformationeel beperkte aminozuuranalogen. De synthese van deze tricyclische fosfonaten

werd ontwikkeld binnen de *SynBioC* groep. De cycloadditie vertoonde grote stereoselectiviteit. De IMDAF verknoping gebeurde *exo*. Bij de derivaten van het type **xxvii**, waarbij de allylgroep fungeert als dienofiel, werd een mengsel van isomeren gevormd door onvolledige kinetische controle van de positie van het fosfonaat als tethersubstituent. Het majorisomeer **xxix**, met de *C*(2)-fosfonaat-substituent in *exo* positie, werd omgezet naar het minor *endo* isomeer **xxxi** onder thermodynamische controle via een retro-Diels-Alder reactie. Voor derivatieven van het type **xxxiii**, met een acylgroep als dienofiel, werd slechts één isomeer **xxxiv** waargenomen.

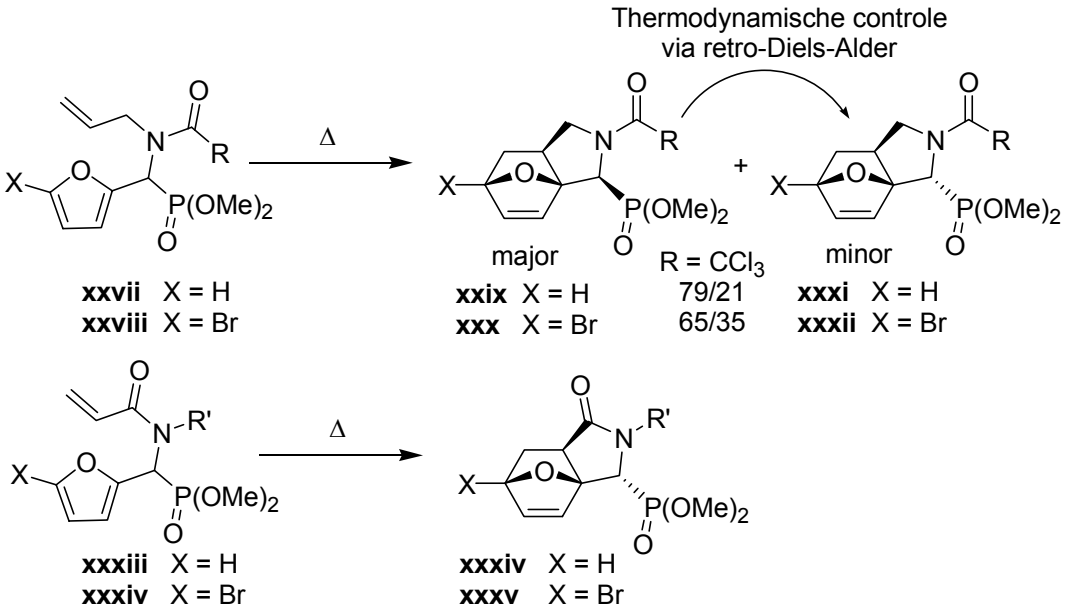

Deze kinetische en thermodynamische controle werd computationeel gereproduceerd. Bij derivaten met de acylgroep als dienofiel vereisen de isomeren met een fosfonaat groep in *exo* positie een grotere afwijking van hun minima dan de *endo* isomeren en de *exo* isomeren vertonen meer sterische hindering in de gemodelleerde transitie-toestanden. Dit zorgt voor specifieke vorming van het *endo* isomeer **xxxiv**. Voor amino fosfonaten **xxvii** vereisen de *endo* and *exo* positie ongeveer dezelfde amiderotatie en is er een subtiel energieverschil dat een hoger berekeningsniveau vereist.

De mogelijkheden van deze IMDAF reactie werden verder uitgebreid. Zo reduceerde een broomsubstituent op de 5-plaats van het furan (zoals in **xxxiv**) de reactieduur van de ringsluiting met 40 %, maar er werd geen significant effect waargenomen op de π-diastereofaciale selectiviteit van IMDAF reactie van **xxviii**.

De acylering van de aminofosfonaten **xxxvi** met maleïnezuuranhydride en IMDAF reactie verliepen in één stap. Aan de hand van IR en NMR spectra kon duidelijk worden aangetoond dat de acylering plaatsvond voor de ringsluiting, er een *exo* verknoping was in het IMDAF adduct en de fosfonaatgroep bij voorkeur een *endo* oriëntatie had.

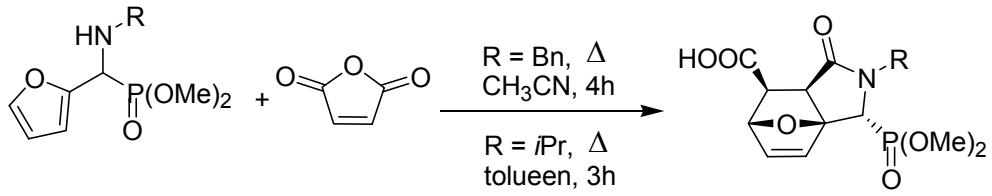

xxxvi

xxxvii R = Bn, 67 %
R = *i*Pr, 63 %

Een belangrijke transformatie van deze 7-oxabicyclo[2.2.1]heptenen in de synthese van biologisch actieve moleculen is de splitsing van de zuurstofbrug van het oxanorborneen tot gefunctionaliseerde cyclohexeenderivaten.

Verschillende reactiecondities werden gevonden voor de ringopening van oxanorborneen **xxix** en een aantal analogen. Gebruik van $FeCl_3$ en $TiCl_4$ als Lewis zuren resulteerde in de ringopening zonder volledige oxidatie van de zesring. Via aromatisatie gaan de stereocentra die gevormd werden door de stereoselectieve IMDAF reactie immers verloren. Coaten van de Fe-katalysator op montmorilloniet K10 vereenvoudigde de opwerking, maar versnelde de aromatisatie.

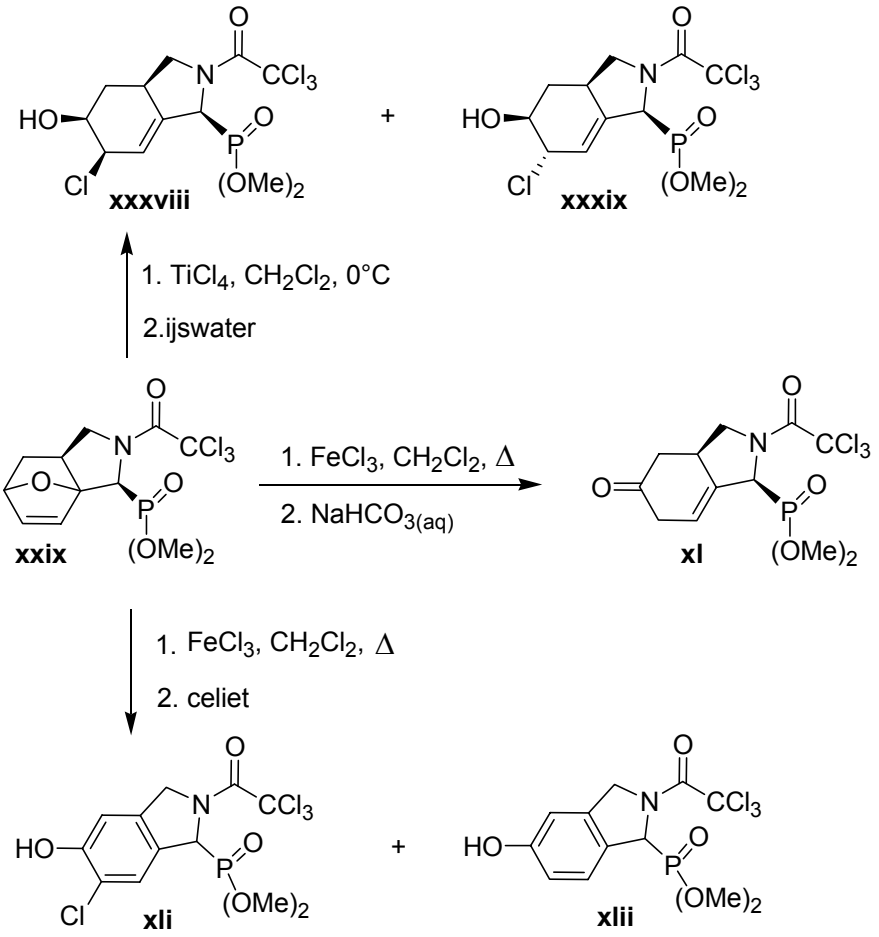

Een computationele studie van de complexatie en het breken van de C-O binding toonde dat de energiebarrière voor de $FeCl_3$-gekatalyseerde reactie hoger is dan voor de $TiCl_4$-gekatalyseerde reactie. Het verschillend gedrag van beide katalysatoren kan gelinkt worden met hun affiniteit om complexen te vormen met oxide anionen. Dit gedrag valt samen met de stabiliteitscorrelatie voor organometaalcomplexen gebaseerd op het hard-zacht zuur-baseprincipe van Pearson. Bij gebruik van $TiCl_4$ wordt een chloride anion ingevoegd ter neutralisatie van het allylische carbocation. Bij $FeCl_3$ stabiliseert het oxide anion zelf het allylische carbocation en verloopt de verdere reactie via een 2-staps 1,2-hydrideshift.

In deze thesis werden nieuwe azaheterocyclische verbindingen met biologisch potentieel gesynthetiseerd vertrekkende van pyroglutamaten en α-amino fosfonaten. Voor verschillende syntheseroutes waar de experimenteel opgebouwde chemische intuïtie tekort schiet, werden computationele studies uitgevoerd om de stereoselectiviteit van de reactie te verklaren en om de mogelijke reactiepaden te evalueren. Dezelfde methodologieën kunnen

gebruikt worden op een meer voorspellende manier en kunnen uitgebreid worden met meer geavanceerde technieken.

In de intramoleculaire Diels-Alder reactie, bijvoorbeeld, hebben de samenstelling van de tether en zijn substituenten vaak tegengestelde effecten op de (π-dia)stereoselectiviteit van de reactie. De gebruikte methodologie kon de waargenomen productratio verklaren en kan in de toekomst gebruikt worden om de selectiviteit van analoge reacties te voorspellen, zelfs van inverse electron demand Diels-Alder reacties waarvoor de analyse van de transitietoestand van groter belang is. De methode kan ook verder uitgebreid worden door solventeffecten in rekening te brengen.

Hetzelfde geldt voor de reacties waarin zowel transitiemetalen als s- en p-blok elementen gebruikt worden, maar hiervoor is verdere benchmarking van de methode nodig.

Computationele studies kunnen bijdragen tot het optimaliseren van de experimentele reacties, maar de chemische intuïtie is nog steeds nodig om mogelijke reactiepaden voor te stellen of om de belangrijke reactiecoördinaten aan te duiden. Deze synergie tussen experimentele en computationele chemie maakt toekomstig onderzoek boeiend, uitdagend, soms frustrerend, maar veelbelovend.

References

[1] Head-Gordon, M.; Artacho, E. *Physics Today* **2008**, *April*, 58.

[2] Rammeloo, T. PhD, *Ghent University, Faculty of Agricultural and Applied Biological Sciences*, **2003**, p.219.

[3] Stevens, C. V.; Rammeloo, T.; De Kimpe, N. *Synlett* **2001**, *10*, 1519.

[4] Masschelein, K. G. R.; Stevens, C. V.; Dieltiens, N.; Claeys, D.D. *Tetrahedron* **2007**, *63*, 4712.

[5] Dieltiens, N.; Stevens, C. V.; Masschelein, K. G. R.; Rammeloo, T. *Tetrahedron* **2005**, *61*, 6749.

[6] Stevens, C. V.; Dieltiens, N.; Claeys, D. D. *Org. Lett.* **2005**, *7*, 1117.

[7] Stevens, C. V.; Dieltiens, N.; Claeys, D. D. *Org. Lett.* **2005**, *7*, 5347.

[8] Back, P.; Maurois, P.; Dupont, C.; Pages, N.; Stables, J. P.; Gressens, P.; Evrard, P.; Vamecq, J. *J. Neurosci.* **1998**, *18*, 4363.

[9] Dieltiens, N.; Claeys, D. D., Zhdankin, V. V.; Nemykin, V. N.; Allaert, B.; Verpoort, F.; Stevens, C. V. *Eur. J. Org. Chem.* **2006**, 2649.

[10] Haces, A.; Breitman, T. R.; Driscoll, J. S. *J. Med. Chem.* **1987**, *30*, 405.

[11] Verstraelen, T.; Van Houteghem, M.; Van Speybroeck, V.; Waroquier, M. *J. Chem. Inf. Model.* **2008**, *48*, 2414.

[12] Van Meenen, E.; Moonen, K.; Acke, D.; Stevens, C. V. *Arkivoc* **2006**, 31.

[13] Moonen, K. PhD, *Ghent University, Faculty of Bioscience Engineering*, **2006**, p.239.

[14] Knabe, J.; Baldauf, J.; Ahlhelm, A. *Pharmazie* **1997**, *52*, 912.

[15] Luer, M. S. *Neurol. Res.* **1998**, *20*, 178.

[16] Rodgers, T. R.; Lamontagne, M. P.; Markovac, A.; Ash, A. B. *J. Med. Chem.* **1977**, *20*, 591.

[17] Somsak, L.; Kovacs, L.; Toth, M.; Osz, E.; Szilagyi, L.; Gyorgydeak, Z.; Dinya, Z.; Docsa, T.; Toth, B.; Gergely, P. *J. Med. Chem.* **2001**, *44*, 2843.

[18] Bazil, C. W.; Pedley, T. A. *Annu. Rev. Med.* **1998**, *49*, 135.

[19] Pham, T. Q.; Pyne, S. G.; Skelton, B. W.; Whitet, A. H. *J. Org. Chem.* **2005**, *70*, 6369.

[20] Ware, E. *Chem. Rev.* **1950**, *46*, 403.

[21] Meusel, M.; Gütschow, M. *Org. Prep. Proced. Int.* **2004**, *36*, 391.

[22] Urech, F. *Justus Liebigs Ann. Chem.* **1873**, *165*, 99.

[23] Bucherer, H. T.; Brandt, W. *J. Prakt. Chem.* **1934**, *140*, 129.

[24] Beller, M.; Eckert, M.; Moradi, W. A.; Neumann, H. *Angew. Chem., Int. Ed.* **1999**, *38*, 1454.

[25] Bhat, B. A.; Dhar, K. L.; Puri, S. C.; Spiteller, M. *Synlett* **2006**, 2723.

[26] Montagne, C.; Shipman, M. *Synlett* **2006**, 2203.

[27] Alsina, J.; Scott, W. L.; O'Donnell, M. J. *Tetrahedron Lett.* **2005**, *46*, 3131.

[28] Driscoll, J. S. US Patent 330509, **1989**.

[29] Kukhar, V. P.; Hudson, H. R. *"Aminophosphonic and Aminophosphinic Acids, Chemistry and Biological Acitivity"*, John Wiley & Sons, Ltd., New York **2000**, p 634.

[30] Ordonez, M.; Rojas-Cabrera, H.; Cativiela, C. *Tetrahedron* **2009**, *65*, 17.

[31] Vanderhoydonck, B. PhD, *Ghent University, Faculty of Bioscience Engineering*, **2005**, p.281.

[32] Redmore, D. *Chem. Rev.* **1971**, *71*, 315.

[33] Moonen, K.; Laureyn, I.; Stevens, C. V. *Chem. Rev.* **2004**, *104*, 6177.

[34] Diels, O.; Alder, K. *Ber. Dtsch. Chem. Ges.* **1929**, *62*, 554.

[35] a) Lipshutz, B. H. *Chem. Rev.* **1986**, *86*, 795; b) Wenkert, E.; Moeller, P. D. R.; Piettre, S. R. *J. Am. Chem. Soc.* **1988**, *110*, 7188; c) Domingo, L. R.; Picher, M. T.; Aurell, M. J. *J. Phys. Chem. A* **1999**, *103*, 11425; d) Lautens, M.; Fillion, E. *J. Org. Chem.* **1996**, *61*, 7994.

[36] Houk, K. N.; Gonzales, J. ; Li, Y. *Acc. Chem. Res.* **1995**, *28*, 81.

[37] Woodward, R. B.; Hoffmann, R. *Angew. Chem. Int. Ed. Engl.* **1969**, *8*, 781.

[38] Fukui, K. *Chemistry Nobel lecture* **1981**, pp. 26.

[39] Klopman, G. *J. Am. Chem. Soc.* **1968**, *90*, 223.

[40] a) Salem, L. *J. Am. Chem. Soc.* **1968**, *90*, 543; b) Salem, L. *J. Am. Chem. Soc.* **1968**, *90*, 553.

[41] Brown, F. K.; Houk, K. N. *Tetrahedron Lett.* **1984**, *25*, 4609.

[42] Hoffmann, R.; Woodward, R. B. *J. Am. Chem. Soc.* **1965**, *87*, 4388.

[43] Houk, K. N. *J. Am. Chem. Soc.* **1973**, *95*, 4092.

[44] Robiette, R.; Marchand-Brynaert, J.; Peeters, D. *J. Org. Chem.* **2002**, *67*, 6823.

[45] Spino, C.; Pesant, M.; Dory, Y. *Angew. Chem. Int. Ed.* **1998**, *37*, 3262.

[46] Ciganek, E. Chapter 1 "The Intramolecular Diels-Alder Reaction" in "Organic Reactions" *Vol. 32*, Ed. Dauben G. W., p 1-100.

[47] Brown, F. K.; Houk, K. N. *Tetrahedron Lett.* **1985**, *26*, 2297.

[48] Cayzer, T. N.; Wong, L. S.-M.; Turner, P.; Paddon-Row, M. N.; Sherburn, M. S. *Chem. Eur. J.* **2002**, *8*, 739.

[49] De Clercq, P. J.; Van Royen, L. A. *Synth. Comm.* **1979**, *9*, 771.

[50] Fischer, K.; Hünig, S. *J. Org. Chem.* **1987**, *52*, 564.

[51] Namboothiri, I. N. N.; Ganesh, M.; Mobin, S. M.; Cojocaru, M. *J. Org. Chem.* **2005**, *70*, 2235.

[52] a) Zubkov, F. I.; Boltukhina, E. V.; Turchin, K. F.; Borisov, R. S.; Varlamov, A. V. *Tetrahedron* **2005**, *61*, 4099; b) Varlamov, A. V.; Zubkov, F. I.; Boltukhina, E. V.; Sidorenko, N. V.; Borisov, R. S. *Tetrahedron Lett.* **2003**, *44*, 3641.

[53] Bilovic, D. *Croat. Chem. Acta* **1966**, *38*, 293. (Abstract)

[54] Gschwend, H. W.; Hillman, M. J.; Kisis, B.; Rodebaugh, R. K. *J. Org. Chem.* **1976**, *41*, 104.

[55] Parker, K. A.; Adamchuk, M. R. *Tetrahedron Lett.* **1978**, *19*, 1689.

[56] Gschwend, H. W.; Lee, A. O.; Meier, H.-P. *J. Org. Chem.* **1973**, *38*, 2169.

[57] Bilovic, D.; Stojanac, Z.; Hahn, V. *Tetrahedron Lett.* **1964**, *31-32*, 2071. (Abstract)

[58] Choony, N.; Dadabhoy, A.; Sammes, P. G. *J. Chem. Doc. Perkin Trans. 1* **1998**, 2017.

[59] a) Sternbach, D. D.; Rossana, D. M. *Tetrahedron Lett.* **1982**, *23*, 303; b) Sternbach, D. D.; Rossana, D. M.; Onan, K. D. *Tetrahedron Lett.* **1985**, *26*, 591.

[60] Jung, M. E.; Street, L. J. *J. Am. Chem. Soc.* **1984**, *106*, 8327.

[61] Jung, M. E.; Gervay, J. *J. Am. Chem. Soc.* **1991**, *113*, 224.

[62] Jung, M. E.; Kiankarimi, M. *J. Org. Chem.* **1998**, *63*, 2968.

[63] Jung, M. E. *Synlett* **1999**, *S1*, 843.

[64] Bruice, T. C.; Pandit, U. K. *J. Am. Chem. Soc.* **1960**, *82*, 5858.

[65] Parrill, A. L.; Dolata, D. P. *J. Mol. Stru. (Theo)* **1996**, *370*, 187.

[66] a) Danforth, C.; Nicholson, A. W.; James, J. C.; Loudon, G. M. *J. Am. Chem. Soc.* **1976**, *98*, 4275; b) Winans, R. E.; Wilcox, C. F. Jr. *J. Am. Chem. Soc.* **1976**, *98*, 4281.

[67] a) Bur, S. K.; Lynch, S. M.; Padwa. A. *Org. Lett.* **2002**, *4*, 473; b) Padwa, A.; Ginn, J. D.; Bur, S. K.; Eidell, C. K.; Lynch, S. M. *J. Org. Chem.* **2002**, *67*, 3412.

[68] Hayashi, T.; Kawakami, Y.; Konno, K.; Takayama, H. *J. Chem. Soc., Perkin Trans. I* **1993**, 2387. (Abstract)

[69] Ghelfi, F.; Parsons, A. F.; Tommasini, D.; Mucci, A. *Eur. J. Org. Chem.* **2001**, 1845.

[70] Mukaiyama, T.; Tsuji, T.; Iwasawa, N. *Chem. Lett.* **1979**, 697.

[71] Mukaiyama, T.; Iwasawa, N. *Chem. Lett.* **1981**, 29.

[72] a) Paddon-Row, M. N.; Sherburn, M. S. *Chem. Comm.* **2000**, 2215; b) Tantillo, D. J.; Houk, K. N.; Jung, M. E. *J. Org. Chem.* **2001**, *66*, 1938.

[73] Schleyer Ragué von P.; Maerker C.; Dransfeld, A.; Jiao, H.; Hommes Eikema van, N. J. R. *J. Am. Chem. Soc.* **1996**, *118*, 6317.

[74] Dinadayalane, T. C.; Vijaya, R.; Smitha, A.; Sastry, G. N. *J. Phys. Chem. A* **2002**, *106*, 1627.

[75] Pienazek, S. N., Houk, K. N. *Angew. Chem., Int. Ed. Engl.* **2006**, *45*, 1442.

[76] Crawford, K. R.; Bur, S. K.; Straub, C. S.; Padwa, A. *Org. Lett.* **2003**, 3337.

[77] Padwa, A.; Crawford, K. R.; Straub, C. S.; Pieniazek, S. N.; Houk, K. N. *J. Org. Chem.* **2006**, *71*, 5432.

[78] Jung, M. E.; Truc, V.C. *Tetrahedron Lett.* , *29*, 6059.

[79] Bovenschulte, E.; Metz, P.; Henkel, G. *Angew. Chem, Int. Ed. Engl.* **1989**, *28*, 202.

[80] Grootaert, W. M.; De Clercq, P. J. *Tetrahedron Lett.* **1982**, *23*, 3291.

[81] Appendino, G.; Hoflack, J.; De Clercq, P. J.; Chiari, G.; Calleri, M. *Tetrahedron* **1988**, 44, 4605.

[82] Nuyttens, F.; Hoflack, J.; Appendino, G.; De Clercq, P. J. *Synlett* **1995**, *1*, 105.

[83] a) Best, W. M.; Wege, D. *Aust. J. Chem.* **1986**, *39*, 635; b) Best, W. M.; Wege, D. *Aust. J. Chem.* **1986**, *39*, 647.

[84] Prajapati, D.; Borthakur, D. R.; Sandhu, J. S. *J. Chem. Soc. Perkin Trans. I* **1993**, 1197. (Abstract)

[85] Roush, W. R.; Gillis, H. R.; Ko, A. I. *J. Am. Chem. Soc.* **1982**, *104*, 2269.

[86] Zylber, J.; Tubul, A.; Brun, P. *Tetrahedron: Asymmetry* **1995**, *6*, 377.

[87] Benningshof, J. C. J.; Blaauw, R. H.; van Ginkel, A. E.; van Maarseveen, J. H.; Rutjes, F. P. J. T.; Hiemstra, H. *J. Chem. Soc. Perkin Trans. I* **2002**, 1693.

[88] Woo, S.; Keay, B. A. *Tetrahedron: Asymmetry* **1994**, *5*, 1411.

[89] a) Zhang, H. J.; Padwa, A. *Org. Lett.* **2006**, *8*, 247; b) Padwa, A.; Ginn, J. D. *J. Org. Chem.* **2005**, *70*, 5197; c) Wang, Q.; Padwa, A. *Org. Lett.* **2004**, *6*, 2189; d) Kouznetsov, V. V.; Zubkov, F. I.; Cruz, U. M.; Voskressensky, L. G.; Mendez, L. Y. V.; Astudillo, L.; Stashenko, E. E. *Lett. Org. Chem.* **2004**, *1*, 37; e) Fokas, D.; Patterson, J. E.; Slobodkin, G.; Baldino, C. M. *Tetrahedron Lett.* **2003**, *44*, 5137; f) Padwa, A.; Eidell, C. K.; Lynch, S. M. *Heterocycles* **2002**, *58*, 227; g) Padwa, A.; Dimitroff, M.; Liu, B. *Org. Lett.* **2000**, *2*, 3233; h) Sprague, P. W.; Heikes, J. E.; Gougoutas, J. Z.; Malley, M. F.; Harris, D. N.; Greenberg, R. *J.*

Med. Chem. **1985**, *28*, 1580; i) Sneden, A. T. *Synlett* **1993**, *5*, 313; j) Yu, S. Y.; Beese, G.; Keay, B. A. *J. Chem. Soc. Perk. Trans. 1* **1992**, 2729.

[90] Vogel, P.; Cossy, J.; Plumet, J.; Arjona, O. *Tetrahedron* **1999**, *55*, 13521.

[91] Hernándes, J. E.; Fernándes, S.; Arias, G. *Synth. Commun.* **1988**, *18*, 2055.

[92] Le Goanvic, D.; Lallemand, M.-C.; Tillequin, F.; Martens T. *Tetrahedron Lett.* **2001**, *42*, 5175.

[93] Padwa, A.; Wang, Q. *J. Org. Chem.* **2006**, *71*, 3210.

[94] Yang, W.; Koreeda, M. *J. Org. Chem.* **1992**, *57*, 3836.

[95] Lee, M.; Moritomo, H.; Kanematsu, K. *Tetrahedron* **1996**, *52*, 8169.

[96] Claeys, S.; Van Haver, D.; De Clercq, P. J.; Milanesio, M.; Viterbo, D. *Eur. J. Org. Chem.*, **2002**, 1051.

[97] Padwa, A.; Brodney, M. A.; Dimitroff, M. *J. Org. Chem.* **1998**, *63*, 5304.

[98] Ginn, J. D.; Lynch, S. M.; Padwa, A. *Tetrahedron Lett.* **2000**, *41*, 9387.

[99] Padwa, A.; Ginn, J. D. *J. Org. Chem.* **2005**, *70*, 5197.

[100] Wu, H.-J.; Ying, F.-H.; Shao, W.-D. *J. Org. Chem.* **1995**, *60*, 6168.

[101] Lautens, M., et al., *Tetrahedron Lett.*, **1990**, *31*, 3253.

[102] Arjona, O.; de Dios, A.; de la Pradilla, R. F.; Plumet, J.; Viso, A. *J. Org. Chem.* **1994**, *59*, 3906.

[103] Woo, S.; Keay, B. A. *Synthesis* **1996**, 669.

[104] Nakamura, M.; Matsuo, K.; Inoue, T.; Nakamura, E. *Org. Lett.* **2003**, *5*, 1373.

[105] Lautens, M.; Renaud, J.-L.; Hiebert, S. *J. Am. Chem. Soc.* **2000**, 122, 1804.

[106] a) Lautens, M.; Fagnou, K. *PNAS* **2004**, *101*, 5455; b) Lautens, M.; Fagnou, K.; Taylor, M. *Org. Lett.* **2000**, *2*, 1677; c) Lautens, M. ; Fagnou, K. *Tetrahedron* **2001**, *57*, 5067; d) Lautens, M.; Dockendorff, C.; Fagnou, K.; Malicki, A. *Org. Lett.*, **2002**, *4*, 1311.

[107] Padwa, A.; Wang, Q. *J. Org. Chem.* **2006**, *71*, 7391.

[108] Fier, S.; Sullivan, R. W.; Rickborn, B. *J. Org. Chem.* **1988**, *53*, 2353.

[109] a) Gupta, A.; Rodrigo, R. *J. Chem. Soc., Chem. Commun.* **1989**, 959; b) Forsey, S. P.; Rajapaksa, D.; Taylor, N. J.; Rodrigo, R. *J. Org. Chem.* **1989**, *54*, 4280.

[110] Weeratunga, G.; Rajapaksa, D.; Rodrigo, R. *J. Org. Chem.* **1985**, *50*, 5905.

[111] Claeys, D. D. Master Thesis, *Ghent University, Faculty of Bioscience Engineering*, **2005**, p.90.

[112] Marquez, V. E.; Kelley, J. A.; Driscoll, J. S. *J. Org. Chem.* **1980**, *45*, 5308.

[113] Guillon, J.; Sonnet, P.; Boulouard, M.; Dallemagne, P.; Miel, H.; Daoust, M.; Rault, S. *J. Heterocyclic Chem.* **1998**, *35*, 535.

[114] Heckendorn, R.; Winkler, T. *J. Heterocyclic Chem.* **2000**, *37*, 111-114.

[115] Senior, M. M.; Chan, T.-M.; Li, G.; Huang, Y.; Stamford, A. *Magn. Reson. Chem.* **2007**, *45*, 240.

[116] Najera, C.; Yus, M. *Tetrahedron: Asymm.* **1999**, *10*, 2245.

[117] Ezquerra, J.; Pedregal, C.; Yruretagoneya, B.; Rubio, A.; Carreno, M. C.; Escribano, A.; Garcia Ruano, J. L. *J. Org. Chem*. **1995**, *60*, 2925.

[118] Dieltiens, N. Master Thesis, *Ghent University, Faculty of Agricultural and Applied Biological Sciences*, **2003**, p.75.

[119] Brana, M. F.; Garranzo, M.; Perez-Castells, J. *Tetrahedron Lett.* **1998**, *39*, 6569.

[120] Guillena, G.; Mancheno, B.; Najera, C.; Ezquerra, J.; Pedegral, C. *Tetrahedron* **1998**, *54*, 9447.

[121] Rigo, B.; Kolocouris, A. *J. Heterocyclic Chem.* **1996**, *33*, 1233.

[122] Evnin, A. B.; Lam, A.; Blyskal, J. *J. Org. Chem.* **1970**, *35*, 3097.

[123] Dyatkin, A. B. *Tetrahedron Lett.* **1997**, *38*, 2065.

[124] Andreeff, M.; Stone, R.; Michaeli, J.; Young, C. W.; Tong, W. P.; Sogoloff, H.; Ervin, T.; Kufe, D.; Rifkind, R. A.; Marks, P. A. *Blood* **1992**, *80*, 2604.

[125] Breslow, R.; Jursic, B.; Yan, Z. F.; Friedman, E.; Leng, L.; Ngo, L.; Rifkind, R. A.; Marks, P. A. *Proc. Nat. Acad. Sci. U.S.A.* **1991**, *88*, 5542.

[126] Breslow, R.; Belvedere, S.; Gershell, L. *Helv. Chim. Acta* **2000**, *83*, 1685.

[127] Poupaert, J. H.; Mergen, F. Lerot, T. *Bull. Soc. Chim. Belg.* **1988**, *97*, 469.

[128] Fürstner, A.; Muller, T. *J. Org. Chem.* **1998**, *63*, 424.

[129] Scholl, M.; Ding, S.; Lee, C. W.; Grubbs, R. H. *Org. Lett.* **1999,** *1*, 953.

[130] Fürstner, A.; Thiel, O. R.; Kindler, N.; Bartkowska, B. *J. Org. Chem.* **2000**, *65*, 7990.

[131] Schwab, P.; France, M. B.; Ziller, J. W.; Grubbs, R. H. *Angew. Chem. Int. Ed. Engl.* **1995**, *34*, 2039.

[132] Lee, C. W.; Grubbs, R. H. *Org. Lett.* **2000**, *2*, 2145.

[133] Mucci, A.; Parenti, F.; Schenetti, L. *Eur. J. Org. Chem.* **2002**, 938.

[134] Claeys, D. D.; Verstraelen, T.; Pauwels, E.; Stevens, C. V.; Waroquier, M.; Van Speybroeck, V. *J. Comput. Chem.*, submitted.

[135] Allaert, B.; Ledoux, N.; Dieltiens, N.; Vander Mierde, H.; Stevens, C. V.; Van Der Voort, P.; Verpoort, F. *Catal. Commun.* **2008**, *9*, 1054.

[136] Castoldi, D.; Caggiano, L.; Panigada, L.; Sharon, O.; Costa, A. M.; Gennari, C. *Chem. Eur. J.* **2006**, *12*, 51.

[137] VandeVondele, J.; Krack, M.; Mohamed, F.; Parrinello, M.; Chassaing, T.; Hutter, J. *Comput. Phys. Commun.* **2005**, *167*, 103.

[138] Repasky, M. P.; Chandrasekhar, J.; Jorgensen, W. L. *J. Comput. Chem.* **2002**, *23*, 1601.

[139] Nose, S. *J. Chem. Phys.* **1984**, *81*, 511.

[140] Nose, S. *Mol. Phys.* **1984**, *52*, 255.

[141] Liwo, A.; Czaplewski, C.; Oldziej, S.; Scheraga, H. A. *Curr. Opin. Struct. Biol.* **2008**, *18*, 134.

[142] Christen, M.; van Gunsteren, W. F. *J. Comput. Chem.* **2008**, *29*, 157.

[143] Frenkel, D.; Smit, B. *"Understanding Molecular Simulation: From Algorithms to Applications"*, Academic Press, San Diego **2002**.

[144] von der Lieth, C. W.; Kozar, T.; Hull, W. E. *J. Mol. Struct. (Theochem)* **1997**, *395*, 225.

[145] Hess, B. *Phys. Rev. E* **2000**, *62*, 8438.

[146] Hess, B. *Phys. Rev. E* **2002**, *65*, 031910-1.

[147] Allen, M. P.; Tildesley, D. J. *"Computer Simulation of Liquids"*, Oxford University Press, New York, **1989**; Chapter 2.

[148] Kabsch, W. *Acta. Cryst.* **1976**, *32*, 922.

[149] Kennard, R. W.; Stone, L. A. *Technometrics* **1969**, 11, 137.

[150] Frish, M. J. et al. Gaussian 03, Revision C.02, Gaussian, Inc., Wallingford CT, **2004**.

[151] Becke, A. D. *J. Chem. Phys.* **1993**, *98*, 5648.

[152] Stephens, P. J.; Devlin, F. J.; Chabalowski, C. F.; Frish, M. J. *J. Phys. Chem.* **1994**, *98*, 11623.

[153] a) Ditchfield, R.; Hehre, W. J.; Pople, J. A. *J. Chem. Phys.* **1971**, *54*, 724; b) Hehre, W. J.; Ditchfield, R.; Pople, J. A. *J. Chem. Phys.* **1972**, *56*, 2257; c) Hariharan, P. C.; Pople, J. A. *Theor. Chem. Acc.* **1973**, *28*, 213; d) Hariharan, P. C.; Pople, J. A. *Mol. Phys*. **1974**, *27*, 209; e) Gordon, M. S. *Chem. Phys. Lett.* **1980**, *76*, 163; f) Francl, M. M.; Pietro, W. J.; Hehre, W. J.; Binkley, J. S.; DeFrees, D. J.; Pople, J. A.; Gordon, M. S. *J. Chem. Phys.* **1982**, *77*, 3654.

[154] a) Møller, C.; Plesset, M. S. *Phys. Rev.* **1934**, *46*, 0618; b) Head-Gordon, M.; Pople, J. A.; Frisch, M. J. *Chem. Phys. Lett.* **1988**, *153*, 503; c) Saebø, S.; Almlöf, J. *Chem. Phys. Lett.* **1989**, *154*, 83; d) Frisch, M. J.; Head-Gordon, M.; Pople, J. A. *Chem. Phys. Lett.* **1990**, *166*, 275; e) Frisch, M. J.; Head-Gordon, M.; Pople, J. A. *Chem. Phys. Lett.* **1990**, *166*, 281; f) Head-Gordon, M.; Head-Gordon, T. *Chem. Phys. Lett.* **1994**, *220*, 122.

[155] Cremer, D.; Pople, J. A. *J. Am. Chem. Soc.* **1975**, *97*, 1354.

[156] Poupaert, J. H.; Lhoëst, G. *Bull. Soc. Chim. Belg.* **1979**, *88*, 339.

[157] Lin, M.-J.; Sun, C.-M. *Tetrahedron Lett.* **2003**, *44*, 8739.

[158] Teng, X.; Degterev, A.; Jagtap, P.; Xing, X.; Choi, S.; Denu, R.; Yuan, J.; Cuny, G. D. *Bioorg. Med. Chem. Lett.* **2005**, *15*, 5039.

[159] Wang, Z. D.; Sheikh, S.; Zhang, Y. *Molecules* **2006**, *11*, 739.

[160] Vanhoecke, B. PhD, *Ghent University, Faculty of Medicine and Health Sciences*, **2006**, p.122.

[161] Vanhoecke, B.; Derycke, L.; Van Marck, V.; Depypere, H.; De Keukeleire, D.; Bracke, M. *Int. J. Cancer* **2005**, *117*, 889.

[162] Hubert, J. C.; Steege, W.; Speckamp, W. N.; Huisman, H. O. *Synth. Comm.* **1971**, *1*, 103.

[163] Duggan, M. E.; Imagire, J. S. *Synthesis* **1989**, 131.

[164] Walker, M. A. *J. Org. Chem.* **1995**, *60*, 5352.

[165] Martin, S. F.; Follows, B. C.; Hergenrother, P. J.; Franklin, C. L. *J. Org. Chem.* **2000**, *65*, 4509.

[166] Sainz-Diaz, C. I.; Galvez-Ruano, E.; Hernandez-Laguna, A.; Bellanato, J. *J. Org. Chem.* **1995**, *60*, 74.

[167] Marcotte, F.-A.; Rombouts, F. J. R.; Lubell, W. D. *J. Org. Chem.* **2003**, *68*, 6984.

[168] Merten, R.; Weber, C. *Chem. Ber.* **1969**, *102*, 2143.

[169] Khailova, N. A.; Shaimardanova, A. A.; Saakyan, G. M.; Zyablikova, T. A.; Azancheev, N. M.; Krivolapov, D. B.; Gubaidullin, A. T.; Litvinov, I. A.; Musin, R. Z.; Chmutova, G. A.; Pudovik, M. A.; Pudovik, A. N. *Russian Journal of General Chemistry* **2003**, *73*, 1213.

[170] Krelaus, R.; Westermann, B. *Tetrahedron Lett.* **2004**, *45*, 5987.

[171] Fiorelli, C.; Savoia, D. *J. Org. Chem.* **2007**, *72*, 6022.

[172] Fu, G. C.; Nguyen, S. T. ; Grubbs, R. H. *J. Am. Chem. Soc.* **1993**, *115*, 9856.

[173] Fürstner, A.; Langemann, K. *J. Am. Chem. Soc.* **1997**, *119*, 9130.

[174] Fürstner, A. *Topics in Catalysis* **1997**, *4*, 285.

[175] Bocelli, G.; Catellani M.; Cugini, F.; Ferraccioli, R. *Tetrahedron Lett.* **1999**, *40*, 2623.

[176] Moonen, K.; Dieltiens, N.; Stevens, C. V. *J. Org. Chem.* **2006**, *71*, 4006.

[177] Correa, A.; Cavallo, L. *J. Am. Chem. Soc.* **2006**, *128*, 13352.

[178] a) Becke, A. D. *Phys. Rev. A* **1988**, *38*, 3098; b) Perdew, J. P. *Phys. Rev. B* **1986**, *33*, 8822; c) Perdew, J. P. *Phys. Rev. B* **1986**, *34*, 7406.

[179] Schaefer, A.; Horn, H.; Ahlrichs, R. *J. Chem. Phys.* **1992**, *97*, 2571.

[180] a) Haeusermann, U.; Dolg, M.; Stoll, H.; Preuss, H. *Mol. Phys.* **1993**, *78*, 1211; b) Kuechle, W.; Dolg, M.; Stoll, H.; Preuss, H. *J. Chem. Phys.* **1994**, *100*, 7535; c) Leininger, T.; Nicklass, A.; Stoll, H.; Dolg, M.; Schwerdtfeger, P. *J. Chem. Phys.* **1996**, *105*, 1052.

[181] Correa, A. *Private Communication*

[182] Benitez, D.; Goddard, W. A. *J. Am. Chem. Soc.* **2005**, *127*, 12218.

[183] a) Leyssens, T.; Peeters, D. *J. Mol. Struct. (Theochem)* **2004**, *673*, 79; b) Leyssens, T.; Peeters, D. *J. Mol. Struct. (Theochem)* **2004**, *686*, 71.

[184] Robiette, R.; Defacqz, N.; Peeters, D.; Marchand-Brynaert, J. *Curr. Org. Synth.* **2005**, *2*, 453.

[185] Guner, V.; Khuong, K. S.; Leach, A. G.; Lee, P. S.; M.; Bartberger, M. D.; Houk, K. N. *J. Phys. Chem. A* **2003**, *107*, 11445.

[186] Adamo, C.; Barone, V. *J. Chem. Phys.* **1998,** *108*, 664.

[187] Zhao, Y.; Lynch, B. J.; Truhlar, D. G. *J. Phys. Chem. A* **2004**, *108*, 2715.

[188] a) Pople, J. A.; Seeger, R.; Krishnan, R. *Int. J. Quant. Chem. Symp.* **1977**, *11*, 149; b) Pople, J. A.; Binkley, J. S.; Seeger, R. *Int. J. Quant. Chem. Symp.* **1976**, *10*, 1.

[189] a) Pople, J. A.; Krishnan, R.; Schlegel, H. B.; Binkley, J. S. *Int. J. Quant. Chem.* **1978**, *14*, 545; b) Bartlett, R. J.; Purvis, G. D. *J. Quant. Chem.* **1978**, *14*, 561; c) Purvis, G. D.; Bartlett, R. J. *J. Chem. Phys.* **1982**, *76*, 1910; d) Scuseria, G. E.; Janssen, C. L.; Schaefer III, H. F. *J. Chem. Phys.* **1988**, *89*, 7382; e) Scuseria, G. E.; Schaefer III, H. F. *J. Chem. Phys.* **1989**, *90*, 3700.

[190] Seeman, J. I. *Chem. Rev.* **1983**, *2*, 83.

[191] Van Speybroeck, V.; Moonen, K.; Hemelsoet, K.; Stevens, C. V.; Waroquier, M. *J. Am. Chem. Soc.* **2006**, *128*, 8468.

[192] Kraicheva, I.; Stefanova, R.; Borisov, G. *Phosphorus, Sulfur Silicon Relat. Elem.* **1993**, *79*, 107.

[193] Bilovic, D. *Croat. Chem. Acta* **1968**, *40*, 15.

[194] Kachkovskyi, G. O.; Kolodiazhnyi, O. I. *Tetrahedron* **2007**, *63*, 12576.

[195] Milkiewicz, K. L.; Neagu, I. B.; Parks, D. J. *Tetrahedron Lett.* **2003**, *44*, 7341.

[196] Branchadell, V.; Oliva, A. *J. Am. Chem. Soc.* **1992**, *114*, 4357.

[197] a) Siodmiak, M.; Frenking, G.; Korkin, A. *J. Mol. Model.* **2000**, *6*, 413; b) Ananthavel, S. P.; Hedge, M. S. *J. Phys. Chem. A* **1997**, *101*, 1680; c) Bongini, A.; Cardillo, G.; Gentilucci, L.; Tomascini, C. *J. Org. Chem.* **1997**, *62*, 9148.

[198] Pelzer, S.; Kauf, T.; van Wüllen C.; Christoffers, J. *J. Organomet. Chem.* **2003**, *684*, 308.

[199] Miranda, P. O.; Carballo, R. M.; Ramirez, M. A.; Martin, V. S.; Padron, J. I. *Arkivoc* **2007**, *iv*, 331.

[200] Roman, B. I. Thesis, *KAHO*, **2006**, p.123

[201] Günther, H. "*NMR spectroscopy: basic principles, concepts, and applications in chemistry*", 2nd ed, John Wiley & Sons Ltd., Chichester **1996**, p 228-233.

[202] Keinan, E.; Mazur, Y. *J. Org. Chem.* **1978**, *43*, 1978.

[203] Jempty, T. C.; Gogins, K. A. Z.; Mazur, Y.; Miller, L. L. *J. Org. Chem.* **1981**, *46*, 4545.

[204] Choudary, B. M.; Sudha, Y. *Synth. Commun.* **1996**, *26*, 2989.

[205] Lakouraj, M. M.; Movassagh, B.; Fasihi, J. *Synth. Commun.* **2000**, *30*, 821.

[206] Nagendrappa, G. *Resonance* **2002**, *7*, 64.

[207] Choudary, B. M.; Chowdari, N. S.; Kantam, M. L. *Tetrahedron* **2000**, *56*, 7291.

[208] Hart, M. P.; Brown, D. R. *J. Mol. Catal. A: Chemical* **2004**, *212*, 315.

[209] Laszlo, P.; Mathy, A. *Helv. Chim. Acta* **1987**, *70*, 577.

[210] Pai, S. G.; Bajpai, A. R.; Deshpande, A. B.; Samant, S. D. *Synth. Commun.* **1997**, *27*, 2267.

[211] Pai, S. G.; Bajpai, A. R.; Deshpande, A. B.; Samant, S. D. *J. Mol. Catal. A: Chemical* **2000**, *156*, 233.

[212] Lakouraj, M.; Movassagh, B.; Fasihi, J. *J. Chem. Research (S)* **2001**, 378.

[213] Elkhayat, Z.; Safir, I.; Castellote, I.; Retailleau, P.; Arseniyadis, S. *Org. Lett.* **2008**, *10*, 2219.

[214] Evans, D. A.; Urpi, F.; Somers, T. C.; Stephen Clark, J.; Bilodeau M. T. *J. Am. Chem. Soc.* **1990**, *112*, 8215.

[215] Mudiganti, N. V. S.; Claessens, S.; De Kimpe, N. *Tetrahedron* **2009**, *65*, 1716.

[216] a) Grimme, S. *J. Comput. Chem.* **2004**, *25*, 1463; b) Grimme, S. *J. Comput. Chem.* **2006**, *27*, 1787.

[217] Neese, F. ORCA – an ab initio, density functional and semiempirical program package, version 2.6.35, Max-Planck institute for bioinorganic chemistry, Mülheim an der Ruhr, Germany, **2008**.

[218] a) Hay, P. J.; Wadt, W. R. *J. Chem. Phys.* **1985**, *82*, 270; b) Hay, P. J.; Wadt, W. R. *J. Chem. Phys.* **1985**, *82*, 299.

[219] a) Wachters, A.; J. H. *J. Chem. Phys.* **1970**, *52*, 1033; b) Hay, P. J. *J. Chem. Phys.* **1977**, *66*, 4377; c) Raghavachari, K.; Trucks, G. W. *J. Chem. Phys.* **1989**, *91*, 1062.

[220] a) McLean, A. D.; Chandler, G. S. *J. Chem. Phys.* **1980**, *72*, 5639; b) Raghavachari, K.; Binkley, J. S.; Seeger, R.; Pople, J. A. *J. Chem. Phys.* **1980**, *72*, 650.

[221] Schultz, N. E.; Zhao, Y.; Truhlar, D. G. *J. Phys. Chem. A* **2005**, *109*, 11127.

[222] Bühl, M.; Kabrede, H. *J. Chem. Theory Comput.* **2006**, *2*, 1282.

[223] Jensen, K. P.; Roos, B. O.; Ryde, U. *J. Chem. Phys.* **2007**, *126*, 014103.

[224] Jensen, K. P. *Inorg. Chem.* **2008**, *47*, 10357.

[225] Tao, J.; Perdew, J. P.; Staroverov, V. N.; Scuseria, G. E. *Phys. Rev. Lett.* **2003**, *91*, 146401.

[226] Staroverov, V. N.; Scuseria, G. E.; Tao, J.; Perdew, J. P. *J. Chem. Phys.* **2003**, *119*, 12129.

[227] Te Velde, G.; Bickelhaupt, F. M.; Baerends, E. J.; Fonseca Guerra, C.; Van Gisbergen, S. J. A.; Snijders, J. G.; Ziegler, T. *J. Comput. Chem.* **2001**, *22*, 931.

[228] Bach, R. D.; Shobe, D. S.; Schlegel, H. B.; Nagel, C. J. *J. Phys. Chem.* **1996**, *100*, 8770.

[229] Poll, T.; Metter, J. O.; Helmchen, G. *Angew. Chem. Int. Ed. Engl.* **1985**, *24*, 112.

[230] Webb, S. P.; Gordon, M. S. *J. Am. Chem. Soc.* **1999**, *121*, 2552.

[231] Jovari, P.; Meszaros, G.; Pusztai, L.; Svab, E. *J. Chem. Phys.* **2001**, *114*, 8082.

[232] Scholz, G.; Curtiss, L. A. *J. Mol. Struct. (Theochem)* **2000**, *507*, 245.

[233] Vertes, A.; Nagy-Czako, I.; Burger, K. *J. Phys. Chem.* **1978**, *82*, 1469.

[234] Keck, G. E.; Castellino, S. *J. Am. Chem. Soc.* **1986**, *108*, 3847.

[235] Assfeld, X.; Garcia, J.; Garcia, J. I.; Mayoral, J. A.; Grazia Proietti, M.; Ruiz-Lopez, M. F.; Sanchez, M. C. *J. Org. Chem.* **1996**, *61*, 1636.

[236] Plietker, B. *"Iron Catalysis in Organic Chemistry: Reactions and Applications"*, Wiley-VCH, Weinheim, **2008**; Chapter 1.

[237] Frenking, G.; Wichmann, K.; Fröhlich, N.; Loschen, C.; Lein, M.; Frunzke, J.; Rayon, V. M. *Coord. Chem. Rev.* **2003**, *238-239*, 55.

[238] Nii, K.; Tagami, K.; Kijima, M.; Munakata, T.; Ooi, T.; Kusumi, T. *Bull. Chem. Soc. Jpn.* **2008**, *81*, 562.

[239] Kettle, S. F. A. "Coordination Compounds", Thomas Nelson & Sons Ltd., Sunbury-on-Thames **1969**, chapter 4.

[240] Ahrland, S.; Chatt, J.; Davies, N. R. *Quart. Rev. Chem. Soc.* **1958**, *12*, 265.

[241] Pearson, R. G. *J. Am. Chem. Soc.* **1963**, *85*, 3533.

[242] Dieltiens, N. PhD, *Ghent University, Faculty of Bioscience Engineering*, **2007**, p.211.

[243] Sobczyk, K.; Siemion, I. Z. *Pol. J. Chem.* **1980**, *54*, 1833.

[244] Suzuki, T.; Tomioka, T.; Tuzimura, K. *Can. J. Biochem.* **1977**, *55*, 521.

[245] Takahashi, A.; Matsuoka, H.; Uda, Y. *Environ. Mutagen. Res.* **2004**, *26*, 1.

Appendices

Appendix 1: The Curtin-Hammet Principle

Appendix 2: Papers

The Curtin-Hammet Principle

The majority of chemical reactions is preceded by much faster conformational pre-equilibria. In Figure 1 the free energy diagram is given of a stereospecific reaction that yields product D from one conformational isomer A and a different product C from another conformational isomer B. The two stereoisomers A and B interconvert rapidly relative to the rate of product formation.

The product ratio in this kinetically controlled reaction will not be proportional to the conformational distribution of the reactants, but is controlled by the difference in standard molar free energies $\delta\Delta G^{0\#}$ of the respective transition states.

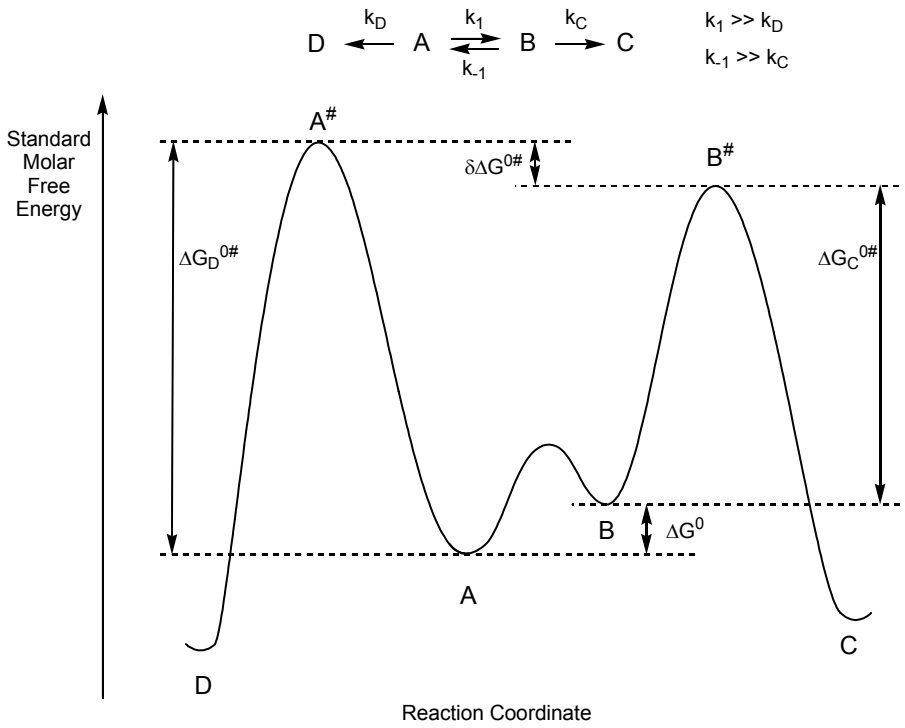

Figure 1. Free-energy profile for the stereospecific formation of products from two rapidly interconverting conformers

The proof can be found e.g. in the book "*The Physical Basis of Organic Chemistry*".[1]

[1] Maskill, H. "*The Physical Basis of Organic Chemistry*", 2nd ed, Oxford University Press Inc., New York **1995**, p 293-300.

--- Paper I ---

Christian V. Stevens,* Nicolai Dieltiens, and Diederica D. Claeys

"Straightforward Ring Expansion of Pyroglutamates to Perhydro-1,3-diazepine-2,4-diones"

Organic Letters **2005**, Vol. 7, 1117-1119

Christian V. Stevens,* Nicolai Dieltiens, and Diederica D. Claeys

"Additions and Corrections"

Organic Letters **2005**, Vol. 7, 5347-5348

ORGANIC LETTERS

2005
Vol. 7, No. 6
1117−1119

Straightforward Ring Expansion of Pyroglutamates to Perhydro-1,3-diazepine-2,4-diones

Christian V. Stevens,* Nicolai Dieltiens, and Diederica D. Claeys

Research group SynBioC, Department of Organic Chemistry, Faculty of Bioscience Engineering, Ghent University, Coupure links 653, B-9000 Gent, Belgium

chris.stevens@ugent.be

Received January 11, 2005

ABSTRACT

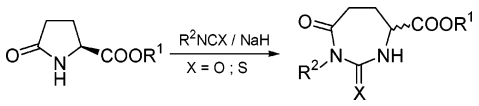

Perhydro-1,3-diazepine-2,4-diones are rare and can only be prepared, up to now, by special methods. A new one-step protocol was developed, comprising N-carbamoylation using an isocyanate followed by intramolecular ring expansion. This new methodology provides a straightforward access to this interesting seven-membered skeleton.

Diazepines are a class of compounds exhibiting a wide range of biological activity. Most common are the 1,4-benzodiazepines which have received much attention since the early 1960s because of their value in psychotherapy (e.g., diazepam, the active compound in Valium, which shows strong CNS depressant properties). Since then, they have been reported to have anxiolytic activity,[1] anticonvulsant activity,[2] and antitumor activity,[3] and later on their herbicidal properties were disclosed.[4] Recently 1,4-diazepine-5-ones were synthesized by the intramolecular transamidation of β-lactams with tethered amines using single-mode microwave irradiation.[5]

The 1,3-diazepines have been studied to a lesser extent although they also show some interesting activities. A seven-membered cyclic urea scaffold, for example, was found to be a potent inhibitor of the HIV-1 protease[6] and a ring-expanded nucleoside containing the 1,3-diazepine moiety, a competitive inhibitor of both adenosine deaminase and guanase.[7] 1,3-Diazepine-2,4-diones **2** (Figure 1), however,

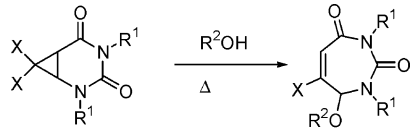

Figure 1. Synthesis of 1,3-diazepine-2,4-diones by ring expansion of halocarbene adducts of uracil derivatives.

are rare[8] and can, up to now, only be prepared by special methods involving photochemical[9] or thermal ring expansion of the halocarbene adducts of 1,3-disubstituted uracil derivatives **1** by heating in the presence of alcohols in a sealed

(1) Wright, W. B.; Brabander, H. J.; Greenblatt, E. N.; Day, I. P.; Hardy, R. A. *J. Med. Chem.* **1978**, *21*, 1087−1089.

(2) De Martino, G.; Massa, S.; Corelli, F. *Eur. J. Med. Chem.-Chim. Ther.* **1983**, *18*, 347−350.

(3) Jones, G. B.; Davey, C. L.; Jenkins, T. C.; Kamal, A.; Kneale, G. G.; Neidle, S.; Webster, G. D.; Thurston, D. E. *Anti-Cancer Drug. Des.* **1990**, *5*, 249−264.

(4) Karp, G. M.; Manfredi, M. C.; Guaciaro, M. A.; Ortlip, C. L.; Marc, P.; Szamosi, I. T. *J. Agric. Food Chem.* **1997**, *45*, 493−500 and references therein.

(5) Vasudevan, A.; Villamil, C. I.; Djuric, S. W. *Org. Lett.* **2004**, *6*, 3361−3364.

(6) Lam, P. Y.; Jadhav, P. K.; Eyermann, C. J.; Hodge, C. N.; Ru, Y.; Bacheler, L. T.; Meek, J. L.; Otto, M. J.; Rayner, M. M.; Wong, Y. N.; Chang, C. H.; Wever, P. C.; Jackson, D. A.; Sharpe, T. R.; Erickson-Vittanen, S. *Science* **1994**, *263*, 380−384.

(7) Wang, L.; Hosmane, R. S. *Bioorg. Med. Chem. Lett.* **2001**, *11*, 2893−2896.

(8) Katritzky, A. R.; Rees, C. W. In *Comprehensive Heterocyclic Chemistry*; Lwowski, W., Ed.; Pergamon Press: Oxford, 1984; Vol. 7, pp 605−608.

(9) Kunida, T.; Witkop, B. *J. Am. Chem. Soc.* **1971**, *93*, 3478−3487.

10.1021/ol050050e CCC: $30.25
Published on Web 02/11/2005

tube.[10] Another known method involves the cyclization, in a low yield, of *N*,*N*′-dichloroglutaric diamides (synthesized from glutaric diamides and Cl_2 gas) with triethylamine.[11]

In the past, 1-carbamoyl-2-pyrrolidinones **3** were incorrectly identified as perhydro-1,3-diazepine-2,4-diones **4** (Figure 2).

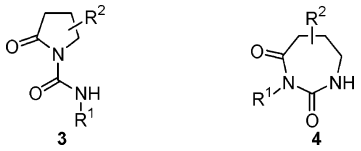

Figure 2. 1-Carbamoyl-2-pyrrolidinones **3** and perhydro-1,3-diazepine-2,4-diones **4**.

For example, the natural product squamolone was originally identified as a seven-membered ring (of type **4**) but later turned out to be a five-membered ring (of type **3**).[12] Also a claim of the preparation of these seven-membered rings by cyclization of 4-ureidobutyric acids with thionyl chloride[13] was later corrected by another research group.[14]

During our research on pyroglutamates for the development of agrochemicals and pharmaceutically interesting azaheterocyclic skeletons,[15] we found that when the sodium salt of an alkylpyroglutamate **5** is treated with 1 equiv of an isocyanate, reaction occurs both on the N-atom and on the C2-atom resulting in a complex mixture of different compounds. However, when a mixture of **5** with an isocyanate is treated with NaH in diethyl ether, a precipitate is formed during the reaction, which after workup proved to be the sodium salt of the expected carbamoyllactam **6** in high purity (Scheme 1). If the reaction is performed in THF on the other

Scheme 1. Synthesis of Perhydro-1,3-diazepine-2,4-diones by Intramolecular Ring Expansion of Pyroglutamates

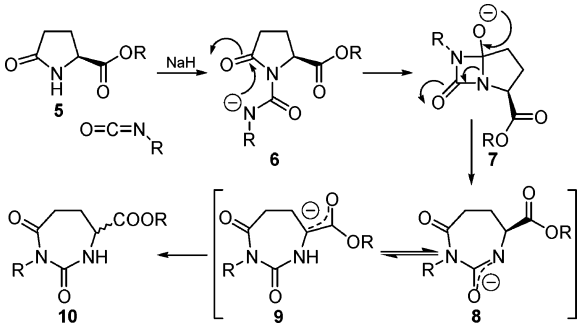

hand, no precipitate is formed and after workup a compound was isolated which gave a different but very similar ^{1}H NMR

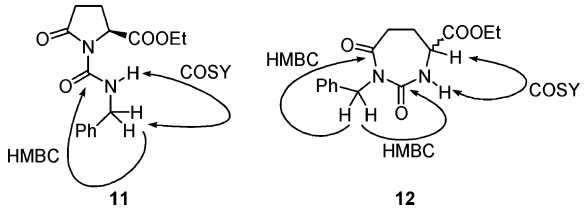

Figure 3. Most important COSY and HMBC couplings of **11** and **12**.

spectrum. It was assumed that intermediate **6**, which is apparently soluble in THF, reacts intramolecularly by a nucleophilic attack on the lactam ring with formation of the unstable intermediate **7**. This intermediate decomposes with loss of ring strain to form the seven-membered ring anions **8** and **9**. These anions are in equilibrium with each other, causing racemization of the chiral center (this was proven

Table 1. Synthesis of Perhydro-1,3-diazepine-2,4-diones by a One-Step Carbamoylation−Ring Expansion Sequence

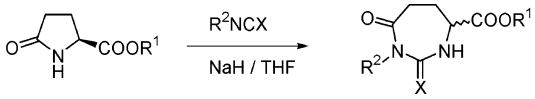

	R^1	isocyanate	product	yield (%)[a]
1	Bn	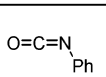	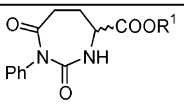	56
2	Bn	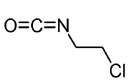	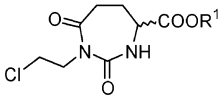	93
3	Bn	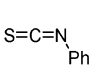	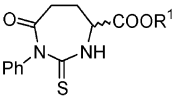	42
4	Et	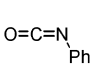	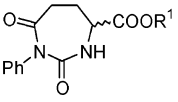	89
5	Et	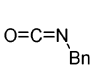	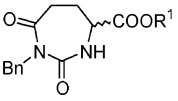	87
6	Et	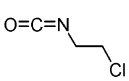	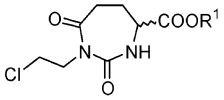	81
7	Et	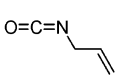	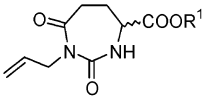	48
8	Me	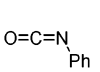	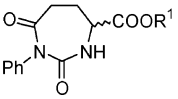	81

[a] Isolated yield after flash chromatography or recrystallization.

(10) Thiellier, H. P. M.; Koomen, G. J.; Pandit, U. K. *Tetrahedron* **1977**, *33*, 2603−2607.
(11) Brandner, A. *Synthesis* **1982**, *11*, 973−974.
(12) Marquez, V. E.; Kelley, J. A.; Driscoll, J. S. *J. Org. Chem.* **1980**, *45*, 5308−5312.

by quenching the reaction with D_2O) and upon workup resulted in **10** as a 1:1 mixture of its enantiomers. In contrast, the isolated carbamoyllactams **6** are still optically active.

Since we now had both the five-membered ring **6** and what we believed to be **10** in hands, it was easy to compare all the spectral data. Although both ^1H NMR and ^{13}C-spectra clearly showed they were two different compounds, no conclusions could be made judging these spectra alone. The decisive proof was given by comparing both COSY- and HMBC-coupled spectra (Figure 3).

In the case of **11**, there is a coupling in the COSY spectrum between the proton on the N-atom and the two protons of the benzyl group, the proton on nitrogen appears as an incompletely resolved triplet. In the case of **12**, however, the proton on the N-atom couples with the proton next to the ester function and not with the protons of the benzyl group, proving that the benzyl group is attached to a tertiary nitrogen. Furthermore, in the HMBC spectrum, the protons of the benzyl group of **11** only couple to the urea carbonyl (easily distinguishable from both other carbonyl groups) whereas in the case of **12** they couple to both the urea and the lactam carbonyl.

Since it is was established that the perhydro-1,3-diazepine-2,4-dione was synthesized, the same methodology was performed on other combinations of pyroglutamate esters and isocyanates (Table 1).

We were pleased to find that different esters underwent the reaction, although in some cases, traces of carbamoyllactam could be observed due to the poor solubility of this intermediate in THF. This is probably the reason the benzyl ester formed a perhydro 4-oxo-2-thioxo-1,3-diazepine with phenyl isothiocyanate (entry 3) whereas the ethyl ester only gave the five-membered ring.[16]

In conclusion, a new and very straightforward one-step approach was developed toward these interesting perhydro-1,3-diazepine-2,4-diones. Since the pyroglutamate skeleton can easily be functionalized on different positions with control of the stereochemistry,[17] this new approach offers the possibility of efficiently synthesizing a collection of highly functionalized small molecules which is important for diversity-oriented synthesis, a concept that has recently gained importance.[18] Further research will be reported in due course.

Acknowledgment. Financial support for this research from the Bijzonder Onderzoeksfonds (Research Fund, Ghent University) is gratefully acknowledged.

Supporting Information Available: All carbon spectra of the new compounds synthesized and their complete characterization. This material is available free of charge via the Internet at http://pubs.acs.org.

OL050050E

(13) Guillon, J.; Sonnet, P.; Boulouard, M.; Dallemagne, P.; Miel, H.; Daoust, M.; Rault, S. *J. Heterocycl. Chem.* **1998**, *35*, 535−539.

(14) Heckendorn, R.; Winkler, T. *J. Heterocycl. Chem.* **2000**, *37*, 111−114.

(15) Stevens, C. V.; Rammeloo, T.; De Kimpe, N. *Synlett* **2001**, 1519−1522.

(16) **Typical Experimental Procedure for Synthesis of Perhydro-1,3-diazepine-2,4-diones.** The pyroglutamate ester (3 mmol) was dissolved into THF (30 mL, freshly distilled from Na metal). To this solution was added the isocyanate (3.3 mmol) followed by NaH (3.3 mmol, washed with hexanes). The reaction was allowed to stir under nitrogen atmosphere at room temperature for 16 h. The reaction was quenched by addition of saturated aqueous NH_4Cl until the pH was neutral. The mixture was extracted with EtOAc, and the organics were dried ($MgSO_4$) and filtered. The solvent was removed in vacuo, and the residue was purified by flash chromatography (silica gel; hexane/EtOAc).

(17) Najera, C.; Yus, M. *Tetrahedron: Asymmetry* **1999**, *10*, 2245−2303.

(18) Schreiber, S. L. *Science* **2000**, *287*, 1964−1969.

ORGANIC LETTERS

2005
Vol. 7, No. 23
5347−5348

Additions and Corrections

Volume 7, 2005

Christian V. Stevens,* Nicolai Dieltiens, and Diederica D. Claeys

Straightforward Ring Expansion of Pyroglutamates to Perhydro-1,3-diazepine-2,4-diones.

Page 1117. The incorrect product was reported in this paper. X-ray analysis after publication shows that the products are not perhydro-1,3-diazepine-2,4-diones, but are hydantoins which were formed by a ring-closing−ring-opening sequence and which have almost identical NMR spectra. A paper is in preparation stating this misinterpretation and proving the structure of the hydantoins by X-ray analysis.

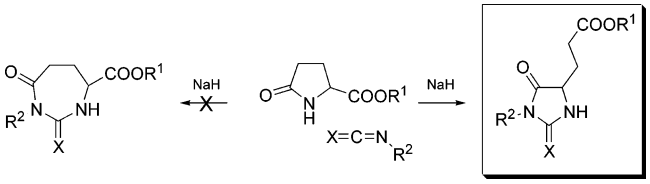

OL052428E

10.1021/ol052428e
Published on Web 10/14/2005

Volume 7, 2005

Amit K. Mandal, John S. Schneekloth, Jr., and Craig M. Crews*

Stereoselective Assembly of a 1,3-Diene via Coupling between an Allenic Acetate and a (*B*)-Alkylborane: Synthetic Studies on Amphidinolide B1.

Page 3646. In Scheme 2, the positioning of TBSO is incorrect for compound **10** and fragment **2**. The correct version of Scheme 2 is below:

Scheme 2. Retrosynthetic Analysis

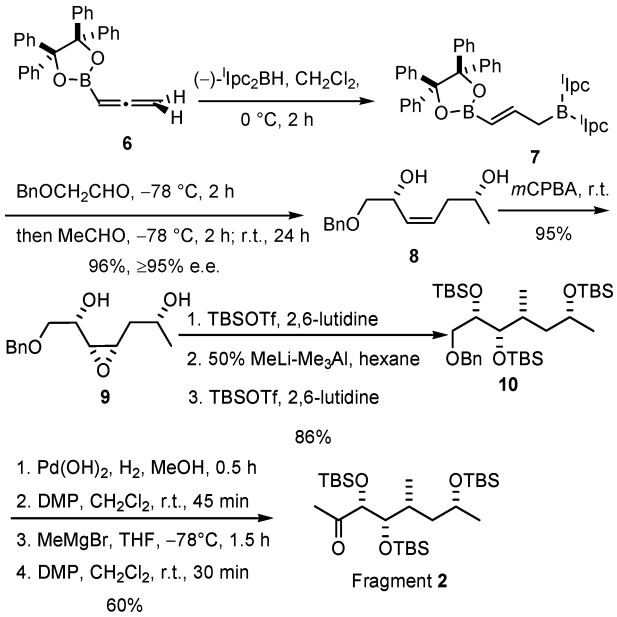

OL052513M

10.1021/ol052513m
Published on Web 10/21/2005

--- Paper II ---

Kurt G. R. Masschelein, Christian V. Stevens,* Nicolai Dieltiens
and Diederica D. Claeys

"Exploiting the regioselectivity of pyroglutamate alkylations
for the synthesis of 6-azabicyclo[3.2.1]octanes and
4-azabicyclo[3.3.0]octanes"

Tetrahedron **2007**, Vol. 63, 4712–4724

Available online at www.sciencedirect.com
ScienceDirect
Tetrahedron
Tetrahedron 63 (2007) 4712–4724

Exploiting the regioselectivity of pyroglutamate alkylations for the synthesis of 6-azabicyclo[3.2.1]octanes and 4-azabicyclo[3.3.0]octanes

Kurt G. R. Masschelein, Christian V. Stevens,* Nicolai Dieltiens and Diederica D. Claeys†

Research Group SynBioC, Department of Organic Chemistry, Faculty of Bioscience Engineering, Ghent University, Coupure Links 653, B-9000 Ghent, Belgium

Received 25 January 2007; revised 14 March 2007; accepted 15 March 2007
Available online 18 March 2007

Abstract—Depending on the *N*-protecting group of pyroglutamates, the reactivity can be directed to the formation of 6-azabicyclo[3.2.1]-octanes or 4-azabicyclo[3.3.0]octanes, which are conformationally restricted glutamate analogues.

1. Introduction

Azabicyclic systems have been extensively used in recent years as key structural components of various pharmaceutical agents. Consequently, flexible methods for the construction of different azabicycles are of considerable interest.

Among the wide variety of alkaloids, both the 6-azabicyclo[3.2.1]octanes **1** and 4-azabicyclo[3.3.0]octanes **2** have received a lot of attention synthetically (Fig. 1).

Prominent among the early synthetic methods for the preparation of 6-azabicyclo[3.2.1]octane derivatives **1** are the Hofmann–Löffler–Freytag reaction of monocyclic *N*-chloro amines[1] and the reductive cyclisation of aminobenzoic acids or benzamides.[2] More recently, several highly efficient strategies based on rearrangements,[3] cycloadditions[4] and multicomponent couplings have been reported.[5]

The formation of the pyrrolizidine framework **2** generally takes place by cyclisation of a conveniently substituted pyrrolidine moiety. Several types of processes have been reviewed, such as radical and ionic cyclisations.[6] Other procedures such as Claisen-like intramolecular acylation involving α-pyrrolidinyl sulfones,[7] ring-closing metathesis of disubstituted ethenyl pyrrolidines,[8] or intramolecular titanium-mediated coupling reactions of α-substituted succinimides[9] have been described. Other processes include the cis allylation of a chiral lactam skeleton derived from D-malic acid,[10] cyclisations of *N*-propargylaminyl radicals[11] and cycloaddition processes including tandem inter[4+2]/inter[3+2]-additions,[12] hetero Diels–Alder reactions,[13] [2+2]-cycloadditions[14] and 1,3-dipolar cycloadditions.[15] Recently, some other processes for the synthesis of the pyrrolizidine skeleton were described in the literature.[16]

1 2

Figure 1.

During our research on azabicyclic compounds, pyroglutamates were selected for the construction of conformationally restricted molecules. Over the years, pyroglutamates have received a lot of attention because of their importance in several domains and as a versatile starting material for the synthesis of both natural and unnatural products.[17] Intensive study on glutamate analogues resulted in specific inhibitors of different receptor types of the mammalian central nervous system.[18] It has also been used for the synthesis of pyrrolidine alkaloids,[19] kainoids,[20] (−)-bulgecinine,[21] (−)-domoic acid,[22] enantiomerically pure glycine and proline derivatives,[23] a wide variety of non-proteinogenic amino acids,[24] etc. The attractiveness of pyroglutamate as a building block is connected to the fact that the site of alkylation can be directed by changing the protecting group on nitrogen. Alkylation of *N*-Boc protected pyroglutamates results in C-4 functionalised derivatives, whereas alkylation of *N*-benzyl or *N*-unprotected pyroglutamates occurs at the 2-position.[25]

* Corresponding author. Tel.: +32 (0)9 2645957; fax: +32 (0)9 2646243; e-mail: chris.stevens@ugent.be
† Diederica D. Claeys is aspirant of the FWO-Vlaanderen.

0040–4020/$ - see front matter © 2007 Elsevier Ltd. All rights reserved.
doi:10.1016/j.tet.2007.03.084

2. Results

2.1. Synthesis of the 6-azabicyclo[3.2.1]octane skeleton by ring closure from C-4 to C-2

Recently we observed that *N*-Boc protected pyroglutamates, substituted at the C-4 position with no or poor electrophilic moieties, undergo a Boc migration.[26] This reaction prevented the synthesis of bicyclic skeletons by alkylation at C-4 followed by ring closure to C-2. Since the Boc migration is competitive with ring closure from C-4 to C-2, a better electrophilic moiety, 3-chloro-2-chloromethyl-1-propene, was introduced at C-4. In this case only ring closure was observed leading to compound **4** in good yield and comprising a new skeleton (Scheme 1).

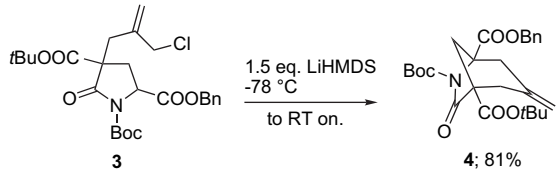

Scheme 1.

2.2. Synthesis of the 6-azabicyclo[3.2.1]octane skeleton by ring closure from C-2 to C-4

The competing Boc migration prompted us to change the site of ring closure. If an unprotected pyroglutamate is properly functionalised at the C-2 position, subsequent protection with a Boc group (activation of C-4) and treatment with base could also lead to the 6-azabicyclo[3.2.1]octane skeleton.

As we have recently shown, treating a mixture of a pyroglutamate and an electrophile with 2.1 equiv of LiHMDS at −40 °C in THF results in C-2 functionalisation without any reaction on the N-atom.[27] Again, we chose 3-chloro-2-chloromethyl-1-propene as electrophile since the allylic positions increase its electrophilic properties and would thus facilitate both alkylation and ring closure. In order to prevent reaction at the N-atom and accompanying cyclisation to a pyrrolizidinone structure, it is crucial to limit the reaction time to 1 h at −40 °C and 2 h at room temperature. If the reaction was stirred overnight, about 25% of the compound had already cyclised.

In order to activate the C-4 position, compounds **5** were protected with a Boc group under standard conditions using Boc-anhydride and DMAP as a catalyst in acetonitrile at 0 °C. Unfortunately, treating derivatives **6** with 1.1 equiv of LiHMDS at −78 °C did not result in the desired cyclisation to **7**. Only unreacted starting material could be recovered. This lack of reactivity could result from the ability of the Li cation to form a six-membered ring counter-ion complex **8** (Li complex) giving additional stability to the C-4 anion, effectively preventing it from reacting further (Scheme 2).[28] If this extra stabilisation indeed prevents the formation of bicyclic compound **7**, changing to KHMDS as a base should circumvent this problem since the bigger potassium cation does not fit as well in the six-membered ring conformation as the Li cation. Indeed we observed that treating **6** with 1.1 equiv of KHMDS at −78 °C for 2 h resulted in complete conversion to the desired compounds **7**.

Further functionalisation of compound **7b** was performed by treating it with ozone in CH_2Cl_2/MeOH (95/5) at −78 °C and subsequent work-up with Me_2S leading to compound **9** in 60% yield after purification, a new type of constrained glutamic acid analogue (Scheme 3).

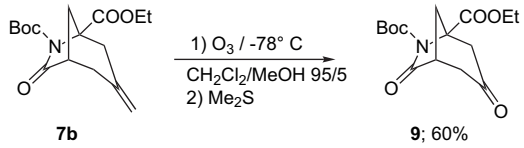

Scheme 3.

2.3. A one-pot synthesis of the 6-azabicyclo[3.2.1]octane skeleton

Because the abovementioned synthetic strategies involve several steps to get to the 6-azabicyclo[3.2.1]octane skeleton, a one-pot strategy for its synthesis was studied. Therefore, *N*-benzyl protected pyroglutamates **10** were treated with 2.1 equiv of LiHMDS and 1.1 equiv of 3-chloro-2-chloromethyl-1-propene. The first equivalent of LiHMDS

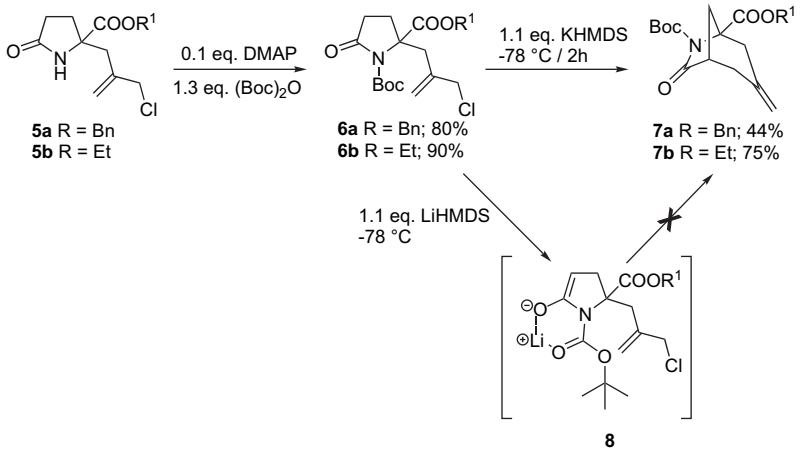

Scheme 2.

deprotonates the C-2 position, which reacts with the electrophile. The second equivalent of LiHMDS then deprotonates at C-4 leading to ring closure. After purification, the 6-azabicyclo[3.2.1]octane **11** was indeed isolated, although in rather poor yields (Scheme 4).

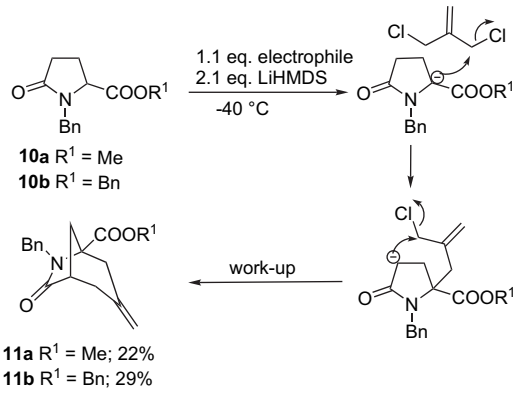

Scheme 4.

In the same way, the 7-azabicyclo[4.2.1]nonane skeleton could be synthesised with 2,3-bis(iodomethyl)-1,3-butadiene **12**[29] as electrophile (Scheme 5). Although the yields of this one-pot strategy were quite poor, a seven-membered ring, which is normally not easily formed, could be obtained.

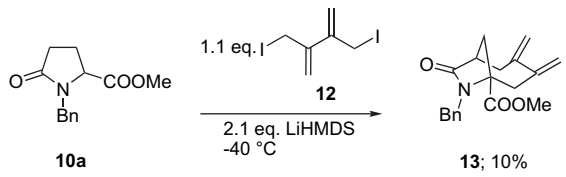

Scheme 5.

Till now, the 7-azabicyclo[4.2.1]nonane skeleton was mainly used in the synthesis of some *Gelsemium* alkaloids, such as gelsemine, gelsedine and gelsemicine. Several synthetic strategies have been published to construct these pharmaceutically interesting products.[30]

2.4. Pyroglutamides: another regioselectivity

Although the one-pot strategy for the 6-azabicyclo[3.2.1]-octane and 7-azabicyclo[4.2.1]nonane skeleton was successful, the yields after purification were rather low. During earlier research at our laboratory, we observed that formation of an anion at C-2 resulted in fragmentation of the pyroglutamate.[26] This was confirmed by the detection of benzyl alcohol when using benzyl pyroglutamate as starting material. Therefore, the corresponding pyroglutamides **15** were synthesised since it was expected that these compounds would fragment less easily (Scheme 6).

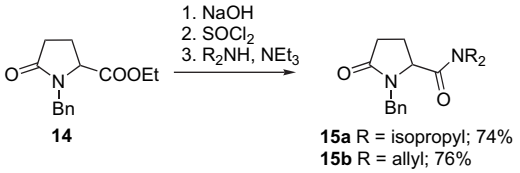

Scheme 6.

Using the pyroglutamides **15** in the same one-pot strategy as mentioned above for the corresponding pyroglutamates, a different regioselectivity was observed. Instead of the formation of the 6-azabicyclo[3.2.1]octane skeleton, double alkylation at C-4 was observed (Scheme 7).

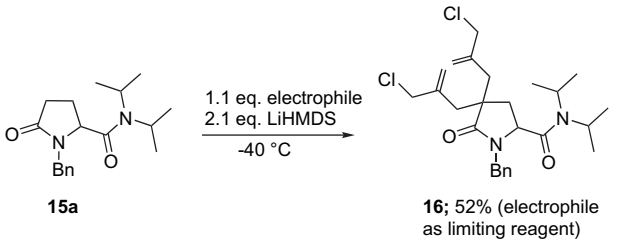

Scheme 7.

Apparently, the most acidic (and the least sterically hindered) protons of *N*-benzyl pyroglutamides are located at the 4-position. With this in mind, treatment of **15b** with 3 equiv of base and 2 equiv of electrophile could lead to the 1-substituted 6-azabicyclo[3.2.1]octane skeleton **18** (Scheme 8). This reaction was indeed successful; although a conversion of 56% was observed, only a 25% yield was obtained after chromatography.

The substitution pattern at the 1-position of the 6-azabicyclo[3.2.1]octane skeleton could be varied by a preceding alkylation at the 4-position of the *N*-benzyl pyroglutamides with subsequent ring closure. To mention one example, **15a** was substituted at the 4-position with a benzyl group after alkylation with benzylbromide. When treating the purified product **19** with 3-chloro-2-chloromethyl-1-propene as electrophile and LiHMDS as base, compound **21** was isolated, besides **19** and **20** (Scheme 9). Apparently, the alkylation and ring closure appears to be slow. The disappointing yield after purification discouraged further efforts in this direction.

2.5. Synthesis of the 4-azabicyclo[3.3.0]octane skeleton by ring closure from C-2 to N

The synthesis of the 4-azabicyclo[3.3.0]octane skeletons **22a** and **22b** was performed by treating **5a** and **5b** (no Boc protection) with 1.5 equiv of NaH in refluxing THF for 16 h and subsequent bulb-to-bulb distillation (Scheme 10).

The pyrrolizidinone **22b** was easily converted to the amino alcohol **23**, a member of an interesting class of compounds,[31] in 70% yield by treatment with $LiAlH_4$ in refluxing THF and subsequent bulb-to-bulb distillation. Compound **22b** was also converted to pyrrolizidinedione **24** by ozonisation followed by work-up with Me_2S (Scheme 11).

Besides pyrrolizidinones, we were also able to construct an indolizidine skeleton applying the same methodology. Treating a mixture of pyroglutamate **25** and *cis*-1,4-dichloro-2-butene with 2.1 equiv of LiHMDS in THF at −40 °C resulted in a mixture, which consists of compounds **26** and **27** in a 1/3 ratio (Scheme 12). Treatment of this mixture with 1 equiv of NaH in refluxing THF resulted in complete cyclisation of **26**. Indolizidine **27** was obtained in 24% yield

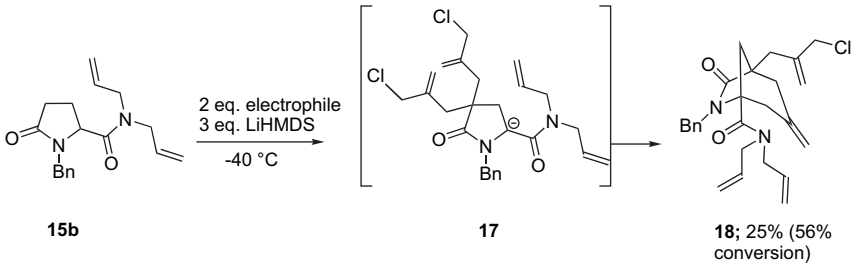

Scheme 8.

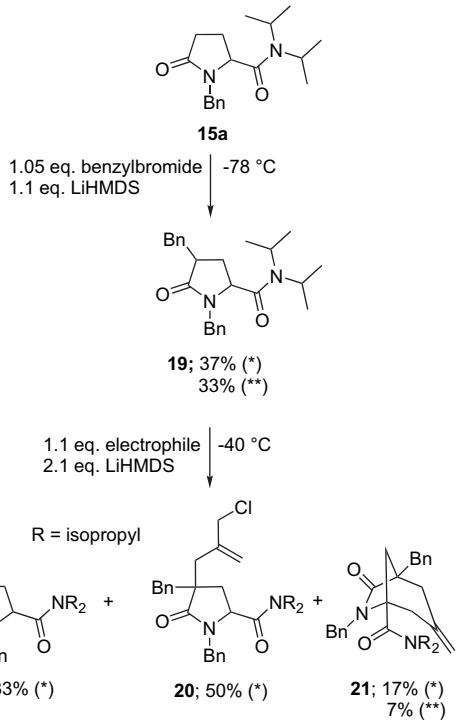

Scheme 9. (*) Observed in ^{1}H NMR of crude mixture; (**) after purification.

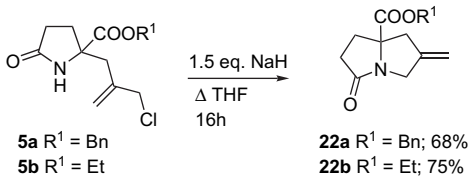

Scheme 10.

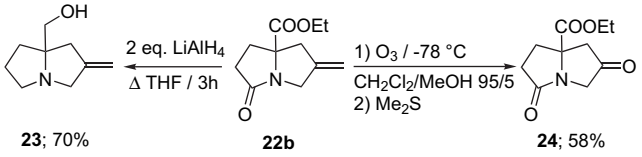

Scheme 11.

after purification by column chromatography. The low yield of this procedure can be explained by a severe loss of material during purification.

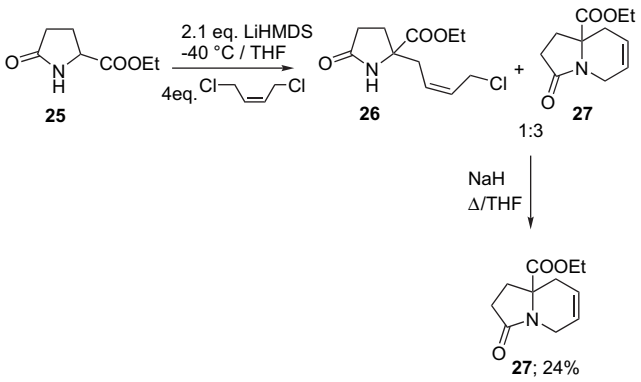

Scheme 12.

2.6. Evaluation of chiral induction during alkylation

Having this new entry to interesting azabicyclic molecules in hand, the possibility of chiral induction during alkylation was evaluated. Moeller and Rutledge have described an electrochemical method for the enantioselective alkylation of the (+)-menthyl ester of pyroglutamic acid.[32] The ester of (*S*)-pyroglutamic acid and (−)-menthol or (+)-fenchol was prepared using DCC as a coupling agent and DMAP as a catalyst (Scheme 13).

Unfortunately, treatment of **29a** with 2.1 equiv of LiHMDS at −40 °C resulted in complete fragmentation of the ester. Only menthol could be identified in the organic fraction. Treatment of a mixture of **29b** and 3-chloro-2-chloromethyl-1-propene with 2.1 equiv of LiHMDS resulted in a mixture of **30** and **31** in a 3/2 ratio. This mixture was quantitatively converted to pyrrolizidinone **31** upon treatment with NaH in refluxing THF. To our disappointment, **31** was obtained as a mixture of both diastereoisomers with a diastereomeric excess of only 12% (after chromatography and crystallisation). In the crude reaction mixture no diastereomeric excess was observed, showing that the chiral fenchol group has no effect on the diastereoselectivity of the alkylation (Scheme 14).

In conclusion, we have shown that both the 6-azabicyclo[3.2.1]octane and 4-azabicyclo[3.3.0]octane skeletons are accessible from the same precursor depending on the protecting group on the N-atom. Although this approach is straightforward and interesting, the difficulty in purification of the products, reducing the yields considerably, stays problematic. The advantage, however, is the limited number of steps needed to construct these interesting skeletons starting from a readily available precursor.

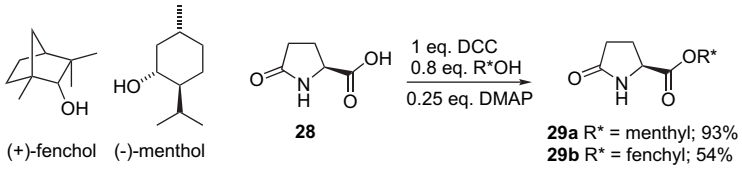

Scheme 13.

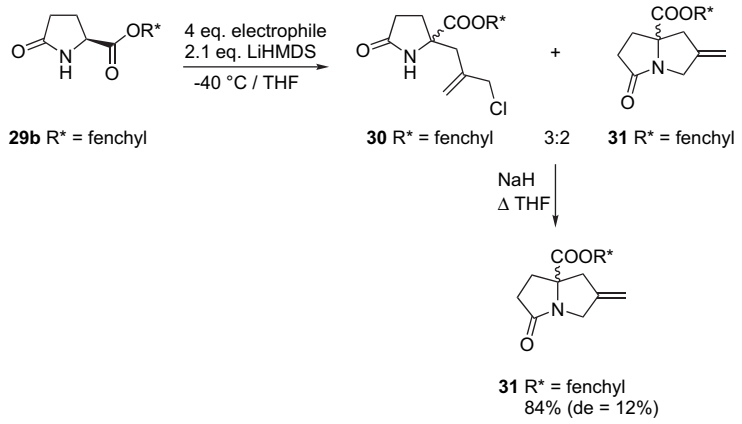

Scheme 14.

3. Experimental

3.1. General

High-resolution ^{1}H NMR (270 MHz or 300 MHz) and ^{13}C NMR (68 MHz or 75 MHz) spectra were run with a Jeol JNM-EX 270 NMR spectrometer or on a Jeol JNM-EX 300 NMR spectrometer. Peak assignments were obtained with the aid of DEPT, 2D-HETCOR, 2D-HSQC and 2D-COSY spectra. The compounds were diluted in deuterated solvents and the used solvent is indicated for each compound. Mass spectra were recorded on a Varian MAT 112 spectrometer (70 eV), using either GC–MS coupling or a direct inlet system. Some volatile samples were recorded on an HP 6890 GC coupled with a HP 5973 MSD (Mass selective detector; quadrupole). Mass spectra of molecules with a high molecular weight were recorded on an Agilent 1100 Series VS (ES, 4000 V) mass spectrometer. The elemental analysis was performed with a Perkin–Elmer 2400 Elemental Analyser. High-resolution mass spectra were recorded on a Finnigan MAT 95 XP-API-GC-Trap tandem Mass spectrometer system (ES, 5000 V). IR-spectra were obtained from a Perkin–Elmer Spectrum One infrared spectrometer. For liquid samples the spectra were collected by preparing a thin film of compound between two sodium chloride plates. The crystalline compounds were mixed with potassium bromide and pressed until a transparent potassium bromide plate was obtained. Melting points of crystalline compounds were measured with a Büchi 540 apparatus and are uncorrected. The purification of reaction mixtures was performed by chromatography using a glass column with silica gel (Across, particle size: 0.035–0.070 mm, pore diameter: ca. 6 nm).

3.2. Typical experimental procedure for the alkylation of pyroglutamates at the C-4 position with di-*tert*-butyldicarbonate and an alkyl halide

A Boc-protected pyroglutamate ester (7.8 mmol) is dissolved in THF (30 mL, freshly distilled from Na metal) and cooled in an acetone bath to −78 °C. At this temperature and under a nitrogen atmosphere, 15.6 mL (15.6 mmol, 2 equiv) of a 1 M LiHMDS solution is added while stirring is continued at this temperature. After 2 h, 11.7 mmol of di-*tert*-butyldicarbonate (1.5 equiv) is added (dissolved in 10 mL of THF) and the reaction mixture is allowed to warm to room temperature. The reaction is quenched with 5 mL of saturated NH_4Cl/NH_4OH solution and 40 mL of water is added. The mixture is extracted with diethyl ether and dried with $MgSO_4$. After filtration and evaporation of the solvent the crude product is purified by means of chromatography.

The purified 4-substituted *N*-Boc pyroglutamate (2.3 mmol) is dissolved in 10 mL of dry THF and kept under a positive N_2-pressure. KO^{t}Bu (2.5 mmol, 1.1 equiv) is added and the mixture is stirred for 30 min when 4.6 mmol of electrophile (2 equiv) is added. The reaction mixture is subsequently refluxed overnight. After cooling, the solution is poured in water and extracted with diethyl ether. The organic layers are combined and dried with $MgSO_4$. Filtering off the drying agent and evaporating the solvent lead to a mixture, which is purified by chromatography to remove the excess of electrophile.

3.2.1. Synthesis of 2-benzyl 1,4-di-*tert*-butyl-4-[2-(chloromethyl)-2-propenyl]-5-oxo-1,2,4-pyrrolidinetricarboxylate (3). The product was obtained as an oil (yield: 60%).

^{1}H NMR (270 MHz, $CDCl_3$) δ: Major: 1.41 (9H, s, *t*-Bu), 1.43 (9H, s, *t*-Bu), 2.32 (1H, dd, J=13.6, 10.2 Hz, CH_AH$_B$ ring), 2.52 (1H, d, J=15.5 Hz, CH_AH$_B$C=CH$_2$), 2.93 (1H, dd, J=13.6, 2.0 Hz, CH$_A$$H_B$ ring), 3.09 (1H, d, J=15.5 Hz, CH$_A$$H_B$C=CH$_2$), 3.92 (2H, s, CH$_2$Cl), 4.61 (1H, dd, J=10.2, 2.0 Hz, CH ring), 5.01 (1H, br s, C=CH_AH$_B$), 5.13 (1H, d, J=12.2 Hz, CH_AH$_B$Ph), 5.19 (1H, br s, C=CH$_A$$H_B$), 5.24 (1H, d, J=12.5 Hz, CH$_A$$H_B$Ph), 7.36 (5H, s, Ph). Minor: 1.41 (9H, s, *t*-Bu), 1.44 (9H, s, *t*-Bu), 1.96 (1H, dd, J=13.8, 6.9 Hz, CH_AH$_B$ ring), 2.60 (1H, d, J=16.0 Hz, CH_AH$_B$C=CH$_2$), 2.88 (1H, dd, J=13.8, 8.9 Hz, CH$_A$$H_B$ ring), 3.01 (1H, d, J=16 Hz, CH$_A$$H_B$C=CH$_2$), 3.99 (2H, s, CH$_2$Cl), 4.64 (1H, dd, J=8.9, 6.9 Hz, CH ring), 4.86 (1H, br s, C=CH_AH$_B$), 5.20 (1H, d, J=13.2 Hz, CH_AH$_B$Ph), 5.24 (1H, d, J=13.2 Hz, CH$_A$$H_B$Ph), 5.28 (1H, br s, C=CH$_A$$H_B$), 7.36 (5H, s, Ph). ^{13}C NMR (68 MHz, $CDCl_3$) δ: Major 28.21 (*t*-Bu), 28.32 (*t*-Bu), 31.61 (CH$_2$ ring), 39.43 (CH$_2$), 48.88 (CH$_2$Cl), 56.91 (CH, C-2), 57.22 (C$_{quat}$, C-4), 67.98 (*C*H$_2$Ph), 83.88 (C$_{quat}$, *t*-Bu), 84.37 (C$_{quat}$, *t*-Bu), 119.35 (C=CH$_2$), 129.04 (CH), 129.15 (CH), 135.72 (C$_{quat}$, Ph), 140.93 (C=CH$_2$), 149.60 (C=O, Boc), 168.09 (C=O), 170.49 (C=O), 170.73 (C=O), 171.54 (C=O). Minor: 28.25 (*t*-Bu), 28.47 (*t*-Bu), 30.39 (CH$_2$ ring), 37.38 (CH$_2$), 48.99 (CH$_2$Cl), 57.22 (CH), 57.45 (C$_{quat}$, C-4), 67.98 (*C*H$_2$Ph), 83.99 (C$_{quat}$, *t*-Bu), 84.71 (C$_{quat}$, *t*-Bu), 119.01 (C=CH$_2$), 129.18 (CH), 129.25 (CH), 135.47 (C$_{quat}$, Ph), 140.93 (C=CH$_2$), 149.60 (C=O, Boc), 168.89 (C=O), 170.73 (C=O), 170.93 (C=O), 171.54 (C=O). IR (cm^{-1}) ν_{max}: 1795, 1725. MS *m*/*z* (%): (ES, Pos) no M$^+$, 354 (30), 352 (85), 91 (100). Chromatography: Hex/EtOAc (64/36). $C_{26}H_{34}ClNO_7$: calcd C 61.47, H 6.75, N 2.76; found C 61.59, H 6.89, N 2.59.

3.3. Synthesis of 5-benzyl 1,6-di-*tert*-butyl-3-methylene-7-oxo-6-azabicyclo[3.2.1]octane-1,5,6-tricarboxylate (4)

2-Benzyl-1,4-di-*tert*-butyl-4-[2-(chloromethyl)-2-propenyl]-5-oxo-1,2,4-pyrrolidinetricarboxylate **3** of 0.28 g (0.55 mmol) was dissolved in 4 mL of dry THF and kept under a positive N_2-pressure during the reaction. The mixture was cooled to −78 °C and 0.66 mL of a LiHMDS solution (0.66 mmol, 1 M solution in hexanes, 1.2 equiv) was added and the solution was slowly allowed to warm up to room temperature overnight keeping the flask in the acetone bath. After quenching the reaction with NH_4Cl/NH_4OH solution, an extra amount of 10 mL of water was added and the reaction mixture was extracted with diethyl ether (3×40 mL). The organic phases were combined and dried with $MgSO_4$. Filtering off the $MgSO_4$ and evaporating the solvent gave the crude product as an oil and was further purified by column chromatography. 5-Benzyl-1,6-di-*tert*-butyl-3-methylene-7-oxo-6-azabicyclo[3.2.1]-octane-1,5,6-tricarboxylate **4** of 0.21 g was obtained as an oil (yield: 81%).

^{1}H NMR (270 MHz, $CDCl_3$) δ: 1.42 (9H, s, *t*-Bu), 1.48 (9H, s, *t*-Bu), 1.96 (1H, d, J=11.2 Hz, CH_AH$_B$), 2.45 (1H, d, J=13.9 Hz, CH_CH$_D$), 2.65 (1H, dd, J=14.4, 1.0 Hz, CH_EH$_F$), 2.79 (1H, d, J=11.2 Hz, CH$_A$$H_B$), 2.87 (1H, d, J=13.9 Hz, CH$_C$$H_D$), 3.04 (1H, d, J=14.4 Hz, CH$_E$$H_F$), 4.94 (1H, br s, C=C$H_AH_B$), 5.00 (1H, br s, C=CH$_A$$H_B$), 5.19 (1H, d, J=12.2 Hz, CH_AH$_B$Ph), 5.24 (1H, d, J=12.2 Hz, CH$_A$$H_B$Ph), 7.35 (5H, br s, Ph). ^{13}C NMR (68 MHz, $CDCl_3$) δ: 27.78 (*t*-Bu), 27.89 (*t*-Bu), 37.48 (CH$_2$), 38.10 (CH$_2$), 41.10 (CH$_2$), 56.24 (C$_{quat}$, C-4), 64.71 (C$_{quat}$, C-2), 67.40 (*C*H$_2$Ph), 82.68 (C$_{quat}$, *t*-Bu), 83.95 (C$_{quat}$, *t*-Bu), 117.30 (C=CH$_2$), 128.28 (CH), 128.50 (CH), 128.61 (CH), 135.00 (C$_{quat}$, Ph), 138.36 (C=CH$_2$), 148.80 (C=O, Boc), 167.54 (C=O), 169.86 (C=O), 170.10 (C=O), 177.59 (C=O). IR (cm^{-1}) ν_{max}: 1795, 1728. MS *m*/*z* (%): (ES, Pos) no M$^+$, 316 (M$^+$−COO^{t}Bu, 100), 91 (15). Chromatography: Hex/EtOAc (90/10) R_f=0.31. $C_{26}H_{33}NO_7$: calcd C 66.22, H 7.05, N 2.97; found C 66.17, H 6.87, N 3.11.

3.4. Typical experimental procedure for the alkylation of pyroglutamates at the 2-position

A Boc-protected pyroglutamate ester (12 mmol) is dissolved in THF (15 mL, freshly distilled from Na metal) and the alkyl halide (48 mmol, 4 equiv) is added. The mixture is cooled to −40 °C under a N_2 atmosphere. Over a period of 30–40 min, 25.2 mL of a LiHMDS solution (25.2 mmol, 1 M solution in hexanes, 2.1 equiv) is added at this temperature. The reaction mixture is allowed to stir at room temperature for an additional 2 h. The reaction is quenched by addition of saturated aqueous NH_4Cl until the pH is neutral. The mixture is extracted with EtOAc, and the organic fractions are dried ($MgSO_4$) and filtered. The solvent is removed under reduced pressure.

3.4.1. Synthesis of benzyl 2-(2-chloromethyl-2-propenyl)-5-oxopyrrolidine-2-carboxylate (5a). Recrystallised from hexanes. White crystals (yield: 40%).

^{1}H NMR (270 MHz, $CDCl_3$) δ: 2.17–2.24 (1H, m, CH_AH$_B$ ring, C-3), 2.37–2.50 (3H, m, CH$_A$$H_B$ ring, C-3+CH$_2$ ring, C-4), 2.57 (1H, d, J=14.5 Hz, CH_AH$_B$C=CH$_2$), 2.96 (1H, d, J=14.5 Hz, CH$_A$$H_B$C=CH$_2$), 3.96 (2H, s, CH$_2$Cl), 5.02 (1H, s, C=C$H_AH_B$), 5.20 (1H, d, J=12.0 Hz, CH_AH$_B$Ph), 5.23 (1H, d, J=12.0 Hz, CH$_A$$H_B$Ph), 5.30 (1H, s, C=CH$_A$$H_B$), 7.40 (5H, s, Ph). ^{13}C NMR (68 MHz, $CDCl_3$) δ: 29.61 (CH$_2$ ring, C-3), 31.25 (CH$_2$ ring, C-4), 41.71 (*C*H$_2$C=CH$_2$), 48.37 (CH$_2$Cl), 65.14 (C$_{quat}$, C-2), 67.65 (COO*C*H$_2$Ph), 120.09 (C=*C*H$_2$), 128.52 (CH, Ph), 128.68 (CH, Ph), 134.89 (C$_{quat}$, Ph), 139.67 (*C*=CH$_2$), 172.97 (C=O), 177.18 (C=O). IR (cm^{-1}) ν_{max}: 1701 (C=O), 1735 (C=O). MS *m*/*z* (%): 308 (M+H$^+$, 100), 257 (7), 91 (Bn$^+$, 7). Chromatography: Hex/EtOAc (25/75) R_f=0.45. Mp: 47.3–50.3 °C. HRMS calcd for $C_{16}H_{18}{}^{35}ClNO_3$ (M+H$^+$) 308.1048, found 308.1036.

3.4.2. Synthesis of ethyl 2-(2-chloromethyl-2-propenyl)-5-oxopyrrolidine-2-carboxylate (5b). White crystals (yield: 62%).

^{1}H NMR (270 MHz, $CDCl_3$) δ: 1.31 (3H, t, J=7.1 Hz, CH$_2$C*H*$_3$), 2.12–2.22 (1H, m, CH_AH$_B$ ring, C-4), 2.37–2.54 (3H, m, CH$_A$$H_B$ ring, C-4+CH$_2$ ring, C-3), 2.54 (1H, d, J=14.5 Hz, CH_AH$_B$C=CH$_2$), 2.94 (1H, d, J=14.5 Hz, CH$_A$$H_B$C=CH$_2$), 4.00 (2H, s, CH$_2$Cl), 4.22 (2H, q, J=7.1 Hz, C*H*$_2$CH$_3$), 5.06 (1H, s, C=CH_AH$_B$), 5.33 (1H, s, CH$_A$$H_B$), 6.41 (1H, br s, NH). ^{13}C NMR (68 MHz, $CDCl_3$) δ: 14.11 (CH$_2$*C*H$_3$), 29.69 (CH$_2$ ring, C-3), 31.23 (CH$_2$ ring, C-4), 41.74 (*C*H$_2$C=CH$_2$), 48.41 (CH$_2$Cl),

61.99 (CH_2CH_3), 65.07 (C_{quat}, C-2), 120.03 (C=CH_2), 139.91 (C=CH_2), 173.19 (C=O, ring), 177.21 (C=O, COOEt). IR (cm^{-1}) ν_{max}: 1707 (C=O), 1741 (C=O). MS *m/z* (%): 246 ($M+H^+$, 100). Mp: 55.4–56.6 °C. HRMS calcd for $C_{11}H_{16}{}^{35}ClNO_3$ ($M+H^+$) 246.0891, found 246.0894.

3.5. Typical experimental procedure for the Boc protection of 5a and 5b

The pyroglutamate ester **5** (12 mmol) is dissolved in acetonitrile (20 mL). The flask is cooled in an ice bath. To this solution are added DMAP (1.2 mmol, 0.1 equiv) and di-*tert*-butyldicarbonate (15.6 mmol, 1.3 equiv) dissolved in acetonitrile (15 mL). The mixture is allowed to stir overnight after which H_2O (5 mL) and brine (5 mL) are added. The mixture is extracted twice with diethyl ether, and the organic fractions are dried ($MgSO_4$) and filtered. The solvent is removed under reduced pressure.

3.5.1. Synthesis of benzyl 2-(2-chloromethyl-2-propenyl)-1-(*tert*-butoxycarbonyl)-5-oxopyrrolidine-2-carboxylate (6a). Brown oil (yield: 80%).

^{1}H NMR (270 MHz, $CDCl_3$) δ: 1.46 (9H, s, *t*-Bu), 2.01–2.10 (1H, m, CH_AH_B ring, C-3), 2.15–2.24 (1H, m, CH_AH_B ring, C-3), 2.45–2.56 (2H, m, CH_2 ring, C-4), 2.82 (1H, d, J=15.0 Hz, CH_AH_BC=CH_2), 3.33 (1H, d, J=15.0 Hz, CH_AH_BC=CH_2), 3.97 (1H, d, J=12.0 Hz, CH_AH_BCl), 4.04 (1H, d, J=12.0 Hz, CH_AH_BCl), 5.11 (1H, s, C=CH_AH_B), 5.15 (1H, d, J=12.2 Hz, CH_AH_BPh), 5.23 (1H, d, J=12.2 Hz, CH_AH_BPh), 5.40 (1H, s, C=CH_AH_B), 7.35 (5H, s, Ph). ^{13}C NMR (68 MHz, $CDCl_3$) δ: 26.61 (CH_2 ring, C-3), 27.80 (*t*-Bu), 30.75 (CH_2 ring, C-4), 36.69 (CH_2C=CH_2), 48.71 (CH_2Cl), 67.60 (CH_2Ph+C_{quat}, C-2), 84.29 (C_{quat}, *t*-Bu), 121.60 (C=CH_2), 128.37 (CH, Ph), 128.61 (CH, Ph), 128.70 (CH, Ph), 134.95 (C_{quat}, Ph), 140.05 (C=CH_2), 149.32 (C=O), 172.25 (C=O), 173.83 (C=O). ^{13}C NMR (68 MHz, C_6D_6) δ: 27.03 (CH_2 ring, C-3), 28.27 (*t*-Bu), 31.02 (CH_2 ring, C-4), 37.07 (CH_2C=CH_2), 49.16 (CH_2Cl), 67.74 (C_{quat}, C-2), 67.87 (CH_2Ph), 83.79 (C_{quat}, *t*-Bu), 121.44 (C=CH_2), 136.24 (C_{quat}, Ph), 141.11 (C=CH_2), 150.96 (C=O), 172.76 (C=O), 172.85 (C=O). IR (cm^{-1}) ν_{max}: 1720 (C=O), 1746 (C=O), 1791 (C=O). MS *m/z* (%): no M^+, 308 (M−Boc+H^+), 201 (21), 199 (7), 91 (12). Chromatography: Hex/EtOAc (60/40) R_f=0.33. $C_{21}H_{26}ClNO_5$: calcd C 61.84, H 6.42, N 3.43; found C 61.80, H 6.68, N 3.46.

3.5.2. Synthesis of ethyl 2-(2-chloromethyl-2-propenyl)-1-(*tert*-butoxycarbonyl)-5-oxopyrrolidine-2-carboxylate (6b). Brown oil (yield: 90%).

^{1}H NMR (300 MHz, $CDCl_3$) δ: 1.28 (3H, t, J=7.1 Hz, CH_2CH_3), 1.51 (9H, s, *t*-Bu), 2.03–2.26 (2H, m, CH_2 ring, C-3), 2.37–2.64 (2H, m, CH_2 ring, C-4), 2.79 (1H, d, J=15.0 Hz, CH_AH_BC=CH_2), 3.29 (1H, d, J=15.0 Hz, CH_AH_BC=CH_2), 3.97 (1H, d, J=12.1 Hz, CH_AH_BCl), 4.03 (1H, d, J=12.1 Hz, CH_AH_BCl), 4.18–4.25 (2H, m, CH_2CH$_3$), 5.11 (1H, s, C=CH_AH_B), 5.40 (1H, s, C=CH_AH_B). ^{13}C NMR (75 MHz, $CDCl_3$) δ: 14.14 (CH_2CH_3), 26.81 (CH_2 ring, C-3), 27.93 (*t*-Bu), 30.87 (CH_2 ring, C-4), 36.76 (CH_2C=CH_2), 48.83 (CH_2Cl), 62.04 (CH_2CH_3), 67.65 (C_{quat}, C-2), 121.63 (C=CH_2), 140.22 (C=CH_2), 149.41 (C=O, Boc), 172.54 (C=O, ring), 174.08 (C=O, COOEt). IR (cm^{-1}) ν_{max}: 1721 (C=O), 1742 (C=O), 1791 (C=O). MS *m/z* (%): no M^+, 246 (M−Boc+H^+, 100), 210 (15), 172 (15), 136 (10). $C_{16}H_{24}ClNO_5$: calcd C 55.57, H 7.00, N 4.05; found C 55.76, H 7.19, N 4.10.

3.6. Typical experimental procedure for the synthesis of 7a and 7b

The pyroglutamate ester **6** (12 mmol) is dissolved in THF (15 mL, freshly distilled from Na metal). The mixture is cooled to −78 °C under a N_2 atmosphere. Over a period of 5 min, 25.2 mL of a KHMDS solution (25.2 mmol, 1 M solution in toluene, 1.1 equiv) is added at this temperature. The reaction mixture is allowed to stir for an additional 2 h at −78 °C. The reaction is quenched by addition of saturated aqueous NH_4Cl until the pH is neutral. The mixture is extracted twice with diethyl ether (25 mL), and the organic fractions are dried ($MgSO_4$) and filtered. The solvent is removed under reduced pressure. The products are purified by chromatography.

3.6.1. Synthesis of 5-benzyl 6-(*tert*-butyl)-3-methylene-7-oxo-6-azabicyclo[3.2.1]octane-5,6-dicarboxylate (7a). Brown oil (yield: 44%).

^{1}H NMR (270 MHz, $CDCl_3$) δ: 1.42 (9H, s, *t*-Bu), 1.87 (1H, d, J=11.2 Hz, CH_AH_B, C-4), 2.37 (1H, d, J=11.2 Hz, CH_AH_B, C-4), 2.34–2.41 (1H, m, CH_AH_B, C-8), 2.58 (1H, d, J=14.2 Hz, CH_AH_B, C-8), 2.72 (1H, d, J=14.9 Hz, CH_AH_B, C-2), 2.75–2.79 (1H, m, CH, C1), 3.04 (1H, d, J=14.9 Hz, CH_AH_B, C-2), 4.91–5.20 (2H, m, C=CH_2), 5.18 (1H, d, J=12.4 Hz, CH_AH_BPh), 5.20 (1H, d, J=12.4 Hz, CH_AH_BPh), 7.35 (5H, br s, Ph). ^{13}C NMR (68 MHz, $CDCl_3$) δ: 27.83 (*t*-Bu), 35.76 (CH_2, C-8), 38.15 (CH_2, C-2), 38.45 (CH_2, C-4), 42.55 (CH, C1), 66.18 (C_{quat}, C-3), 67.31 (CH_2Ph), 83.57 (*t*-Bu, C_{quat}), 116.69 (C=CH_2), 128.30 (CH, Ph), 128.52 (CH, Ph), 128.66 (CH, Ph), 135.04 (C_{quat}, Ph), 139.12 (C=CH_2), 148.89 (C=O, Boc), 170.55 (C=O), 174.12 (C=O). IR (cm^{-1}) ν_{max}: 1716 (C=O), 1747 (C=O), 1790 (C=O). MS *m/z* (%): 272 (M−Boc+H^+, 100), 91 (7). Chromatography: Hex/EtOAc (70/30) R_f=0.27. $C_{21}H_{25}NO_5$: calcd C 67.91, H 6.78, N 3.77; found C 67.88, H 6.82, N 3.59.

3.6.2. Synthesis of 5-ethyl 6-(*tert*-butyl)-3-methylene-7-oxo-6-azabicyclo[3.2.1]octane-5,6-dicarboxylate (7b). Brown oil (yield: 75%).

^{1}H NMR (300 MHz, $CDCl_3$) δ: 1.28 (3H, t, J=7.2 Hz, CH_2CH_3), 1.47 (9H, s, *t*-Bu), 1.86 (1H, d, J=11.3 Hz, CH_AH_B, C-4), 2.34–2.41 (2H, m, CH_AH_B, C-4+CH_AH_B, C-8), 2.59 (1H, br d, J=14.3 Hz, CH_AH_B, C-8), 2.69 (1H, dd, J=15.0, 1.9 Hz, CH_AH_B, C-2), 2.76–2.82 (1H, m, CH, C1), 3.00 (1H, d, J=15.0 Hz, CH_AH_B, C-2), 4.21 (2H, m, CH_2CH$_3$), 4.90–5.95 (2H, m, C=CH_2). ^{13}C NMR (75 MHz, $CDCl_3$) δ: 13.99 (CH_2CH_3), 27.78 (*t*-Bu), 35.66 (CH_2, C-8), 38.06 (CH_2, C-2), 38.40 (CH_2, C-4), 42.49 (CH, C1), 61.52 (CH_2CH_3), 66.07 (C_{quat}, C-3), 83.24 (C_{quat}, *t*-Bu), 116.34 (C=CH_2), 139.35 (C=CH_2), 148.74 (C=O, Boc), 170.60 (C=O), 174.22 (C=O). IR (cm^{-1})

ν_{max}: 1716 (C=O), 1742 (C=O), 1790 (C=O). MS *m/z* (%): no M^+, 210 (M−Boc+H^+, 100), 136 (7). Chromatography: Hex/EtOAc (70/30) R_f=0.21. $C_{16}H_{23}NO_5$: calcd C 62.12, H 7.49, N 4.53; found C 62.07, H 7.42, N 4.55.

3.7. Synthesis of 5-ethyl 6-(*tert*-butyl)-3,7-dioxo-6-azabicyclo[3.2.1]octane-5,6-dicarboxylate (9)

Compound **7b** (1.6 mmol) is dissolved in a mixture of CH_2Cl_2 (10 mL, freshly distilled from CaH_2) and methanol (0.5 mL). The mixture is cooled to −78 °C. Ozone is bubbled through until the mixture remains blue. Air is bubbled through the mixture to remove the excess of ozone after which dimethylsulfide (3.24 mmol, 2 equiv) is added. The flask is put in the freezer (−20 °C) for an overnight period. The mixture is washed twice with brine (10 mL). The aqueous layer is extracted once with CH_2Cl_2 (10 mL). The combined organic fractions are dried ($MgSO_4$) and filtered. The solvent is removed under reduced pressure. The product is purified by chromatography and a brown oil is obtained (yield: 60%).

^{1}H NMR (300 MHz, $CDCl_3$) δ: 1.30 (3H, t, J=7.2 Hz, CH_2CH_3), 1.47 (9H, s, *t*-Bu), 2.10 (1H, d, J=11.8 Hz, CH_AH_B, C-4), 2.52–2.61 (2H, m, CH_AH_B, C-4+CH_AH_B, C-8), 2.75 (1H, br d, J=18.4 Hz, CH_AH_B, C-8), 2.97–3.02 (1H, m, CH, C1), 3.00 (1H, d, J=18.6 Hz, CH_AH_B, C-2), 3.18 (1H, br d, J=18.6 Hz, CH_AH_B, C-2), 4.22 (1H, dq, J=13.8, 7.0 Hz, $CH_AH_BCH_3$), 4.23 (1H, dq, J=13.8, 7.0 Hz, $CH_AH_BCH_3$). ^{13}C NMR (75 MHz, $CDCl_3$) δ: 13.99 (CH_2CH_3), 27.81 (*t*-Bu), 37.03 (CH_2, C-4), 40.39 (CH, C1), 42.68 (CH_2, C-8), 45.93 (CH_2, C-2), 62.26 (CH_2CH_3), 65.52 (C_{quat}, C-3), 84.56 (C_{quat}, *t*-Bu), 148.38 (C=O, Boc), 169.42 (C=O), 173.20 (C=O), 204.53 (C=O, C-3). IR (cm^{-1}) ν_{max}: 1721 (C=O), 1745 (C=O), 1790 (C=O). MS *m/z* (%): no M^+, 212 (M−Boc+H^+, 100), 166 (7). Chromatography: Hex/EtOAc (50/50) R_f=0.24. $C_{15}H_{21}NO_6$: calcd C 57.87, H 6.80, N 4.50; found C 58.03, H 6.95, N 4.44.

3.8. Typical experimental procedure for the synthesis of 11a, 11b and 13

The pyroglutamate ester **10** (4.29 mmol) is dissolved in THF (15 mL, freshly distilled from Na metal) and the alkyl halide (4.72 mmol, 1.1 equiv) is added. The mixture is cooled to −40 °C under a N_2 atmosphere. Over a period of 30–40 min, 9 mL of a LiHMDS solution (9.01 mmol, 1 M solution in hexanes, 2.1 equiv) is added at this temperature. The reaction mixture is allowed to stir at room temperature for an additional 2 h. The reaction is quenched by addition of saturated aqueous NH_4Cl. An extra amount of 15 mL of water is added and the mixture is extracted with EtOAc (3×15 mL). The organic fractions are dried ($MgSO_4$) and filtered. The solvent is removed under reduced pressure and the crude product is purified by chromatography.

3.8.1. Synthesis of methyl 6-benzyl-3-methylene-7-oxo-6-azabicyclo[3.2.1]octane-5-carboxylate (11a).

Brown oil (yield: 22%).

^{1}H NMR (300 MHz, $CDCl_3$) δ: 1.83 (1H, d, J=11.0 Hz, CH_AH_B, C-8), 2.32 (1H, d, J=14.3 Hz, CH_AH_B, C-2), 2.44 (1H, dd, J=17.7, 2.0 Hz, CH_AH_B, C-4), 2.51–2.61 (3H, m, CH_AH_B, C-8+CH_AH_B, C-2+CH_AH_B, C-4), 2.74–2.77 (1H, m, CH, C1), 3.43 (3H, s, CH_3), 4.22 (1H, d, J=15.0 Hz, CH_AH_BPh), 4.55 (1H, d, J=15.0 Hz, CH_AH_BPh), 4.63 (1H, d, J=2.0 Hz, C=CH_AH_B), 4.90 (1H, d, J=2.0 Hz, C=CH_AH_B), 7.19–7.30 (5H, m, Ph). ^{13}C NMR (75 MHz, $CDCl_3$) δ: 35.14 (CH_2, C-2), 37.29 (CH_2, C-4), 40.00 (CH, C1), 40.18 (CH_2, C-8), 44.18 (CH_2Ph), 52.23 (CH_3), 66.39 (C_{quat}, C-5), 116.93 (C=CH_2), 127.33 (CH, Ph), 128.11 (CH, Ph), 128.73 (CH, Ph), 136.90 (C_{quat}, Ph), 138.95 (C=CH_2), 171.03 (C=O), 176.77 (C=O). IR (cm^{-1}) ν_{max}: 1702 (C=O), 1740 (C=O). MS *m/z* (%): (ES, pos) 286 (M+H^+, 100). Chromatography: Hex/EtOAc (70/30) R_f=0.19. HRMS calcd for $C_{17}H_{19}NO_3$ (M+H^+) 286.1438, found 286.1441.

3.8.2. Synthesis of benzyl 6-benzyl-3-methylene-7-oxo-6-azabicyclo[3.2.1]octane-5-carboxylate (11b).

Brown oil (yield: 29%).

^{1}H NMR (300 MHz, $CDCl_3$) δ: 1.83 (1H, d, J=11.0 Hz, CH_AH_B, C-8), 2.31 (1H, br d, J=14.3 Hz, CH_AH_B, C-2), 2.46 (2H, br s, CH_2, C-4), 2.51–2.60 (2H, m, CH_AH_B, C-8+CH_AH_B, C-2), 2.71–2.75 (1H, m, CH, C1), 4.33 (1H, d, J=15.1 Hz, NCH_AH_BPh), 4.43 (1H, d, J=15.1 Hz, NCH_AH_BPh), 4.55 (1H, br s, C=CH_AH_B), 4.75 (1H, d, J=12.4 Hz, OCH_AH_BPh), 4.87 (1H, br s, C=CH_AH_B), 5.01 (1H, d, J=12.4 Hz, OCH_AH_BPh), 7.14–7.36 (10H, m, Ph). ^{13}C NMR (75 MHz, $CDCl_3$) δ: 35.11 (CH_2, C-2), 37.45 (CH_2, C-4), 40.12 (CH, C1), 40.25 (CH_2, C-8), 44.17 (NCH_2Ph), 66.60 (C_{quat}, C-5), 67.19 (OCH_2Ph), 116.97 (C=CH_2), 127.37 (CH, Ph), 128.11 (CH, Ph), 128.37 (CH, Ph), 128.54 (CH, Ph), 128.60 (CH, Ph), 128.91 (CH, Ph), 134.91 (C_{quat}, Ph), 136.86 (C_{quat}, Ph), 138.85 (C=CH_2), 170.45 (C=O), 176.67 (C=O). IR (cm^{-1}) ν_{max}: 1649 (C=C), 1704 (C=O), 1735 (C=O). MS *m/z* (%): (ES, pos) 362 (M+H^+, 100). Chromatography: Hex/EtOAc (70/30) R_f=0.33. HRMS calcd for $C_{23}H_{23}NO_3$ (M+H^+) 362.1751, found 362.1749.

3.8.3. Synthesis of methyl 7-benzyl-3,4-dimethylene-8-oxo-7-azabicyclo[4.2.1]-nonane-6-carboxylate (13).

White crystals (yield: 10%).

^{1}H NMR (300 MHz, $CDCl_3$) δ: 2.05 (1H, d, J=12.7 Hz, CH_AH_B, C-9), 2.54–2.62 (3H, m, CH_AH_B, C-9+CH_AH_B, C-2+CH_AH_B, C-5), 2.79–2.84 (2H, m, CH, C1+CH_AH_B, C-2), 2.96 (1H, br d, J=14.9 Hz, CH_AH_B, C-5), 3.29 (3H, s, CH_3), 4.01 (1H, d, J=15.1 Hz, CH_AH_BPh), 4.70 (1H, d, J=15.1 Hz, CH_AH_BPh), 4.79 (1H, br s, C^4=CH_AH_B), 4.82 (1H, t, J=1.9 Hz, C^3=CH_AH_B), 4.85 (1H, d, J=1.4 Hz, C^4=CH_AH_B), 4.90 (1H, br s, C^3=CH_AH_B), 7.19–7.31 (5H, m, Ph). ^{13}C NMR (75 MHz, $CDCl_3$) δ: 33.87 (CH_2, C-9), 38.37 (CH, C1), 39.42 (CH, C-2), 42.89 (CH_2, C-5), 44.29 (CH_2, CH_2Ph), 52.25 (CH_3), 67.61 (C_{quat}, C-6), 115.43 (C^3=CH_2), 117.76 (C^4=CH_2), 127.20 (CH, Ph), 128.18 (CH, Ph), 128.54 (CH, Ph), 136.97 (C_{quat}, Ph), 145.45 (C^3=CH_2), 148.13 (C^4=CH_2), 172.07 (C=O), 178.13 (C=O). IR (cm^{-1}) ν_{max}: 1625 (C=C), 1698 (C=O), 1737 (C=O). MS *m/z* (%): (ES, pos) 312 (M+H^+, 100). Chromatography: Hex/EtOAc (70/30) R_f=0.25. Mp: 114–117 °C. HRMS calcd for $C_{19}H_{21}NO_3$ (M+H^+) 312.1594, found 312.1591.

3.9. Typical experimental procedure for the synthesis of 15a and 15b

To 28.83 mmol of pyroglutamate **14** is added 14.4 mL of a 2 N NaOH solution (28.83 mmol, 1.0 equiv). After stirring overnight at room temperature the solvent is removed under reduced pressure. The sodium salt of 1-benzyl-5-oxopyrrolidine-2-carboxylic acid is obtained in 99% yield.

To a suspension of 20.75 mmol 1-benzyl-5-oxopyrrolidine-2-carboxylic acid in 30 mL CH_2Cl_2 is added 62.25 mmol (3 equiv) $SOCl_2$. The reaction mixture is allowed to stir at room temperature for 30 min. After removal of the solvent under reduced pressure, 19.9 mmol of 1-benzyl-5-oxopyrrolidine-2-carbonyl chloride is obtained (yield: 96%).

To a solution of 6.33 mmol of 1-benzyl-5-oxopyrrolidine-2-carbonyl chloride in 15 mL CH_2Cl_2 is added 12.7 mmol of triethylamine (2.0 equiv) and 12.7 mmol of amine (2.0 equiv). After stirring for 1 h at room temperature, 25 mL of water is added. The reaction mixture is extracted with CH_2Cl_2 (3×20 mL). The organic fractions are combined and dried with $MgSO_4$. After filtration and evaporation under reduced pressure, 1-benzyl-*N*,*N*-dialkyl-5-oxopyrrolidine-2-carboxamides are obtained.

3.9.1. Synthesis of 1-benzyl-*N*,*N*-diisopropyl-5-oxopyrrolidine-2-carboxamide (15a). Brown powder (yield: 74%).

^{1}H NMR (300 MHz, $CDCl_3$) δ: 0.90 (3H, d, J=6.6 Hz, CH_3), 1.12 (3H, d, J=6.6 Hz, CH_3), 1.39 (3H, d, J=6.6 Hz, CH_3), 1.44 (3H, d, J=6.6 Hz, CH_3), 1.79–1.89 (1H, m, CH_AH$_B$ ring, C-3), 2.11–2.24 (1H, m, CH$_A$$H_B$ ring, C-3), 2.37–2.47 (1H, m, CH_AH$_B$ ring, C-4), 2.54–2.65 (1H, m, CH$_A$$H_B$ ring, C-4), 3.32–3.50 (1H, m, NCH), 3.59 (1H, sept, J=6.6 Hz, NCH), 3.87 (1H, d, J=14.6 Hz, CH_AH$_B$Ph), 4.04 (1H, d, J=8.8, 3.9 Hz, CH ring, C-2), 5.19 (1H, d, J=14.6 Hz, CH$_A$$H_B$Ph), 7.19–7.33 (5H, m, Ph). ^{13}C NMR (75 MHz, $CDCl_3$) δ: 19.21 (CH_3), 20.45 (CH_3), 20.56 (CH_3), 20.77 (CH_3), 22.89 (CH_2 ring, C-3), 29.88 (CH_2 ring, C-4), 45.53 (*C*H$_2$Ph), 46.19 (NCH), 47.82 (NCH), 57.12 (CH ring, C-2), 127.72 (CH, Ph), 128.68 (CH, Ph), 129.02 (CH, Ph), 136.21 (C_{quat}, Ph), 169.07 (C=O), 175.25 (C=O). IR (cm^{-1}) ν_{max}: 1634 (C=O), 1682 (C=O). MS *m*/*z* (%): (ES, pos) 303 (M+H$^+$, 100). Mp: 100.5–102.5 °C. HRMS calcd for $C_{18}H_{26}N_2O_2$ (M+H$^+$) 303.2067, found 303.2079.

3.9.2. Synthesis of 1-benzyl-*N*,*N*-diallyl-5-oxopyrrolidine-2-carboxamide (15b). Brown oil (yield: 76%).

^{1}H NMR (300 MHz, $CDCl_3$) δ: 1.87–1.97 (1H, m, CH_AH$_B$ ring, C-3), 2.14–2.27 (1H, m, CH$_A$$H_B$ ring, C-3), 2.39–2.49 (1H, m, CH_AH$_B$ ring, C-4), 2.57–2.72 (1H, m, CH$_A$$H_B$ ring, C-4), 3.52 (1H, dd, J=17.6, 5.0 Hz, CH_AH$_B$CH=CH$_2$), 3.66 (1H, dd, J=17.6, 3.9 Hz, CH$_A$$H_B$CH=CH$_2$), 3.76 (1H, d, J=14.9 Hz, CH_AH$_B$Ph), 3.89 (1H, dd, J=15.1, 6.2 Hz, CH_AH$_B$CH=CH$_2$), 4.07 (1H, dd, J=15.1, 5.8 Hz, CH$_A$$H_B$CH=CH$_2$), 4.15 (1H, dd, J=9.0, 3.7 Hz, CH ring, C-2), 4.93–5.07 (2H, m, CH$_2$CH=CH_2), 5.11–5.23 (2H, m, CH$_2$CH=CH_2), 5.20 (1H, d, J=14.9 Hz, CH$_A$$H_B$Ph), 5.41–5.53 (1H, m, CH$_2$C*H*=CH$_2$), 5.68–5.81 (1H, m, CH$_2$C*H*=CH$_2$), 7.17–7.35 (5H, m, Ph). ^{13}C NMR (75 MHz, $CDCl_3$) δ: 23.33 (CH_2 ring, C-3), 29.70 (CH_2 ring, C-4), 45.31 (*C*H$_2$Ph), 48.41 (*C*H$_2$CH=CH$_2$), 48.49 (*C*H$_2$CH=CH$_2$), 56.19 (CH ring, C-2), 117.14 (CH$_2$CH=*C*H$_2$), 118.05 (CH$_2$CH=*C*H$_2$), 127.70 (CH, Ph), 128.51 (CH, Ph), 128.71 (CH, Ph), 132.16 (CH$_2$*C*H=CH$_2$), 132.59 (CH$_2$*C*H=CH$_2$), 136.16 (C_{quat}, Ph), 170.76 (C=O), 175.44 (C=O). IR (cm^{-1}) ν_{max}: 1656 (C=O), 1690 (C=O). MS *m*/*z* (%): (ES, pos) 299 (M+H$^+$, 100). HRMS calcd for $C_{18}H_{22}N_2O_2$ (M+H$^+$) 299.1754, found 299.1761.

3.10. Synthesis of 1-benzyl-4,4-bis-(2-chloromethyl-allyl)-*N*,*N*-diisopropyl-5-oxopyrrolidine-2-carboxamide (16)

1-Benzyl-*N*,*N*-diisopropyl-5-oxopyrrolidine-2-carboxamide **15a** (0.75 g, 2.48 mmol) is dissolved in THF (10 mL, freshly distilled from Na metal) and 0.34 g of 3-chloro-2-chloromethyl-1-propene (2.73 mmol, 1.1 equiv) is added. The mixture is cooled to −40 °C under a N_2 atmosphere. Over a period of 30–40 min, 5.2 mL of a LiHMDS solution (5.2 mmol, 1 M solution in hexanes, 2.1 equiv) is added at this temperature. The reaction mixture is allowed to stir at room temperature for an additional 2 h. The reaction is quenched by addition of saturated aqueous NH_4Cl. An extra amount of 15 mL of water is added and the mixture is extracted with EtOAc (3×15 mL), and the organic fractions are dried ($MgSO_4$). After filtration, the solvent is removed under reduced pressure. Purification by chromatography gives 0.34 g of 1-benzyl-4,4-bis-(2-chloromethyl-allyl)-*N*,*N*-diisopropyl-5-oxopyrrolidine-2-carboxamide (yield: 29%). When considering the electrophile as limiting reagent, the yield is 52%.

^{1}H NMR (300 MHz, $CDCl_3$) δ: 0.88 (3H, d, J=6.6 Hz, CH_3), 1.12 (3H, d, J=6.6 Hz, CH_3), 1.38 (3H, d, J=6.6 Hz, CH_3), 1.45 (3H, d, J=6.6 Hz, CH_3), 1.92 (1H, dd, J=13.2, 5.2 Hz, CH_AH$_B$ ring, C-3), 2.21 (1H, dd, J=13.2, 9.6 Hz, CH$_A$$H_B$ ring, C-3), 2.30 (1H, d, J=14.2 Hz, CH_AH$_B$(C=CH$_2$)CH$_2$Cl), 2.32 (1H, d, J=14.2 Hz, CH_AH$_B$(C=CH$_2$)CH$_2$Cl), 2.62 (1H, d, J=14.2 Hz, CH$_A$$H_B$(C=CH$_2$)CH$_2$Cl), 2.76 (1H, d, J=14.2 Hz, CH$_A$$H_B$(C=CH$_2$)CH$_2$Cl), 3.36 (1H, sp, J=6.6 Hz, NCH), 3.52 (1H, sept, J=6.6 Hz, NCH), 3.84 (1H, dd, J=9.6, 5.2 Hz, CH ring, C-2), 4.01 (1H, d, J=14.3 Hz, CH_AH$_B$Ph), 4.02 (2H, s, 2×CH_AH$_B$Cl), 4.07 (2H, s, 2×CH$_A$$H_B$Cl), 5.04 (2H, s, 2×C=C$H_AH_B$), 5.16 (1H, d, J=14.3 Hz, CH$_A$$H_B$Ph), 5.30 (2H, s, 2×C=CH$_A$$H_B$), 7.14–7.34 (5H, m, Ph). ^{13}C NMR (75 MHz, $CDCl_3$) δ: 20.26 (CH_3), 20.44 (CH_3), 20.52 (CH_3), 20.66 (CH_3), 30.92 (CH_2 ring, C-3), 40.72 (*C*H$_2$(C=CH$_2$)CH$_2$Cl), 41.00 (*C*H$_2$(C=CH$_2$)CH$_2$Cl), 46.02 (N*C*H$_2$Ph), 46.11 (NCH), 47.29 (C_{quat} ring, C-4), 47.96 (NCH), 48.78 (CH_2Cl), 48.87 (CH_2Cl), 54.55 (CH ring, C-2), 119.03 (C=*C*H$_2$), 119.79 (C=*C*H$_2$), 127.87 (CH, Ph), 128.71 (2×CH, Ph), 129.40 (2×CH, Ph), 135.41 (C_{quat}, Ph), 141.38 (*C*=CH$_2$), 141.57 (*C*=CH$_2$), 168.64 (C=O), 176.70 (C=O). IR (cm^{-1}) ν_{max}: 1649 (C=O), 1683 (C=O). MS *m*/*z* (%): (ES, pos) 480/482/484 (M+H$^+$, 100). Chromatography: Hex/EtOAc (85/15) R_f=0.17. HRMS calcd for $C_{26}H_{36}{}^{35}Cl_2N_2O_2$ (M+H$^+$) 479.2227, found 479.2212.

3.11. Synthesis of 6-benzyl-1-(2-chloromethyl-allyl)-*N*,*N*-diallyl-3-methylene-7-oxo-6-azabicyclo[3.2.1]-octane-5-carboxamide (18)

1-Benzyl-*N*,*N*-diisopropyl-5-oxopyrrolidine-2-carboxamide **15a** of 0.25 g (0.84 mmol) is dissolved in THF (5 mL, freshly distilled from Na metal) and 0.21 g of 3-chloro-2-chloromethyl-1-propene (1.68 mmol, 2.0 equiv) is added. The mixture is cooled to −40 °C under a N_2 atmosphere. Over a period of 30–40 min, 2.5 mL of LiHMDS (2.5 mmol, 1 M solution in hexanes, 3.0 equiv) is added at this temperature. The reaction mixture is allowed to stir at room temperature for an additional 2 h. The reaction is quenched by addition of saturated aqueous NH_4Cl. An extra amount of 10 mL water is added and the mixture is extracted with EtOAc (3×10 mL). The organic fractions are dried ($MgSO_4$) and filtered. The solvent is removed under reduced pressure. A crude reaction mixture of 0.34 g is obtained (conversion: 56%). After purification by chromatography, 0.09 g of 6-benzyl-1-(2-chloromethyl-allyl)-*N*,*N*-diallyl-3-methylene-7-oxo-6-azabicyclo[3.2.1]octane-5-carboxamide **18** is obtained as white crystals (yield: 25%).

^{1}H NMR (300 MHz, $CDCl_3$) δ: 1.74 (1H, d, J=11.6 Hz, CH_AH$_B$, C-8), 2.16 (1H, d, J=13.6 Hz, CH_AH$_B$, C-4), 2.28 (1H, d, J=14.3 Hz, CH_AH$_B$(C=CH$_2$)CH$_2$Cl), 2.30 (1H, d, J=13.6 Hz, CH$_A$$H_B$, C-4), 2.44–2.50 (2H, m, CH_AH$_B$, C-2+CH$_A$$H_B$, C-8), 2.78 (1H, d, J=14.3 Hz, CH$_A$$H_B$(C=CH$_2$)CH$_2$Cl), 2.80 (1H, d, J=14.9 Hz, CH$_A$$H_B$, C-2), 2.94 (1H, dd, J=17.6, 4.7 Hz, CH_AH$_B$CH=CH$_2$), 3.39 (1H, dd, J=13.8, 7.7 Hz, CH_AH$_B$CH=CH$_2$), 3.96 (1H, d, J=12.1 Hz, CH_AH$_B$Cl), 4.03 (1H, d, J=12.1 Hz, CH$_A$$H_B$Cl), 4.17 (1H, d, J=14.6 Hz, CH_AH$_B$Ph), 4.18–4.24 (2H, m, 2×CH$_A$$H_B$CH=CH$_2$), 4.30 (1H, d, J=14.6 Hz, CH$_A$$H_B$Ph), 4.41 (1H, br s, C^3=CH_AH$_B$), 4.74 (1H, br s, C^3=CH$_A$$H_B$), 4.98–5.20 (4H, m, 2×CH$_2$CH=CH_2), 5.07 (1H, br s, CH$_2$(C=CH_AH$_B$)CH$_2$Cl), 5.29 (1H, br s, CH$_2$(C=CH$_A$$H_B$)CH$_2$Cl), 5.44–5.60 (1H, m, CH$_2$CH=CH$_2$), 5.60–5.79 (1H, m, CH$_2$CH=CH$_2$), 7.24–7.35 (5H, m, Ph). ^{13}C NMR (75 MHz, $CDCl_3$) δ: 36.34 (*C*H$_2$(C=CH$_2$)CH$_2$Cl), 39.27 (CH$_2$, C-2), 42.02 (CH$_2$, C-8), 42.80 (CH$_2$, C-4), 45.52 (N*C*H$_2$Ph), 48.04 (C$_{quat}$, C1), 48.80 (*C*H$_2$CH=CH$_2$), 49.06 (CH$_2$Cl), 49.99 (*C*H$_2$CH=CH$_2$), 66.63 (C$_{quat}$, C-5), 116.65 (C^3=*C*H$_2$), 117.57 (CH$_2$CH=*C*H$_2$), 118.74 (CH$_2$CH=*C*H$_2$), 118.86 (CH$_2$(C=*C*H$_2$)CH$_2$Cl), 127.80 (CH, Ph), 128.33 (2×CH, Ph), 130.06 (2×CH, Ph), 132.51 (CH$_2$*C*H=CH$_2$), 132.86 (CH$_2$*C*H=CH$_2$), 136.41 (C$_{quat}$, Ph), 139.35 (C$_{quat}$, C-3), 141.05 (CH$_2$(*C*=CH$_2$)CH$_2$Cl), 169.14 (C=O), 177.13 (C=O). IR (cm^{-1}) ν_{max}: 1625 (C=O), 1691 (C=O). MS *m*/*z* (%): (ES, pos) 440/442 (M+H$^+$, 100). Chromatography: Hex/EtOAc (70/30) R_f= 0.56. Mp: 109–111 °C. HRMS calcd for $C_{26}H_{31}{}^{35}ClN_2O_2$ (M+H$^+$) 439.2147, found 439.2142.

3.12. Typical experimental procedure for the synthesis of 22a and 22b

In an oven dry flask, NaH (0.11 g of a 60% suspension in mineral oil washed with hexanes, 3.32 mmol, 1.2 equiv) is dispersed in THF (5 mL, freshly distilled from Na metal). To this dispersion derivative **5** (2.77 mmol, 1 equiv), dissolved in THF (10 mL), is added. The mixture is refluxed under a N_2 atmosphere for 16 h. Very carefully water (5 mL) is added and the mixture is extracted with diethyl ether (3×20 mL). The combined organic fractions are dried ($MgSO_4$) and filtered. The solvent is removed under reduced pressure. The compound is purified by bulb-to-bulb distillation.

3.12.1. Synthesis of benzyl 2-methylene-5-oxotetrahydro-1*H*-pyrrolizine-7a(5*H*)-carboxylate (22a). Colourless oil (yield: 68%).

^{1}H NMR (270 MHz, $CDCl_3$) δ: 2.05–2.17 (1H, m, CH_AH$_B$, C-7), 2.33–2.79 (4H, m, CH$_2$, C-6+CH$_A$$H_B$, C-7+C$H_AH_B$, C1), 3.05 (1H, d, J=15.5 Hz, CH$_A$$H_B$, C1), 3.71 (1H, d, J=15.7 Hz, CH_AH$_B$, C-3), 4.28 (1H, d, J=15.7 Hz, CH$_A$$H_B$, C-3), 5.01–5.07 (2H, m, C=CH_2), 5.17 (2H, s, CH_2Ph), 7.28–7.37 (5H, m, Ph). ^{13}C NMR (68 MHz, $CDCl_3$) δ: 31.37 (CH$_2$, C-7), 33.30 (CH$_2$, C-6), 43.85 (CH$_2$, C1), 46.54 (CH$_2$, C-3), 67.84 (*C*H$_2$Ph), 72.87 (C$_{quat}$, C-7a), 109.22 (C=*C*H$_2$), 127.96 (CH, Ph), 128.48 (CH, Ph), 128.66 (CH, Ph), 135.27 (C$_{quat}$, Ph), 145.17 (*C*=CH$_2$), 172.94 (C=O), 174.23 (C=O). IR (cm^{-1}) ν_{max}: 1703 (C=O), 1736 (C=O). MS *m*/*z* (%): 272 (M+H$^+$, 100). Bp: 145–160 °C/0.13 mbar. HRMS calcd for $C_{16}H_{17}NO_3$ (M+H$^+$) 272.1281, found 272.1285.

3.12.2. Synthesis of ethyl 2-methylene-5-oxotetrahydro-1*H*-pyrrolizine-7a(5*H*)-carboxylate (22b). Colourless oil (yield: 75%).

^{1}H NMR (270 MHz, $CDCl_3$) δ: 1.27 (3H, t, J=7.1 Hz, CH$_2$CH_3), 2.07–2.19 (1H, m, CH_AH$_B$, C-7), 2.40–2.82 (4H, m, CH$_2$, C-6+CH_AH$_B$, C1+CH$_A$$H_B$, C-7), 3.05 (1H, d, J=15.5 Hz, CH$_A$$H_B$, C1), 3.73 (1H, d, J=15.8 Hz, CH_AH$_B$, C-3), 4.21 (2H, q, J=7.1 Hz, CH_2CH$_3$), 4.29 (1H, d, J=15.8 Hz, CH$_A$$H_B$, C-3), 5.03–5.08 (2H, m, C=CH_2). ^{13}C NMR (68 MHz, $CDCl_3$) δ: 14.12 (CH$_2$*C*H$_3$), 31.48 (CH$_2$, C-7), 33.33 (CH$_2$, C-6), 43.86 (CH$_2$, C1), 46.49 (CH$_2$, C-3), 61.80 (*C*H$_2$CH$_3$), 72.79 (C$_{quat}$, C-7a), 109.06 (C=*C*H$_2$), 145.32 (*C*=CH$_2$), 173.15 (C=O), 174.23 (C=O). IR (cm^{-1}) ν_{max}: 1708 (C=O), 1732 (C=O). MS *m*/*z* (%): 210 (M+H$^+$, 100). Bp: 80–90 °C/0.01 mbar. HRMS calcd for $C_{11}H_{15}NO_3$ (M+H$^+$) 210.1125, found 210.1134.

3.13. Synthesis of (2-methylenetetrahydro-1*H*-pyrrolizin-7a(5*H*)-yl)methanol (23)

In an oven dry flask, 0.23 g of $LiAlH_4$ (5.8 mmol, 2 equiv) is dispersed in THF (10 mL, freshly distilled from Na metal). The flask is put in an ice bath under a N_2 atmosphere. To this dispersion derivative **22b** (2.9 mmol, 1 equiv), dissolved in THF (10 mL), is added. The ice bath is removed and the mixture is refluxed for 3 h under a N_2 atmosphere. Very carefully water is added until all remaining $LiAlH_4$ is decomposed. The mixture is filtered over a combination $MgSO_4$/Celite (50/50) and the solvent is removed under reduced pressure. The compound is purified by bulb-to-bulb distillation and a colourless oil is obtained (yield: 70%).

^{1}H NMR (300 MHz, $CDCl_3$) δ: 1.62–1.94 (4H, m, CH$_2$, C-6+CH$_2$, C-7), 2.32 (1H, dd, J=15.8, 2.0 Hz, CH_AH$_B$, C1), 2.43 (1H, ddd, J=15.8, 2.1, 1.5 Hz, CH$_A$$H_B$, C1),

2.60–2.69 (1H, m, CH_AH$_B$, C-5), 3.02–3.10 (1H, m, CH$_A$$H_B$, C-5), 3.24 (1H, d, J=13.5 Hz, CH_AH$_B$, C-3), 3.25 (1H, d, J=10.9 Hz, CH_AH$_B$OH), 3.27 (1H, d, J=10.9 Hz, CH$_A$$H_B$OH), 3.61 (1H, d, J=13.5 Hz, CH$_A$$H_B$, C-3), 4.87–4.92 (2H, m, C=CH_2). ^{13}C NMR (75 MHz, $CDCl_3$) δ: 25.18 (CH_2, C-6), 34.45 (CH_2, C-7), 41.26 (CH_2, C1), 55.54 (CH_2, C-5), 59.12 (CH_2, C-3), 66.56 (CH_2OH), 74.32 (C$_{quat}$, C-7a), 106.13 (C=CH$_2$), 149.07 (C=CH$_2$). IR (cm^{-1}) ν_{max}: 3368 (br OH). MS m/z (%): 154 (M+H$^+$, 100). Bp: 80–100 °C/0.27 mbar. HRMS calcd for $C_9H_{15}NO$ (M+H$^+$) 154.1226, found 154.1229.

3.14. Synthesis of ethyl 2,5-dioxotetrahydro-1*H*-pyrrolizine-7a(5*H*)-carboxylate (24)

Compound **22b** (1.2 mmol) is dissolved in a mixture of CH_2Cl_2 (10 mL, freshly distilled from CaH_2) and methanol (0.5 mL). The mixture is cooled to −78 °C. Ozone is bubbled through until the mixture remains blue. Air is bubbled through the mixture to remove the excess of ozone after which dimethylsulfide (2.3 mmol, 2 equiv) is added. The flask is put in the freezer (−20 °C) for an overnight period. The mixture is washed twice with brine (10 mL). The aqueous layer is extracted once with CH_2Cl_2 (10 mL). The combined organic fractions are dried ($MgSO_4$) and filtered. The solvent is removed under reduced pressure. After purification by chromatography, a brown oil is obtained (yield: 58%).

^{1}H NMR (300 MHz, $CDCl_3$) δ: 1.26 (3H, t, J=7.1 Hz, CH$_2$CH_3), 2.16 (1H, ddd, J=12.9, 11.1, 9.5 Hz, CH_AH$_B$, C-6), 2.40–2.49 (1H, m, CH_AH$_B$, C-7), 2.52 (1H, d, J=18.0 Hz, CH_AH$_B$, C1), 2.74–2.88 (1H, m, CH$_A$$H_B$, C-7), 2.97–2.99 (1H, m, CH$_A$$H_B$, C-6), 2.97 (1H, d, J=18.0 Hz, CH$_A$$H_B$, C1), 3.54 (1H, d, J=18.5 Hz, CH$_A$H$_B$, C-3), 4.10 (1H, d, J=18.5 Hz, CH$_A$$H_B$, C-3), 4.23 (2H, q, J=7.1 Hz, CH_2CH$_3$). ^{13}C NMR (75 MHz, $CDCl_3$) δ: 14.05 (CH$_2$$CH_3$), 31.57 ($CH_2$, C-7), 31.66 ($CH_2$, C-6), 48.52 ($CH_2$, C1), 49.74 ($CH_2$, C-3), 62.48 ($CH_2CH_3$), 68.95 (C$_{quat}$, C-7a), 171.53 (C=O), 174.44 (C=O), 208.87 (C=O). IR (cm^{-1}) ν_{max}: 1709 (C=O), 1738 (C=O), 1765 (C=O). MS m/z (%): 212 (M+H$^+$, 100). Chromatography: Hex/EtOAc (35/65) R_f=0.16. HRMS calcd for $C_{10}H_{13}NO_4$ (M+H$^+$) 212.0917, found 212.0918.

3.15. Synthesis of 26 and 27

The procedure is the same as for the synthesis of derivatives **5**. After work-up, a mixture of compounds **26** and **27** is obtained. This mixture is treated with NaH in THF and stirred at room temperature for 16 h. The work-up is the same as described for the synthesis of **22**. After chromatography a brown oil is obtained (yield: 24%).

3.15.1. Synthesis of ethyl 3-oxo-2,3,5,8-tetrahydro-8a(1*H*)-indolizine-carboxylate (27). ^{1}H NMR (300 MHz, $CDCl_3$) δ: 1.22 (3H, t, J=7.0 Hz, CH$_2$CH_3), 1.95–2.06 (1H, m, CH_AH$_B$, C1), 2.18 (1H, br d, J=15.9 Hz, CH_AH$_B$, C-8), 2.28–2.51 (3H, m, CH$_A$$H_B$, C1+CH$_2$, C-2), 2.96 (1H, ddd, J=15.9, 5.4 Hz, J=1.9 Hz, CH$_A$$H_B$, C-8), 3.66 (1H, dd, J=19.0, 1.4 Hz, CH_AH$_B$, C-5), 4.14 (1H, dq, J=10.9, 7.0 Hz, CH_AH$_B$CH$_3$), 4.17 (1H, dq, J=10.9, 7.0 Hz, CH$_A$$H_BCH_3$), 4.21 (1H, dd, J=19.0, 2.5 Hz, CH$_A$$H_B$, C-5), 5.65–5.77 (2H, m, CH, C-6+CH, C-7). ^{13}C NMR (75 MHz, $CDCl_3$) δ: 14.19 (CH$_2$$CH_3$), 29.17 ($CH_2$, C1), 31.19 ($CH_2$, C-2), 34.52 ($CH_2$, C-8), 40.02 ($CH_2$, C-5), 61.81 ($CH_2CH_3$), 64.33 (C$_{quat}$, C-8a), 122.92 (CH, C-7), 123.53 (CH, C-6), 173.14 (C=O), 174.66 (C=O). IR (cm^{-1}) ν_{max}: 1701 (C=O), 1732 (C=O). MS m/z (%): 210 (M+H$^+$, 100). Chromatography: Hex/EtOAc (10/90) R_f=0.30. HRMS calcd for $C_{11}H_{15}NO_3$ (M+H$^+$) 210.1125, found 210.1128.

3.15.2. Synthesis of ethyl 2-[(2*Z*)-4-chloro-2-butenyl]-5-oxopyrrolidine-2-carboxylate (26). ^{1}H NMR (300 MHz, $CDCl_3$) δ: 1.30 (3H, t, J=7.1 Hz, CH$_2$CH_3), 2.08–2.13 (1H, m, CH_AH$_B$ ring, C-3), 2.29–2.48 (3H, m, CH$_2$ ring, C-4+CH$_A$$H_B$), 2.57 (1H, dd, J=14.4, 7.3 Hz, CH_AH$_B$HC=CH), 2.67 (1H, dd, J=14.4, 8.5 Hz, CH$_A$$H_B$HC=CH), 4.05 (1H, d, J=8.0 Hz, CH_AH$_B$Cl), 4.03–4.25 (3H, m, CH$_A$$H_B$Cl+C$H_2CH_3$), 5.48–5.57 (1H, m, C$HCH_2$Cl), 5.81–5.89 (1H, m, HC=CHCH$_2$Cl), 6.39 (1H, br s, NH). ^{13}C NMR (75 MHz, $CDCl_3$) δ: 14.16 (CH$_2$$CH_3$), 29.79 (CH$_2$ ring, C-3), 30.30 (CH$_2$ ring, C-4), 36.32 (CH$_2$HC=CH$_2$), 38.76 (CH$_2$Cl), 61.99 (CH$_2$CH$_3$), 65.14 (C$_{quat}$ ring, C-2), 126.90 (CH$_2$HC=CH), 130.06 (HC=CHCH$_2$Cl), 172.94 (C=O), 177.18 (C=O). IR (cm^{-1}) ν_{max}: 1703 (C=O), 1732 (C=O). MS m/z (%): 246 (M+H$^+$, 100). Chromatography: Hex/EtOAc (10/90) R_f=0.30. HRMS calcd for $C_{11}H_{16}{}^{35}ClNO_3$ (M+H$^+$) 246.0891, found 246.0898.

3.16. Synthesis of (2*S*)-[L-(−)-menthyl]-5-oxopyrrolidine-2-carboxylate (29a)

To a solution of (2*S*)-pyroglutamic acid (6.46 g, 50 mmol) in dry CH_2Cl_2 (100 mL, freshly distilled from CaH_2) is added L-(−)-menthol (6.26 g, 40 mmol, 0.8 equiv). Afterwards DMAP (1.52 g, 12.5 mmol, 0.25 g equiv) and DCC (10.34 g, 50 mmol, 1 equiv) are added. The mixture is allowed to stir for 16 h, the volatiles are removed under reduced pressure and the product is purified by chromatography. A yellow oil is obtained (yield: 93%).

^{1}H NMR (300 MHz, $CDCl_3$) δ: 0.76 (3H, d, J=6.9 Hz, CH$_3$, C-9′), 0.90 (3H, d, J=7.2 Hz, CH$_3$, C-10′), 0.92 (3H, d, J=6.3 Hz, CH$_3$, C-7′), 0.8–1.13 (3H, m, CH_AH$_B$, C-2′+CH_AH$_B$, C-5′+CH_AH$_B$, C-6′), 1.36–1.56 (2H, m, CH, C1′+CH, C-4′), 1.64–1.74 (2H, m, CH$_A$$H_B$, C-5′+CH$_A$$H_B$, C-6′), 1.84 (1H, septd, J=7.1, 2.8 Hz, CH, C-8′), 1.93–2.01 (1H, m, CH$_A$$H_B$, C-2′), 2.13–2.45 (1H, m, CH_AH$_B$, C-3), 2.33–2.41 (2H, m, CH$_2$, C-4), 2.43–2.55 (1H, m, CH$_A$$H_B$, C-3), 4.61 (1H, dd, J=8.7, 5.4 Hz, CH, C-2), 4.78 (1H, dt, J=10.7, 4.4 Hz, CH, C-3′), 5.98 (1H, br s, NH). ^{13}C NMR (75 MHz, $CDCl_3$) δ: 16.33 (CH$_3$, C-9′), 20.82 (CH$_3$, C-10′), 22.04 (CH$_3$, C-7′), 23.40 (CH$_2$, C-5′), 25.13 (CH$_2$, C-3), 26.41 (CH, C-8′), 29.29 (CH$_2$, C-4), 31.45 (CH, C1′), 34.16 (CH$_2$, C-6′), 40.78 (CH$_2$, C-2′), 46.96 (CH, C-4′), 55.48 (CH, C-2), 75.85 (CH, C-3′), 171.64 (C=O), 177.68 (C=O). IR (cm^{-1}) ν_{max}: 1711 (C=O, br), 2871, 2951, 3110, 3230. MS m/z (%): (ES, pos) 268 (M+H$^+$, 53), 225 (7). Chromatography: Hex/EtOAc (30/70) R_f=0.30. Polarimetry: $[\alpha]_{546}$ −77.3 (1.022 g/100 mL, CH_2Cl_2, 27 °C). HRMS calcd for $C_{15}H_{25}NO_3$ (M+H$^+$) 268.1907, found 268.1910.

3.17. Synthesis of (2*S*)-[(1*R*,2*R*,4*S*)-fenchyl]-5-oxopyrrolidine-2-carboxylate (29b)

The procedure is identical as for the synthesis of **29a**. White crystals are obtained (yield: 54%).

^{1}H NMR (300 MHz, $CDCl_3$) δ: 0.78 (3H, s, CH_3), 1.05 (3H, s, CH_3), 1.11 (3H, s, CH_3), 1.22 (1H, d, J=10.4 Hz, CH_AH$_B$, C-6′); 1.44–1.51 (1H, m, CH_AH$_B$, C-5′), 1.60 (1H, d, J=10.4 Hz, CH$_A$$H_B$, C-6′), 1.07–1.16 and 1.53–1.74 (4H, m, CH$_A$$H_B$, C-5′+CH$_2$, C-7′+CH, C-4′), 2.17–2.32 (1H, m, CH_AH$_B$, C-3), 2.35–2.42 (2H, m, CH$_2$, C-4), 2.44–2.58 (1H, m, CH$_A$$H_B$, C-3), 4.29 (1H, dd, J=8.2, 5.2 Hz, CH, C-2), 4.42 (1H, d, J=1.7 Hz, CH, C-2′), 6.31 (1H, br s, NH). ^{13}C NMR (75 MHz, $CDCl_3$) δ: 19.38 (CH_3), 20.19 (CH_3), 25.23 (CH_2, C-5′), 25.81 (CH_2, C-3), 26.68 (CH_2, C-6′), 29.29 (CH_2, C-4), 29.69 (CH_3), 39.58 (C_{quat}, C-3′), 41.34 (CH_2, C-7′), 48.35 (C_{quat}, C1′), 48.44 (CH, C-4′), 55.68 (CH, C-2), 87.60 (CH, C-2′), 172.34 (C=O, lactam), 177.65 (C=O, ester). IR (cm^{-1}) ν_{max}: 1709 (C=O), 1736 (C=O), 3432 (NH). MS *m/z* (%): (ES, Pos) 266 (M+H$^+$, 100). Chromatography: Hex/EtOAc (20/80) R_f=0.31. Mp: 78.0–81.5 °C. Polarimetry: $[\alpha]_{546}$ +39.60 (1.01 g/100 mL, CH_2Cl_2, 27 °C). HRMS calcd for $C_{15}H_{23}NO_3$ (M+H$^+$) 266.1751, found 266.1757.

3.18. Synthesis of [(1*R*,2*R*,4*S*)-fenchyl]-2-(2-chloromethyl-allyl)-5-oxopyrrolidine-2-carboxylate (30)

The procedure is identical as for the synthesis of **5a** and **5b**. Upon work-up a mixture of **30** and **31** is obtained. In the crude reaction mixture no diastereomeric excess was observed. After purification (chromatography and crystallisation in hexanes) compound **30** is obtained as white crystals (yield: 20%, diastereomeric excess 12%).

^{1}H NMR (300 MHz, $CDCl_3$) δ: Major (in italic), minor, overlap (underlined): 0.78 (6H, s, CH_3), 1.03 (3H, s, CH_3), *1.05* (3H, s, CH_3), 1.08–1.19 (2H, m, CH_AH$_B$, C-7′), 1.11 (6H, s, CH_3), 1.22 (2H, d, J=10.3 Hz, CH_AH$_B$, C-6′), 1.40–1.54 (2H, m, CH$_A$$H_B$, C-7′), 1.60 (2H, d, J=10.3 Hz, CH$_A$$H_B$, C-6′), 1.66–1.72 (2H, m, CH_AH$_B$, C-5′), 1.71 (2H, s, CH, C-4′), 1.72–1.75 (2H, m, CH$_A$$H_B$, C-5′), 2.16–2.25 (2H, m, CH_AH$_B$, C-3), 2.38–2.43 (4H, m, CH_2, C-4), 2.46–2.55 (2H, m, CH$_A$$H_B$, C-3), 2.55 (2H, d, J=15.0 Hz, CH_AH$_B$C=CH$_2$), 2.95 (2H, d, J=15.0 Hz, CH$_A$$H_B$C=CH$_2$), 4.02 (4H, d, J=0.6 Hz, CH_2Cl), 4.38 (2H, t, J=2.1 Hz, CH, C-2′), *5.06* (1H, s, C=CH$_A$H$_B$), 5.07 (1H, s, C=CH$_A$H$_B$), 5.35 (2H, s, C=CH$_A$$H_B$), 6.38 (2H, s, NH). ^{13}C NMR (75 MHz, $CDCl_3$) δ: Major (in italic), minor, overlap (underlined): 19.81 (CH_3), *19.91* (CH_3), 20.64 (CH_3), *20.72* (CH_3), 26.12 (CH_2, C-7′), 26.96 (CH_2, C-5′), 29.89 (CH_3), 29.95 (CH_2, C-4), *31.86* (CH_2, C-3), 32.01 (CH_2, C-3), 39.94 (C_{quat}, C-3′), *41.60* (CH_2, C-6′), 41.77 (CH_2, C-6′), 42.01 (CH_2HC=CH_2), 48.35 (CH, C-4′), 48.53 (CH, C-4′), *48.82* (C_{quat}, C1′), 48.93 (C_{quat}, C1′), 49.04 (CH_2Cl), *65.41* (C_{quat}, C-2), 65.56 (C_{quat}, C-2), 88.58 (CH, C-2′), *119.99* (C=CH_2), 120.16 (C=CH_2), 140.26 (C=CH$_2$), 173.98 (C=O), 177.11 (C=O). IR (cm^{-1}) ν_{max}: 1699 (C=O), 1745 (C=O), 3193 (br NH). MS *m/z* (%): (ES, pos) 354/356 (M+H$^+$, 100). Chromatography: Hex/EtOAc (40/60) R_f=0.42. Mp: 95 °C. Polarimetry: $[\alpha]_{546}$ +30.41 (0.88 g/100 mL, CH_2Cl_2, 27 °C). HRMS calcd for $C_{19}H_{28}{}^{35}ClNO_3$ (M+H$^+$) 354.1830, found 354.1823.

3.19. Synthesis of [(1*R*,2*R*,4*S*)-fenchyl]-2-methylene-5-oxotetrahydropyrrolizine-7a-carboxylate (31)

The procedure is identical as for the synthesis of **22**. In the crude reaction mixture no diastereomeric excess was observed. After purification (chromatography and crystallisation) white crystals are obtained (yield: 84%, diastereomeric excess 12%).

^{1}H NMR (300 MHz, $CDCl_3$) δ: Major (in italic), minor, overlap (underlined): *0.74* (3H, s, CH_3), 0.75 (3H, s, CH_3), 1.01 (3H, s, CH_3), *1.03* (3H, s, CH_3), 1.11 (6H, s, CH_3), 1.14–1.75 (14H, m, CH, C-4′+CH_2, C-5′+CH_2, C-6′+CH_2, C-7′), 2.08–2.20 (2H, m, CH_AH$_B$, C-7), 2.43–2.54 (4H, m, CH_AH$_B$, C-6 and CH_AH$_B$, C1), 2.62–2.71 (2H, m, CH$_A$$H_B$, C-7), 2.71–2.86 (2H, m, CH$_A$$H_B$, C-6), 3.06 (2H, pseudo t, J=14.2 Hz, CH$_A$$H_B$, C1), *3.73* (1H, d, J=15.7 Hz, CH_AH$_B$, C-3), 3.74 (1H, d, J=15.7 Hz, CH_AH$_B$, C-3), 4.31 (2H, d, J=15.7 Hz, CH$_A$$H_B$, C-3), *4.36* (1H, s, CH, C-2′), 4.37 (1H, s, CH, C-2′), 5.06–5.10 (4H, m, C=CH_2). ^{13}C NMR (75 MHz, $CDCl_3$) δ: Major (in italic), minor, overlap (underlined): 19.37 (CH_3), *19.48* (CH_3), 20.09 (CH_3), 25.84 (CH_2, C-7′), 26.84 (CH_2, C-5′), 29.63 (CH_3), 31.86 (CH_2, C-7), 33.55 (CH_2, C-6), *33.63* (CH_2, C-6), 39.52 (C_{quat}, C-3′), 41.26 (CH_2, C-6′), *43.98* (CH_2, C1), 44.26 (CH_2, C1), 46.61 (CH_2, C-3), 48.32 (CH, C-4′), 48.38 (CH, C-4′ of C_{quat}, C1′), 48.43 (CH, C-4′ of C_{quat}, C1′), 73.16 (C_{quat}, C-7a), 88.02 (CH, C-2′), *88.08* (CH, C-2′), 109.28 (C=CH_2), 145.55 (C=CH$_2$), *173.56* (C=O), 173.70 (C=O), 174.10 (C=O), *174.20* (C=O). IR (cm^{-1}) ν_{max}: 1709 (C=O), 1732 (C=O). MS *m/z* (%): (ES, Pos) 318 (M+H$^+$, 100). Chromatography: Hex/EtOAc (40/60) R_f=0.43. Mp: 214–217 °C. Polarimetry: $[\alpha]_{546}$ +21.93 (0.23 g/100 mL, CH_2Cl_2, 27 °C). HRMS calcd for $C_{19}H_{27}NO_3$ (M+H$^+$) 318.2064, found 318.2051.

Acknowledgements

We thank the BOF (Bijzonder Onderzoeksfonds Universiteit Gent, Research Fund Ghent University), the IWT (Instituut voor de Aanmoediging van Innovatie door Wetenschap en Technologie in Vlaanderen, Institute for the Promotion of Innovation by Science and Technology in Flanders) and the FWO (Fonds voor Wetenschappelijk Onderzoek Vlaanderen, Fund for Scientific research Flanders) for financial support of this research.

References and notes

1. Gassman, P. G.; Fox, B. L. *J. Org. Chem.* **1967**, *32*, 3679.
2. (a) Augustine, R. L.; Vag, L. A. *J. Org. Chem.* **1975**, *40*, 1074; (b) Furstoss, R.; Esposito, G.; Teissier, P.; Waegell, B. *Bull. Soc. Chim. Fr.* **1974**, 2485; (c) Philip, A.; Pitner, J. B.; Joo, Y. J.; Triggle, D. J.; Carroll, F. I. *J. Chem. Soc., Chem. Commun.* **1990**, 984.
3. (a) Holmes, A. B.; Raithby, P. R.; Thompson, J.; Baxter, A. J. G.; Dixon, J. *J. Chem. Soc., Chem. Commun.* **1983**, 1490; (b) Bussmann, R.; Heesing, A. *Tetrahedron Lett.* **1986**,

27, 561; (c) Rigby, J. H.; Pigge, F. C. *Tetrahedron Lett.* **1996**, *37*, 2201; (d) Davies, H. M. L.; Cao, G. *Tetrahedron Lett.* **1998**, *39*, 5943.
4. (a) Rigby, J. H.; Pigge, F. C. *Synlett* **1996**, 631; (b) Oppolzer, W.; Bieber, L.; Francotte, E. *Tetrahedron Lett.* **1979**, *20*, 4537; (c) Tomisawa, H.; Hongo, H.; Hatano, T.; Nakano, H.; Fujita, R. *Chem. Pharm. Bull.* **1987**, *35*, 530; (d) Quirante, J.; Vila, X.; Bonjoch, J.; Kozikowski, A. P.; Johnson, K. M. *Bioorg. Med. Chem.* **2004**, *12*, 1383.
5. Neumann, H.; Jacobi von Wangelin, A.; Gördes, D.; Spannenberg, A.; Baumann, W.; Beller, M. *Tetrahedron* **2002**, *58*, 2381.
6. Despinoy, X. L. M.; McNab, H. *Tetrahedron* **2000**, *56*, 6359.
7. (a) Vicente, J.; Arrayás, R. G.; Carretero, J. C. *Tetrahedron Lett.* **1999**, *40*, 6083; (b) Lindsay, K. B.; Tang, M.; Pyne, S. G. *Synlett* **2002**, 731.
8. Rambaud, L.; Compain, P.; Martin, O. R. *Tetrahedron: Asymmetry* **2001**, *12*, 1807.
9. Kim, S.-H.; Park, Y.; Choo, H.; Cha, J. K. *Tetrahedron Lett.* **2002**, *43*, 6657.
10. Yoda, H.; Egawa, T.; Takabe, K. *Tetrahedron Lett.* **2003**, *44*, 1643.
11. Hasegawa, H.; Senboku, H.; Kajizuka, Y.; Orito, K.; Tokuda, M. *Tetrahedron* **2003**, *59*, 827 and references cited herein.
12. (a) Denmark, S. E.; Herbert, S. E. *J. Am. Chem. Soc.* **1998**, *120*, 7357; (b) White, J. D.; Hrnciar, P.; Yokochi, A. F. T. *J. Am. Chem. Soc.* **1998**, *120*, 7359; (c) Denmark, S. E.; Martinborough, E. A. *J. Am. Chem. Soc.* **1999**, *121*, 3046; (d) Denmark, S. E.; Hurd, A. R. *Org. Lett.* **1999**, *1*, 1311; (e) Denmark, S. E.; Hurd, A. R. *J. Org. Chem.* **2000**, *65*, 2875; (f) Denmark, S. E.; Herbert, B. *J. Org. Chem.* **2000**, *65*, 2887; (g) Denmark, S. E.; Cottell, J. J. *J. Org. Chem.* **2001**, *66*, 4276.
13. Gallos, J. K.; Sarli, V. C.; Stathakis, C. I.; Koftis, T. V.; Nachmia, V. R.; Coutoli-Argyropoulou, E. *Tetrahedron* **2002**, *58*, 9351.
14. de Faria, A. R.; Salvador, E. L.; Correia, C. R. D. *J. Org. Chem.* **2002**, *67*, 3651.
15. (a) Lombardo, M.; Fabbroni, S.; Trombini, C. *J. Org. Chem.* **2001**, *66*, 1264; (b) Holzapfel, C. W.; Crous, R. *Heterocycles* **1998**, *48*, 1337; (c) Brandi, A.; Cicchi, S.; Cordero, F. M.; Frignoli, R.; Goti, A.; Picasso, S.; Vogel, P. *J. Org. Chem.* **1995**, *60*, 6806; (d) McCaig, A. E.; Wightman, R. H. *Tetrahedron Lett.* **1993**, *34*, 3939; (e) McCaig, A. E.; Meldrum, K. P.; Wightman, R. H. *Tetrahedron* **1998**, *54*, 9429; (f) Kuban, J.; Kolarovic, A.; Fisera, L.; Jaeger, V.; Humpa, O.; Pronayova, N. *Synlett* **2001**, 1866; (g) Hall, A.; Meldrum, K. P.; Theron, P. R.; Wightman, R. H. *Synlett* **1997**, 123; (h) Goti, A.; Cicchi, S.; Cacciarini, M.; Cardona, F.; Fedi, V.; Brandi, A. *Org. Lett.* **2001**, *3*, 1367; (i) Goti, A.; Cicchi, S.; Cacciarini, M.; Cardona, F.; Fedi, V.; Brandi, A. *Eur. J. Org. Chem.* **2000**, 3633; (j) Epperson, M. T.; Gin, D. Y. *Angew. Chem., Int. Ed.* **2002**, *41*, 1778; (k) Cardona, F.; Faggi, E.; Liguori, F.; Cacciarini, M.; Goti, A. *Tetrahedron Lett.* **2003**, *44*, 2315; (l) Carmona, A. T.; Wightman, R. H.; Robina, I.; Vogel, P. *Helv. Chim. Acta* **2003**, *86*, 3066; (m) Azizian, J.; Karimi, A. R.; Dastkhan, R.; Mohammadi, A. A.; Mohammadizadeh, M. R. *J. Chem. Res.* **2004**, 347.
16. (a) Pearson, W. H.; Dietz, A.; Stoy, P. *Org. Lett.* **2004**, *6*, 1005; (b) Gensini, M.; de Meijere, A. *Chem.—Eur. J.* **2004**, *10*, 785; (c) Lemaire, S.; Giambastiani, G.; Prestat, G.; Poli, G. *Eur. J. Org. Chem.* **2004**, 2840; (d) Jin, J. Y.; Zheng, M. H.; Wu, X.; Tian, G. R. *Synth. Commun.* **2004**, *34*, 3191; (e) Izquierdo, I.; Plaza, M. T.; Yanez, V. *Tetrahedron: Asymmetry* **2005**, *16*, 3887; (f) Van Speybroeck, V.; De Kimpe, N.; Waroquier, M. *J. Org. Chem.* **2005**, *70*, 3674; (g) Vanecko, J. A.; West, F. G. *Org. Lett.* **2005**, *7*, 2949.
17. Najera, C.; Yus, M. *Tetrahedron: Asymmetry* **1999**, *10*, 2245.
18. (a) Valli, M. J.; Schoepp, D. D.; Wright, R. A.; Johnson, B. G.; Kingston, A. E.; Tomlinson, R.; Monn, J. A. *Bioorg. Med. Chem. Lett.* **1998**, *8*, 1985; (b) Danbolt, N. C. *Prog. Neurobiol.* **2001**, *65*, 1.
19. (a) Ikota, N. *Tetrahedron Lett.* **1992**, *33*, 2553; (b) Rosset, S.; Célérier, J. P.; Lhommet, G. *Tetrahedron Lett.* **1991**, *32*, 7521.
20. Ezquerra, J.; Escrabino, A.; Rubio, A.; Remuinan, M. J.; Vaquero, J. J. *Tetrahedron Lett.* **1995**, *34*, 6149.
21. Ohta, T.; Hosoi, A.; Nozoe, S. *Tetrahedron Lett.* **1988**, *29*, 329.
22. Ohfune, Y.; Tomita, M. J. *J. Am. Chem. Soc.* **1982**, *104*, 3511.
23. Van Betsbrugge, J.; Van Den Nest, W.; Verheyden, P.; Tourwé, D. *Tetrahedron* **1998**, *54*, 1753.
24. Hanessian, S.; McNaughton-Smith, G.; Lombart, H.; Lubell, W. *Tetrahedron* **1997**, *53*, 12789.
25. Braña, M. F.; Garranzo, M.; Pérez-Castells, J. *Tetrahedron Lett.* **1998**, *39*, 6569.
26. Dieltiens, N.; Stevens, C. V.; Masschelein, K. G. R.; Rammeloo, T. *Tetrahedron* **2005**, *61*, 6749.
27. (a) Dieltiens, N.; Claeys, D. D.; Zhdankin, V. V.; Nemykin, V. N.; Allaert, B.; Verpoort, F.; Stevens, C. V. *Eur. J. Org. Chem.* **2006**, 2649; (b) Guillena, G.; Mancheno, B.; Najera, C.; Ezquerra, J.; Pedregal, C. *Tetrahedron* **1998**, *54*, 9447.
28. Stevens, C. V.; Rammeloo, T.; De Kimpe, N. *Synlett* **2001**, 1519.
29. Hamon, D. P. G.; Spurr, P. R. *Synthesis* **1981**, *11*, 873.
30. (a) Newcombe, N. J.; Fang, Y.; Vijn, R. J.; Hiemstra, H.; Speckamp, W. N. *J. Chem. Soc., Chem. Commun.* **1994**, 767; (b) Dutton, J. K.; Steel, R. W.; Tasker, A. S.; Popsavin, V.; Johnson, A. P. *J. Chem. Soc., Chem. Commun.* **1994**, 765; (c) Kuzmich, D.; Wu, S. C.; Ha, D.-C.; Lee, C.-S.; Ramesh, S.; Atarashi, S.; Choi, J.-K.; Hart, D. J. *J. Am. Chem. Soc.* **1994**, *116*, 6943; (d) Fukuyama, T.; Gang, L. *J. Am. Chem. Soc.* **1996**, *118*, 7426; (e) Atarashi, S.; Choi, J.-K.; Ha, D.-C.; Hart, D. J.; Kuzmich, D.; Lee, C.-S.; Ramesh, S.; Wu, S. C. *J. Am. Chem. Soc.* **1997**, *119*, 6226; (f) Baldwin, S. W.; Doll, R. J. *Tetrahedron Lett.* **1979**, *20*, 3275; (g) Hamer, N. K. *J. Chem. Soc., Chem. Commun.* **1990**, 102; (h) Kende, A. S.; Luzzio, M. J.; Mendoza, J. S. *J. Org. Chem.* **1990**, *55*, 918; (i) Takayama, H.; Tominaga, Y.; Kitajama, M.; Aimi, N.; Sakai, S. *J. Org. Chem.* **1994**, *59*, 4381; (j) Beyersbergen van Henegouwen, W. G.; Fieseler, R. M.; Rutjes, F. P. J. T.; Hiemstra, H. *Angew. Chem., Int. Ed.* **1999**, *38*, 2214; (k) Beyersbergen van Henegouwen, W. G.; Fieseler, R. M.; Rutjes, F. P. J. T.; Hiemstra, H. *J. Org. Chem.* **2000**, *65*, 8317.
31. Holliday, M. W.; Abreo, M. A.; Gunn, D. E.; Lin, N.-H.; Garvey, D. S.; Ryther, K.; Lebold, S. A.; Elliot, R. L.; He, Y.; Wasiak, J. T.; Bai, H.; Dart, M. J.; Ehrlich, P. P.; Li, Y.; Kincaid, J. F.; Schkeryantz, J. M.; Lynch, J. K. PCT Int. Appl. CAN 131:73563, 1999.
32. Moeller, K. D.; Rutledge, L. D. *J. Org. Chem.* **1992**, *57*, 6360.

--- Paper III ---

Nicolai Dieltiens, Diederica D. Claeys, Bart Allaert, Francis Verpoort and Christian V. Stevens*

"Synthesis of 1,3-dioxo-hexahydropyrido[1,2-c][1,3]diazepine carboxylates, a new bicyclic skeleton formed by ring expansion–RCM methodology"

Chem. Commun., **2005**, 4477–4478

Synthesis of 1,3-dioxo-hexahydropyrido[1,2-*c*][1,3]diazepine carboxylates, a new bicyclic skeleton formed by ring expansion–RCM methodology†

Nicolai Dieltiens,[a] Diederica D. Claeys,[a] Bart Allaert,[b] Francis Verpoort[b] and Christian V. Stevens*[a]

Received (in Cambridge, UK) 20th June 2005, Accepted 14th July 2005
First published as an Advance Article on the web 4th August 2005
DOI: 10.1039/b508663a

A short and elegant synthetic pathway was developed for the synthesis of 1,3-dioxo-hexahydropyrido[1,2-*c*][1,3]diazepine carboxylates, a new 1,3-diazepan-2,4-dione containing bicyclic moiety, starting from pyroglutamate esters.

Ever since the importance of diazepines in psychotherapy was discovered in the early 1960s, this class of azaheterocyclic compounds has received a lot of attention from the scientific community. Besides their CNS depressant properties, a wide variety of derivatives possess activities ranging from anxiolytic[1] to anticonvulsant[2] and from antitumor[3] to herbicidal properties.[4] Very recently, 1,4-diazepan-2,5-diones were disclosed as novel inhibitors of LFA-1 (lymphocyte function-associated antigen-1).[5] Among the different classes of diazepines, the 1,3-diazepines have been studied to a minor extent although their derivatives show some interesting activities too, *i.e.* inhibition of the HIV-1 protease,[6,7] adenosine deaminase and guanase.[8] 1,3-Diazepan-2,4-diones, or perhydro-1,3-diazepine-2,4-diones, however, are rare and no straightforward synthetic method for their preparation existed until recently we discovered that this interesting skeleton can be prepared in one step by intramolecular transamidation of pyroglutamates after reaction with isocyanates.[9] During our ongoing research to use ring-closing metathesis for the construction of agrochemically and pharmaceutically interesting azaheterocyclic skeletons,[10] we wanted to evaluate the possibility of using RCM for the construction of hexahydropyridodiazepines, because most of the bioactive diazepines contain one or more fused rings in order to reduce the flexibility of the 7-membered ring. This would produce a new interesting heterocyclic skeleton **1** (Fig. 1), since very similar skeletons are described in the literature with very promising properties.

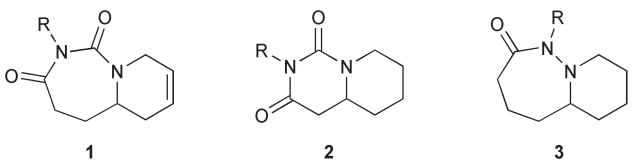

Fig. 1

The six-membered analogue **2**, for example, is a crucial part of a variety of compounds that are CCK (cholecystokinin) receptor antagonists,[11] ligands for 5-HT (5-hydroxytryptamine) receptors,[12] antibacterial agents,[13] antiarrhythmics[14] and herbicides.[15] Derivatives containing the diazepinone core **3** are patented as inhibitors of neutral endopeptidase and angiotensin converting enzyme.[16]

Our strategy to synthesise this heterocyclic skeleton **1**, started from a pyroglutamate ester **4** (Fig. 2). The first step is functionalisation at the C2 position **5**. Carbamoylation and immediate ring expansion would provide the seven-membered motif **6**. Subsequent *N*-alkylation **7** and RCM would provide the envisaged compounds **8**. This strategy provides the possibility of introducing a variety of substituents at four positions and thus would be ideal to synthesise a library of highly functionalised molecules.

Although alkylation of pyroglutamates at the C2 position has been described before,[17] this method is rather impractical with the need for stringent time and temperature control. It was found that excellent results can be obtained when a mixture of the pyroglutamate and the electrophile is treated with 2.1 equivalents of LiHMDS at −40 °C (Scheme 1). When using several equivalents of electrophile, no *N*-alkylation was observed. This methodology, however, cannot be followed if base-sensitive electrophiles are used (*e.g.* in the case of **5e** and **5f**). When using the benzyl ester, however, small amounts of benzyl alcohol were formed caused by fragmentation of the ester.[18] Therefore, all subsequent reactions were carried out on the ethyl ester.

Next the ring expansion was performed with different isocyanates (Scheme 2). In almost all cases, small amounts of carbamoyllactam **9** were formed together with the desired

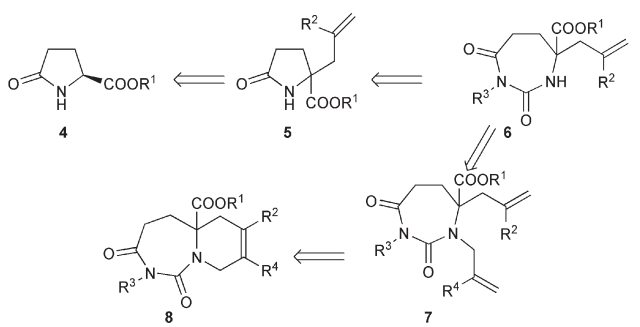

Fig. 2 Retrosynthetic analysis of bicyclic skeleton **8**.

[a]*Research group SynBioC, Department of Organic Chemistry, Faculty of Bioscience Engineering, Ghent University, Coupure links 653, B-9000, Ghent, Belgium. E-mail: chris.stevens@ugent.be; Fax: +32-9-2646243; Tel: +32-9-2645957*
[b]*Division of Organometallics and Catalysis, Department of Inorganic and Physical Chemistry, Ghent University, Krijgslaan 281 (S-3), B-9000, Ghent, Belgium*

† Electronic supplementary information (ESI) available: experimental section, complete spectral characterisation of all compounds and copies of carbon spectra of the end compounds. See http://dx.doi.org/10.1039/b508663a

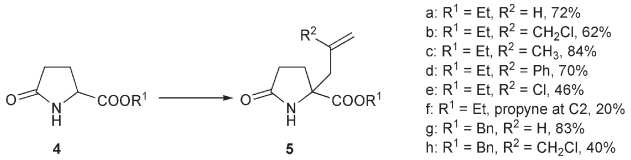

Scheme 1 *Reagents and conditions*: 4 equiv. electrophile, 2.1 equiv. LiHMDS, THF, 30 min at −40 °C then 2 h at rt.

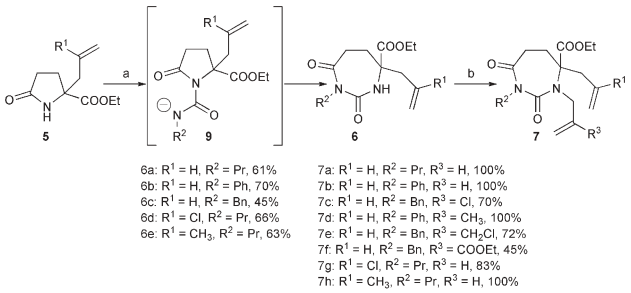

Scheme 2 *Reagents and conditions*: (a) R^2NCO, NaH, THF, rt; (b) electrophile, K_2CO_3, acetone, reflux.

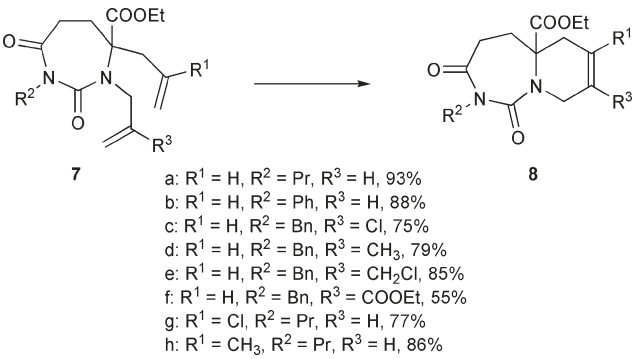

Scheme 3 *Reagents and conditions*: for entries a, b, d, e and h: 5% Grubbs' 2nd generation catalyst, CH_2Cl_2, reflux, 2 h; for entry f: 5% Hoveyda–Grubbs' 2nd generation catalyst, CH_2Cl_2, reflux, 2 h; for entries c and g: 5% Grubbs' 2nd generation catalyst, benzene, reflux, 14 h.

7-membered ring **6** thus requiring purification. It was observed that bulky R^1 substituents (*e.g.* phenyl, morpholinomethyl) prevent the pyroglutamate from reacting with the isocyanate even under more drastic conditions (reflux in DMF). In these cases only unreacted starting material could be recovered.

Also compound **5f**, with a propyne substituent at C2, gave a mixture of compounds upon reaction with isocyanates and was therefore not further used. The 1,4-functionalised 1,3-diazepan-2,4-diones **6** obtained in this fashion proved to be rather poor nucleophiles. Treatment with strong bases did not lead to alkylation but resulted in partial decomposition of the starting material. The only way to alkylate these intermediates at N3 in good yield was to reflux them with 2 equivalents of electrophile and 5 equivalents of finely ground K_2CO_3 in acetone for several days (Scheme 2). Finally, ring-closing metathesis on substrates **7** provided the envisaged bicyclic structures **8** in excellent yield (Scheme 3).

The second generation Grubbs' and Hoveyda–Grubbs' catalysts provide the possibility of performing RCM on a variety of substrates with different substituents on the double bond. Substrates with a vinylic[19] or allylic chloride (**8c**, **8e**, **8g**) or an extra ester-functionality (**8f**) thus provide the possibility of further functionalisation.

In short, we have developed an efficient four step protocol for the synthesis of highly functionalised 1,3-dioxo-hexahydropyrido-[1,2-*c*][1,3]diazepine carboxylates, a new bicyclic skeleton which allows further functionalisation.

The authors thank the BOF (Bijzonder Onderzoeksfonds Universiteit Gent, Research Fund of Ghent University) for financial support of this research.

Notes and references

1 W. B. Wright, H. J. Brabander, E. N. Greenblatt, I. P. Day and R. A. Hardy, *J. Med. Chem.*, 1978, **21**, 1087.
2 G. De Martino, S. Massa and F. Corelli, *Eur. J. Med. Chem.-Chim. Ther.*, 1983, **18**, 347.
3 G. B. Jones, C. L. Davey, T. C. Jenkins, A. Kamal, G. Kneale, S. Neidle, G. D. Webster and D. E. Thurston, *Anti-cancer Drug Des.*, 1990, **5**, 249.
4 G. M. Karp, M. C. Manfredi, M. A. Guaciaro, C. L. Ortlip, P. Marc and I. T. Szamosi, *J. Agric. Food Chem.*, 1997, **45**, 493.
5 S. Wattanasin, J. Kallen, S. Myers, Q. Guo, M. Sabio, C. Ehrhardt, R. Albert, U. Hommel, G. Weckbecker, K. Welzenbach and G. Weitz-Schmidt, *Bioorg. Med. Chem. Lett.*, 2005, 1217.
6 P. Y. Lam, P. K. Jadhav, C. J. Eyermann, C. N. Hodge, Y. Ru, L. T. Bacheler, J. L. Meek, M. J. Otto, M. M. Rayner, Y. N. Wong, C. H. Chang, P. C. Wever, D. A. Jackson, T. R. Sharpe and S. Erickson-Vittanen, *Science*, 1994, **263**, 380.
7 For a recent discussion on privileged skeletons for HIV-protease inhibitors see: E. Specker, J. Böttcher, H. Lilie, A. Heine, A. Schoop, G. Müller, N. Griebenow and G. Klebe, *Angew. Chem., Int. Ed.*, 2005, **44**, 2.
8 L. Wang and R. S. Hosmane, *Bioorg. Med. Chem. Lett.*, 2001, **11**, 2893.
9 C. V. Stevens, N. Dieltiens and D. D. Claeys, *Org. Lett.*, 2005, **7**, 1117.
10 N. Dieltiens, C. V. Stevens, D. De Vos, B. Allaert, R. Drozdzak and F. Verpoort, *Tetrahedron Lett.*, 2004, **45**, 8995; N. Dieltiens, C. V. Stevens, B. Allaert and F. Verpoort, *ARKIVOC*, 2005, **I**, 92. For a recent review on RCM see: A. Fürstner, *Angew. Chem., Int. Ed.*, 2000, **39**, 3012. Recent articles concerning the use of RCM for the synthesis of azaheterocycles: T. J. Donohoe, A. J. Orr, K. Gosby and M. Bingham, *Eur. J. Org. Chem.*, 2005, **10**, 1969; S. Varray, R. Lazaro, J. Martinez and F. Lamaty, *Eur. J. Org. Chem.*, 2002, **14**, 2308. For a recent review on the use of RCM for the synthesis of azaheterocycles see: A. Deiters and S. F. Martin, *Chem. Rev.*, 2004, **104**, 2199.
11 S. Ballaz, A. Barber, A. Fortuño, J. Del Rio, M. Martin-Martinez, I. Gomez-Monterrey, R. Herranz, R. Gonzalez-Muñiz and M. T. Garcia-Lopez, *Br. J. Pharmacol.*, 1997, **121**, 759; M. Latorre, J. M. Bartolomé-Nebreda, M. T. Garcia-Lopez, R. Gonzalez-Muñiz, R. Herranz, J. Del Rio and E. Cenarruzabeitia, *Pharmacology*, 2004, **72**, 68; P. Munoz-Ruiz, M. T. Garcia-Lopez, E. Cenarruzabeitia, J. Del Rio, M. Dufresne, M. Foucaud, D. Fourmy and R. Herranz, *J. Med. Chem.*, 2004, **47**, 5318 (and references cited therein).
12 F. Herold, J. Kleps, I. Wolska and G. Nowak, *Il Farmaco*, 2002, **57**, 959.
13 E. L. Ellsworth, H. D. H. Showalter, K. M. Hutchings and D. Q. Nguyen, *PCT Int. Appl.*, 2002, CAN 138:14071.
14 K. W. Fowler and R. J. Chorvat, *US Pat.*, 1987, CAN 107:176063.
15 M. Schaefer and K. Drauz, *Ger. Offen.*, 1994, CAN 120:270444.
16 D. E. Ryono and C. Q. Sun, *Eur. Pat. Appl.*, 1996, CAN 126:131476.
17 G. Guillena, I. Mico, C. Najera, J. Ezquerra and C. Pedregal, *An. Quim., Int. Ed.*, 1996, **92**, 362.
18 The fragmentation of pyroglutamates under basic conditions has been observed by us before: N. Dieltiens, C. V. Stevens, K. G. R. Masschelein and T. Rammeloo, *Tetrahedron*, 2005, **61**, 6749.
19 For the first report on RCM on substrates with a vinylic chloride see: W. Chao and S. Weinreb, *Org. Lett.*, 2003, **5**, 2505.

--- Paper IV ---

Nicolai Dieltiens, Diederica D. Claeys, Viktor V. Zhdankin, Victor N. Nemykin,
Bart Allaert, Francis Verpoort, and Christian V. Stevens*

"The Pyroglutamate Hydantoin Rearrangement"

Eur. J. Org. Chem. **2006**, 2649–2660

DOI: 10.1002/ejoc.200600051

The Pyroglutamate Hydantoin Rearrangement

Nicolai Dieltiens,[a] Diederica D. Claeys,[a][‡] Viktor V. Zhdankin,[b] Victor N. Nemykin,[b] Bart Allaert,[c] Francis Verpoort,[c] and Christian V. Stevens*[a]

Keywords: Nitrogen heterocycles / Lactams / Fused-ring systems / Rearrangement / Pyroglutamates / Hydantoins / Ring-closing metathesis / Isocyanates

When a mixture of a pyroglutamate and an isocyanate in THF is treated with NaH, a ring transformation occurs leading to functionalised hydantoins. The novel reaction involves a ring-closing ring-opening sequence providing a new and straightforward access to an interesting class of heterocyclic compounds. Furthermore, starting from pyroglutamates allows the synthesis of highly substituted hydantoins under very mild conditions. This ring transformation in combination with ring-closing metathesis is used in a four-step reaction sequence for the synthesis of multi-functionalised bicyclic hydantoin derivatives.

Introduction

Pyroglutamates and their transformations have received a lot of attention over the years because of their importance in several domains. Pyroglutamic acid (**1**) (Figure 1) is a very useful and versatile starting material for the synthesis of both natural and unnatural products.[1] Intensive study of glutamate analogues resulted in specific inhibitors of different receptor types of the mammalian central nervous system.[2,3] It has also been used for the synthesis of pyrrolidine alkaloids,[4,5] kainoids,[6] (–)-bulgecinine,[7] (–)-domoic acid,[8] enantiomerically pure glycine and proline derivatives,[9] a wide variety of non-proteinogenic amino acids,[10] etc. During the last decade, hydantoins (or imidazolidine-2,4-diones, **2**) have been extensively studied and are reported to possess a wide range of biological activities. Phenetoin (5,5-diphenylhydantoin, **3**) for example was already synthesised in 1908[11] and is now still the drug of choice for the treatment of certain types of epileptic seizures.[12] They have not only proven useful in human medicine (antiarrhytmic,[13] anticonvulsant,[14,15] antitumour,[16] antidiabetic,[17,18] antimuscarinic,[19] ... activity), but also in the agrochemical sector (herbicidal and fungicidal activity).[20] In recent years many new synthetic approaches have been developed towards this interesting heterocycle.[21–27] In this article we wish to report on the single-step transformation of pyroglutamates to hydantoins, and the use of this ring transformation in combination with ring-closing metathesis for the synthesis of heavily substituted bicyclic hydantoin derivatives.

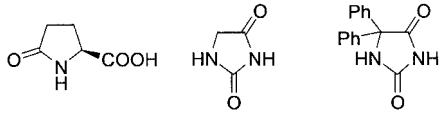

1 2 3

Figure 1. Pyroglutamic acid (**1**), the hydantoin nucleus (**2**) and phenetoin (**3**).

Results and Discussion

The Pyroglutamate Hydantoin Rearrangement

During our research on pyroglutamates for the development of agrochemicals and pharmaceutically interesting azaheterocyclic skeletons, we found that when the sodium salt of an alkyl pyroglutamate **4** is treated with 1 equivalent of an isocyanate, reaction occurs both on the N atom and on the C2 atom resulting in a complex mixture of different compounds. However, when a mixture of **4** with an isocyanate is treated with NaH in diethyl ether, a precipitate is formed during the reaction, which after workup proved to be the sodium salt of the expected carbamoyllactam **5** in high purity (Scheme 1). On the other hand, if the reaction is performed in THF no precipitate is formed, and after workup a compound was isolated which gave a different but very similar ^{1}H NMR spectrum. It was assumed that intermediate **5** (Scheme 1), which is apparently soluble in THF, reacts intramolecularly by a nucleophilic attack on

[a] Research group Synbioc, Department of Organic Chemistry, Faculty of Bioscience Engineering, Ghent University, Coupure links 653, 9000 Ghent, Belgium
Fax: +32-9-2646243
E-mail: chris.stevens@ugent.be
[b] Department of Chemistry, University of Minnesota Duluth, Duluth, Minnesota 55812, USA
[c] Division of Organometallics and Catalysis, Department of Inorganic and Physical Chemistry, Ghent University, Krijgslaan 281 (S-3), 9000 Ghent, Belgium
[‡] D. D. C. is aspirant of the FWO (Fund for Scientific Research Flanders)

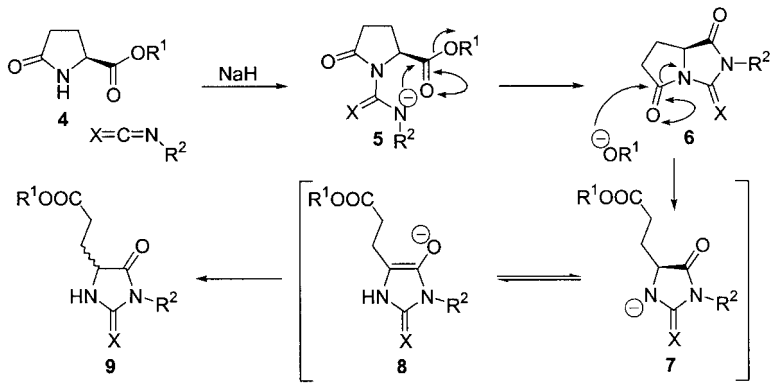

Scheme 1.

the carbonyl of the ester function followed by expulsion of an alkoxide anion resulting in the formation of the bicyclic intermediate **6**. The alkoxide anion in turn can open this bicyclic intermediate with formation of the anions **7** and **8**. These anions are in equilibrium with each other, causing racemisation of the chiral centre (this was proven by quenching the reaction with D_2O). Upon work up this resulted in the hydantoin derivatives **9** as a 1:1 mixture of its enantiomers.

In contrast, the isolated carbamoyllactams **10** (R^1 = Et, R^2 = Bn) and **11** (R^1 = Et, R^2 = Ph)[28] are still optically active. Because we now had both the carbamoyllactam **10** and the hydantoin derivative **9e** in hand, it was easy to compare all the spectroscopic data. From their structures it is obvious that they would have very similar ^{1}H NMR and ^{13}C NMR spectra, hence no conclusions could be made judging these spectra alone. The decisive proof was given by comparing both COSY (Correlated Spectroscopy) and HMBC (Heteronuclear Multiple Bound Correlation) coupled spectra (Figure 2). In the case of **10**, there is a coupling in the COSY spectrum between the proton on the N atom and the two protons of the benzyl group, the proton on nitrogen appears as an incompletely resolved triplet. In the case of **9e**, however, the proton on the N atom couples with the proton next to the carbonyl and not with the protons of the benzyl group, proving that the benzyl group is attached to a tertiary nitrogen. Furthermore, in the HMBC spectrum, the protons of the benzyl group of **10** only couple to the urea carbonyl (easily distinguishable from both other carbonyl groups), whereas in the case of **9e** they couple to both the urea and the lactam carbonyl.

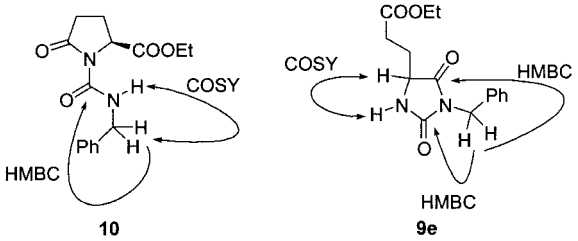

Figure 2. Characteristic COSY and HMBC couplings of **10** and **9e**.

Table 1. Synthesis of hydantoin derivatives **9** by ring transformation of pyroglutamates **4**.

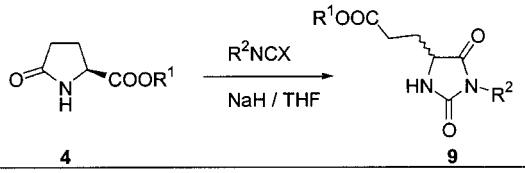

	R^1	Isocyanate	hydantoin	yield (%)
a	Bn	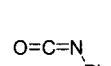	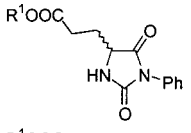	56
b	Bn	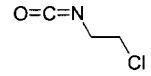	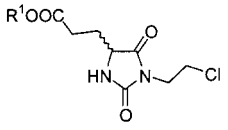	50
c	Bn	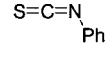	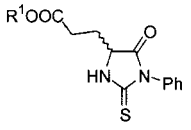	42
d	Et	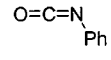	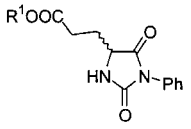	89
e	Et	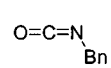	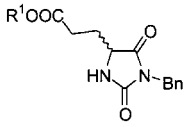	87
f	Et	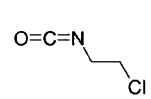	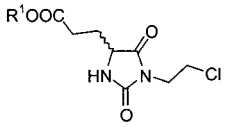	81
g	Et	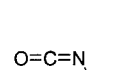	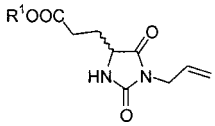	48
h	Me		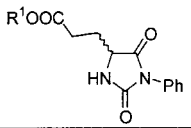	81

Since it was established that the hydantoin was synthesised, the same methodology was performed on other combinations of pyroglutamate esters and isocyanates (Table 1).

We were pleased to find that different esters underwent the same reaction, although, in some cases, traces of carbamoyllactam could be observed due to the poor solubility of this intermediate in THF. This is probably the reason why the benzyl ester formed a hydantoin with phenyl isothiocyanate (Entry 3), whereas the ethyl ester only gave the thiocarbamoylated pyroglutamate.

Synthesis of Bicyclic Hydantoin Derivatives

Having discovered this ring transformation and established its general nature, we wanted to use this reaction as the key step in the synthesis of more complex hydantoins. Our goal was the synthesis of a new series of more constrained bicyclic derivatives **15**. These compounds have attracted the attention of a number of research groups due to their potential biological application and as a template in organic synthesis.[29,30] Our strategy to synthesise this heterocyclic skeleton, started from a pyroglutamate ester **4** (Scheme 2). The first step is functionalisation at the C2 position, which afforded compound **12**. Next carbamoylation and immediate ring transformation would provide the hydantoin derivatives **13**. Subsequent *N*-alkylation to afford **14** and RCM would provide the envisaged compounds **15**.[31] This strategy provides the possibility of varying substituents at four positions and thus would be ideal to synthesise a library of highly functionalised molecules.

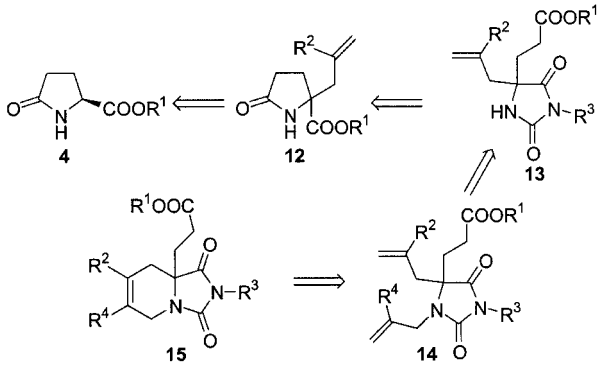

Scheme 2. Retrosynthetic analysis of bicyclic hydantoin derivatives **15**.

Although alkylation of pyroglutamates at the C2 position has been described before,[32] this method is rather unpractical with the need for stringent time and temperature control. It was found that excellent results can be obtained when a mixture of the pyroglutamate and the electrophile is treated with 2.1 equivalents of LiHMDS at –40 °C (Scheme 3). Even when using several equivalents of electrophile, no *N*-alkylation was observed. This methodology however, can not be followed if base-sensitive electrophiles are used (e.g. in case of **12e** and **12f**). When using the benzyl ester, however, small amounts of benzyl alcohol were formed caused by fragmentation of the ester. This kind of fragmentation has been observed before.[33] Therefore, all following reactions were carried out on the ethyl ester.

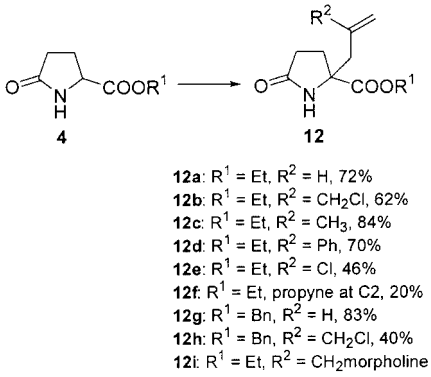

12a: R^1 = Et, R^2 = H, 72%
12b: R^1 = Et, R^2 = CH_2Cl, 62%
12c: R^1 = Et, R^2 = CH_3, 84%
12d: R^1 = Et, R^2 = Ph, 70%
12e: R^1 = Et, R^2 = Cl, 46%
12f: R^1 = Et, propyne at C2, 20%
12g: R^1 = Bn, R^2 = H, 83%
12h: R^1 = Bn, R^2 = CH_2Cl, 40%
12i: R^1 = Et, R^2 = CH_2morpholine

Scheme 3. Reagents and conditions: 4 equiv. electrophile, 2.1 equiv. LiHMDS, THF, 30 min at –40 °C, then 2 h at room temp.

The ring transformation was then performed using different isocyanates (Scheme 4). In almost all cases, small amounts of the carbamoyllactam **16** were formed together with the desired hydantoins **13** thus requiring purification. It was observed that bulky R^2 substituents (e.g. **12d** and **12i**) prevent the pyroglutamate from reacting with the isocyanate even under more drastic conditions (reflux in DMF). In these cases only unreacted starting material could be recovered. Also compound **12f**, with a propyne substituent at C2, gave a mixture of compounds upon reaction with isocyanates and was therefore not further used.

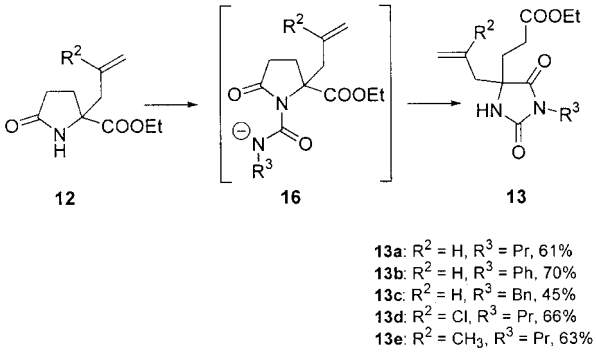

13a: R^2 = H, R^3 = Pr, 61%
13b: R^2 = H, R^3 = Ph, 70%
13c: R^2 = H, R^3 = Bn, 45%
13d: R^2 = Cl, R^3 = Pr, 66%
13e: R^2 = CH_3, R^3 = Pr, 63%

Scheme 4. Reagents and conditions: R^3NCO, NaH, THF, room temp., 16 h.

As is the case for the derivatives **9**, 2D-spectra confirm the structure of compounds **13** (Figure 3). An example is shown in Figure 3: In the HMBC spectrum of **13c**, the protons of the allyl substituent, of the benzyl group and on the N atom couple to the same carbon at δ = 175.0 ppm.

The hydantoins **13** obtained in this fashion proved to be rather poor nucleophiles. Treatment with strong bases did not lead to alkylation, but resulted in partial decomposition of the starting material. The only way to alkylate these com-

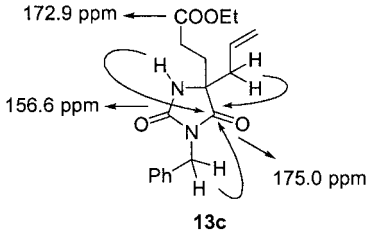

Figure 3. Characteristic HMBC couplings of **13c** and chemical shifts of the carbonyl carbon atoms.

pounds at N1 in good yield was to reflux them with 2 equivalents of electrophile and 5 equivalents of finely ground K_2CO_3 in acetone for several days (Scheme 5).

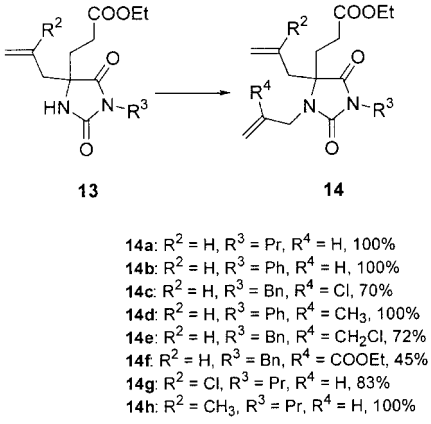

Scheme 5. Reagents and conditions: electrophile, K_2CO_3, acetone, reflux.

Finally, ring-closing metathesis on substrates **14** provided the envisaged bicyclic structures **15** in excellent yields (Table 2). The second-generation Grubbs' catalyst **16**[34] and Hoveyda–Grubbs' catalyst **17**[35] (Figure 4) provide the possibility of performing RCM on a variety of substrates with different substituents on the double bond. Substrates with a vinylic or allylic chloride (**15c**, **15e**, **15g**) or an extra ester functionality (**15f**) thus provide the possibility of further functionalisation.[36]

Figure 5 shows the structure obtained by X-ray analysis of derivative **15b**. As expected, the five-membered cycle is planar with the typical C=O bonds of 1.21 Å. The observed torsion angle of 44.05° between the five-membered and the phenyl rings (C3–N4–C7–C12) confirms the non-coplanar configuration of these molecular fragments. The annelated partially saturated six-membered ring (C1–N2–C14–C15–C16–C17) has the pseudo-envelope conformation in which

Table 2. Synthesis of bicyclic hydantoin derivatives using RCM.

	substrate **14**	RCM product **15**	Yield (%)
a	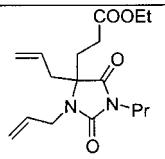	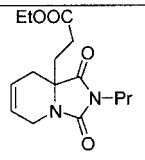	93
b	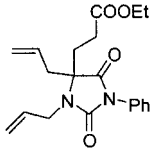	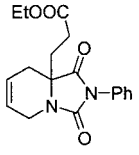	88
c	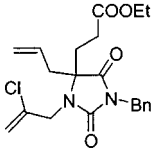	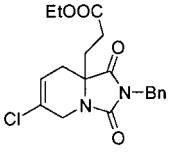	75
d	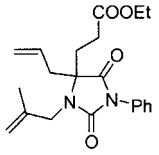	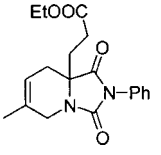	79
e	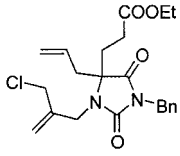	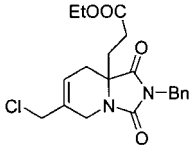	85
f	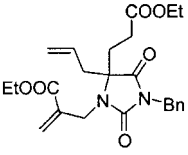	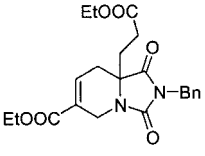	55
g	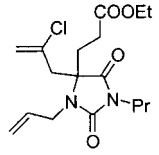	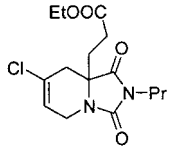	77
h	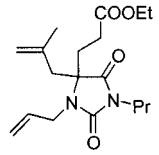	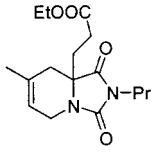	86

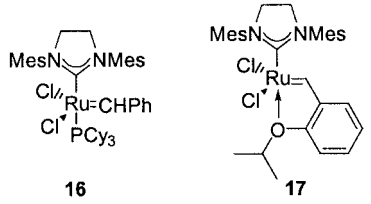

Figure 4. Second-generation Grubbs' catalyst **16** and Hoveyda-Grubbs' catalyst **17**.

all atoms but C1 are in the same plane with the observed C15–C14–N2–C1 torsion angle of 39.07°. An observed C15–C16 bond length of 1.371 Å clearly indicates the presence of the double bond between these atoms formed by the RCM reaction. The ester fragment adopts a typical zigzag conformation with the expected bond lengths. Finally, we were not able to find any significant intra- and intermolecular interactions in the crystal packing of the compound **15b**.

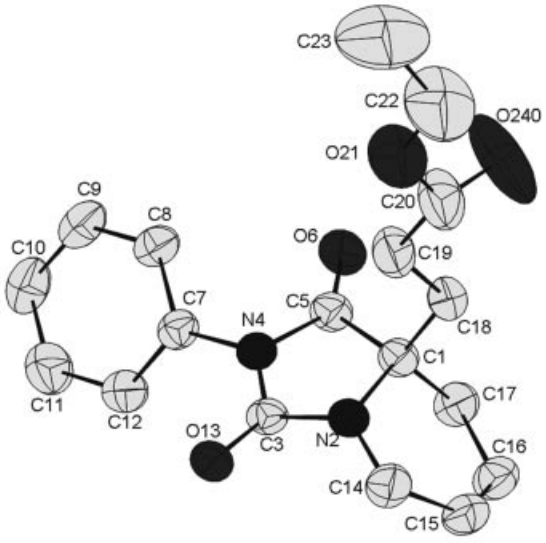

Figure 5. X-ray structure of bicyclic derivative **15b**.[37]

Conclusions

In the present study we have described a new ring transformation of pyroglutamates leading to hydantoins in one step in good to high yields. This rearrangement proceeds through a ring-closing ring-opening sequence. Furthermore, the general nature of this rearrangement was proven using different pyroglutamate esters and isocyanates. The rearrangement was used in a reaction sequence in combination with ring-closing metathesis for the synthesis of multifunctionalised bicyclic hydantoins, expanding the synthetic scope and utility of pyroglutamates.

Experimental Section

General Remarks: High-resolution ^{1}H NMR (270 MHz) and ^{13}C NMR (68 MHz) spectra were run with a Jeol JNM-EX 270 NMR spectrometer or with a Jeol JNM-EX 300 NMR spectroscopy. Peak assignments were obtained with the aid of DEPT, 2D-HETCOR, 2D-COSY spectra. The compounds were diluted in deuterated solvents and the used solvent is indicated for each compound. Low-resolution mass spectra were recorded with an Agilent 1100 Series VS. (ES = 4000 V) mass spectrometer. IR spectra were obtained with a Perkin–Elmer Spectrum One infrared spectrometer. For liquid samples the spectra were collected by preparing a thin film of compound between two sodium chloride plates. The crystalline compounds were mixed with potassium bromide and pressed until a transparent potassium bromide plate was obtained. Melting points of crystalline compounds were measured with a Büchi 540 apparatus and are uncorrected. The elemental analysis was performed with a Perkin–Elmer 2400 Elemental Analyzer. The purification of reaction mixtures was performed by flash chromatography using a glass column with silica gel (Across, particle size 0.035–0.070 mm, pore diameter ca. 6 nm). Single crystals of compound **15b** as colourless plates were grown by slow evapouration of its $CDCl_3$ solution. The X-ray data were collected with a Rigaku AFC-7R diffractometer using graphite-monochromated Mo-K_α radiation (λ = 0.71073 Å) at 293 K. Psi-scan absorption corrections were applied to the data using TeXsan 10.3b program.[38] The structures were solved by direct methods (SIR-92) and refined by full-matrix least-squares on F^2 using Crystals for Windows program.[39] All of the non-hydrogen atoms were refined anisotropically. Selected data: **15b:** $C_{18}H_{20}N_2O_4$, M = 328.37, triclinic, space group $P\bar{1}$, a = 8.2050(16), b = 9.5970(19), c = 12.045(2) Å; α = 77.59(3), β = 79.65(3), γ = 67.39(3)°, V = 850.2(4) Å ^{3}, Z = 2, T = 293 K, μ = 0.091 mm^{-1}, 4215 reflections measured, 3037 unique (R_{int} = 0.0832); final R_1 = 0.051, R_w = 0.129.

CCDC-287973 contains the supplementary crystallographic data for this paper. These data can be obtained free of charge from The Cambridge Crystallographic Data Centre via www.ccdc.cam.ac.uk/data_request/cif.

Typical Experimental Procedure for the Alkylation of Pyroglutamates at the 2-Position: The pyroglutamate ester (12 mmol) was dissolved in THF (15 mL, freshly distilled from Na metal) and the alkyl halide (48 mmol) was added. The mixture was cooled to –40 °C under N_2. Over a period of 30–40 min, LiHMDS (25.2 mmol, solution in hexane) was added at this temperature. The mixture was stirred at room temperature for an additional 2 h and the reaction then quenched by addition of saturated aqueous NH_4Cl until the pH was neutral. The mixture was extracted with EtOAc, and the organics were dried ($MgSO_4$) and filtered. The solvent was removed in vacuo.

Ethyl 2-Allyl-5-oxopyrrolidine-2-carboxylate (12a): Yield: 1.70 g (72%). ^{1}H NMR (270 MHz, $CDCl_3$): δ = 1.29 (t, J = 7.1 Hz, 3 H, CH_2CH_3), 2.07–2.17 (m, 1 H, $COCH_2CH_AH_B$), 2.35–2.51 (m, 4 H, $COCH_2CH_AH_B$ + CCH_AH_B), 2.63–2.71 (m, 1 H, CCH_AH_B), 4.22 (q, J = 7.1 Hz, 2 H, CH_2CH_3), 5.14–5.21 (m, 2 H, $CH{=}CH_2$), 5.69 (dddd, J = 6.5 Hz, J = 7.9 Hz, J = 10.9 Hz, J = 16.2 Hz, 1 H, $CH{=}CH_2$), 6.35 (br s, 1 H, NH) ppm. ^{13}C NMR (68 MHz, $CDCl_3$): δ = 14.20 (CH_2CH_3), 29.88 ($COCH_2CH_2$), 30.04 ($COCH_2$), 43.38 ($CH_2CH{=}CH_2$), 61.72 (CH_2CH_3), 65.35 (C_q), 120.41 ($CH{=}CH_2$), 131.19 ($CH{=}CH_2$), 173.19 (NHC=O), 177.25 (C=OO) ppm. MS: m/z (%) = 198 (100) [M + H$^+$]. IR: $\tilde{\nu}_{max}$ = 1711 (br C=O) cm^{-1}. $C_{10}H_{15}NO_3$ (197.23): calcd. C 60.90, H 7.67, N 7.10; found C 60.74, H 7.77, N 7.09.

Ethyl 5-Oxo-2-(2-chloromethylprop-2-enyl)pyrrolidine-2-carboxylate (12b): Yield: 1.83 g (62%). M.p. 55.4–56.6 °C. ^{1}H NMR (270 MHz, $CDCl_3$): δ = 1.31 (t, J = 7.1 Hz, 3 H, CH_2CH_3), 2.12–2.22 (m, 1 H, $COCH_2CH_AH_B$), 2.37–2.54 (m, 3 H, $COCH_2CH_AH_B$), 2.54 (d, J =14.5 Hz, 1 H, CCH_AH_B), 2.94 (d, J =14.5 Hz, 1 H, CCH_AH_B), 4.00 (s, 2 H, CH_2Cl), 4.22 (q, J =7.1 Hz, 2 H, CH_2CH_3), 5.06 (s, 1 H, $C{=}CH_AH_B$), 5.33 (s, 1 H, $C{=}CH_AH_B$), 6.41 (br s, 1 H, NH) ppm. ^{13}C NMR (68 MHz, $CDCl_3$): δ = 14.11 (CH_2CH_3), 29.69 ($COCH_2CH_2$), 31.23 ($COCH_2$), 41.74 (CCH_2), 48.41 (CH_2Cl), 61.99 (CH_2CH_3), 65.07 (C_q), 120.03 ($C{=}CH_2$), 139.91 ($C{=}CH_2$), 173.19 (NHC=O), 177.21 (C=OO) ppm. MS: m/z (%) = 246.0/248.0 (100) [M + H$^+$]. IR: $\tilde{\nu}_{max}$ = 1707 (C=O), 1741 (C=O) cm^{-1}. $C_{11}H_{16}ClNO_3$ (245.70): calcd. C 53.77, H 6.56, N 5.70; found C 53.73, H 6.43, N 5.66.

Ethyl 2-(2-Methylprop-2-enyl)-5-oxopyrrolidine-2-carboxylate (12c): Yield: 2.13 g (84%). ^{1}H NMR (300 MHz, $CDCl_3$): δ = 1.30 (t, J = 7.2 Hz, 3 H, CH_3), 1.72 (s, 3 H, CH_3), 2.09–2.19 (m, 1 H, $COCH_AH_B$), 2.35–2.52 (m, 3 H, $COCHAH_BCH_2$), 2.37 (dd, J = 2.6 Hz, J = 13.7 Hz, 1 H, CCH_AH_BC), 2.69 (d, J = 13.7 Hz, 1 H, CCH_AH_BC), 4.21 (q, J = 7.2 Hz, 2 H, $CH_AH_BCH_3$), 4.76 (s, 1 H, $C{=}CH_AH_B$), 4.92 (s, 1 H, $C{=}CH_AH_B$), 6.27 (br s, 1 H, NH) ppm. ^{13}C NMR (75 MHz, $CDCl_3$): δ = 14.19 (CH_2CH_3), 23.57 (CH_3), 29.69 ($COCH_2CH_2$), 31.66 ($COCH_2$), 47.11 (CCH_2C), 61.88 (CH_2CH_3), 65.02 (C_q), 116.11 ($C{=}CH_2$), 139.96 ($CH_3C{=}CH_2$), 173.52 (HNC=O), 176.72 (C=OO) ppm. IR: $\tilde{\nu}_{max}$ = 1647 (C=C), 1706 (C=O), 1735 (C=O), 3220 (br NH) cm^{-1}. MS: m/z (%) = 212.8

(100) [M + H$^+$]. $C_{11}H_{17}NO_3$ (211.26): calcd. C 62.54, H 8.11, N 6.63; found C 62.36, H 8.13, N 6.59.

Ethyl 5-Oxo-2-(2-phenylprop-2-enyl)pyrrolidine-2-carboxylate (12d): Yield: 2.30 g (70%). M.p. 73.4–74.4 °C. ^{1}H NMR (300 MHz, $CDCl_3$): δ = 1.12 (t, J = 7.2 Hz, 3 H, CH_3), 2.05–2.17 (m, 1 H, COCH_AH$_B$), 2.23–2.36 (m, 2 H, COCH$_2$CH_2), 2.23–2.49 (m, 1 H, COCH$_A$$H_B$), 2.86 (d, J = 13.6 Hz, 1 H, CCH_AH$_B$C), 3.21 (d, J = 12.1 Hz, 1 H, CCH$_A$$H_B$C), 3.75 (q, J = 7.2 Hz, 1 H, CH_AH$_B$CH$_3$), 3.76 (q, J = 7.2 Hz, 1 H, CH$_A$$H_BCH_3$), 5.15 (s, 1 H, C=C$H_AH_B$), 5.33 (d, J = 1.4 Hz, 1 H, C=CH$_A$$H_B$), 5.98 (br s, 1 H, NH), 7.29–7.35 (m, 5 H, Ph) ppm. ^{13}C NMR (75 MHz, $CDCl_3$): δ = 13.97 (CH_3), 29.60 (COCH$_2$$CH_2$), 31.49 (CO$CH_2$), 45.05 (C$CH_2$C), 61.69 ($CH_2CH_3$), 65.46 ($C_q$), 118.52 (C=$CH_2$), 126.69 ($CH_{ar}$), 128.15 ($CH_{ar}$), 128.55 ($CH_{ar}$), 140.54 ($C$=CH$_2$), 143.68 ($C_{q,ar}$), 172.87 (HNC=O), 176.42 (C=OO) ppm. IR: $\tilde{\nu}_{max}$ = 1728 (C=O), 1744 (C=O), 3203 (br NH) cm^{-1}. MS: m/z (%) = 274.3 (100) [M + H$^+$]. Chromatography [Hex/EtOAc (4:6)]: R_f = 0.21. $C_{16}H_{19}NO_3$ (273.33): calcd. C 70.31, H 7.01, N 5.12; found C 70.10, H 7.04, N 5.04.

Benzyl 2-Allyl-5-oxopyrrolidine-2-carboxylate (12g): Yield: 2.58 g (83%). ^{1}H NMR (270 MHz, $CDCl_3$): δ = 2.09–2.16 (m, 1 H, COCH$_2$CH_AH$_B$), 2.33–2.47 (m, 4 H, COCH_2CH$_A$$H_B$ + CCH_AH$_B$), 2.66 (dd, J = 6.4 Hz, J = 13.7 Hz, 1 H, CCH$_A$$H_B$), 5.09–5.16 (m, 2 H, CH=CH_2), 5.17 (s, 2 H, CH_2Ph), 5.61 (dddd, J = 6.6 Hz, J = 8.3 Hz, J = 10.4 Hz, J = 16.7 Hz, 1 H, CH=CH$_2$), 7.33–7.37 (m, 5 H, Ph) ppm. ^{13}C NMR (68 MHz, $CDCl_3$): δ = 29.72 (COCH$_2$$CH_2$), 30.17 (CO$CH_2$), 43.45 (C$CH_2$), 65.28 ($C_q$), 67.53 ($CH_2$Ph), 120.81 (CH=$CH_2$), 128.41 ($CH_{ar}$), 128.71 ($CH_{ar}$), 130.78 ($CH$=CH$_2$), 135.09 ($C_{q,ar}$), 172.85 (NHC=O), 176.91 (C=OO) ppm. MS: m/z (%) = 260 (100) [M + H$^+$]. IR: $\tilde{\nu}_{max}$ = 1703 (C=O), 1736 (C=O) cm^{-1}. Chromatography [Hex/EtOAc (25:75)]: R_f = 0.31. $C_{15}H_{17}NO_3$ (259.30): calcd. C 69.48, H 6.61, N 5.40; found C 69.13, H 6.52, N 5.37.

Benzyl 5-Oxo-2-(2-chloromethylprop-2-enyl)pyrrolidine-2-carboxylate (12h): Yield: 1.48 g (40%). M.p. 47.3–50.3 °C.^{1}H NMR (270 MHz, $CDCl_3$): δ = 2.17–2.24 (m, 1 H, COCH$_2$CH_AH$_B$), 2.37–2.50 (m, 3 H, COCH_2CH$_A$$H_B$), 2.57 (d, J =14.5 Hz, 1 H, CCH_AH$_B$), 2.96 (d, J =14.5 Hz, 1 H, CCH$_A$$H_B$), 3.96 (s, 2 H, CH$_2$Cl), 5.02 (s, 1 H, C=C$H_AH_B$), 5.20 (d, J =12.0 Hz, 1 H, CH_AH$_B$Ph), 5.23 (d, J =12.0 Hz, 1 H, CH$_A$$H_B$Ph), 5.30 (s, 1 H, C=CH$_A$$H_B$), 7.40 (s, 5 H, Ph) ppm. ^{13}C NMR (68 MHz, $CDCl_3$): δ = 29.61 (COCH$_2$$CH_2$), 31.25 (CO$CH_2$), 41.71 (C$CH_2$), 48.37 ($CH_2$Cl), 65.14 ($C_q$), 67.65 ($CH_2$Ph), 120.09 (C=$CH_2$), 128.52 ($CH_{ar}$), 128.68 ($CH_{ar}$), 134.89 ($C_{q,ar}$), 139.67 ($C$=CH$_2$), 172.97 (NHC=O), 177.18 (C=OO) ppm. MS: m/z (%) = 308.0/310.0 (100) [M + H$^+$], 257 (7), 91 (7) [Bn$^+$]. IR: $\tilde{\nu}_{max}$ = 1701 (C=O), 1735 (C=O) cm^{-1}. Chromatography [Hex/EtOAc (25:75)]: R_f = 0.45. $C_{16}H_{18}ClNO_3$ (307.77): calcd. C 62.44, H 5.89, N 4.55; found C 62.28, H 5.78, N 4.47.

Typical Experimental Procedure for the Alkylation of Pyroglutamates at the 2-Position with Base Sensitive Electrophiles: The pyroglutamate ester (12 mmol) was dissolved in THF (15 mL, freshly distilled from Na metal) and the solution was cooled to –40 °C under N_2. LiHMDS (25.2 mmol, solution in hexane) was added at this temperature and the mixture was stirred for 20 min followed by addition of the alkyl halide (48 mmol, dissolved in 5 mL of dry THF). The mixture was stirred at room temperature for an additional 2 h and the reaction then quenched by addition of saturated aqueous NH_4Cl until the pH was neutral. The mixture was extracted with EtOAc, and the organics were dried ($MgSO_4$) and filtered. The solvent was removed in vacuo, and the residue was purified by flash chromatography (silica gel; hexane/EtOAc).

Ethyl 2-(2-Chloroprop-2-enyl)-5-oxopyrrolidine-2-carboxylate (12e): Yield: 1.28 g (46%). M.p. 90.3° C. ^{1}H NMR (300 MHz, $CDCl_3$): δ = 1.30 (t, J = 7.2 Hz, 3 H, CH_3), 2.13–2.23 (m, 1 H, COCH_AH$_B$), 2.36–2.43 (m, 2 H, COCH$_2$CH_2), 2.46–2.56 (m, 1 H, COCH$_A$$H_B$), 2.71 (d, J = 14.3 Hz, 1 H, CCH_AH$_B$C), 3.05 (d, J = 14.3 Hz, 1 H, CCH$_A$$H_B$C), 4.22 (q, J = 7.2 Hz, 1 H, CH_AH$_B$CH$_3$), 4.23 (q, J = 7.2 Hz, 1 H, CH$_A$$H_BCH_3$), 5.25 (t, J = 0.7 Hz, 1 H, C=CH_AH$_B$), 5.35 (d, J = 1.4 Hz, 1 H, C=CH$_A$$H_B$), 6.29 (br s, 1 H, NH) ppm. ^{13}C NMR (75 MHz, $CDCl_3$): δ = 14.18 (CH_3), 29.31 (COCH$_2$$CH_2$), 31.58 (CO$CH_2$), 48.13 (C$CH_2$C), 62.23 ($CH_2CH_3$), 64.72 ($C_q$), 117.85 (C=$CH_2$), 136.20 ($C$Cl=CH$_2$), 172.51 (HNC=O), 176.52 (C=OO) ppm. IR: $\tilde{\nu}_{max}$ = 1636 (.C=C), 1715 (C=O), 1741 (C=O), 3195 (br NH) cm^{-1}. MS: m/z (%) = 232.7/234.7 (100) [M + H$^+$]. $C_{10}H_{14}ClNO_3$ (231.68): calcd. C 51.84, H 6.09, N 6.05; found C 51.44, H 6.26, N 6.10.

Ethyl 5-Oxo-2-prop-2-ynylpyrrolidine-2-carboxylate (12f): Yield: 0.47 g (20%). ^{1}H NMR (300 MHz, $CDCl_3$): δ = 1.31 (t, J = 7.2 Hz, 3 H, CH_3), 2.08 (t, J = 2.2 Hz, 1 H, CH), 2.12–2.52 (m, 4 H, COCH_2CH_2), 2.61 (dd, J = 14.3 Hz, J = 2.2 Hz, 1 H, CCH_AH$_B$C), 2.82 (dd, J = 14.3 Hz, J = 2.2 Hz, 1 H, CCH$_A$$H_B$C), 4.25 (q, J = 7.2 Hz, 2 H, CH_2CH$_3$), 5.25 (t, J = 0.7 Hz, 1 H, C=CH_AH$_B$), 7.01 (br s, 1 H, NH) ppm. ^{13}C NMR (75 MHz, $CDCl_3$): δ = 14.13 (CH_3), 29.09 (COCH$_2$$CH_2$), 29.79 (C$CH_2$C + CO$CH_2$), 62.15 ($CH_2CH_3$), 64.67 ($C_q$), 72.11 (CH), 78.21 (C), 172.33 (HNC=O), 177.36 (C=OO) ppm. IR: $\tilde{\nu}_{max}$ = 1705 (br C=O), 2120 (alkyne), 3283 (br NH) cm^{-1}. MS: m/z (%) = 391.7, (100) [2M + H$^+$]. Chromatography [Hex/EtOAc (2:8)]: R_f = 0.3. $C_{10}H_{13}NO_3$ (195.22): calcd. C 61.53, H 6.71, N 7.18; found C 61.73, H 6.77, N 7.13.

Ethyl 2-[2-(Morpholin-4-ylmethyl)prop-2-enyl]-5-oxopyrrolidine-2-carboxylate (12i): Ethyl 5-oxo-2-(2-chloromethylprop-2-enyl)pyrrolidine-2-carboxylate (4 mmol) was dissolved in THF (20 mL, freshly distilled from Na metal). Morpholine (10 mmol) was added and the mixture was refluxed until TLC analysis showed that all starting material was consumed. Then the mixture was cooled and aqueous $NaHCO_3$ (15 mL) was added. The mixture was extracted with EtOAc, and the organics were dried ($MgSO_4$) and filtered. The solvent was removed in vacuo, and the residue was purified by flash chromatography. Yield: 0.71 g (60%). ^{1}H NMR (300 MHz, $CDCl_3$): δ = 1.27 (t, J = 7.2 Hz, 3 H, CH_3), 1.98–2.08 (m, 1 H, COCH_AH$_B$), 2.23 (d, J = 13.5 Hz, 1 H, CCH_AH$_B$C), 2.31–2.56 (m, 7 H, COCH$_A$$H_BCH_2$ + CH_2NCH_2), 2.75 (d, J = 12.1 Hz, 1 H, NCH_AH$_B$C), 2.94 (d, J = 12.1 Hz, 1 H, NCH$_A$$H_B$C), 2.98 (d, J = 13.5 Hz, 1 H, CCH$_A$$H_B$C), 3.68–3.87 (m, 4 H, C$H_2OCH_2$), 4.16 (q, J = 7.2 Hz, 2 H, CH_2CH$_3$), 5.01 (s, 1 H, C=CH_AH$_B$), 5.07 (s, 1 H, C=CH$_A$$H_B$), 9.19 (br s, 1 H, NH) ppm. ^{13}C NMR (75 MHz, $CDCl_3$): δ = 14.35 (CH_3), 30.26 (COCH$_2$$CH_2$), 32.76 (CO$CH_2$), 47.54 (C$CH_2$C), 53.31 ($CH_2NCH_2$), 61.49 ($CH_2CH_3$), 65.37 (C$CH_2$N), 65.94 ($C_q$), 66.73 ($CH_2OCH_2$), 122.43 (C=$CH_2$), 139.22 ($C$=CH$_2$), 173.71 (HNC=O), 176.77 (C=OO) ppm. IR: $\tilde{\nu}_{max}$ = 1705 (C=O), 1734 (C=O), 3270 (br NH) cm^{-1}. MS: m/z (%) = 297.8 (100) [M + H$^+$]. Chromatography: First 100% EtOAc until R_f = 0.27 then strip with CH_2Cl_2 + 5% MeOH. $C_{15}H_{24}N_2O_4$ (296.36): calcd. C 60.79, H 8.16, N 9.45; found C 60.46, H 8.16, N 9.39.

Typical Experimental Procedure for the Hydantoin Formation from Pyroglutamates: The pyroglutamate ester (5 mmol) was dissolved in THF (40 mL, freshly distilled from Na metal) and the isocyanate (5.5 mmol) was added followed by NaH (5.5 mmol, washed with hexanes). The mixture was stirred at room temperature for 16 h. The reaction was quenched by addition of saturated aqueous NH_4Cl until the pH was neutral. Then the mixture was extracted with EtOAc, and the organics were dried ($MgSO_4$) and filtered. The solvent was removed in vacuo, and the residue was purified by

recrystallisation in case of solids or by flash chromatography (silica gel; hexane/EtOAc) in case of liquids.

Benzyl 3-(2,5-Dioxo-1-phenyl-imidazolidin-4-yl)propanoate (9a): Yield: 0.95 g (56%). M.p. 144,5–145,4 °C. ^{1}H NMR (300 MHz, $CDCl_3$): δ = 2.10–2.22 (m, 1 H, CHCH_AH$_B$), 2.27–2.38 (m, 1 H, CHCH$_A$$H_B$), 2.59 (t, J = 7.1 Hz, 2 H, CH_2CO), 4.25 (br t, J = 5.6 Hz, 1 H, CHCO), 5.13 (s, 2 H, CH_2Ph), 6.36 (br s, 1 H, NH), 7.33–7.48 (m, 10 H, 2 × Ph) ppm. ^{13}C NMR (75 MHz, $CDCl_3$): δ = 27.43 (CH_2), 30.18 (CH_2), 56.68 (CH), 67.34 (OCH_2), 126.59 (CH_{arom}), 128.79 (CH_{arom}), 128.85 (CH_{arom}), 128.93 (CH_{arom}), 129.11 (CH_{arom}), 129.57 (CH_{arom}), 131.75 ($C_{q.\ arom}$) 135.86 ($C_{q.\ arom}$), 156.69 (NC=ON), 172.83 (C=O), 172.99 (C=O) ppm. MS (ES, Neg): m/z (%) = 337.2 (100) [M – H$^+$]. IR (KBr): $\tilde{\nu}_{max}$ = 1699 (C=O), 1715 (C=O), 1781 (C=O), 3256 (br NH) cm^{-1}. $C_{19}H_{18}N_2O_4$ (338.36): calcd. C 67.36, H 5.36, N 8.28; found C 67.03, H 5.43, N 8.27.

Benzyl 3-[1-(2-Chloro-ethyl)-2,5-dioxo-imidazolidin-4-yl]propanoate (9b): Yield: 0.81 g (50%). ^{1}H NMR (300 MHz, $CDCl_3$): δ = 1.99–2.11 (m, 1 H, CHCH_AH$_B$), 2.14–2.28 (m, 1 H, CHCH$_A$$H_B$), 2.52 (t, J = 7.4 Hz, 2 H, CH_2CO), 3.68 (t, J = 5.9 Hz, 2 H, CH_2Cl), 3.77–3.82 (m, 2 H, NCH_2), 4.13 (br t, J = 6.1 Hz, 1 H, CH), 5.10 (s, 2 H, CH_2Ph), 7.12 (br s, 1 H, NH), 7.27–7.38 (m, 5 H, Ph) ppm. ^{13}C NMR (75 MHz, $CDCl_3$): δ = 26.92 (CH_2), 29.54 (CH_2), 40.13 (CH_2N or CH_2Cl), 40.74 (CH_2N or CH_2Cl), 56.44 (CH), 66.90 (OCH_2), 128.44 (CH_{arom}), 128.59 (CH_{arom}), 128.83 (CH_{arom}), 135.77 ($C_{q.\ arom}$), 157.44 (NC=ON), 172.67 (C=O), 173.80 (C=O) ppm. MS (ES, Neg): m/z (%) = 323.3/325.2 (100) [M – H$^+$]. IR (KBr): $\tilde{\nu}_{max}$ = 1714 (br, C=O), 1777 (C=O), 3320 (NH) cm^{-1}. $C_{15}H_{17}ClN_2O_4$ (324.76): calcd. C 55.48, H 5.28, N 8.63; found C 55.45, H 5.36, N 8.62.

Benzyl 3-(5-Oxo-1-phenyl-2-thioxo-imidazolidin-4-yl)propanoate (9c): Yield: 0.74 g (42%). M.p. 157 °C. ^{1}H NMR (300 MHz, $CDCl_3$): δ = 2.13–2.26 (m, 1 H, CHCH_AH$_B$), 2.33–2.44 (m, 1 H, CHCH$_A$$H_B$), 2.58–2.65 (m, 2 H, CH_2CO), 4.35 (dd, J = 5.1 Hz and J = 6.5 Hz, 1 H, CH), 5.16 (s, 2 H, CH_2Ph), 7.28–7.53 (m, 10 H, 2 × Ph), 7.66 (br s, 1 H, NH) ppm. ^{13}C NMR (75 MHz, $CDCl_3$): δ = 26.61 (CH_2), 29.85 (CH_2), 59.00 (CH), 67.10 (OCH_2), 128.25 ($CH_{arom.}$), 128.50 ($CH_{arom.}$), 128.56 ($CH_{arom.}$), 128.69 ($CH_{arom.}$), 129.18 ($CH_{arom.}$), 129.32 ($CH_{arom.}$), 132.54 ($C_{q.\ arom.}$), 135.29 ($C_{q.\ arom.}$), 172.69 (C=O) 173.20 (C=O), 183.71 (C=S) ppm. MS (ES, Neg): m/z (%) = 353.2 (100) [M – H$^+$]. IR (KBr): $\tilde{\nu}_{max}$ = 1697 (C=S), 1719 (C=O), 1750 (C=O), 3233 (NH) cm^{-1}. $C_{19}H_{18}N_2O_3S$ (354.42): calcd. C 64.39, H 5.12, N 7.90; found C 64.15, H 5.30, N 7.82.

Ethyl 3-(2,5-Dioxo-1-phenyl-imidazolidin-4-yl)propanoate (9d): Yield: 1.23 g (89%). M.p. 84–85 °C. ^{1}H NMR (300 MHz, $CDCl_3$): δ = 1.26 (t, J = 7.2 Hz, 3 H, CH_3), 2.08–2.20 (m, 1 H, CHCH_AH$_B$), 2.26–2.37 (m, 1 H, CHCH$_A$$H_B$), 2.53 (t, J = 6.9 Hz, 2 H, $COCH_2$), 4.16 (q, J = 7.2 Hz, 2 H, CH_2CH$_3$), 4.26 (dt, J = 1.3 Hz and J = 5.7 Hz, 1 H, CH), 6.31 (br s, 1 H, NH), 7.31–7.50 (m, 5 H, Ph) ppm. ^{13}C NMR (75 MHz, $CDCl_3$): δ = 14.14 (CH_3), 26.96 (CH_2), 29.53 (CH_2), 56.20 (CH), 60.95 (OCH_2), 126.21 (CH_{arom}), 128.33 (CH_{arom}), 129.12 (CH_{arom}), 131.38 ($C_{q.\ arom}$), 156.62 (NC=ON), 172.62 (C=O), 172.67 (C=O) ppm. MS (70 eV, ES, Neg): m/z (%) = 275.3 (100) [M – H$^+$]. IR (KBr): $\tilde{\nu}_{max}$ = 1713 (C=O), 1728 (C=O), 1774 (C=O), 3272 (NH) cm^{-1}. $C_{14}H_{16}N_2O_4$ (276.29): calcd. C 60.86, H 5.84, N 10.14; found C 60.84, H 5.76, N 10.05.

Ethyl 3-(1-Benzyl-2,5-dioxo-imidazolidin-4-yl)propanoate (9e): Yield: 1.26 g (87%). M.p. 92 °C. ^{1}H NMR (300 MHz, $CDCl_3$): δ = 1.24 (t, J = 7.2 Hz, 3 H, CH_3), 1.93–2.06 (m, 1 H, CHCH_AH$_B$), 2.15–2.26 (m, 1 H, CHCH$_A$$H_B$), 2.42 (t, J = 7.2 Hz, 2 H, $COCH_2$), 4.07–4.08 (m, 1 H, CH), 4.12 (q, J = 7.2 Hz, 2 H, CH_2CH$_3$), 4.64 (s, 2 H, CH_2Ph), 6.29 (br s, 1 H, NH), 7.25–7.39 (m, 5 H, Ph) ppm. ^{13}C NMR (75 MHz, $CDCl_3$): δ = 14.12 (CH_3), 26.84 (CH_2), 29.51 (CH_2), 42.14 (CH_2N), 56.35 (CH), 60.86 (OCH_2), 127.89 (CH_{arom}), 128.39 (CH_{arom}), 128.65 (CH_{arom}), 135.96 ($C_{q.\ arom}$), 157.43 (NC=ON), 172.65 (C=O), 173.49 (C=O) ppm. MS (ES, Neg): m/z (%) = 289.2 (100) [M – H$^+$]. IR (KBr): $\tilde{\nu}_{max}$ = 1708 (C=O), 1732 (C=O), 1778 (C=O), 3448 (br NH) cm^{-1}. $C_{15}H_{18}N_2O_4$ (290.31): calcd. C 62.02, H 6.25, N 9.65; found C 61.80, H 6.19, N 9.72.

Ethyl 3-[1-(2-Chloro-ethyl)-2,5-dioxo-imidazolidin-4-yl]propanoate (9f): Yield: 1.06 g (81%). ^{1}H NMR (300 MHz, $CDCl_3$): δ = 1.27 (t, J = 7.2 Hz, 3 H, CH_3), 2.01–2.13 (m, 1 H, CHCH_AH$_B$), 2.18–2.30 (m, 1 H, CHCH$_A$$H_B$), 2.49 (t, J = 7.4 Hz, 2 H, $COCH_2$), 3.75 (t, J = 6.1 Hz, 2 H, CH_2Cl), 3.84–3.89 (m, 2 H, NCH_2), 4.14 (q, J = 7.2 Hz, 2 H, CH_2CH_3), 4.20 (t, J = 6.1 Hz, 1 H, CH), 7.18 (br s, 1 H, NH) ppm. ^{13}C NMR (75 MHz, $CDCl_3$): δ = 14.37 (CH_3), 26.99 (CH_2), 29.58 (CH_2), 40.17 (CH_2N of CH_2Cl), 40.73 (CH_2N of CH_2Cl), 56.54 (CH), 61.14 (OCH_2), 157.42 (NC=ON), 172.93 (C=O), 173.91 (C=O) ppm. MS (ES, Neg): m/z (%) = 261.2/263.2 (100) [M – H$^+$]. IR (NaCl): $\tilde{\nu}_{max}$ = 1714 (C=O), 1778 (C=O) cm^{-1}. $C_{10}H_{15}ClN_2O_4$ (262.69): calcd. C 45.72, H 5.76, N 10.66; found C 45.70, H 5.71, N 10.63.

Ethyl 3-(1-Allyl-2,5-dioxo-imidazolidin-4-yl)propanoate (9g): Yield: 0.57 g (48%). ^{1}H NMR (300 MHz, $CDCl_3$): δ = 1.26 (t, J = 6.9 Hz, 3 H, CH_3), 1.99–2.10 (m, 1 H, CHCH_AH$_B$), 2.17–2.28 (m, 1 H, CHCH$_A$$H_B$), 2.48 (t, J = 7.4 Hz, 2 H, $COCH_2$), 4.13 (q, J = 6.9 Hz, 2 H, CH_2CH$_3$), 4.11 (d, J = 13.9 Hz, 1 H, NCH_AH$_B$), 4.17 (d, J = 13.9 Hz, 1 H, NCH$_A$$H_B$), 4.09–4.19 (m, 1 H, CH), 5.17–5.24 (m, 2 H, HC=CH_2), 5.76–5.88 (m, 1 H, HC=CH$_2$), 7.25 (br s, 1 H, NH) ppm. ^{13}C NMR (75 MHz, $CDCl_3$): δ = 14.31 (CH_3), 27.05 (CH_2), 29.60 (CH_2), 40.41 (NCH_2), 56.48 (CH), 61.02 (OCH_2), 117.94 (HC=CH$_2$), 131.34 (HC=CH$_2$), 157.65 (NC=ON), 172.81 (C=O), 173.70 (C=O) ppm. MS (ES, Neg): m/z (%) = 239.3 (100) [M – H$^+$]. IR (KBr): $\tilde{\nu}_{max}$ = 1646 (C=C), 1719 (br C=O), 1775 (C=O), 3316 (NH) cm^{-1}. $C_{11}H_{16}N_2O_4$ (240.26): calcd. C 54.99, H 6.71, N 11.66; found C 54.63, H 6.73, N 11.63.

Methyl 3-(2,5-Dioxo-1-phenyl-imidazolidin-4-yl)propanoate (9h): Yield: 1.06 g (81%). M.p. 103–104 °C. ^{1}H NMR (300 MHz, $CDCl_3$): δ = 1.85–2.22 (m, 1 H, CHCH_AH$_B$), 2.25–2.39 (m, 1 H, CHCH$_A$$H_B$), 2.52–2.58 (m, 2 H, CH_2CO), 3.70 and 3.71 (2×s, 3 H, CH_3), 4.23–4.28 (m, 1 H, CH), 6.45–6.71 (1 H, br s, NH), 7.36–7.50 (5 H, m, Ph) ppm. ^{13}C NMR (75 MHz, $CDCl_3$): δ = 27.35 (CH_2), 29.66 (CH_2), 52.41 (OCH_3), 56.54 (CH), 126.59 (CH_{arom}), 128.75 (CH_{arom}), 129.53 (CH_{arom}), 131.74 ($C_{q.\ arom}$), 157.04 (NC=ON), 172.98 (C=O), 173.48 (C=O) ppm. MS (ES, Pos): m/z (%) = 263.3 (100) [M + H$^+$]. IR (KBr): $\tilde{\nu}_{max}$ = 1707 (C=O), 1725 (C=O), 1775 (C=O), 3233 (NH) cm^{-1}. $C_{13}H_{14}N_2O_4$ (262.26): calcd. C 59.54, H 5.38, N 10.68; found C 59.81, H 5.21, N 10.71.

Ethyl 3-(4-Allyl-2,5-dioxo-1-propylimidazolidin-4-yl)propanoate (13a): Yield: 0.86 g (61%). ^{1}H NMR (300 MHz, $CDCl_3$): δ = 0.92 (t, J = 7.4 Hz, 3 H, $CH_2CH_2CH_3$), 1.25 (t, J = 7.2 Hz, 3 H, CH_3), 1.63 (sext, J = 7.4 Hz, 2 H, $CH_2CH_2CH_3$), 2.03–2.29 (m, 4 H, $COCH_2CH_2$), 2.43 (dd, J = 14.0 Hz, J = 7.4 Hz, 1 H, CH_AH$_B$CH), 2.50 (dd, J = 14.0 Hz, J = 7.6 Hz, 1 H, CH$_A$$H_B$CH), 3.44 (t, J = 7.4 Hz, 2 H, CH_2CH$_2$CH$_3$), 4.13 (q, J = 7.2 Hz, 2 H, CH_2CH$_3$), 5.16 (s, 1 H, HC=CH_AH$_B$), 5.20 (d, J = 3.3 Hz, 1 H, HC=CH$_A$$H_B$), 5.59–5.73 (m, 1 H, H$C$=CH$_2$), 5.88 (br s, 1 H, NH) ppm. ^{13}C NMR (75 MHz, $CDCl_3$): δ = 11.23 ($CH_2CH_2CH_3$), 14.21 (CH_3), 21.52 ($CH_2CH_2CH_3$), 28.74 ($COCH_2$), 31.05 ($COCH_2CH_2$), 40.36 ($CH_2CH_2CH_3$), 41.57 (CCH_2), 61.04 (CH_2CH_3), 64.38 (C_q), 121.34 (HC=CH$_2$), 130.02 (HC=CH$_2$), 156.97 (NC=ON), 172.86 (C=OO), 175.29 (HNC=O) ppm. IR: $\tilde{\nu}_{max}$ = 1642 (C=C), 1713 (br C=O),

1775 (C=O) cm^{-1}. MS: *m/z* (%) = 283.3 (100) $[M+H^+]$. Chromatography [Hex/EtOAc (1:1)]: R_f = 0.42. $C_{14}H_{22}N_2O_4$ (282.34): calcd. C 59.56, H 7.85, N 9.92; found C 59.16, H 7.75, N 9.89.

Ethyl 3-(4-Allyl-2,5-dioxo-1-phenylimidazolidin-4-yl)propanoate (13b): Yield: 1.11 g (70%). ^{1}H NMR (300 MHz, $CDCl_3$): δ = 1.25 (t, *J* = 7.1 Hz, 3 H, CH_3), 2.12–2.30 (m, 2 H, $COCH_2CH_2$), 2.37–2.41 (m, 2 H, $COCH_2CH_2$), 2.51 (dd, *J* = 13.8 Hz, *J* = 7.2 Hz, 1 H, CH_AH_BCH), 2.62 (dd, *J* = 13.8 Hz, *J* = 7.7 Hz, 1 H, CH_AH_BCH), 4.15 (q, *J* = 7.1 Hz, 2 H, CH_2CH_3), 5.23 (s, 1 H, $HC=CH_AH_B$), 5.27 (d, *J* = 1,9 Hz, 1 H, $HC=CH_ACH_B$), 5.70–5.84 (m, 1 H, $HC=CH_2$), 6.09 (br s, 1 H, NH), 7.32–7.50 (m, 5 H, Ph) ppm. ^{13}C NMR (75 MHz, $CDCl_3$): δ = 14.24 (CH_3), 28.90 ($COCH_2$), 31.29 ($COCH_2CH_2$), 41.75 (CCH_2), 61.17 (CH_2CH_3), 64.49 (C_q), 121.73 ($HC=CH_2$), 126.32 ($CH_{arom.}$), 128.51 ($CH_{arom.}$), 129.24 ($CH_{arom.}$), 129.86 ($HC=CH_2$), 131.44 ($C_{q\ arom.}$) ppm. 155.76 (NC=ON), 172.84 (C=OO), 174.23 (HNC=O). IR: $\tilde{\nu}_{max}$ = 1719 (C=O), 1781 (C=O) cm^{-1}. MS: *m/z* (%) = 317.3 (100) $[M+H^+]$. Chromatography: Hex/EtOAc (1:1) R_f = 0.33. $C_{17}H_{20}N_2O_4$ (316.35): calcd. C 64.54, H 6.37, N 8.86; found C 64.42, H 6.46, N 8.76.

Ethyl 3-(4-Allyl-1-benzyl-2,5-dioxoimidazolidin-4-yl)propanoate (13c): Yield: 0.74 g (45%). ^{1}H NMR (300 MHz, $CDCl_3$): δ = 1.22 (t, *J* = 7.1 Hz, 3 H, CH_3), 2.05–2.20 (m, 4 H, $COCH_2CH_2$), 2.39 (dd, *J* = 14.0 Hz, *J* = 7.3 Hz, 1 H, CH_AH_BCH), 2.47 (dd, *J* = 14.0 Hz, *J* = 7.4 Hz, 1 H, CH_AH_BCH), 4.09 (q, *J* = 7.1 Hz, 2 H, CH_2CH_3), 4.62 (s, 2 H, CH_2Ph), 5.02–5.12 (m, 2 H, $HC=CH_2$), 5.46–5.60 (m, 1 H, $HC=CH_2$), 6.05 (br s, 1 H, NH), 7.23–7.37 (m, 5 H, Ph) ppm. ^{13}C NMR (75 MHz, $CDCl_3$): δ = 14.19 (CH_3), 28.67 ($COCH_2$), 31.08 ($COCH_2CH_2$), 41.52 (CCH_2), 42.35 (CH_2Ph), 61.01 (CH_2CH_3), 64.55 (C_q), 121.36 ($HC=CH_2$), 127.97 ($CH_{arom.}$), 128.55 ($CH_{arom.}$), 128.66 ($CH_{arom.}$), 129.83 ($HC=CH_2$), 136.03 ($C_{q\ arom.}$) ppm. 156.55 (NC=ON), 172.87 (C=OO), 175.04 (HNC=O). IR: $\tilde{\nu}_{max}$ = 1713 (C=O), 1774 (C=O) cm^{-1}. MS: *m/z* (%) = 331.2 (100) $[M+H^+]$. Chromatography [Hex/EtOAc (55:45)]: R_f = 0.22. $C_{18}H_{22}N_2O_4$ (330.38): calcd. C 65.44, H 6.71, N 8.48; found C 65.39, H 6.90, N 8.43.

Ethyl 3-[4-(2-Chloroprop-2-enyl)-2,5-dioxo-1-propylimidazolidin-4-yl]propanoate (13d): Yield: 1.05 g (66%). ^{1}H NMR (300 MHz, $CDCl_3$): δ = 0.93 (t, *J* = 7.4 Hz, 3 H, $CH_2CH_2CH_3$), 1.24 (t, *J* = 7.2 Hz, 1.5 H, CH_3), 1.25 (t, *J* = 7.2 Hz, 1.5 H, CH_3), 1.64 (sext, *J* = 7.4 Hz, 2 H, $CH_2CH_2CH_3$), 2.11–2.20 (m, 2 H, $COCH_2CH_2$), 2.23–2.35 (m, 2 H, $COCH_2CH_2$), 2.77 (d, *J* = 14.6 Hz, 1 H, CCH_AH_BC), 2.87 (d, *J* = 14.6 Hz, 1 H, CCH_AH_BCH), 3.45 (t, *J* = 7.4 Hz, 2 H, $CH_2CH_2CH_3$), 4.12 (q, *J* = 7.2 Hz, 1 H, $CH_AH_BCH_3$), 4.13 (q, *J* = 7.2 Hz, 2 H, $CH_AH_BCH_3$), 5.28 (s, 1 H, $HC=CH_AH_B$), 5.34 (d, *J* = 3.3 Hz, 1 H, $HC=CH_AH_B$), 6.48 (br s, 1 H, NH) ppm. ^{13}C NMR (75 MHz, $CDCl_3$): δ = 11.28 ($CH_2CH_2CH_3$), 14.18 (CH_3), 21.35 ($CH_2CH_2CH_3$), 28.54 ($COCH_2$), 31.34 ($COCH_2CH_2$), 40.53 ($CH_2CH_2CH_3$), 45.97 (CCH_2), 61.05 (CH_2CH_3), 63.80 (C_q), 118.37 ($HC=CH_2$), 135.25 ($HC=CH_2$), 156.90 (NC=ON), 172.55 (C=OO), 174.75 (HNC=O) ppm. IR: $\tilde{\nu}_{max}$ = 1633 (C=C), 1717 (br C=O), 1777 (C=O) cm^{-1}. MS: *m/z* (%) = 317.7/319.8 (100) $[M+H^+]$. Chromatography [Hex/EtOAc (6:4)]: R_f = 0.26. $C_{14}H_{21}ClN_2O_4$ (316.78): calcd. C 59.08, H 6.68, N 8.84; found C 58.97, H 6.78, N 8.74.

Ethyl 3-[4-(2-Methylprop-2-enyl)-2,5-dioxo-1-propylimidazolidin-4-yl]propanoate (13e): Yield: 0.93 g (63%). ^{1}H NMR (300 MHz, $CDCl_3$): δ = 0.92 (t, *J* = 7.4 Hz, 3 H, $CH_2CH_2CH_3$), 1.25 (t, *J* = 7.2 Hz, 1.5 H, CH_3), 1.26 (t, *J* = 7.2 Hz, 1.5 H, CH_3), 1.62 (sext, *J* = 7.4 Hz, 2 H, $CH_2CH_2CH_3$), 1.73 (s, 3 H, CCH_3), 2.08–2.28 (m, 4 H, $COCH_2CH_2$), 2.38 (d, *J* = 13.6 Hz, 1 H, CCH_AH_BC), 2.55 (d, *J* = 13.6 Hz, 1 H, CCH_AH_BCH), 3.43 (dt, *J* = 2.8 Hz, *J* = 7.4 Hz, 2 H, $CH_2CH_2CH_3$), 4.13 (q, *J* = 7.2 Hz, 2 H, CH_2CH_3), 4.79 (s, 1 H, $C=CH_AH_B$), 4.91 (d, *J* = 1.1 Hz, 1 H, $C=CH_AH_B$), 6.04 (br s, 1 H, NH) ppm. ^{13}C NMR (75 MHz, $CDCl_3$): δ = 11.26 ($CH_2CH_2CH_3$), 14.19 (CH_3), 21.42 ($CH_2CH_2CH_3$), 24.30 (CH_3), 28.76 ($COCH_2$), 31.83 ($COCH_2CH_2$), 40.42 ($CH_2CH_2CH_3$), 44.62 (CCH_2), 61.07 (CH_2CH_3), 64.79 (C_q), 116.98 ($C=CH_2$), 138.75 ($C=CH_2$), 157.39 (NC=ON), 172.87 (C=OO), 175.46 (HNC=O) ppm. IR: $\tilde{\nu}_{max}$ = 1646 (C=C), 1713 (br C=O), 1772 (C=O) cm^{-1}. MS: *m/z* (%) = 297.8 (100) $[M+H^+]$. Chromatography [Hex/EtOAc (4:6)]: R_f = 0.42. $C_{15}H_{24}N_2O_4$ (296.36): calcd. C 60.79, H 8.16, N 9.45; found C 60.54, H 8.00, N 9.36.

Typical Experimental Procedure for the Carbamoyllactam Formation from Pyroglutamates: The pyroglutamate ester (1.9 mmol) was dissolved in diethyl ether (10 mL, freshly distilled from Na metal) and the isocyanate (1.9 mmol) was added followed by NaH (2.09 mmol, washed with hexanes). The mixture was stirred at room temperature for 1 h. Then the reaction was quenched by addition of saturated aqueous NH_4Cl until the pH was neutral. The mixture was extracted with diethyl ether, and the organics were dried ($MgSO_4$) and filtered. The solvent was removed in vacuo.

(2*S*) Ethyl 1-Benzylcarbamoyl-5-oxopyrrolidine-2-carboxylate (10): Yield: 0.38 g (69%). $[a]_D$ = –6.0 (*c* = 3.0, CH_2Cl_2). ^{1}H NMR (300 MHz, $CDCl_3$): δ = 1.26 (t, *J* = 7.2 Hz, 3 H, CH_3), 1.96–2.06 (m, 1 H, $CHCH_AH_B$), 2.22–2.36 (m, 1 H, $CHCH_AH_B$), 2.51 (ddd, *J* = 3.4 Hz, *J* = 9.4 Hz, *J* = 18.2 Hz, 1 H, $COCH_AH_B$), 2.70 (dt, *J* = 8.9, *J* = 18.2 Hz, 1 H, CH_AH_B), 4.22 (q, *J* = 7.2 Hz, 2 H, OCH_2), 4.45 (dd, *J* = 5.9 Hz, *J* = 15.3 Hz, 1 H, NCH_AH_B), 4.50 (dd, *J* = 5.9 Hz, *J* = 15.3 Hz, 1 H, NCH_AH_B), 4.77 (dd, *J* = 2.8 Hz, *J* = 9.6 Hz, 1 H, CH), 7.20–7.33 (m, 5 H, Ph), 8.70 (br t, *J* = 5.9 Hz, 1 H, NH) ppm. ^{13}C NMR (75 MHz, $CDCl_3$): δ = 13.92 (CH_3), 21.07 ($CHCH_2$), 31.58 ($COCH_2$), 43.54 (NCH_2), 58.03 (CH), 61.54 (OCH_2), 127.19 (CH_{arom}), 127.29 (CH_{arom}), 128.45 (CH_{arom}), 137.97 ($C_{q,arom}$), 152.22 (NC=ON), 171.26 (COO), 176.37 (NC=O) ppm. MS (ES, Pos): *m/z* (%) = 291.3 (100) $[M+H^+]$. IR: $\tilde{\nu}_{max}$ = 1694 (C=O), 1723 (C=O), 1746 (C=O), 3314 (br NH) cm^{-1}. $C_{15}H_{18}N_2O_4$ (290.31): calcd. C 62.02, H 6.25, N 9.65; found C 61.69, H 5.93, N 9.68.

(2*S*) Ethyl 1-Fenylcarbamoyl-5-oxopyrrolidine-2-carboxylate (11): Yield: 0.47 g (89%). $[a]_D$ = –19.7 (*c* = 1.3, CH_2Cl_2). M.p. 104.2–107.6 °C. ^{1}H NMR (300 MHz, $CDCl_3$): δ = 1.3 (t, *J* = 7.2 Hz, 3 H, CH_3), 2.11 (dddd, *J* = 2.9 Hz, *J* = 3.2 Hz, *J* = 9.6 Hz, *J* = 13.4 Hz, 1 H, $CHCH_AH_B$), 2.39 (dddd, *J* = 9.7 Hz, *J* = 9.7 Hz, *J* = 9.8 Hz, *J* = 13.4 Hz, 1 H, $CHCH_AH_B$), 2.65 (ddd, *J* = 3.2 Hz, *J* = 9.7 Hz, *J* = 17.7 Hz, 1 H, $COCH_AH_B$), 2.84 (ddd, *J* = 9.6 Hz, *J* = 9.8 Hz, *J* = 17.7 Hz, 1 H, $COCH_AH_B$), 4.26 (q, *J* = 7.2 Hz, 2 H, OCH_2), 4.87 (dd, *J* = 2.9 Hz, *J* = 9.7 Hz, 1 H, CH), 7.10–7.53 (m, 5 H, Ph), 10.42 (br s, NH) ppm. ^{13}C NMR (75 MHz, $CDCl_3$): δ = 14.11 (CH_3), 21.13 ($CHCH_2$), 31.96 ($COCH_2$), 58.20 (CH), 61.88 (OCH_2), 120.16 (CH_{arom}), 124.27 (CH_{arom}), 129.00 (CH_{arom}), 137.17 ($C_{q,arom}$), 149.57 (NC=ON), 171.19 (COO), 176.71 (NCO) ppm. MS (ES, Pos): *m/z* (%) = 277.2 (100) $[M+H^+]$. IR: $\tilde{\nu}_{max}$ = 1702 (C=O), 1717 (C=O), 1739 (C=O), 3300 (br NH) cm^{-1}. $C_{14}H_{16}N_2O_4$ (276.11): calcd. C 60.86, H 5.84, N 10.14; found C 61.48, H 5.69, N 10.21.

Typical Experimental Procedure for the *N*-Alkylation of Ethyl 3-[1,4-Dialkyl-2,5-dioxo-1-imidazolidin-4-yl]propanoates (13): The hydantoin (**13**) (3 mmol) was dissolved in acetone (10 mL) and the alkyl halide (9 mmol) was added followed by K_2CO_3 (15 mmol, finely ground). The mixture was refluxed until TLC analysis showed that all starting material was consumed. The mixture was filtered and the solvent was removed in vacuo. If necessary the

residue was purified by flash chromatography (silica gel; hexane/EtOAc).

Ethyl 3-(3,4-Diallyl-2,5-dioxo-1-propylimidazolidin-4-yl)propanoate (14a): Yield: 0.97 g (100%). ^{1}H NMR (300 MHz, $CDCl_3$): δ = 0.91 (t, J = 7.4 Hz, 3 H, $CH_2CH_2CH_3$), 1.24 (t, J = 7.2 Hz, 3 H, CH_3), 1.61 (sext, J = 7.3 Hz, 2 H, $CH_2CH_2CH_3$), 2.05–2.20 (m, 4 H, $COCH_2CH_2$), 2.46–2.60 (m, 2 H, CCH_2), 3.44 (dt, J = 7.4 Hz, J = 1.7 Hz, 2 H, NCH_2CH_2), 3.82 (dd, J = 15.6 Hz, J = 6.9 Hz, 1 H, NCH_AH_BCH), 4.01 (dd, J = 15.6 Hz, J = 6.5 Hz, 1 H, NCH_AH_BCH), 4.11 (q, J = 7.2 Hz, 2 H, CH_2CH_3), 5.10–5.35 (m, 4 H, 2×HC=CH_2), 5.42–5.56 (m, 1 H, HC=CH_2), 5.85–5.99 (m, 1 H, HC=CH_2) ppm. ^{13}C NMR (75 MHz, $CDCl_3$): δ = 11.35 ($CH_2CH_2CH_3$), 14.22 (CH_3), 21.57 ($CH_2CH_2CH_3$), 28.33 ($COCH_2$), 29.77 ($COCH_2CH_2$), 39.54 (CCH_2CH), 40.58 ($CH_2CH_2CH_3$), 42.87 (NCH_2CH), 60.90 (CH_2CH_3), 68.09 (C_q), 118.93 (HC=CH_2), 121.01 (HC=CH_2), 129.88 (HC=CH_2), 133.32 (HC=CH_2), 156.39 (NC=ON), 172.05 (C=OO), 174.19 (NC=O) ppm. IR: $\tilde{\nu}_{max}$ = 1643 (C=C), 1709 (C=O), 1735 (C=O), 1768 (C=O) cm^{-1}. MS: m/z (%) = 323.3 (100) [M + H$^+$]. Chromatography [Hex/EtOAc (6:4)]: R_f = 0.52. $C_{17}H_{26}N_2O_4$ (322.40): calcd. C 63.33, H 8.13, N 8.69; found C 62.98, H 8.01, N 8.66.

Ethyl 3-(3,4-Diallyl-2,5-dioxo-1-phenylimidazolidin-4-yl)propanoate (14b): Yield: 1.07 g (100%). ^{1}H NMR (300 MHz, $CDCl_3$): δ = 1.24 (t, J = 7.1 Hz, 3 H, CH_3), 2.14–2.38 (m, 4 H, $COCH_2CH_2$), 2.60 (dd, J = 14.2 Hz, J = 6.5 Hz, 1 H, CCH_AH_B), 2.67 (dd, J = 14.2 Hz, J = 8.0 Hz, 1 H, CCH_AH_B), 3.91 (dd, J = 15.4 Hz, J = 6.9 Hz, 1 H, NCH_AH_BCH), 4.09 (dd, J = 15.4 Hz, J = 6.6 Hz, 1 H, NCH_AH_BCH), 4.13 (q, J = 7.1 Hz, 2 H, CH_2CH_3), 5.19–5.40 (m, 4 H, 2×HC=CH_2), 5.57–5.71 (m, 1 H, HC=CH_2), 5.92–6.06 (m, 1 H, HC=CH_2), 7.32–7.48 (m, 5 H, Ph) ppm. ^{13}C NMR (75 MHz, $CDCl_3$): δ = 14.24 (CH_3), 28.48 ($COCH_2$), 29.97 ($COCH_2CH_2$), 39.78 (CCH_2CH), 43.16 (NCH_2CH), 61.00 (CH_2CH_3), 68.18 (C_q), 119.28 (HC=CH_2), 121.42 (HC=CH_2), 126.22 ($CH_{arom.}$), 128.35 ($CH_{arom.}$), 129.13 ($CH_{arom.}$), 129.77 (HC=CH_2), 131.52 ($C_{q\ arom.}$) ppm. 133.04 (HC=CH_2), 155.22 (NC=ON), 171.99 (C=OO), 173.23 (NC=O). IR: $\tilde{\nu}_{max}$ = 1642 (C=C), 1717 (br C=O), 1772 (C=O) cm^{-1}. MS: m/z (%) = 357.2 (100) [M + H$^+$]. $C_{20}H_{24}N_2O_4$ (356.42): calcd. C 67.40, H 6.79, N 7.86; found C 67.08, H 6.74, N 7.84.

Ethyl 3-[4-Allyl-1-benzyl-3-(2-chloroprop-2-enyl)-2,5-dioxo-1-phenylimidazolidin-4-yl]propanoate (14c): Yield: 0.85 g (70%). ^{1}H NMR (300 MHz, $CDCl_3$): δ = 1.22 (t, J = 7.0 Hz, 3 H, CH_3), 2.00–2.28 (m, 4 H, $COCH_2CH_2$), 2.50 (dd, J = 14.5 Hz, J = 7.2 Hz, 1 H, CCH_AH_B), 2.58 (dd, J = 14.5 Hz, J = 7.3 Hz, 1 H, CCH_AH_B), 3.90 (d, J = 15.8 Hz, 1 H, NCH_AH_BC), 4.09 (q, J = 7.0 Hz, 2 H, CH_2CH_3), 4.27 (d, J = 15.8 Hz, 1 H, NCH_AH_BC), 4.62 (d, J = 14.4 Hz, 1 H, NCH_AH_BPh), 4.68 (d, J = 14.4 Hz, 1 H, NCH_AH_BPh), 4.93–5.10 (m, 2 H, HC=CH_2), 5.28–5.39 (m, 1 H, HC=CH_2), 5.42 (d, J = 1.8 Hz, 1 H, C=CH_AH_B), 5.50 (d, J = 1.8 Hz, 1 H, C=CH_AH_B), 7.25–7.39 (m, 5 H, Ph) ppm. ^{13}C NMR (75 MHz, $CDCl_3$): δ = 14.22 (CH_3), 28.33 ($COCH_2$), 29.95 ($COCH_2CH_2$), 39.54 (CCH_2CH), 42.79 (NCH_2Ph), 46.50 (NCH_2C), 60.84 (CH_2CH_3), 68.38 (C_q), 116.72 (C=CH_2), 121.28 (HC=CH_2), 128.06 ($CH_{arom.}$), 128.67 ($CH_{arom.}$), 128.75 ($CH_{arom.}$), 129.44 (HC=CH_2), 135.88 ($C_{q\ arom.}$) ppm. 137.45 (CCl), 156.52 (NC=ON), 172.03 (C=OO), 173.73 (NC=O). IR: $\tilde{\nu}_{max}$ = 1635 (C=C), 1713 (br C=O), 1772 (C=O) cm^{-1}. MS: m/z (%) = 405.2 (100) [M + H$^+$], 407.2 (29) [M + H$^+$]. Chromatography [Hex/EtOAc (7:3)]: R_f = 0.35. $C_{21}H_{25}ClN_2O_4$ (404.89): calcd. C 62.30, H 6.22, N 6.92; found C 62.55, H 6.14, N 6.86.

Ethyl 3-[4-Allyl-3-(2-methylprop-2-enyl)-2,5-dioxo-1-phenylimidazolidin-4-yl]propanoate (14d): Yield: 1.11 g (100%). ^{1}H NMR (300 MHz, $CDCl_3$): δ = 1.24 (t, J = 7.2 Hz, 3 H, CH_3), 1.86 (s, 3 H, CCH_3), 2.18–2.38 (m, 4 H, $COCH_2CH_2$), 2.63–2.67 (m, 2 H, CH_2CH), 3.86 (d, J = 15.3 Hz, 1 H, NCH_AH_BC), 4.03 (d, J = 15.3 Hz, 1 H, NCH_AH_BC), 4.12 (q, J = 7.2 Hz, 2 H, CH_2CH_3), 4.96 (s, 1 H, C=CH_AH_B), 5.02 (s, 1 H, C=CH_AH_B), 5.19 (d, J = 3.9 Hz, 1 H, HC=CH_AH_B), 5.24 (d, J = 10.7 Hz, 1 H, HC=CH_AH_B), 5.55–5.69 (m, 1 H, HC=CH_2), 7.31–7.48 (m, 5 H, Ph) ppm. ^{13}C NMR (75 MHz, $CDCl_3$): δ = 14.23 (CH_3), 20.89 (CCH_3), 28.53 ($COCH_2$), 29.95 ($COCH_2CH_2$), 39.72 (CCH_2CH), 46.41 (NCH_2C), 60.97 (CH_2CH_3), 68.44 (C_q), 114.96 (C=CH_2), 121.42 (HC=CH_2), 126.17 ($CH_{arom.}$), 128.32 ($CH_{arom.}$), 129.12 ($CH_{arom.}$), 129.83 (HC=CH_2), 131.65 ($C_{q\ arom.}$) ppm. 141.50 (C=CH_2), 155.80 (NC=ON), 172.00 (C=OO), 173.33 (NC=O). IR: $\tilde{\nu}_{max}$ = 1717 (br C=O), 1773 (C=O) cm^{-1}. MS: m/z (%) = 371.2 (100) [M + H$^+$]. $C_{21}H_{26}N_2O_4$ (370.44): calcd. C 68.09, H 7.07, N 7.56; found C 67.93, H 6.97, N 7.55.

Ethyl 3-{4-Allyl-1-benzyl-3-[2-(chloromethyl)prop-2-enyl]-2,5-dioxoimidazolidin-4-yl}propanoate (14e): Yield: 0.90 g (72%). ^{1}H NMR (300 MHz, $CDCl_3$): δ = 1.22 (t, J = 7.1 Hz, 3 H, CH_3), 2.01–2.20 (m, 4 H, $COCH_2CH_2$), 2.48 (dd, J = 14.5 Hz, J = 7.4 Hz, 1 H, CCH_AH_BCH), 2.56 (dd, J = 14.5 Hz, J = 6.9 Hz, 1 H, CCH_AH_BCH), 3.89–4.12 (m, 4 H, NCH_2CCH_2Cl), 4.09 (q, J = 7.1 Hz, 2 H, CH_2CH_3), 4.64 (s, 2 H, NCH_2Ph), 4.79–5.08 (m, 2 H, HC=CH_2), 5.23 (s, 1 H, C=CH_AH_B), 5.23–5.37 (m, 1 H, HC=CH_2), 5.37 (s, 1 H, C=CH_AH_B), 7.25–7.40 (m, 5 H, Ph) ppm. ^{13}C NMR (75 MHz, $CDCl_3$): δ = 14.22 (CH_3), 28.32 ($COCH_2$), 29.71 ($COCH_2CH_2$), 39.52 (CCH_2CH), 42.21 (NCH_2CH), 42.73 (NCH_2Ph), 45.98 (CH_2Cl), 60.89 (CH_2CH_3), 68.55 (C_q), 118.50 (C=CH_2), 121.27 (HC=CH_2), 128.06 ($CH_{arom.}$), 128.69 ($CH_{arom.}$), 128.78 ($CH_{arom.}$), 129.51 (HC=CH_2), 135.94 ($C_{q\ arom.}$) ppm. 140.87 (C=CH_2), 156.81 (NC=ON), 171.87 (C=OO), 173.94 (NC=O). IR: $\tilde{\nu}_{max}$ = 1710 (br C=O), 1769 (C=O) cm^{-1}. MS: m/z (%) = 419.2/421.3 (100) [M + H$^+$]. Chromatography [Hex/EtOAc (6:4)]: R_f = 0.63. $C_{22}H_{27}N_2O_4$ (418.91): calcd. C 63.08, H 6.50, N 6.69; found C 62.94, H 6.55, N 6.72.

Ethyl 2-{[5-Allyl-3-benzyl-5-(3-ethoxy-3-oxopropyl)-2,4-dioxoimidazolidin-1-yl]methyl}acrylate (14f): Yield: 0.60 g (45%). ^{1}H NMR (300 MHz, $CDCl_3$): δ = 1.16–1.32 (m, 6 H, 2×CH_2CH_3), 1.94–2.15 (m, 4 H, $COCH_2CH_2$), 2.60 (dd, J = 14.2 Hz, J = 6.5 Hz, 1 H, CCH_AH_B), 2.52 (d, J = 7.2 Hz, 2 H, CCH_2), 4.02–4.16 (m, 3 H, NCH_AH_B + CH_2CH_3), 4.19–4.26 (m, 3 H, NCH_AH_B + CH_2CH_3), 4.64 (s, 2 H, CH_2Ph), 4.91–5.07 (m, 2 H, HC=CH_2), 5.22–5.36 (m, 1 H, HC=CH_2), 5.99 (d, J = 0.8 Hz, 1 H, C=CH_AH_B), 6.42 (s, 1 H, C=CH_AH_B), 7.24–7.39 (m, 5 H, Ph) ppm. ^{13}C NMR (75 MHz, $CDCl_3$): δ = 14.21 (2×CH_3), 28.36 ($COCH_2$), 29.75 ($COCH_2CH_2$), 39.40 (CCH_2CH), 39.75 (NCH_2CH), 42.67 (CH_2Ph), 60.79 (CH_2CH_3), 61.36 (CH_2CH_3), 68.43 (C_q), 121.09 (HC=CH_2), 128.00 ($CH_{arom.}$), 128.64 ($CH_{arom.}$), 128.73 ($CH_{arom.}$), 129.60 (C=CH_2), 129.67 (HC=CH_2), 136.02 ($C_{q\ arom.}$) ppm. 156.64 (NC=ON), 165.99 (CC=O), 171.85 (C=OO), 174.00 (NC=O). IR: $\tilde{\nu}_{max}$ = 1662 (C=C), 1711 (br C=O), 1770 (C=O) cm^{-1}. MS: m/z (%) = 443.2 (100) [M + H$^+$]. Chromatography [Hex/EtOAc/ether (9:1:2)]: R_f = 0.07. $C_{24}H_{30}N_2O_4$ (442.50): calcd. C 65.14, H 6.83, N 6.33; found C 65.09, H 6.85, N 6.23.

Ethyl 3-[3-Allyl-4-(2-chloroprop-2-enyl)-2,5-dioxo-1-propylimidazolidin-4-yl]propanoate (14g): Yield: 0.89 g (83%). ^{1}H NMR (300 MHz, $CDCl_3$): δ = 0.92 (t, J = 7.4 Hz, 3 H, $CH_2CH_2CH_3$), 1.24 (t, J = 7.1 Hz, 1.5 H, CH_3), 1.25 (t, J = 7.1 Hz, 1.5 H, CH_3), 1.63 (sext, J = 7.4 Hz, 2 H, $CH_2CH_2CH_3$), 2.01–2.25 (m, 4 H, $COCH_2CH_2$), 2.80 (d, J = 14.9 Hz, 1 H, CCH_AH_B), 2.95 (d, J = 14.9 Hz, 1 H, CCH_AH_B), 3.42 (dt, J = 7.4 Hz, J = 11.8 Hz, 1 H, $NCH_AH_BCH_2$), 3.48 (dt, J = 7.4 Hz, J = 11.8 Hz, 1 H, $NCH_AH_BCH_2$), 3.65 (dd, J = 15.6 Hz, J = 7.8 Hz, 1 H,

NCH_AH$_B$CH), 4.11 (q, J = 7.1 Hz, 2 H, CH_2CH$_3$), 4.28 (dd, J = 15.6 Hz, J = 5.5 Hz, 1 H, NCH$_A$$H_B$CH), 5.19–5.35 (m, 4 H, C=CH_2 + HC=CH_2), 5.89–6.02 (m, 1 H, HC=CH$_2$) ppm. ^{13}C NMR (75 MHz, CDCl$_3$): δ = 11.32 (CH$_2$CH$_2$$CH_3$), 14.19 (CH$_3$), 21.32 (CH$_2$$CH_2CH_3$), 27.92 (CO$CH_2$), 30.32 (COCH$_2$$CH_2$), 40.70 ($CH_2CH_2CH_3$), 43.54 (C$CH_2$C + NCH$_2$CH), 60.84 ($CH_2CH_3$), 67.49 (C$_q$), 118.14 (C=$CH_2$), 119.02 (HC=$CH_2$), 133.13 (H$C$=CH$_2$), 135.09 ($C$=CH$_2$), 156.14 (NC=ON), 171.73 (C=OO), 173.45 (NC=O) ppm. IR: $\tilde{\nu}_{max}$ = 1632 (C=C), 1709 (C=O), 1735 (C=O), 1770 (C=O) cm^{-1}. MS: m/z (%) = 357.7/359.7 (100) [M + H$^+$]. Chromatography [Hex/EtOAc (2:1)]: R_f = 0.43. C$_{17}$H$_{25}$ClN$_2$O$_4$ (356.84): calcd. C 57.22, H 7.06, N 7.85; found C 56.89, H 6.90, N 7.83.

Ethyl 3-[3-Allyl-4-(2-methylprop-2-enyl)-2,5-dioxo-1-propylimidazolidin-4-yl]propanoate (14h): Yield: 1.01 g (100%). ^{1}H NMR (300 MHz, CDCl$_3$): δ = 0.91 (t, J = 7.4 Hz, 3 H, CH$_2$CH$_2$CH_3), 1.24 (t, J = 7.2 Hz, 3 H, CH$_3$), 1.61 (sext, J = 7.4 Hz, 2 H, CH$_2$CH_2CH$_3$), 1.63 (s, 3 H, CCH$_3$), 1.96–2.22 (m, 4 H, COCH_2CH_2), 2.49 (d, J = 14.4 Hz, 1 H, CCH_AH$_B$), 2.57 (d, J = 14.4 Hz, 1 H, CCH$_A$$H_B$), 3.41 (dt, J = 7.4 Hz, J = 13.5 Hz, 1 H, NCH_AH$_B$CH$_2$), 3.45 (dt, J = 7.4 Hz, J = 13.5 Hz, 1 H, NCH$_A$$H_BCH_2$), 3.61 (dd, J = 15.4 Hz, J = 7.7 Hz, 1 H, NCH_AH$_B$CH), 4.11 (q, J = 7.2 Hz, 2 H, CH_2CH$_3$), 4.21 (ddt, J = 15.4 Hz, J = 5.5 Hz, J = 1.4 Hz, 1 H, NCH$_A$$H_B$CH), 4.72 (d, J = 0.8 Hz, 1 H, C=CH_AH$_B$), 4.86 (t, J = 1.5 Hz, 1 H, C=CH$_A$$H_B$), 5.20 (dd, J = 9.9 Hz, J = 0.8 Hz, 1 H, HC=CH_AH$_B$), 5.31 (dq, J = 17.0 Hz, J = 1.4 Hz, 1 H, HC=CH$_A$$H_B$), 5.87–6.00 (m, 1 H, HC=CH$_2$) ppm. ^{13}C NMR (75 MHz, CDCl$_3$): δ = 11.34 (CH$_2$CH$_2$$CH_3$), 14.24 (CH$_3$), 21.45 (CH$_2$$CH_2CH_3$), 23.67 (C$CH_3$), 28.13 (CO$CH_2$), 30.88 (COCH$_2$$CH_2$), 40.58 ($CH_2CH_2CH_3$), 42.45 (C$CH_2$C), 43.23 (N$CH_2$CH), 60.82 ($CH_2CH_3$), 67.97 (C$_q$), 116.58 (C=$CH_2$), 118.96 (HC=$CH_2$), 133.19 (H$C$=CH$_2$), 138.77 ($C$=CH$_2$), 156.32 (NC=ON), 172.00 (C=OO), 174.39 (NC=O) ppm. IR: $\tilde{\nu}_{max}$ = 1645 (C=C), 1708 (C=O), 1735 (C=O), 1767 (C=O) cm^{-1}. MS: m/z (%) = 337.8 (100) [M + H$^+$]. C18 H$_{28}$N$_2$O$_4$ (336.43): calcd. C 64.26, H 8.39, N 8.33; found C 64.22, H 8.55, N 8.28.

Typical Experimental Procedure for the Synthesis of Ethyl 3-(2,6-Dialkyl-1,3-dioxo-2,3,5,8-tetrahydroimidazo[1,5-*a*]pyridin-8a(1*H*)-yl)propanoates (15): The hydantoin **14** (0.6 mmol) was dissolved in CH$_2$Cl$_2$ (10 mL, freshly distilled from CaH$_2$) and the second generation Grubbs' catalyst (0.03 mmol) was added. The mixture was refluxed under N$_2$ for 4 h. The residue was adsorbed onto silica gel by removal of the solvent in vacuo and purified by flash chromatography (silica gel; hexane/EtOAc).

Ethyl 3-[1,3-Dioxo-2-propyl-2,3,5,8-tetrahydroimidazo[1,5-*a*]pyridin-8a(1*H*)-yl]propanoate (15a): Yield: 0.16 g (93%). ^{1}H NMR (300 MHz, CDCl$_3$): δ = 0.93 (t, J = 7.4 Hz, 3 H, CH$_3$ pr), 1.24 (t, J = 7.1 Hz, 3 H, CH$_2$CH_3), 1.66 (sext, J = 7.4 Hz, 2 H, NCH$_2$CH_2), 2.05–2.33 (m, 6 H, COCH_2CH_2 and CCH_2), 3.49 (dt, J = 7.4 Hz, J = 1.6 Hz, 2 H, NCH_2CH$_2$), 3.56 (d, J = 18.2 Hz + small splitting, 1 H, NCH_AH$_B$), 4.10 (q, J = 7.1 Hz, 2 H, CH_2CH$_3$), 4.41 (d, J = 18.2 Hz + small splitting, 1 H, NCH$_A$$H_B$), 5.78 (t, J = 1.9 Hz + small splitting, 2 H, HC=CH) ppm. ^{13}C NMR (75 MHz, CDCl$_3$): δ = 11.22 (CH$_3$ pr), 14.15 (CH$_2$$CH_3$), 21.53 (CH$_2$ pr), 28.43 (COCH$_2$), 28.80 (COCH$_2$$CH_2$), 31.65 (C$CH_2$CH), 37.71 (NCH$_2$), 40.37 (NCH$_2$ pr), 60.28 (C$_q$), 60.87 (CH$_2$CH$_3$), 121.59 (CH), 123.27 (CH), 155.15 (NC=ON), 172.39 (C=OO), 175.74 (NC=O) ppm. IR: $\tilde{\nu}_{max}$ = 1656 (C=C), 1709 (br C=O), 1771 (C=O) cm^{-1}. MS: m/z (%) = 295.2 (100) [M + H$^+$]. Chromatography [Hex/EtOAc (6:4)]: R_f = 0.25. C$_{15}$H$_{22}$N$_2$O$_4$ (294.35): calcd. C 61.21, H 7.53, N 9.52; found C 60.92, H 7.62, N 9.48.

Ethyl 3-[1,3-Dioxo-2-phenyl-2,3,5,8-tetrahydroimidazo[1,5-*a*]pyridin-8a(1*H*)-yl]propanoate (15b): Yield: 0.17 g (88%). M.p. 110–113 °C. ^{1}H NMR (300 MHz, CDCl$_3$): δ = 1.23 (t, J = 7.2 Hz, 3 H, CH$_2$CH_3), 2.19–2.56 (m, 6 H, COCH_2CH_2 and CCH_2), 3.65 (d, J = 19.9 Hz + small splitting, 1 H, NCH_AH$_B$), 4.12 (q, J = 7.2 Hz, 2 H, CH_2CH$_3$), 4.48 (d, J = 19.9 Hz, 1 H, NCH$_A$$H_B$), 5.78 (m, 1 H, CH), 7.35–7.50 (m, 5 H, Ph) ppm. ^{13}C NMR (75 MHz, CDCl$_3$): δ = 14.22 (CH$_2$$CH_3$), 28.94 (CO$CH_2$), 28.99 (COCH$_2$$CH_2$), 31.83 (C$CH_2$CH), 38.04 (NCH$_2$), 60.39 (C$_q$), 61.08 ($CH_2CH_3$), 121.71 (CH), 123.25 (CH), 126.25 (CH$_{arom.}$), 128.32 (CH$_{arom.}$), 129.16 (CH$_{arom.}$), 131.65 (C$_{q\ arom.}$), 153.99 (NC=ON), 172.42 (C=OO), 174.62 (NC=O) ppm. IR: $\tilde{\nu}_{max}$ = 1721 (br C=O), 1775 (C=O) cm^{-1}. MS: m/z (%) = 329.2 (100) [M + H$^+$]. Chromatography [Hex/EtOAc (7:3)]: R_f = 0.21. C$_{18}$H$_{20}$N$_2$O$_4$ (328.36): calcd. C 65.84, H 6.14, N 8.53; found C 65.70, H 6.34, N 8.45.

Ethyl 3-[2-Benzyl-6-chloro-1,3-dioxo-2,3,5,8-tetrahydroimidazo[1,5-*a*]pyridin-8a(1*H*)-yl]propanoate (15c): Instead of refluxing in CH$_2$Cl$_2$, the reaction is refluxed in dry benzene for 16 hours. Yield: 0.17 g (75%). ^{1}H NMR (300 MHz, CDCl$_3$): δ = 1.20 (t, J = 7.1 Hz, 3 H, CH$_3$), 2.00–2.33 (m, 4 H, COCH_2CH_2), 2.39–2.41 (m, 2 H, CH_2CH), 3.63 (dq, J = 17.9 Hz, J = 2.6 Hz, 1 H, NCH_AH$_B$CCl), 4.07 (q, J = 7.1 Hz, 2 H, CH_2CH$_3$), 4.49 (dq, J = 17.9 Hz, J = 2.2 Hz, 1 H, NCH$_A$$H_B$CCl), 4.67 (s, 2 H, NC$H_2$Ph), 5.86 (dq, J = 1.6 Hz, J = 3.5 Hz, 1 H, CH), 7.27–7.39 (m, 5 H, Ph) ppm. ^{13}C NMR (75 MHz, CDCl$_3$): δ = 14.19 (CH$_3$), 28.48 (COCH$_2$), 28.71 (COCH$_2$$CH_2$), 32.61 (C$CH_2$CH), 41.87 (NCH$_2$C), 42.64 (N$CH_2$Ph), 60.07 (C$_q$), 61.02 ($CH_2CH_3$), 119.28 (CH), 127.31 (CCl), 128.14 (CH$_{arom.}$), 128.52 (CH$_{arom.}$), 128.83 (CH$_{arom.}$), 135.91 (C$_{q\ arom.}$), 154.51 (NC=ON), 172.20 (C=OO), 174.49 (NC=O) ppm. IR: $\tilde{\nu}_{max}$ = 1660 (C=C), 1714 (br C=O), 1775 (C=O) cm^{-1}. MS: m/z (%) = 377.2/379.2 (100) [M + H$^+$]. Chromatography [Hex/EtOAc (7:3)]: R_f = 0.29. C$_{19}$H$_{21}$ClN$_2$O$_4$ (376.83): calcd. C 60.56, H 5.62, N 7.43; found C 60.44, H 5.74, N 7.37.

Ethyl 3-[6-Methyl-1,3-dioxo-2-phenyl-2,3,5,8-tetrahydroimidazo[1,5-*a*]pyridin-8a(1*H*)-yl]propanoate (15d): Yield: 0.16 g (79%). ^{1}H NMR (300 MHz, CDCl$_3$): δ = 1.23 (t, J = 7.2 Hz, 3 H, CH$_2$CH_3), 1.76 (s, 3 H, CCH_3), 2.19–2.52 (m, 6 H, COCH_2CH_2 and CCH_2), 3.50 (d, J = 18.0 Hz, 1 H, NCH_AH$_B$), 4.12 (q, J = 7.2 Hz, 2 H, CH_2CH$_3$), 4.34 (d, J = 18.0 Hz, 1 H, NCH$_A$$H_B$), 5.51 (t, J = 1.9 Hz, 1 H, CH), 7.35–7.49 (m, 5 H, Ph) ppm. ^{13}C NMR (75 MHz, CDCl$_3$): δ = 14.22 (CH$_2$$CH_3$), 20.21 (C$CH_3$), 28.79 (CO$CH_2$), 29.05 (COCH$_2$$CH_2$), 31.89 (C$CH_2$CH), 41.39 (NCH$_2$), 60.29 (C$_q$), 61.07 ($CH_2CH_3$), 116.05 (CH), 126.26 (CH$_{arom.}$), 128.31 (CH$_{arom.}$), 129.16 (CH$_{arom.}$), 130.57 (CCH$_3$), 131.68 (C$_{q\ arom.}$), 153.96 (NC=ON), 172.51 (C=OO), 174.74 (NC=O) ppm. IR: $\tilde{\nu}_{max}$ = 1721 (br C=O), 1775 (C=O) cm^{-1}. MS: m/z (%) = 343.2 (100) [M + H$^+$]. Chromatography [Hex/EtOAc (7:3)]: R_f = 0.29. C$_{19}$H$_{22}$N$_2$O$_4$ (342.39): calcd. C 66.65, H 6.48, N 8.18; found C 66.25, H 6.39, N 8.17.

Ethyl 3-[2-Benzyl-6-(chloromethyl)-1,3-dioxo-2,3,5,8-tetrahydroimidazo[1,5-*a*]pyridin-8a(1*H*)-yl]propanoate (15e): Yield: 0.20 g (85%). ^{1}H NMR (300 MHz, CDCl$_3$): δ = 1.20 (t, J = 7.1 Hz, 3 H, CH$_2$CH_3), 2.05–2.21 (m, 4 H, COCH_2CH_2), 2.23–2.43 (m, 2 H, CCH$_2$), 3.59 (dq, J = 18.0 Hz, J = 2.4 Hz, 1 H, NCH_AH$_B$), 4.05 (s, 2 H, CH$_2$Cl), 4.07 (q, J = 7.1 Hz, 2 H, CH_2CH$_3$), 4.54 (d, J = 18.0 Hz, 1 H, NCH$_A$$H_B$), 4.67 (d, J = 15.0 Hz, 1 H, NCH_AH$_B$Ph), 4.68 (d, J = 15.0 Hz, 1 H, NCH$_A$$H_B$Ph), 5.88 (q-like, J = 2.4 Hz, 1 H, CH), 7.28–7.41 (m, 5 H, Ph) ppm. ^{13}C NMR (75 MHz, CDCl$_3$): δ = 14.21 (CH$_2$$CH_3$), 28.62 (CO$CH_2$), 28.73 (COCH$_2$$CH_2$), 31.58 (C$CH_2$CH), 38.38 (NCH$_2$), 42.56 (N$CH_2$Ph), 45.83 (CH$_2$Cl), 60.30 (C$_q$), 60.97 ($CH_2CH_3$), 121.85 (CH), 128.06 (CH$_{arom.}$), 128.55 (CH$_{arom.}$), 128.80 (CH$_{arom.}$), 131.45 (CCH$_2$Cl), 136.08 (C$_{q\ arom.}$), 154.77 (NC=ON), 172.33 (C=OO), 175.00 (NC=O) ppm. IR: $\tilde{\nu}_{max}$ = 1713 (br C=O), 1771 (C=O) cm^{-1}. MS:

m/*z* (%) = 391.2/393.2 (100) [M + H$^+$]. Chromatography [Hex/EtOAc (7:3)]: R_f = 0.18. $C_{20}H_{23}ClN_2O_4$ (390.86): calcd. C 61.46, H 5.93, N 7.17; found C 61.19, H 5.85, N 7.13.

Ethyl 2-Benzyl-8a-(3-ethoxy-3-oxopropyl)1,3-dioxo-1,2,3,5,8,8a-hexahydroimidazo[1,5-*a*]pyridine-6-carboxylate (15f): Instead of the second generation Grubbs' catalyst, the second generation Hoveyda-Grubbs' catalyst is used for this reaction. Yield: 0.14 g (55%). ^{1}H NMR (300 MHz, $CDCl_3$): δ = 1.20 (t, *J* = 7.2 Hz, 3 H, CH_2CH_3), 1.30 (t, *J* = 7.0 Hz, 3 H, CH_2CH_3), 2.04–2.17 (m, 4 H, $COCH_2CH_2$), 2.41 (dq, *J* = 18.4 Hz, *J* = 2.8 Hz, 1 H, CCH_AH_B), 2.54 (dd, *J* = 18.4 Hz, *J* = 5.5 Hz, 1 H, CCH_AH_B), 3.73 (ddt, *J* = 18.7 Hz, *J* = 3.7 Hz, *J* = 4.1 Hz, 1 H, NCH_AH_B), 4.07 (q, *J* = 7.2 Hz, 2 H, CH_2CH_3), 4.21 (dq, *J* = 10.6 Hz, *J* = 7.0 Hz, 1 H, $CH_AH_BCH_3$), 4.25 (dq, *J* = 10.6 Hz, *J* = 7.1 Hz, 1 H, $CH_AH_BCH_3$), 4.68 (s, 2 H, NCH_2Ph), 4.70 (dt, *J* = 18.7 Hz, *J* = 1.9 Hz, 1 H, NCH_AH_B), 6.98 (dd, *J* = 5.8 Hz, *J* = 2.2 Hz, 1 H, CH), 7.29–7.59 (m, 5 H, Ph) ppm. ^{13}C NMR (75 MHz, $CDCl_3$): δ = 14.19 (CH_2CH_3), 14.27 (CH_2CH_3), 28.61 ($COCH_2$), 28.76 ($COCH_2CH_2$), 32.09 (CCH_2CH), 36.91 (NCH_2), 42.58 (NCH_2Ph), 59.92 (C_q), 60.99 (CH_2CH_3), 61.16 (CH_2CH_3), 128.09 (CH), 128.35 (CH), 128.80 (CH), 133.42 (HC=C), 136.03 (HC=*C*), 137.67 ($C_{q,ar}$), 154.61 (NC=ON), 164.28 ($CCOOEt$), 172.13 (C=OO), 174.68 (NC=O) ppm. IR: $\tilde{\nu}_{max}$ = 1659 (C=C), 1716 (br C=O), 1774 (C=O) cm^{-1}. MS: *m*/*z* (%) = 415.3 (100) [M + H$^+$]. Chromatography: first Hex/EtOAc (3:1) until R_f = 0.26, then strip with EtOAc + 5% CH_2Cl_2. $C_{22}H_{26}N_2O_4$ (414.45): calcd. C 63.76, H 6.32, N 6.76; found C 63.54, H 6.51, N 6.72.

Ethyl 3-[7-Chloro-1,3-dioxo-2-propyl-2,3,5,8-tetrahydroimidazo[1,5-*a*]pyridin-8a(1*H*)-yl]propanoate (15g): Instead of refluxing in CH_2Cl_2, the reaction is refluxed in dry benzene for 16 hours. Yield: 0.15 g (77%). ^{1}H NMR (300 MHz, $CDCl_3$): δ = 0.93 (t, *J* = 7.4 Hz, 3 H, $CH_2CH_2CH_3$), 1.24 (t, *J* = 7.2 Hz, 3 H, CH_2CH_3), 1.66 (sext, *J* = 7.4 Hz, 2 H, NCH_2CH_2), 2.07–2.36 (m, 4 H, $COCH_2CH_2$), 2.51 (d, *J* = 17.4 Hz, 1 H, CCH_AH_BC), 2.64 (dq, *J* = 17.4 Hz, *J* = 3.1 Hz, 1 H, CCH_AH_BC), 3.49 (dt, *J* = 7.4 Hz, *J* = 2.2 Hz, 2 H, NCH_2CH_2), 3.61 (dq, *J* = 18.4 Hz, *J* = 3.2 Hz, 1 H, NCH_AH_B), 4.11 (q, *J* = 7.2 Hz, 2 H, CH_2CH_3), 4.49 (dt, *J* = 18.4 Hz, *J* = 3.2 Hz, 1 H, NCH_AH_B), 5.90 (q, *J* = 3.2 Hz, 1 H, CH) ppm. ^{13}C NMR (75 MHz, $CDCl_3$): δ = 11.26 (CH_3 pr), 14.21 (CH_2CH_3), 21.52 (CH_2 pr), 28.70 ($COCH_2CH_2$), 38.16 (NCH_2), 38.77 (CCH_2C), 40.64 (NCH_2 pr), 61.08 (CH_2CH_3), 61.55 (C_q), 120.17 (CH), 126.86 (CCl), 154.97 (NC=ON), 172.20 (C=OO), 174.29 (NC=O) ppm. IR: $\tilde{\nu}_{max}$ = 1663 (C=C), 1713 (br C=O), 1774 (C=O) cm^{-1}. MS: *m*/*z* (%) = 329.8/331.7 (100) [M + H$^+$]. Chromatography [Hex/EtOAc (2:1)]: R_f = 0.43. $C_{15}H_{21}ClN_2O_4$ (328.79): calcd. C 54.79, H 6.44, N 8.52; found C 54.57, H 6.59, N 8.52.

Ethyl 3-[7-Methyl-1,3-dioxo-2-propyl-2,3,5,8-tetrahydroimidazo[1,5-*a*]pyridin-8a(1*H*)-yl]propanoate (15h): Yield: 0.16 g (86%). ^{1}H NMR (300 MHz, $CDCl_3$): δ = 0.93 (t, *J* = 7.4 Hz, 3 H, $CH_2CH_2CH_3$), 1.24 (t, *J* = 7.2 Hz, 3 H, CH_2CH_3), 1.66 (sext, *J* = 7.4 Hz, 2 H, NCH_2CH_2), 1.74 (s, 3 H, CCH_3), 2.05–2.24 (m, 6 H, $COCH_2CH_2$ and CCH_2), 3.49 (dt, *J* = 7.4 Hz, *J* = 1.7 Hz, 2 H, NCH_2CH_2), 3.51 (dddd, *J* = 17.9 Hz, *J* = 12.5 Hz, *J* = 4.6 Hz, *J* = 2.2 Hz, 1 H, NCH_AH_B), 4.10 (q, *J* = 7.2 Hz, 2 H, CH_2CH_3), 4.36 (d, *J* = 17.9 Hz, 1 H, NCH_AH_B), 5.44 (s, 1 H, CH) ppm. ^{13}C NMR (75 MHz, $CDCl_3$): δ = 11.29 (CH_3 pr), 14.22 (CH_2CH_3), 21.60 (CH_2 pr), 23.51 (CCH_3), 28.55 ($COCH_2$), 28.85 ($COCH_2CH_2$), 36.38 (CCH_2C), 37.72 (NCH_2), 40.42 (NCH_2 pr), 60.93 (C_q + CH_2CH_3), 116.78 (CH), 129.42 (C), 155.24 (NC=ON), 172.48 (HNC=O), 175.81 (C=OO) ppm. ^{13}C NMR (75 MHz, C_6D_6): δ = 11.05 (CH_3 pr), 13.92 (CH_2CH_3), 21.60 (CH_2 pr), 22.93 (CCH_3), 28.73 ($COCH_2$), 28.85 ($COCH_2CH_2$), 35.95 (CCH_2C), 37.43 (NCH_2), 40.12 (NCH_2 pr), 60.41 (CH_2CH_3), 60.64 (C_q), 116.83 (CH), 128.83 (C), 154.98 (NC=ON), 171.90 (C=OO), 175.26 (NC=O) ppm. IR: $\tilde{\nu}_{max}$ = 1712 (br C=O), 1770 (C=O) cm^{-1}. MS: *m*/*z* (%) = 309.8 (100) [M + H$^+$]. Chromatography [Hex/EtOAc (7:3)]: R_f = 0.27. $C_{16}H_{24}N_2O_4$ (308.37): calcd. C 62.32, H 7.84, N 9.08; found C 62.38, H 8.00, N 9.10.

Acknowledgments

The authors thank the BOF (Bijzonder Onderzoeksfonds Universiteit Gent, Research Fund Ghent University) and the FWO (Fonds voor Wetenschappelijk Onderzoek - Vlaanderen, Fund for Scientific Research – Flanders) for financial support of this research.

[1] C. Najera, M. Yus, *Tetrahedron: Asymmetry* **1999**, *10*, 2245–2303.
[2] M. J. Valli, D. D. Schoepp, R. A. Wright, B. G. Johnson, A. E. Kingston, R. Tomlinson, J. A. Monn, *Bioorg. Med. Chem. Lett.* **1998**, *8*, 1985–1990.
[3] N. C. Danbolt, *Prog. Neurobiol.* **2001**, *65*, 1–105.
[4] N. Ikota, *Tetrahedron Lett.* **1992**, *33*, 2553–2556.
[5] S. Rosset, J. P. Célérier, G. Lhommet, *Tetrahedron Lett.* **1991**, *32*, 7521–7524.
[6] J. Ezquerra, A. Escrabino, A. Rubio, M. J. Remuinan, J. J. Vaquero, *Tetrahedron Lett.* **1995**, *36*, 6149–6152.
[7] T. Ohta, A. Hosoi, S. Nozoe, *Tetrahedron Lett.* **1988**, *29*, 329–332.
[8] Y. Ohfune, M. J. Tomita, *J. Am. Chem. Soc.* **1982**, *104*, 3511–3513.
[9] J. Van Betsbrugge, W. Van Den Nest, P. Verheyden, D. Tourwé, *Tetrahedron* **1998**, *54*, 1753–1762.
[10] S. Hanessian, G. McNaughton-Smith, H. Lombart, W. Lubell, *Tetrahedron* **1997**, *53*, 12789–12854.
[11] H. Biltz, *Ber. Dtsch. Chem. Ges.* **1908**, 1379–1393.
[12] P. Back, P. Maurois, C. Dupont, N. Pages, J. P. Stables, P. Gressens, P. Evrard, *J. Neurosci.* **1998**, *18*, 4363–4373.
[13] J. Knabe, J. Baldauf, A. Ahlhelm, *Pharmazie* **1997**, *52*, 912–919.
[14] M. S. Luer, *Neurol. Res.* **1998**, *20*, 178–182.
[15] S. Sholl, A. Koch, D. Henning, G. Kempter, E. Kleinpeter, *Struct. Chem.* **1999**, *10*, 355–366.
[16] T. R. Rodgers, M. P. LaMontagne, A. Markovac, A. B. Ash, *J. Med. Chem.* **1977**, *20*, 591–594.
[17] R. Sarges, P. J. Oates, *Prog. Drug. Res.* **1993**, *40*, 99–159.
[18] L. Somsak, L. Kovacs, M. Toth, E. Ösz, L. Szilagyi, Z. Györgydeak, Z. Dinya, T. Docsa, B. Toth, P. Gergely, *J. Med. Chem.* **2001**, *44*, 2843–2848.
[19] C. W. Bazil, T. A. Pedley, *Annu. Rev. Med.* **1998**, *49*, 135–162.
[20] C. J. Mappes, E.-H. Pommer, C. Rentzea, B. Zeeh, (BASF A.-G., Fed. Rep. Ger.). US Patent 4,198,423, **1980**, *Chem. Abstr.* **1980**, *93*, 71784.
[21] J. Charton, S. Delarue, S. Vendeville, M.-A. Debreu-Fontaine, S. Girault-Mizzi, C. Sergheraert, *Tetrahedron Lett.* **2001**, *42*, 7559–7561.
[22] W. Zhang, Y. Lu, *Org. Lett.* **2003**, *5*, 2555–2558.
[23] G. G. Muccioli, J. H. Poupaert, J. Wouters, B. Norberg, W. Poppitz, G. K. E. Scriba, D. M. Lambert, *Tetrahedron* **2003**, *59*, 1301–1307.
[24] M. Meusel, A. Ambrozak, T. K. Hecker, M. Gütschow, *J. Org. Chem.* **2003**, *68*, 4684–4692.
[25] J. Charton, A. C. Gassiot, P. Melnyk, S. Girault-Mizzi, C. Sergheraert, *Tetrahedron Lett.* **2004**, *45*, 7081–7085.
[26] A. Volonterio, C. Ramirez de Arellano, M. Zanda, *J. Org. Chem.* **2005**, *70*, 2161–2170.
[27] S. Manku, D. P. Curran, *J. Org. Chem.* **2005**, *70*, 4470–4473.

[28] For a study on the carbamoylation of some pyroglutamic derivatives see: P. Cauliez, D. Fasseur, D. Couturier, *J. Heterocycl. Chem.* **1996**, *33*, 1233–1237.
[29] A. B. Evnin, A. Lam, J. Blyskal, *J. Org. Chem.* **1970**, *35*, 3097–3105.
[30] A. B. Dyatkin, *Tetrahedron Lett.* **1997**, *38*, 2065–2066.
[31] For our previous work on RCM for the synthesis of azaheterocyclic molecules see: a) N. Dieltiens, C. V. Stevens, D. De Vos, B. Allaert, R. Drozdzak, F. Verpoort, *Tetrahedron Lett.* **2004**, *45*, 8995–8998; b) N. Dieltiens, C. V. Stevens, B. Allaert, F. Verpoort, *Arkivoc* **2005**, *i*, 92–97.
[32] G. Guillena, I. Mico, C. Najera, J. Ezquerra, C. Pedregal, *Anales de Quimica Int. Ed.* **1996**, *92*, 362–369.
[33] N. Dieltiens, C. V. Stevens, K. G. R. Masschelein, T. Rammeloo, *Tetrahedron* **2005**, *61*, 6749–6756.
[34] M. Scholl, S. Ding, C. W. Lee, R. H. Grubbs, *Org. Lett.* **1999**, *1*, 953–956.
[35] A. M. Hoveyda, D. G. Gillingham, J. J. Van Veldhuizen, O. Kataoka, S. B. Garber, J. S. Kingsburry, J. P. A. Harrity, *Org. Biomol. Chem.* **2004**, *2*, 8–23.
[36] For a recent review on the use of RCM for the synthesis of azaheterocycles see: A. Deiters, S. F. Martin, *Chem. Rev.* **2004**, *104*, 2199–2238.
[37] For clarity only one part of the disorder is shown: O240 is disordered with a 56:44 ratio.
[38] TeXsan 10.3b program, Rigaku Inc. **1997**.
[39] P. W. Betteridge, J. R. Carruthers, R. I. Copper, K. Prout, D. J. Watkin, *J. Appl. Crystallogr.* **2003**, *36*, 1487.

Received: January 20, 2006
Published Online: April 3, 2006

--- Paper V ---

Nicolai Dieltiens, Diederica D. Claeys, and Christian V. Stevens*

"Synthesis of *N*(3),*N*'(3)-Polymethylene-bis-hydantoins and Their Macrocyclic Derivatives"

J. Org. Chem. **2006**, Vol.71, 3863–3868

JOC*Article*

Synthesis of *N*(3),*N*′(3)-Polymethylene-bis-hydantoins and Their Macrocyclic Derivatives

Nicolai Dieltiens, Diederica D. Claeys,† and Christian V. Stevens*

Research group Synbioc, Department of Organic Chemistry, Faculty of Bioscience Engineering, Ghent University, Coupure links 653, B-9000 Ghent, Belgium

chris.stevens@ugent.be

Received February 22, 2006

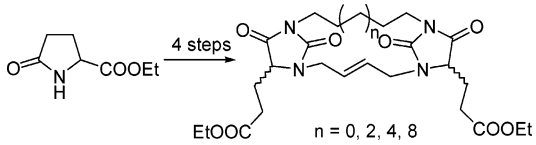

An efficient and straightforward two-step approach toward *N*(3),*N*′(3)-polymethylene-bis-hydantoins was developed. As a first step, a pyroglutamate is reacted with a diisocyanate to produce a bis-carbamoyllactam. The second step is a double-ring transformation by treatment of this bis-carbamoyllactam with KO*t*Bu in ethanol. In this fashion N(3),N′(3)-polymethylene-bis-hydantoins are produced in two quantitative steps and under very mild conditions. When properly derivatized, these compounds can be converted to their macrocyclic derivatives upon treatment with 5 mol % of second-generation Grubbs' catalyst. These macrocyclic derivatives are so far not described in the literature. It was proven that exclusively (*E*)-isomers are formed.

Introduction

The exploration of privileged structures in drug discovery has gained significant popularity in pharmaceutical chemistry over the years. Hydantoins (or imidazolidine-2,4-diones, **1**) have been extensively studied and are reported to possess a wide range of biological activities (Figure 1). Phenetoin (5,5-diphenylhydantoin, **2**), for example, was already synthesized in 1908[1] and is now still the drug of choice for the treatment of certain types of epileptic seizures.[2] They have proven useful not only in human medicine (antiarrhythmic,[3] anticonvulsant,[4] antitumor,[5] antidiabetic,[6] and antimuscarinic activity,[7] etc.) but also in the agrochemical sector (herbicidal and fungicidal activity).[8] In recent years, many new synthetic approaches have been developed toward this interesting heterocycle.[9−15]

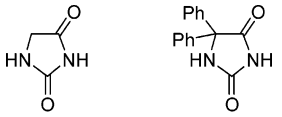

FIGURE 1. Hydantoin nucleus **1** and phenetoin **2**.

Recently, we described the pyroglutamate−hydantoin rearrangement.[16] It was found that treating pyroglutamates **3** with NaH in the presence of isocyanates or isothiocyanates in THF

† D.D.C. is aspirant of the Fund for Scientific Research Flanders (FWO Vlaanderen).

(1) Biltz, H. *Chem. Ber.* **1908**, 1379−1393.
(2) Back, P.; Maurois, P.; Dupont, C.; Pages, N.; Stables, J. P.; Gressens, P.; Evrard, P. *J. Neurosci.* **1998**, *18*, 4363−4373.
(3) Knabe, J.; Baldauf, J.; Ahlhelm, A. *Pharmazie* **1997**, *52*, 912−919.
(4) (a) Luer, M. S. *Neurol. Res.* **1998**, *20*, 178−182. (b) Sholl, S.; Koch, A.; Henning, D.; Kempter, G.; Kleinpeter, E. *Struct. Chem.* **1999**, *10*, 355−366.
(5) Rodgers, T. R.; LaMontagne, M. P.; Markovac, A.; Ash, A. B. *J. Med. Chem.* **1977**, *20*, 591−594.
(6) (a) Sarges, R.; Oates, P. J. *Prog. Drug. Res.* **1993,** *40*, 99−159. (b) Somsak, L.; Kovacs, L.; Toth, M.; Ösz, E.; Szilagyi, L.; Györgydeak, Z.; Dinya, Z.; Docsa, T.; Toth, B.; Gergely, P. *J. Med. Chem.* **2001**, *44*, 2843−2848.
(7) Bazil, C. W.; Pedley, T. A. *Annu. Rev. Med.* **1998,** *49*, 135−162.
(8) Mappes, C. J.; Pommer, E.-H.; Rentzea, C.; Zeeh, B. (BASF A.-G., Fed. Rep. Ger.). US Patent 4,198,423, 1980; *Chem. Abstr.* **1980**, *93*, 71784.
(9) Charton, J.; Delarue, S.; Vendeville, S.; Debreu-Fontaine, M.-A.; Girault-Mizzi, S. Sergheraert. C. *Tetrahedron Lett.* **2001**, *42*, 7559−7561.
(10) Zhang, W.; Lu, Y. *Org. Lett.* **2003**, *5*, 2555−2558.
(11) Muccioli, G. G.; Poupaert, J. H.; Wouters, J. Norberg, B.; Poppitz, W.; Scriba, G. K. E.; Lambert, D. M. *Tetrahedron* **2003**, *59*, 1301−1307.
(12) Meusel, M.; Ambrozak, A.; Hecker, T. K.; Gütschow, M. *J. Org. Chem.* **2003**, *68*, 4684−4692.
(13) Charton, J.; Gassiot, A. C.; Melnyk, P.; Girault-Mizzi, S. Sergheraert, C. *Tetrahedron Lett.* **2004**, *45*, 7081−7085.
(14) Volonterio, A.; Ramirez de Arellano, C.; Zanda, M. *J. Org. Chem.* **2005**, *70*, 2161−2170.
(15) Manku, S.; Curran, D. P. *J. Org. Chem.* **2005**, *70*, 4470−4473.
(16) Dieltiens, N.; Claeys, D. D.; Zhdankin, V. V.; Nemykin, V. N.; Allaert, B.; Verpoort, F.; Stevens, C. V. *Eur. J. Org. Chem.* **2006**, in press.

10.1021/jo060370r CCC: $33.50
Published on Web 04/22/2006

SCHEME 1

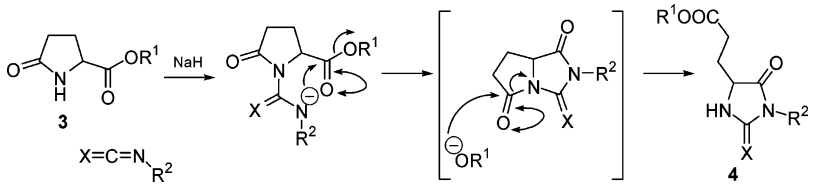

SCHEME 2

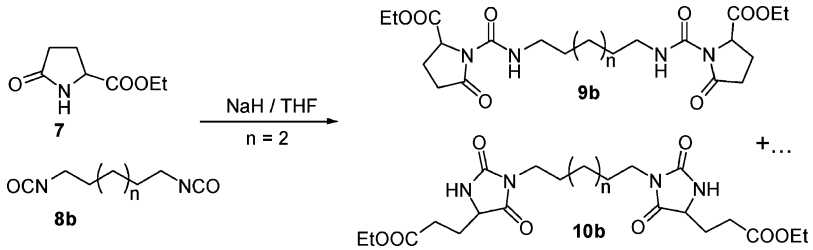

produces hydantoins **4** in high yield via a ring-closing−ring-opening sequence (Scheme 1).

In this paper, we disclose the application of this ring transformation for the synthesis of *N*(3),*N*′(3)-polymethylene-bis-hydantoins. Several of these bis-hydantoins **5** have been evaluated as hexamethylenebis(acetamide) analogues (HMBA, **6**) (Figure 2). HMBA is an agent that induces differentiation of certain types of tumor cells to nonmalignant phenotypes. This implies that it works not by killing the cancer cells but by inducing them to differentiate and to express characteristics of the normal nontransformed counterpart. This is a promising approach to cancer therapy, potentially without many of the disadvantages of cytotoxic agents. HMBA has even had some modest success in clinical trials. The doses required to achieve sufficient blood levels in human patients, however, led to some undesirable side effects. It was found that compounds **5a** and **5d** were 10 times more potent than HMBA itself, but the activity of **5b** however was low, probably due to its insolubility.[17−19] Compound **5c** was found to show antiepileptic activity in the maximal electroshock seizure test.[20]

The synthesis of these compounds usually involves the reaction of a hydantoin with a *ω*-dihaloalkane under basic conditions. The problem with this reaction is the need for N(3)-selective alkylation and the yield which is usually quite low. Starting from pyroglutamates would avoid the problem of N(3)-selectivity and also allows the synthesis of highly functionalized derivatives since pyroglutamates can easily be derivatized.[16,21−24]

Results and Discussion

Following our protocol for the ring transformation of pyroglutamates, a mixture of ethylpyroglutamate **7** and diisocyanate **8b** in THF was treated with NaH (Scheme 2). It was found, however, that a mixture of compounds was obtained. Besides the desired compound **10b**, the dicarbamoyllactam **9b** was observed in the ^{1}H NMR of the crude reaction mixture accompanied by a variety of compounds probably resulting from the attack of the formed alkoxide anion on the second isocyanate after reaction with the first isocyanate functionality.

To avoid these undesired reactions, it seemed necessary to make a short synthetic detour. Previous observations had shown that the formed sodium salt of the carbamoylated lactam precipitates from diethyl ether, effectively preventing it from reacting further.[25] Thus, it would be possible to isolate the carbamoylated intermediate and attempt the ring transformation in a separate step. As expected, the double sodium salts **11** precipitates from solution after treating a mixture of **7** and **8** with NaH in ether and provided derivatives **9** in quantitative yield and good purity after acidic workup (Scheme 3).

The double-ring transformation from **9** to **10** did not proceed as smoothly as anticipated. Treatment of **9** with strong bases such as NaH and KO-*t*-Bu in THF at room temperature or at reflux did not result in the desired conversion. Switching to ethanol as a solvent in combination with NaOH or KO-*t*-Bu as a base however, resulted in clean and complete double transformation to the bis-hydantoins **10** within 1 h at room temperature (Scheme 4). Derivatives **10** are obtained as a viscous oil after acidic workup but can be crystallized from THF to afford white powders.

Special attention is required when distinguishing between 1-carbamoyl-2-pyrrolidines **9** and hydantoins **10**. Indeed, from their structures it is obvious that straightforward ^{1}H NMR and

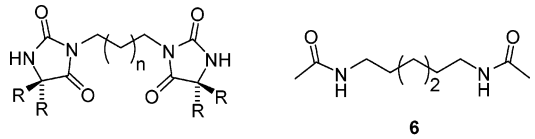

5a n = 4, R = Me
5b n = 4, R = Ph
5c n = 0, R = Ph
5d n = 3, R = Me

FIGURE 2. Bis-hydantoins **5** and HMBA **6**.

(17) Haces, A.; Breitman, T. R. Driscoll, J. S. *J. Med. Chem.* **1987**, *30*, 405−409.
(18) Breslow, R. Jursic, B.; Yan, Z. F.; Friedman, E.; Leng, L.; Ngo, L.; Rifkind, R. A.; Marks, P. A. *Proc. Natl. Acad. Sci. U.S.A.* **1991**, *88*, 5542−5546.
(19) Breslow, R.; Belvedere, S.; Gershell, L. *Helv. Chim. Acta* **2000**, *83*, 1685−1692.
(20) Poupaert, J. H.; Mergen, F. Lerot, T. *Bull. Soc. Chim. Belg.* **1988**, *97*, 469−470.
(21) Braña, M. F.; Garranzo, M.; Pérez-Castells, J. *Tetrahedron Lett.* **1998**, *39*, 6569−6572.
(22) Najera, C.; Yus, M. *Tetrahedron: Asymmetry* **1999**, *10*, 2245−2303.
(23) Stevens, C. V.; Rammeloo, T.; De Kimpe, N. *Synlett.* **2001**, *10*, 1519−1522.
(24) Dieltiens, N.; Stevens, C. V.; Masschelein, K. G. R.; Rammeloo, T. *Tetrahedron* **2005**, *61*, 6749−6756.
(25) Stevens, C. V.; Dieltiens, N.; Claeys, D. D. *Org. Lett.* **2005**, *7*, 1117−1119.

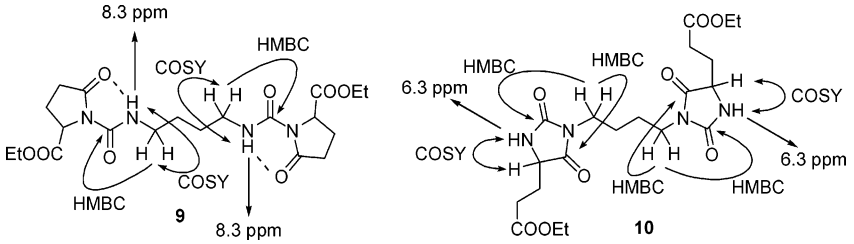

FIGURE 3. Most important COSY and HMBC couplings in **9a** and **10a**.

SCHEME 3

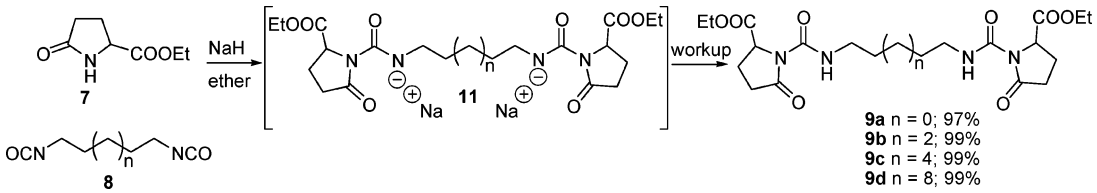

SCHEME 4

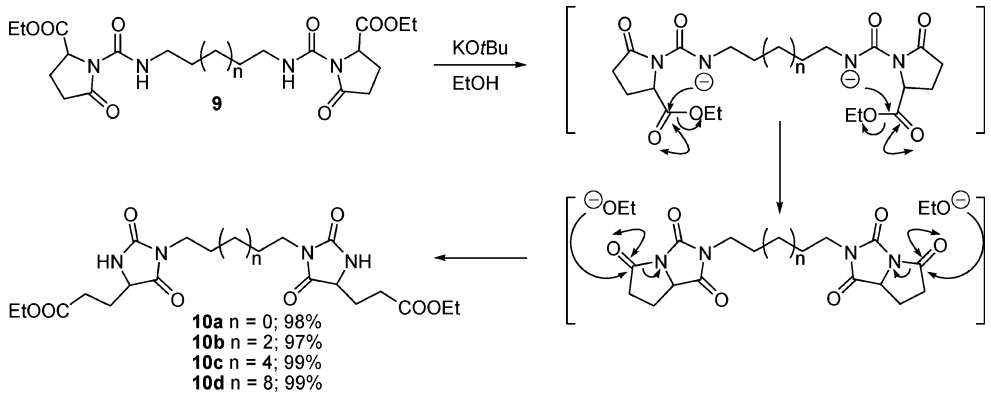

SCHEME 5

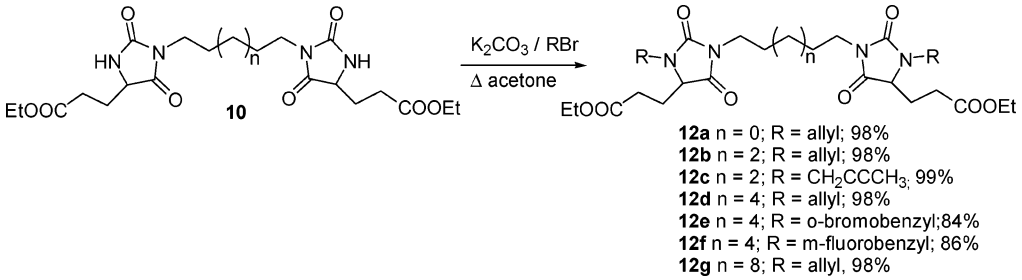

^{13}C NMR measurements are not sufficient to distinguish between the two. However, having both compounds in hand, two-dimensional spectroscopy clearly allowed the unambiguous determination (Figure 3). In the case of **9**, there is a coupling in the COSY spectrum between the NH protons and the CH_2 next to the nitrogen. On the other hand, the NH protons of **10** show a coupling to the proton next to the carbonyl and not to the CH_2, proving that this methylene is connected to a tertiary nitrogen. Furthermore, the protons of the CH_2 next to nitrogen of **9** only couple to the urea carbonyl in the HMBC (heteronuclear multiple bound correlation) spectrum, whereas in the case of **10** they couple to both the urea and the lactam carbonyl. Another distinctive feature is the shift of the NH-protons. Intramolecular hydrogen bridge formation in **9** to the lactam carbonyl causes a downfield shift, resulting in a typical value of 8.3 ppm, whereas the value in the case of **10** is typically around 6.3 ppm.

As we reported before, the hydantoins can easily be further functionalized by refluxing in acetone with a proper electrophile in the presence of finely ground K_2CO_3.[16] The same conditions proved to work perfectly on the dimers, and in this fashion several derivatives could be prepared in near-quantitative yields (Scheme 5). The only losses occur during purification by flash chromatography, which is only necessary to remove the excess of electrophile in the case of **12e** and **12f**. For all other derivatives, it is sufficient to filter off the solids and evaporate the volatiles in vacuo.

One of the challenges of medicinal chemistry is the enhancement of the affinity of a given ligand for its target by decreasing its degrees of freedom, thereby reducing the cost in entropy. To prevent free rotation around the central polymethylene axis, we wanted to evaluate the possibility to use ring-closing metathesis (RCM) for the macrocyclization of derivatives

SCHEME 6

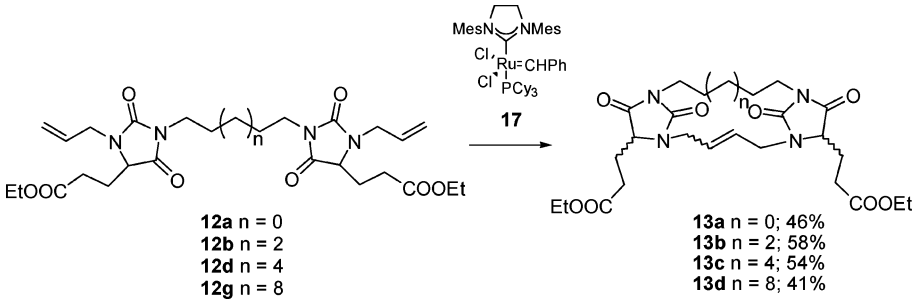

SCHEME 7

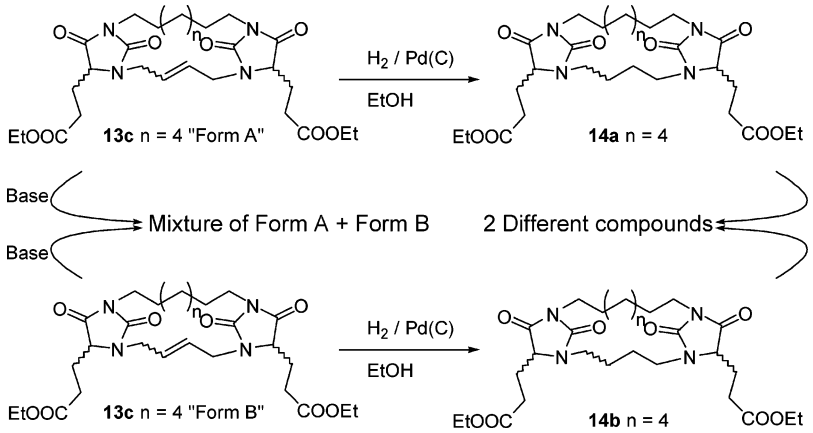

12a,**b**,**d**,**g**.[26,27] Fürstner and co-workers have proven that substrates devoid of any conformational constraints can be efficiently cyclized by RCM to macrocyclic products and that neither the conformational predisposition nor the ring size formed is a major concern. The decisive parameters are the presence of polar relay substituents, their proper distance to the alkene groups, and the low steric hindrance close to the double bonds.[28] Since all of these requirements are met in these substrates, macrocyclization was expected to pose no special problems. Indeed, it was found that treating derivatives **12a**,**b**,**d**,**g** with a catalytic amount of the second-generation Grubbs' catalyst **17** (5 mol %) resulted in quantitative conversion to macrocyclic derivatives **13** after 16 h of reflux in CH_2Cl_2 (Scheme 6). A significant drop in yield, however, was observed during purification by flash chromatography, probably caused by the high polarity of these compounds.

It is known that when using RCM as a macrocyclization method, usually (*E*,*Z*) mixtures of cyclized compounds are formed. In this case, two separate signals (1:1 ratio) were observed for the alkene protons of derivatives **13**. This, however, does not mean that an (*E*,*Z*) mixture is formed, since in this particular case, both **12** and **13** have two racemic centers and, thus, the two observed signals could belong to another diastereoisomer. Moreover, $^3J_{HH}$ coupling constants, which are normally used to distinguish *trans* and *cis* isomers, are absent since the macrocycles are symmetrical entities and as a consequence the two alkene protons do not couple with each other. They appear as small triplets. It was, however, possible to separate the two forms of compound **13c** by flash chromatography. Now it was possible to prove whether form A and form B were diastereoisomers or (*E*,*Z*)-isomers. First, it was observed that treatment with base of one form of **13c** resulted in equilibration to the mixture of both forms (Scheme 7). Second, hydrogenation of form A and form B gave two different compounds. This can only be the case if the two compounds were diastereoisomers since the (*E*,*Z*)-isomers should have produced the same hydrogenation product.

The question rose whether the *trans*- or *cis*-fused cycles were produced. The presence of only one isomer around the double bound can be explained by secondary metathesis reactions. In a kinetic study, Grubbs has proven that macrocycles isomerize to produce a thermodynamically controlled (*E*/*Z*) ratio regardless the stereochemistry of the initial alkene.[29] Although usually a mixture of both isomers is isolated, Fürstner has already reported that only the (*E*)-isomer is formed in some cases.[30] A stereoselective approach to macrocyclic (*E*)- and (*Z*)-isomers is possible using ring-closing alkyne metathesis (RCAM).[31] In the first case, the macrocyclic alkyne is converted to the (*E*)-isomer

(26) For our previous work on using RCM for the synthesis of azaheterocycles, see: (a) Dieltiens, N.; Stevens, C. V.; De Vos, D.; Allaert, B.; Drozdzak, R.; Verpoort, F. *Tetrahedron Lett.*, **2004**, *45*, 8995−8998. (b) Dieltiens, N.; Stevens, C. V.; Allaert, B.; Verpoort, F. *Arkivoc* **2005**, *i*, 92−97.

(27) For recent reviews on RCM, see: Fürstner, A. *Angew. Chem., Int. Ed.* **2000**, *39*, 3012−3043. Grubbs, R. H. *Tetrahedron* **2004,** *60*, 7117−7140. Dragutan, I.; Dragutan, V.; Filip, P. *Arkivoc* **2005**, *x*, 105−129. Nicolaou, K. C.; Bulger, P. G.; Sarlah, D. *Angew. Chem., Int. Ed.* **2005**, *44*, 4490−4527. For a recent review on the use of RCM for the synthesis of azaheterocycles, see: Deiters, A.; Martin, S. F. *Chem. Rev.* **2004**, *104*, 2199−2238.

(28) (a) Fürstner, A.; Langeman, K. *J. Org. Chem.* **1996**, *61*, 3942−3943. (b) Fürstner, A. *Top. Catal.* **1997**, *4*, 285−299. (c) Fürstner; A.; Müller, T. *J. Org. Chem.* **1998**, *63*, 424−425 and references cited therein.

(29) (a) Lee, C. W.; Grubbs, R. H. *Org. Lett.* **2000**, *2*, 2145−2147. For a computational study, see: (b) Vyboishchikov, S. F.; Thiel, W. *Chem. Eur. J.* **2005**, *11*, 3921−3935.

(30) Fürstner, A.; Thiel, O. R.; Kindler, N.; Bartkowska, B. *J. Org. Chem.* **2000**, *65*, 7990−7995.

(31) For a review on RCAM, see: Fürstner, A. *Angew. Chem., Int. Ed.* **2000**, *39*, 3012−3043.

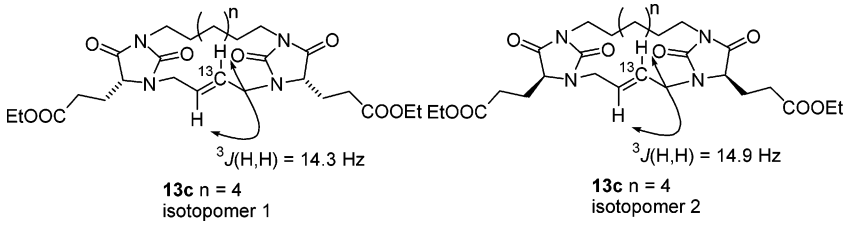

FIGURE 5. $^3J_{H,H}$ coupling of the ^{13}C satellites of both isotopomers of **13c**.

SCHEME 8

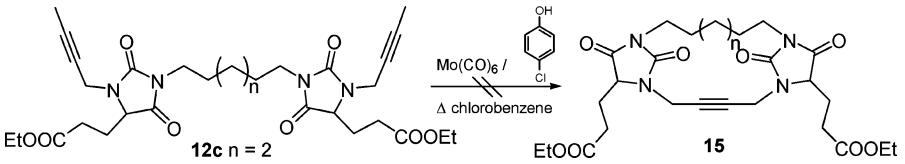

by *trans*-selective hydrosilylation and subsequent protodesilylation.[32] In the second case, the macrocyclic alkyne is converted to the (*Z*)-isomer by Lindlar reduction.[33] In this perspective, derivative **12c** was prepared and was treated with a mixture of $Mo(CO)_6$ and *p*-chlorophenol as an "instant" catalyst system under an Ar atmosphere (Scheme 8).[34] Unfortunately, even after prolonged reaction times only starting material could be recovered.

In a further attempt to selectively synthesize the *trans*- and the *cis*-isomer, derivative **10c** was refluxed in two separate experiments with *trans*-1,4-dichloro-2-butene and *cis*-1,4-dichloro-2-butene. Only in the second case was some reaction observed, resulting in a mixture that was tentatively identified as a mixture of starting material, monoalkylated material, and cyclized material (<10%). The last two components proved impossible to separate, but a ^{13}C-spectrum of this mixture proved it to be different from compound **13c**, suggesting that the macrocycles produced by RCM are in the *trans*-geometry. The fact that these derivatives are so difficult to cyclize again proves the importance of RCM as the macrocyclization method and of the functional group as an essential relay in order to accomplish this.[35] Probably chelation complexes of type **16** are formed during metathesis, effectively bringing the two alkene moieties in the correct position (Figure 4).

A more decisive confirmation of the *trans*-geometry was obtained by looking at the ^{13}C satellites of the alkene protons of one pair of enantiomers of **13c** (Figure 5).[36] When one of the two alkene carbon atoms is a ^{13}C-isotope, the symmetry is lost due to the presence of a magnetically active ^{13}C in place of an inactive ^{12}C. In this case, the two isotopomers give two separate signals (br d, 5.14 ppm, 14.3 Hz and br d, 5.12 ppm, 14.9 Hz). They are not each others mirror image because of the two other chiral centers. A $^3J_{H,H}$ coupling of 14.3 and 14.9 Hz is observed, pointing to the *trans*-geometry.[37]

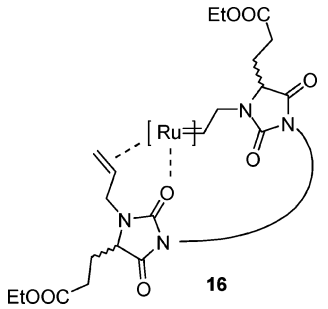

FIGURE 4. Possible chelation complex formed during metathesis.

Conclusions

A short and high-yield approach was developed to *N*(3),*N*′-(3)-polymethylene-bis-hydantoins. This two-step approach consists of carbamoylation of a pyroglutamate and subsequent double-ring transformation. After proper functionalization, these dimers can be cyclized by ring-closing metathesis using the second-generation Grubbs' catalyst. It was proven that only the *trans*-isomers are isolated.

Experimental Section

1. Synthesis of Derivatives 9. As a representative example, the synthesis of ethyl 1-({[4-({[2-(ethoxycarbonyl)-5-oxopyrrolidin-1-yl]carbonyl}amino)butyl]amino}carbonyl)-5-oxopyrrolidine-2-carboxylate **9a** is described. Ethyl pyroglutamate **7** (5 g, 31.8 mmol) was dissolved in diethyl ether (100 mL, freshly distilled from Na metal) and kept under a positive N_2-pressure. To this solution was added 1,4-diisocyanatobutane (2.23 g, 15.9 mmol) followed by NaH (0.92 g, 38.2 mmol, washed with hexanes). The reaction was allowed to stir under nitrogen atmosphere at room temperature for 1 h. The reaction was quenched by the addition of saturated aqueous NH_4Cl until the pH was neutral. The mixture was extracted with EtOAc, and the organics were dried ($MgSO_4$) and filtered. The solvent was removed in vacuo. Compound **9a** was obtained as a viscous oil in quantitative yield.

Ethyl 1-({[4-({[2-(ethoxycarbonyl)-5-oxopyrrolidin-1-yl]carbonyl}amino)butyl]amino}carbonyl)-5-oxopyrrolidine-2-carboxylate 9a: ^1H NMR (300 MHz, $CDCl_3$) δ 1.29 (6H, t, J = 7.2 Hz), 1.60 (4H, t, J = 3.0 Hz), 2.00−2.10 (2H, m), 2.25−2.45 (2H, m), 2.57 (2H, ddd, J = 17.6 Hz, J = 3.4 Hz, J = 9.5 Hz), 2.74 (2H, ddd, J = 17.6 Hz, J = 9.9 Hz, J = 9.9 Hz), 3.23−3.40 (4H,

(32) Lacombe, F.; Radkowski, K.; Seidel, G.; Fürstner, A *Tetrahedron* **2004**, *60*, 7315−7324.

(33) (a) Fürstner, A.; Guth, O.; Rumbo, A.; Seidel, G. *J. Am. Chem. Soc.* **1999**, *121*, 11108−11113. (b) Fürstner, A.; Mathes, C.; Lehmann, C. W. *Chem. Eur. J.* **2001**, *7*, 5299−5317.

(34) Mortreux, A.; Blanchard, M. *J. Chem. Soc., Chem. Commun.* **1974**, 786−787.

(35) (a) Fürstner, A.; Langemann, K. *Synthesis* **1997**, 792−803. (b) Fürstner, A.; Thiel, O. R.; Lehmann, C. W. *Organometallics* **2002**, *21*, 331−335.

(36) For clarity the diastereoisomer with the two ester groups in a *cis* position is depicted.

(37) For articles concerning the recovery of $^3J_{H,H}$, see: (a) Mucci, A.; Parenti, F.; Schenetti, L. *Eur. J. Org. Chem.* **2002**, 938−940. (b) Janssen, C. E.; Krause, N. *Eur. J. Org. Chem.* **2005**, 2322−2329.

m), 4.24 (4H, q, $J = 7.2$ Hz), 4.77 (2H, dd, $J = 9.5$ Hz, $J = 2.6$ Hz), 8.31 (2H, t, $J = 5.5$ Hz); ^{13}C NMR (75 MHz, $CDCl_3$) δ 14.2, 21.3, 27.0, 31.9, 39.5, 58.2, 61.7, 152.3, 171.5, 176.5; IR (NaCl, cm^{-1}) ν_{max} 1694 (C═O), 1721 (br C═O), 3317 (NH); MS (70 eV) *m*/*z* 455.7 ($M^+ + 1$, 100); HRMS calcd for $C_{20}H_{30}N_4O_8$ ($M + H^+$) 455.2136, found 455.2148.

2. Synthesis of Derivatives 10. As a representative example, the synthesis of 3-(1-{4-[4-(2-ethoxycarbonylethyl)-2,5-dioxoimidazolidin-1-yl]butyl}-2,5-dioxoimidazolidin-4-yl)propionic acid ethyl ester **10a** is described. Compound **9a** (7.23 g, 15.9 mmol) was dissolved in absolute ethanol (75 mL) and kept under a positive N_2 pressure. To this solution was added KO-*t*-Bu (3.92 g, 35 mmol). The reaction was allowed to stir under nitrogen atmosphere at room temperature for 1 h. The reaction was quenched by the addition of saturated aqueous oxalic acid until the pH was acidic. The ethanol was removed in vacuo, and the residue was extracted with EtOAc, the organics were dried ($MgSO_4$) and filtered. The solvent was removed in vacuo. For the crystallization, the product was dissolved in a minimal amount of boiling THF and hexane was added until the solution remained cloudy. The flask was put in the freezer and afterward the solids were filtered. This procedure was repeated until no more precipitate was formed. Compound **10a** was obtained in quantitative yield.

3-(1-{4-[4-(2-Ethoxycarbonylethyl)-2,5-dioxoimidazolidin-1-yl]butyl}-2,5-dioxoimidazolidin-4-yl)propionic acid ethyl ester 10a: white powder; mp 124−127 °C; ^{1}H NMR (300 MHz, $CDCl_3$) δ 1.26 (6H, t, $J = 7.2$ Hz), 1.63 (4H, br s), 2.03 (2H, ddt, $J = 13.9$ Hz, $J = 7.2$ Hz, $J = 7.3$ Hz), 2.20 (2H, ddt, $J = 13.9$ Hz, $J = 7.3$ Hz, $J = 6.3$ Hz), 2.47 (2H, t, $J = 7.3$ Hz), 3.52 (4H, br s), 4.14 (4H, q, $J = 7.2$ Hz), 4.10 (2H, dd, $J = 7.2$ Hz, $J = 6.3$ Hz), 6.29 (2H, s); ^{13}C NMR (75 MHz, $CDCl_3$) δ 14.3, 25.2, 26.9, 29.9, 38.0, 56.4, 61.1, 157.4, 172.9, 173.7; IR (KBr, cm^{-1}) ν_{max} 1713 (br C═O), 1764 (C═O), 3249 (NH); MS (70 eV) *m*/*z* 455.7 ($M^+ + 1$, 100); HRMS calcd for $C_{20}H_{30}N_4O_8$ ($M + H^+$) 455.2136, found 455.2148.

3. Synthesis of Derivatives 12. As a representative example, the synthesis of 3-(3-allyl-1-{4-[3-allyl-4-(2-ethoxycarbonylethyl)-2,5-dioxoimidazolidin-1-yl]butyl}-2,5-dioxoimidazolidin-4-yl)propionic acid ethyl ester **12a** is described. Compound **10a** (7.23 g, 15.9 mmol) was dissolved in acetone (75 mL). To this solution were added K_2CO_3 (11 g, 79.5 mmol) and allyl bromide (7.70 g, 63.6 mmol). This mixture was refluxed until TLC showed complete consumption of the starting material. The mixture was filtered, and the solvent was removed in vacuo. Compound **12a** was obtained as a viscous oil in quantitative yield.

3-(3-Allyl-1-{4-[3-allyl-4-(2-ethoxycarbonylethyl)-2,5-dioxoimidazolidin-1-yl]butyl}-2,5-dioxoimidazolidin-4-yl)propionic acid ethyl ester 12a: ^{1}H NMR (300 MHz, $CDCl_3$) δ 1.26 (6H, t, $J = 7.2$ Hz), 1.64 (4H, br s), 2.00−2.12 (2H, m), 2.18−2.42 (6H, m), 3.53 (4H, br s), 3.62 (2H, dd, $J = 15.7$ Hz, $J = 7.4$ Hz), 4.01 (2H, dd, $J = 3.0$ Hz, $J = 6.6$ Hz), 4.13 (4H, q, $J = 7.2$ Hz), 4.34 (2H, dd, $J = 15.7$ Hz, $J = 5.0$ Hz), 5.24 (2H, d, $J = 4.7$ Hz), 5.28 (2H, s), 5.70−5.83 (2H, m); ^{13}C NMR (75 MHz, $CDCl_3$) δ 14.3, 23.8, 25.3, 28.2, 38.3, 43.5, 57.8, 60.9, 119.5, 131.8, 156.3, 172.4, 172.6; IR (NaCl, cm^{-1}) ν_{max} 1645 (C═C), 1709 (br C═O), 1769 (C═O); MS (70 eV) *m*/*z* 535.7 ($M^+ + 1$, 100); HRMS calcd for $C_{26}H_{38}N_4O_8$ ($M + H^+$) 535.2762, found 535.2769.

4. Synthesis of Derivatives 13. As a representative example, the synthesis of 3-[18-(2-ethoxycarbonylethyl)-8,17,19,20-tetraoxo-1,6,9,16-tetraazatricyclo[14.2.1.1^{6,9}]icos-3-en-7-yl]propionic acid ethyl ester **13b** is described. Compound **12b** (0.2 g, 0.36 mmol) was dissolved in CH_2Cl_2 (20 mL, freshly distilled from CaH_2), and the second-generation Grubbs' catalyst (0.015 g, 0.018 mmol) was added. The reaction was allowed to reflux for 16 h under a N_2 atmosphere. The product was coated on silica gel by removal of the solvent in vacuo and purified by flash chromatography (silica gel; hexane/EtOAc). Compound **13a** is obtained as a 1:1 mixture of the two diastereoisomers (combined yield 46%) which can be separated and obtained as viscous oils.

3-[18-(2-Ethoxycarbonylethyl)-8,17,19,20-tetraoxo-1,6,9,16-tetraazatricyclo[14.2.1.1^{6,9}]icos-3-en-7-yl]propionic acid ethyl ester 13b, diastereoisomer 1: TLC R_f 0.42 (petroleum ether/ethyl acetate, 2:8); ^{1}H NMR (300 MHz, $CDCl_3$) δ 1.15−1.30 (4H, m), 1.24 (6H, t, $J = 7.2$ Hz), 1.62−1.74 (4H, m), 2.00−2.16 (2H, m), 2.17−2.52 (6H, m), 3.43−3.49 (4H, m), 3.57 (2H, ddd, $J = 13.8$ Hz, $J = 6.3$ Hz, $J = 3.9$ Hz), 4.04 (2H, dd, $J = 2.9$ Hz, $J = 6.5$ Hz), 4.11 (4H, q, $J = 7.2$ Hz), 4.35 (2H, d, $J = 16.0$ Hz), 5.35 (2H, t, $J = 2.2$ Hz); ^{13}C NMR (75 MHz, $CDCl_3$) δ 14.2, 23.6, 27.5, 27.8, 28.5, 39.6, 41.8, 57.7, 60.9, 126.3, 157.0, 172.6, 172.7; IR (NaCl, cm^{-1}) ν_{max}: 1709 (C═O), 1769 (C═O); MS (70 eV) *m*/*z* 535.2 ($M^+ + 1$, 100); HRMS calcd for $C_{26}H_{38}N_4O_8$ ($M + H^+$) 535.2762, found 535.2772.

Diastereoisomer 2: TLC R_f 0.38 (petroleum ether/ethyl acetate, 2:8); ^{1}H NMR (300 MHz, $CDCl_3$) δ 1.16−1.35 (4H, m), 1.26 (6H, t, $J = 7.2$ Hz), 1.58−1.75 (4H, m), 1.97−2.09 (2H, m), 2.13−2.55 (6H, m), 3.43−3.49 (4H, m), 3.48 (2H, ddd, $J = 13.3$ Hz, $J = 6.4$ Hz, $J = 3.8$ Hz), 3.58 (2H, ddd, $J = 13.3$ Hz, $J = 3.9$ Hz, $J = 3.8$ Hz), 3.68 (2H, dt, $J = 16.2$ Hz, $J = 2.4$ Hz), 4.04 (2H, dd, $J = 3.6$ Hz, $J = 7.2$ Hz), 4.09 (2H, d, $J = 16.2$ Hz), 4.14 (4H, q, $J = 7.2$ Hz), 5.63 (2H, t, $J = 2.4$ Hz); ^{13}C NMR (75 MHz, $CDCl_3$) δ 14.3, 24.3, 26.8, 27.6, 28.6, 38.9, 42.4, 58.1, 60.9, 128.2, 156.9, 172.7, 173.0; IR (NaCl, cm^{-1}) ν_{max} 1709 (C═O), 1768 (C═O); MS (70 eV) *m*/*z* 535.2 ($M^+ + 1$, 100); HRMS calcd for $C_{26}H_{38}N_4O_8$ ($M + H^+$) 535.2762, found 535.2779.

Acknowledgment. Financial support of this research by the BOF (Bijzonder Onderzoeksfonds Universiteit Gent, Research Fund Ghent University) and by the FWO (Fonds voor Wetenschappelijk Onderzoek - Vlaanderen, Fund for Scientific Research - Flanders) is gratefully acknowledged.

Supporting Information Available: General information and spectroscopic data of all compounds synthesized with complete peak assignment. Copies of the ^{13}C NMR spectra of all compounds. This material is available free of charge via the Internet at http://pubs.acs.org.

JO060370R

--- Paper VI ---

Diederica D. Claeys, Christian V. Stevens,* and Nicolai Dieltiens

"The Formation of *trans*-Fused Macrocycles from *N*3,*N*3'-Polymethylenebis-(hydantoins) by Ring-Closing Metathesis"

Eur. J. Org. Chem. **2008**, 171–179

DOI: 10.1002/ejoc.200700836

The Formation of *trans*-Fused Macrocycles from N^3,$N^{3'}$-Polymethylenebis-(hydantoins) by Ring-Closing Metathesis

Diederica D. Claeys,[a][‡] Christian V. Stevens,*[a] and Nicolai Dieltiens[a]

Keywords: Nitrogen heterocycles / Lactams / Macrocycles / Rearrangement / Pyroglutamates / Hydantoins / Ring-closing metathesis / Isocyanates

A straightforward ring transformation giving polymethylenebis(hydantoins) was extended, as these are HMBA analogues. Firstly, ethyl or allyl pyroglutamate was carbamoylated with a diisocyanate. Upon treatment with KO*t*Bu in allyl alcohol the bis(carbamoyllactam) rearranged to give the hydantoin, which was followed by the ring-opening of the pyrrolidinone with formation of the allyl ester. These compounds were subsequently ring-closed in the presence of second-generation Grubbs' catalyst to form macrocycles containing the ester functionality in the ring. It was established by HSQC experiments with inverse detection that only the *E* isomers were formed in the cases of the 24- and 26-membered heterocycles.

Introduction

Hydantoins, first identified as products of undesired side-reactions in peptide chemistry, have attracted much interest in drug discovery because of their wide range of therapeutic properties, which include, among others, antiarrhythmic,[1] anticonvulsant,[2] antitumour,[3] antidiabetic[4] and antimuscarinic[5] activities. Several clinically important pharmaceuticals, such as phenytoin (**1**, Figure 1), which is used to treat certain types of epileptic seizures,[6] and nilutamide (**2**), an antiandrogen medication used in the treatment of prostate cancer, are based upon this heterocyclic scaffold. Hydantoins are useful not only for human medicine, but also in agriculture. Hydantocidin (**3**) is a naturally occurring spirohydantoin with herbicidal activities,[7] while iprodion (**4**) is a commercially used fungicide.

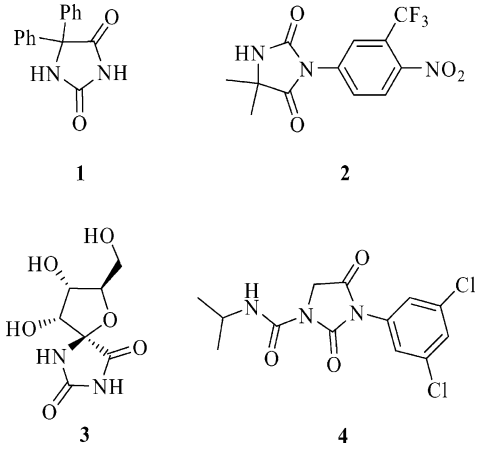

Figure 1. Phenytoin (**1**), nilutamide (**2**), hydantocidin (**3**) and iprodion (**4**).

Hydantoins may be regarded as cyclic ureides of α-amino acids, and these two types of compounds are readily interconvertible. A number of methods to synthesise hydantoins exist.[8,9] Treatment of α-amino acids, nitriles or amides with alkali cyanates is used mainly for the preparation of hydantoins with substituents at their C-5 positions, but also for N^1-substituted hydantoins. Treatment of free α-amino acids, esters or nitriles with isocyanates is valuable when hydantoins substituted at their N-3 positions are desired. Urea can be treated with α-amino acids, α-hydroxy acids, α-hydroxy nitriles, α-dicarbonyl compounds or unsaturated acids. Further, a range of other methods starting from amino acids or derivatives with carbonic acid derivatives such as phosgene, alkyl chloroformates or 1,1′-carbonyldiimidazole (CDI) have been described, while another general method is the Bucherer–Bergs synthesis of 5-substituted hydantoins from aldehydes and ketones through the action of potassium cyanide and ammonium carbonate. New synthetic methods are still being developed or older ones further investigated; they include palladium-catalysed reactions,[10] rearrangement reactions of 2,3-epoxydiaryl ketones[11] and modified Bucherer–Bergs reactions with nitriles and organometallic reagents.[12] In solid-phase synthesis the hydantoins are mostly synthesised from natural and unnatural acyclic α-amino acids or dipeptides as starting materials.[13]

[a] Research group SynBioC, Department of Organic Chemistry, Faculty of Bioscience Engineering, Ghent University, Coupure links 653, 9000 Ghent, Belgium
Fax: +32-9-2646243
E-mail: chris.stevens@ugent.be
[‡] Ph.D. fellow of the Research Foundation – Flanders (FWO).

Several N^3,$N^{3'}$-polymethylenebis(hydantoins) have been evaluated as hexamethylenebis(acetamide) (HMBA) analogues. HMBA is a compound that induces cancer cells to differentiate to a less malignant phenotype, which provides an attractive area for the development of new anticancer drugs. These differentiation agents are expected to exhibit reduced toxicity relative to conventional chemotherapeutic agents, since the mechanism is not primarily based on cytotoxity. HMBA had some modest success in a phase II clinical trial.[14] Relatively high drug concentrations, of the order of 5 mM, are required, but HMBA suffers from dose-related toxicity and has a short biological lifetime as it undergoes rapid deacetylation and rapid renal clearance.[15] The bis(hydantoin) **5a** (Figure 2) was about 10 times more potent than HMBA. The phenytoin analogue **5b** was very insoluble, which may have limited its activity.[16,17]

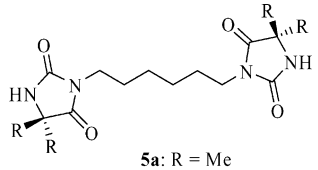

Figure 2. Bis(hydantoins) as HMBA analogues.

The bis(hydantoins) were synthesised through *N*-3-selective alkylation of the hydantoins with 1,6-dihalohexanes. The associated problems of selectivity and the low yields can be circumvented using the protocol described below.

Recently we reported on the pyroglutamate–hydantoin rearrangement:[18] when a solution of pyroglutamate and iso(thio)cyanate is treated with NaH in THF, ring-closure to the hydantoin occurs, with simultaneous ring-opening of the pyrrolidinone (Scheme 1). With this reaction in ether as a solvent, the intermediate sodium salt of the *N*-carbamoylated pyroglutamate precipitates and can be easily isolated. These products of the double ring-transformation can be converted into bicyclic hydantoin derivatives[18] and macrocycles.[19]

In view of the promising results of earlier biotesting by chick heart invasion assay,[20] in which some bis(hydantoins) with hexa- and octamethylene spacers showed anti-invasive activity at a concentration of 10 μM,[21] the allyl esters of the bis(hydantoins) were synthesised and further ring-closed by ring-closing metathesis (RCM).[22,23] In this library of compounds, the ester function is incorporated in the macrocyclic ring, endowing the molecule with lower polarity. Esterification is also a bioreversible chemical derivatisation and is most popular for drugs containing carboxy or hydroxy functions. This was used in, for example, the synthesis of prodrugs to D-prolines, where ester derivatives as well as further macrocyclic ring-closed products were evaluated.[24]

For the macrocycles that we have previously synthesised it was shown that only the *trans* isomers were formed.[19] This was also evaluated for the 24- and 26-membered rings described below. As these ring structures are symmetrical entities, $^3J_{H,H}$ coupling constants do not appear in the ^{1}H NMR spectra of these compounds, but can be recovered by using ^{1}H- and ^{13}C-correlated spectra obtained by inverse detection techniques.[25]

Results and Discussion

The hydantoins **11** were synthesised by the previously described two-step protocol,[19] since the more straightforward one-step ring-closing ring-opening (Scheme 1) did not go to completion in THF and some side reactions resulting from the attack of the alkoxide anions on the isocyanates occurred. NaH was therefore added to a mixture of allyl pyroglutamate, synthesised by a Dean–Stark esterification reaction, and diisocyanate in dry ether (Scheme 2). Almost immediately after the addition of the base, a white precipitate was formed. The reaction was quenched with saturated NH_4Cl solution after two hours. Stirring of the bis(carbamoyllactam) **11a** in allyl alcohol with 2.1 equiv. KO*t*Bu afforded the bis(hydantoin) **12a**.

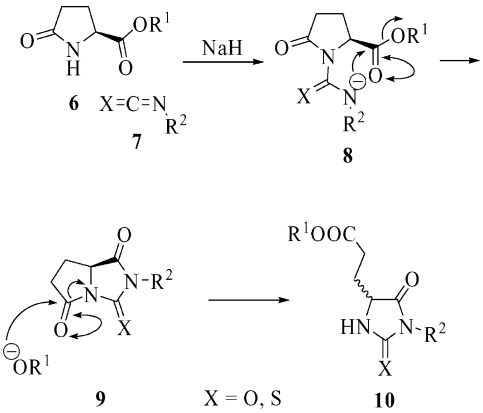

Scheme 1.

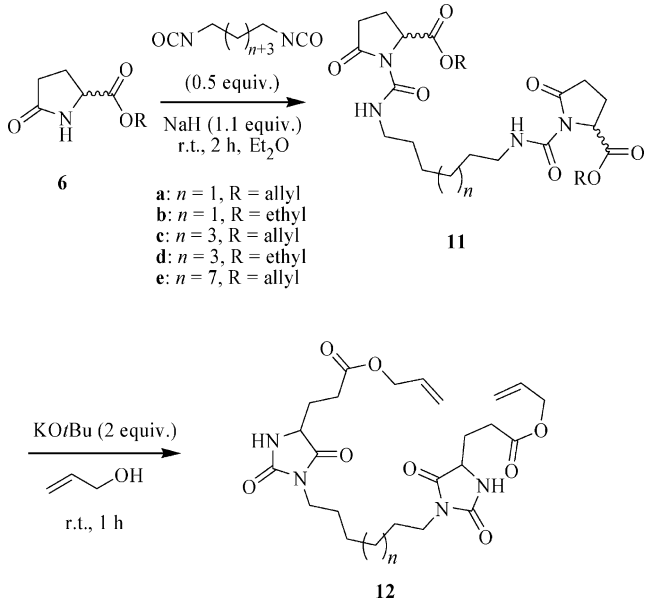

Scheme 2.

It was investigated whether one could start from ethyl pyroglutamate and perform a transesterification simultaneously with the pyroglutamate–hydantoin rearrangement (Table 1). For this purpose the ethyl pyroglutamate was carbamoylated in ether with 1,6-diisocyanatohexane and then rearranged in allyl alcohol by treatment with KO*t*Bu. This sequence resulted in pure bis(hydantoin) **12b** in a slightly higher yield – 85% in comparison with 71% – for the complete sequence in Scheme 2. Unfortunately, though, this protocol could not be used successfully for diisocyanates with longer alkyl chains, since not only carbamoylation, but also rearrangement had started even during the intended preparation of **11d**. This is in contrast with our previous results with short-chain alkylisocyanates and arylisocyanates, which did not rearrange even after stirring overnight in ether. After workup, the hydantoin, which in this case is the side-product, could be precipitated in diethyl ether (34% yield) while the carbamoylated product had to be purified by column chromatography (48% yield, **11d**). The rearrangement resulted in **12d** in high yield.

Table 1. Yields of carbamoylation and rearrangement of pyroglutamate **6**.

n	Path A, R = allyl		Path B, R = ethyl	
	Carbamoylation	Rearrangement	Carbamoylation	Rearrangement
1	**11a** 83%	**12a** 86%	**11b** 93%	**12b** 91%
3		**12c** 86%[a]	**11d** 48%[b]	**12d** 96%
7	**11e** 91%	**12e** 49%[c]		

[a] Product **11c** was not purified from the mixture with **12c**. [b] Drop in yield due to purification of **11d** from the crude mixture with the hydantoin by column chromatography. [c] Purified by column chromatography.

Also in the case of allyl pyroglutamate, prolonged stirring in ether causes the sodium salts of the carbamoylated lactams (**11c** and **11e**) to rearrange partially to the hydantoins (**12c** and **12e**), though the crude mixtures could be further used for the rearrangement in allyl alcohol. The rearrangement in ether can be limited by shortening the reaction time to 30 minutes and by using a 0.1 to 0.2 M concentration of the pyroglutamate. The limited reaction time is important, as side reactions occur with, for example, the nucleophilic alkoxide anions. Moreover, it is very important to work under dry conditions, as the presence of water leads to the formation of carbamic acids, which after decarboxylation produce amines, which add to isocyanates to form urea derivatives. These can be precipitated in ether, but column chromatography is needed to achieve complete purity.

The obtained hydantoins can be further derivatised by alkylation at nitrogen (Scheme 3). To introduce *N*-benzyl groups, the imidazolidinediones **12** were heated at reflux overnight in acetone with an excess of electrophile (mostly the corresponding bromide) and finely ground K_2CO_3. The alkylation had a 100% conversion, but the chromatographic removal of the excess of electrophile caused the yield to drop. For the methylation, iodomethane and NaH in DMF were used. The yields presented in Scheme 3 are those after purification of **13**.

The *N*-alkylation also serves as protection methodology for the *N*-lactam to prevent deactivation of the catalyst used for the cyclisation. RCM is a powerful method to synthesise macrocyclic products; substrates devoid of any conformational constraints can be cyclised by it. Neither the conformational predisposition of the substrates nor the ring-size play a decisive role, but the presence of polar relay substituents, their distance from the alkene groups and low steric hindrance close to the double bond are important.[26] The ring-closure was carried out by use of 5 mol-% of second-generation Grubbs' catalyst **16** (Figure 3).[27] Simply heating the compounds at reflux overnight together with the ruthenium catalyst resulted in quantitative conversion to the macrocycles.

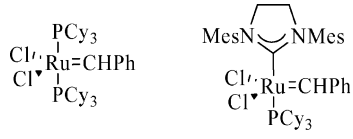

15 **16**

Figure 3. First- and second-generation Grubbs' catalysts.

Usually RCM results in mixtures of *E* and *Z* isomers, but in some cases only *E* isomers have been formed.[28] The use of the fully saturated second-generation Grubbs' catalyst **16** affords much higher *E*/*Z* ratios than the use of the standard Grubbs' carbene **15**.[29] This is caused by the ability of **16** to isomerise the initial product under the reaction

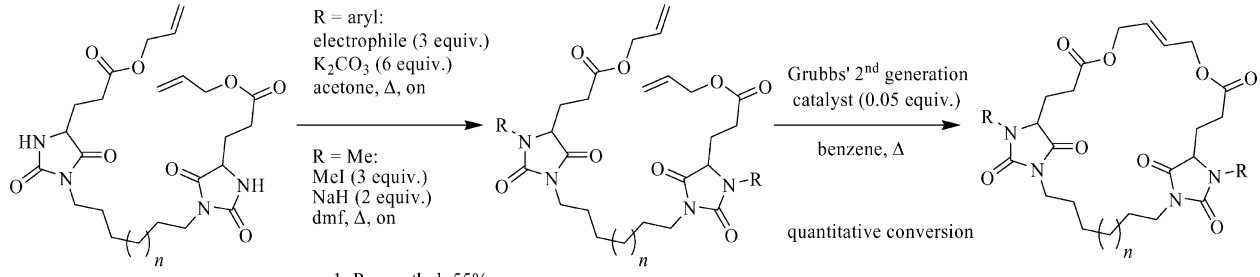

12 **13** **14**

a: *n* = 1, R = methyl, 55%
b: benzyl, 73%
c: *p*-bromobenzyl, 78%
d: *n* = 3, R = *p*-chlorobenzyl, 68%
e: *p*-bromobenzyl, 54%
f: *n* = 7, R = benzyl, 55%

Scheme 3.

conditions, thereby progressively enriching the mixture in the thermodynamically favoured *E* isomer.[30]

Also in this case, two separate signals for the alkene protons of derivatives **14** were observed. Since these macrocycles **14** have two chiral centres, these can be diastereomers as well. Usually the *E* and *Z* isomers are distinguished through their $^3J_{H,H}$ NMR coupling constants, but these are absent as the macrocycles are symmetrical. These $^3J_{H,H}$ coupling constants, however, can be recovered when an H,C-inverse-detection spectrum is acquired without carbon-decoupling during acquisition. In the inverse-detected H,C-correlation spectra, the major component due to signals coming from H bonded to ^{12}C, which represents 99% of the total number of C atoms in normal ^1H NMR spectra, is suppressed. By doing this, the $^3J_{H,H}$ coupling constants between equivalent protons can be observed.[25]

The diastereomers of **14a** and **14c** were separated by preparative thin-layer chromatography (TLC), though chromatography again caused a large drop in yield. For **14c**, coupling constants of 17.4 and 18.1 Hz were observed, pointing to *trans* geometries for both isomers.

Further evidence that a mixture of diastereomers rather than *E* and *Z* isomers is formed was provided by an experiment in which one of the diastereomers of **13e** was isolated in pure form by column chromatography. This so-called "diastereomer" is actually a mixture of two enantiomers, which cannot be distinguished in the NMR spectra. Heating of this diastereomer at reflux with Grubbs' catalyst **16** gave one product in the ^{13}C NMR spectrum, so only the *E* or the *Z* isomer was formed, as otherwise two products should have been observed in the ^{13}C NMR spectrum. The coupling constant of **14e** was 17.7 Hz, again pointing to the formation of the *E* isomer.

Conclusions

The pyroglutamate hydantoin rearrangement has been used to construct $N^3,N^{3'}$- polymethylenebis(hydantoins), which are HMBA analogues and showed anti-invasive activity in the chick heart assay. The biological data will be published in due course. After *N*-alkylation or *N*-arylation, the bis(hydantoins) were ring-closed to form 24- to 30-membered macrocycles, again indicating the power of ring-closing metathesis. The use of second-generation Grubbs' catalyst **16** resulted in exclusive formation of the *trans* isomers, as was confirmed by undecoupled HSQC.

Experimental Section

General Remarks: High-resolution ^1H NMR (300 MHz) and ^{13}C NMR (75 MHz) spectra were run with a Jeol EX300 Eclipse NMR spectrometer. Peak assignments were obtained with the aid of 2D-HSQC, 2D-HMBC and 2D-COSY spectra. The compounds were diluted in deuterated solvents, and the solvent used is indicated for each compound. Low-resolution mass spectra were recorded with an Agilent 1100 Series VS (ES = 4000 V) mass spectrometer. IR spectra were obtained with a Perkin–Elmer Spectrum One infrared spectrometer. The samples were collected by preparing a thin film of compound between two sodium chloride plates. Crystalline compounds were mixed with KBr and pressed in a transparent plate. Melting points of crystalline compounds were measured with a Büchi 540 apparatus and have not been corrected. The elemental analysis was performed with a Perkin–Elmer 2400 Elemental Analyzer. The purification of reaction mixtures was performed by column chromatography in a glass column with silica gel (Across, particle size 0.035–0.070 mm, pore diameter ca. 6 nm). Removal of the Grubbs' catalyst was achieved by preparative thin-layer chromatography.

In the next part the procedures and spectroscopic data are given for the different types of reaction. The amounts in grams were used for the synthesis of the products that are given just underneath the procedures.

Typical Experimental Procedure for the Carbamoylation of Pyroglutamates at Nitrogen: The pyroglutamate ester (2.48 g, 14.66 mmol) was dissolved in dry diethyl ether (70 mL, freshly distilled from Na metal), the diisocyanate (1.24 g, 7.37 mmol) was added by syringe, and the mixture was briefly stirred. After addition of NaH (0.36 g, 15.00 mmol) the reaction mixture was stirred under nitrogen for 0.5 to 2 hours, while a white precipitate formed. The reaction was then quenched with saturated NH_4Cl solution until the pH was neutral or slightly acidic. The mixture was extracted three times with EtOAc, and the organic layers were dried with $MgSO_4$ and filtered. Compound **11c** was further purified by column chromatography. The allyl ester derivatives can be used without purification in the subsequent rearrangement reaction, as they appear with the rearranged product.

Allyl 1-{6-[(2-Allyloxycarbonyl-5-oxopyrrolidin-1-ylcarbonyl)-amino]hexylcarbamoyl}-5-oxopyrrolidine-2-carboxylate (11a): Yield 83%, 3.08 g. ^1H NMR (300 MHz, $CDCl_3$): δ = 1.30–1.40 (m, 4 H, CH_2CH_2), 1.50–1.60 (m, 4 H, $2\times CH_2CH_2N$), 2.01–2.11 (m, 2 H, $2\times CH_aH_b$, ring), 2.28–2.42 (m, 2 H, $2\times CH_aH_b$, ring), 2.57 (ddd, J = 17.7, 9.4, 3.3 Hz, 2 H, $2\times CH_aH_bCO$), 2.75 (dt, J = 17.7, 9.9 Hz, 2 H, $2\times CH_aH_bCO$), 3.18–3.37 (m, 4 H, $2\times NCH_2$), 4.68 (br d, J = 5.7 Hz, 4 H, $2\times OCH_2$), 4.82 (dd, J = 9.6, 2.8 Hz, 2 H, $2\times CH$), 5.26 (ddd, J_{cis} = 10.5, 2.3, 1.1 Hz, 2 H, $2\times =CH_aH_b$), 5.35 (ddd, J_{trans} = 17.3, 2.3, 1.4 Hz, 2 H, $2\times =CH_aH_b$), 5.92 (ddt, J_{trans} = 17.3 Hz, J_{cis} = 10.5 Hz and J_{vic} = 5.7 Hz, 2 H, $2\times CH=CH_2$), 8.28 (t, J = 5.2 Hz, 2 H, $2\times NH$) ppm. ^{13}C NMR (75 MHz, $CDCl_3$): δ = 21.25 ($2\times CH_2$, ring), 26.46 (CH_2CH_2), 29.47 ($2\times CH_2CH_2N$), 31.83 ($2\times CH_2CO$), 39.80 ($2\times NCH_2$), 58.10 ($2\times CH$), 66.14 ($2\times OCH_2$), 118.89 ($2\times =CH_2$), 131.43 ($2\times CH=CH_2$), 152.18 ($2\times C$=O, urea), 171.17 ($2\times C$=O, ester), 176.32 ($2\times C$=O, lactam) ppm. IR (NaCl): $\tilde{\nu}_{max}$ = 1651 (C=C), 1689 (C=O), 1719 (C=O), 1745 (C=O), 3317 (NH) cm^{-1}. MS: *m/z* (%) = 507 (100) $[M + H]^+$. $C_{24}H_{34}N_4O_8$ (506.55): calcd. C 56.91, H 6.77, N 11.06; found C 57.14, H 6.41, N 11.38.

Ethyl 1-{6-[(2-Ethoxycarbonyl-5-oxopyrrolidin-1-ylcarbonyl)-amino]hexylcarbamoyl}-5-oxopyrrolidine-2-carboxylate (11b): Yield 93%, 1.43 g, white powder, m.p. 79 °C. ^1H NMR (300 MHz, $CDCl_3$): δ = 1.29 (t, J = 7.2 Hz, 6 H, $2\times CH_3$), 1.32–1.38 (m, 4 H, CH_2CH_2), 1.50–1.59 (m, 4 H, $2\times CH_2CH_2N$), 1.99–2.09 (m, 2 H, $2\times CH_aH_b$, ring), 2.27–2.41 (m, 2 H, $2\times CH_aH_b$, ring), 2.57 (ddd, J = 17.6, 9.4, 3.3 Hz, 2 H, $2\times CH_aH_bCO$), 2.74 (dt, J = 17.6, 9.9 Hz, 2 H, $2\times CH_aH_bCO$), 3.18–3.37 (m, 4 H, $2\times NCH_2$), 4.24 (q, J = 7.2 Hz, 4 H, $2\times OCH_2$), 4.78 (dd, J = 9.4, 2.8 Hz, 2 H, $2\times CH$), 8.28 (t, J = 5.5 Hz, 2 H, $2\times NH$) ppm. ^{13}C NMR (75 MHz, $CDCl_3$): δ = 14.21 ($2\times CH_3$), 21.37 ($2\times CH_2$, ring), 26.58 (CH_2CH_2), 29.60 ($2\times CH_2CH_2N$), 31.98 ($2\times CH_2CO$), 39.91 ($2\times NCH_2$), 58.26 ($2\times CH$), 61.80 ($2\times OCH_2$), 152.32 ($2\times C$=O, urea), 171.61 ($2\times C$=O, ester), 176.49 ($2\times C$=O, lactam) ppm. IR

(NaCl): $\tilde{\nu}_{max}$ = 1693 (C=O), 1722 (C=O), 1742 (C=O), 3320 (NH) cm^{-1}. MS: *m*/*z* (%) = 483 (100) [M + H]$^+$. $C_{22}H_{34}N_4O_8$ (482.53): calcd. C 54.76, H 7.10, N 11.61; found C 54.47, H 7.26, N 11.45.

The mixture of **11c** and the rearranged product was used without purification.

Ethyl 1-{6-[(2-Ethoxycarbonyl-5-oxopyrrolidin-1-ylcarbonyl)-amino]octylcarbamoyl}-5-oxopyrrolidine-2-carboxylate (11d): Yield 48%, 0.50 g; the rearranged product was also formed. ^{1}H NMR (300 MHz, $CDCl_3$): δ = 1.26–1.32 (m, 14 H, 2×C*H*$_3$, CH_2CH_2), 1.50–1.58 (m, 4 H, 2×CH_2CH_2N), 2.00–2.10 (m, 2 H, 2×CH_aH$_b$, ring), 2.28–2.42 (m, 2 H, 2×CH$_a$*H*$_b$, ring), 2.57 (ddd, *J* = 17.6, *J* = 9.4, 3.3 Hz, 2 H, 2×CH_aH$_b$CO), 2.75 (dt, *J* = 17.6, 9.9 Hz, 2 H, 2×CH$_a$*H*$_b$CO), 3.19–3.36 (m, 4 H, 2×NCH_2), 4.24 (q, *J* = 7.2 Hz, 4 H, 2×OCH_2), 4.77 (dd, *J* = 9.4, 2.8 Hz, 2 H, 2×C*H*), 8.29 (t, *J* = 5.5 Hz, 2 H, 2×N*H*) ppm. ^{13}C NMR (75 MHz, $CDCl_3$): δ = 14.08 (2×*C*H$_3$), 21.22 (2×*C*H$_2$, ring), 26.70 (*C*H$_2$CH$_2$), 29.09 (*C*H$_2$CH$_2$CH$_2$*C*H$_2$), 29.51 (2×*C*H$_2$CH$_2$N), 31.85 (2×*C*H$_2$CO), 39.85 (2×N*C*H$_2$), 58.14 (2×*C*H), 61.62 (2×O*C*H$_2$), 152.19 (2×*C*=O, urea), 171.48 (2×*C*=O, ester), 176.39 (2×*C*=O, lactam) ppm. IR (NaCl): $\tilde{\nu}_{max}$ = 1692 (C=O), 1721 (C=O), 1744 (C=O), 3316 (NH) cm^{-1}. MS: *m*/*z* (%) = 511 (100) [M + H]$^+$. Chromatography: R_f = 0.20 (PE/EtOAc, 1:1). $C_{24}H_{38}N_4O_8$ (510.58): calcd. C 56.46, H 7.50, N 10.97; found C 56.59, H 7.51, N 11.04.

Allyl 1-{6-[(2-Allyloxycarbonyl-5-oxopyrrolidin-1-ylcarbonyl)-amino]dodecylcarbamoyl}-5-oxopyrrolidine-2-carboxylate (11e): Yield 91%, 0.63 g. ^{1}H NMR (300 MHz, $CDCl_3$): δ = 1.25–1.36 [m, 16 H, 2×N(CH$_2$)$_2$(CH_2)$_4$], 1.49–1.56 (m, 4 H, 2×CH_2CH$_2$N), 2.07 (ddt, *J* = 13.1, *J* = 9.8, 2.9 Hz, 2 H, 2×CH_aH$_b$, ring), 2.28–2.42 (m, 2 H, 2×CH$_a$*H*$_b$, ring), 2.57 (ddd, *J* = 17.6, *J* = 9.3, 3.2 Hz, 2 H, 2×CH_aH$_b$CO), 2.75 (dt, *J* = 17.6, 9.8 Hz, 2 H, 2×CH$_a$*H*$_b$CO), 3.19–3.37 (m, 4 H, 2×NCH_2), 4.66–4.69 (m, 4 H, 2×OCH_2), 4.82 (dd, *J* = 9.6, 2.9 Hz, 2 H, 2×C*H*), 5.27 (dbrq, *J* = 10.6, 1.4 Hz, 2 H, 2×=CH_aH$_b$), 5.35 (dbrq, J_{trans} = 17.2, 1.4 Hz, 2 H, 2×=CH$_a$*H*$_b$), 5.92 (ddt, J_{trans} = 17.2, J_{cis} = 10.6, J_{vic} = 5.7 Hz, 2 H, 2×C*H*=CH$_2$), 8.28 (t, *J* = 5.2 Hz, 2 H, 2×N*H*) ppm. ^{13}C NMR (75 MHz, $CDCl_3$): δ = 21.25 (2×*C*H$_2$, ring), 26.86 (*C*H$_2$CH$_2$), 29.27 (2×*C*H$_2$), 29.51 (2×*C*H$_2$), 29.54 (2×*C*H$_2$), 29.57 (2×*C*H$_2$CH$_2$N), 31.86 (2×*C*H$_2$CO), 39.99 (2×N*C*H$_2$), 58.11 (2×*C*H), 66.14 (2×O*C*H$_2$), 118.91 (2×=*C*H$_2$), 131.41 (2×*C*H=CH$_2$), 152.16 (2×*C*=O, urea), 171.20 (2×*C*=O, ester), 176.32 (2×*C*=O, lactam) ppm. IR (NaCl): $\tilde{\nu}_{max}$ = 1695 (C=O), 1722 (C=O), 1745 (C=O), 3323 (NH) cm^{-1}. MS: *m*/*z* (%) = 591 (100) [M + H]$^+$. $C_{30}H_{46}N_4O_8$ (590.71): calcd. C 61.00, H 7.85, N 9.48; found C 60.62, H 7.62, N 9.41.

Typical Experimental Procedure for the Rearrangement of Carbamoylated Pyroglutamates 11 to Hydantoins 12: The pyroglutamate ester **11** (1.40 g, 2.76 mmol) was dissolved in allyl alcohol (20 mL) and KO*t*Bu (0.65 g, 5.79 mmol) was added. The mixture was stirred at room temperature for 1 hour, protected from moisture with a $CaCl_2$ tube. The reaction mixture was quenched with a saturated NH_4Cl solution, extracted with EtOAc, dried with $MgSO_4$ and filtered. Removal of the solvent yielded the product. Product **12a** was crystallised from EtOAc, **12b** and **12c** were crystallised from dry acetone, and **12e** was further purified by column chromatography.

Allyl 3-(1-{6-[4-(2-Allyloxycarbonylethyl)-2,5-dioxoimidazolidin-1-yl]hexyl}-2,5-dioxoimidazolidin-4-yl)propionate (12a and 12b): Yield 86%, 1.20 g and 91%, 0.42 g, white crystals, m.p. 99–103 °C. ^{1}H NMR (300 MHz, $CDCl_3$): δ = 1.28–1.39 (m, 4 H, CH_2CH_2), 1.56–1.68 (m, 4 H, 2×CH_2CH$_2$N), 1.98–2.10 (m, 2 H, 2×CH_aH$_b$CH$_2$CO), 2.17–2.29 (m, 2 H, 2×CH$_a$*H*$_b$CH$_2$CO), 2.51 (t, *J* = 7.2 Hz, 4 H, 2×CH_2CO), 3.48 (t, *J* = 7.2 Hz, 4 H, 2×NCH_2), 4.10 (brt, *J* = 5.8 Hz, 2 H, 2×C*H*), 4.60 (d, *J* = 5.8 Hz, 4 H, 2×OCH_2), 5.26 (dq, J_{cis} = 10.5, 1.1 Hz, 2 H, 2×=CH_aH$_b$), 5.32 (dq, J_{trans} = 17.1, 1.5 Hz, 2 H, 2×=CH$_a$*H*$_b$), 5.91 (ddt, J_{trans} = 17.1, J_{cis} = 10.5, J_{vic} = 5.8 Hz, 2 H, 2×C*H*=CH$_2$), 6.00 (brs, 2 H, 2×N*H*) ppm. ^{13}C NMR (75 MHz, $CDCl_3$): δ = 26.12 (*C*H$_2$*C*H$_2$), 26.81 (2×*C*H$_2$CH$_2$CO), 27.82 (2×*C*H$_2$CH$_2$N), 29.68 (2×*C*H$_2$CO), 38.51 (2×N*C*H$_2$), 56.25 (2×*C*H), 65.65 (2×O*C*H$_2$), 118.83 (2×=*C*H$_2$), 131.78 (2×*C*H=CH$_2$), 157.28 (2×*C*=O, urea), 172.45 (2×*C*=O, ester), 173.54 (2×*C*=O, lactam) ppm. IR (KBr): $\tilde{\nu}_{max}$ = 1650 (C=C), 1732 (C=O), 1771 (C=O), 3234 (NH) cm^{-1}. MS: *m*/*z* (%) = 505 (100) [M + H]$^+$. $C_{24}H_{34}N_4O_8$ (506.55): calcd. C 56.91, H 6.77, N 11.06; found C 56.82, H 6.82, N 10.99.

Allyl 3-(1-{8-[4-(2-Allyloxycarbonylethyl)-2,5-dioxoimidazolidin-1-yl]octyl}-2,5-dioxoimidazolidin-4-yl)propionate (12c and 12d): Yield 86%, 1.05 g from **6a** and 96%, 50 mg, white powder, m.p. 89 °C. ^{1}H NMR (300 MHz, $CDCl_3$): δ = 1.22–1.35 [m, 8 H, 2×N(CH$_2$)$_2$-(CH_2)$_2$], 1.54–1.64 (m, 4 H, 2×NCH$_2$CH_2), 1.99–2.10 (m, 2 H, 2×CH_aH$_b$CH), 2.18–2.29 (m, 2 H, 2×CH$_a$*H*$_b$CH), 2.51 (t, *J* = 7.2 Hz, 4 H, 2×CH_2CO), 3.47 (t, *J* = 7.3 Hz, 4 H, 2×NCH_2), 4.10 (brt, *J* = 5.4 Hz, 2 H, 2×C*H*), 4.59 (brd, *J* = 5.8 Hz, 4 H, 2×OCH_2), 5.26 (dq, J_{cis} = 10.4, 1.4 Hz, 2 H, 2×=CH_aH$_b$), 5.32 (dq, J_{trans} = 17.2, 1.4 Hz, 2 H, 2×=CH$_a$*H*$_b$), 5.91 (ddt, J_{trans} = 17.2, J_{cis} = 10.4, J_{vic} = 5.8 Hz, 2 H, 2×C*H*=CH$_2$), 6.31 (s, 2 H, 2×N*H*) ppm. ^{13}C NMR (75 MHz, $CDCl_3$): δ = 26.64 [2×N(CH$_2$)$_3$-*C*H$_2$], 26.93 (2×*C*H$_2$CH), 28.06 (2×NCH$_2$*C*H$_2$), 29.02 [2×N(CH$_2$)$_2$*C*H$_2$], 29.69 (2×*C*H$_2$CO), 38.79 (2×N*C*H$_2$), 56.32 (2×*C*H), 65.74 (2×O*C*H$_2$), 118.90 (2×=*C*H$_2$), 131.91 (2×*C*H=CH$_2$), 157.65 (2×*C*=O, urea), 172.54 (2×*C*=O, ester), 173.73 (2×*C*=O, lactam) ppm. IR (NaCl): $\tilde{\nu}_{max}$ = 1649 (C=C), 1706 (C=O), 1774 (C=O), 3310 (NH) cm^{-1}. MS: *m*/*z* (%) = 535 (100) [M + H]$^+$. $C_{26}H_{38}N_4O_8$ (534.60): calcd. C 58.41, H 7.16, N 10.48; found C 58.14, H 7.33, N 10.39.

Allyl 3-(1-{12-[4-(2-Allyloxycarbonylethyl)-2,5-dioxoimidazolidin-1-yl]dodecyl}-2,5-dioxoimidazolidin-4-yl)propionate (12e): Yield 49%, 0.16 g, oil. ^{1}H NMR (300 MHz, $CDCl_3$): δ = 1.22–1.28 [m, 16 H, 2×N(CH$_2$)$_2$(CH_2)$_4$], 1.47–1.64 (m, 4 H, 2×CH_2CH$_2$N), 1.99–2.11 (m, 2 H, 2×CH_aH$_b$CH), 2.17–2.30 (m, 2 H, 2×CH$_a$*H*$_b$CH), 2.51 (t, *J* = 7.3 Hz, 4 H, 2×CH_2CO), 3.47 (t, *J* = 7.2 Hz, 4 H, 2×NCH_2), 4.11 (t, *J* = 5.9 Hz, 2 H, 2×C*H*), 4.59 (brd, *J* = 5.8 Hz, 4 H, 2×OCH_2), 5.25 (dq, J_{cis} = 10.4, 1.4 Hz, 2 H, 2×=CH_aH$_b$), 5.32 (dq, J_{trans} = 17.1, 1.4 Hz, 2 H, 2×=CH$_a$*H*$_b$), 5.91 (ddt, J_{trans} = 17.1, J_{cis} = 10.4, J_{vic} = 5.8 Hz, 2 H, 2×C*H*=CH$_2$), 6.74 (s, 2 H, 2×N*H*) ppm. ^{13}C NMR (75 MHz, $CDCl_3$): δ = 26.74 [2×N(CH$_2$)$_2$-*C*H$_2$], 26.87 (2×*C*H$_2$CH), 28.09 (2×*C*H$_2$CH$_2$N), 29.16 [2×N(CH$_2$)$_3$*C*H$_2$], 29.49 [2×*C*H$_2$CO and 2×N(CH$_2$)$_4$(*C*H$_2$)$_2$], 38.78 (2×N*C*H$_2$), 56.21 (2×*C*H), 65.62 (2×O*C*H$_2$), 118.72 (2×=*C*H$_2$), 131.88 (2×*C*H=CH$_2$), 157.84 (2×*C*=O, urea), 172.40 (2×*C*=O, ester), 173.78 (2×*C*=O, lactam) ppm. IR (NaCl): $\tilde{\nu}_{max}$ = 1651 (C=C), 1710 (C=O), 1733 (C=O), 1774 (C=O), 3337 (NH) cm^{-1}. MS: *m*/*z* (%) = 591 (100) [M + H]$^+$. Chromatography: R_f = 0.01 (PE/EtOAc, 5:2). $C_{30}H_{46}N_4O_8$ (590.71): calcd. C 61.00, H 7.85, N 9.48; found C 61.19, H 7.87, N 9.30.

Typical Procedure for the *N*-Alkylation of Hydantoins. Synthesis of 13a: The bis(hydantoin) (0.12 g, 0.24 mmol) was dissolved in THF (7 mL). Iodomethane (0.10 g, 0.70 mmol) was added by syringe, followed by NaH (0.02 g, 0.83 mmol). The mixture was stirred overnight, protected from moisture with a $CaCl_2$ tube. The reaction was quenched with a saturated NH_4Cl solution, extracted with EtOAc, dried with $MgSO_4$, filtered and coated on silica for column chromatography.

Allyl 3-(1-{6-[4-(2-Allyloxycarbonylethyl)-3-methyl-2,5-dioxoimidazolidin-1-yl]hexyl}-3-methyl-2,5-dioxoimidazolidin-4-yl)propionate (13a): Yield 55%, 71 mg, yellowish oil. ^{1}H NMR (300 MHz, $CDCl_3$): δ = 1.27–1.37 (m, 4 H, CH_2CH_2), 1.54–1.64 (m, 4 H, 2×CH_2CH$_2$N), 2.02–2.19 (m, 2 H, 2×CH_aH$_b$CH$_2$CO), 2.20–2.34 (m, 2 H, 2×CH$_a$$H_bCH_2$CO), 2.30–2.53 (m, 4 H, 2×CH_2CO), 2.93 (s, 6 H, 2×NCH_3), 3.47 (brt, J = 7.3 Hz, 4 H, 2×NCH_2), 3.91 (dd, J = 6.5, 3.2 Hz, 2 H, 2×CH), 4.58 (brd, J = 5.8 Hz, 4 H, 2×OCH_2), 5.25 (dbrq, J = 10.5, 1.2 Hz, 2 H, 2×=CH_aH$_b$), 5.32 (dbrq, J = 17.2, 1.2 Hz, 2 H, 2×=CH$_a$$H_b$), 5.90 (ddt, J_{trans} = 17.2, J_{cis} = 10.5, J_{vic} = 5.8 Hz, 2 H, 2×CH=CH$_2$) ppm. ^{13}C NMR (75 MHz, $CDCl_3$): δ = 23.73 (2×CH$_2$CH$_2$CO), 26.18 (CH$_2$$CH_2$), 27.85 (2×$CH_3$), 27.93 (2×$CH_2CH_2$N), 28.11 (2×$CH_2$CO), 38.78 (2×NCH$_2$, alkyl), 60.05 (2×$C$H), 65.55 (2×OCH$_2$), 118.68 (2×=$CH_2$), 131.89 (2×$C$H=CH$_2$), 156.62 (2×$C$=O, urea), 171.98 (2×$C$=O, ester), 172.36 (2×$C$=O, lactam) ppm. IR (NaCl): $\tilde{\nu}_{max}$ = 1709 (C=O), 1732 (C=O), 1770 (C=O) cm^{-1}. MS: m/z (%) = 535 (100) [M + H]$^+$. Chromatography: R_f = 0.01 (PE/EtOAc, 4:1). $C_{26}H_{38}N_4O_8$ (534.60): calcd. C 58.41, H 7.16, N 10.48; found C 58.37, H 7.18, N 10.14.

Typical Procedure for the *N*-Alkylation of Hydantoins. Synthesis of 13b–e: The bis(hydantoin) (0.32 g, 0.63 mmol) was dissolved in dry acetone (6 mL, dried with K_2CO_3 and distilled). The aryl bromide (0.32 g, 1.87 mmol) and K_2CO_3 (0.52 g, 3.76 mmol) were added and the mixture was heated at reflux overnight, protected from moisture with a $CaCl_2$ tube. The solution was cooled to room temperature, and the precipitate was filtered and coated on silica for column chromatography.

Allyl 3-(1-{6-[4-(2-Allyloxycarbonylethyl)-3-benzyl-2,5-dioxoimidazolidin-1-yl]hexyl}-3-benzyl-2,5-dioxoimidazolidin-4-yl)propionate (13b): Yield 73%, 0.52 g, yellow oil. ^{1}H NMR (300 MHz, $CDCl_3$): δ = 1.31–1.42 (m, 4 H, CH_2CH_2), 1.58–1.68 (m, 4 H, 2×CH_2CH$_2$N), 2.01–2.13 (m, 2 H, 2×CH_aH$_b$CH$_2$CO), 2.16–2.27 (m, 2 H, 2×CH$_a$$H_bCH_2$CO), 2.25–2.42 (m, 4 H, 2×CH_2CO), 3.51 (brt, J = 7.2 Hz, 4 H, 2×NCH_2, alkyl), 3.82 (dd, J = 6.2, 2.9 Hz, 2 H, 2×CH), 4.10 (d, J = 15.3 Hz, 2 H, 2×NCH_aH$_b$, benzyl), 4.55 (brd, J = 5.8 Hz, 4 H, 2×OCH_2), 4.97 (d, J = 15.3 Hz, 2 H, 2×NCH$_a$$H_b$, benzyl), 5.23 (dbrq, J_{cis} = 10.5, 1.2 Hz, 2 H, 2×=CH_aH$_b$), 5.30 (dbrq, J_{trans} = 17.2, 1.2 Hz, 2 H, 2×=CH$_a$$H_b$), 5.89 (ddt, J_{trans} = 17.2, J_{cis} = 10.5, J_{vic} = 5.8 Hz, 2 H, 2×CH=CH$_2$), 7.25–7.37 (m, 10 H, 10×CH_{ar}) ppm. ^{13}C NMR (75 MHz, $CDCl_3$): δ = 23.45 (2×CH$_2$CH$_2$CO), 26.13 (CH$_2$$CH_2$), 27.86 (2×$CH_2CH_2$N or 2×$CH_2$CO), 27.95 (2×$CH_2CH_2$N or 2×$CH_2$CO), 38.79 (2×NCH$_2$, alkyl), 44.59 (2×NCH$_2$, benzyl), 57.31 (2×$C$H), 65.42 (2×OCH$_2$), 118.54 (2×=$CH_2$), 128.09 (2×$CH_{ar}$), 128.20 (4×$CH_{ar}$), 128.96 (4×$CH_{ar}$), 131.90 (2×$C$H=CH$_2$), 135.59 (2×$C_{ar,quat.}$), 156.63 (2×$C$=O, urea), 171.84 (2×$C$=O, ester), 172.28 (2×$C$=O, lactam) ppm. IR (NaCl): $\tilde{\nu}_{max}$ = 1649 (C=C), 1707 (C=O), 1734 (C=O), 1768 (C=O) cm^{-1}. MS: m/z (%) = 687 (100) [M + H]$^+$. Chromatography: R_f = 0.02 (PE/EtOAc, 4:1). $C_{38}H_{46}N_4O_8$ (686.79): calcd. C 66.45, H 6.75, N 8.16; found C 66.10, H 6.46, N 8.09.

Allyl 3-(1-{6-[4-(2-Allyloxycarbonylethyl)-3-(4-bromobenzyl)-2,5-dioxoimidazolidin-1-yl]hexyl}-3-(4-bromobenzyl)-2,5-dioxoimidazolidin-4-yl)propionate (13c): Yield 78%, 0.17 g, yellowish oil. ^{1}H NMR (300 MHz, $CDCl_3$): δ = 1.31–1.40 (m, 4 H, CH_2CH_2), 1.57–1.67 (m, 4 H, 2×CH_2CH$_2$N), 1.97–2.09 (m, 2 H, 2×CH_aH$_b$CH$_2$CO), 2.16–2.25 (m, 2 H, 2×CH$_a$$H_bCH_2$CO), 2.25–2.45 (m, 4 H, 2×CH_2CO), 3.50 (brt, J = 7.2 Hz, 4 H, 2×NCH_2, alkyl), 3.82 (dd, J = 6.6, 3.0 Hz, 2 H, 2×CH), 4.10 (d, J = 15.3 Hz, 2 H, 2×NCH_aH$_b$, benzyl), 4.56 (brd, J = 5.8 Hz, 4 H, 2×OCH_2), 4.88 (d, J = 15.3 Hz, 2 H, 2×NCH$_a$$H_b$, benzyl), 5.22–5.28 (m, 2 H, 2×=CH_aH$_b$), 5.26–5.34 (m, 2 H, 2×=CH$_a$$H_b$), 5.89 (ddt, J_{trans} = 16.7, J_{cis} = 10.3, J_{vic} = 5.8 Hz, 2 H, 2×CH=CH$_2$), 7.16 (d, J = 8.4 Hz, 4 H, 4×CH_{ar}), 7.48 (d, J = 8.4 Hz, 4 H, 4×CH_{ar}) ppm. ^{13}C NMR (75 MHz, $CDCl_3$): δ = 23.81 (2×CH$_2$CH$_2$CO), 26.36 (CH$_2$$CH_2$), 28.10 (2×$CH_2CH_2$N), 28.20 (2×$CH_2$CO), 39.09 (2×NCH$_2$, alkyl), 44.34 (2×NCH$_2$, benzyl), 57.67 (2×$C$H), 65.78 (2×OCH$_2$), 118.93 (2×=$CH_2$), 122.44 (2×$C_{ar,quat.}$), 130.21 (4×$CH_{ar}$), 132.07 (2×$C$H=CH$_2$), 132.39 (4×$CH_{ar}$), 134.94 (2×$C_{ar,quat.}$), 156.88 (2×$C$=O, urea), 172.12 (2×$C$=O, ester), 172.40 (2×$C$=O, lactam) ppm. IR (NaCl): $\tilde{\nu}_{max}$ = 1705 (C=O), 1732 (C=O), 1768 (C=O) cm^{-1}. MS: m/z (%) = 843/845/847 (100) [M + H]$^+$. Chromatography: R_f = 0.17 (PE/EtOAc, 5:3). $C_{38}H_{44}Br_2N_4O_8$ (844.59): calcd. C 54.04, H 5.25, N 6.63; found C 53.81, H 5.29, N 6.32.

Allyl 3-(1-{8-[4-(2-Allyloxycarbonylethyl)-3-(4-chlorobenzyl)-2,5-dioxoimidazolidin-1-yl]octyl}-3-(4-chlorobenzyl)-2,5-dioxoimidazolidin-4-yl)propionate (13d): Yield 68%, 51 mg. ^{1}H NMR (300 MHz, $CDCl_3$): δ = 1.22–1.34 [m, 8 H, 2×N(CH$_2$)$_2$(CH_2)$_2$], 1.56–1.66 (m, 4 H, 2×NCH$_2$CH_2), 1.98–2.10 (m, 2 H, 2×CH_aH$_b$CH), 2.17–2.26 (m, 2 H, 2×CH$_a$$H_b$CH), 2.24–2.45 (m, 4 H, 2×CH_2CO), 3.50 (td, J = 7.4, 1.8 Hz, 4 H, 2×NCH_2, alkyl), 3.81 (dd, J = 6.5, 2.9 Hz, 2 H, 2×CH), 4.11 (d, J = 15.3 Hz, 2 H, 2×NCH_aH$_b$, benzyl), 4.56 (d, J = 5.8 Hz, 4 H, 2×OCH_2), 4.90 (d, J = 15.3 Hz, 2 H, 2×NCH$_a$$H_b$, benzyl), 5.25 (brd, J_{cis} = 10.8 Hz, 2 H, 2×=CH_aH$_b$), 5.31 (brd, J_{trans} = 16.9 Hz, 2 H, 2×=CH$_a$$H_b$), 5.89 (ddt, J_{trans} = 16.9, J_{cis} = 10.8, J_{vic} = 5.8 Hz, 2 H, 2×CH=CH$_2$), 7.22 (d, J = 8.3 Hz, 4 H, 4×CH_{ar}), 7.32 (d, J = 8.3 Hz, 4 H, 4×CH_{ar}) ppm. ^{13}C NMR (75 MHz, $CDCl_3$): δ = 23.63 (2×CH$_2$CH), 26.71 [2×N(CH$_2$)$_3$$CH_2$], 28.03 (2×NCH$_2$$CH_2$ or 2×CH$_2$CO), 28.09 (2×NCH$_2$$CH_2$ or 2×CH$_2$CO), 29.03 [2×N(CH$_2$)$_2$$CH_2$], 39.13 (2×NCH$_2$, alkyl), 44.12 (2×NCH$_2$, benzyl), 57.51 (2×$C$H), 65.65 (2×OCH$_2$), 118.78 (2×=$CH_2$), 129.29 (4×$CH_{ar}$), 129.76 (4×$CH_{ar}$), 131.93 (2×$C$H=CH$_2$), 134.19 (2×$C_{ar,quat.}$), 134.31 (2×$C_{ar,quat.}$), 156.80 (2×$C$=O, urea), 172.01 (2×$C$=O, ester or lactam), 172.30 (2×C=O, lactam or ester) ppm. IR (NaCl): $\tilde{\nu}_{max}$ = 1708 (C=O), 1733 (C=O), 1769 (C=O) cm^{-1}. MS: m/z (%) = 781/783/785 (100) [M – H]$^+$. Chromatography: R_f = 0.37 (PE/EtOAc, 4:3). $C_{40}H_{48}Cl_2N_4O_8$ (783.74): calcd. C 61.30, H 6.17, N 7.15; found C 61.23, H 6.44, N 6.84.

Allyl 3-(1-{8-[4-(2-Allyloxycarbonylethyl)-3-(4-bromobenzyl)-2,5-dioxoimidazolidin-1-yl]octyl}-3-(4-bromobenzyl)-2,5-dioxoimidazolidin-4-yl)propionate (13e): Yield 54%, 0.16 g. ^{1}H NMR (300 MHz, $CDCl_3$): δ = 1.24–1.38 [m, 8 H, 2×N(CH$_2$)$_2$(CH_2)$_2$], 1.56–1.66 (m, 4 H, 2×NCH$_2$CH_2), 1.98–2.10 (m, 2 H, 2×CH_aH$_b$CH), 2.17–2.26 (m, 2 H, 2×CH$_a$$H_b$CH), 2.24–2.45 (m, 4 H, 2×CH_2CO), 3.43–3.57 (m, 4 H, 2×NCH_2, alkyl), 3.82 (dd, J = 6.6, 3.0 Hz, 2 H, 2×CH), 4.10 (d, J = 15.4 Hz, 2 H, 2×NCH_aH$_b$, benzyl), 4.56 (dt, J = 5.8, 1.4 Hz, 4 H, 2×OCH_2), 4.89 (d, J = 15.4 Hz, 2 H, 2×NCH$_a$$H_b$, benzyl), 5.25 (dq, J_{cis} = 10.5, 1.2 Hz, 2 H, 2×=CH_aH$_b$), 5.31 (dq, J_{trans} = 17.1, 1.4 Hz, 2 H, 2×=CH$_a$$H_b$), 5.89 (ddt, J_{trans} = 17.1, J_{cis} = 10.5, J_{vic} = 5.8 Hz, 2 H, 2×CH=CH$_2$), 7.16 (d, J = 8.4 Hz, 4 H, 4×CH_{ar}), 7.47 (d, J = 8.4 Hz, 4 H, 4×CH_{ar}) ppm. ^{13}C NMR (75 MHz, $CDCl_3$): δ = 23.53 (2×CH$_2$CH), 26.60 [2×N(CH$_2$)$_3$$CH_2$], 27.93 (2×NCH$_2$$CH_2$ or 2×CH$_2$CO), 27.97 (2×NCH$_2$$CH_2$ or 2×CH$_2$CO), 28.92 [2×N(CH$_2$)$_2$$CH_2$], 39.01 (2×NCH$_2$, alkyl), 44.08 (2×NCH$_2$, benzyl), 57.41 (2×$C$H), 65.52 (2×OCH$_2$), 118.66 (2×=$CH_2$), 122.18 (2×$C_{ar,quat.}$), 129.98 (4×$CH_{ar}$), 131.84 (2×$C$H=CH$_2$), 132.13 (4×$CH_{ar}$), 134.74 (2×$C_{ar,quat.}$), 156.68 (2×$C$=O, urea), 171.87 (2×$C$=O, ester or lactam), 172.15 (2×C=O, lactam or ester) ppm. IR (NaCl): $\tilde{\nu}_{max}$ = 1706 (C=O), 1734 (C=O), 1769 (C=O) cm^{-1}. MS: m/z (%) = 871/873/875 (100)

$[M + H]^+$. Chromatography: R_f = 0.11 (PE/EtOAc, 2:1). $C_{40}H_{48}Br_2N_4O_8$ (872.64): calcd. C 55.05, H 5.54, N 6.42; found C 55.45, H 5.93, N 6.05.

Allyl 3-(1-{12-[4-(2-Allyloxycarbonylethyl)-3-benzyl-2,5-dioxoimidazolidin-1-yl]dodecyl}-3-benzyl-2,5-dioxoimidazolidin-4-yl)propionate (13f): Yield 55%, 52 mg, oil. ^{1}H NMR (300 MHz, $CDCl_3$): δ = 1.22–1.34 [m, 16 H, 2× N(CH_2)$_2$(CH_2)$_4$], 1.57–1.67 (m, 4 H, 2× CH_2CH$_2$N), 2.01–2.13 (m, 2 H, 2× CH_aH$_b$CH), 2.17–2.28 (m, 2 H, 2× CH$_a$$H_b$CH), 2.30–2.26 (m, 4 H, 2× CH_2CO), 3.51 (td, J = 7.4, 2.2 Hz, 4 H, 2× NCH_2), 3.81 (dd, J = 6.2, 3.2 Hz, 2 H, 2× CH), 4.08 (d, J = 15.3 Hz, 2 H, 2× NCH_aH$_b$, benzyl), 4.56 (dt, J = 5.8, 1.4 Hz, 4 H, 2× OCH_2), 5.00 (d, J = 15.3 Hz, 2 H, 2× NCH$_a$$H_b$, benzyl), 5.24 (dq, J_{cis} = 10.5, 1.4 Hz, 2 H, 2× =CH_aH$_b$), 5.30 (dq, J_{trans} = 17.1, 1.4 Hz, 2 H, 2× =CH$_a$$H_b$), 5.91 (ddt, J_{trans} = 17.1, J_{cis} = 10.5, J_{vic} = 5.8 Hz, 2 H, 2× CH=CH$_2$), 7.24–7.38 (m, 10 H, 10× CH_{ar}) ppm. ^{13}C NMR (75 MHz, $CDCl_3$): δ = 23.47 (2× CH$_2$CH), 26.75 [2× N(CH_2)$_2$-CH$_2$], 27.99 (2× CH$_2$CO), 28.08 (2× CH$_2$CH$_2$N), 29.15 [2× N(CH_2)$_3$$CH_2$], 29.50 [2× N($CH_2$)$_4$($CH_2$)$_2$], 39.09 (2× NC$H_2$, alkyl), 44.63 (2× NC$H_2$, benzyl), 57.32 (2× CH), 65.50 (2× OCH_2), 118.60 (2× =CH$_2$), 128.16 (2× C$H_{ar, para}$), 128.24 (4× CH_{ar}), 129.02 (4× CH$_{ar}$), 131.90 (2× CH=CH$_2$), 135.63 (2× $C_{ar,quat.}$), 156.76 (2× C=O, urea), 171.93 (2× C=O, ester), 172.38 (2× C=O, lactam) ppm. IR (NaCl): $\tilde{\nu}_{max}$ = 1709 (C=O), 1735 (C=O), 1769 (C=O) cm^{-1}. MS: m/z (%) = 771 (100) $[M + H]^+$. Chromatography: R_f = 0.29 (PE/EtOAc, 2:1). $C_{44}H_{58}N_4O_8$ (770.95): calcd. C 68.55, H 7.58, N 7.27; found C 68.47, H 7.90, N 7.19.

Typical Procedure for the Ring-Closing Metathesis Reaction of Bis(hydantoins) 14: Bis(hydantoin) **14** (0.11 g, 0.16 mmol) was dissolved in benzene (20 mL) and brought to reflux temperature. Then the second-generation Grubbs' catalyst (0.0068 g, 0.008 mmol) was added. The reaction was heated at reflux overnight, shielded from moisture with a $CaCl_2$ tube. Traces of catalyst were removed by preparative thin layer chromatography (TLC) and in the cases of compounds **14a** and **14c** diastereomers were separated; **14d** yielded one single diastereomer.

10,25-Dimethyl-15,20-dioxa-1,8,10,25-tetraazatricyclo[22.2.1.1^{8,11}]-octacos-17-ene-9,14,21,26,27,28-hexaone (14a): Yield (before TLC) 99%, 80 mg.

Diastereomer 1: Oil. ^{1}H NMR (300 MHz, $CDCl_3$): δ = 1.27–1.40 (m, 4 H, CH_2CH_2), 1.54–1.69 (m, 4 H, 2× CH_2CH$_2$N), 2.14–2.49 (m, 8 H, 2× CH_2CH_2CO), 2.87 (s, 6 H, 2× NCH_3), 3.39–3.49 (m, 2 H, 2× NCH_aH$_b$, alkyl), 3.51–3.62 (m, 2 H, 2× NCH$_a$$H_b$, alkyl), 3.89 (t, J = 3.7 Hz, 2 H, 2× CH), 4.55 (brd, J = 10.9 Hz, 2 H, 2× OCH_aH$_b$), 4.63 (brd, J = 10.9 Hz, 2 H, 2× OCH$_a$$H_b$), 5.76 (t, J = 2.9 Hz, 2 H, 2× =CH_2) ppm. ^{13}C NMR (75 MHz, $CDCl_3$): δ = 23.42 (2× CH$_2$CH$_2$CO), 26.55 (CH$_2$CH_2), 27.83 (2× CH$_2$CH$_2$N), 28.06 and 28.18 (2× CH$_3$, 2× CH$_2$CO), 39.09 (2× CH$_2$N), 60.81 (2× CH), 63.94 (2× OCH_2), 127.73 (2× = CH), 156.90 (2× C=O, urea), 172.03 (2× C=O, ester), 172.25 (2× C=O, lactam) ppm. IR (NaCl): $\tilde{\nu}_{max}$ = 1706 (C=O), 1732 (C=O), 1768 (C=O) cm^{-1}. MS: m/z (%) = 507 (100) $[M + H]^+$. Chromatography: R_f = 0.26 (EtOAc/Et_2O, 1:1). $C_{24}H_{34}N_4O_8$ (506.55): calcd. C 56.91, H 6.77, N 11.06; found C 57.26, H 7.11, N 10.71.

Diastereomer 2: Oil. ^{1}H NMR (300 MHz, $CDCl_3$): δ = 1.28–1.37 (m, 4 H, CH_2CH_2), 1.51–1.70 (m, 4 H, 2× CH_2CH$_2$N), 2.23–2.38 (m, 8 H, 2× CH_2CH_2CO), 2.90 (s, 6 H, 2× NCH_3), 3.41–3.59 (m, 4 H, 2× NCH_2, alkyl), 3.88–3.91 (m, 2 H, 2× CH), 4.50–4.66 (m, 4 H, 2× OCH_2), 5.78 (brt, J = 2.9 Hz, 2 H, 2× =CH) ppm. ^{13}C NMR (75 MHz, $CDCl_3$) by difference spectrum reaction mixture and first fraction: δ = 23.48 (2× CH$_2$CH$_2$CO), 26.52 (CH$_2$CH_2), 27.96 (2× CH$_2$CH$_2$N or 2× CH$_3$ or 2× CH$_2$CO), 28.08 (2× CH$_2$CH$_2$N or 2× CH$_3$ or 2× CH$_2$CO), 38.96 (2× NCH_2, alkyl), 60.49 (2× CH), 63.88 (2× OCH_2), 127.49 (2× =CH), 156.73 (2× C=O, urea), 171.95 (2× C=O, ester), 172.30 (2× C=O, lactam) ppm. IR (NaCl) of the reaction mixture: $\tilde{\nu}_{max}$ = 1708 (C=O), 1733 (C=O), 1769 (C=O) cm^{-1}. MS: m/z (%) = 507 (100) $[M + H]^+$. Chromatography: R_f = 0.21 (EtOAc/Et_2O, 1:1). $C_{24}H_{34}N_4O_8$ (506.55): calcd. C 56.91, H 6.77, N 11.06; found C 57.14, H 6.88, N 10.73.

10,25-Dibenzyl-15,20-dioxa-1,8,10,25-tetraazatricyclo[22.2.1.1^{8,11}]-octacos-17-ene-9,14,21,26,27,28-hexaone (14b): Mixture of diastereomers. Yield 95%, 0.10 g, oil. ^{1}H NMR (300 MHz, $CDCl_3$): δ = 1.28–1.43 (m, 4 H, CH_2CH_2), 1.56–1.74 (m, 4 H, 2× CH_2CH$_2$N), 2.14–2.41 (m, 8 H, 2× CH_2CH_2CO), 3.41–3.65 (m, 4 H, 2× NCH_2, alkyl), 3.78–3.81 (m, 2 H, 2× CH), 3.98 (dd, J = 15.3, 8.1 Hz, 2 H, 2× NCH_aH$_b$, benzyl), 4.54–4.72 (m, 4 H, 2× OCH_2), 5.00 (brd, J = 15.3 Hz, 2 H, 2× NCH$_a$$H_b$, benzyl), 5.79 (t, J = 2.8 Hz, 2 H, 2× =CH), 7.22–7.38 (m, 10 H, 10× CH_{ar}) ppm. ^{13}C NMR (75 MHz, $CDCl_3$): δ = 23.07 and 23.16 (2× CH$_2$CH$_2$CO), 26.55 (CH$_2$CH_2), 27.83 and 27.93 (2× CH$_2$CH$_2$N), 28.08 and 28.22 (2× CH$_2$CO), 39.04 and 39.16 (2× NCH_2, alkyl), 44.45 and 44.52 (2× NCH_2, benzyl), 57.38 and 57.47 (2× CH), 63.85 and 63.96 (2× OCH_2), 127.47 and 127.75 (2× =CH), 128.19, 128.32 and 128.34 (6× CH_{ar}), 129.03 (4× CH$_{ar}$), 135.47 (2× $C_{ar,quat.}$), 156.73 and 156.83 (2× C=O, urea), 172.00 and 172.12 (2× C=O, ester), 172.30 (2× C=O, lactam) ppm. IR (NaCl): $\tilde{\nu}_{max}$ = 1708 (C=O), 1733 (C=O), 1768 (C=O) cm^{-1}. MS: m/z (%) = 659 (100) $[M + H]^+$. Chromatography: R_f = 0.6 (PE/EtOAc, 1:4). $C_{36}H_{42}N_4O_8$ (658.74): calcd. C 65.64, H 6.43, N 8.51; found C 65.79, H 6.76, N 8.15.

10,25-Bis(4-bromobenzyl)-15,20-dioxa-1,8,10,25-tetraazatricyclo-[22.2.1.1^{8,11}]octacos-17-ene-9,14,21,26,27,28-hexaone (14c): Yield (before TLC) 99%, 83 mg.

Diastereomer 1: Oil. ^{1}H NMR (300 MHz, $CDCl_3$): δ = 1.25–1.43 (m, 4 H, CH_2CH_2), 1.56–1.72 (m, 4 H, 2× CH_2CH$_2$N), 2.11–2.46 (m, 8 H, 2× CH_2CH_2CO), 3.43–3.52 (m, 2 H, 2× NCH_aH$_b$, alkyl), 3.55–3.66 (m, 2 H, 2× NCH$_a$$H_b$, alkyl), 3.76–3.80 (m, 2 H, 2× CH), 3.95 (d, J = 15.3 Hz, 2 H, 2× NCH_aH$_b$, benzyl), 4.57 (brd, J = 11.6 Hz, 2 H, 2× OCH_aH$_b$), 4.67 (brd, J = 11.6 Hz, 2 H, 2× OCH$_a$$H_b$), 4.92 (d, J = 15.3 Hz, 2 H, 2× NCH$_a$$H_b$, benzyl), 5.78 (t, J = 2.9 Hz, 2 H, 2× =CH), 7.12 (d, J = 8.3 Hz, 4 H, 4× CH_{ar}), 7.47 (d, J = 8.3 Hz, 4 H, 4× CH_{ar}) ppm. ^{13}C NMR (75 MHz, $CDCl_3$): δ = 23.05 (2× CH$_2$CH$_2$CO), 26.51 (CH$_2$CH_2), 27.77 (2× CH$_2$CH$_2$N or 2× CH$_2$CO), 28.17 (2× CH$_2$CH$_2$N or 2× CH$_2$CO), 39.19 (2× NCH_2, alkyl), 43.85 (2× NCH_2, benzyl), 57.50 (2× CH), 63.99 (2× OCH_2), 122.28 (2× $C_{ar,quat.}$), 127.72 (2× = CH), 130.07 (4× CH_{ar}), 132.21 (4× CH$_{ar}$), 134.47 (2× $C_{ar,quat.}$), 156.80 (2× C=O, urea), 172.12 (4× C=O, ester and lactam) ppm. IR (NaCl): $\tilde{\nu}_{max}$ = 1706 (C=O), 1733 (C=O), 1768 (C=O) cm^{-1}. Chromatography: R_f = 0.29 (PE/EtOAc, 1:1).

Diastereomer 2: Oil. ^{1}H NMR (300 MHz, $CDCl_3$): δ = 1.25–1.41 (m, 4 H, CH_2CH_2), 1.56–1.72 (m, 4 H, 2× CH_2CH$_2$N), 2.15–2.40 (m, 8 H, 2× CH_2CH_2CO), 3.45–3.62 (m, 4 H, 2× NCH_2, alkyl), 3.79 (t, J = 3.9 Hz, 2 H, 2× CH), 3.99 (d, J = 15.4 Hz, 2 H, 2× NCH_aH$_b$, benzyl), 4.59–4.60 (m, 4 H, 2× OCH_2), 4.91 (d, J = 15.4 Hz, 2 H, 2× NCH$_a$$H_b$, benzyl), 5.78 (brt, J = 2.8 Hz, 2 H, 2× =CH), 7.14 (d, J = 8.3 Hz, 4 H, 4× CH_{ar}), 7.48 (d, J = 8.3 Hz, 4 H, 4× CH_{ar}) ppm. ^{13}C NMR (75 MHz, $CDCl_3$): δ = 23.16 (2× CH$_2$CH$_2$CO), 26.46 (CH$_2$CH_2), 27.88 (2× CH$_2$CH$_2$N or 2× CH$_2$CO), 28.02 (2× CH$_2$CH$_2$N or 2× CH$_2$CO), 39.06 (2× NCH_2, alkyl), 43.96 (2× NCH_2, benzyl), 57.45 (2× CH), 63.90 (2× OCH_2), 122.28 (2× $C_{ar,quat.}$), 127.43 (2× =CH), 130.04 (4× CH_{ar}), 132.22 (4× CH_{ar}), 134.51 (2× $C_{ar,quat.}$), 156.71

(2× *C*=O, urea), 171.98 (2× *C*=O, ester), 172.12 (2× *C*=O, lactam) ppm. IR (NaCl): $\tilde{\nu}_{max}$ = 1706 (C=O), 1733 (C=O), 1768 (C=O) cm^{-1}. Chromatography: R_f = 0.23 (PE/EtOAc, 1:1). MS: *m/z* (%) = 813/815/817 (100) $[M - H]^+$. $C_{36}H_{40}Br_2N_4O_8$ (816.53): calcd. C 52.95, H 4.94, N 6.86; found C 53.34, H 5.23, N 6.54.

12,27-Bis(4-chlorobenzyl)-17,22-dioxa-1,10,12,27-tetraazatricyclo-[24.2.1.1^{10,13}]triacont-19-ene-11,16,23,28,29,30-hexaone (14d): Mixture of diastereomers. Yield (before TLC) 99%, 39 mg. ^{1}H NMR (300 MHz, $CDCl_3$): δ = 1.22–1.37 [m, 8 H, 2× $N(CH_2)_2(CH_2)_2$], 1.58–1.68 (m, 4 H, 2× NCH_2CH_2), 2.14–2.37 (m, 8 H, 2× CH_2CH_2CO), 3.43–3.55 (m, 2 H, 2× NCH_aH_b, alkyl), 3.52–3.66 (m, 2 H, 2× NCH_aH_b, alkyl), 3.80 (brs, 2 H, 2× *CH*), 3.99 (brd, *J* = 15.3 Hz, 2 H, 2× NCH_aH_b, benzyl), 4.47–4.71 (m, 4 H, 2× OCH_2), 4.94 (dd, *J* = 15.3, 2.6 Hz, 2 H, 2× NCH_aH_b, benzyl), 5.80 (t, *J* = 2.9 Hz, 2 H, 2× =CH), 7.19 (d, *J* = 7.8 Hz, 4 H, 4× CH_{ar}), 7.32 (d, *J* = 7.8 Hz, 4 H, 4× CH_{ar}) ppm. ^{13}C NMR (75 MHz, $CDCl_3$): δ = 23.02 (2× CH_2CH), 26.87 [2× $N(CH_2)_3CH_2$], 27.81 (2× NCH_2CH_2 or 2× CH_2CO), 27.97 (2× NCH_2CH_2 or 2× CH_2CO), 29.19 [2× $N(CH_2)_2CH_2$], 39.30 (2× NCH_2, alkyl), 43.94 (2× NCH_2, benzyl), 57.54 (2× *C*H), 64.21 (2× OCH_2), 127.79 (2× =*C*H), 129.35 (4× CH_{ar}), 129.82 (4× CH_{ar}), 134.08 (2× $C_{ar,quat.}$), 134.29 (2× $C_{ar,quat.}$), 156.89 (2× *C*=O, urea), 172.10 (4× *C*=O, lactam and ester) ppm. IR (NaCl): $\tilde{\nu}_{max}$ = 1707 (C=O), 1735 (C=O), 1769 (C=O) cm^{-1}. MS: *m/z* (%) = 755/757/759 (100) $[M + H]^+$. Chromatography: R_f = 0.3 (PE/EtOAc, 1:1). $C_{38}H_{44}Cl_2N_4O_8$ (755.68): calcd. C 60.40, H 5.87, N 7.41; found C 60.76, H 6.14, N 7.12.

12,27-Bis(4-bromobenzyl)-17,22-dioxa-1,10,12,27-tetraazatricyclo-[24.2.1.1^{10,13}]triacont-19-ene-11,16,23,28,29,30-hexaone (14e): One diastereomer. Yield (before TLC) 99%, 0.12 g, oil. ^{1}H NMR (300 MHz, $CDCl_3$): δ = 1.25–1.37 [m, 8 H, 2× $N(CH_2)_2(CH_2)_2$], 1.57–1.69 (m, 4 H, 2× NCH_2CH_2), 2.14–2.35 (m, 8 H, 2× CH_2CH_2CO), 3.43–3.52 (m, 2 H, 2× NCH_aH_b, alkyl), 3.55–3.64 (m, 2 H, 2× NCH_aH_b, alkyl), 3.80 (brs, 2 H, 2× *CH*), 3.97 (brd, *J* = 15.2 Hz, 2 H, 2× NCH_aH_b, benzyl), 4.47–4.70 (m, 4 H, 2× OCH_2), 4.92 (dd, *J* = 15.2, 2.3 Hz, 2 H, 2× NCH_aH_b, benzyl), 5.80 (t, *J* = 2.9 Hz, 2 H, 2× =CH), 7.13 (d, *J* = 8.4 Hz, 4 H, 4× CH_{ar}), 7.47 (d, *J* = 8.4 Hz, 4 H, 4× CH_{ar}) ppm. ^{13}C NMR (75 MHz, $CDCl_3$): δ = 22.89 (2× CH_2CH), 26.77 [2× $N(CH_2)_3CH_2$], 27.71 (2× NCH_2CH_2 or 2× CH_2CO), 27.86 (2× NCH_2CH_2 or 2× CH_2CO), 29.09 [2× $N(CH_2)_2CH_2$], 39.19 (2× NCH_2, alkyl), 43.87 (2× NCH_2, benzyl), 57.42 (2× *C*H), 64.11 (2× OCH_2), 122.28 (2× $C_{ar,quat.}$), 127.67 (2× =*C*H), 130.04 (4× CH_{ar}), 132.21 (4× CH_{ar}), 134.47 (2× $C_{ar,quat.}$), 156.77 (2× *C*=O, urea), 171.98 (4× *C*=O, lactam and ester) ppm. IR (NaCl): $\tilde{\nu}_{max}$ = 1710 (C=O), 1737 (C=O), 1769 (C=O) cm^{-1}. MS: *m/z* (%) = 843/845/847 (100) $[M + H]^+$. Chromatography: R_f = 0.35 (PE/EtOAc, 1:1). $C_{38}H_{44}Br_2N_4O_8$ (844.59): calcd. C 54.04, H 5.25, N 6.63; found C 54.31, H 5.48, N 6.25.

16,31-Dibenzyl-21,26-dioxa-1,14,16,31-tetraazatricyclo-[28.2.1.1^{14,17}]tetratriacont-23-ene-15,20,27,32,33,34-hexaone (14f): Mixture of diastereomers. Yield (before TLC) 99%, 54 mg, oil. ^{1}H NMR (300 MHz, $CDCl_3$): δ = 1.22–1.34 [m, 16 H, 2× $N(CH_2)_2(CH_2)_4$], 1.59–1.69 (m, 4 H, 2× CH_2CH_2N), 2.14–2.33 (m, 8 H, 2× CH_2CH_2CO), 3.45–3.63 (m, 4 H, 2× NCH_2), 3.79–3.81 (m, 2 H, 2× *CH*), 4.08 (d, *J* = 15.1 Hz, 2 H, 2× NCH_aH_b, benzyl), 4.49–4.67 (m, 4 H, 2× OCH_2), 5.00 (brd, *J* = 15.1 Hz, 2 H, 2× NCH_aH_b, benzyl), 5.81 (t, *J* = 2.8 Hz, 2 H, 2× =CH), 7.23–7.37 (m, 10 H, 10× CH_{ar}) ppm. ^{13}C NMR (75 MHz, $CDCl_3$): δ = 23.08 (2× CH_2CH), 26.47 [2× $N(CH_2)_2CH_2$], 27.67 (2× CH_2CO), 27.88 (2× CH_2CH_2N), 28.98 [2× $N(CH_2)_3CH_2$], 29.02 and 29.12 [2× $N(CH_2)_4(CH_2)_2$], 39.09 (2× NCH_2, alkyl), 44.61 (2× NCH_2, benzyl), 57.35 (2× *C*H), 64.22 (2× OCH_2), 128.06 and 128.26 (2× =*C*H), 128.38 and 129.10 (10× CH_{ar}), 135.55 (2× $C_{ar,quat.}$), 156.92 (2× *C*=O, urea), 171.96 (2× *C*=O, ester), 172.30 (2× *C*=O, lactam) ppm. IR (NaCl): $\tilde{\nu}_{max}$ = 1709 (C=O), 1736 (C=O), 1769 (C=O) cm^{-1}. MS: *m/z* (%) = 743 (100) $[M + H]^+$. Chromatography: R_f = 0.3 (PE/EtOAc, 1:1). $C_{42}H_{54}N_4O_8$ (742.90): calcd. C 67.90, H 7.33, N 7.54; found C 68.17, H 7.55, N 7.28.

Acknowledgments

The authors are indebted to the Research Foundation – Flanders (FWO) for financial support of this research.

[1] J. Knabe, J. Baldauf, A. Ahlhelm, *Pharmazie* **1997**, *52*, 912–919.
[2] M. S. Luer, *Neurol. Res.* **1998**, *20*, 178–182.
[3] T. R. Rodgers, M. P. Lamontagne, A. Markovac, A. B. Ash, *J. Med. Chem.* **1977**, *20*, 591–594.
[4] L. Somsak, L. Kovacs, M. Toth, E. Osz, L. Szilagyi, Z. Györgydeak, Z. Dinya, T. Docsa, B. Toth, P. Gergely, *J. Med. Chem.* **2001**, *44*, 2843–2848.
[5] C. W. Bazil, T. A. Pedley, *Annu. Rev. Med.* **1998**, *49*, 135–162.
[6] P. Bac, P. Maurois, C. Dupont, N. Pages, J. P. Stables, P. Gressens, P. Evrard, J. Vamecq, *J. Neurosci.* **1998**, *18*, 4363–4373.
[7] T. Q. Pham, S. G. Pyne, B. W. Skelton, A. H. Whitet, *J. Org. Chem.* **2005**, *70*, 6369–6377.
[8] E. Ware, *Chem. Rev.* **1950**, *46*, 403–470.
[9] M. Meusel, M. Gutschow, *Org. Prep. Proced. Int.* **2004**, *36*, 391–443.
[10] M. Beller, M. Eckert, W. A. Moradi, H. Neumann, *Angew. Chem. Int. Ed.* **1999**, *38*, 1454–1457.
[11] B. A. Bhat, K. L. Dhar, S. C. Puri, M. Spiteller, *Synlett* **2006**, 2723–2726.
[12] C. Montagne, M. Shipman, *Synlett* **2006**, 2203–2206.
[13] J. Alsina, W. L. Scott, M. J. O'Donnell, *Tetrahedron Lett.* **2005**, *46*, 3131–3135.
[14] M. Andreeff, R. Stone, J. Michaeli, C. W. Young, W. P. Tong, H. Sogoloff, T. Ervin, D. Kufe, R. A. Rifkind, P. A. Marks, *Blood* **1992**, *80*, 2604–2609.
[15] R. Breslow, B. Jursic, Z. F. Yan, E. Friedman, L. Leng, L. Ngo, R. A. Rifkind, P. A. Marks, *Proc. Natl. Acad. Sci. USA* **1991**, *88*, 5542–5546.
[16] J. S. Driscoll, US Patent 330509, **1989**.
[17] A. Haces, T. R. Breitman, J. S. Driscoll, *J. Med. Chem.* **1987**, *30*, 405–409.
[18] N. Dieltiens, D. D. Claeys, V. V. Zhdankin, V. N. Nemykin, B. Allaert, F. Verpoort, C. V. Stevens, *Eur. J. Org. Chem.* **2006**, 2649–2660.
[19] N. Dieltiens, D. D. Claeys, C. V. Stevens, *J. Org. Chem.* **2006**, *71*, 3863–3868.
[20] B. W. Vanhoecke, H. T. Depypere, A. De Beyter, S. K. Sharma, V. S. Parmar, D. De Keukeleire, M. E. Bracke, *Pure Appl. Chem.* **2005**, *77*, 65–74.
[21] N. Dieltiens, PhD, *Ghent University*, *Faculty of Bioscience Engineering*, **2007**, p. 211.
[22] For general reviews on RCM see: a) H.-G. Schmalz, *Angew. Chem. Int. Ed. Engl.* **1995**, *34*, 1833–1836; b) M. Schuster, S. Blechert, *Angew. Chem. Int. Ed. Engl.* **1997**, *36*, 2036–2056; c) I. Dragutan, V. Dragutan, P. Filip, *Arkivoc* **2005**, *X*, 105–129; d) A. Fürstner, *Angew. Chem. Int. Ed.* **2000**, *39*, 3012–3043; e) R. H. Grubbs, S. Chang, *Tetrahedron* **1998**, *54*, 4413–4450; f) R. Drozdzak, B. Allaert, N. Ledoux, I. Dragutan, V. Dragutan, F. Verpoort, *Coord. Chem. Rev.* **2005**, *249*, 3055–3074; g) K. C. Nicolaou, P. G. Bulger, D. Sarlah, *Angew. Chem. Int. Ed.* **2005**, *44*, 4490–4527; h) E. Colacino, J. Martinez, F. Lamaty, *Coord. Chem. Rev.* **2007**, *251*, 726–764.

[23] For a review on the synthesis of oxygen- and nitrogen-containing heterocycles by RCM see: A. Deiters, S. F. Martin, *Chem. Rev.* **2004**, *104*, 2199–2238.
[24] J. Huwyler, R. Jakob-Roetne, S. M. Poli, CH Patent WO03051836, **2003**.
[25] A. Mucci, F. Parenti, L. Schenetti, *Eur. J. Org. Chem.* **2002**, 938–940.
[26] A. Fürstner, T. Muller, *J. Org. Chem.* **1998**, *63*, 424–425.
[27] M. Scholl, S. Ding, C. W. Lee, R. H. Grubbs, *Org. Lett.* **1999**, *1*, 953–956.
[28] A. Fürstner, O. R. Thiel, N. Kindler, B. Bartkowska, *J. Org. Chem.* **2000**, *65*, 7990–7995.
[29] P. Schwab, M. B. France, J. W. Ziller, R. H. Grubbs, *Angew. Chem. Int. Ed. Engl.* **1995**, *34*, 2039–2041.
[30] C. W. Lee, R. H. Grubbs, *Org. Lett.* **2000**, *2*, 2145–2147.

Received: September 6, 2007
Published Online: November 22, 2007

--- Paper VII ---

Diederica D. Claeys, Kristof Moonen, Bart I. Roman, Victor N. Nemykin, Viktor V. Zhdankin, Michel Waroquier, Veronique Van Speybroeck,* and Christian V. Stevens*

"Synthesis of Tricyclic Phosphonopyrrolidines via IMDAF: Experimental and Theoretical Investigation of the Observed Stereoselectivity"

J. Org. Chem. **2008**, Vol. 73, 7921-7927

JOC Article

Synthesis of Tricyclic Phosphonopyrrolidines via IMDAF: Experimental and Theoretical Investigation of the Observed Stereoselectivity

Diederica D. Claeys,[†,§,||] Kristof Moonen,[†] Bart I. Roman,[†,||] Victor N. Nemykin,[‡] Viktor V. Zhdankin,[‡] Michel Waroquier,[§] Veronique Van Speybroeck,*[,§] and Christian V. Stevens*[,†]

Research Group SynBioC, Department of Organic Chemistry, Faculty of Bioscience Engineering, Ghent University, Coupure links 653, B-9000 Ghent, Belgium, Department of Chemistry and Biochemistry, University of Minnesota, Duluth, Minnesota 55812, and Center for Molecular Modeling, Ghent University, Proeftuinstraat 86, B-9000 Ghent, Belgium

chris.stevens@ugent.be; veronique.vanspeybroeck@ugent.be

Received May 28, 2008

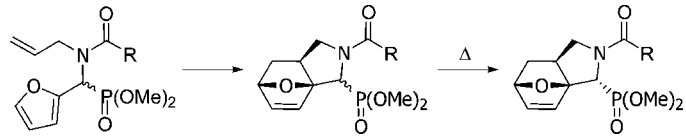

During the synthesis of tricyclic phosphonopyrrolidines via intramolecular Diels−Alder reactions of 1-acylamino(furan-2-yl)methyl phosphonates, two isomers are formed in most cases. The presence of a short three-atom tether together with spectroscopic data, including difference NOE, revealed that the cycloaddition occurred *exo*, but the phosphonate substituent on the tether had an *exo* or *endo* orientation. This was confirmed via X-ray analysis. A thermodynamic preference for the product with the phosphonate function in the *endo* position was observed experimentally and was confirmed theoretically. Density functional theory methods and several high-level post Hartree−Fock procedures were used to rationalize the observed isomer ratio of the IMDAF-reactions. This was done for two different types of reagents: with the activating carbonyl group in the tether or as a substituent on the tether. For the first type of molecules there is a large steric hindrance of the bulky tether substituents that disfavors the *exo*-isomer. In the latter case, there was a very small energy difference between the transition states causing a mixture of epimers being formed.

Introduction

Since the discovery of the biological activity of aminoalkylphosphonates, e.g., as enzyme inhibitors with antibacterial, plant growth regulatory, and neuromodulatory activities,[1] many researchers have also focused their attention on conformationally constrained azaheterocyclic phosphonates.[2] This paper reveals the synthesis of tricyclic 2-phosphonopyrrolidines via intramolecular Diels−Alder reaction of carefully designed furanyl-α-aminophosphonates. Furans can undergo Diels−Alder reactions as the 4π diene components despite their aromaticity and hence expected decrease in reactivity,[3] both inter- and intramolecularly.[4] Furthermore, the IMDAF reaction (intramolecular Diels−Alder reaction of furan) is particularly attractive as two or more rings can be constructed in a single step with high regio- and stereocontrol, providing a convenient entry into polycyclic targets including natural products[5] like prostaglandins[5h,i] and terpenoids.[5j] The 7-oxabicyclo[2.2.1]heptane skeleton, formed here, is present in biologically active natural products, but moreover, the 7-oxanorbornanes and their unsaturated deriva-

* To whom correspondence should be addressed. (C.V.S.) Fax: +32-9-2646243. Tel: +32-9-2645957. (V.V.S.) Fax: +32-9-2646697. Tel: +32-9-2646558.
† Department of Organic Chemistry, Ghent University.
‡ University of Minnesota.
§ Center for Molecular Modeling, Ghent University.
|| D.D.C. and B.I.R. are Ph.D. fellow of the Research Foundation - Flanders (FWO - Vlaanderen).

(1) Kafarski, P.; Lejczak, B. *Phosphorus, Sulfur, Silicon Relat. Elem.* **1991**, *63*, 193–215, and references therein.

(2) (a) Moonen, K.; Laureyn, I.; Stevens, C. V. *Chem. Rev.* **2004**, *104*, 6177–6215. (b) Redmore, D. *Chem. Rev.* **1971**, *71*, 315–337. (c) Robiette, R.; Defacqz, N.; Peeters, D.; Marchand-Brynaert, J. *Curr. Org. Synth.* **2005**, *2*, 453–477.

(3) (a) Lipshutz, B. H. *Chem. Rev.* **1986**, *86*, 795–819. (b) Wenkert, E.; Moeller, P. D. R.; Piettre, S. R. *J. Am. Chem. Soc.* **1988**, *110*, 7188–7194. (c) Domingo, L. R.; Picher, M. T.; Aurell, M. J. *J. Phys. Chem. A* **1999**, *103*, 11425–11430. (d) Lautens, M.; Fillion, E. *J. Org. Chem.* **1996**, *61*, 7994–7995.

(4) Kappe, C. O.; Murphree, S. S.; Padwa, A. *Tetrahedron* **1997**, *53*, 14179–14233.

10.1021/jo801138s CCC: $40.75 © 2008 American Chemical Society
Published on Web 09/12/2008

tives can undergo a variety of reactions making them quite useful synthetic intermediates in the synthesis of natural products and analogues.[6]

While absolute stereocontrol of substituents on the diene or dienophile is often observed, this is not the case for tether substituents, which regularly give mixtures of both isomers.[7] A detailed spectroscopic elucidation of the products and their stereochemistry was performed using DIFNOE-NMR and X-ray analysis. In order to explain the origin of selectivity or duality of both isomers, theoretical calculations were conducted. They can reveal whether the process is thermodynamically or kinetically preferred and elucidate the effect of the position of the carbonyl group on the stereoselectivity. Previous studies have shown that steric interactions and ring strain in the transition states are the source of stereoselectivity in intramolecular Diels−Alder reactions.[8] Tether substitutions, ring constraints, and (planar) functional groups are known to alter the conformational distribution and to restrict the rotations.[9,10] The possible influence of these factors was first investigated on a compound with the carbonyl group incorporated in the tether, as a 100% selectivity was observed in that case, using DFT methods: B3LYP,[11] mPW1PW91,[12] and BB1K.[13] The same DFT methods, MP2,[14] MP3,[15] and CCSD[16] procedures were used for these compounds where both isomers were formed.

Experimental Results and Discussion

The suitability of 1-(allylamino)-1-(furan-2-yl)methyl phosphonates **5** for the IMDAF reaction was investigated. From previous research it was shown that, when aminoalkyl phosphonate **1** (Figure 1) was acylated at nitrogen, there was a hindered rotation about the C^1-N bond.[17] It is, however, an unresolved issue whether this rotational barrier would allow, hinder, or proliferate the Diels−Alder reaction.

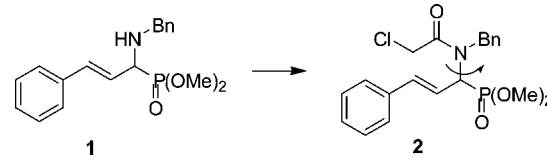

FIGURE 1. Hindered rotation after acylation of the amine.

The aminoalkyl phosphonates were synthesized following our previously reported protocol.[18] Subsequent acylations yielded the corresponding amides **5** in high purity (Scheme 1). With pivaloyl chloride, however, complex mixtures were obtained under different reaction conditions.

This acyl group induces both a steric and an electronic advantage to obtain a reactive substrate for the IMDAF reaction. When 1-(allylamino)-1-(furan-2-yl)methyl phosphonate **4** was refluxed overnight in toluene, only minimal amounts, 16%, of Diels−Alder adducts could be detected using the typical peaks of $C^6H_aH_b$ at 1.4 and 1.7 ppm. Prolonged refluxing only resulted in a breakdown of the starting material. However, when the corresponding amides (**5a**−**e**) were refluxed in toluene, complete conversion to the ring-closed products was observed. In all cases, a mixture of isomers (**6′** and **6″**) was formed, the identity of which will be discussed further in this paper (Scheme 1). Experiments with toluene and acetonitrile showed that the first one was the solvent of choice in most cases: a faster formation of product and smaller amounts of side products were observed, probably due to the higher boiling point of toluene.

The order of reactivity was in accordance with the results reported previously for similar substrates **7** without the phosphonate group[19] (Scheme 1). With a chloroacetyl group, 20 h of reflux was required, while the ring-closed product **6e** was already formed during the acylation at room temperature and subsequent aqueous workup.

In our work, however, a remarkable influence of the phosphonate group could be observed. While amides **8a** and **8c** could only be obtained in low yield[19] because of the poor conversion (Table 1), the corresponding phosphono amides **6** gave complete conversion. However, column chromatography caused big losses of the product due to the presence of a polar group such as the phosphonate group. The positive influence of increased tether substitution on IMDAF reactions is often attributed to the geminal dialkyl substitution and explained by the Thorpe−Ingold effect, the reactive rotamer, or the facilitated transition effect.[4,20] The hindered rotation we already observed in the synthesis of phosphono-β-lactams[17] will be further investigated.

The structure of the tricyclic pyrrolidines was confirmed by its 2D DQFCOSY, HSQC, and HMBC spectra (Supporting Information) and compared with the data from compounds **8**. The ^{1}H NMR spectrum is characterized by a large difference

(5) (a) Zhang, H. J.; Padwa, A. *Org. Lett.* **2006**, *8*, 247–250. (b) Padwa, A.; Ginn, J. D. *J. Org. Chem.* **2005**, *70*, 5197–5206. (c) Wang, Q.; Padwa, A. *Org. Lett.* **2004**, *6*, 2189–2192. (d) Kouznetsov, V. V.; Zubkov, F. I.; Cruz, U. M.; Voskressensky, L. G.; Mendez, L. Y. V.; Astudillo, L.; Stashenko, E. E. *Lett. Org. Chem.* **2004**, *1*, 37–39. (e) Fokas, D.; Patterson, J. E.; Slobodkin, G.; Baldino, C. M. *Tetrahedron Lett.* **2003**, *44*, 5137–5140. (f) Padwa, A.; Eidell, C. K.; Lynch, S. M. *Heterocycles* **2002**, *58*, 227–242. (g) Padwa, A.; Dimitroff, M.; Liu, B. *Org. Lett.* **2000**, *2*, 3233–3235. (h) Sprague, P. W.; Heikes, J. E.; Gougoutas, J. Z.; Malley, M. F.; Harris, D. N.; Greenberg, R. *J. Med. Chem.* **1985**, *28*, 1580–1590. (i) Sneden, A. T. *Synlett* **1993**, *5*, 313–322. (j) Yu, S. Y.; Beese, G.; Keay, B. A. *J. Chem. Soc., Perkin Trans. 1* **1992**, 2729–2731.

(6) Vogel, P.; Cossy, J.; Plumet, J.; Arjona, O. *Tetrahedron* **1999**, *55*, 13521–13624.

(7) (a) Namboothiri, I. N. N.; Ganesh, M.; Mobin, S. M.; Cojocaru, M. *J. Org. Chem.* **2005**, *70*, 2235–2243. (b) Zubkov, F. I.; Boltukhina, E. V.; Turchin, K. F.; Borisov, R. S.; Varlamov, A. V. *Tetrahedron* **2005**, *61*, 4099–4113. (c) Varlamov, A. V.; Zubkov, F. I.; Boltukhina, E. V.; Sidorenko, N. V.; Borisov, R. S. *Tetrahedron Lett.* **2003**, *44*, 3641–3643.

(8) (a) Weingarten, M. D.; Prein, M.; Price, A. T.; Snyder, J. P.; Padwa, A. *J. Org. Chem.* **1997**, *62*, 2001–2010. (b) Turner, C. I.; Williamson, R. M.; Paddon-Row, M. N.; Sherburn, M. S. *J. Org. Chem.* **2001**, *66*, 3963–3969. (c) Tantillo, D. J.; Houk, K. N.; Jung, M. E. *J. Org. Chem.* **2001**, *66*, 1938–1940.

(9) Jung, M. E.; Gervay, J. *J. Am. Chem. Soc.* **1991**, *113*, 224–232.

(10) Bur, S. K.; Lynch, S. M.; Padwa, A. *Org. Lett.* **2002**, *4*, 473–476.

(11) (a) Becke, A. D. *J. Chem. Phys.* **1993**, *98*, 5648–5652. (b) Stephens, P. J.; Devlin, F. J.; Chabalowski, C. F.; Frish, M. J. *J. Phys. Chem.* **1994**, *98*, 11623–11627.

(12) Adamo, C.; Barone, V. *J. Chem. Phys.* **1998**, *108*, 664–675.

(13) (a) Zhao, Y.; Lynch, B. J.; Truhlar, D. G. *J. Phys. Chem. A* **2004**, *108*, 2715–2719. (b) BB95/6-31+G(d) IOp(3/76=0580004200).

(14) (a) Head-Gordon, M.; Pople, J. A.; Frisch, M. J. *Chem. Phys. Lett.* **1988**, *153*, 503–506. (b) Frisch, M. J.; Head-Gordon, M.; Pople, J. A. *Chem. Phys. Lett.* **1990**, *166*, 275–280. (c) Frisch, M. J.; Head-Gordon, M.; Pople, J. A. *Chem. Phys. Lett.* **1990**, *166*, 281–289. (d) Head-Gordon, M.; Head-Gordon, T. *Chem. Phys. Lett.* **1994**, *220*, 122–128. (e) Saebo, S.; Almlof, J. *Chem. Phys. Lett.* **1989**, *154*, 83–89.

(15) (a) Pople, J. A.; Seeger, R.; Krishnan, R. *Int. J. Quant. Chem. Symp.* **1977**, *11*, 149–163. (b) Pople, J. A.; Binkley, J. S.; Seeger, R. *Int. J. Quant. Chem. Symp.* **1976**, *10*, 1–19.

(16) (a) Pople, J. A.; Krishnan, R.; Schlegel, H. B.; Binkley, J. S. *Int. J. Quantum Chem.* **1978**, *14*, 545–560. (b) Bartlett, R. J.; Purvis, G. D. *J. Quant. Chem.* **1978**, *14*, 561–581. (c) Purvis, G. D.; Bartlett, R. J. *J. Chem. Phys.* **1982**, *76*, 1910–1918. (d) Scuseria, G. E.; Janssen, C. L.; Schaefer, H. F., III. *J. Chem. Phys.* **1988**, *89*, 7382–7387. (e) Scuseria, G. E.; Schaefer, H. F., III. *J. Chem. Phys.* **1989**, *90*, 3700–3703.

(17) (a) Van Speybroeck, V.; Moonen, K.; Hemelsoet, K.; Stevens, C. V.; Waroquier, M. *J. Am. Chem. Soc.* **2006**, *128*, 8468–8478. (b) Stevens, C. V.; Vekemans, W.; Moonen, K.; Rammeloo, T. *Tetrahedron Lett.* **2003**, *44*, 1619–1622. (c) Moonen, K.; Stevens, C. V. *Synthesis* **2005**, 3603–3612.

(18) Van Meenen, E.; Moonen, K.; Acke, D.; Stevens, C. V. *Arkivoc* **2006**, *i*, 31–45.

(19) Ghelfi, F.; Parsons, A. F.; Tommasini, D.; Mucci, A. *Eur. J. Org. Chem.* **2001**, 1845–1852.

(20) (a) Bruice, T. C.; Pandit, U. K. *J. Am. Chem. Soc.* **1960**, *82*, 5858–5865. (b) Parrill, A. L.; Dolata, D. P. *THEOCHEM* **1996**, *370*, 187–202.

SCHEME 1

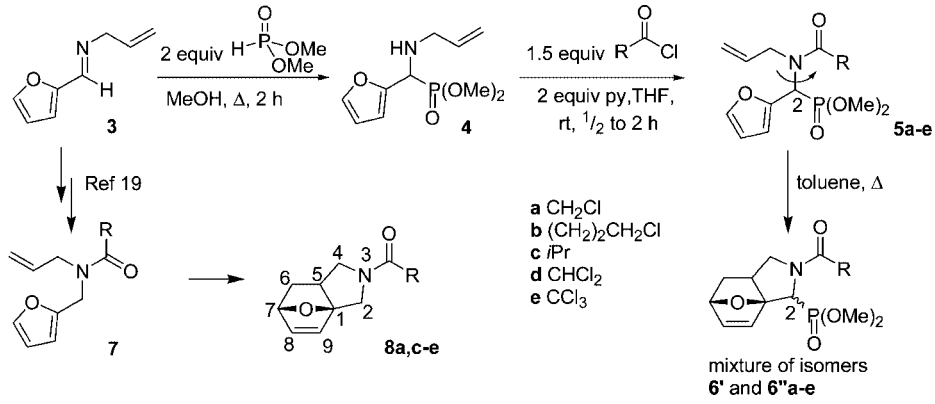

TABLE 1. Acylation and IMDAF Reaction of 1-(Allylamino)-1-(furan-2-yl)methyl Phosphonate 4

no.	R	yield of **5** (%)	conversion/yield of **6**[a] (%)	isomer ratio **6″/6′**	time (h)	*T* (°C)	conversion/yield of **7** to **8**[b] (%)
a	CH_2Cl	99	100/75	27/73	20	110	43/40
b	$(CH_2)_2CH_2Cl$	88	100/47	20/80	4.5	110	
c	*i*Pr	88	100/53	17/83	7	110	62/60
d	$CHCl_2$	96	100/94	35/65	3	110	100/97
e	CCl_3	99[c]	100/99	21/79	1[c]	82	100/99

[a] The reported yields are those of isolated products after column chromatography or crystallization. [b] 30−40 h of reflux in acetonitrile (results from ref 19). [c] The cycloadduct formed at room temperature during acylation and subsequent workup. The obtained mixture of **5e** and **6e** was further refluxed for 1 h to obtain complete conversion to **6e**.

in chemical shift of both NCH_2 protons, clearly indicating that they are on opposite sides of a rigid ring system. Similar to pyrrolidines **8**, the phosphonopyrrolidines **6** were isolated as a mixture of two isomers, indicated as **6′** and **6″** for the major and minor isomer, respectively. Ghelfi and co-workers showed, based on a NOESY experiment, that the configuration of the tricyclic skeleton in **8** was *exo* and that the two isomers were amide rotamers.[19] The description *exo* is used if the group attached to a nonbridgehead atom is pointing toward the oxa-bridge and *endo* if it is pointing away from it. In the case of phosphonopyrrolidines **6**, the isomers might originate from three diverse structural properties: *endo*- or *exo*-annulation, amide rotamers, or configuration of the C^2-center. Most studies using similar substrates show exclusive formation of the *exo*-adduct when the reaction is performed under thermodynamic control.[4,5,7,10,19,21] *Endo*-fused, kinetic products are normally formed under high-pressure-mediated conditions.[7a] Nevertheless, it is reasonable to suggest the appearance of an *endo*-fused isomer next to the *exo*-fused isomer based on the results of Tromp and co-workers.[22] They found that more steric substituents on the tether can favor *endo*-addition. Therefore, the bulky phosphonate group may be able to alter the reaction selectivity, yielding a mixture of both adducts. However, having a close look at the ^{1}H NMR and DQFCOSY data of both isomers **6′** and **6″**, the differences in the multiplicities and coupling constants are found to be too little to be the result of an opposite configuration at the C^5-bridgehead. Comparison with typical coupling constants from similar compounds revealed the presence of an *exo*-fused skeleton in both isomers (Figure 2).

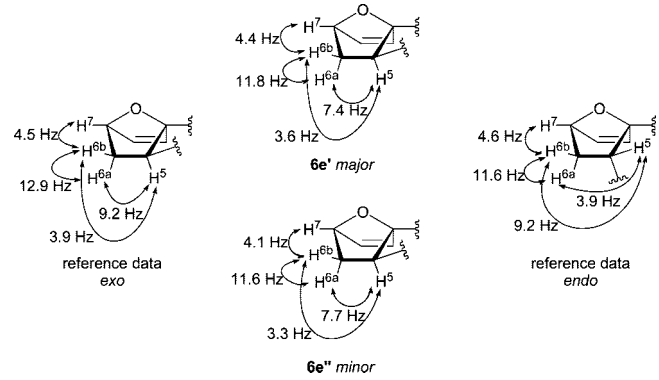

FIGURE 2. Comparison of typical coupling constants from literature sources (refs 22 and 23) with those measured in both isomers of pyrrolidine **6**.

In a further attempt to reveal the identity of the two isomers, they were separated by recrystallization in acetone or diethyl ether, giving the pure major isomer. The filtrate contained a mixture of both isomers from which the minor isomer could be recovered using column chromatography. Both isomers were stable at room temperature for at least 1 month, so no amide rotation is expected to occur during NMR acquisition. Furthermore, no rotamers were observed in the NMR spectra for the open precursors **5**. Therefore, it was concluded that the observed isomers were not rotamers but originated from an incomplete stereocontrol of the IMDAF-reaction at C^2.

In order to reveal the position of the phosphonate group, DIFNOE experiments were performed on both isomers. Considerable nuclear Overhauser effects were observed between C^5H and C^6H_α and C^4H_α, confirming the *exo*-fused skeleton of both isomers (Figure 3). A clear difference between both isomers was observed, however, when the nuclear Overhauser effect at C^2H was studied: the bulky phosphonate is *exo*-oriented in the major isomer **6e′**. These results were confirmed using X-ray analysis (Figure 3).

(21) (a) Pedrosa, R.; Sayalero, S.; Vicente, M.; Casado, B. *J. Org. Chem.* **2005**, *70*, 7273–7278. (b) Padwa, A.; Ginn, J. D.; Bur, S. K.; Eidell, C. K.; Lynch, S. M. *J. Org. Chem.* **2002**, *67*, 3412–3424. (c) Paulvannan, K.; Chen, T.; Jacobs, J. W. *Synlett* **1999**, 1609–1611.

(22) Tromp, R. A.; Brussee, J.; van der Gen, A. *Org. Biomol. Chem.* **2003**, *1*, 3592–3599.

(23) (a) Feringa, B. L.; Gelling, O. J.; Melters, L. *Tetrahedron Lett.* **1990**, *31*, 7201–7204. (b) Van Royen, L. A.; Mijngheer, R.; De Clercq, P. J. *Tetrahedron Lett.* **1983**, *24*, 3145–3148.

SCHEME 2

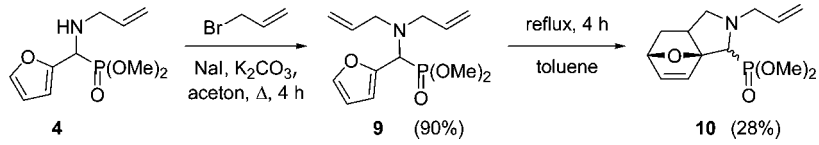

SCHEME 3

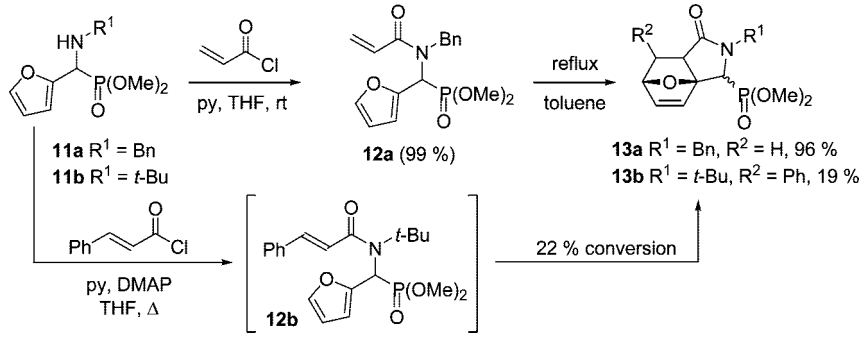

Furthermore, the observed stereoisomer ratio may be the result of thermodynamic control and may not be the isomer ratio formed in the initial reaction mixture. Equilibration can occur under thermal conditions via a consecutive retro-Diels−Alder, Diels−Alder reaction. To investigate this kind of behavior, pure samples of major **6e′** and minor **6e″** were heated in toluene (110 °C). No change at all occurred to the minor isomer **6e″** over a 20 h period. The major isomer **6e'** on the other hand, was slowly converted to the minor isomer **6e″**. After 1 h at 110 °C, only 2% conversion was observed. This did not reflect at all the 21/79 ratio observed after 1 h at 110 °C starting from the open precursor **5e**. When heating was continued for 20 h, 95% conversion to **6e″** was observed. The slow conversion of the major isomer to the minor isomer suggests retrocycloaddition of the less stable cycloadduct. This is in agreement with the stereochemistry generally observed during IMDAF reactions: when a single bulky substituent is present in the tether, the most stable cycloadduct will be formed in such a way as to minimize nonbonded interactions.[7a]

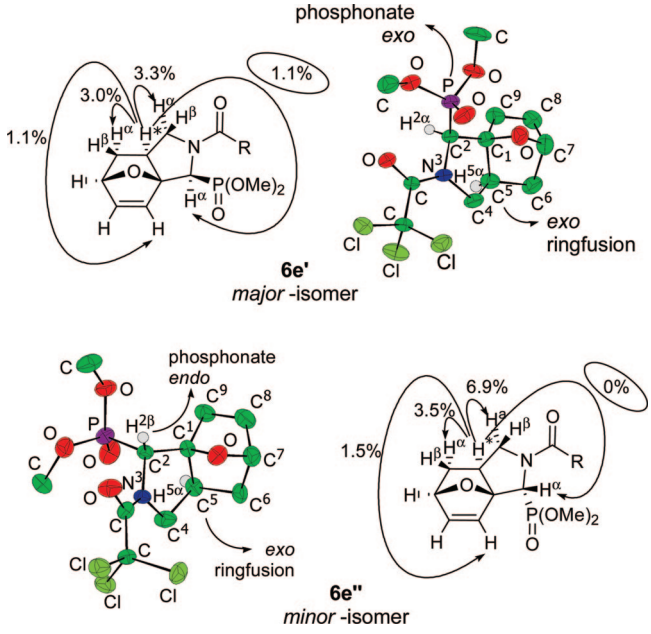

FIGURE 3. Stereochemical analysis of isomers **6e′** and **6e″**. The percentage of nuclear Overhauser effect with irradiation of C^5H is indicated. The X-ray structures of both isomers are depicted as well.

Solvent effects may have an influence on the *endo*/*exo* selectivity.[24] Therefore, an experiment was set up to test this latter effect in the laboratory for the IMDAF reaction leading to pyrrolidine **6e**. Methanol, acetonitrile, and toluene were used as solvents at 65 °C leading to an *endo*/*exo* ratio of 18, 26, and 33%, respectively, after 2.25 h. So, the solvent does not cause an inversion of stereoselectivity, but it causes some change on the *endo*/*exo* ratio; the *endo* ratio increases with a decrease of the solvent polarity.

An additional experiment was performed using a substrate without an amide substituent. *N*-Allyl aminoalkyl phosphonate **4** was allylated using an excess of allyl bromide in the presence of NaI. After refluxing for 4 h in acetone, a mixture of diallylamine **9** and the ring-closed product **10** was obtained (Scheme 2). This mixture was then refluxed in toluene during 4 h, yielding the ring-closed product **10**. Notwithstanding the presence of the chiral *CHP*-center, only one isomer could be detected by NMR. Therefore, the relative stereochemistry at the *CHP*-center was apparently fixed during the ring-closure reaction or equilibration via retrocycloaddition was fast in this case.

This was also observed when the amide group was included in the tricyclic skeleton. In this case, the dienophiles were inserted during alkylation using cinnamoyl and acryloyl chloride. The corresponding pyrrolidinones **13** were obtained as single isomers upon refluxing the amides **12** in toluene or THF (Scheme 3). However, the stereochemistry of the two stereocenters could not be determined via DIFNOE experiments. Refluxing of **13a** in toluene during 60 h did not result in formation of the other epimer. In this case the acylation of the sterically hindered *tert*-butylamine derivative succeeded, but only with a very low degree of conversion and was followed by ring closure in the same reaction step.

To conclude the experimental part learns that for compounds **6** with the acyl group as a substituent on the tether, two isomers were formed, which are epimers at the C^2-center. The major isomer, with the phosphonate in *exo*-position, is the thermody-

(24) (a) Kong, S.; Evanseck, J. D. *J. Am. Chem. Soc.* **2000**, *122*, 10418–10427. (b) Moreau, Y.; Loos, P.-F.; Assfeld, X. *Theor. Chem. Acc.* **2004**, *112*, 228–239. (c) Acevedo, O.; Jorgensen, W. L. *J. Chem. Theory Comput.* **2007**, *3*, 1412–1419.

SCHEME 4. Computationally Studied IMDAF Reactions

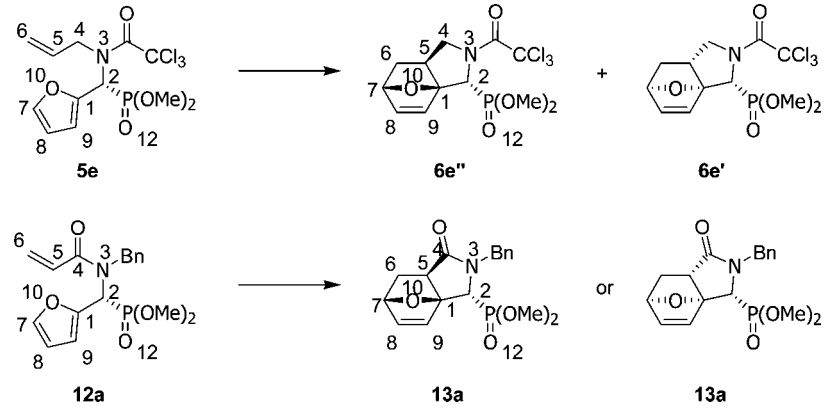

namically less stable one. For the products **13** with the carbonyl group being part of the tether, only one isomer was formed. This isomer could not be converted into the other C^2-epimer by refluxing it in toluene.

Computational Details

All ab initio calculations were carried out with the GAUSSIAN 03 software package.[25] All geometries have been optimized at the B3LYP[11] level with the 6-31+G* basis set and were followed by frequency calculations that confirmed the nature of the stationary points and were used in the thermochemical analysis. Diffuse functions were added as phosphorus is a third-row element.[26] Previous studies have shown B3LYP is very accurate for many Diels−Alder reactions and performs well in reproducing the effects on activation energies but shows systematic errors for hetero systems and incorrectly predicts the strain of the norbornene framework, leading to an underestimation of the reaction exothermicity.[27,28]

As a correct energy calculation of the TSs was relevant because of the small preference for one of the epimers, single-point energies were calculated with new generation functionals, i.e., mPW1PW91[12] and BB1K[13] as well as with post-HF MP2[14] and MP3[15] methods, and these numbers were validated against CCSD.[16]

Theoretical Results and Discussion

As the tricyclic phosphonopyrrolidine **6e** was most easily formed, an X-ray was taken of both these isomers, and to have a means for comparison, **6e** was used for the calculation as well. In addition, the acryloyl derivative **13a** was used because only one isomer was formed in excellent yield. The reactions considered and the numbering of atoms are presented in Scheme 4.

Until now, we have always mentioned the formation of one or two isomers, but actually two or four different isomers are present (keeping in mind that the stereochemistry at positions 1, 5, and 7 are linked), since they appear as enantiomeric couples. The *R*-isomer was used for the calculations. For the product only the *exo*-oriented tether was modeled, which was based on the known stereochemical preference of the reaction. From now on, *exo* and *endo* always point at the orientation of the phosphonate group on the C^2-position of the tether, respectively, pointing toward the oxabridge or away from it.

TABLE 2. Relative[a] Electronic (SCF without ZPE Corrections) and Free Energies at 383.8 K (kJ/mol) for the Stationary Points of the IMDAF Reaction of 12a to 13a with 6-31+G(d) Basis Set

	B3LYP		BB1K		mPW1PW91	
	ΔE	ΔG	ΔE	ΔG	ΔE	ΔG
12a	0.0	0.0	0.0	0.0	0.0	0.0
TS *endo*	111.3	118.5	98.0	105.3	89.1	96.4
TS *exo*	125.6	133.8	113.8	122.0	103.8	112.0
13a *endo*	−24.6	−6.1	−72.9	−54.4	−67.3	−48.8
13a *exo*	−8.9	11.6	−57.8	−37.2	−51.5	−31.0

[a] Relative to the energy of the reactant.

i. Formation of Pyrrolidinone 13a. The relative energies and free energies of the *endo*- and *exo*-cycloadducts **13a** and their respective TSs, with respect to the reactant, are given in Table 2. The product with the phosphonate in the *endo*-position is energetically more stable than the *exo*-analogue due to reduced steric hindrance between the phosphonate group and the oxanorbornene and a higher distance between the electronegative oxygens of the phosphonate—in which the double-bonded *O* is most electronegative—and the oxabridge of the oxanorbornene skeleton. These distances are given in Table 3.

B3LYP is known to have problems with calculating the energy of the oxanorbornene skeleton.[11,27] In this case, the relative free energies of the cycloadducts are too high and ΔG of the *exo*-isomer is even positive. Nevertheless, the energy difference between them can be used as a good indicator for their relative energetic stability, as the strain is about the same in both the *endo*- and the *exo*-isomer. This was confirmed by the good correspondence with the single-point energy calculations using the mPW1PW91[12] and BB1K[13] functional.

The absence of a nuclear Overhauser effect between C^5H and C^2H cannot completely exclude the *exo*-position of the phosphonate, mainly because this NOE effect was small for the *exo*-isomer of pyrrolidine **6e**. An experimental indication that the *endo*-isomer is formed indeed can be deduced from the coupling constant J_{HP} of the proton at C^2 of product **6e**: for the *exo*-isomer this is 14.0 Hz, for the *endo*-isomer 4.7 Hz. Thus, the value of 5.5 Hz found for pyrrolidinone **13a** also points in the direction of the *endo*-isomer.

(25) Frish, M. J. et al. Gaussian 03, Revision C.02; Gaussian, Inc.: Wallingford; CT, 2004; see the Supporting Information for the full reference.
(26) (a) Leyssens, T.; Peeters, D. *THEOCHEM* **2004**, *673*, 79–86. (b) Leyssens, T.; Peeters, D. *THEOCHEM* **2004**, *686*, 71–82.
(27) Guner, V.; Khuong, K. S.; Leach, A. G.; Lee, P. S.; Bartberger, M. D.; Houk, K. N. *J. Phys. Chem. A* **2003**, *107*, 11445–11459.
(28) (a) Domingo, L. R.; Aurell, M. J.; Arno, M.; Saez, J. A. *J. Org. Chem.* **2007**, *72*, 4220–4227. (b) Pieniazek, S. N.; Houk, K. N. *Angew. Chem.* **2006**, *118*, 1470–1473. (c) Pieniazek, S. N.; Houk, K. N. *Angew. Chem., Int. Ed.* **2006**, *45*, 1442–1445. (d) Padwa, A.; Crawford, K. R.; Straub, C. S.; Pieniazek, S. N.; Houk, K. N. *J. Org. Chem.* **2006**, *71*, 5432–5439. (e) Dinadayalane, T. C.; Vijaya, R.; Smitha, A.; Sastry, G. N. *J. Phys. Chem. A* **2002**, *106*, 1627–1633. (f) Domingo, L. R.; Picher, M. T.; Andrés, J. *J. Org. Chem.* **2000**, *65*, 3473–3477.

TABLE 3. Geometric Parameters for the Stationary Points of the IMDAF Reaction of 12a to 13a of the B3LYP/6-31+G(d)-Optimized Structures (Distances in Å, Angles in deg)

	$a_{O^{10}P^{11}}$	$a_{O^{10}O^{12}}$	$a_{O^{10}O_{Cl}}$ [a]	$a_{H_{Bn}O^{12}}$ [b]	$a_{H_{ar}O^{12}}$ [c]	$\varphi C^1C^2NC^4$	$\varphi C^2NC^4C^5$	$\varphi O^{10}C^1C^2N$
12a	4.06	4.56	4.56	4.51	4.68	120.68	−168.43	−27.15
TS *endo*	4.08	5.22	4.30	2.46	3.37	−12.49	−12.99	−71.79
TS *exo*	3.21	4.61	2.93	2.37	2.51	18.04	6.05	70.33
13a *endo*	4.09	5.23	4.27	2.52	3.21	−10.81	−6.09	−84.27
13a *exo*	3.17	4.57	2.88	2.45	2.52	16.70	1.22	80.94

[a] O_{cl} is the oxygen of the methoxy groups closest to the oxabridge. [b] H_{Bn} is the H-atom at the benzylic position closest to O^{12}. [c] H_{ar} is the aromatic hydrogen atom closest to O^{12}.

TABLE 4. Relative[a] Electronic (SCF without ZPE Corrections) and Free Energies at 354.8 K (kJ/mol) for the Stationary Points of the IMDAF Reaction of 5e to 6e with 6-31+G(d) Basis Set

	B3LYP		BB1K		mPW1PW91		MP2		MP3		CCSD	
	ΔE	ΔG	ΔE	ΔG	ΔE	ΔG	ΔE	ΔG	ΔE	ΔG	ΔE	ΔG
5e	0.0	0.0	0.0	0.0	0.0	0.0						
TS *endo*	101.5	113.7	87.7	100.0	80.6	92.8	1.4	1.9	1.0	1.5	1.0	1.6
TS *exo*	101.9	113.6	85.4	97.2	78.7	90.4	0.0	0.0	0.0	0.0	0.0	0.0
6e *endo*	−26.0	−1.8	−76.2	−52.1	−67.7	−43.6						
6e *exo*	−12.3	9.5	−63.8	−42.0	−54.6	−32.9						

[a] Relative to the energy of the reactant for DFT methods and to the TS *exo* for MPx and CCSD.

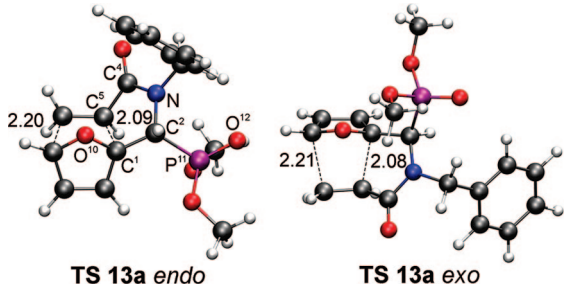

FIGURE 4. Structures of the TSs of the *endo*- and *exo*-isomer of **13a** at B3LYP/6-31+G(d). Distances in angstroms.

Both pathways were then explored to find an explanation for the formation of a single isomer of pyrrolidinone **13a** (Table 2). This IMDAF reaction has a large energy barrier toward the TS, which is in agreement with the high temperature required for the reaction. At 110 °C, the precursor rotamers will be in equilibrium and the kinetic isomer ratio of the cycloadducts will depend only on the difference in the free energy of the TS of both isomers (Curtin−Hammett principle[29]). The TSs are depicted in Figure 4, and relevant geometrical parameters for TSs and precursors are given in Table 3. The free energy of the TS for the *exo*-isomer is higher than for the *endo*-isomer by 15−17 kJ/mol depending on the functional; causing the exclusive formation of the *endo*-isomer.

To trace the origin of this energetic difference, we took a closer look at the TSs and reactant. The major differences between the TSs of the different isomers are the dihedral angles $\varphi O^{10}C^1C^2N$ and $\varphi C^1C^2NC^4$. The first one corresponds to the rotation of the furan group and has an opposite value for both isomers. The latter is associated with the hindered C^2-N rotation we described previously.[17] This rotation has a barrier of about 70 kJ/mol at the HF/3-21+g* level and shows two minima at −45° and at 115° that have about the same energy. The *exo*-TS needs a larger distortion of the dihedral angle, and this might be one of the origins for the higher energy of the TS. This increase can be attributed to steric interactions, mainly of the benzyl and furan group with the phosphonate moiety as can be seen from the distances given in Table 3. The rotational potential in terms of the dihedral angle $\varphi C^1C^2NC^4$ was calculated at a B3LYP/6-31+G(d) level of theory and is given as Figure S1 in the Supporting Information.

TABLE 5. Geometric Parameters for the Stationary Points of the IMDAF Reaction of 5e to 6e of the B3LYP/6-31+G(d)-Optimized Structures (Distances in Å, Angles in deg)

	$a_{O^{10}P^{11}}$	$a_{O^{10}O^{12}}$	$a_{O^{10}O_{Cl}}$ [a]	$\varphi C^1C^2NC^4$	$\varphi C^2NC^4C^5$	$\varphi O^{10}C^1C^2N$
5e	3.14	3.50	3.07	−43.52	80.24	85.95
TS *endo*	4.08	4.59	4.54	−32.26	8.59	−61.61
TS *exo*	3.06	3.42	2.96	−23.02	49.33	92.05
6e *endo*	4.09	4.57	4.58	−25.18	8.19	−75.71
6e *exo*	3.02	3.37	2.90	−15.51	35.78	98.58

[a] O_{cl} is the oxygen of the methoxy groups closest to the oxabridge.

For formation of pyrrolidinone **13a** we find exclusive formation of the *endo*-isomer corresponding to the experimental results of full selectivity, irrespective of the functional used.

ii. Formation of Pyrrolidines 6e. The energies and important geometrical parameters of the stationary points in the cycloaddition to the *exo*- and *endo*-isomer of **6e** are given in Tables 4 and 5. Again, B3LYP underestimates the free energy of the reaction, but the energy difference between both epimers is independent of the functional. The *endo*-cycloadduct is energetically preferred in order to minimize the steric hindrance and electrostatic repulsion between the phosphonate group and the oxabridge of the oxanorbornene skeleton. These distances between the oxygen atoms are listed in Table 5. The energy difference between the *endo*- and *exo*-isomer of pyrrolidinone **13a** is of the same order of magnitude as for the pyrrolidine **6e**. If the retro-Diels−Alder reaction is possible, this difference in stability between the two isomers can explain the conversion of the major isomer into the minor isomer under thermodynamic control.

Next, we wanted to unravel the experimentally observed isomer ratio during the synthesis of pyrrolidine **6e**. To test whether the Curtin−Hammet[29] conditions are fulfilled, the reaction was followed in methanol. Methanol was chosen because of its lower boiling point which does not allow the retro-Diels−Alder reaction to occur, as observed experimentally. Moreover, the ^{31}P NMR peaks of both isomers are better

(29) Seeman, J. I. *Chem. Rev.* **1983**, *2*, 83–134.

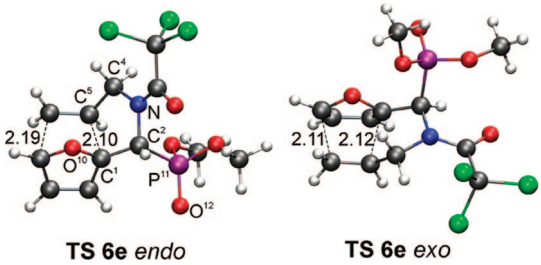

FIGURE 5. Structures of the TSs of the *endo*- and *exo*-isomer of **6e** at B3LYP/6-31+G(d). Distances in angstroms.

resolved. As the ratio of major and minor isomer remained constant throughout the course of the reaction, the Curtin−Hammet principle holds. So again the relative energies of the TSs were studied. The structures and parameters are given in Figure 5 and Tables 4 and 5. The energetic difference of both TSs is very small and depends on the functional. Therefore, a higher level of theory was used to calculate these subtle differences. MP2[14] and MP3[15] calculations predict indeed a lower free energy of the *exo*-TS by 1.9 to 1.5 kJ/mol, and these figures were validated using a CCSD[16] calculation. This confirms the formation of a mixture of the *endo*- and *exo*-cycloadduct.

The retro-Diels−Alder reaction of the *exo*-isomer has an activation free energy that is, depending on the method, 33−42 kJ/mol more than the forward reaction and indicates that the slow thermodynamic conversion of the *exo*- isomer to the *endo*-epimer is possible.

The theoretical study for formation of pyrrolidine **6e** indeed shows that the *endo*-cycloadduct is thermodynamically preferred and that there is a competition between the formation of both isomers. CCSD calculations confirm the experimentally observed preference for the epimer in which the phosphonate group is oriented toward the oxa-bridge.

Conclusions

The IMDAF-reaction of 1-acyl-1-alkylamino(furan-2-yl)-methyl phosphonates results in complex azaheterocyclic phosphonates in a small number of synthetic steps. These products might be used as novel conformationally constrained amino acid analogues. The presence of a phosphonate substituent on the tether raises the conversion of the IMDAF reaction significantly. Furthermore, a high degree of stereocontrol is observed during the cycloaddition reaction. Only the *exo*-fused products were obtained. For derivatives containing the carbonyl group in the tether two isomers were formed, originating from incomplete stereocontrol of the phosphite addition. If the allyl group serves as dienophile, four isomers are formed resulting from an incomplete kinetic control of the position of the phosphonate as tether substituent during the IMDAF reaction. However, the most stable stereoisomers, having an *endo*-oriented phosphonate group, are formed under thermodynamic control.

This kinetic and thermodynamic control could be computationally reproduced. With the acyl group functioning as dienophile the isomers with the phosphonate group in the *exo*-position require a larger distortion from their minimum energy precursor than the *endo*-isomers and are sterically more hindered, as can be seen in their respective TSs. For aminophosphonates **5** with the allyl group as dienophile the *endo*- and *exo*-position require about the same amide rotation and there is a subtle energy difference that requests a high level of theory calculation. From the calculations, it is clear that B3LYP fails to estimate the reaction free energy of these strained cycloadducts.

Experimental Section

Typical Procedure for the Synthesis of α-Aminophosphonates 4 and 11a,b. See ref 18.

Typical Procedure for the Acylation of α-Aminophosphonates (5 and 12a,b). To a solution of 5 mmol of 1-aminoalkyl phosphonate in 10 mL of dry THF were added 10 mmol of pyridine and a solution of the acid chloride of choice in 2 mL of dry THF under a nitrogen atmosphere. The reaction mixture was stirred for 0.5−2 h at room temperature. It was washed with saturated $NaHCO_{3(aq)}$ and then with a 1 M $HCl_{(aq)}$ solution. After drying with $MgSO_4$, filtration of the solids, and evaporation of the solvent under reduced pressure, the product was obtained in high purity.

Synthesis of Tricyclic Phosphonopyrrolidines. Procedure for the Preparation of Dimethyl (3-Allyl-10-oxa-3-azatricyclo-[5.2.1.0^{1,5}]dec-8-en-2-yl)phosphonate (10). A mixture of α-aminophosphonate **4** (5 mmol), allyl bromide (15 mmol), sodium iodide (15 mmol), and potassium carbonate (35 mmol) was refluxed in 5 mL of acetone. After 4 h, the mixture was cooled to room temperature; the insoluble salts were filtered off, and the filtrate was evaporated under reduced pressure. This resulted in a mixture of diallylamine **9** (90%) and the ring-closed product. Refluxing in toluene completed the IMDAF reaction. Product **10** was purified using column chromatography (EtOAc, $R_f = 0.25$) which caused the yield to drop to 28%.

Procedure for the Preparation of Dimethyl (3-tert-Butyl-4-oxo-6-phenyl-10-oxa-3-azatricyclo[5.2.1.0^{1,5}]dec-8-en-2-yl)phosphonate (13b). A solution of 5 mmol of 1-(*tert*-butylamino)-1-(furan-2-yl)methyl phosphonate (**11b**) and 10 mmol of pyridine in 12 mL of dry THF was stirred at room temperature under a nitrogen atmosphere. A solution of 7.5 mmol of cinnamoyl chloride in 3 mL of dry THF was added. The mixture was then refluxed for 7 h. It was washed with saturated $NaHCO_{3(aq)}$ solution and then with 1 M $HCl_{(aq)}$ and dried with $MgSO_4$. After filtration of the solids and evaporation of the solvent under reduced pressure, a brown oil was obtained from which the ring-closed product could be obtained in pure form using column chromatography.

Typical Procedure for the IMDAF Reaction (6 and 13a). A solution of 3.5 mmol of a suitable 1-(alkylamino)-1-(furan-2-yl)methyl phosphonate in 14 mL of toluene was refluxed until complete disappearance of the starting material was obtained (monitoring by ^{31}P NMR). Then the solvent was removed under reduced pressure, and the corresponding adducts were obtained in good purity. Further purification could be performed using column chromatography or crystallization from ether or acetone.

Acknowledgment. We thank the Research Foundation - Flanders (Fonds voor Wetenschappelijk Onderzoek - Vlaanderen) and the research board of Ghent University for financial support of this research.

Supporting Information Available: General experimental methods, experimental procedures, spectroscopic data of all new compounds with detailed peak assignments, crystallographic information files of **6e′** and **6e″**, computational data, and full reference. This material is available free of charge via the Internet at http://pubs.acs.org.

JO801138S

Curriculum vitae

Personalia

Diederica Claeys
Berouw 78
9000 Gent

diederica.claeys@UGent.be

Bio-engineer Chemistry
° 24/11/1982, Ninove

Education

Secondary School:	Latin-mathematics (1994-2000) Sint-Aloysiuscollege, Ninove
University:	Master of Bioscience Engineering: Chemistry (2000-2005) Ghent University, graduated with great distinction
Erasmus:	University of Helsinki (September-December 2003)
Master Thesis:	'Reactivity and Ring Expansion of Pyroglutamate Derivatives' Promoter: Prof. Dr. ir. C. Stevens Research Group SynBioC, Department of Organic Chemistry
PhD Training:	Ghent University (2006-2009) Organometallic Chemistry Introduction to Quantum Chemistry Molecular Modelling Molecular Simulations of Biosystems Presentation Techniques University of Amsterdam (January 2008) Understanding Molecular Simulations

Career

Ph.D. Fellow of the Research Foundation – Flanders (01/10/2005 - Present)
Department of Organic Chemistry, Faculty of Bioscience Engineering, Ghent University
Title:'Combination of Experimental and Computational Chemistry in the Synthesis of New Azaheterocycles'
Promoters: Prof. dr. ir. C. Stevens, Research Group SynBioC, Department of Organic Chemistry, Faculty of Bioscience Engineering, Ghent University
Prof. dr. ir. V. Van Speybroeck, Centre for Molecular Modeling, Ghent University

Publications

Conformational Sampling of Macrocyclic Alkenes Using a Kennard-Stone Based Algorithm
Claeys, D.D.; Verstraelen, T.; Pauwels, E.; Stevens, C.V.; Waroquier, M.; Van Speybroeck, V. *J. Comput. Chem.*, submitted

Synthesis of Tricyclic Phosphonopyrrolidines via IMDAF: Experimental and Theoretical Investigation of the Observed Stereoselectivity
Claeys, D.D.; Moonen, K.; Roman, B.I.; Nemykin, V.N.; Zhdankin, V.V.; Waroquier, M.; Van Speybroeck, V.; Stevens, C.V. *J. Org. Chem.*, **2008**, *73*, 7921.

The Formation of *trans*-Fused Macrocycles from N^3,$N^{3'}$-Polymethylenebis(hydantoins) by Ring-Closing Metathesis
Claeys, D.D.; Stevens, C.V.; Dieltiens, N. *Eur. J. Org. Chem.*, **2008**, *1*, 171.

Exploiting the Regioselectivity of Pyroglutamate Alkylations for the Synthesis of 6-Azabicyclo[3.2.1]octanes and 4-Azabicyclo[3.3.0]octanes
Masschelein, K.G.R.; Stevens, C.V.; Dieltiens, N.; Claeys, D.D. *Tetrahedron*, **2007**, *63*, 4712.

The Pyroglutamate Hydantoin Rearrangement
Dieltiens, N.; Claeys, D.D.; Zhdankin, V.V.; Nemykin, V.N.; Allaert, B.; Verpoort, F.; Stevens, C.V. *Eur. J. Org. Chem.*, **2006**, *11*, 2649.

Synthesis of *N*(3),*N'*(3)-Polymethylene-bis-hydantoins and Their Macrocyclic Derivatives
Dieltiens, N.; Claeys, D.D.; Stevens, C.V. *J. Org. Chem.*, **2006**, *71*, 3863.

Synthesis of 1,3-dioxo-hexahydropyrido[1,2-*c*][1,3]diazepine carboxylates, a new bicyclic skeleton formed by ring expansion-RCM methodology
Dieltiens, N.; Claeys, D.D.; Allaert, B.; Verpoort, F.; Stevens, C.V. *Chem. Comm.*, **2005**, *35*, 4477.

Straightforward Ring Expansion of Pyroglutamates to Perhydro-1,3-diazepine-2,4-diones
Stevens, C.V.; Dieltiens, N.; Claeys, D.D. *Org. Lett.*, **2005**, *7*, 1117.
Additions and Corrections:
Stevens, C.V.; Dieltiens, N.; Claeys, D.D. *Org. Lett.*, **2005**, *7*, 5347.

Participation to Conferences

Oral Presentation:

The Formation of *Trans*-Fused Macrocycles from N(3),N'(3)-Polymethylenebishydantoins Using Second-Generation Grubbs' Catalyst
Claeys, D.D.; Dieltiens, N.; Stevens, C.V.; Van Speybroeck, V.; Waroquier, M. *NCCC*, March 3-5, 2008, Noordwijkerhout, The Netherlands

Posters:

Cleavage of the Oxanorbornene Oxygen Bridge with Lewis Acids: Computaion and Experiment
Claeys, D.D.; Moonen, K.; Roman, B.I.; Van De Caveye, P.; Van Speybroeck, V.; Waroquier, M.; Stevens, C.V. *13th International Congress of Quantum Chemistry ICQC*, June 22-27, 2009, Helsinki, Finland

Use of Ring-Closing Metathesis to Form *trans*-Fused Macrocyclic Bis(hydantoins): Synthesis and Theory
Claeys, D.D.; Dieltiens, N.; Stevens, C.V.; Van Speybroeck, V.; Waroquier, M. *11th Belgian Organic Synthesis Symposium BOSS XI*, July 13-18, 2008, Ghent – Belgium

A Combined Experimental and Theoretical Investigation of the Stereoselectivity in the Synthesis of Azaheterocyclic Phosphonates
Claeys, D.D.; Moonen, K.; Roman, B.I.; Van Speybroeck, V.; Waroquier, M.; Stevens, C.V. 12th *Sigma-Aldrich Organic Synthesis Meeting*, December 4-5, 2008, Sol Cress – Spa – Belgium

The Formation of *Trans*-Fused Macrocycles from N(3),N'(3)-Polymethylenebishydantoins Using Ring-Closing Metathesis
Claeys, D.D.; Dieltiens, N.; Stevens, C.V.; Van Speybroeck, V.; Waroquier, M. *9de Vlaams Jongerencongres van de Chemie*, April 4, 2008, Antwerp, Belgium

Synthesis of Functionalised Bicyclic Hydantoin Derivatives via a Ring Transformation-RCM Sequence
Dieltiens, N.; Claeys, D.D.; Stevens, C.V. *9th Sigma-Aldrich Organic Synthesis Meeting*, December 1-2, 2005, Sol Cress – Spa – Belgium

Abstracts at Conferences

Exploiting the Regioselectivity of Pyroglutamate Alkylations
Masschelein, K.G.R.; Dieltiens, N.; Claeys, D.D.; Rammeloo, T.; Stevens, C.V. *10th Sigma-Aldrich Organic Synthesis Meeting*, December 7-8, 2005, Sol Cress – Spa – Belgium

Straightforward Ring Opening of Pyroglutamates for the Synthesis of Perhydro 2,4-dioxo-1,3-diazepines
Stevens, C.V.; Dieltiens, N.; Claeys, D.D. *6th Annual Florida Heterocyclic Course and Conference*, March 3-6, 2005, University of Florida, Gainsville, US

Straightforward Synthesis of Complex Hydantoin Derivatives via a Rearrangement-RCM Sequence
Dieltiens, N.; Claeys, D.D.; Stevens, C.V. *Journées Nord-Ouest Européennes des Jeunes Chercheurs*, April 13-14, 2006, Villeneuve d'Ascq, France